SERI/CP - 622-1096
UC CATEGORY: 61a

SPECIALISTS' WORKSHOP ON
FAST PYROLYSIS OF BIOMASS
PROCEEDINGS

OCTOBER 19-22, 1980

FOXPINE INN

COPPER MOUNTAIN, COLORADO

SPONSORED BY:

SOLAR ENERGY RESEARCH INSTITUTE

FOR THE

U.S. DEPARTMENT OF ENERGY

Table of Contents

Other Considerations

PREFACE

The Solar Energy Research Institute (SERI) is deeply committed to the thermal conversion of biomass to fuels and petrochemicals. One of the most promising techniques involves the very rapid pyrolysis of biomass and this specialists' workshop was organized to explore in depth the phenomena of fast pyrolysis. This workshop brought together most of those who are currently working in or have published significant findings in the area of fast pyrolysis of biomass or biomass-derived materials, with the goal of attaining a better understanding of the dominant mechanisms which produce olefins, oxygenated liquids, char, and tars. In addition, background papers were given in hydrocarbon pyrolysis, "slow" pyrolysis of biomass, and techniques for powdered-feedstock preparation in order that the other papers did not need to introduce in depth these concepts in their presentations for continuity. In general, the authors were requested to present summaries of experimental data with as much interpretation of that data as possible with regard to mechanisms and process variables such as heat flux, temperatures, partial pressure, feedstock, particle size, heating rates, residence time, etc. The attendees were limited primarily to the other authors in order to have a small informal gathering. After presentation of all the papers, time was set aside for a round table discussion of the pyrolysis mechanisms and how they can be manipulated to produce valuable fuel and petrochemical products. The discussion also addressed those research areas which would be most fruitful to the future application of fast pyrolysis of biomass and biomass-derived materials to more useful fuels and petrochemicals. The round table discussion was off the record to encourage as much discussion as possible. It is hoped that these proceedings will constitute a useful reference volume to those pursuing fast pyrolysis. In order to make the proceedings available as soon as possible, the individual papers were not subjected to editing by SERI and are reproduced herein as they were submitted by the authors.

The financial support and technical direction of Simon Friedrich of the Biomass Energy Systems Division of the U.S. Department of Energy through Don Stevens and Gary Schiefelbein of Pacific Northwest Laboratories of Richland, WA are gratefully acknowledged.

James Diebold
Biomass Thermal Conversion
and Exploratory Branch
SERI

WORKSHOP SUMMARY

James Diebold, Workshop Chairman
SERI, Golden, CO 80401

This workshop brought together what is believed to be most of the individuals who have been or who are now involved with the study of the fast pyrolysis of biomass. These individuals have approached fast pyrolysis with a number of different methods and reaction conditions. As evidenced by the relative yields of char, tar, oxygenated liquids, and gases (including olefins), it appears that different reaction conditions favor different product distributions.

There was a general agreement that very rapid heating of the biomass to temperatures above 700°C greatly increased the gas yields at the expense of the char and tars favored at low heating rates and low final temperatures. The actual measurement of the heating rate of the biomass during fast pyrolysis is quite difficult due to the relatively short time involved with the very high heating rates, e.g., at 10,000°C/s the biomass is pyrolyzed in 30 to 50 milliseconds. This difficulty in temperature measurement of the pyrolyzing biomass is reflected by the differences in kinetic parameters derived by different researchers utilizing different experimental techniques.

Another complicating factor in comparing pyrolysis data from several sources is that there has been very little, if any, attempt to standardize the feedstocks used in fast pyrolysis. Thus, it has been difficult to separate the effects of feedstock from experimental apparatus and techniques. To obtain a uniform sample of a heterogeneous material such as hygroscopic biomass presents a real, non-trivial problem due to differences in moisture content, lignin/cellulose/homocellulose ratios, volatile oils or terpene content, ash content, and ash composition within even the same species or the same plant. For example, a pine tree will have a high concentration of pitch near an old injury, which would be expected to greatly increase the olefin content of the pyrolysis gases. Refined biomass products such as microcrystalline cellulose and powdered Kraft lignin are thought to be very uniform materials, but since they are not chemically the same as raw biomass their use does not necessarily lead to valid conclusions relative to the pyrolysis of unprocessed biomass materials. The use of a central repository having several "standardized" biomass feedstocks would help in the comparison of pyrolysis data. The "standardization", storage, and distribution of the feedstocks would require a significant effort for which none of the attendees currently had resources available. Until a central biomass repository is established, the most practical, low cost solution to the non-uniform feedstock problem may well be to use the highly processed, microcrystalline cellulose as a standard to compare different pyrolysis techniques and process conditions. The evaluation of more practical biomass feedstocks would then be relative to this standard cellulosic feedstock in the same reactor

and process conditions. The use of a standard in this way will increase the experimentation a bit, but several researchers have already reported fast pyrolysis results with this type of "standard" material.

The chemical mechanisms involved in the fast pyrolysis of biomass are not yet well understood. However, in an attempt to visualize the general effect of process variables, the overall mechanisms shown below are thought to have sufficient validity for consideration. Of considerable importance in the visualization of biomass pyrolysis is that there are many competing reactions which result in different products. These many reactions may be divided into two major categories: molecule splitting versus molecule building. The molecule building reactions are favored by the close proximity of the molecules found in condensed phases (liquid or solid) or by higher partial pressures which encourage bimolecular reactions. The molecule splitting or cracking reactions are favored by a separation of the molecules, e.g., a low partial pressure in the vapor phase, which makes the bimolecular reactions less probable. Figure 1 illustrates this pyrolysis concept where the desired route to olefins is shown as a horizontal sequence of reactions within the rectangular box. In this desired sequence, the biomass is first depolymerized to a sufficiently low molecular weight to allow it to vaporize from the liquid primary tar surface. High surface temperatures and a low partial pressure for the tar vapors encourage this volatilization to occur before the primary tar liquids rearrange and/or polymerize to more thermally stable secondary tar liquids. These primary and secondary tar liquids are apparently quite viscous at low pyrolysis temperatures and can retain many of the macroscopic features of the biomass cell walls. If the secondary tar liquids are not quickly heated to higher temperatures, they further polymerize and rearrange to form solid charcoal (having macroscopic cellular features, water, and carbon oxides. The primary tar vapors will tend to form vapor-phase derived tars by polymerization if the temperatures are only moderately high and/or if the partial pressure is high. Transient oxygenated fragments in the vapor phase are formed by cracking any of the previously mentioned tars or the refractory water soluble oxygenated compounds. These transient fragments would be very active species and rapidly crack to form hydrogen, carbon oxides, and hydrocarbons if the temperatures are high and the partial pressures are low. Higher partial pressures of these active species encourage the molecular building processes which result in the vapor-phase-derived tar and the refractory water solubles. The vapor-phase-derived tars can undergo further molecular growth with extended residence times, high temperatures and partial pressures to form a vapor-phase-derived, solid carbon black (which can condense into 1 μm spheres and then form agglomerates of up to about 200 μm in diameter). The olefins are relatively inert with respect to the other gases, but can undergo vapor phase polymerization to form aromatic liquids and polyaromatic solids (carbon black) with high temperatures, high partial pressures, and long residence times. The temperatures, times, and partial pressures in Figure 1 should only be considered qualitative at this time; future work in fast pyrolysis

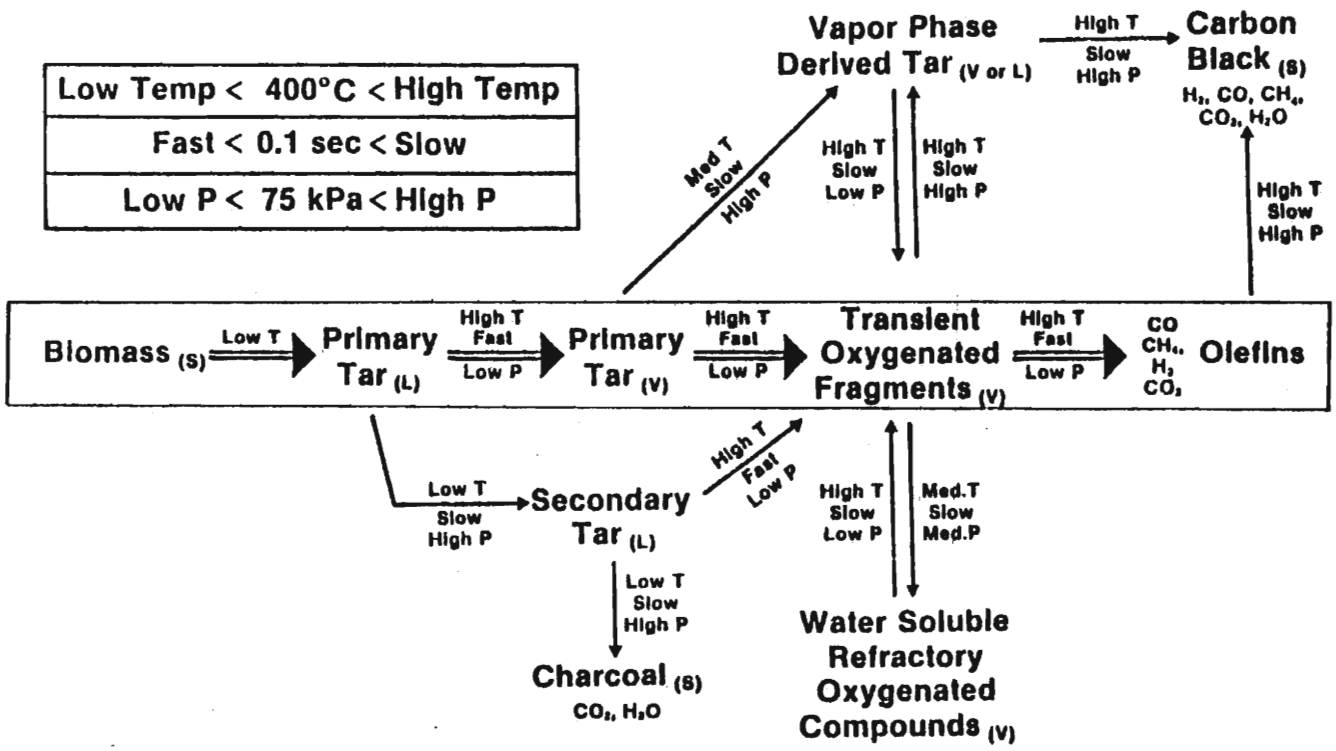

FIG. 1. REACTIONS COMPETING WITH FAST PYROLYSIS REACTIONS

will help to better quantitatively establish these values as well as to modify some of these proposed mechanisms. It should be noted that not all of the attendees were in agreement with these overall mechanisms, but at the moment the concepts seem to explain most of the experimental results reported at the workshop.

Other areas for future research efforts which were discussed by the attendees included tar and char characterization, heat transfer, and feedstock preparation including the possibility of prehydrogenation followed by pyrolysis.

PERSPECTIVES IN HEAT TRANSFER REQUIREMENTS AND MECHANISMS FOR FAST PYROLYSIS

T.B. Reed, J.P. Diebold, and R. Desrosiers

SERI, Golden, CO

ABSTRACT

When biomass is heated slowly it produces charcoal, tars and gases, but as the heating rate increases less char is produced and at sufficiently high rates very little, if any, char is produced. Since the slowest step in gasification of biomass is the conversion of char to gas, rapid heating of biomass will be very important in gasification processes.

Methods of attaining the high heat fluxes of interest in fast pyrolysis are discussed and put into relative order of magnitude perspective. The concept of transfer by solid convection is introduced for consideration as a practical method for fast pyrolysis. Equations are presented which describe a non-char forming pyrolysis model as a function of heat flux, time, and thermal properties of the biomass.

INTRODUCTION

In the last few years it has become increasingly evident that the yields of volatiles from the pyrolysis of biomass (and coal) increase with the rate of heating [1,2,3]. In fact, there now seems to be good evidence that at sufficiently high heating rates, cellulose and probably all biomass can be nearly all converted to volatiles [4,5]. Since once formed, the conversion of char to gas is the most difficult step in gasification of biomass or coal, the absence of char has far reaching implications for the future of gasification.

If we accept the conclusion that sufficiently rapid heating can completely convert biomass to volatile materials only, we should then examine all possible methods for achieving high heat transfer rates and determine which ones are likely to hold the most promise for practical fast pyrolysis systems. We summarize many possible methods and examine their suitability below.

HEAT TRANSFER CHARACTERISTICS OF FAST PYROLYSIS OF BIOMASS

Energy Requirements

Thermogravimetric (TGA) experiments show that pyrolysis of dry biomass begins at about 200°C and is essentially complete at 500°C. The energy required in this temperature range is more difficult to

estimate because it varies, depending upon the products formed. In slow pyrolysis the techniques of differential scanning calorimetry (DSC) show that pyrolysis can be exothermic (self-heating) over a part of this temperature range if char is formed [6].

Under the rapid heating conditions of fast pyrolysis however, it has not been possible to measure the heat consumed in vaporizing biomass. For the sake of argument, consider fast pyrolysis to be a sequence of steps involving sensible and latent heating of the biomass. Consider that the biomass is first sensibly heated without undergoing phase changes or chemical reactions. At the reaction temperature, the biomass is depolymerized to form a solid which subsequently melts. If the temperature is high enough, the melted biomass can then vaporize. The melting and vaporization may actually occur as a single step (sublimation). Since enthalpy is a point function and independent of path, the energy required for a single-step or a two-step path to the vapor state would be identical. The overall standard heat of reaction of fast pyrolysis (reactants starting at 25°C and the final products ending up at 25°C) was determined by the work of Diebold and Benham at the Naval Weapons Center, China Lake, CA to be essentially zero with municipal-trash derived organics. The heat required to produce vapors from biomass is given by:

$$\Delta h_p = c\Delta T + \Sigma x_i \Delta h_{m_i} + \Sigma x_i \Delta h_{v_i} + [\Sigma x_i \Delta h_{f_i} - \Delta h_{f_{feedstock}}] \quad (1)$$

where c is the heat capacity of the solid biomass, ΔT is the increase in temperature of the biomass needed for pyrolysis, Δh_{m_i} is the heat of melting of each liquid species, Δh_{v_i} is the heat of vaporization of each vapor species and x_i is the mass fraction of each product species, and Δh_f is the heat of formation of each species in the solid phase.

Unfortunately, the number of species in the vapor phase is enormous; the heats of formation and vaporization are not known and the vaporization occurs over a range of temperature. We can obtain an estimate for the heat of fast pyrolysis from the following approximation. The heat capacity of biomass is about 2.7 J/g°C. Thus, it requires about 1350 J/g to sensibly heat biomass to 500°C without chemical reaction, melting, vaporization, or pyrolysis. Assume that the average molecular weight of the vapors is 100 and that vaporization occurs at 500°C. From Trouton's rule to estimate the heat of vaporization and Reed's rule to estimate the heat of melting, the entropy of sublimation is 104 J/mole °K. From this we estimate the heat of sublimation of biomass is 803 J/g. Then the heat required to vaporize biomass would be 2157 J/g or about 2000 J/g, if the energy associated with the chemical reactions is negligible. This corresponds to a little more than 10% of the heat of combustion of the biomass.

If however, the pyrolysis step does not require the vaporization of the decomposition product and a mechanical means is used to wipe the tars away, then the heat input to the biomass is less. If the primary tars have a higher molecular weight than the vapors, say an average molecular weight of 162, using Reed's rule their heat of fusion would be estimated to be about 40 J/g at 500°C. Using the same sensible heat as before of 1350 J/g, the pyrolysis to tar liquids would require 1390 J/g or about 1400 J/g which is about a third less than required for pyrolysis followed by vaporization. Subsequent vaporization of the tar liquids would require the same total input of energy to the system as in the above example, but considerably less energy would need to be transferred to the decomposing biomass itself.

Heat Flux Requirement

There are a large number of competing reactions involved with fast pyrolysis. For example, if the initially formed tar molecules do not vaporize quickly enough, they will have a tendency to crosslink and form thermally stable larger tar molecules which in turn can eventually form char. The relative rates of the volatile-forming and the char-forming reactions have been studied extensively. The volatile forming reaction is favored over the char forming reaction by a ratio of only two to one at 300°C, but at 600°C the volatile forming reaction is favored by fifty to one [7]. Thus, if the heating rate is very fast so that the biomass spends an insignificant amount of time at the lower temperatures, nearly all volatiles can be produced. Since volatiles are more apt to be the precursors of olefins than is char, high heat fluxes causing very rapid heating rates are therefore desirable to produce olefins from biomass. With very thin, two-dimensional cellulose samples blackened with 2% carbon black, it has been found that radiant heat fluxes of 6.3 W/cm^2 produced 33 per cent by weight char whereas 46 W/cm^2 reduced the char produced to 3% and 12,500 W/cm^2 further reduced the char level to about 1% [1]. Three-dimensional biomass samples will require significantly higher heat fluxes to achieve the same degree of volatization due to heat sink effects. Thus, the central problem of fast pyrolysis is to supply about 2000 J/g to a biomass surface at about 500°C with a flux somewhat above 50 W/cm^2.

Ablative Cooling

The physical mechanism of fast pyrolysis appears to be one of ablative cooling. As the surface temperature of the biomass increases to that necessary for pyrolysis, depolymerization of the lignocellulosic material produces a liquid tar on that surface. If the liquid tar is not mechanically removed and is allowed to remain on the biomass surface, it will absorb a considerable amount of energy as it further pyrolyzes and/or vaporizes. The initial presence of the pyrolysis products and their subsequent movement away from the biomass surface form a protective film which adversely affects the ability to transfer heat into the biomass. This mechanism is called ablative cooling and is the mechanism that

enables rockets to reenter the atmosphere while sacrificing their ablatively cooled nose cones. In fact, wet wood was demonstrated to have a resistance to high heat fluxes superior to that of most solid materials including quartz or sapphire. While it is difficult to estimate the magnitude of this effect without specifying an exact experiment, calculations for transpirational cooling (a similar phenomenon) show a decrease of the heat transfer coefficient to 10% or less under conditions of strong transpirational (and ablational) cooling [8]. Gaseous heat transfer from flames and arcs to any surface tends to have a low efficiency [9]. Due to the outward movement of gases it is expected that heat transfer will be even lower to pyrolyzing biomass surfaces. On the other hand, radiation heating can reach the biomass surface through the transpirational boundary layer provided that the gases formed are not opaque at the active wavelengths. Solid conduction and convection are more complex. While the gases and liquids formed interfere with heat transfer, the pressures and velocities involved can rapidly remove these products from the interface. It may be possible to pyrolyze only to the liquid phase and to remove that liquid from the pyrolyzing solid prior to vaporization and/or further cracking.

Transient Heating

Consider a rod (such as a wooden dowel) heated uniformly at one end only and vaporizing with a surface regression rate of ν. The temperature T at a distance x from this end is given by

$$\phi = \frac{T - T_o}{T_p - T_o} = \tfrac{1}{2}\left[\operatorname{erfc}\left(\frac{x + \nu t}{2(\alpha t)^{1/2}}\right) + e^{\frac{-\nu x}{\alpha}} \operatorname{erfc}\left(\frac{x - \nu t}{2(\alpha t)^{1/2}}\right)\right] \qquad (2)$$

where, α is the thermal diffusivity of the material ($\alpha = \frac{k}{\rho c}$, ρ is the density, k is the thermal conductivity and c is the heat capacity), T_o is the initial temperature of the rod, and T_p is the temperature of pyrolysis. The temperature profiles at specified times are shown in Fig. 1.

Fortunately, after a relatively short time the temperature reaches the steady state described by

$$\phi = e^{\frac{-\nu x}{\alpha}} \qquad (3)$$

It is possible to calculate various characteristic thermal states from this distribution and the thermal properties of the biomass.

The steady state pyrolysis velocity is related to the rate of heat input I in $J/cm^2 s$ by

$$\nu = I/\rho \Delta h_p \qquad (4)$$

The limiting temperature in eq. (2) can be integrated to give the

FIGURE 1. HEAT PENETRATION IN PYROLYSIS

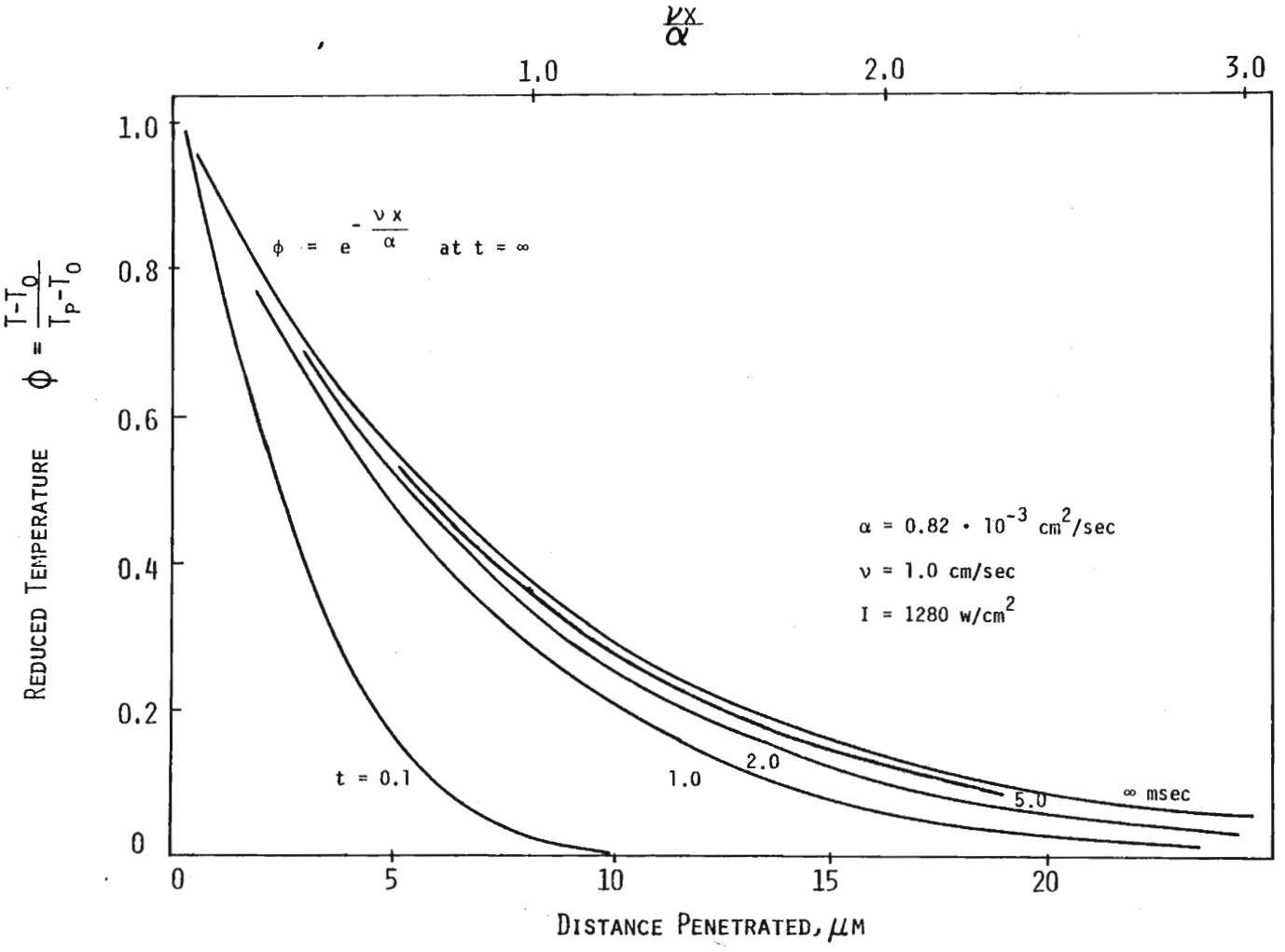

quantity of heat, q in J/cm^2 which must enter the biomass before T_p is reached at the surface

$$q = It_o = \rho c \int_0^\infty (T - T_o)dx = (T_p - T_o) \frac{k\rho\Delta h_p}{I} \qquad (5)$$

The time to reach steady state, t_o, is calculated from the heat transfer and this heat input according to

$$t_o = \frac{q}{I} = \frac{(T_p - T_o)\, k\rho\Delta h_p}{I^2} \qquad (6)$$

Note that this time is inversely proportional to the square of the heat transfer rate, thus putting a high premium on heat transfer rate.

Although the thermal wave in Fig. 1 extends to ∞, a straight line approximation intersecting the x axis at $\frac{\nu x}{\alpha} = 2$ would have nearly the same heat content, h_o, under this curve. We define the heat penetration as this distance where

$$x_o = \frac{2\alpha}{\nu} \qquad (7)$$

We illustrate these thermal parameters in Table I using the thermal properties of yellow pine, and for comparison purposes use velocities of 10^{-3} cm/s as typical of slow pyrolysis (10) and 1 cm/s as typical of fast pyrolysis.

Note particularly that the heat penetration is exceedingly small for fast pyrolysis. This small amount of heat penetration may appear to be contradictory, but is the result of the biomass-surface regression rate being nearly equal to the rate of heat penetration. Char formation is thought to be a much slower reaction than tar formation in fast pyrolysis. For slow pyrolysis, the hot layer available for pyrolysis is 1000 times larger with a significant amount of time spent at low pyrolysis temperatures where the char forming reaction dominates to form large amounts of char and lesser amounts of volatile tars.

HEAT TRANSFER MECHANISMS

Heating with Atoms, Photons and Electrons

Heat can be transferred to a surface by a flux of atoms (as in a gaseous flame), photons (as in a furnace), or electrons (as in electron welding) or by combinations of these mechanisms. Various

TABLE I

THERMAL PARAMETERS IN SLOW & FAST PYROLYSIS (YELLOW PINE)

SYMBOL	QUANTITY	RELATION	SLOW	FAST	UNITS
ν	Pyrolysis Rate	-	10^{-3}	1	cm/s
I	Heat Transfer	$\nu\Delta h_p$	1.3	1280	W/cm^2
x_o	Heat Penetration	$2\alpha/\nu$	16,000	16	μm
q	Heat in Wood	$k\ T/\nu$	370	0.73	J/cm^2
t_o	Time to T_p	q/I	570	0.6×10^{-3}	s
	Heating Rate	$\frac{dT}{dt}$	1	8×10^5	$^oC/s$

Assumptions: $c = 2.8\ J/g\ ^oC$; $\Delta h_p = 2000\ J/g$; $T_p = 500^oC$, $\rho = 0.64\ g/cm^3$

$k = 1.47 \times 10^{-3}\ \frac{J\ cm}{^oC\ s\ cm^2}$; $\alpha = 0.82 \times 10^{-3}\ cm^2/s$

devices using these mechanisms are illustrated in Fig. 2 [9]. We will first comment on the three mechanisms briefly before examining their application to biomass.

In the discussion of heat transfer from directed energy flows to a surface, it is important to distinguish between the energy flux, E, and that which is actually transferred, I. The ratio of the two is the heat transfer efficiency, $\eta = I/E$. It is also important to distinguish between the role of temperature and heat transfer. Although the temperature of the beam must be higher than that of the surface for heat to flow, and in general, the higher the temperature difference the higher the flow; there are situations in which a higher temperature difference decreases heat flow (e.g., the Leidenfrost effect as exemplified by water "dancing" on a very hot surface). It is important to recognize that pyrolysis depends on I, the actual heat transferred to the surface, not on T_s, the temperature of the source or E, the available energy flux. Although biomass heating rates are often listed in degrees/sec, it is important to recognize that this is usually the rise time of the heat source or of a temperature sensor, not of the biomass. We seldom actually know what temperatures exist at the biomass surface itself during such experiments, especially at very high heating rates which involve values of t_o of less than 100 ms.

Gaseous Convection Heating

Heat Transfer by gaseous convection is a relatively difficult approach to attain high heat fluxes. As indicated in Fig. 3, with a temperature difference of 500°C, the free convective heat flux can be as low as 0.3 W/cm^2 and gradually increases to a little over 1 W/cm^2 as the velocity of the gases approaches that of forced convection (1 W/cm^2 = 3175 BTU/ft^{2}hr). With the same temperature difference, forced convective heat fluxes can be as high as 14 W/cm^2 which is about the same as the radiative heat flux from a 1000°C black body. However if the biomass particle is pyrolyzing to produce a cloud of gas and vapors which surround the particle, the heat transfer by convection will be very severely reduced because of transpirational cooling.

Higher heat transfer rates can be achieved with impinging flames. In a typical Bunsen flame the energy flux of the flowing gases just above the cone is about 400 W/cm^2 for a flame velocity of 10^3 cm/s [9]. Measurements of actual heat transfer to cold surfaces from such flames show that the heat transfer efficiency in the projected area of the flame is about 10% thus giving a directed heat transfer of about 40 W/cm^2. While useful for making coffee or soldering, in general, this heat transfer rate is too low for most industrial applications. In particular, such a flame directed at a large piece of wood would produce charcoal and volatiles and so is too low in intensity for "fast pyrolysis" directed at producing only volatiles from other than very small or thin particles of biomass.

Fig. 2

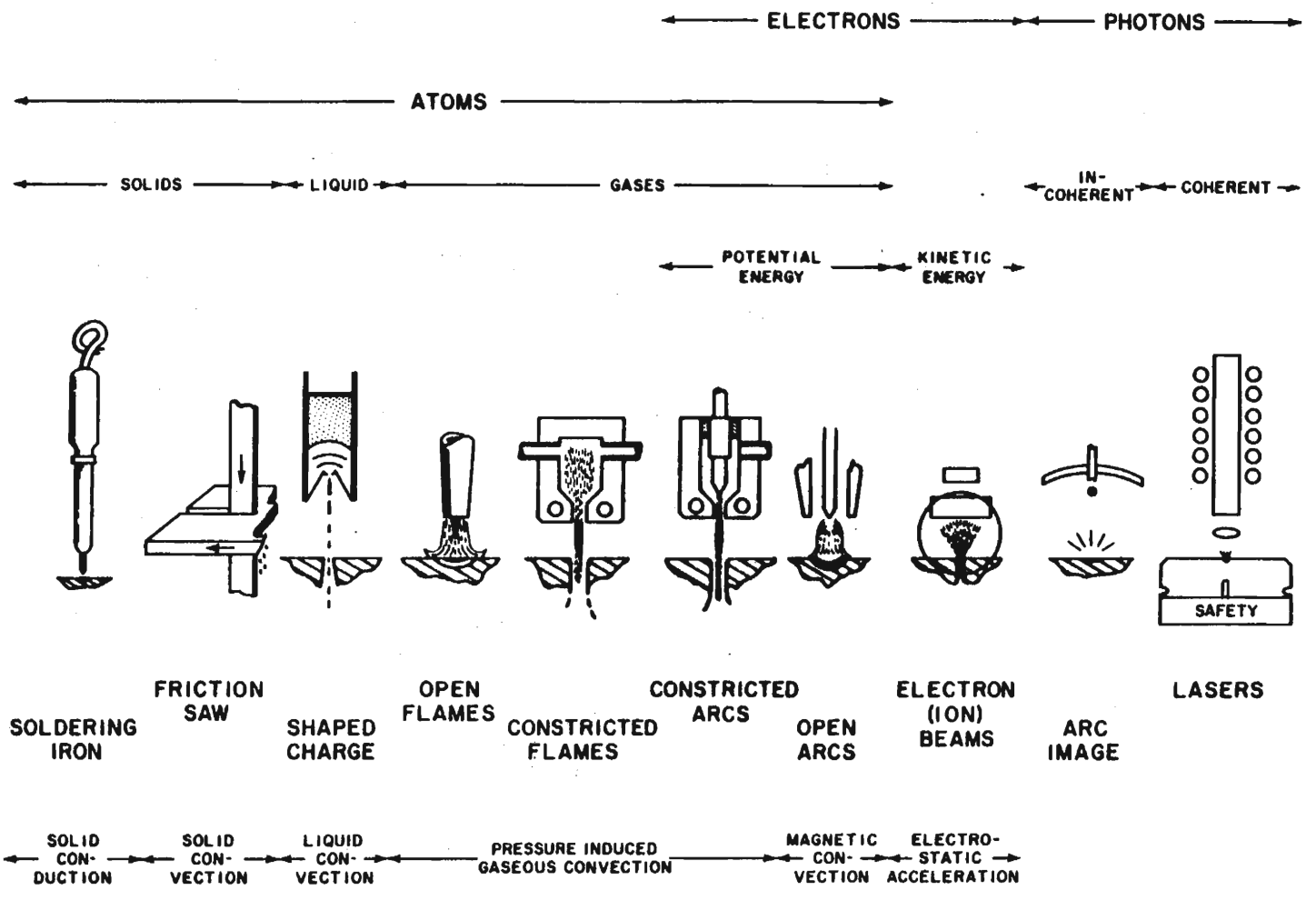

DIRECTED HEAT TRANSFER FROM ATOMS, ELECTRONS & IONS

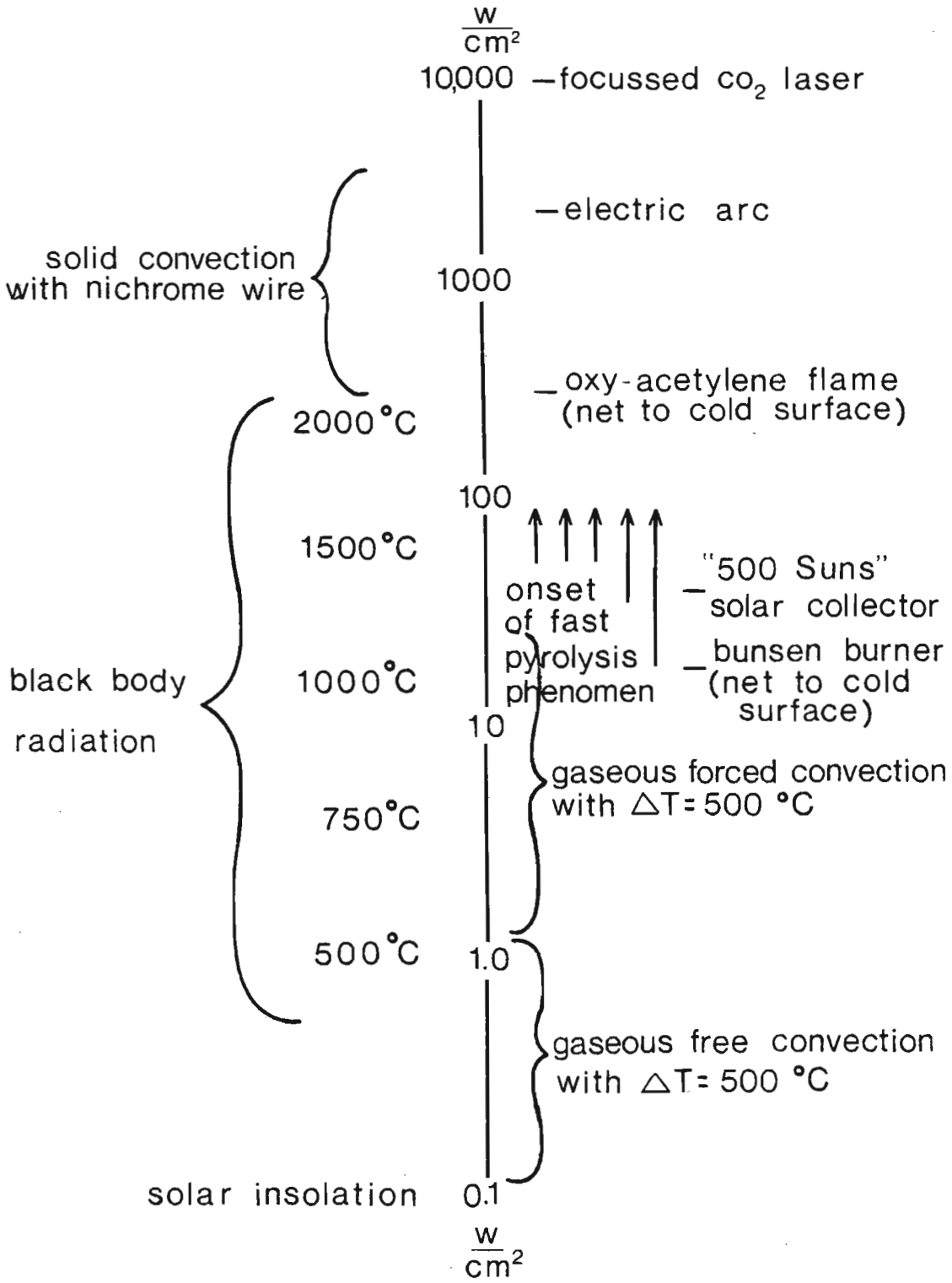

FIG. 3. HEAT TRANSFER PERSPECTIVES

The flame heat transfer intensity can be increased a factor of ten by using oxygen instead of air (increasing flame velocity) or by using jet burners such as rocket engines. These higher intensities come close to converting wood or cellulose completely to volatiles and have been used in ornamental wood erosion, where the different relative rates of the volatilization of spring and summer wood produces ridges of the more resistant wood. In general, the low efficiencies of heat transfer from directed flames make them unsuitable for fast pyrolysis.

Most of the devices of Fig. 2 are unsuitable for fast pyrolysis for various theoretical or practical reasons. Electric arcs and electron beams are difficult for biomass heating because biomass is not an electrical conductor. Liquid jets transfer too much momentum and would be too costly for fast pyrolysis, though they might be used in cutting wood in special instances.

Solid Conduction and Convection

The conduction of heat from a solid has the potential for delivering high heating rates and a familiar device relying on solid heat conduction is the soldering iron. The amount of heat transferred by solid heat conduction is proportional to the thermal conductivity and to the temperature difference, but inversely proportional to the thickness involved. A high thermal conductivity metal (such as tungsten) at high temperatures is capable of delivering heat at 10^4 W/cm^2, with a temperature difference of 2000°C and a 2 mm thickness, and so could be considered for fast pyrolysis. The materials and control problems in such a heat source would be formidable, however.

Convection is generally thought of as the motion of liquid or gases, but in a sense, a moving hot wire is a solid convection heat transfer agent. With a 0.025 cm diameter wire, moving at a velocity of 20 cm/s, we have achieved rapid pyrolysis of wood in the laboratory with penetration rates of about 3 cm/s (11). If we assume a heat of pyrolysis requirement of 2000 J/g, this implies a heating rate of 3500 W/cm^2 from this moving wire.

Radiation Heat Transfer

The heat delivered by radiation has a very wide range. Black body (incoherent) radiation delivers heat proportional to the absolute temperature raised to the fourth power. A furnace at 1000°C delivers a maximum heat flux of 14.9 W/cm^2, which we think may be marginal for fast pyrolysis and so it is common experience that a large piece of wood will char during pyrolysis in such a furnace. The temperature of the sun is about 5500°K and the heat flux at the surface of the sun is 5,200 W/cm^2, far above the requirement for fast pyrolysis. However, since we are a considerable distance from the sun, the heat flux actually received at the earth's surface is closer to about 0.11 W/cm^2. Point focusing solar collectors can achieve about 500 suns, or a heat flux of 55 W/cm^2 and so could marginally achieve fast pyrolysis.

The laser (producing coherent radiation) is not limited by the laws of black body radiation and has in practice reached steady heat transfer intensities of 10^6 W/cm^2 and pulsed values a thousand times higher. Carbon dioxide lasers can easily be focused to give 10^4 W/cm^2 fluxes and are now being used to produce art objects of carved wood using fast pyrolysis. Unfortunately, the cost and efficiency of lasers at present prevents them from being a practical heat source except in such special applications.

Fluidized Bed

Heat transfer in a fluidized bed has the characteristics of many of the previously mentioned heat transfer mechanisms. With a mildly, fluidized bed, the pyrolyzing particles are surrounded by hot radiating bed-particles. However, the heat capacity of the bed-particles is small so that a relatively large number of them must be used to transfer heat from the source to the biomass if a high uniform temperature is to be maintained. With an increase in bed turbulence, the importance of heat transfer by gaseous convection and intermittent solid-solid conduction is increased. With very high turbulence as in entrained flow, the bed-particles may be superfluous particularly if the heat source is the hot wall of the reactor. If the bed-particles have a high velocity relative to the biomass, the high heat transfer rates achievable with solid convection may be attained unless the bed-particles become attached to the biomass to form a protective coating.

Momentum Transfer During Fast Pyrolysis

In all heat transfer processes there is also a necessary associated momentum transfer. For photons and electrons, this momentum transfer can be very small but it is higher with gases and can be very high with liquids and solids. The momentum transfer can be very important in removing the products of pyrolysis such as tar and/or any char that may form, in order to permit further pyrolysis.

Bulk Heating of Biomass

The above mechanisms describe the transfer of heat to a surface by molecules, atoms, electrons, and photons. In addition, one can envisage the bulk heating of materials, and a widely used example of such heating is induction heating in which currents are induced in metals and semiconductors for very rapid heating.

Microwave heating (as in microwave ovens) is another example of bulk heating in which the high frequency field couples to the dielectric moment of the material being heated by displacement currents. Unfortunately biomass has a relatively low dielectric constant which presents difficulties in using this heat transfer mechanism.

A second bulk heating method is the adiabatic compression of biomass in which a sudden application of pressure generates internal heat through friction and gas heating. This mechanism is important in the

densification of biomass for fuel, but would not be useful for fast pyrolysis because of the necessary confinement of the biomass.

CONCLUSION

We have listed here the various mechanisms that are available for the surface and bulk heating of biomass and shown those that are most suitable for fast pyrolysis. These are high velocity gas flames, direct conduction, solid convection, fluidized beds, and radiant heating. The use of conduction and solid convection, in particular, would appear to be a very fruitful area for additional consideration because very high heat fluxes are readily available with relatively inexpensive technology (e.g., compared to electrically operated lasers).

REFERENCES

1. Lincoln, K.A. "Flash-Pyrolysis of Solid-Fuel Materials by Thermal Radiation", Pyrodynamics, Vol. 2, pp. 133-143 (1965).

2. Llewellen, P.C., W.A. Peters, and J.B. Howard "Cellulose Pyrolysis Kinetics and Char Formation Mechanisms", Fire and Explosion Research: Sixteenth Symposium on Combustion. The Combustion Institute, pp. 1471-80 (1976).

3. Antal, M.J. Jr., W.E. Edwards, H.L. Friedman, F.E. Rogers "A Study of the Steam Gasification of Organic Wastes" University Grant No. R804836010 to Princeton University by U.S. EPA, IERL, Cincinnati, Ohio 45268.

4. Diebold, J.P. "Preliminary Results in the Fast Pyrolysis of Biomass to Lower Olefins", Petroleum Chemistry Division of ACS Symposium on "Alternate Feedstocks for Petrochemicals", Las Vegas, NV, August 24-29, 1980. (Also appears in more detail in Solar Energy Research Institute report SERI/TR-332-586, June 1980).

5. Diebold, J.P. "Thermochemical Conversion of Biomass to Gasoline. September 1980 Update" DOE's 11th Biomass Thermochemical Conversion Contractor's Meeting at Pacific Northwest Laboratories (September 23, 1980).

6. Milne, T. "A Survey of Biomass Gasification. Volume II - Principles of Gasification", Solar Energy Research Institute. Chapter 5. SERI/TR 33-239 (1979).

7. Bradbury, A., Y. Sakai, F. Shafizadeh "A Kinetic Model for Pyrolysis of Cellulose", J. Appl. Polym. Sci., 23, 3271-80 (1979).

8. Eckert, E.R.G., R.M. Drake, Jr. "Analysis of Heat and Mass Transfer", McGraw Hill, 1972, p. 453.

9. Reed, T.B. "Directed Heating with Atoms, Electrons and Photons", ASM Technological report NY 9.1.62; or Science and Industry (N.V. Philips' Gloeilampenfabrieken) 12 1 (1965).

10. Schaffer, E.L. "An Approach to the Mathematical Prediction of Temperature Rise within a Semi-infinite Wood Slab subjected to High Temperature Conditions", Pyrodynamics, 2, 117-132 [1965).

11. Diebold, J.P. "Ablative Pyrolysis of Macroparticles of Biomass", Proceedings of the Specialists Workshop on the Fast Pyrolysis of Biomass, Copper Mountain, CO October 19-21, 1980.

THEORY OF HYDROCARBON PYROLYSIS TO FORM OLEFINS

S. Narayanan
Stone & Webster Engineering Corporation
Boston, Massachusetts 02107

INTRODUCTION

The basic concept of a "mechanism" of a reaction is to postulate a procedure by which a particular reaction proceeds. One can have many mechanisms postulated. There are two basic approaches in the literature with regard to the pyrolysis of hydrocarbons, they are radical modelling and the molecular schemes.

Radical Modelling. Rice [1] postulated a radical mechanism which is successfully applied to hydrocarbon pyrolysis and is used to predict yields at low conversion levels. It postulates that hydrocarbon decomposition is initiated by the formation of a radical, which being active abstracts a hydrogen atom from the parent alkane and it subsequently decomposes to an olefin and a radical. This propagates the reaction. Radical interaction tends to terminate the reaction.

Molecular Schemes. For very complex reactions, where the radical formation is too difficult to determine experimentally or theoretically, a molecular mechanism is postulated and tested. This mechanism simply involves evaluating all plausible reactions of a decomposing hydrocarbon.

A generalized reaction rate for many reaction steps put together, known as global reaction rate, of a decomposing component is arrived at only experimentally. Most hydrocarbons decompose by a first order type relation. Accordingly one can write:

$$\frac{dc}{dt} = kc \qquad (1)$$

where $k = Ae^{-E/RT}$

Once we know the rate coefficient for a particular decomposition reaction, we can find out a given time how much of the component will be converted for a given temperature.

Examining the level of conversion of a component becomes difficult when the compound decomposing is a complex one. Therefore, some generalized techniques have to be developed to predict conversion.

Most organic compounds, when heated above 450°C, decompose into simpler products. Such thermal decompositions have been studied extensively. The evidence so far accumulated has shown that several classes of organic compounds, such as hydrocarbons, ketones, aldehydes, ethers, and amines, decompose homogeneously and by an approximately first-order relationship. Self-inhibition (decrease in calculated first-order rate constant with increasing conversion) is sometimes observed. The energies of activation of these processes lie in the range between 50,000 and 67,000 calories/g-mole.

The occurrence of free radicals as intermediates in cracking reactions has been well established by now. Rice and Herzfeld [2] developed a free radical mechanism, which was later modified by Kossiakoff and Rice [3] to predict the product distribution from hydrocarbon decomposition reactions. This theory also gives plausible explanation for the approximately first-order kinetic relationship and the experimental activation energy, which is considerably lower than the carbon-carbon bond energy.

Rice-Herzfeld-Kossiakoff Mechanism

The strength of the carbon-carbon bond in paraffins is 80 kcal/g-mole, whereas the carbon-hydrogen bond is 100 kcal/g-mole. Rice indicates that because of this 20 kcal/g-mole difference in the bond energies, the decomposition of a paraffin will exclusively involve the rupture of the carbon-carbon bond to produce two free radicals. The yields of the products from the cracking would then depend upon the subsequent reactions of these free radicals formed in the primary step. An important limitation of this mechanism is that it is valid for small conversions only. Any organic compound, unless it is one of the few very simple ones, can yield a great variety of compounds which will in turn decompose; if, therefore, more than a small fraction of the original compound is decomposed, the whole problem will become hopelessly involved.

According to Rice, the primary decomposition products can be estimated from experimental measurements in which the conversion of the feed is kept below 20 percent. The main features of the theory are as follows. As a first step, it is assumed that a hydrogen atom is removed from a paraffin molecule by attack by an alkyl radical. The radical thus formed is assumed to dissociate unimolecularly into an olefin and a free radical through the rupture of the much weaker carbon- carbon bonds. Since the methyl and ethyl radicals are much more stable than the higher radicals, the free radicals so formed, with the exception of the methyl and ethyl radicals, decompose very rapidly into olefins leaving methyl groups, ethyl groups or atomic hydrogen. These small radicals are then assumed to form methane, ethane, or hydrogen, by abstracting a hydrogen from the original paraffins and thus continuing the chain. The following additional assumptions are made:

(a) The large radical formed in the primary step decomposes without reacting with any other hydrocarbon. This implies that the rate constant of the bimolecular reaction is much smaller than the unimolecular dissociation rate constant.

(b) The kind of initial radicals formed depends upon the number and nature of the carbon-hydrogen bonds present. The activation energy of the removal of a secondary and tertiary hydrogen are assumed to be, respectively, 2 and 4 kcals less than required for the removal of a primary hydrogen. The frequency factors for all reactions are assumed to be the same. The initial rate of formation of each type of radical is taken to be proportional to the rate constant for that reaction multiplied by the number of bonds of that type present in the original hydrocarbon.

(c) In order to improve the agreement of the theoretical predictions with the experimentally measured values, Kossiakoff and Rice later modified the theory.

small saturated molecule and a new radical. Radicals may also stabilize themselves by decomposing to ethylene and another reaction species, (E.2), and (E.4).

Termination: Reaction chain is ended by the collision of free radicals to either combine or disproportionate to stable molecules (E.5).

In hydrocarbon pyrolysis, main reaction products usually originate from the chain propagation steps. Thus, for ethane pyrolysis methane, ethylene and hydrogen would be the major reaction products.

The first reaction, (E.1), is known as the initiation reaction. (E.2), (E.3), and (E.4) are known as the propagation reactions and (E.5) is known as the termination reaction. Besides these a host of other side reactions have been observed by chemists which are established as occuring at higher temperatures of 800°C and the like.

$$C_2H_4 + H^* \rightleftharpoons C_2H_3^* + H_2 \qquad \text{(E.6)}$$

$$C_2H_3^* \rightleftharpoons C_2H_2 + H^*$$

Further radical reaction schemes involving the formation of carbon and its reaction have also been reported as:

$$C_2H_2 \longrightarrow 2C + H_2 \qquad \text{(E.7)}$$

$$C + H_2O \longrightarrow CO + H_2$$

The overall reaction ethane is considered as

$$C_2H_6 \rightleftharpoons C_2H_4 + H_2$$

The forward reaction is favored at lower partial pressures.

Propane Cracking

The thermal cracking propane has been established to proceed as follows:

$C_3H_8 \longrightarrow CH_3^* + C_2H_5^*$	Initiation	(P.1)
$C_2H_5^* + C_3H_8 \longrightarrow C_2H_6 + C_3H_7^*$	Propagation	(P.2)
$H^* + C_3H_8 \longrightarrow H_2 + C_3H_7^*$	Propagation	(P.3)
$CH_3^* + C_3H_8 \longrightarrow CH_4 + C_3H_7^*$	Propagation	(P.4)
$C_3H_7^* \longrightarrow CH_3^* + C_2H_4$	Propagation	(P.5)
$C_3H_7^* \longrightarrow H^* + C_3H_6$	Propagation	(P.6)
$C_3H_7^* + CH_3^* \longrightarrow CH_4 * C_3H_6$ or C_4H_{10}	Termination	(P.7)
$CH_3^* + CH_3^* \longrightarrow C_2H_6$	Termination	(P.8)

Comparing this with that of ethane decomposition scheme, we observe with increasing paraffinic series the reaction steps are becoming more complex. Simple overall stoichimetric relations for propane are:

$$C_3H_8 \longrightarrow C_3H_6 + H_2 \qquad \text{(P.9)}$$

$$C_3H_8 \longrightarrow C_2H_4 + CH_4 \qquad \text{(P.10)}$$

N-Butane Cracking

Normal butane decomposition follows the following mechanism.

$C_4H_{10} \longrightarrow 2C_2H_5^*$	Initiation	(NB.1)
$C_4H_{10} + C_2H_5^* \longrightarrow C_2H_6 + C_4H_9^*$	Propagation	(NB.2)
$C_4H_{10} + C_2H_5^* \longrightarrow C_2H_4 + C_4H_{10} + H^*$		(NB.3)
$C_4H_{10} + H^* \longrightarrow H_2 + C_4H_9^*$		(NB.4)
$C_4H_9^* \longrightarrow C_2H_4 + C_2H_5^*$		(NB.5)
$C_4H_9^* \longrightarrow C_3H_6 + CH_3^*$	Propagation	(NB.6)
$C_4H_{10} + CH_3^* \longrightarrow CH_4 + C_4H_9^*$		(NB.7)
$2CH_3^* \longrightarrow C_2H_6$	Termination	(NB.8)
$2C_2H_5^* \longrightarrow C_4H_{10}\ (C_2H_4 + C_2H_6)$		(NB.9)
$2C_4H_9^* \longrightarrow C_8H_{18}\ (C_4H_8 + C_4H_{10})$		(NB.10)
$CH_3^* + C_4H_9^* \longrightarrow C_5H_{12};\ C_2H_5 + C_4H_9^* \rightarrow C_6H_{14}$		(NB.11)

Comparing the sets of reaction, the normal butane cracking has a larger number of reaction steps. This brings out the point; namely, the reactions' sequence multiplies with increasing carbon number of the paraffin series. The relative speed of the reactions or radical concentrations are too difficult to determine.

Simple overall reactions of N-Butane can be written as:

$$nC_4H_{10} \longrightarrow 2C_2H_4 + H_2 \qquad \text{(NB.12)}$$

$$nC_4H_{10} \longrightarrow C_2H_4 + C_2H_6 \qquad \text{(NB.13)}$$

$$nC_4H_{10} \longrightarrow C_3H_6 + CH_4 \qquad \text{(NB.14)}$$

Iso-Butane Cracking

While normal butane has a (primary) carbon-carbon rupture, iso is more refractory and accordingly its decomposition does not involve major (secondary) carbon-carbon break up.

$$iC_4H_{10} \longrightarrow iC_4H_9^* + H^* \qquad \text{(iB.1)}$$

In their modification they assume that any free radical with six or more carbon atoms, prior to rupture, can coil around and react with itself to produce an isomer.

(d) The free radicals formed in the isomerization step are then assumed to break at the carbon-carbon bond relative to the free radical site. If there is more than one such bond, the mechanism which forms a radical of greater stability is preferred.

The theory has been developed with observations made on paraffins containing up to six carbon atoms. It cannot be used for higher paraffins without proper verification. A number of simplifications have been made to reduce the number of reactions possible and as such it cannot be expected to give precise results. However, the theory provides good agreement with the broad nature of experimental facts.

As shown below, this mechanism gives a plausible explanation for the approximate nature of the decomposition process and also predicts an activation energy much less than the energy required to break a carbon-carbon bond. Considering the case in which only one carbon-carbon bond in the free radical is broken before the resulting radical is converted into a paraffin, we have the following steps:

			E kcal/g-mole	
$M \xrightarrow{K_1} R_1+R_1'$	radical formation		80	(2)
$R_1+M \xrightarrow{K_2} R_1H+R_2$	Hydrogen transfer		8	(3)
$R_2 \xrightarrow{K_3} RO_1+d_1$	fission		38	(4)
$R_1+R_2 \xrightarrow{K_4} R_1R_2$	products chain termination		0	(5)

In the first step, the decomposing hydrocarbon, M, splits into two free radicals which involves the rupture of a carbon-carbon bond.

The radical R_1' is assumed to play no part in the reaction. In the second step the radical R_1 abstracts a hydrogen from the parent molecule to form a molecule and a large free radical R_2. Fission at a carbon-carbon bond in the third step converts the R_2 radical into an olefin ($O1_1$) and a small radical which continues the chain. Termination occurs through the collision of R_1 and R_2.

Woinsky [4] simulated the kinetics of thermal cracking of high molecular weight normal paraffins on a digital computer. The products and free radicals heavier than the ethyl radical were lumped into various groups depending on whether they were olefins or paraffins and whether they were heavier or lighter than the feed. The primary reactions involved could thus be represented by 32 equations. Secondary reactions were neglected and as such the model is applicable at low conversions only. The rate constants for the intermediate reactions were approximated from the literature.

This model, although more detailed than the mechanism proposed by Rice, has a number of limitations. With the exception of hydrogen, methane and ethane, the model does not give individual values of the product yields and a number of constants in the model have been assigned arbitrary values. Moreover, the predictions from the model will be only as good as the frequency factors and activation energies used to determine the rate constants for the intermediate reactions, which to date have not been determined very accurately. However, considering the approximations involved, the results presented by Woinsky were in good agreement with the experimental data.

Gavalas [5] presented a mechanism that uses the chain propagation reactions alone to determine the concentrations of the various species in the reacting system. The initiation and termination reactions were taken to have an effect only on the overall kinetics. All possible reactions were written in matrix notation and by using both the long chain approximation and the customarily made steady-state approximation, the resulting set of simultaneous differential equations could be solved on a digital computer. In theory, this method is capable of handling large sets of reactions. It can even take into account the polymerization, isomerization, and the reaction of olefins with free radicals. However, due to the limited knowledge of intermediate rate constants, this method is of little value.

LIGHT HYDROCARBON CRACKING

Ethane Cracking

Ethane is the most suitable feedstock for ethylene production for it has a high ultimate yield of ethylene. Ethane is recovered from refinery or natural gas or obtained as a by-product during naphtha or gas oil cracking. The simplified mechanism by which ethane cracking proceeds is expressed as

$$C_2H_6 \rightleftharpoons 2CH_3^* \qquad \text{(E.1)}$$

$$CH_3^* + C_2H_6 \longrightarrow CH_4 + C_2H_5* \qquad \text{(E.2)}$$

$$C_2H_5* \rightleftharpoons C_2H_4 + H* \qquad \text{(E.3)}$$

$$C_2H_6 + H* \rightleftharpoons H_2 + C_2H_5* \qquad \text{(E.4)}$$

$$2\ C_2H_5^* \longrightarrow C_4H_{10} \text{ or } C_2H_4 + C_2H_6 \qquad \text{(E.5)}$$

It is interesting to note that the radicals CH_3^*, H* and C_2H_5* because of their high reactivity initiate, propagate, and terminate the reactions. The formation of H* radical is something characteristic to ethane cracking.

Initiation: Free radicals are produced by the rupture of parent molecule at its weakest bond, (E.1).

Propagation: Newly formed radicals abstract H from parent compound to form

$$\longrightarrow iC_3H_7^* + CH_3^*$$

$$iC_4H_9^* \longrightarrow C_3H_6 + CH_3^* \quad \text{(iB.2)}$$

$$iC_4H_9^* \longrightarrow iC_4H_8 + H^* \quad \text{(iB.3)}$$

$$iC_4H_9^* + H^* \longrightarrow iC_4H_8 + H_2 \quad \text{(iB.4)}$$

$$iC_4H_9^* + CH_3^* \longrightarrow iC_4H_8 + CH_4 \quad \text{(iB.5)}$$

$$iC_3H_7^* + H^* \longrightarrow C_3H_6 + H_2 \quad \text{(iB.6)}$$

$$CH_3^* + H^* \longrightarrow CH_4 \quad \text{(iB.7)}$$

$$iC_4H_9^* + H^* \longrightarrow iC_4H_{10} \quad \text{(iB.8)}$$

$$iC_4H_9^* + iC_4H_9^* \longrightarrow C_8H_{18} \quad \text{(iB.9)}$$

LIGHT HYDROCARBON MIXTURES CRACKING

The mixtures' cracking technology is more complicated due to the interaction of the various radical species. When light hydrocarbon mixtures crack, the conversion levels and product yields are influenced by the ability of large radicals effectively to utilize the smaller free radicals, thus during ethane and propane cocracking, propane starts decomposing first. But as the reaction proceeds when ethane starts decomposing, the radicals generated by ethane are preferentially consumed by the propane and propylene formed for its fuller decomposition. The hydrogen radicals produced in greater amount during ethane cracking have greater ability to decompose heavier hydrocarbons and, accordingly, heavier hydrocarbons decompose faster when cracked with ethane or hydrocarbons which produce H* radicals during their decomposition.

HEAVY HYDROCARBON CRACKING

From the studies of vapor phase pyrolysis of individual hydrocarbons, the rate of disappearance of reactant is generally independent of surface to volume ratio of the reactor and pressure. Thus, the disappearance can be considered to be unimolecular and to follow a first order mechanism. The integrated form of the first order equation is

$$k_t\theta = 2.3 \log \left(\frac{1}{1-\alpha}\right) \quad (6)$$

where K_t = rate coefficient, Sec^{-1}, evaluation at temperature t
θ = time in Sec
α = fractional disappearance of reactant

The rate coefficient varies with temperature in accordance with the Arrhenius equation:

$$k = Ae^{-E/RT} \quad (7)$$

The rate coefficient-temperature-conversion relationships similar to those

which hold for light hydrocarbons apply to the constituents found in the heavier feedstocks such as naphtha and gas oils.

While considering the heavier hydrocarbons, it is convenient to relate their rate coefficients to that for normal pentane at the same temperature. If we designate any normal paraffin of carbon number greater than 5 by subscript i

$$k_i = A_i e^{-E_i/RT} \tag{8}$$

$$k_5 = A_5 e^{-E_5/RT} \tag{9}$$

Dividing one by the other

$$\frac{Ki}{k_5} = \frac{Ai}{A_5} e^{(-E_i + E_5)/RT} \tag{10}$$

Study of available data indicates that the activation energies for all normal paraffins of five or more carbon atoms can be assumed to be equal without serious error. Such assumptions causes the exponential factor to become unity so that

$$\frac{ki}{k_5} = \frac{Ai}{A_5} \tag{11}$$

If we further assume that the frequency factor for this class of compound is a power function of carbon number n , as $A = g(n)^h$

where g and h are constants we may write

$$\frac{Ai}{A_5} = \left(\frac{ni}{5}\right)^h = \frac{ki}{k_5} \tag{12}$$

Estimating the values of h for three specific components a curve can be established for a particular family. Such a set of curves for normal paraffins, brancher paraffins, alkyl cyclohexanes, alkyl cyclopentanes, and normal alpha olefins is shown in Fig. 1.

HEAVY HYDROCARBON MIXTURES CRACKING

The distillate feedstocks like naphtha, kerosine, and gas oil are extensively used in commercial practice. Each feedstock contains well over 75 separately identified compounds. So in order to establish their conversion, we may have to know the kinetic rate constants of 75 different species, plus the exact yield from each one. We already observed that even in the pyrolysis of binary mixtures, unpredictable synergistic interactions can result. To develop an exact reaction mechanism amidst all these complications would be a formidable task for distillate feedstocks.

While the measure of the percentage conversion is easy to obtain for pure components, it is a difficult parameter to estimate for a distillate feedstock. A kinetic severity function or KSF is normally used. KSF is a measure of the conversion of distillate related to n-pentane conversion, and indicates how

RATE COEFFICIENT OF PENTANE VERSUS TEMPERATURE AND CARBON

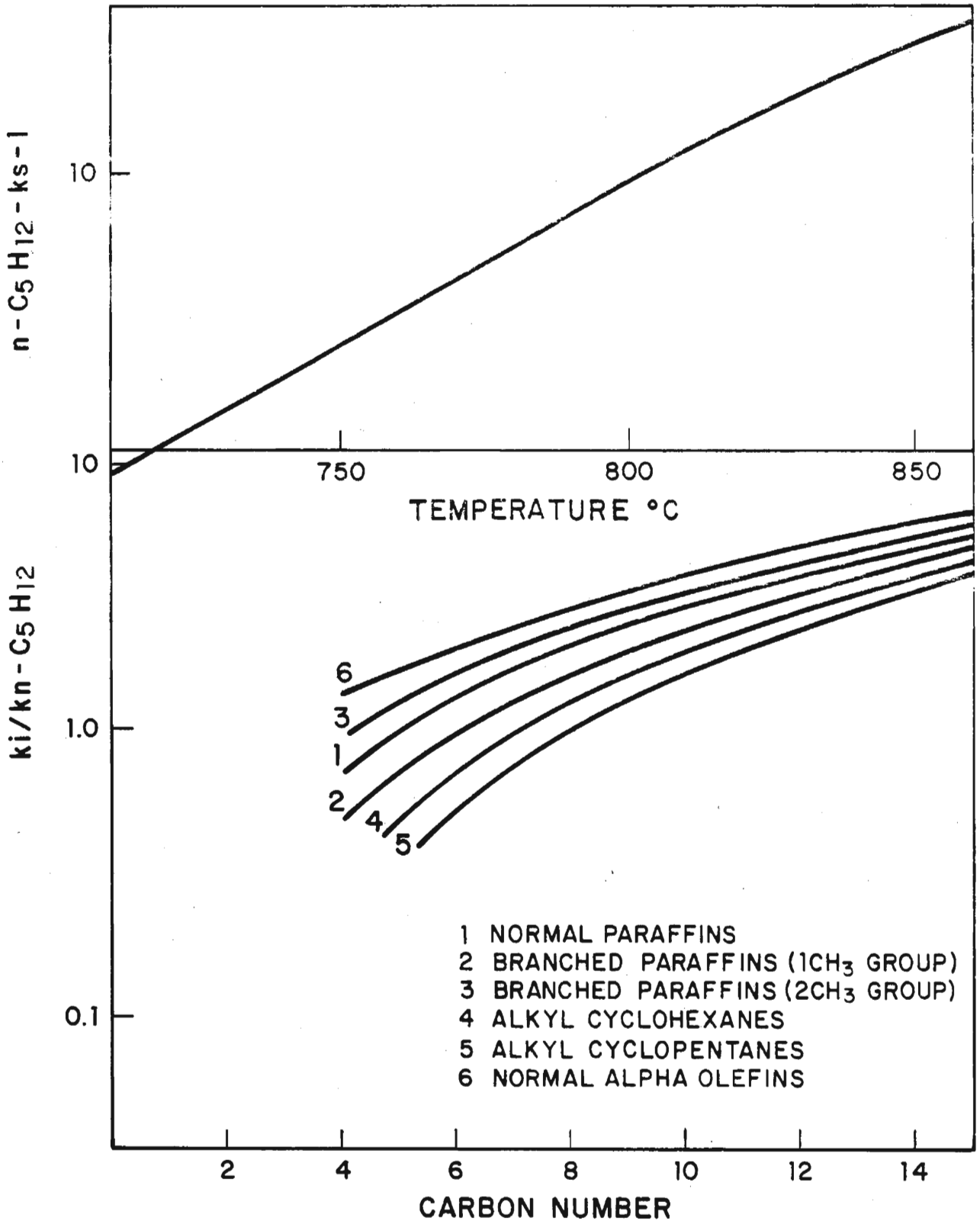

much n-pentane would have converted under identical conditions of temperature and time.

The product distribution is normally presented for distillate feedstocks as a function of severity. A tyical curve for naphtha cracking is shown in Fig. 2. This severity diagram can be divided into three zones. In zone 1, the zone of low severity up to KSF of about 1, the principal reaction in progress are those involved in the primary disappearance of saturates in the feedstocks.

In zone 2, primary reactions continue, but the secondary reactions become dominant. This zone extends up to a KSF of 2.4. Yields of hydrogen, methane, total C_2's, and butadiene continue to increase but at a gradually diminishing rate.

The rates of decomposition of propylene and butylenes reach such levels that their rates of disappearance catch up to and then exceed their rates of formation. As a result, their concentrations in the reaction mixture pass through maxima.

The propylene peak typically occurs at a KSF of about 1.7 for naphtha cracking. The butylene peak usually appears at lower severities, although feedstocks rich in isoparaffins which yield isobutylene on primary decomposition tend to displace the peak to a severity level comparable to the propylene peak.

In zone 3, primary reactions have virtually ceased and all further changes in constitution of the mixture are attributed to secondary reactions. Yields at C_6+ pass through a minimum as the original saturates become exhausted and the formation of stable aromatics from the degradation of propylene and C_4's adds to C_6+ yields as the severity is increased.

The production of hydrogen plus methane continues to rise but the C_2's and butadiene curves eventually pass through maxima. Butadiene yield typically peaks at a KSF of about 2.5, while C_2's pass through a broad maximum at about KSF = 5.

PILOT PLANT SIMULATION

In 1965, Stone & Webster decided to proceed with a laboratory scale hydrocarbon pyrolysis program. The principal objective of this work was to study the pyrolysis reactions, simulate commercial cracking conditions, and to determine the effect of important process variables such as hydrocarbon partial pressure, residence time, and temperature profile on the product yield patterns obtained from different feedstocks. Instrumentation on-line analytical capability was developed for effluent monitoring. Laboratory analytical techniques were adopted from commercial practice for feed and product inspection.

The bench scale pyrolysis unit is as shown in Fig. 3. Hydrocarbon feedstock and water are moved from the feed tanks by positive displacement pumps via separate heaters to the superheater and reactor. The reaction coil is housed in a multi-heating zone electric furnace.

Following the completion of cracking reactions, the products are rapidly quenched, then condensed at ambient temperature. The vapors are sent to an electrostatic precipitator, dried and chilled to -40°F. The cracked gas is

NAPHTHA CRACKING TYPICAL VARIATION OF PRODUCT DISTRIBUTION WITH CRACKING SEVERITY

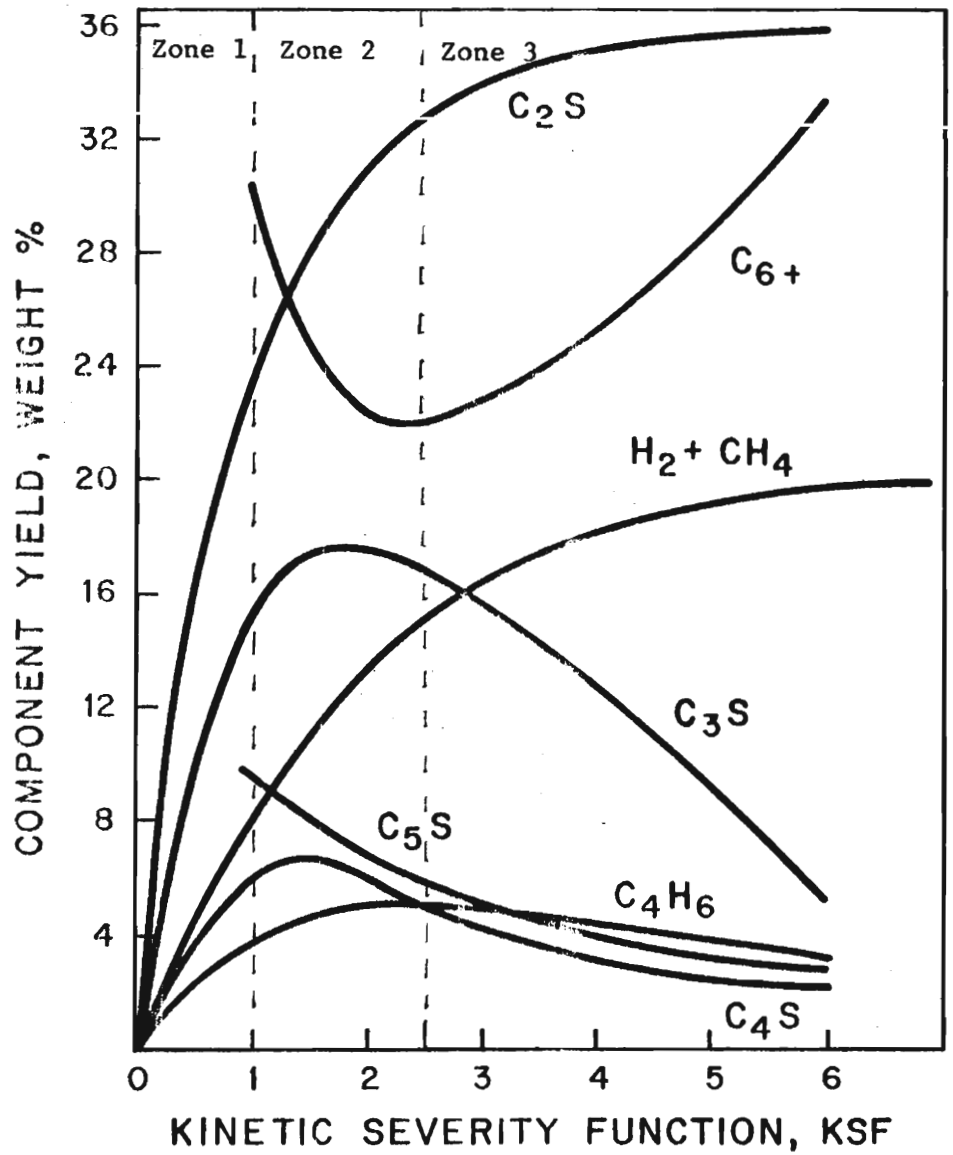

FIGURE 2

bench scale pyrolysis unit

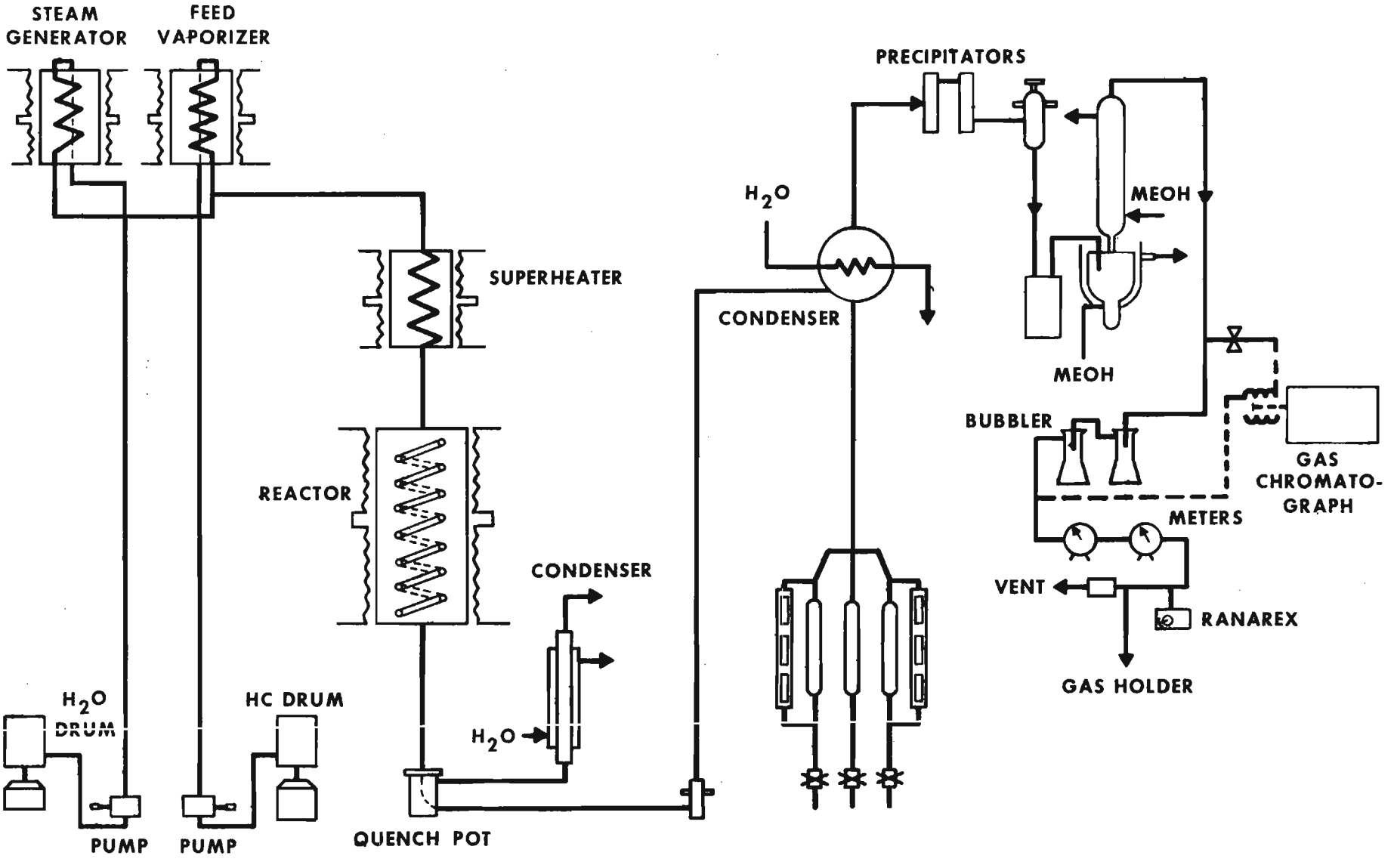

75-5137

FIGURE 3

metered and collected. Liquid products from the condensers are collected and weighed separately allowing complete material balancing.

The features of the pilot plant are tabulated.

Details of Pyrolysis Unit

Reactor type	Helical
Reactor length	Variable 4-120 feet
Furnace	Electrical resistance with six heating zones
Maximum operating temperature	1,000 C
Pressure range	0-5 70 kg/cm^2 g
Hydrocarbon throughout	1-6 kg/h
Dilution steam	1-6 kg/h
Product recovery	Indirect quench Gradual condensation to -40°C Gas collection
Features that can be simulated	Temperature profile Pressure profile Residence time Steam/hydrocarbon ratio Coil outlet pressure
Features that can not be simulated	Mass velocity Reynolds number Heat flux

A variety of feedstocks were used for the bench scale tests. They are listed in Table 1. These include pure components and major feedstocks of commercial interest ranging from light condensates to high vacuum distillates.

The importance of bench scale cracking lies in its ability to reproduce test results and generate dependable simulation of the commercial processes. The long operational history of the bench scale unit proved that both requirements were successfully met. Typical experimental and predicted values are shown in Table 2.

Influence of Residence Time

To obtain the same amount of conversion at a shorter resident time, the temperature level of the reaction has to be increased. This increase in temperature shifts the equilibrium so as to favor higher yields of light olefins. Ethylene yields from ethane, propane, butane, and naphtha cracking at the same conversion level increases when the residence time is decreased. See Fig. 4.

Influence of Hydrocarbon Partial Pressure

The influence of decreasing the hydrocarbon partial pressure provides an environment favoring progress of forward reactions like

$$C_2H_5^* \rightleftharpoons C_2H_4 + H^*$$

SUMMARY OF BENCH SCALE FURNACE TESTS

CONVENTIONAL FEEDSTOCKS	RANGE	NO. TESTS
PURE COMPONENTS	C_2H_6 - C_{14}	180
NGL, NAPHTHAS, RAFFINATES	SG 0.62 - 0.76	200
KEROSENE, AGO, VGO	SG 0.77 - 0.91	150
WAXY DISTILLATES, RESIDUES, CRUDES		20

HYDROGENATED FEEDSTOCKS	COKER & FCC NAPHTHAS AGO VGO PYROLYSIS FUEL OILS	50
SYNTHETIC FEEDSTOCKS	COAL LIQUIDS SYN CRUDE FRACTIONS SHALE OIL	25

TABLE 1

STONE & WEBSTER

COMPARISON OF PREDICTED AND EXPERIMENTAL YIELD PATTERNS FROM BENCH SCALE PYROLYSIS TESTS

COMPONENTS WT. % FEED BASIS

FEED STOCK	HEAVY GAS OIL AND NAPHTHA MIX	
RUN No.	PREDICTED	EXPERIMENTAL SOCA-2
COMPONENTS		
HYDROGEN	0.51	0.58
METHANE	9.57	9.70
ACETYLENE	0.20	0.25
ETHYLENE	21.49	21.25
ETHANE	3.65	3.50
METHYL ACET. + PROPADIENE	0.55	0.48
PROPYLENE	14.09	13.80
PROPANE	0.42	0.46
1,3-BUTADIENE	4.83	4.73
OTHER C_4-s	5.93	6.30
TOTAL C_4 + LIGHTER	61.24	61.00
C_5-400F GASOLINE	25.66	24.60
FUEL OIL	13.10	14.40
TOTAL	100.00	100.00

TABLE 2

TYPICAL ONCE THROUGH ETHYLENE YIELDS

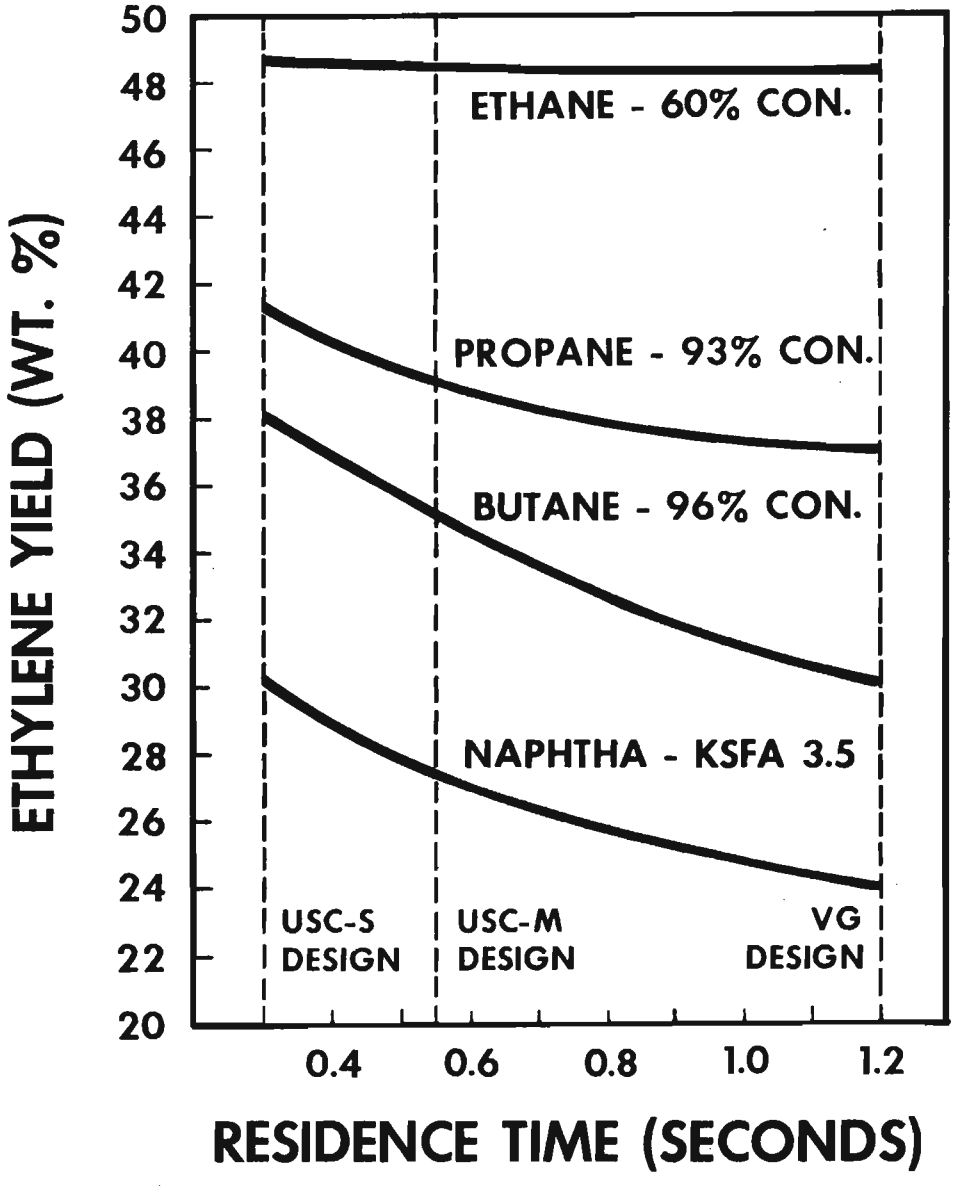

and discouraging the formation of by-products by condensation reaction between radicals. Thus, high ratios of olefins to saturates are favored and ratios of acetylenes and diolefins to mono-olefins tend to increase.

One method of decreasing hydrocarbon partial pressure in industry is to increase the steam to hydrocarbon ratio during pyrolysis. By selecting an optimum steam to hydrocarbon ratio, the formation of heavy liquid, tars, and coke are reduced.

All commercial pyrolysis of hydrocarbons for olefin production is carried out in the presence of steam, which serves three important functions.

1. It lowers the hydrocarbon partial pressure and thereby encourages higher selectivity to the desired olefinic products.

2. It reduces the partial pressure of high boiling aromatic hydrocarbons in the zone of high conversion, lessening the tendency to form coke within the cracking coils and deposit tars on the walls of downstream heat exchange surfaces and piping.

3. It has sufficient oxidizing effect on the tube metal to diminish significantly the catalytic effect of iron and nickel which otherwise would promote carbon forming reactions.

The steam to hydrocarbon ratio varies with the hydrocarbons selected for pyrolysis. A typical set of values are shown below:

Feed	Kg Steam/Kg Hydrocarbon
Ethane	0.3 ~ 0.4
Propane	0.4 ~ 0.5
Naphtha	0.5 ~ 0.6
Gas Oil	0.7 ~ 1.0

In reactors characterized by low pressure drop, the hydrocarbon partial pressure gradually increases through the coil and reaches its maximum at the outlet.

THE DEMONSTRATION UNIT

The bench scale unit was limited, since it could not provide information on the prolonged effect of the furnace unit, the fouling characteristics, the tubular reactor behaviour from start of run to end of run conditions, the heat transfer aspects. Since the efficient utilization of the feedstocks and fuel have to be ascertained before commercial units are designed and built, a logical step was to test the pilot plant results in a semicommercial plant.

Stone & Webster's demonstration unit consisted of a preheat furnace, a furnace filled with commercial sized coils, effluent exchangers, quenching facilities, and a single stage quenching facilities and a single stage of gas compression. The cracking furnace was basically one module of a commercial design with respect to coil dimensions and metallurgy and number, arrangement and type of burners, etc. The effluent heat exchange and quenching systems closely simulated commercial operation. Compressed cracked gas was delivered into an operating ethylene plant for recovery of the contained ethylene as well as other

valuable products. Essential features of this unit are shown in Fig. 5.

From the tests in the demonstration unit, Stone & Webster could not only examine the yield predicted by the pilot plant unit but also could develop a radiant coil which had the best combination of residence time, hydrocarbon partial pressure, and temperature profile leading to an ultra selective coil.

A number of extended duration runs were made to prove the operability of the furnace and to examine the performance transferline exhanger and quench systems when processing a number of feedstocks including heavy gas oils and waxy distillates.

STONE & WEBSTER COMMERCIAL USC FURNACE

With the extensive knowledge of basic theoretical analysis on the pyrolysis reaction examined in the pilot plant and tested out in the demonstration unit, Stone & Webster developed several Ultra Selective Coil designs, capable of pyrolysis many feedstocks to maximize the possible olefinic production. A typical furnace with radiant coil layout is shown in Fig. 6.

Radiant coils are laid out vertically in the furnace and fired from both the sides. The burners are so located to provide uniform heat distribution. The radiant coils absorb as much as 40 percent of the fired duty and the waste heat is recovered in the convection section where the hydrocarbons are preheated. Additional heat recovery in the convection section lend itself to high pressure steam production which provides energy to run the compressors.

Fig. 7 indicates a typical set of tube metal temperature profiles prevailing under those pyrolytic conditions. Precise predictions of these temperature profiles are possible by the understanding of the conversion of the feedstock as it passes along the length of the coil.

The coke formation steps near the walls of the reactor is developed by the temperature profile that prevails on the inside wall of the pyrolysis tube. The coke precursor synthesis procedure is then modeled by examining the possible stable small radicals present at the gas boundary layer and the aromatic molecules. Coking mechanisms are developed and are incorporated along with the mechanistic models of pyrolytic conversion. Such a model then predicts the decomposition of the feedstock from start of run condition to the end of run condition.

Stone & Webster have by now built 90 units all over the world with variety of feedstocks (Table 3). This experience and expertise is available for extension into realms of biomass pyrolysis.

USC demonstration cracking unit carrington, england

cracking section

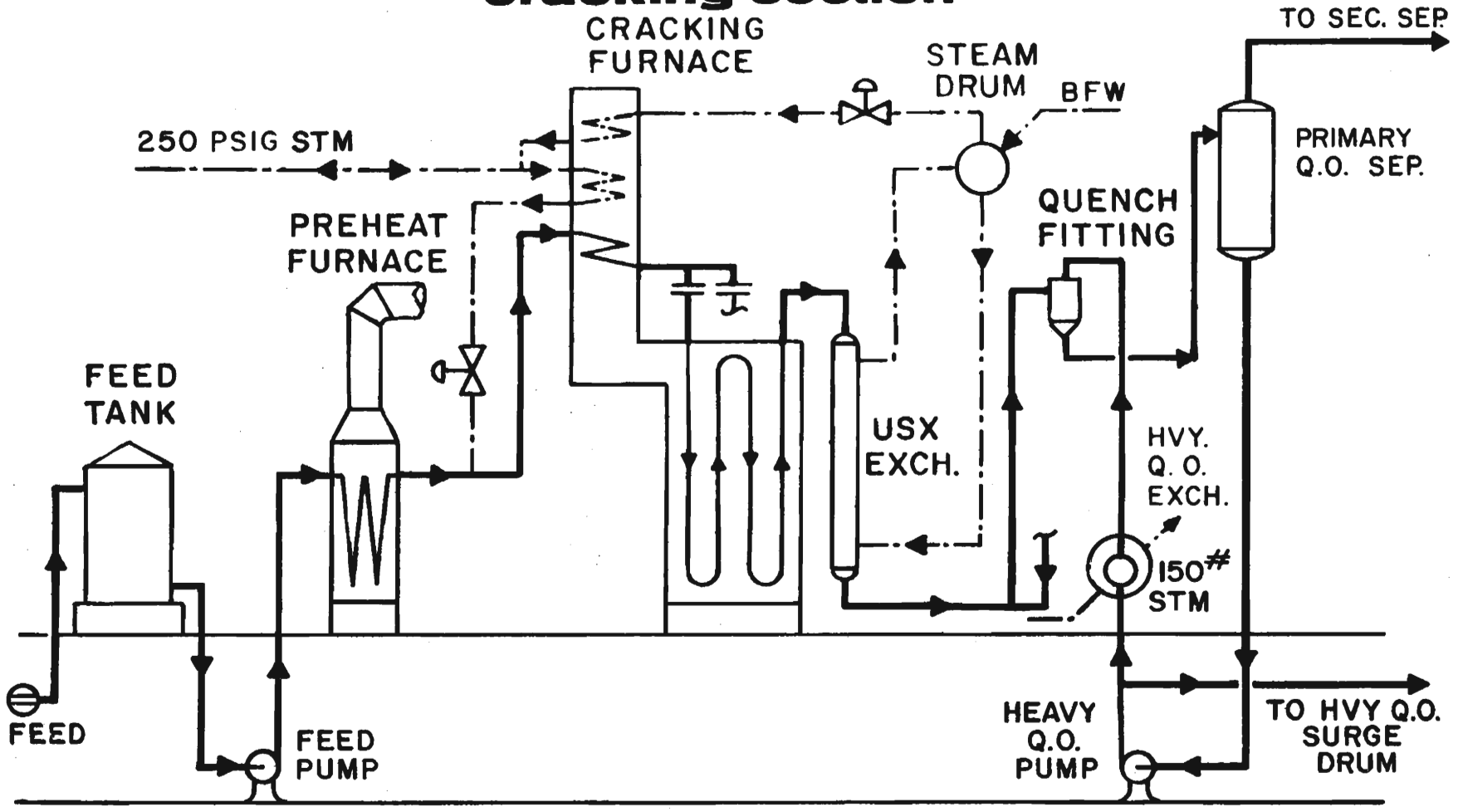

FIGURE 5

STONE & WEBSTER

54858

STONE & WEBSTER USC TYPE CRACKING FURNACE

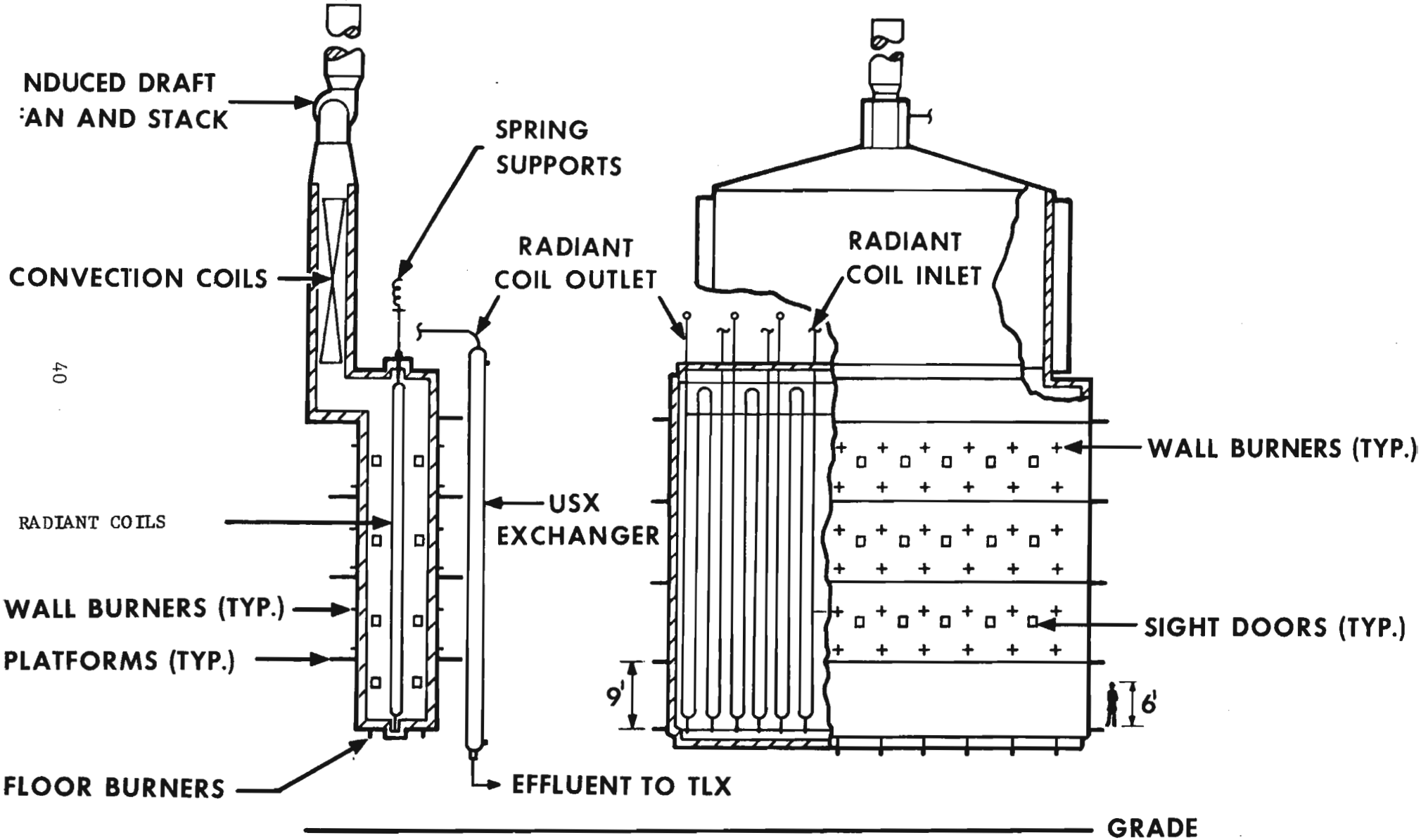

FIGURE 6

STONE & WEBSTER

TUBE METAL TEMPERATURE VS COIL LENGTH

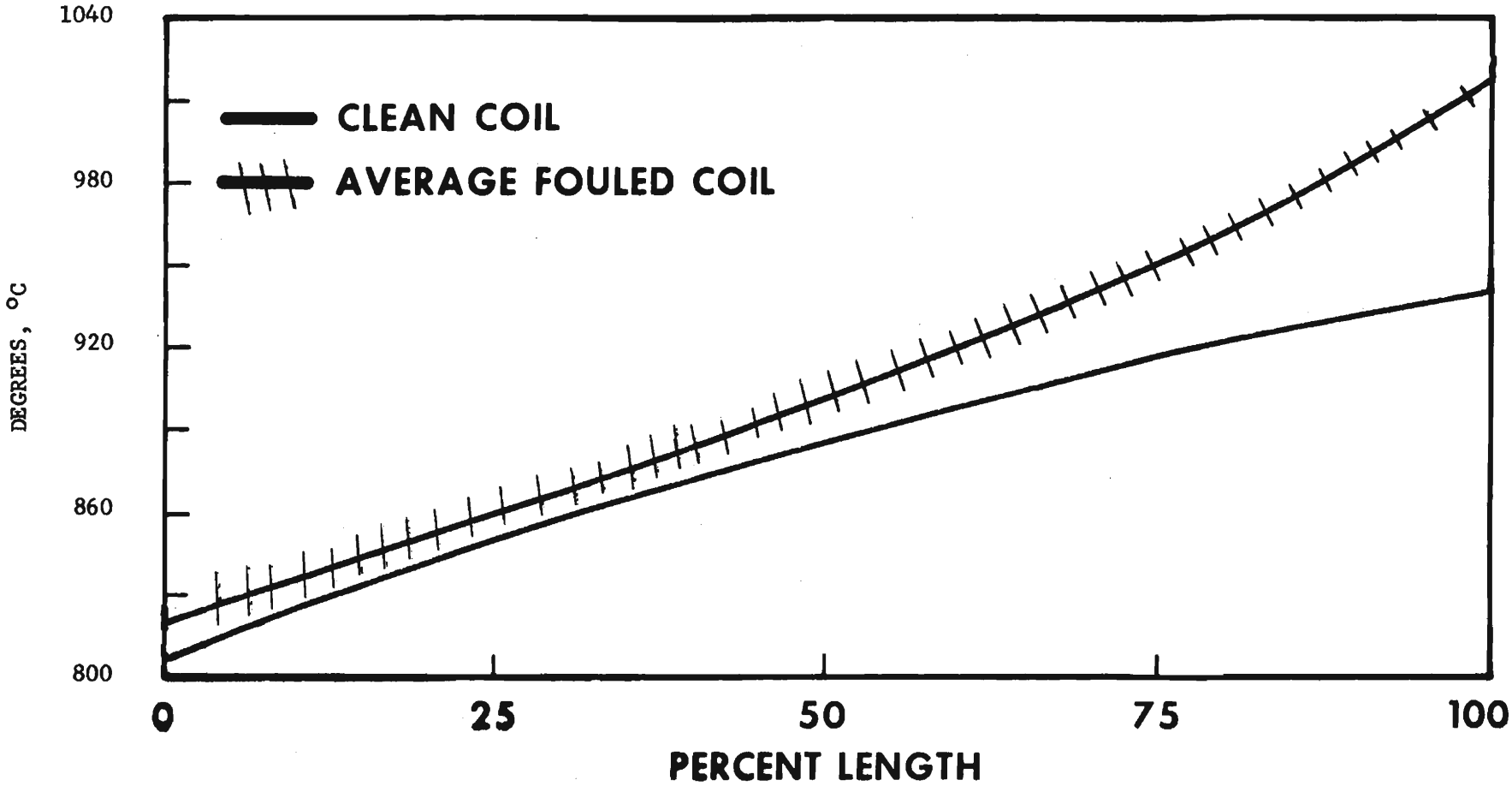

FIGURE 7

USC EXPERIENCE BASED ON :

COMMERCIAL TEST FURNACE	6 YEARS 800 RUNS 40 FEEDSTOCKS
BENCH SCALE FURNACE	12 YEARS 500 TEST SERIES ETHANE THRU 1100°F EP
COMMERCIAL INSTALLATIONS	17 OPERATING 6 DESIGN/CONSTRUCTION 18 BILLION LB/YR C_2H_4
TOTAL STONE & WEBSTER OLEFIN UNITS BUILT	90

TABLE 3

1. Rice, F.O., J. Am. Chem. Soc., Vol. 55 (1933) p. 3035

2. Rice, F.O., Herozfeld, K.F., J.Am. Chem. Soc., Vol. 56 (1934) p. 284

3. Kossiakoff, A., Rice, F.O., J. Am. Chem. Soc., Vol. 65 (1943) p. 590

4. Woinsky, S.G., Ind. Eng. Chem. Proc. Des. and Develop., Vol. 7 (1961) p. 529

5. Gavalas, G.R., Chem. Eng. Sci., Vol. 21 (1966) p. 133

6. "Manufacturing Ethylene," Zdonik, S.B., Green, E.J. & Hallee, L.P. A compendium of articles from Oil and Gas Journal. The Petroleum Publishing Company, Tulsa, Oklahoma.

COMMERCIAL HYDROCARBON CRACKING PRACTICES

R. M. Contractor
E. I. du Pont de Nemours & Company
Central Research & Development Department
Wilmington, Delaware 19898

ABSTRACT

Steam cracking of different hydrocarbons, as practiced commercially, to produce ethylene and other primary chemical feedstocks is summarized. The process technology involved, and the effects of feed quality and the process parameters on product yields are briefly described. The feedstocks trends and feed flexibility for ethylene plants are also discussed.

INTRODUCTION

Pyrolysis, or steam cracking of hydrocarbons, is the primary source of ethylene worldwide. Hydrocarbon feeds as different as ethane to gas oils are used in commercial crackers. Besides ethylene, the cracked products include, in various ratios, other important primary petrochemicals such as propylene, butadiene and BTX as well as fuels ranging from hydrogen and methane to heavy fuel oil. Although the design of an ethylene plant and operating parameters change substantially with different feeds, the same general processing scheme is used. Hydrocarbon feed is cracked in the presence of steam at high temperatures and low pressures in tubular furnace coils. The furnace effluent is rapidly quenched, heat recovered and liquid products separated out. The gaseous products are compressed, acid gases and water are removed and the desired individual products are separated in a series of fractionation steps.

The current installed ethylene capacity in the United States is about 16.8 million tons per year [1]. These ethylene plants also supply large percentages of the nation's propylene and butadiene needs as well as about 10% of benzene demand as petrochemical industry feedstocks. The plants are among the largest, most complex and expensive facilities of the hydrocarbon processing industry. Today's world scale steam crackers often have ethylene capacities in excess of 500,000 tons per year.

PROCESS DESCRIPTION

A block flow diagram of naphtha or gas oil fed ethylene plant is shown in Figure 1. The feed is mixed with steam in a steam-to-hydrocarbon weight ratio of 0.2 to 1.0 range, and the mixture is heated to a cracking temperature of about 750°C to 900°C in a tubular furnace. The steam is basically an inert diluent and is added for two reasons. It lowers the hydrocarbon partial pressure, which improves selectivity to olefins; and it increases the furnace run length by minimizing coke formation on the reactor tube walls. The total residence time in the furnace is generally in the range of 0.2 to 0.7 seconds.

After the cracking reaction has progressed as far as desired, the furnace effluent is rapidly cooled in the transfer line heat exchangers to stop further reaction. The heat is removed as high pressure steam and is used to drive compressor turbines. The cracked products are further cooled in a quench tower by a circulating quench liquor stream. Here, the dilution steam and any liquid products are condensed and separated into different boiling range fractions; additional heat is recovered as well.

The cracked gas is then compressed from a little over atmospheric pressure to around 3500 kPa in a series of multistage compressors. Water and hydrocarbons condensed between stages are separated from the cracked gas in interstage separators and returned to appropriate recovery units. Before the final compression stage, the gas is treated to remove carbon dioxide and hydrogen sulfide, which can contaminate the product and affect further processing. After compression, the cracked gas is dried to remove the last traces of water.

The product recovery section involves chilling the gas and processing it through a sequence of condensate separation, fractionation and heat exchange to recover ethylene, propylene, a butadiene rich C_4 stream, hydrogen and methane. There exists numerous process variations in the product recovery scheme. Small amounts of acetylene in the cracked gases is usually converted to ethane and ethylene by hydrogenation. Other unwanted products such as methyl acetylene and propadiene are also hydrogenated. The location of the acetylene conversion step varies depending on the importance of butadiene recovery. Ethane is usually recycled to extinction. Propane may be recycled or sold as fuel. The C_4 stream may be sent for butadiene extraction and pyrolysis gasoline fraction is hydrotreated and fed to an aromatics extraction unit or used as a blending stock for gasoline.

RAW MATERIAL

Ethane, propane and heavier paraffins recovered from natural gas as well as LPG, naphtha, kerosene and gas oil fraction of virgin crude are the primary feedstocks for steam crackers. A small amount of the nonaromatic raffinate from aromatics extraction units is also

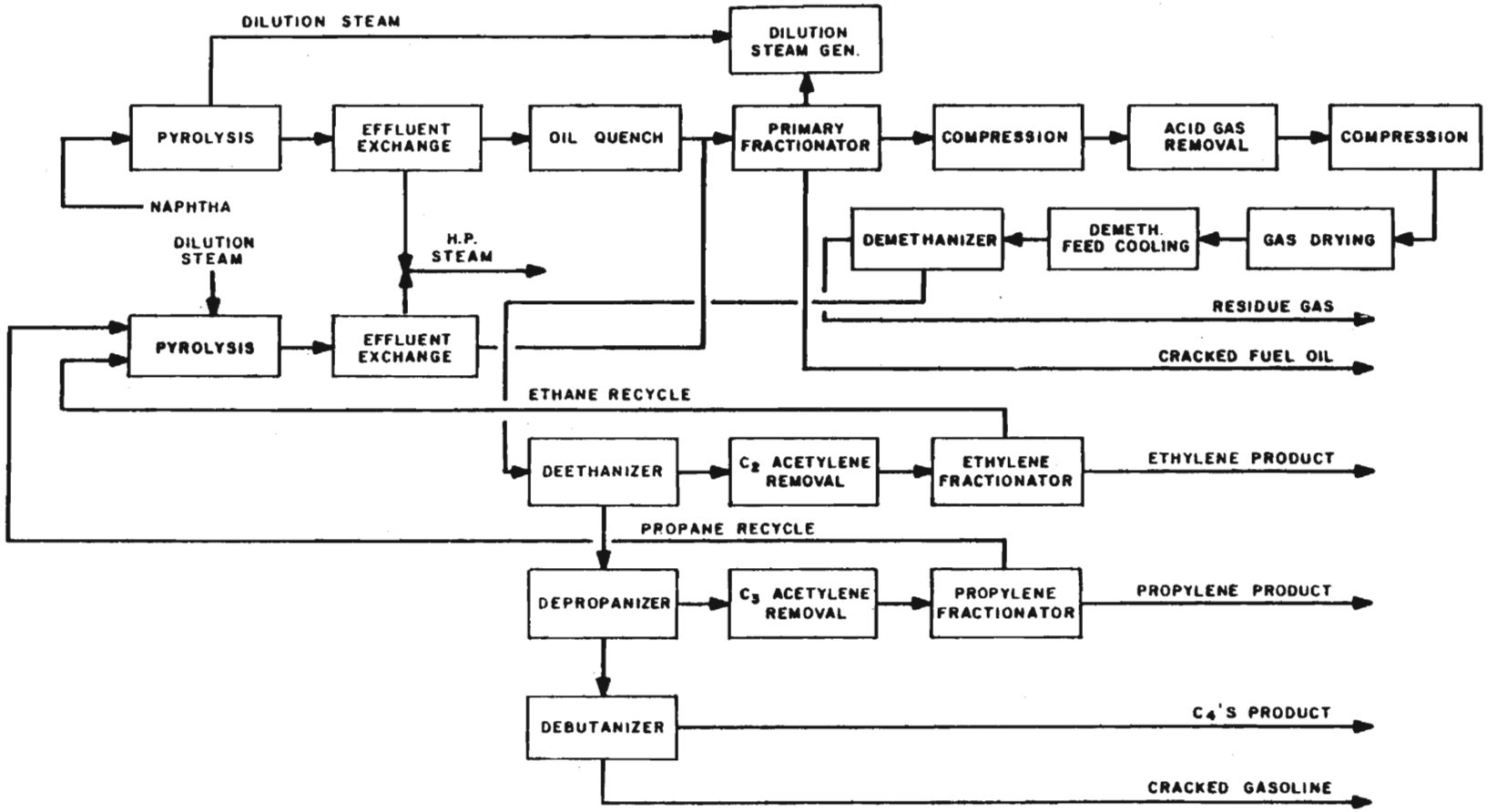

Figure 1 - TYPICAL PROCESSING STEPS OF AN ETHYLENE UNIT CRACKING LIQUID FEEDSTOCKS (2)

used. Although there have been several articles published in technical journals within the last few years regarding the advantages of using vacuum gas oil, as of now it is not a significant factor as a feedstock for the commercial crackers.

Different feeds produce different slates of products. In general, the higher the molecular weight of the feed, the easier it cracks. Thus, ethane crackers give only 50 to 60% conversion per pass under high severity cracking conditions whereas naphtha and gas oils give very high conversions at lower severities [Table I]. Usually, this means that a given furnace, designed for one type of feed, cannot readily be used for other feeds without some penalty.

TABLE I

FEEDSTOCKS FOR OLEFINS PRODUCTION

Feed	% Conv. Pass	% H_2 in Feed	% C_2H_4 Yield	Lb. Feed / Lb. C_2H_4	Steam Feed	Rela. Plant Invest.
Ethane	50-60	20	83	1.2	0.2-0.4	1X
Propane	75-90	18	45	2.2	0.3-0.5	1.15X
n-Butane	95	17.2	41	2.4	0.3-0.5	1.2X
Naphtha	High	15.5	34	2.9	0.5-0.8	1.45X
Gas Oil	High	13.5	27	3.7	0.8-1.0	1.64X
Vac. Gas Oil	High	12.4	21	4.8	1.0-1.2	1.84X

Another important parameter of the feed is its hydrogen/carbon ratio. It is a measure of feedstocks ethylene potential. The lighter hydrocarbons with their higher hydrogen/carbon ratio, or wt.% H_2, give greater ethylene yields. The basic hydrocarbon type in the feed also has an important effect on its crackability and yield pattern. Paraffins are the easiest to crack. Straight chain paraffins give highest ethylene yields whereas branched paraffins give high propylene yields. Cyclo paraffins decompose by ring rupture and give ethylene yields similar to those of iso paraffins. The ring structure of aromatic compounds has a high thermal stability and resists thermal decomposition. However, side chains break off readily resulting in high concentration of benzene in pyrolysis gasoline. Also there are tar and coke forming tendencies due to ring condensation.

The amount of feed required to produce a pound of ethylene increases rapidly with heavier feedstocks. Also, heavy feeds require more diluent steam because of their higher tendency for coking. The product recovery section is considerably more complex for ethylene plants operating on heavy feeds because of large quantities of by-products produced. Thus, for a given ethylene capacity, the size of the plant and investment are significantly higher for heavy feedstocks.

However, besides investment, the selection of the feed for an ethylene plant depends on the relative costs and availability of the feed as well as on the market value of the by-products.

Typical pyrolysis yields of ethylene and other by-products from commercial crackers operating with different feeds are shown in Figure 2. As the feed gets heavier and ethylene yield decreases, yields of other products increase. Some of the by-products such as propylene, butadiene and BTX are high value petrochemicals and the remaining have fuel value. The dotted line in the figure shows the typical split between chemicals and fuels, and indicates that even gas oil crackers can produce over 50% chemical yields. Thus, for a constant ethylene capacity plant, very large quantities of other chemicals and fuel are produced with liquid feeds. Even though ethylene plants are high energy consumers, gas oil crackers make so much fuel product that they are invariably net fuel makers.

MAJOR PROCESS VARIABLES

The typical yield pattern shown in Figure 2 can be significantly altered by changing process conditions. Major process variables affecting yields are cracking severity, residence time and hydrogen partial pressure.

Severity

Severity is a measure of how hard the feed is cracked or how much of the feed is cracked, and is a function of cracking temperature and hydrocarbon residence time in the furnace coil. Figure 3 shows the typical effect of increasing cracking severity on product distribution for a liquid feedstock. As the cracking severity is increased, the yields of H_2, CH_4, ethylene and higher mono olefins, the primary products of the cracking reactions, start increasing. Simultaneously, yields of C_5^+ liquid products start decreasing because of cracking of liquid feed. As the olefins concentration build up in the reactor, they start cracking, hydrogenating, polymerizing and condensing at increasing rate and produce acetylenes, diolefins, light saturates and aromatics. The diolefins and acetylenes would also react further in similar manner. Soon the yields of olefins reach a peak value and then start declining because of these secondary and tertiary reactions. C_4 olefins yields peak first, then C_3 and eventually ethylene. As the olefins yields start declining, the yields of C_5^+ liquid products reach a low value and then start increasing because of polymerization and condensation reactions. Yields of H_2, CH_4 and benzene keep increasing with increased severity because of their high thermal stability. Thus, different product slates can be obtained by selecting different cracking severities. This gives olefins producers some flexibility in responding to market demands. At very high severity, the tar build up in the C_5^+ fraction begins to foul up the reactor and the transfer line heat exchanger at increasing rate. The maximum severity is usually limited by this factor. Very low

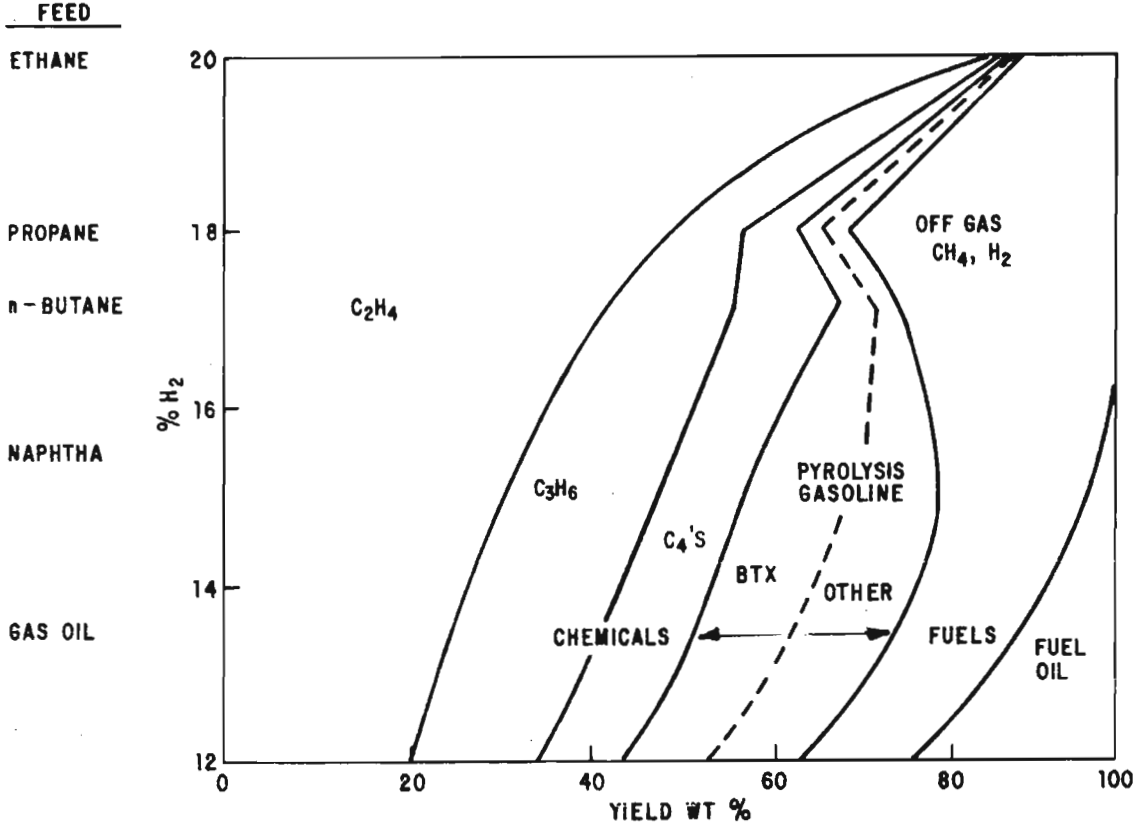

Figure 2 – TYPICAL PYROLYSIS YIELDS FROM DIFFERENT FEEDS

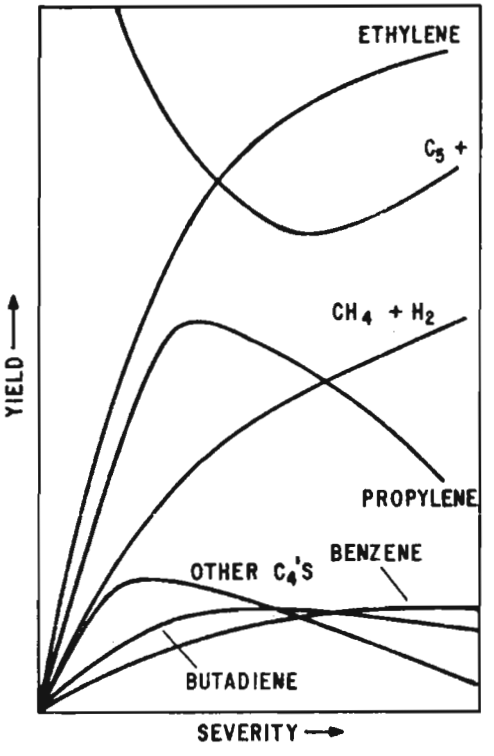

Figure 3– TYPICAL EFFECT OF SEVERITY ON YIELDS

severity decreases the furnace capacity because of poor feed conversion per pass. Also, once the furnace is designed, there is generally not a great deal of flexibility in changing severity without paying some economic penalty.

Residence Time

In general, short residence time favors the desired primary cracking reactions and minimizes the less desired secondary reactions. The selectivity to olefins increases at the expense of fuel products as the residence time decreases. Thus, with advances in tube metallurgy and furnace design, the design residence times in commercial naphtha crackers have been decreasing for the last two decades from about 2 seconds to 0.2 seconds.

Hydrocarbon Partial Pressure

Pyrolysis selectivity towards ethylene and butadiene has been found to be favored by low hydrocarbon partial pressure in the furnace coil. The partial pressure is controlled by the reactor outlet pressure and by the diluent steam to feed ratio. Selected partial pressure is a compromise between steam costs, product gas compression costs and increased ethylene yields. Once again, the hydrocarbon partial pressure cannot be changed to a large extent without paying significant economic penalty, once the plant is designed to operate at a certain partial pressure.

FEEDSTOCK TRENDS

Based on economics and availability, historically, light hydrocarbons recovered from natural gas have been the primary choice as feedstocks for ethylene plants in the United States. In 1975, about 75% of ethylene produced in the nation came from crackers operating on these light hydrocarbon feeds. However, as it became apparent that the United States natural gas production was peaking out, ethylene producers started considering use of naphtha and gas oil for additional capacity. Most new ethylene plants built in the last five years were designed for these liquid feeds. This trend towards use of heavier feedstocks is generally expected to continue in the future [Figure 4].

The situation is reverse in Western Europe and Japan. Traditionally, naphtha has been the feedstock of choice for ethylene plans in these areas because of limited production of natural gas and availability of naphtha at low costs due to lower gasoline demand [Figure 5]. Recently, however, increased amounts of light hydrocarbons are being fed to ethylene plants. The percentage of ethylene produced from these lighter feeds is expected to grow in the future [4,5] with increased availability of NGL and LPG from the North Sea and Middle East and increased demand for naphtha for the growing gasoline market.

Various assumptions and factors normally considered in making these projections are discussed below.

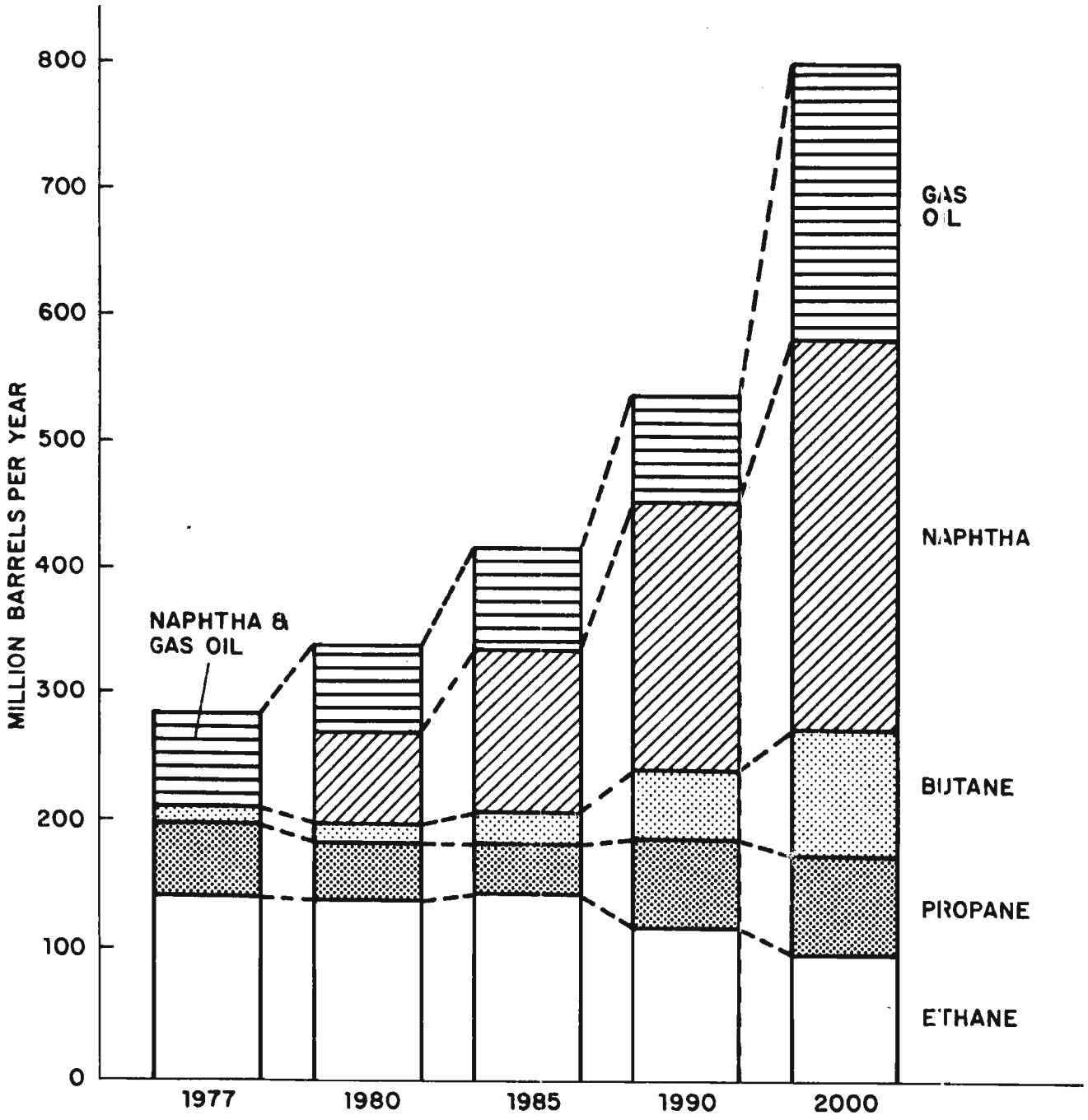

Figure 4 - U.S. OLEFIN PLANT FEEDSTOCKS (3)

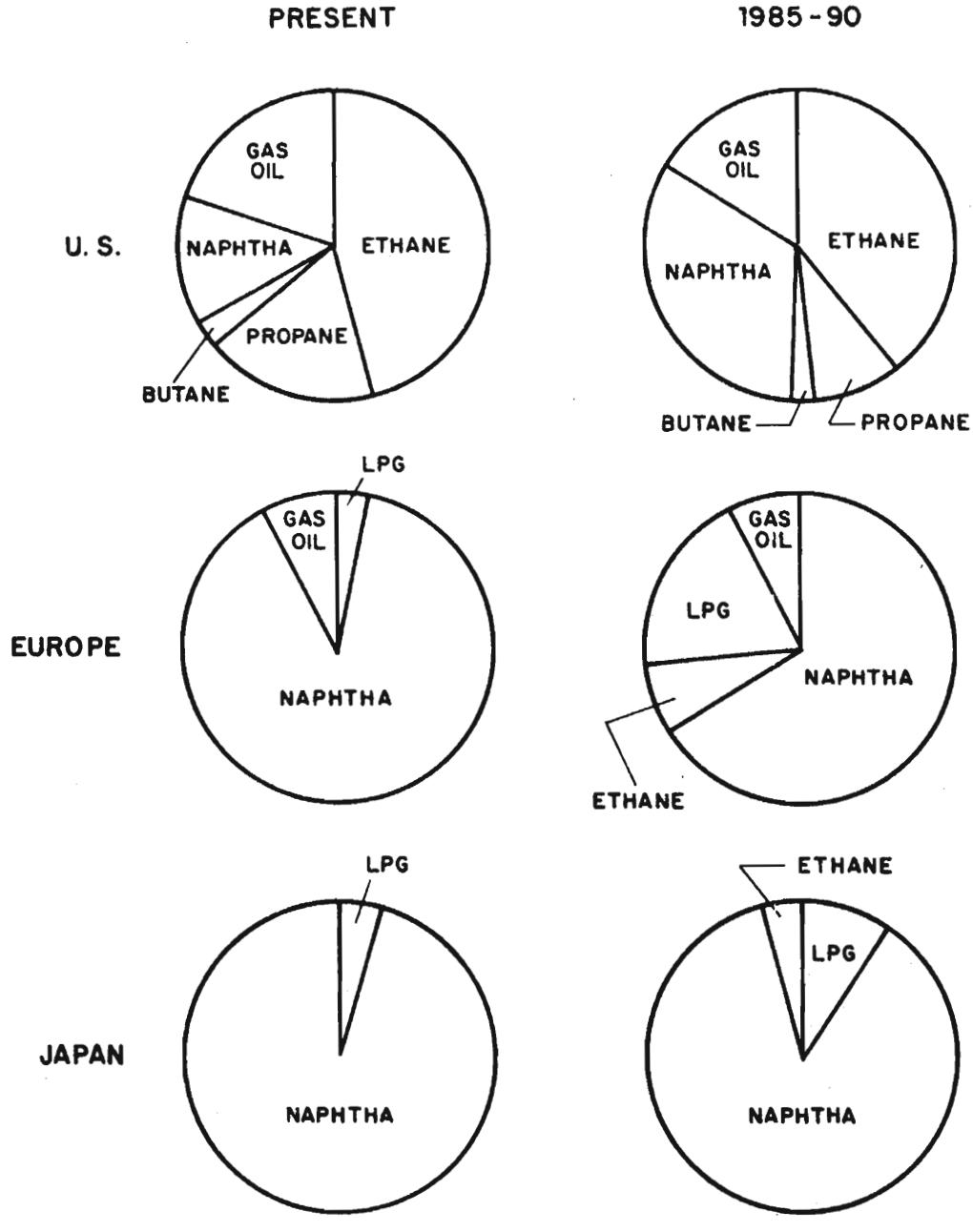

Figure 5 - FEEDSTOCKS FOR ETHYLENE PLANTS

The supply of natural gas liquids is limited. U.S. production of natural gas is expected to decline and the gas is getting drier. World supply of LPG, primarily from Middle East, is expected to greatly increase. U.S. gasoline consumption has peaked, but the phaseout of leaded gasoline and expected rapid increase in demand for premium unleaded gasoline will keep the heavy straight run naphtha and aromatic feedstocks in tight supply. Low octane light virgin naphtha and raffinate of reformate have only fuel value and should be available for ethylene production. Raffinates are, however, rich in iso paraffins which are poor feeds for ethylene production. Distillate demand is expected to keep rising because of increased demand for jet fuel and diesel for automobiles.

It is generally believed that petrochemical producers will be able to compete for these feedstocks with the fuel market. However, temporary glut and shortages will almost certainly develop from time to time in each category. Therefore, ability to use a variety of different feeds for ethylene plants will become increasingly important. Meanwhile, the incentive to use even heavier fractions of crude oil as feedstocks for ethylene production will grow. Several efforts are underway for extending the commercially viable range of feedstocks by developing processes to crack vacuum gas oils, whole crude and even resids [6-9].

FEEDSTOCK FLEXIBILITY

Most existing ethylene plants are designed for a single feed and normally they cannot be operated on a different feed without some penalty. Design of each major area of an ethylene plant changes substantially with a change in feedstock. For example, for a constant capacity ethylene plant, a change to a heavier feed usually:

- Increases the amount of feed and requires higher steam to feed ratio.
- Increases the furnace duty.
- Requires lower severity furnace with lower temperature and shorter residence time.
- Results in lower percentage of heat removed as high pressure steam in transfer line heat exchangers.
- Increases complexity of the quench tower. With liquid feeds, a distillation column is required to separate large quantities of pyrolysis gasoline and fuel oil products.
- Increases average molecular weight of the gaseous products and increases compressor duty.

- Increases complexity of the gaseous product recovery section because of higher flow rates and because of the importance of recovering increased quantity of other olefins.

Also, as ethylene plants are often a part of a major complex with a certain degree of interdependency regarding utilities and materials between the ethylene plant and surrounding facilities, even a minor change in feedstock composition requires prior extensive assessment of its impact. However, ethylene producers usually find ways to crack some amount of other-than-design feed from time to time, sometimes after minor additional investment.

New facilities can be designed to provide significant feedstock flexibility. Although this flexibility increases the plant investment and operating costs, ethylene producers have begun to find it prudent to provide more flexibility, particularly on their newer plants.

REFERENCES

1. Wett, T., "Ethylene Report", The Oil and Gas Journal, Sept. 1980, pp. 59-64.

2. Zdonik, S. B., Bassler, E. J., and Hallee, L. P., "How Feedstocks Affect Ethylene", Hydrocarbon Processing, Feb., 1974, pp. 73-81.

3. Cobb, C. B., "Petrochemicals in an Energy Constrained Economy", Paper presented at 88th National Meeting of AIChE, June 1980, Philadelphia, PA.

4. Scopes, H. M., "Feedstocks in the Eighties: A European Perspective", Paper presented at 88th National Meeting of AIChE, June 1980, Philadelphia, PA.

5. Ichikawa, M. and Kaike, H., "Feedstocks for Japanese Petrochemical Industries", Paper presented at 88th National Meeting of AIChE, June 1980, Philadelphia, PA.

6. Ishikawa, T. and Keister, R. G., "A Petrochemical Alternative - ACR", Hydrocarbon Processing, December 1978, pp. 109-113.

7. Wing, M., "Why not Crack Crude?", Chemtech, January 1980, pp. 20-22.

8. Greene, R. B., "Vacuum Gas Oil Cracking", 9th World Petroleum Congress Proceedings of PD 19 (1), Tokyo, 1975.

9. Kunii, D., et al, "Production of Olefins by Thermal Cracking of Heavy Oils .....", 9th World Petroleum Congress Proceedings of PD 19 (3), Tokyo, 1975.

FLASH PYROLYSIS AND HYDROPYROLYSIS OF COAL

by

Meyer Steinberg and Bharat Bhatt

Process Sciences Division
Department of Energy and Environment
Brookhaven National Laboratory
Upton, New York

October 1980

For presentation at "Specialists"
Workshop on Fast Pyrolysis of Biomass
Copper Mountain, Colorado

This work was performed under the auspices of the Department of Energy, Washington, D.C. under contract DE-AC-02-76CH00016.

FLASH PYROLYSIS AND HYDROPYROLYSIS OF COAL

by

Meyer Steinberg and Bharat Bhatt

Process Sciences Division
Department of Energy and Environment
Brookhaven National Laboratory
Upton, New York

Flash Pyrolysis

Pyrolysis of coal is usually referred to as a process of thermal decomposition in the absence of air or oxygen over a wide range of temperatures. There is a considerable body of literature dating back to early 1920's on the pyrolysis of coal with a rapid growth of interest in the last two decades. It is the purpose of this discussion to briefly summarize the major findings and to bring in the more recent work especially that relating to developing larger scale pyrolysis and rapid hydropyrolysis processes.

Coal is the product of very slow decomposition of organic matter deposited in prehistoric times. The younger coals will have gone through less decomposition and hence will contain more volatile matter than the older coals. The decomposition can be accelerated artificially by increasing the temperature. When heated at conventional rate, (1-10°C/sec) in an inert atmosphere, coal begins to decompose at 350 to 400°C into a carbon rich residue and a hydrogen rich volatile fraction. The volatile fraction consists of various gases and liquids. The amount of volatile matter released and the relative proportions of its various components depend upon the process parameters such as temperature, heat up rate, pressure, particle size, type of coal, etc. Higher heating rates (10^2 to 10^6 °C/sec) tend to increase the volatile yield substantially. Pyrolysis with higher heat up rate is known as flash pyrolysis. The developments in pyrolysis and flash pyrolysis have been reviewed in several publications.[1,2] Various heating methods, such as laser, microwave, flash tube, plasma, electric arc, shock tube, electric current and entraining gas, have been applied in the experimental work.

The amounts of volatile matter obtained by various investigators were compared to the volatile matter content determined by proximate analysis. Their ratio varied from 0.75 to 1.36 for several coals.[1]

Comparison of volatile yields obtained by Mentser et al[3] with the ASTM determined volatile matter is given in Table 1. Volatile yields in excess of the ASTM volatile matter content, were obtained. Figure 1 shows weight loss as a function of temperature for various coals.[3] As the temperature increases, weight loss increases upto a certain temperature, after that a drop in weight loss is observed in a certain range of temperature, before rising again. The fraction of tar and gas obtained for Pittsburgh hvAb coal are shown in Figure 2 as a function of temperature.[3] As the temperature increases, tar yield decreases and gas yield increases. The gas composition for the Pittsburgh hvAb coal as a function of temperature, are shown in Figure 3.[3]

II. Kinetics of Mechanisms

The exact description of the complex decomposition and transport phenomena involved in coal pyrolysis is not yet available. A simple model proposed by many authors is a first order decomposition occuring throughout the particle. The rate constant is typically correlated with temperature by the Arrhenius expression. There is little agreement on the observed rate constants, with several orders of magnitude discrepancy at a given temperature. The value of apparent activation energies vary from 2 to over 50 kcal/mole. Differences in equipment, experimental procedures and various coals used seem to be the reasons for the disagreement.

III. Flash Hydropyrolysis

Following early work, in the 1960's on the rapid gas phase hydrogeneration of coal for the synthesis of liquid hydrocarbons, preliminary bench scale experiments in a 3/4-in. diameter x 8-ft long downflow reactor was undertaken at Brookhaven National Laboratory in 1974.[4] When hydrogenating lignite at temperatures and pressure up to 700°C and 1500 psi, the results indicated significant yields of liquids, especially benzene, and gaseous hydrocarbons, particularly methane and ethane. The liquid yields increased for reaction residence times less than 30 seconds.

Preliminary process design and economic evaluation of a flash hydropyrolysis process[5] indicated a reasonable return on capital investment especially for chemical feedstock production. This gave encouragement to the further investigation and development of a flash hydropyrolysis process (FHP) which featured a one step, non-catalytic, rapid deep hydrogeneration system for conversion of coal to synthetic liquids and gaseous fuels. In late 1976 a larger, versatile, and highly instrumented entrained downflow tubular reactor was constructed and placed into operation.[6,7]

During this period several university research laboratories have contributed to an understanding of the rapid coal hydrogenation reaction, notably, R. Graff et al.[8] at City University of New York and J.B. Howard et al.[9] at MIT. In addition, three federally-supported industrial programs have been undertaken at Cities

Table 1

COMPARISON OF VOLATILE YIELDS FROM RAPID PYROLYSIS
OF VARIOUS COALS WITH ASTM VOLATILE MATTER CONTENTS

Coal Source	Volatile matter content-wt% by ASTM analysis	Volatile matter content-wt% from peak weight loss	Increase factor
Pochontas No. 3	16.8	18.5	1.10
Lower Kittanning	25.3	30.8	1.22
Pittsburgh	35.1	47.9	1.36
Colchester Ill. No. 2	48.0	55.8	1.16
Rock Springs No. 7-1/2	37.7	42.4 (plateau)	1.12

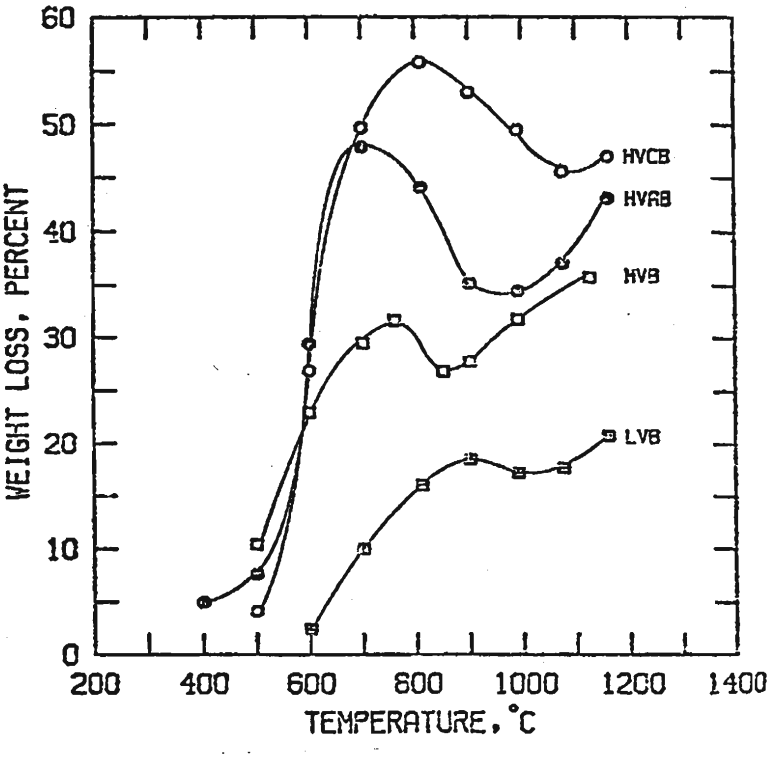

Figure 1. Devolatilization of Bituminous Coals by Rapid Heating (3)

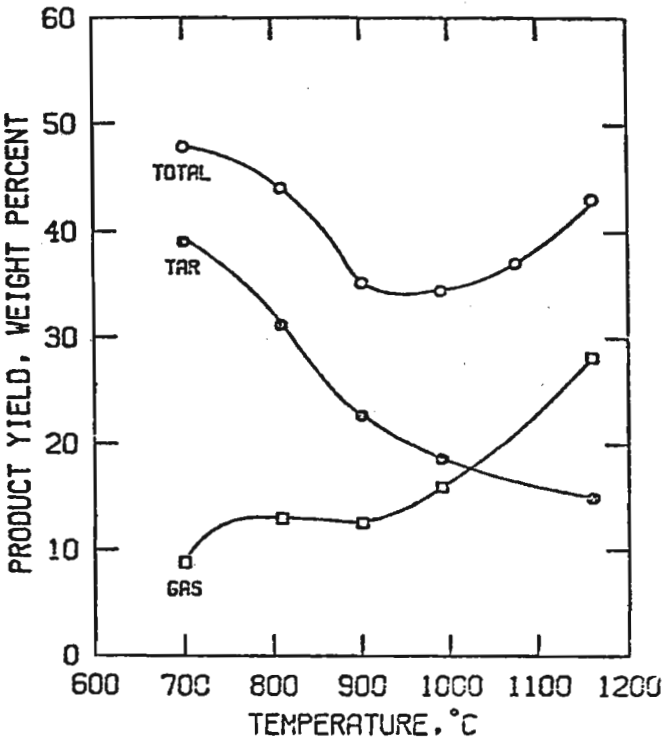

Figure 2. Yields of Tar and Gas from Devolatilization of Pittsburgh hvAb coal (3)

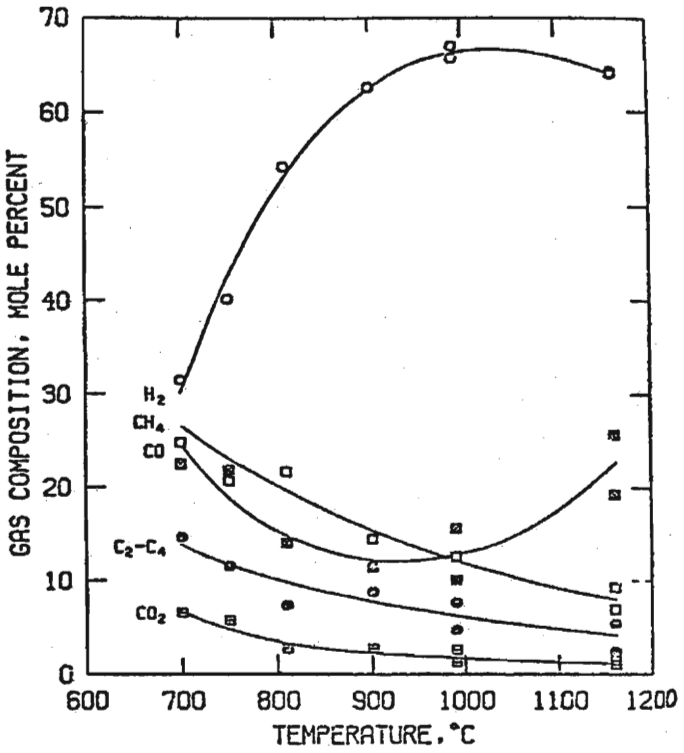

Figure 3. Composition of Gas from Devolatilization of Pittsburgh hvAb coal (3)

Service Research and Development Company on a short residence time (CS-SRT) hydrogenation process,[10] at the Institute of Gas Technology on a high speed riser cracking (IGT-RC) process using a coil reactor[11] and at Rocketdyne Corp. on a rocket type reactor system.[12]

The 1-in. I.D. tubular reactor, 8-ft long, equipped with four sectional clam shell electric heaters followed by 4-ft of cooling section is constructed of Inconel 617, a high Cr-Ni alloy. Hydrogen can be supplied up to 5 lbs/hr and preheated to a maximum of 900°C in a 1/4-in. diameter electrical resistance heated hairpin tube. The reactor tube maximum operating conditions are 4000 psi and 800°C or 2500 psi and 900°C. An on-line process gas chromatograph can analyze 10 chemical components every eight minutes with sample taps every two feet along the length of the reactor and in the traps and vent lines. A char trap maintained at 300°C separates out the char and avoids condensation of liquid hydrocarbons. This is followed by a water-cooled trap which separates the oils ($> C_9$) and a low temperature trap (-40°C) which separates the condensable BTX ($< C_9$). The remaining gases are vented up a stack. A schematic of the apparatus is shown in Figure 4.

The general trend of yields for the FHP conversion of coal (lignite) to products collected at the exit of the tubular reactor are shown for the light liquid product BTX ($< C_9$, mainly benzene) in Figure 5, and for the main gaseous hydrocarbon products, methane and ethane in Figure 6. It appears that the yield (in terms of fraction of carbon converted) of liquid remains at a relatively low level at any given pressure until temperatures in the order of 650°C is reached. The BTX yield tends to rise and reach a maximum in the order of 10% at temperatures ranging from 725°C to 800°C after which the yield declines. Thus, a dynamic equilibrium appears to be established between the formation and the decomposition of the liquid hydrocarbons. In the case of the gaseous hydrocarbons, the yield appears to continually rise both as a function of pressure and temperature reaching values as high as 50 to 60%. However, these are not maximum yields since they have been measured at the reactor exit which is across the entire length of the reactor for coal residence times ranging from about 9 to 12 seconds. The yields have been found to vary along the length of the reactor going through a maximum in a number of cases.

Concerning the flash hydropyrolysis operation, it is calculated that the average coal particle (100 μ dia) heat-up rate from ambient feed temperature to reactor temperature is > 20,000 °C/sec when mixed at the entrance to the reactor with 750°c preheated hydrogen. The average cool-down or quench rate of the reaction mixture from the heated reaction zone, through the air cooled quench zone to the 300°C char trap is approximately 200 °C/sec. However, the initial cool-down rate at the exit of the reaction zone may be higher. The maximum yields were determined from the highest measured value along the length of the reactor using the sample taps. One example of the product yield as a function of coal particle residence times is given

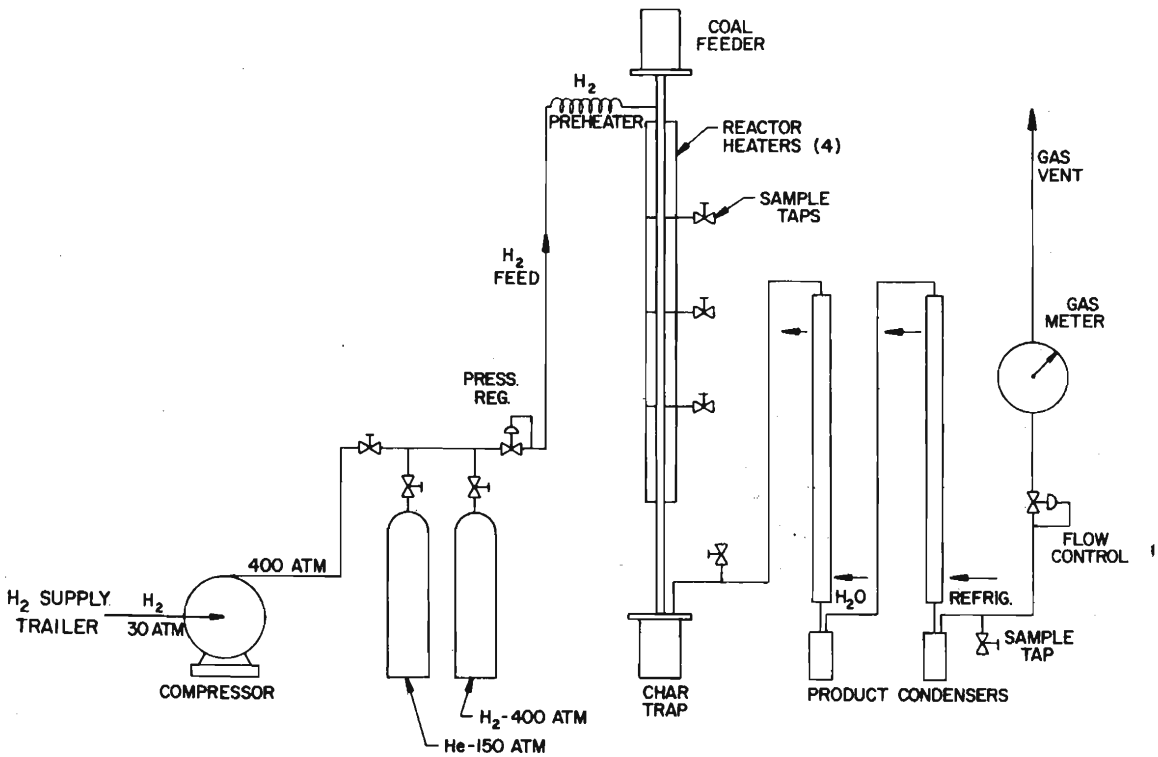

SCHEMATIC FLOWSHEET OF ENTRAINED TUBULAR REACTOR EXPERIMENT

Figure 4

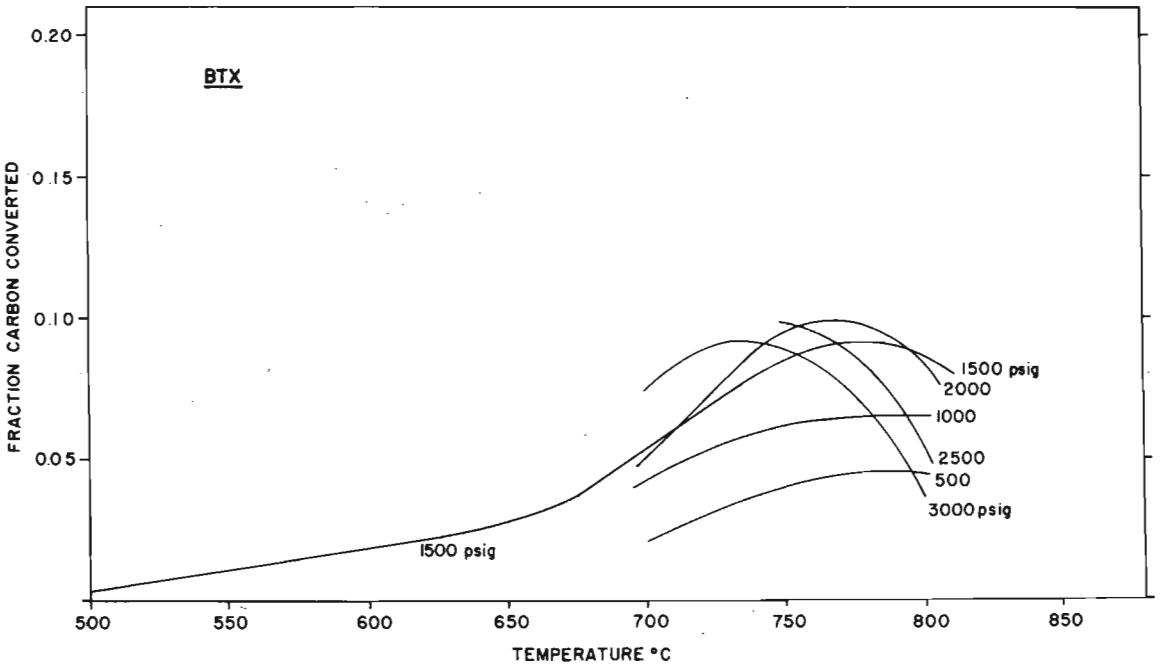

FLASH HYDROPYROLYSIS OF LIGNITE
BTX vs TEMPERATURE
PRESS. 500 - 3000 psig
COAL RESIDENCE TIME 9-12 sec

Figure 5

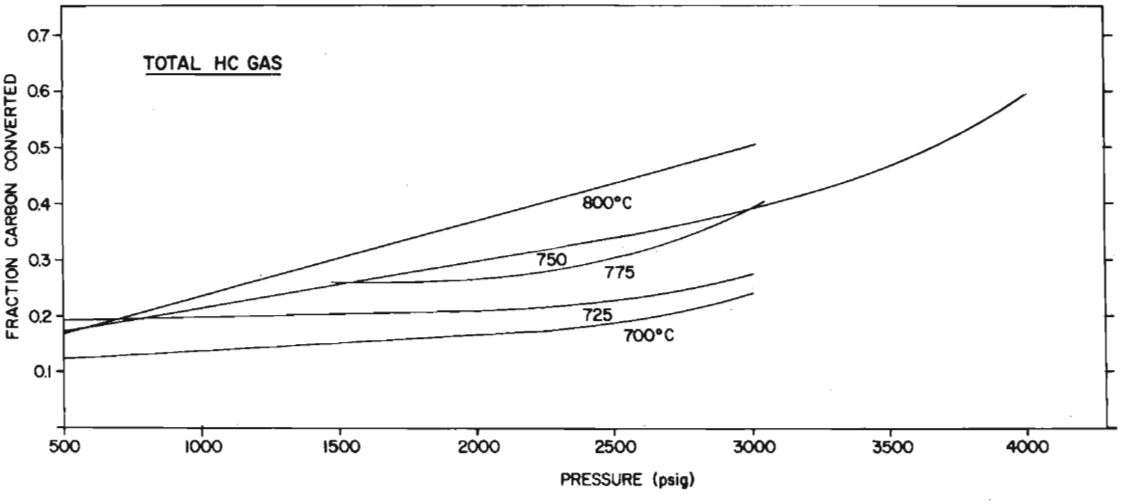

FLASH HYDROPYROLYSIS OF LIGNITE
TOTAL HC GAS vs. PRESSURE
TEMP 700°- 800°C
COAL RESIDENCE TIME 9-12 sec

Figure 6

in Figure 7 at 3000 psi and 825°c. As the residence time increased from 2 to 10 seconds, BTX and ethane yield decreased while methane yield went through a maximum around 7 seconds and this also decreased.

In the temperature range of 750° to 800°C and pressure range of 2000 to 2500 psi, the maximum yield for BTX peaks out at coal particle residence times varying from 2 to 7 seconds with the shorter residence times at the higher temperatures.

Because of the higher boiling range of the heavier oils (> C_9), these are determined only by collection at the end of the reactor. As shown in Figure 8 for North Dakota lignite at temperatures in the range of 725° to 750°C and 2000 psi, the maximum yield of the heavier liquid hydrocarbons (> C_9), is approximately equal to that of the BTX yield. However, above 750°C, the > C_9's decrease much more rapidly with increasing temperature than the BTX. Since one of the probable products of decomposition or hydrocracking of the heavier liquids is BTX, there appears to be a relationship between the measured yields of these two liquid products. At even higher temperatures, (> 775°C) the heavier liquids (> C_9's) decrease rapidly primarily due to hydrogenation and rapid formation of gaseous hydrocarbons.

As the reactor temperature increases above 875°C, the principal product remaining is methane with smaller amounts of ethane. The maximum gaseous hydrocarbon yield occurs between 2.4 and 7 seconds coal particle residence time over a range of pressures as given in Figure 9. The almost linear nature of the curves shows a yield increase of from 2.8 to 3.8% per 100 psi of total system pressure. This pressure effect is thermodynamically in agreement with that predicted for the hydrogen-carbon reaction producing CH_4 and C_2H_6.

Since the feed ratio of hydrogen to coal is usually in the order of 1 lb of hydrogen to 1 lb of coal, the product concentration in the process gas stream are far below thermodynamic equilibrium values. Due to this dilute phase, the methane gas usually is below 5 mole % concentration in the equipment while the equilibrium concentration is 84% at 700°C and 4000 psig and 32% at 900°C and 500 psig. By decreasing the hydrogen to coal feed ratio in the reactor to 0.2 at 2500 psig and 875°C, a methane concentration as high as 33% was observed. The thermodynamic equilibrium concentration under these conditions is 61%, thus, the methane reached 54% of the equilibrium value. At very low feed ratios we have exceeded the equilibrium concentration. The rapid hydropyrolysis of coal is not equilibrium limited.

Two maximum yield runs are shown in Table 2. One run listed is the highest liquid yield run (19.9% liquid and 64.5% total conversion) and the other is the highest gaseous yield run (88.5% gaseous HC and 90.5% total conversion).

Additional data has been obtained with a sub-bituminous coal. The yield structure appears similar. However, the sub-bituminous gave a higher gaseous yield at lower pressures than the lignite.[13]

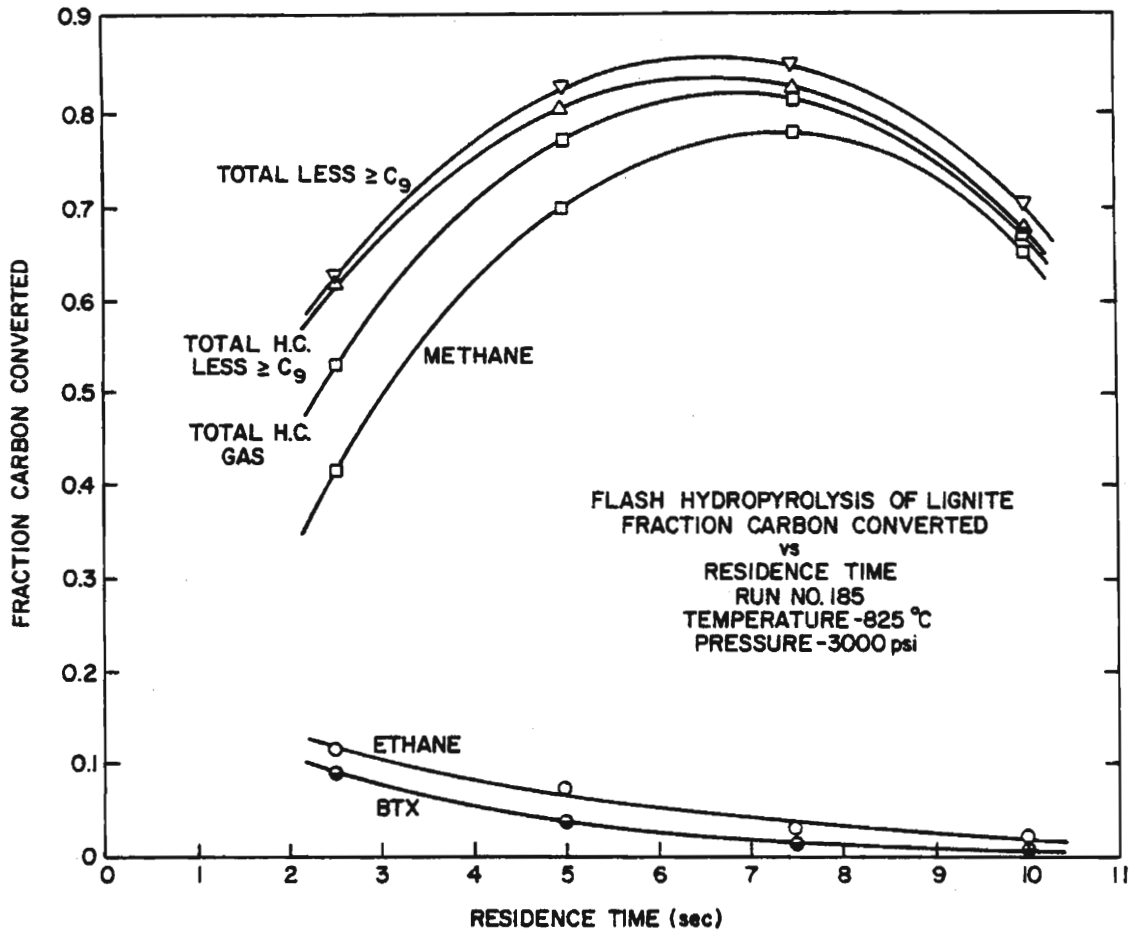
FRACTION CARBON CONVERTED
RESIDENCE TIME (sec)
TOTAL LESS ≥ C9
TOTAL H.C. LESS ≥ C9
TOTAL H.C. GAS
METHANE
ETHANE
BTX
FLASH HYDROPYROLYSIS OF LIGNITE
FRACTION CARBON CONVERTED
vs
RESIDENCE TIME
RUN NO. 185
TEMPERATURE - 825 °C
PRESSURE - 3000 psi

Figure 7

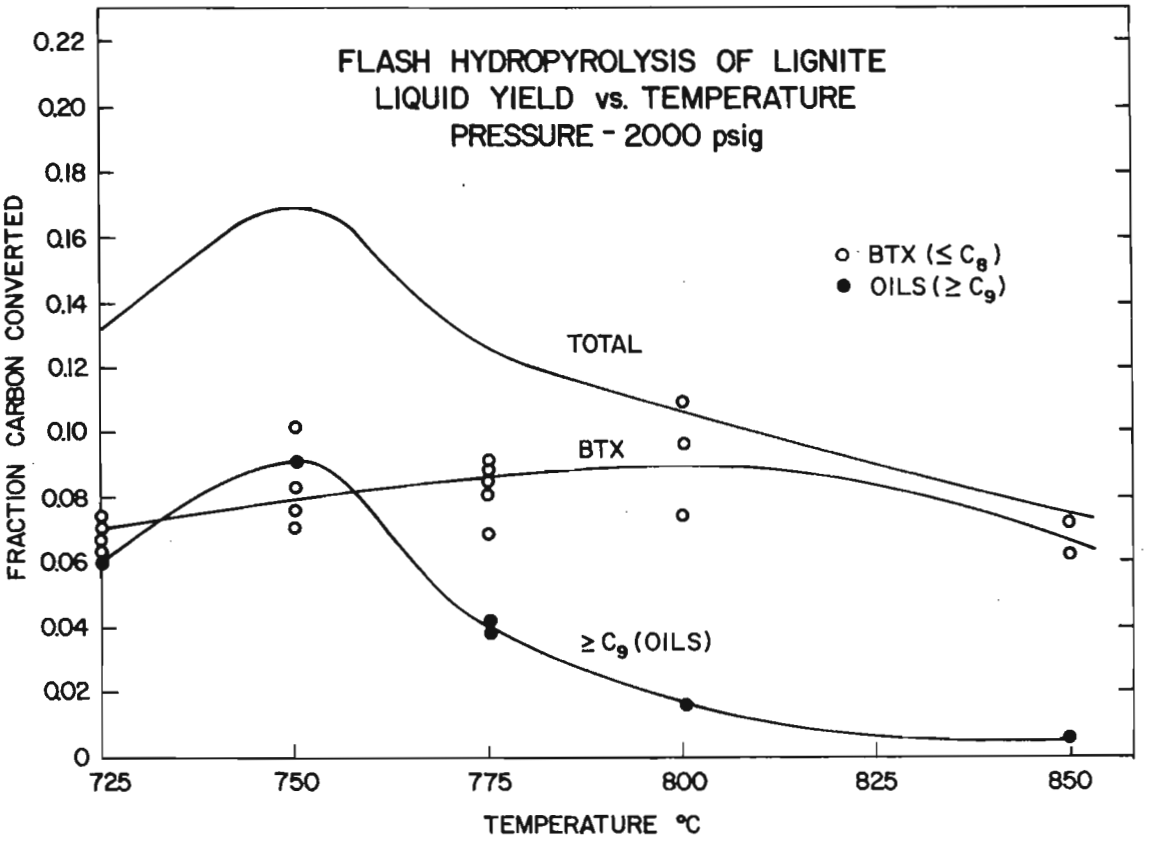
FLASH HYDROPYROLYSIS OF LIGNITE
LIQUID YIELD vs. TEMPERATURE
PRESSURE - 2000 psig
FRACTION CARBON CONVERTED
TEMPERATURE °C
o BTX (≤ C8)
● OILS (≥ C9)
TOTAL
BTX
≥ C9 (OILS)
0.22
0.20
0.18
0.16
0.14
0.12
0.10
0.08
0.06
0.04
0.02
0
725
750
775
800
825
850

Figure 8

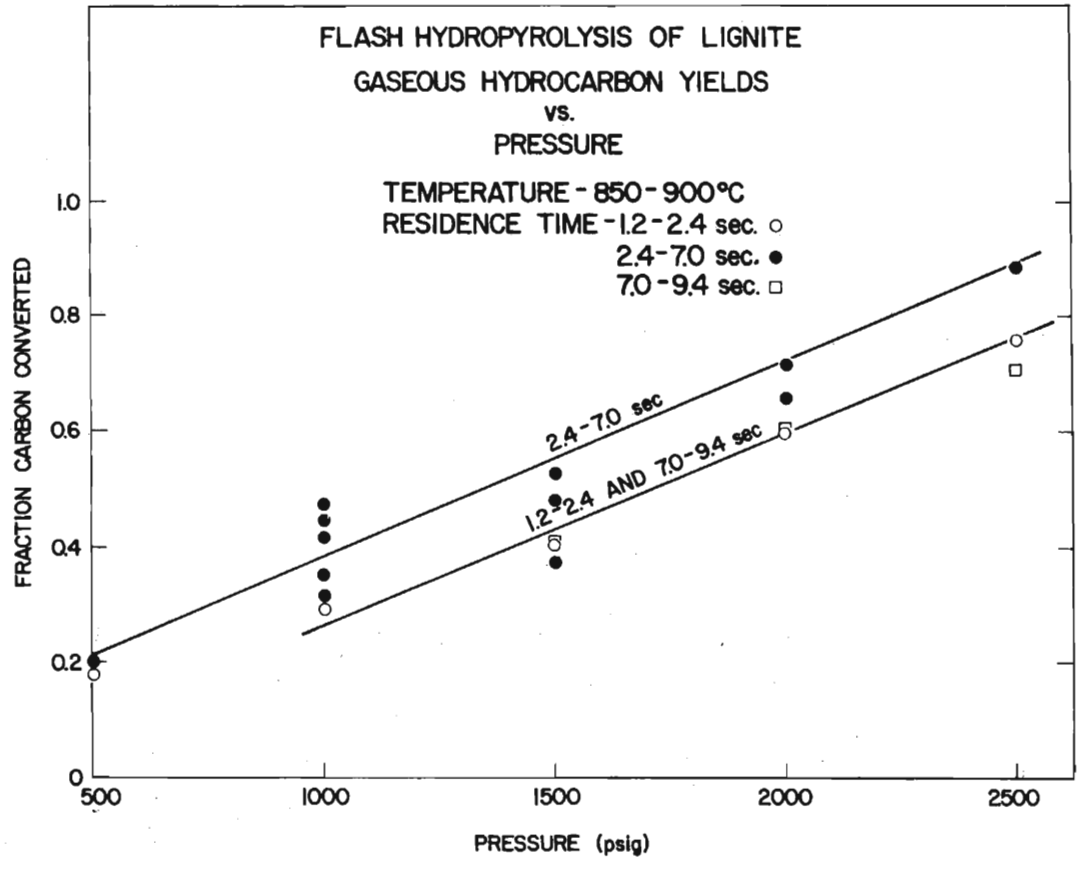
FLASH HYDROPYROLYSIS OF LIGNITE
GASEOUS HYDROCARBON YIELDS
vs.
PRESSURE
TEMPERATURE - 850 - 900°C
RESIDENCE TIME - 1.2 - 2.4 sec. ○
2.4 - 7.0 sec. ●
7.0 - 9.4 sec. □
2.4 - 7.0 sec
1.2 - 2.4 AND 7.0 - 9.4 sec
FRACTION CARBON CONVERTED
0
0.2
0.4
0.6
0.8
1.0
500
1000
1500
2000
2500
PRESSURE (psig)

Figure 9

Table 2

FLASH HYDROPYROLYSIS OF NORTH DAKOTA LIGNITE

Maximum Liquid and Maximum Gas Yield Runs

	Max. Liquid Run	Max. Gas Run
Reactor temp. (^{o}C)	775	875
Reactor pressure (psig)	2000	2500
H_2 feed rate (lb/hr)	0.82	0.88
Coal feed rate (lb/hr)	0.98	0.95
Residence time (sec)	7.1	4.7
Product Yields (% Carbon		
CO	3.4	1.3
CH_4	30.9	88.0
C_2H_6	10.3	0.5
Total HC gas	41.2	88.5
BTX	10.2	0.7
$\geq C_9$	9.7	0.0
Total liquid	19.9	0.7
Total	64.5	90.5
Heat of reaction (kcal/gm coal)	- 0.70	- 1.3
Hydrogen consumption (lb/lb coal)	0.077	0.20
Effective carbon conv. (%)	58.8	62.4
Effective energy eff. (%)	75.9	100.0

The nitrogen and sulfur distribution and balances were measured. The lignite is a relatively low S content coal (0.5% S). With FHP the major portion, 48 to 77% of initial S remains in the char. The oil is found to contain < 0.1% S. For the nitrogen (initial N content is 0.9%), less than half remains in the char and the oil contains < 0.2% N.

Mixing recycled char with the lignite feed and addition of iron oxide to the lignite improved the yield of BTX and ethane.

A reaction model has been developed in an attempt to obtain generalized expressions for the hydrocarbon component yields as a function of pressure, temperature and residence time.[14,15] The results of the non-linear regression analysis show that a first-order chemical reaction model with respect to C conversion, with a production and a decomposition step for each of the major products, satisfactorily describes the dilute phase hydrogenation. The activation energy for the initial products formation was estimated to be about 43,000 cal/mole and the power of hydrogen partial pressure was found to be +0.14. Activation energies indicate mainly a chemical reaction controlled mechanism. The use of these rate equations in conjunction with heat balance expressions are applied to the design of a hydrolysis reaction vessel. Additional experimental, design, and analysis work is needed to obtain a much more detailed understanding of the reactor engineering.

Process design and preliminary economic estimates were made for three versions of the FHP process system:[14] (1) producing only liquid products for motor gasoline fuel, (2) producing both liquid and gaseous hydrocarbon products for motor gasoline and pipeline gas, and (3) producing only gaseous products for pipeline gas. For comparable overall values of coal conversions (62%), the minimum production cost is obtained for the combined production of motor gasoline and pipeline gas. The largest part of the capital cost of the FHP plant, amounting up to 35% of the plant, is required by the equipment needed for recycling and conditioning the hydrogen process gas. The FHP process has the advantage of allowing effective gas-solid and gas-liquid separation operations. The hydrocarbon products can be readily separated from the unconverted char, oils, and process gas by condensation from the gas phase. The FHP system also has the distinct advantage of versatility and process flexibility. The product slate and the production rate of gaseous and liquid hydrocarbon fuel products can be altered in the same reactor by adjusting the reactor operating conditions.

IV. Comparison of Flash Pyrolysis and Hydropyrolysis Systems

An attempt has been made to compare the yields and product distribution from several pyrolysis and hydropyrolysis systems. The data are listed in Table 3.

Table 3

FLASH PYROLYSIS AND HYDROPYROLYSIS OF COAL
COMPARISON OF PROCESSES

Reactor System	Coal Type	Pressure atm	Temp., °C	Heating rate, °C/sec	Residence Time °C/sec	Yield-% Carbon Conversion Total Gas+Liquid	Gas	BTX	Oil	Tar
Electrically heated tube, Muentser et al	Pittsburgh HVB(1973)	vacuum	700	8300	--	50	12	—	—	38
Garret-occidental system--heat with char	Pittsburgh HVB	1 atm (CO_2,H_2)	580	2800	--	42	7	—	—	35
Flash hydropyrolysis entrained flow with H_2 BNL, IGT, CS	Lignite and Sub-bituminous	130 (H_2)	775	20,000	7	60 [1]	40	10	10	--
		170 (H_2)	900	20,000	5	89 [2]	88	1	—	—
Rockwell--short res. time, hydrogen entrainment	Pittsburgh HVB	100 (H_2)	1040	50,000	0.1	60	27	33	total	liquid
		70 (H_2)	980	50,000	2	56	45	11	—	—
Avco gasifier char combustion and steam gasification	Bituminous HVB	37 (H_2O,N_2,CO_2)	1315	>50,000	0.1	49	49 (H_2,CO,CO_2)	—	—	--

1) Liquefaction mode.
2) Gasification mode.

Mentser et al[3] heated small quantities of coal in an electrically heated resistive screen cylinder in vacuum. The heating rate was of the order of 8300°C/sec. Maximum yields of volatile matter including tars and gases were obtained in the range of 700° to 800°C. The volatile matter yields were higher than the ASTM analyses. The tar yields at 700°C are up to 40% of the carbon content in the coal while the gas yields are in the order of 12%. As the temperature increased to 1200°C tar yields decreased and gaseous yields increased.

The Garrett-Occidental System heats coal at a rate of 2800°C/sec with recycled hot char and inert gas.[16] This process which reached pilot plant scale operates at 580°C and near atmospheric pressure. The yield amounted to 35% of the carbon to heavy liquid (tar) products and 7% to gas. The heavy liquids would have to be upgraded by hydrocracking for producing a saleable lighter liquid fuel.

Data for the flash hydrogenation indicate higher heat up rates (20,000°C/sec) in an entrained tubular reactor. For maximizing liquid products, temperatures of 775°C and hydrogen pressure up to 130 atm are required. Liquid yields are up to 20% of carbon converted to benzene and lights oils and 45% to gas of which up to 31% consists of methane. At higher temperatures of 875°C and 170 atm up to 90% of the carbon in the coal can be converted to methane.

A form of a high capacity entrained reactor is the Rockwell[17] design which employs a rocket engine type mixing device for contacting the preheated hydrogen and the coal. In the mode of maximizing gaseous product, 56% of the coal carbon can be converted to gaseous and liquid products (45% to gas and 11.3% to lighter liquids such as benzene) at residence times of 2 seconds. It is also claimed that for very short residence times, on the order of 0.1 sec or less, gas yields are reduced and up to 33% liquids can be obtained. However, these liquids appear to be heavier tarry substances.

The Avco-Gasifier concept[18] is a rapid gasification process using high temperature combustion products in a high temperature pyrolyzer. Unconverted char is combusted with oxygen and the products are mixed in a secondary pyrolyzer with steam. The products are mainly H_2 and CO, which is a synthesis gas useful for subsequent catalytic conversion to hydrocarbons. The overall carbon conversion for the process is 49%.

Summary of Observations

A brief summary of the major findings of pyrolysis and hydropyrolysis are as follows:

1. Rapid pyrolysis of coal usually produces larger yields of volatile matter including liquid and gaseous hydrocarbons than slow pyrolysis.

2. Rapid pyrolysis in vacuum or with an inert atmosphere yields lower conversions of coal to liquid and gaseous hydrocarbons than hydropyrolysis in a hydrogen atmosphere.

3. Pyrolysis in a higher pressure inert atmosphere tends to decrease overall yields.

4. Rapid pyrolysis in an inert atmosphere produces larger amounts of heavier liquids and tars than hydropyrolysis.

5. Hydropyrolysis at higher hydrogen pressures produces higher overall yields.

6. Rapid pyrolysis at higher temperatures tend to decrease yields and produce lower molecular weight species.

7. Rapid hydropyrolysis at higher temperatures produces more gaseous hydrocarbons and lower liquid yields.

8. Longer residence times in rapid hydropyrolysis tends to produce more methane. Shorter residence times tend to produce more liquids. There are optimum residence times for maximizing either liquid or gaseous yields.

9. Pyrolysis in an inert atmosphere at longer residence times tend to increase conversions but then becomes constant after devolatilization is complete.

10. Heating rate is a function of the method of heating. Entrained gas heating with hydrogen produces the highest heating rates and produces the highest yields.

11. Lower rank coals tend to be more reactive and produce higher yields of gaseous and liquid hydrocarbons than higher rank coals.

12. From a process economics point of view, pyrolysis in an inert atmosphere requires the need for a consumer of residual char, and an upgrading of heavier liquids.

13. In a flash hydropyrolysis process, the char can be used to produce hydrogen consumed the process. A considerable fraction of the cost of the process is involved in production, recovery and recycle of hydrogen.

References

1. Anthony, D.B., and Howard, J.A., "Coal Devolatilization and Hydrogasification" AIChE Journal 22, No. 4, 625-56 (1976).

2. Belt, R.J., and Bissett, L.A., "Assessment of Flash Pyrolysis and Hydropyrolysis" METC/RI-79/2 Morgantown Energy Technology Center, West Virginia (July 1978).

3. Mentser, M., O'Donnel, H.J., Ergun, S., and Friedel, R.A., "Devolatilization of Coal by Rapid Heating", ACS Preprint, Division of Fuel Chemistry, Vol. 18, No. 1, pp. 26-35 (1973).

4. Steinberg, M. and Fallon, P., "Coal Liquefaction by Rapid Gas Phase Hydrogenation", BNL 19507, Brookhaven National Laboratory, Upton, New York, (November 1974) and American Chem. Soc., 169th National Meeting (Philadelphia, Pa.), Petroleum Chemistry Division 20, No. 2, pp. 542-52 (April 1975).

5. Steinberg, M., Sheehan, T.V., and Lee, Q.E., "Flash Hydropyrolysis Process for Conversion of Lignite and Gaseous Products", BNL 20915, Brookhaven National Laboratory, Upton, New York (October 1975) and American Chem. Soc., 170th National Meeting (New York, N.Y.), Ind. and Eng. Chem. Division (April 4-9, 1976). Also published in Syn. Fuels Processing, A.H. Pelofsky, editor, Marcel Dekker, Inc., (New York, N.Y.) pp. 163-92 (1977).

6. Fallon, P. and Steinberg, M., "Flash Hydropyrolysis of Coal--The Design, Construction, Operation and Initial Results of a Flash Hydropyrolysis Experimental Unit", BNL 50698 (January 1977) presented at 173rd National American Chem. Soc. Meeting (New Orleans, La.) March 20-25, 1977).

7. Steinberg, M. and Fallon, P., "Flash Hydropyrolysis of Coal", Quarterly Reports Nos. 1 to 5, BNL 50677, 50707, 50779, 50821, 50824 (January 1977 to March 1978).

8. Dobner, S., Graff, R.A., and Squires, A.M., "Flash Hydrogenation of Coal, Yield Structure of Illinois No. 6 Coal at 100 atm.", Fuel 55, 114 (1976).

9. Anthony, D.B. and Howard, J.B., "Coal Devolatilization and Hydrogasification", AIChE J. 22, 625 (1976).

10. Greene, M.I., Ladelfa, C.J., and Bivacca, S.J., "Benzene-Ethylene-SNG from Coal via Short Residence Hydropyrolysis", Cities Service Research and development Company, Cranbury, New Jersey (March 1978) presented at 175th National AIChE Meeting (Anaheim, Calif.) (March 12-17, 1978).

11. Dunca, D.A., Beeson, J.L., and Oberle, R.D., "Research and Development of Rapid Hydrogenation for Coal Conversion to Synthetic Motor Fuels (Rise Cracking of Coal)", FE-2307-34 (August 1978) Institute of Gas Technology, Chicago, Illinois, Annual Report for the period of April 1, 1977 to March 31, 1978.

12. Oberg, C.L., Combs, L.P., and Silverman, J., "Coal Conversion by Flash Hydropyrolysis and Hydrogasification", Proceedings of the 13th Intersociety Energy Conversion Engineering Conference (San Diego, Calif.) 1, pp. 402-8 (August 20-25, 1978).

13. Fallon, P.T., Bhatt, B., and Steinberg, M., "The Flash Hydropyrolysis of Lignite and Sub-Bituminous Coals to both Liquid and Gaseous Products", BNL 26210, Brookhaven National Laboratory, Upton, N.Y. (May 1979) accepted in Fuel Technology (in press).

14. Steinberg, M., Fallon, P., Dang, V.D., Bhatt, B., Ziegler, E., and Lee, Q., BNL 25232, Reaction, "Process and Coal Engineering for the Flash Hydropyrolysis of Coal", BNL 25232, Brookhaven National Laboratory, Upton, New York, (November 1978).

15. Bhatt, B., Fallon, P., and Steinberg, M., "Reaction Modelling and Correlation for Flash Hydropyrolysis of Lignite", BNL 27574, Brookhaven National Laboratory, Upton, N.Y., (March 1980).

16. Sass, A., "Garrett's Coal Pyrolysis Process", Chem. Eng. Progress, 70, No. 1, 72-3 (1974).

17. Silverman, J., Freidman, J., and Kahn, D.R., "The CS/R Advanced SNG Hydrogasification Process", 15th Intersociety of Energy Conversion Engineering Conference (IECEC) Vol. 2, 952-958 (Aug. 18-22, 1980).

18. White, G.A., Stechler, D.B., Rosenberg, C.W., and Gannon, R.E., "Indirect Liquefaction via the Avco Coal Gasification System", 15th IECEC, Vol. 2, 978-84 (Aug. 18-22, 1980).

INTRODUCTION TO PYROLYSIS OF BIOMASS

F. Shafizadeh
Wood Chemistry Laboratory
Department of Chemistry
University of Montana
Missoula, Montana 59812

ABSTRACT

The pyrolytic properties of biomass are controlled by the chemical composition of its major components, namely cellulose, hemicelluloses, and lignin and their minor components including extractives and inorganic materials. Pyrolysis of these materials proceeds through a series of complex, concurrent and consecutive reactions and provides a variety of products.

Pyrolysis of cellulose at lower temperatures (below 300°C) involves reduction in molecular weight, evolution of water, carbon dioxide and carbon monoxide and formation of char. On heating at higher temperatures (300-500°C), the molecule is rapidly depolymerized to anhydroglucose units that further react to provide a tarry pyrolyzate.

At still higher temperatures, the anhydrosugar compounds undergo fission, dehydration, disproportionation and decarboxylation reactions to provide a mixture of low molecular weight, gaseous and volatile products. The composition of these products and mechanism and kinetics of their production have been reported in a series of papers that are summarized in this presentation.

COMPOSITION OF BIOMASS

Pyrolysis of biomass involves different materials and methods and provides a variety of products. An analytical relationship between these factors provides the basic knowledge which is needed for new development.

Biomass consists of different types of dead and living plant cells, the structure and composition of which varies for different parts and species of the plant. The living cells as in the green leaves contain some proteins in their protoplasm, considerable water in the vacuoles which maintains their turgidity and less cellulosic cell wall materials. The woody tissues contain some living (parenchyma) cells, but are largely

composed of dead (prosenchyma) cells which consist of several layers and an intercellular material (middle lamella). Figure 1 shows a diagramic presentation of a wood fiber (tracheid).

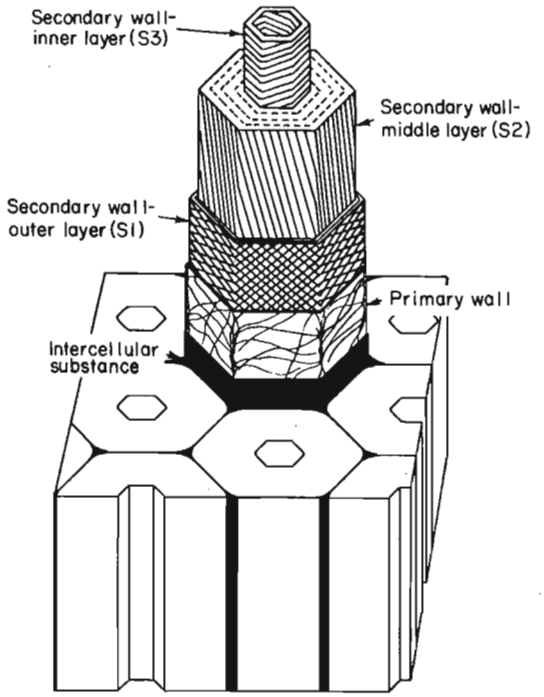

FIG. 1. Diagrammatic presentation of wood fiber (tracheid).

Cellulose microfibrils embedded in a matrix of hemicelluloses and lignin form the main components of the cell walls [1] and biomass in general. In addition to these materials, there are some lipids and hydrocarbons (terpenes) which are soluble in ether and various types of phenolic compounds, carbohydrates and proteins, which may be soluble in benzene, alcohol or water. The leaves and bark generally contain more extractives and less cell wall materials than wood and woody tissues. Table 1 shows the approximate analysis of several types of biomass.

The cellulose component, which is a macromolecule composed of linearly linked β - (1$\longrightarrow$4) D-glucopyranose units, is the same in all types of biomass except for the degree of polymerization (DP). However, the nature of the hemicelluloses and lignin could vary. Aggregation of the linear chains of the cellulose macromolecules within the microfibrils provide a crystalline structure which is highly inert and inaccessible to the chemical reagents. Consequently, it is very difficult to hydrolyze the cellulose molecules by acids or enzymes.

TABLE 1

Approximate Analysis of Some Biomass Species

Species	Total ash	Solvent sol.	Water sol.	Lignin	Hemi-cellulose	Cellulose
Softwood	0.4%	2.0%	--	27.8%	24.0%	41.0%
Hardwood	0.3	3.1	--	19.5	35.0	39.0
Wheat straw	6.6	3.7	7.4	16.7	28.2	39.9
Rice straw	16.1	4.6	13.3	11.9	24.5	30.2
Bagasse	1.6	0.3	--	20.2	38.5	38.1

In contrast to cellulose, the hemicelluloses are amorphous, have a lower DP and could be preferentially hydrolyzed under relatively mild conditions, known as prehydrolysis. Acetyl-4-O-methylglucuronoxylan (xylan) forms the main hemicellulose of the hardwoods and glucomannans (mannan) form the principal hemicellulose of the softwoods.

Lignin is a randomly linked, amorphous, high molecular weight phenolic compound which is more abundant and polymeric in softwoods than in hardwoods. Furthermore, the softwood lignin contains guaiacyl propane units (phenolic groups having one methoxyl group). Hardwood lignin, in addition to this, contains syringyl propane units (with two methoxyl groups). The higher content of acetyl and methoxyl groups in hardwoods explains why this material has been used in destructive distillation processes to obtain acetic acid and methanol.

The soluble components could be removed by stepwise solvent and water extraction, but isolation of the other cell wall components in the native form is very difficult, if not impossible. After the solvent extraction, lignin could be removed by selective oxidation to leave a combination of cellulose a d hemicelluloses called holocellulose. Alternatively, the hemicellulose component could be removed by controlled hydrolysis to leave a combination of cellulose and lignin called lignocellulose. Complete hydrolysis of the carbohydrate leaves the lignin as a dark partially decomposed residue called Klason lignin. It is also possible to break the lignin bonds (presumably with the carbohydrates) so that it could be removed with solvents at high temperatures as organosolv lignin.

COMPETING PYROLYTIC PATHWAYS

Different components of biomass display different thermal properties and the thermal properties of the aggregate represents the sum of its major organic components [2].

As discussed later on rapid heating, the carbohydrates break down at the glycosidic link to provide lower molecular weight volatile pyrolysis products, whereas lignin is mainly charred to a carbonaceous residue. This phenomenon is observed on thermogravimetry of wood and its components shown in Figure 2 [2].

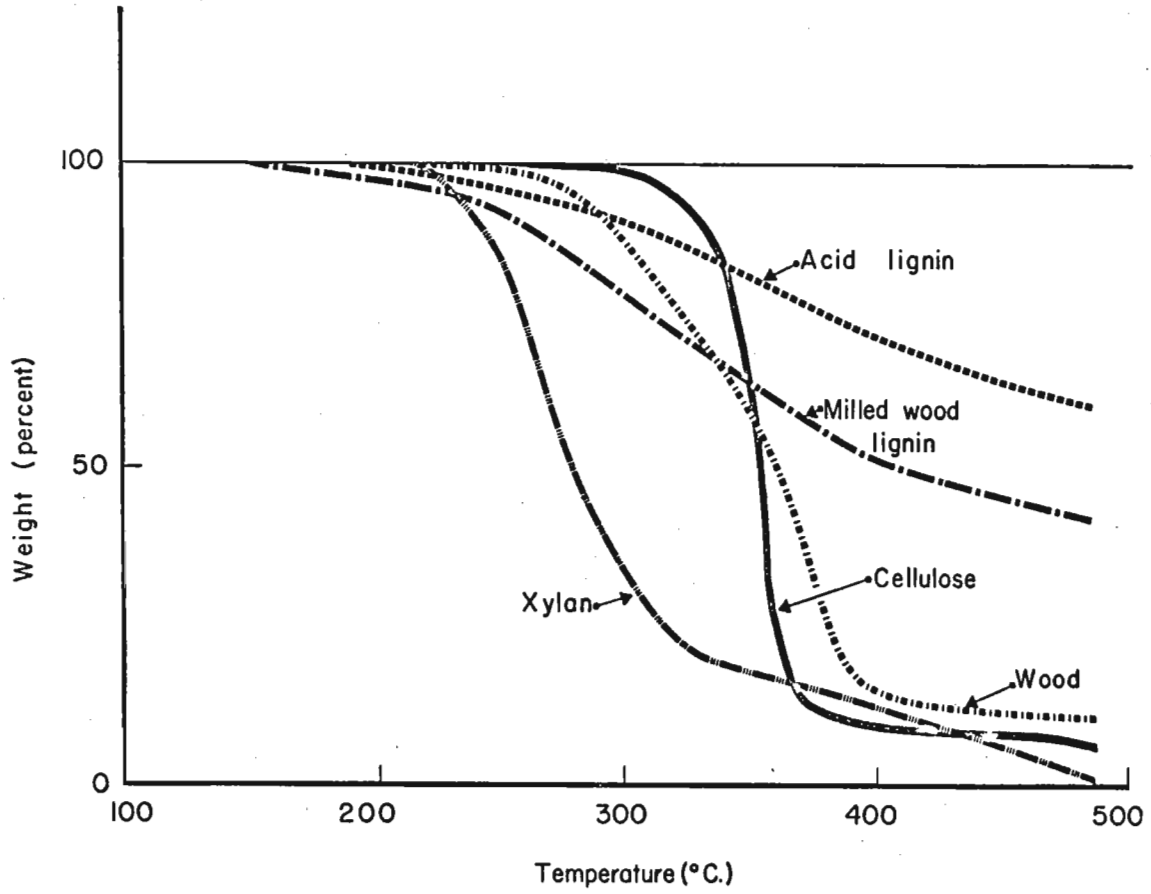

FIG. 2. Thermogravimetry of cottonwood and its components.

Furthermore, thermal properties of the components and aggregate are highly influenced by the presence of inorganic materials and various treatments. As these materials are heated, the availability of sufficient energy for alternative pathways at higher temperatures results in a series of complex, concurrent and consecutive reactions which give a variety of products.

The Arrhenius plot for the rates of weight loss of cellulose in air and nitrogen is shown in Figure 3 [3]. These data indicate a transition at ~ 300°C which reflects the existence of two different pathways. As shown in Figure 4, the rate of pyrolysis followed by weight loss under isothermal conditions, shows an initial period of acceleration and proceeds much faster in air than in an inert atmosphere. As the pyrolysis temperature is increased, the initiation period and the difference between pyrolysis under nitrogen and air gradually diminish and disappear at 310°C when pyrolysis by the second pathway takes over.

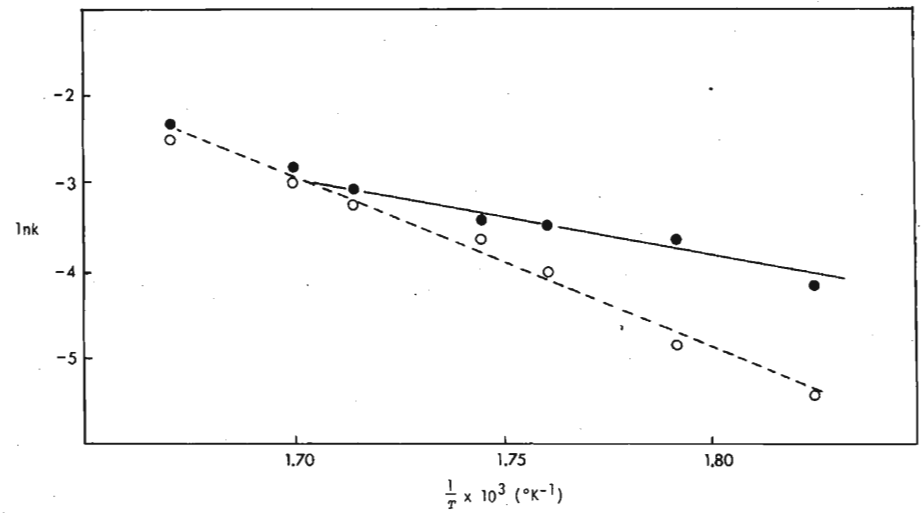

FIG. 3. Arrhenius plot for the first order reaction in the isothermal degradation of cellulose in air (-) and nitrogen (---).

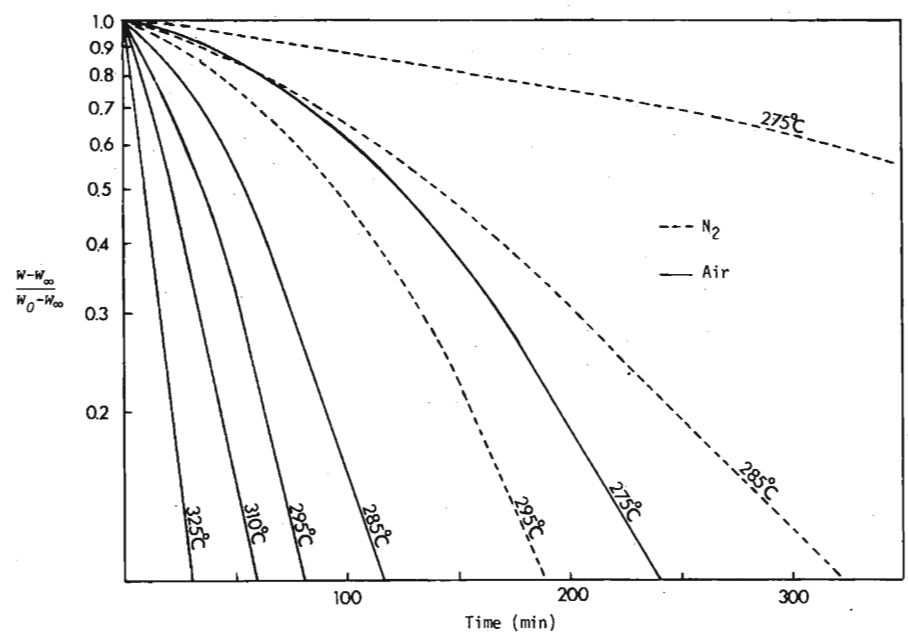

FIG. 4. First order plot for the residual cellulose weight (normalized) versus time. Plots at 310°C and 325°C for air and nitrogen are similar.

The general pathways for pyrolysis of cellulose [4,5] are shown in Figure 5.

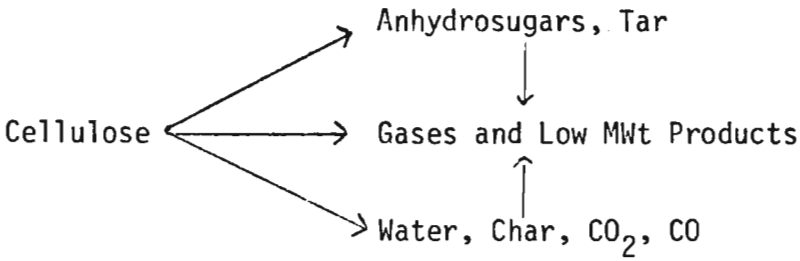

FIG. 5. Competing pathways for cellulose pyrolysis.

LOWER TEMPERATURE REACTIONS

The reactions in the first pathway, which dominates at lower temperatures, involve reduction in molecular weight or DP by bond scission, appearance of free radicals, elimination of water, formation of carbonyl, carboxyl and hydroperoxide groups (especially in air), evolution of carbon monoxide and carbon dioxide, and finally production of a charred residue. The mechanism and kinetics of these reactions which contribute to the overall rates of pyrolysis of cellulosic materials have been individually investigated [3]. Reduction in the degree of polymerization of cellulose on isothermal heating in air or nitrogen at a temperature within the range of 150-190°C has been measured by the visicosity method as shown in Figure 6. This data has been correlated with rates of bond scission given in Table 2 and used for calculating the Arrhenius plot shown in Figure 7.

Figure 8 shows the rate of production of carbon monoxide and carbon dioxide at 170°C in air and in nitrogen. The rate of evolution of these gases is much faster in air than in nitrogen and, furthermore, accelerates on continued heating. It is constructive to compare the initial linear rates for the emission of these gases with the rates of bond scission obtained for depolymerization at 170°C, discussed before. As can be seen in Table 3, for air the rate of bond scission approximately equals the rate of production of carbon dioxide plus carbon monoxide in moles per glucose unit. In nitrogen, however, the rate of bond scission is greater than the combined rates of carbon monoxide and carbon dioxide evolution.

It is assumed that carbon dioxide and carbon monoxide may be formed by decarboxylation and decarbonylation, respectively, as well as by other competing reactions. The significance of the former reactions was determined by measuring the net rate of accumulation of carboxyl and carbonyl groups in cellulose on heating in air at 190°C. The results

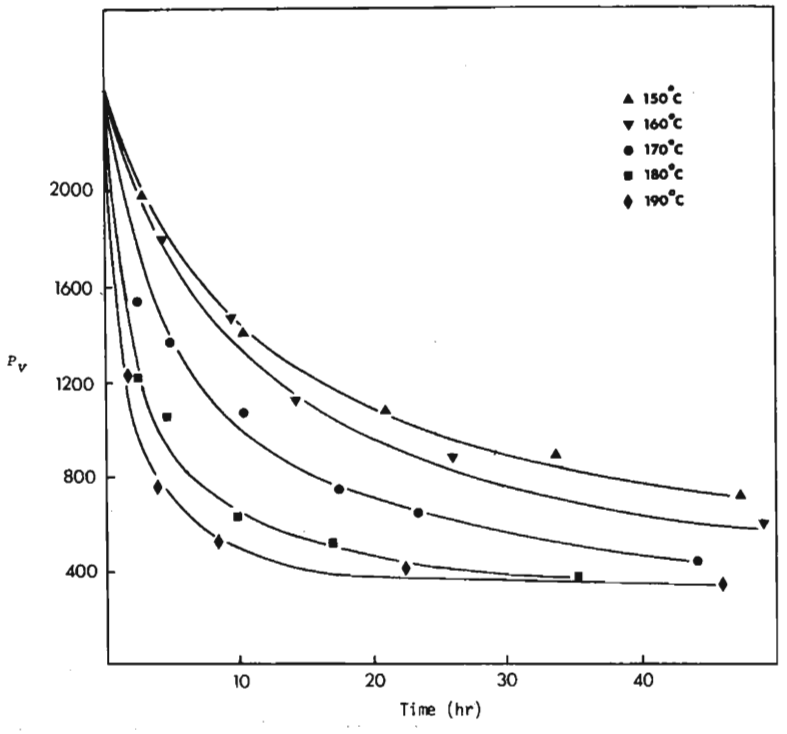

FIG. 6. Viscosity average degrees of polymerization (P_v) of cellulose heated in air at 150°C-190°C.

TABLE 2

Rate Constants for the Depolymerization of Cellulose in Air and Nitrogen

Temperature,°C	$k_0 \times 10^7$ in N_2 mole/162 g min[a]	$k_0 \times 10^7$ in Air mole/162 g min
150	1.1	6.0
160	2.8	8.1
170	4.4	15.0
180	9.8	29.8
190	17.0	48.9

[a] 162g represents 1 mole of monomer unit.

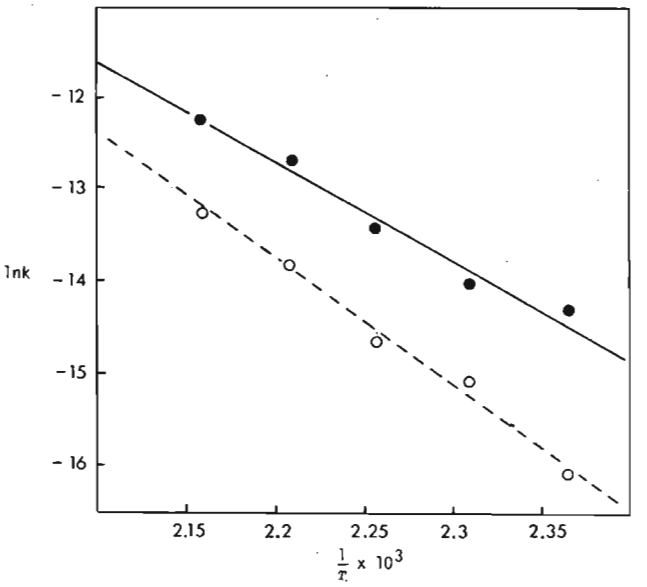

FIG. 7. Arrhenius plot for the rate of bond scission in air (—) and nitrogen (---).

TABLE 3

Initial Rates of Glycosidic Bond Scission and Carbon Monoxide and Carbon Dioxide Formation at 170 °C

Reaction	Rate × 10^5 in N_2, mole/162 g hr	Rate × 10^5 in Air, mole/162 g hr
Bond scission	2.7	9.0
CO evolution	0.6	2.1
CO_2 evolution	0.4	6.4

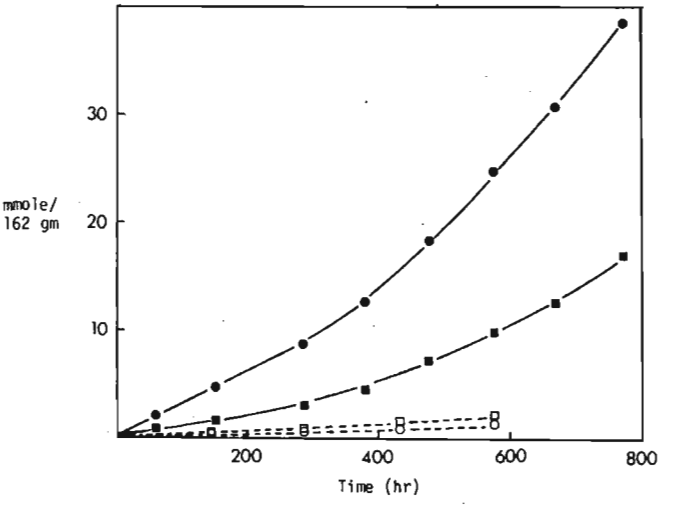

FIG. 8. Yields of CO and CO_2 from heating cellulose at 170°C:(o)CO_2 in N_2; (□)CO in N_2; (●)CO_2 in air; (■)CO in air.

shown in Figure 9 indicate an almost linear rate of formation on heating for 50 hr. On heating for longer periods, the rate of accumulation of carboxyl groups falls off, and the rate of accumulation of aldehyde groups is increased. The latter effect, however, could be due to the sodium chlorite method employed for the oxidation and measurement of the aldehyde groups. These data show the production of carboxylic and aldehyde groups on oxidation of cellulose in air. There was also a very small increase in the number of oxidized functions on heating in nitrogen. In order to check the extent of decarboxylation at the relatively lower pyrolysis temperatures, samples of low-DS (degree of substitution) carboxylcellulose with carboxylgroups at C1, C2 and C3 and C6 were prepared and pyrolyzed. The results shown in Figure 10 are, by and large, inconclusive, except for the sample oxidized at C2 and C3, which showed a definite reduction in carboxyl-group content. Thus, although both carboxyland carbonyl groups, as well as carbon dioxide and carbon monoxide, are formed during low-temperature pyrolysis, the production of the latter compounds could not be directly related to the formation of the former functions.

The thermal degradation of cellulose in air, similar to that of synthetic polymers, may involve a free-radical mechanism. We were not able to observe these radicals, but were able to monitor the formation of hydroperoxide groups on heating cellulose in air. The hydroperoxide functions are simultaneously formed and decomposed, and their concentration rapidly climbs until a steady state is reached. Figure 11 shows

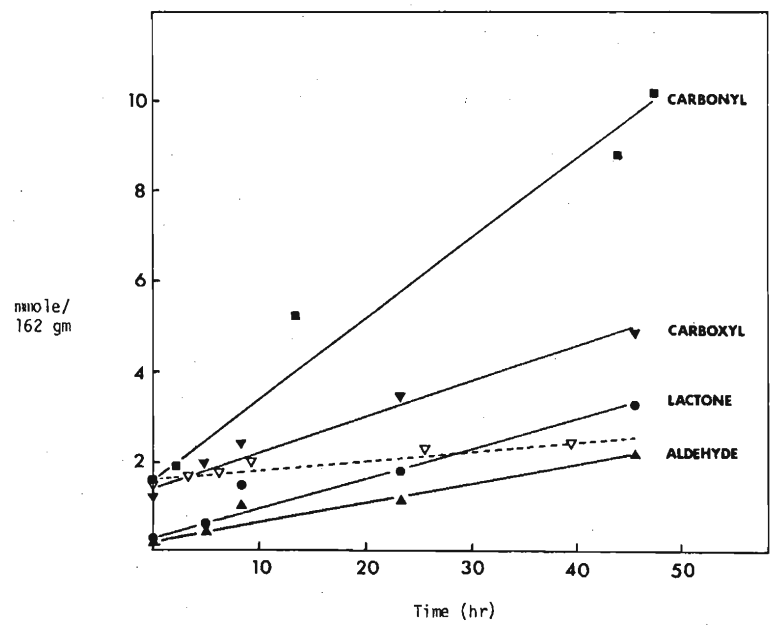

FIG. 9. Incorporation of oxidized groups in cellulose at 190°C---▽--- represents number of lactone and carboxyl groups formed in nitrogen at 190°C.

the development of the steady-state concentration in air at 170°C during a period of about 100 min. It also shows the rate of decay in nitrogen over a similar period. This decay of the hydroperoxide function appeared to follow first-order kinetics with a rate constant of 2.5×10^{-2} min^{-1} at 170°C. From the steady-state concentration of 3.0×10^{-5} mole/162g, the rate of hydroperoxide decomposition is thus 7.5×10^{-7} mole/162 g min. When compared with the initial rate of bond scission in air of 1.5×10^{-6} mole/162 g min at 170°C (Table 2), it is apparent that the hydroperoxide formation could make a significant contribution to bond scisson.

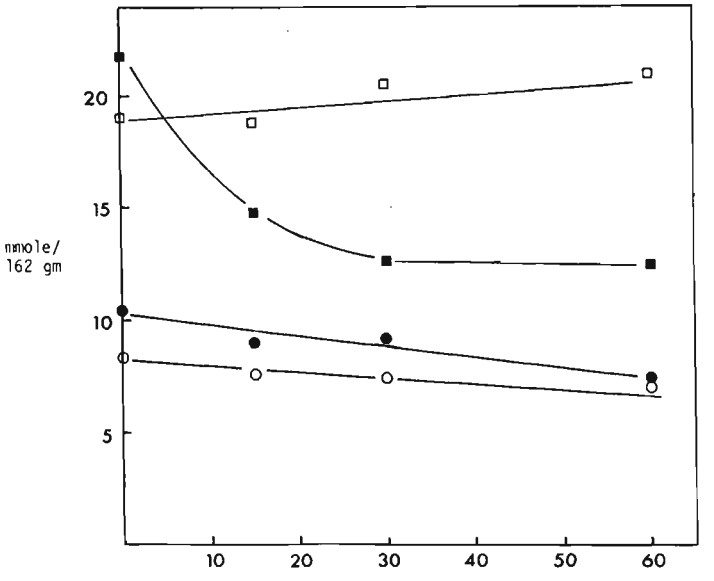

FIG. 10. Effect of heating on carboxyl content of carboxyl celluloses in nitrogen at 190°C. (o) 1-carboxyl cellulose; (■) 2,3-carboxyl cellulose; (□) 6-carboxyl cellulose; (●) prepared by heating cellulose in air at 190°C.

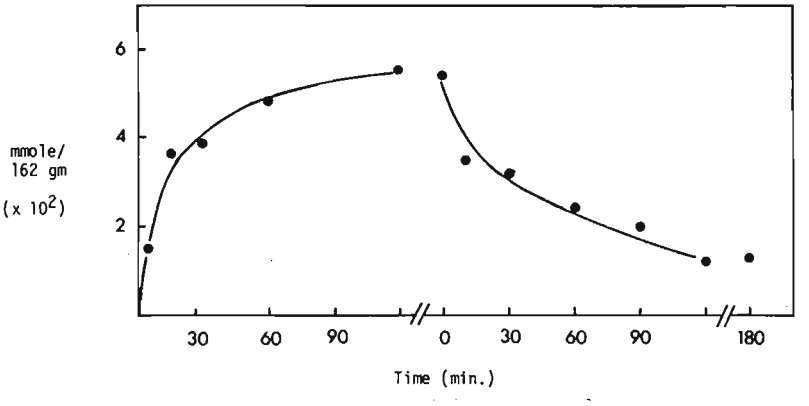

FIG. 11. Rate of formation and decay of hydroperoxide groups in cellulose at 170°C. Formation is in air and decay is in nitrogen.

Based on the above considerations and in analogy with studies on radiation of carbohydrates, it is proposed that three stages are involved in the low temperature pathway; initiation of pyrolysis, propogation and product formation. As shown in Figure 12, the initiation period apparently involves the formation of free radicals facilitated by the presence of oxygen or inorganic impurities. Subsequent reactions of the free radicals could lead to bond scission, oxidation and decomposition of the molecule, producing char, water, carbon monoxide and carbon dioxide. Figure 13 shows the nature of the initiation, propagation, and decomposition reactions involved in the thermal decomposition of cellulose by this pathway.

Initiation

$$\text{Initiator (I)} \xrightarrow{\text{Heat}} \text{I}\cdot$$

$$\text{Cell-H} + O_2 \rightarrow \text{Cell}\cdot + HO_2\cdot$$
$$\text{I}\cdot + O_2 \rightarrow IO_2\cdot$$
$$\text{Cell-H} + \text{I}\cdot \rightarrow \text{Cell}\cdot + \text{IH}$$
$$\text{Cell-H} + IO_2\cdot \rightarrow \text{Cell}\cdot + IO_2H$$

Propagation

$$\text{Cell}\cdot + O_2 \rightarrow \text{Cell}\,O_2\cdot$$
$$\text{Cell}\,O_2\cdot + \text{Cell-H} \rightarrow \text{Cell}\,O_2H + \text{Cell}\cdot$$

Formation of Products

$$\text{Cell}\,O_2H \rightarrow \text{Cell}\,O\cdot, \text{Cell}\,O_2\cdot$$
$$\text{Cell}\,O_2H \rightarrow \text{Products}$$
$$\text{Cell}\,O_2\cdot, \text{Cell}\,O\cdot \rightarrow \text{Products}$$

FIG. 12. The thermal autoxidation of cellulose in air.

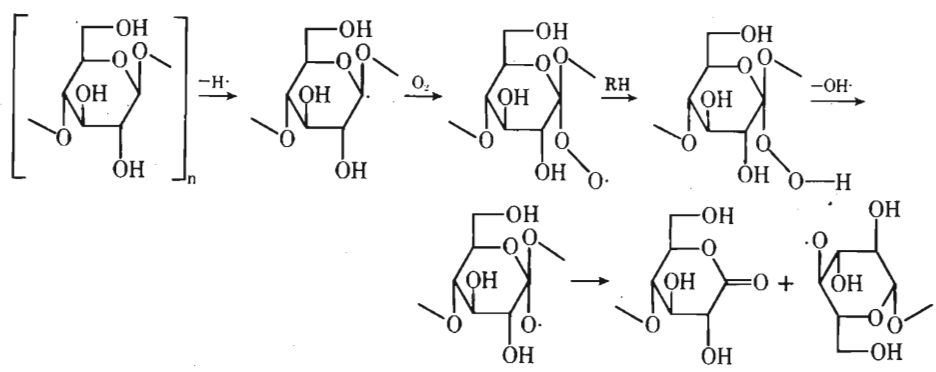

FIG. 13. Possible mechanism of formation and decomposition of cellulose hydroperoxide in air.

TRANSGLYCOSYLATION

At temperatures above 300°C, cellulose is decomposed by an alternative pathway which provides a tarry pyrolyzate containing levoglucosan (1,6-anhydro-β-D-glucopyranose), other anhydroglucose compounds, randomly linked oligosaccharides, and glucose decomposition products [6]. Figure 14 shows the g.l.c. analysis of the tarry pyrolyzate after trimethylsilylation of the free hybroxyl groups [6,7]. The mechanism for the formation of these compounds has been established by extensive investigation of the pyrolytic reactions of phenyl glucosides and other related model compounds. [5,8-10].

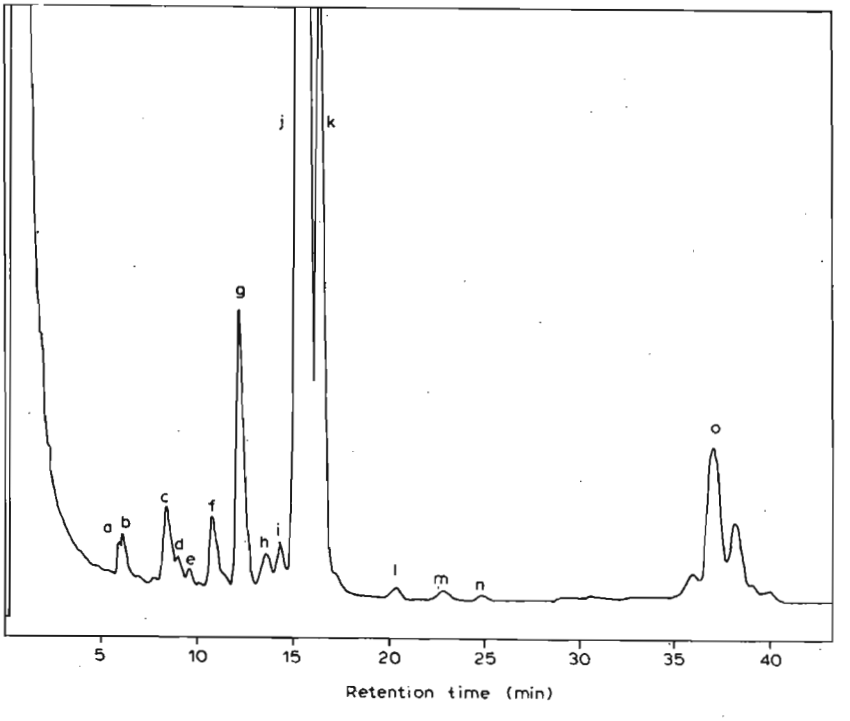

FIG. 14. G.l.c. of tar from pyrolysis of (trimethylsilyl)ated cellulose (column 2, 110 to 275° at 4°/min). [a, 5-(Hydroxymethyl)-2-furaldehyde; b, 1,4:3,6-dianhydro-α-D-glucopyranose; c, 2,3-dihydro-3,5-dihydroxy-6-methyl-4H-pyran-4-one; d, unknown; e, 3,5-dihydroxy-2-methyl-4H-pyran-4-one; f, unknown g, 1,5-anhydro-4-deoxy-D-glycero-hex-1-en-3-ulose; h and i, unknown; j, levoglucosan; k, 1,6-anhydro-β-D-glucofuranose; l, α-D-glucose; m, β-D-glucose; n, 3-deoxy-D-erythro-hexosulose; and o, O-D-glucosyl-levoglucosans.]

It has been shown that pyrolysis of a glycosidic compound as shown in Figure 15 starts with cleavage of the glycosidic group and condensation of the sugar moiety, which is decomposed on further heating. The sequence of these reactions as a function of temperature could be determined by thermogravimetry (TG) [5] and differential thermal analysis (DTA) as shown for phenyl β-D-glucopyranoside in Figure 16.

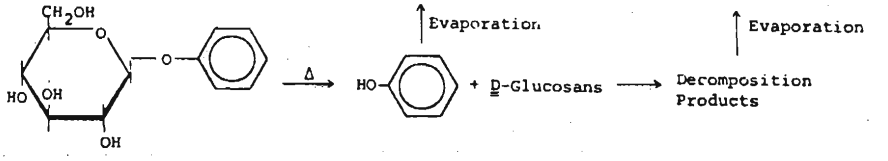

FIG. 15. Pyrolytic reactions of phenyl β-D-glucopyranoside.

The individual reactions which take place within each thermal event, characterized by changes in mass (TG) and/or energy (DTA), are then followed by various scanning or isothermal analytical methods. In Figure 15, cleavage of the phenolic group is established by quantitative recovery of the free phenol and condensation of the sugar unit is established by recovery and chemical analysis of intermediate pyrolysis products [8].

It has been shown that the reaction proceeds through a heterolytic mechanism because it is influenced by variation of the electron density producted through the introduction of various substituents on the aglycone [5,8]. This conclusion eliminated the possibility of a homolytic mechanism (free radical cleavage of the glycosidic bond), although further breakdown and charring of the sugar units involve free radical

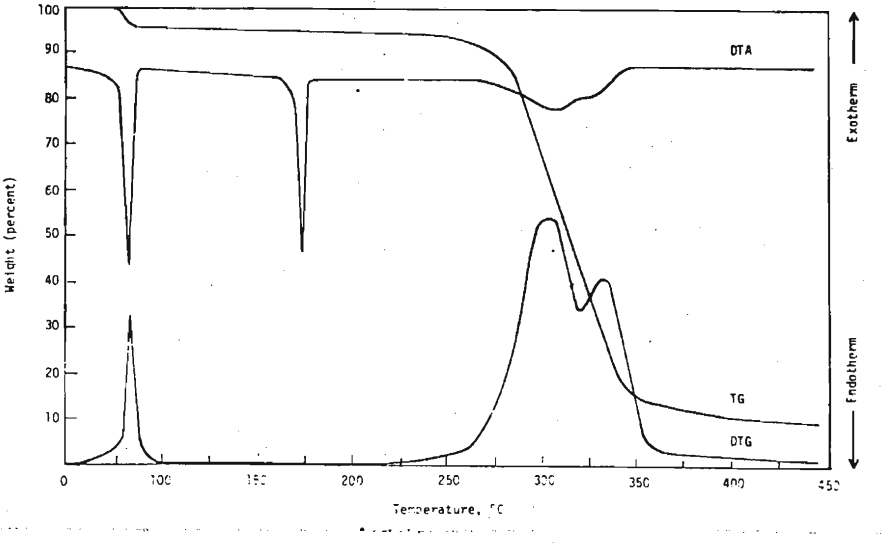

FIG. 16. Thermal analysis of phenyl β-D-glucopyranoside.

formation. It also indicated that the thermolysis, as a heterolytic process, must be sensitive to the effect of acidic and alkaline reagents.

Investigation of a variety of glycosides containing deoxy, amino and acetamido groups and the corresponding fully acetylated compounds [8,9] showed that the substituent on the sugar moiety, in addition to the inductive effect on the glycosidic bond, changes the availability and reactivity of the transglycosylation sites, and the acetylated compounds are considerably more stable than the parent compounds with free hydroxyl groups. These data and production of randomly linked condensation products [8,11] confirmed that the heterolytic cleavage of existing glycosidic bonds proceeds through a transglycosylation process involving nucleophilic displacement of the glycosidic groups by one of the free hydroxyl or amino groups of the sugar molecule. Thermolysis of levoglucosan (1,6-anhydro-β-D-glucopyranose) [6] reducing and non-reducing disaccharides [10] (cellobiose and trehalose), cellulose [6] and xylan [12] and the isolation and structural investigation of the products showed that the transglycosylation reactions give mixtures of anhydrosugars and randomly linked oligosaccharides.

There is a close similarity between the thermolysis of phenyl glucoside (Figures 15 and 16) and the thermolysis of cellulose (Figure 17) which starts at 300°C and proceeds rapidly until most of the substrate is evaporated. Also chromatographic analysis of the tarry pyrolyzate (Figure 14) shows the presence of similar products. These products, as shown in Figure 18, are formed by the intramolecular substitution of the glycosidic linkage in cellulose by one of the free hydroxyl groups (transglycoslylation). Subsequent inter- and intra- molecular transglycosylations provide several anhydrosugars and randomly linked oligosaccharides, which could dehydrate and decompose on further heating. The initial substitution requires changes in the conformation of the sugar units and increased flexibility of the molecule. This could be achieved at the elevated temperatures by reduction of molecular weight, breaking of hydrogen bonds and glass transition which are expected to activate the molecule.

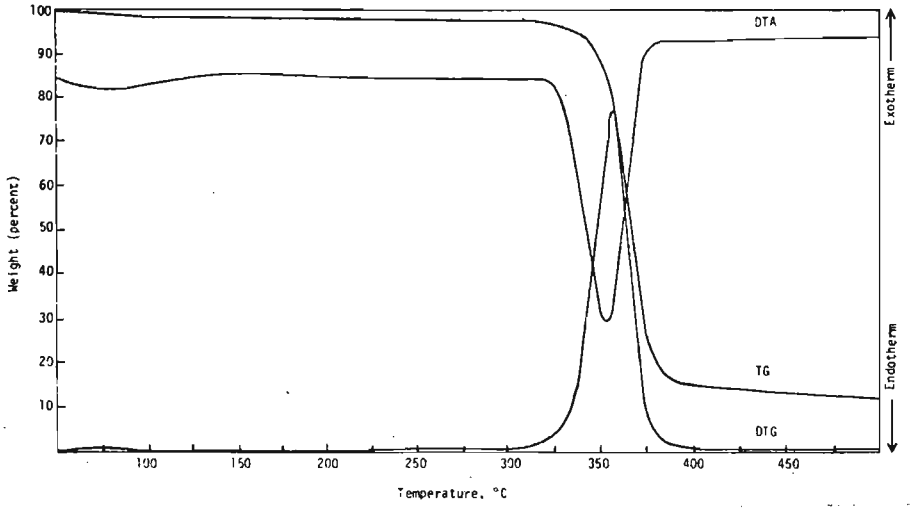

FIG. 17. Thermal analysis of untreated cellulose.

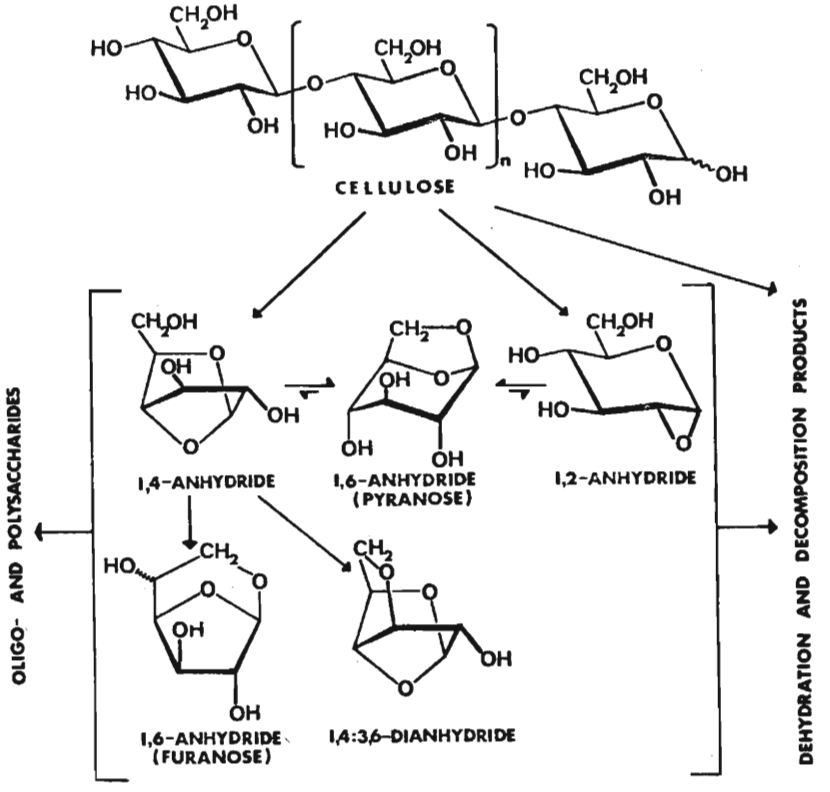

FIG. 18. Pyrolysis of cellulose to anhydrosugars and other compounds by transglycosylation reactions.

KINETICS OF CELLULOSE PYROLYSIS

Kinetic studies have shown that at higher temperatures the tar-forming reactions accelerate rapidly and overshadow the production of char and gases. The data in Table 4 shows the production of diminishing amounts of char and increasing amounts of tar, the anhydrosugars and other compounds (that could be hydrolyzed to reducing sugar) as the oven temperature is raised from 300° to 500°C [13]. At this time, it should be pointed out that evaporation of levoglucosan and the volatile pyrolysis products is highly endothermic (see Figure 17 and Ref. 13). Thus, the increased oven temperature could raise the rate of heat transfer but not necessarily the temperature of the ablating substrate. As shown in Figure 19 [14], the oven temperature is reached when the rapid evaporation and the accompanied change in entropy is over. In other words, at the higher temperatures the pyrolysis process is controlled by the rate of heat transfer rather than the kinetics of the chemical reaction. Material transport presents another major obstacle to the investigation of chemical kinetics, because if the products of primary reactions are not removed, they could undergo further decomposition reactions.

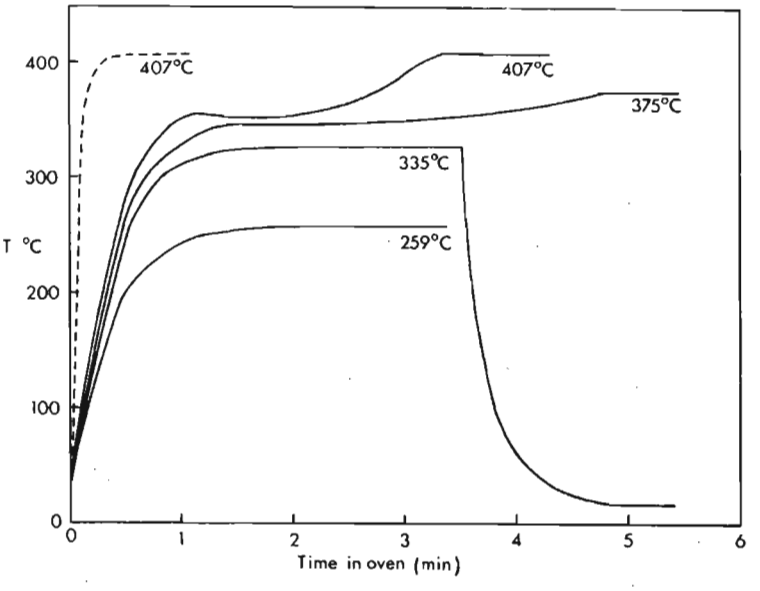

FIG. 19. Temperature of pyrolysis as measured by a thermocouple in cellulose sample. Final temperatures T_f are indicated. (---) temperature measured in empty boat. The cooling curve follows removal of a sample from the oven at 335°C.

Table 5 shows the difference between the yield of different pyrolysis products in vacuum, which removes the primary volatile products, and in nitrogen at atmospheric pressure which allows more decomposition of the anhydrosugars [6]. It also shows the effect of inorganic catalysts in changing the nature of the reactions and products. In view of these considerations, the chemical kinetics of cellulose pyrolysis has been investigated within the limited temperature range of 260-340° and under vacuum in order to obtain chemically meaningful data. Under these conditions, the chemical kinetics of cellulose pyrolysis could be represented by the three reaction model shown in Figure 20 [14]. In this model, it is assumed that the initiation reactions discussed before lead to the formation of an active cellulose, which subsequently

TABLE 4. Effect of temperature on the products from pyrolysis of cellulose powder under vacuum.

Oven Temp (°C)	Pyrolysis Time (min)	Percent Yield from Cellulose				
		Char	Tar	Levo-glucosan	1,6-Anhydro-β-D-gluco-furanose	Reducing Sugar
300	180	21	60	34	4	47
325	60	10	70	38	-	54
350	30	8	70	38	4	52
375	10	6	70	38	-	59
400	5	5	77	39	4	60
425	4	4	78	40	4	59
450	3	4	78	39	4	57
475	3	3	80	38	4	58
500	3	3	81	38	4	57

decomposes by two competitive first order reactions, one yielding anhydrosugars (transglycosylation products) and the other char and a gaseous fraction.

TABLE 5. Analysis of the pyrolysis products of cellulose at 300°C under nitrogen.

Condition	*Atm. pressure*	*1.5 Mm Hg*	*1.5 Mm Hg, 5% $SbCl_3$*
Char	34.2%[a]	17.8%[a]	25.8%[a]
Tar	19.1	55.8	32.5
levoglucosan	3.57	28.1	6.68
1,6-anhydro-β-D-glucofuranose	0.38	5.6	0.91
D-glucose	trace	trace	2.68
hydrolyzable materials	6.08	20.9	11.8

[a] The percentages are based on the original amount of cellulose.

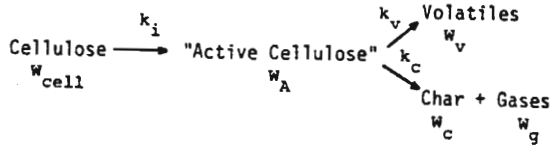

where

$$\frac{-d(W_{cell})}{dt} = k_i[W_{cell}]$$

$$\frac{d(W_A)}{dt} = k_i[W_{cell}] - (k_v + k_c)[W_A]$$

$$\frac{d(W_c)}{dt} = 0.35k_c[W_A]$$

For pyrolysis of pure cellulose under vacuum the rate constants k_i, k_v and k_c were found to correspond with $k_i = 1.7 \times 10^{21} e^{-(58,000/RT)}$ min^{-1} $k_v = 1.9 \times 10^{16} e^{-(47,300/RT)}$ min^{-1} and $k_c = 7.9 \times 10^{11} e^{-(36,000/RT)}$ min^{-1}

FIG. 20. Pyrolysis model for cellulose.

DEHYDRATION REACTIONS

As discussed before, detailed analysis of the pyrolysis tar (see Figures 14 and 18) shows the presence of levoglucosan, its furanose isomer (1,6-anhydro-β-D-glucofuranose) and their transglycosylation products as the main components. In addition to these compounds, the pyrolyzate contains minor amounts of a variety of products formed from dehydration of the glucose units. The dehydration products detected include 3-deoxy-D-erythro-hexos-ulose, 5-(hydroxymethyl)-2-furaldehyde, 2-furaldehyde (furfural), other furan derivatives, levoglucosenone (1,6-anhydro-3,4-dideoxy-β-D-glycero-hex-3-enopyranose, 1,5-anhydro-4-deoxy-D-glycero-hex-1-en-3-ulose and other pyran derivatives. The dehydration products are important as intermediate compounds in char formation.

The 3-deoxy-D-hexosulose, which is the initial dehydration product of hexoses plays a significant role as an intermediate in the production of furan derivatives. Isomers of this compound have been identified among the pyrolysis products of cellulose [6,7], D-glucose, D-fructose and D-xylose [5]. Moreover, the oligosaccharides formed from the pyrolytic transglycosylation of carbohydrate derivatives or the condensation of the reducing sugars often show u.v. and i.r. absorption bands that could be due to the presence of 3-deoxy-hexosulose units or its tautomeric forms [10].

In view of the above considerations, pyrolytic reactions of 3-deoxy-D-erythro-hexosulose (3-deoxy-glucosulose) were investigated with dynamic thermal analysis and parallel chemical methods in order to gain better understanding of the dehydration, rearrangement, decarboxylation and charring, which could ensue after the initial formation of this compound. The resulting data showed that 3-deoxy-D-erythro-hexosulose decomposes rapidly within the range of [15] 100-200°C as compared to D-glucose [16], levoglucosan and glycosides [8] which decompose at the much higher temperatures of 250-350°C. Within this range, a small fraction of the compound gives 5-(hydroxymethyl)-2-furaldehyde, pyruvaldehyde, glycolaldehyde, glyceraldehyde and glucometasaccharinic acid as monomeric products of dehydration, fission and rearrangement; while most of the compound undergoes condensation and chars.

As in aqueous reactions [14], the dehydration reactions are strongly catalyzed by presence of acidic reagents. G.l.c. analysis (see Figure 21) has shown that acid catalyzed pyrolysis of cellulose at ~350°C produces a pyrolyzate containing levoglucosenone (instead of levoglucosan) as the major component and 1,4:3,6-dianhydro-α-D-glucopyranose, 2-furaldehyde and 5-(hydroxymethyl)-2-furaldehyde as minor components [17]. Levoglucosenone, formed by dehydration reactions shown in Figure 22, could be separated by fractional distillation, and is a highly reactive compound that could be obtained by pyrolysis of waste paper, treated with mineral acids. It could be readily converted to a variety of vinyl, substituted and addition compounds. Some of these reactions are already investigated, but the industrial applications of this compound still remain to be explored.

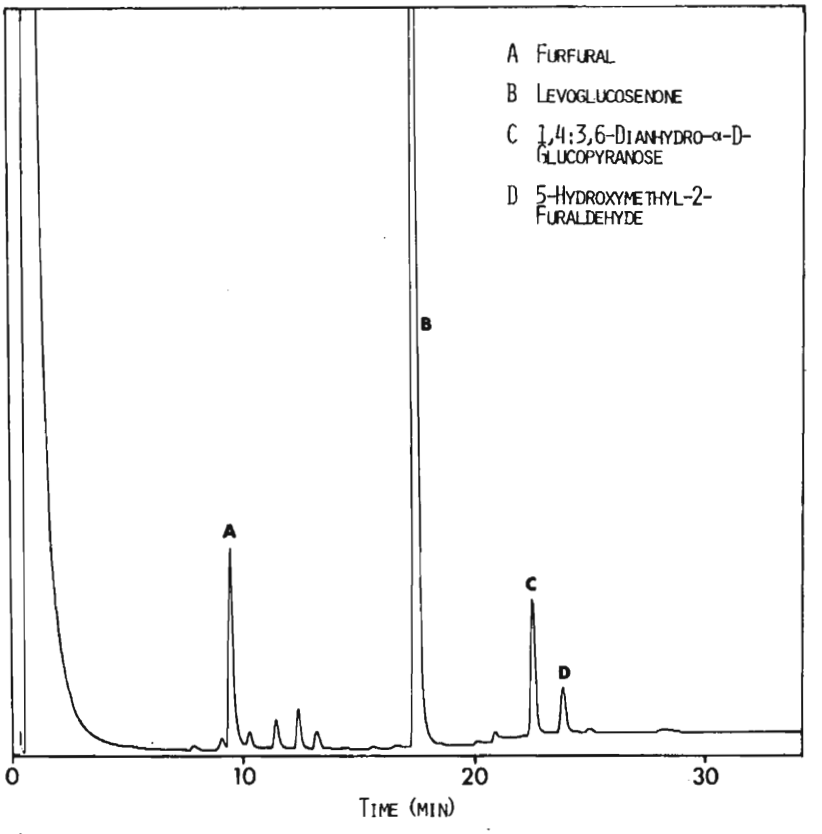

FIG. 21. G.l.c. analysis of the pyrolyzate from cellulose + 2% H_4PO_4 at 350°C.

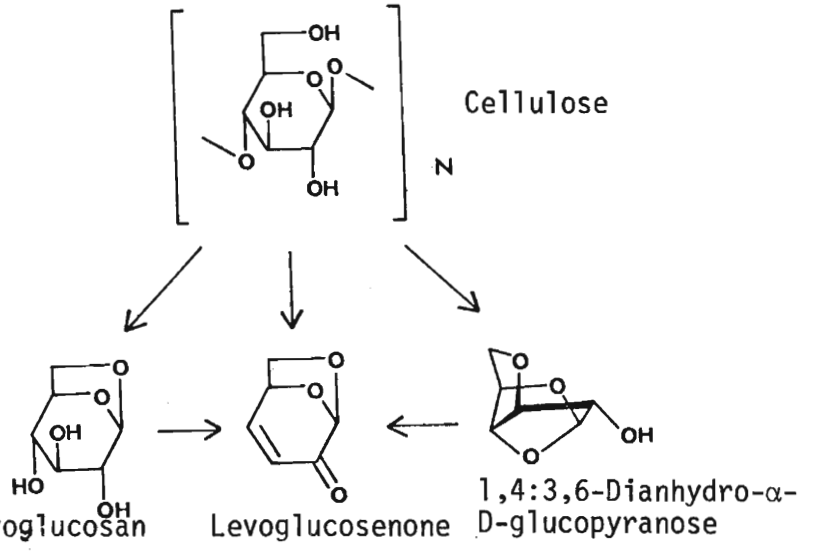

FIG. 22. Dehydration of cellulose and glucose derivatives to levoglucosenone.

FISSION AND DISPROPORTIONATION REACTIONS

On further heating, fission of the sugar units at higher temperatures accompanied by dehydration, disproportionation, decarboxylation and decarbonylation provides a variety of carbonyl, carboxyl and olefinic compounds as well as water, carbon dioxide, carbon monoxide and char [5,18,19]. The analyses of these products are closely similar to those obtained from pyrolysis of levoglucosan shown in Table 6 [20]. These compounds may be divided into three categories. The first category includes furan compounds, water and char, which are the expected products of the better understood acid catalyzed dehydration reactions of carbohydrates under aqueous acid conditions [4]. The second category includes glyoxal, acetaldehyde and other low molecular weight carboxyl compounds, which are similar to the alkaline catalyzed fission products of the sugar molecule formed through the reverse aldol condensation mechanism. The products formed through these pathways are further randomized by disproportionation, decarboxylation, and decarbonylation reactions to provide a third category which is characteristic for the pyrolytic reactions, especially at the elevated temperatures.

TABLE 6. Pyrolysis products of 1,6-Anhydro-β-D-Glucopyranose at 600°C.

Pyrolysis product	Yield		
	Neat	+$ZnCl_2$	+NaOH
Acetaldehyde	1.1	0.3	7.3
Furan	1.0	1.3	1.6
Acrolein	1.7	<0.1	2.6
Methanol	0.3	0.4	0.7
2,3-Butanedione	0.5	0.8	1.6
2-Butenal	0.7	0.2	2.2
1-Hydroxy-2-propanone	0.8	<0.1	1.1
Glyoxal	1.4	<0.1	4.9
Acetic acid	1.7	0.7	1.5
2-Furaldehyde	0.9	3.0	0.4
5-Methyl-2-furaldehyde	0.1	0.3	--
Carbon dioxide	2.9	6.8	5.7
Water	8.7	20.1	14.1
Char	3.9	29.0	16.0
Balance (tar)	74.3	36.8	40.3

In the absence of acidic or alkaline catalysts, both fission and dehydration products are formed. However, as expected, addition of these catalysts promote the formation of one type of product at the expense of the other.

The chemical reactions involved were further investigated by the synthesis of levoglucosan labeled at C1, C2, and C6 and tracing of the major pyrolysis products to theoriginal positions of the sugar molecule [19]. The resulting data shown in Table 7 indicate the major dehydration and fission pathways shown in Figures 23 and 24. These schemes are more complex and less specific than the single pathways generally postulated for normal reactions, because at high temperatures, the energy barrier becomes less significant and the thermal decomposition could proceed through different routes[4].

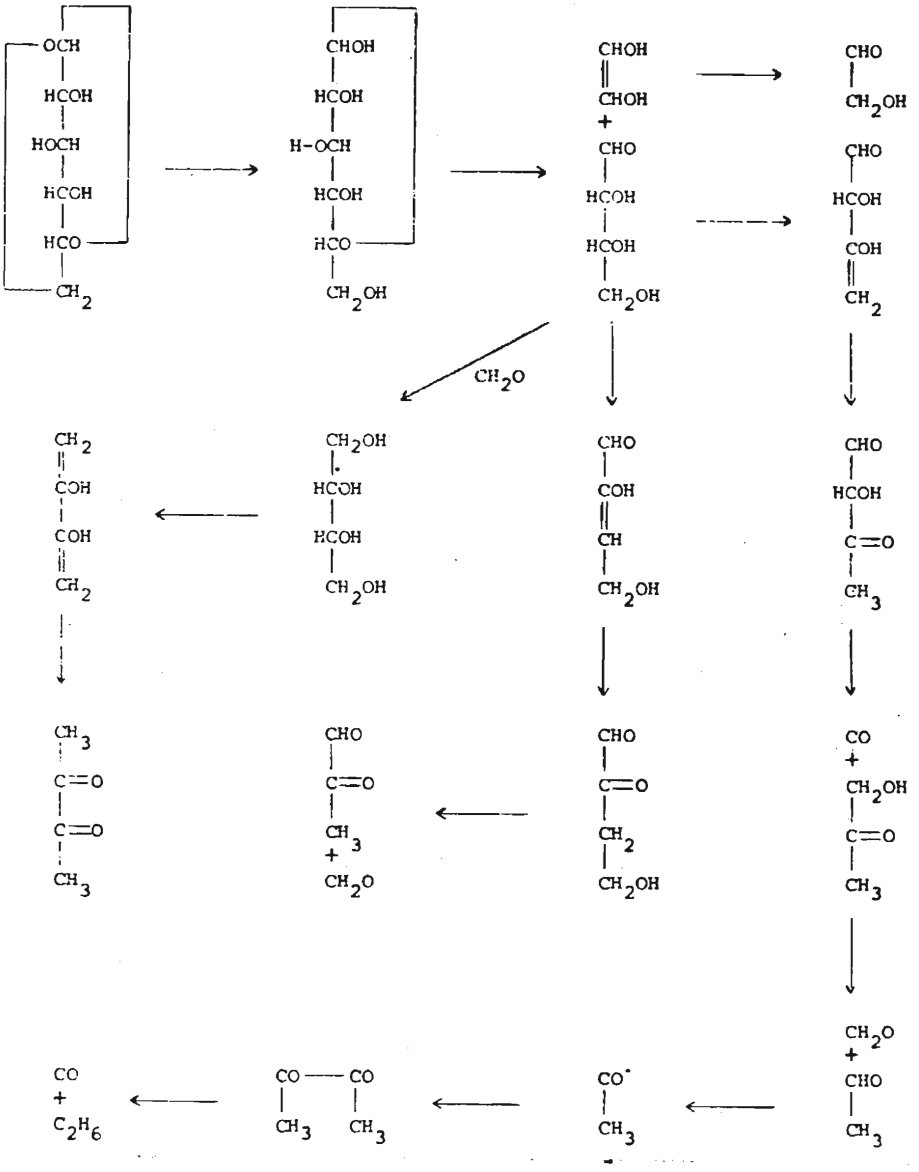

FIG. 23. Degradation of levoglucosan to volatile products.

TABLE 7. Percentage of the pyrolysis products traced to the labeled carbons of 1,6-anhydro-β-D-glucopyranose.

Compound	Neat			5% NaOH			5% $ZnCl_2$		
	1-^{14}C	2-^{14}C	6-^{14}C	1-^{14}C	2-^{14}C	6-^{14}C	1-^{14}C	2-^{14}C	6-^{14}C
2-Furaldehyde	60.8	103.4	35.8	30.2	100.7	73.0	86.0	95.8	16.6
2,3-butanedione	24.8	54.6	31.3	16.5	31.0	56.5	64.8	57.7	26.9
Pyruvaldehyde	27.3	26.3	19.1	23.3	42.0	30.7	49.7	46.7	29.6
Acetaldehyde	10.1	30.5	36.0	6.3	29.2	55.1	4.4	7.3	29.8
Glyoxal	15.4	19.2	6.9	25.5	48.3	36.0	29.5	28.2	28.2
Carbon dioxide	34.3	24.5	6.3	31.2	17.7	8.9	43.7	33.3	9.5
Carbon monoxide	21.1	18.9	16.8	38.4	18.0	13.7	36.7	27.6	11.4

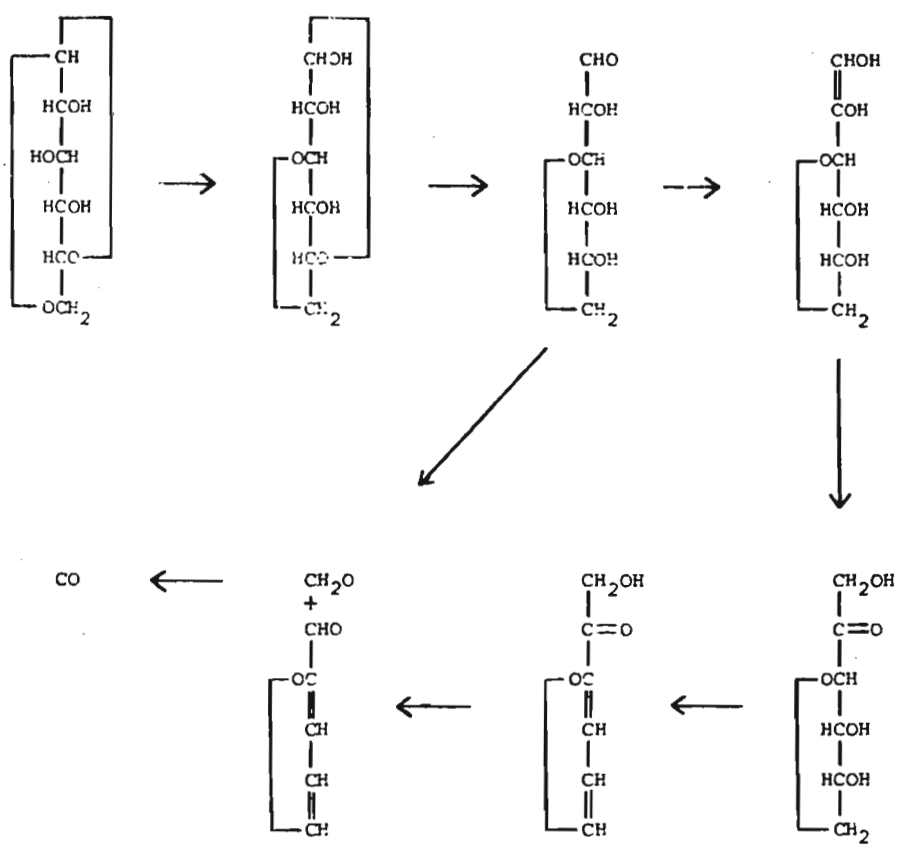

FIG. 24. Production of 2-furaldehyde under alkaline conditions.

CONCLUSIONS

The above data indicate that pyrolysis at lower temperatures (below 300°C) favors the production of char, water, CO_2, and CO; whereas heating at higher temperatures (300-500°C) favors the production of tar, containing anhydrosugars, oligosaccharides and some pyran and furan dehydration products. Flash pyrolysis at still high temperatures (above 500°C) results in the fission, dehydration, disproportionation, decarboxylation and decarbonylation reactions, which provide a mixture of low molecular weight, gaseous or volatile products. Indirect evidence shows that these materials are formed from the secondary reaction of the tar and high temperature interaction of char with water and carbon dioxide (see Figure 5). However, the possibility of direct conversion of cellulose molecules to the low molecular weight fission and disproportionation products could not be entirely eliminated.

ACKNOWLEDGMENT

The author is pleased to acknowledge the contributions of the post-doctoral fellows, research associates and graduent students who are named in the following list of references. He is also grateful to the National Science Foundation and the National Bureau of Standards for their support of this program.

REFERENCES

1. Shafizadeh, F. and McGinnis, G.D. "Morphology and Biogenesis of Cellulose and Plant Cell Walls" Advan. Carbohydr. Chem., 26, 297 (1971).

2. Shafizadeh, F. and McGinnis, G.D. "Chemical Composition and Thermal Analysis of Cottonwood," Carbohyd. Res., 16, 273 (1971).

3. Shafizadeh, F. and Bradbury, A.G.W. "Thermal Degradation of Cellulose in Air and Nitrogen at Low Temperatures," J. Appl. Polym. Sci., 23, 1431 (1979).

4. Shafizadeh, F. "Pyrolysis and Combustion of Cellulosic Materials," Advan. Carbohydr. Chem., 23, 419 (1968).

5. Shafizadeh, F. "Industrial Pyrolysis of Cellulosic Materials," Appl. Polym. Symp., 28, 153 (1975).

6. Shafizadeh, F. and Fu, Y.L. "Pyrolysis of Cellulose," Carbohyd. Res., 29, 113 (1973).

7. Shafizadeh, F., et al. "1,5-Anhydro-4-Deoxy-D-glycero-hex-1-En-3-Ulose and Other Pyrolysis Products of Cellulose," Carbohyd. Res., 67, 433 (1978).

8. Shafizadeh, F. Susott, R.A., and McGinnis, G.D., "Pyrolysis of Substituted Phenyl β-D-glucopyranosides and 2-Deoxy-α-D-arabino-hexopyranosides," Carbohyd. Res., 22, 63 (1972).

9. Shafizadeh, F., Meshriki, M.H., and Susott, R.A., "Thermolysis of Phenyl Glycosides," J. Org. Chem., 38, 1190 (1973).

10. Shafizadeh, F. and Lai, Y.Z., "Thermal Rearrangements of Cellobiose and Trehalose," Carbohyd. Res., 31, 57 (1973).

11. Lai, Y.Z. and Shafizadeh, F., "Thermolysis of Phenyl β-D-glucopyranoside Catalyzed by Zinc Chloride," Carbohyd. Res., 38, 177 (1974).

12. Shafizadeh, F., McGinnis, G.D. and Philpot, C.W., "Thermal Degradation of Xylan and Related Model Compounds," Carbohyd. Res., 25, 23 (1972).

13. Shafizadeh, F., et al., "Production of Levoglucosan and Glucose from Pyrolysis of Cellulosic Materials," J. Appl. Polym., Sci., 23, 3525 (1979).

14. Bradbury, A.G.W., Sakai, Y. and Shafizadeh, F., "A Kinetic Model for Pyrolysis of Cellulose," J. Appl. Polym., Sci., 23, 3271 (1979).

15. Shafizadeh, F. and Lai, Y.Z., "Thermal Degradation of 3-Deoxy-D-erythro-Hexosulose," Carbohyd. Res., 40, 263 (1975).

16. Shafizadeh, F. and Lai, Y.Z., "Base-catalyzed, Pyrolytic Rearrangement of Some Monosaccharides," Carbohyd. Res., 26, 83 (1973).

17. Shafizadeh, F., Furneaux, R.H., and Stevenson, T.T., "Some Reactions of Levoglucosenone," Carbohyd. Res., 71, 169 (1979).

18. Shafizadeh, F., Lai, Y.Z., and McIntyre, C.R., "Thermal Degradation of 6-Chlorocellulose and Cellulose-Zinc Chloride Mixture," J. Appl. Polym. Sci., 22, 1183 (1978).

19. Shafizadeh, F. and Lai, Y.Z., "Thermal Degradation of 1,6-Anhydro-β-D-glucopyranose, J. Org. Chem., 37, 278 (1972).

20. Shafizadeh, F., Philpot, and Ostojic, N., "Thermal Analysis of 1,6-Anhydro-β-D-glucopyranose," Carbohyd. Res., 16, 279 (1971).

DIRECT FORMATION OF PYROLYSIS OIL FROM BIOMASS

by

Herbert M. Kosstrin, Ph.D.
Stone & Webster Engineering Corporation

ABSTRACT

An extensive experimental program of the Fluidized Bed Pyrolysis of Biomass to Clean Energy was carried out by Energy Resources Co. This paper describes the analytical model developed to predict the yield of liquid fuels from biomass. It is found that secondary reactions play a large part in the determination of the final liquid product yeild.

BACKGROUND

The production of liquid fuels from biomass has been accomplished via various means on several pilot plant size reaction systems. Various amounts of pyrolysis oil have been produced by Occidental's Flash Pyrolysis Process [1]Georgia Tech's Fixed Bed Partial Oxidation,[2] Lawrence Berkley's Labs' Acid Hydrolysis[3], and ERCO's Fluidized Bed Pyrolysis Process[4]. The quality and quantity of pyrolysis oils produced by these several processes vary. In addition, reaction conditions within each process will change the output quality and quantity of the pyrolysis oils produced. This change in the quanity and quality of produced pyrolysis oils is due to the effect of secondary reactions. This paper will discuss the work on Fluidized Bed Pyrolysis of Biomass preformed by Energy Resources Co. Inc. (ERCO) of Cambridge, Massachusetts, under EPA contract 68-03-0240.

INTRODUCTION

The production of biomass liquids, as practiced in the ERCO bubbling fluidized bed reaction system, is a rapid pyrolysis. The solids entering the system are well mixed and can have a residence time on the order of several minutes; while the gases and vapors evolved are flowed through the bed in plug flow and have a stay time on the

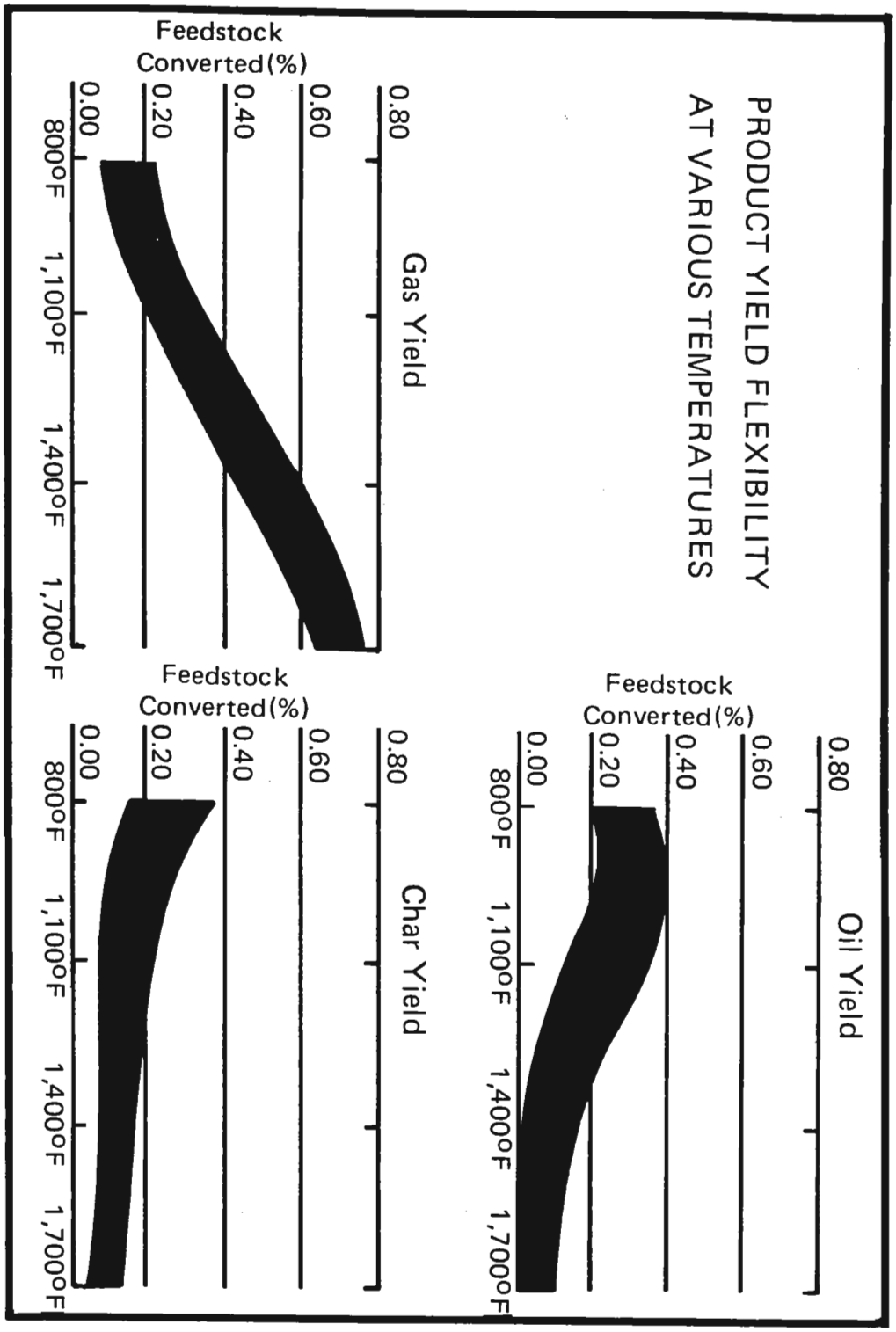

FIGURE 1 Pyrolysis Product Yields

order of seconds. A series of parametric studies were conducted in the ERCO 20 in. diameter fluidized bed pilot facility. The parameters studied were gaseous residence time, particle size, and reaction temperature. Figure 1 shows the data from the pyrolysis of sawdust. It is evident that the major parameter of interest is reaction temperature. Although variations of a factor of three (3) were obtained in gaseous residence time, and of an order of magnitude in particle size, these parameters did not influence the data to the extent of the reaction temperature.

With this experimental data, a reaction model has been developed that predicts the formation of pyrolysis oils from biomass.

MODELING

It is clear from the data obtained that the modeling of pyrolysis behavior in bubbling fluidized beds must account for secondary reactions, referring primarily to cracking and carbon deposition on particles and the associated conversion of part of the oils or tars to char and gases. This requirement arises because the oil yields observed for all of the materials studied decrease with increasing temperature, whereas the amount of oil actually produced as a primary product and observable in simplified experiments that are designed to minimize, or even eliminate secondary reactions, is known to increase monotonically with increasing temperature. In other words, the concept of oil destruction by secondary reactions is required to explain the decrease of oil yield with increasing temperature. Oil lost in this way is assumed to be converted to char and gas. These characteristics of the behavior are illustrated qualitatively in Figure 2 where the solid curves represent product yields from the fluidized bed pyrolyzer and the dashed curves represent yields obtained under simplified conditions of no secondary reactions. Thus, the differences between the two types of yields represent oil destruction by cracking and an associated and equal amount of char plus gas formation. The extent of the secondary reactions is seen to be significant only above some critical temperature, and to increase with increasing temperature until the attainment of the limits imposed by the depletion of the oil and the completion of the primary decomposition.

The general overall reaction mechanism from refuse to final products will follow the general scheme in Figure 3. The refuse is decomposed by a series of n primary reactions into primary products, each of which is acted upon by a series of secondary reactions as displayed in Figure 3. Char is assumed to be formed as the solid residue of the primary reactions and as solid material deposited in the course of secondary reactions.

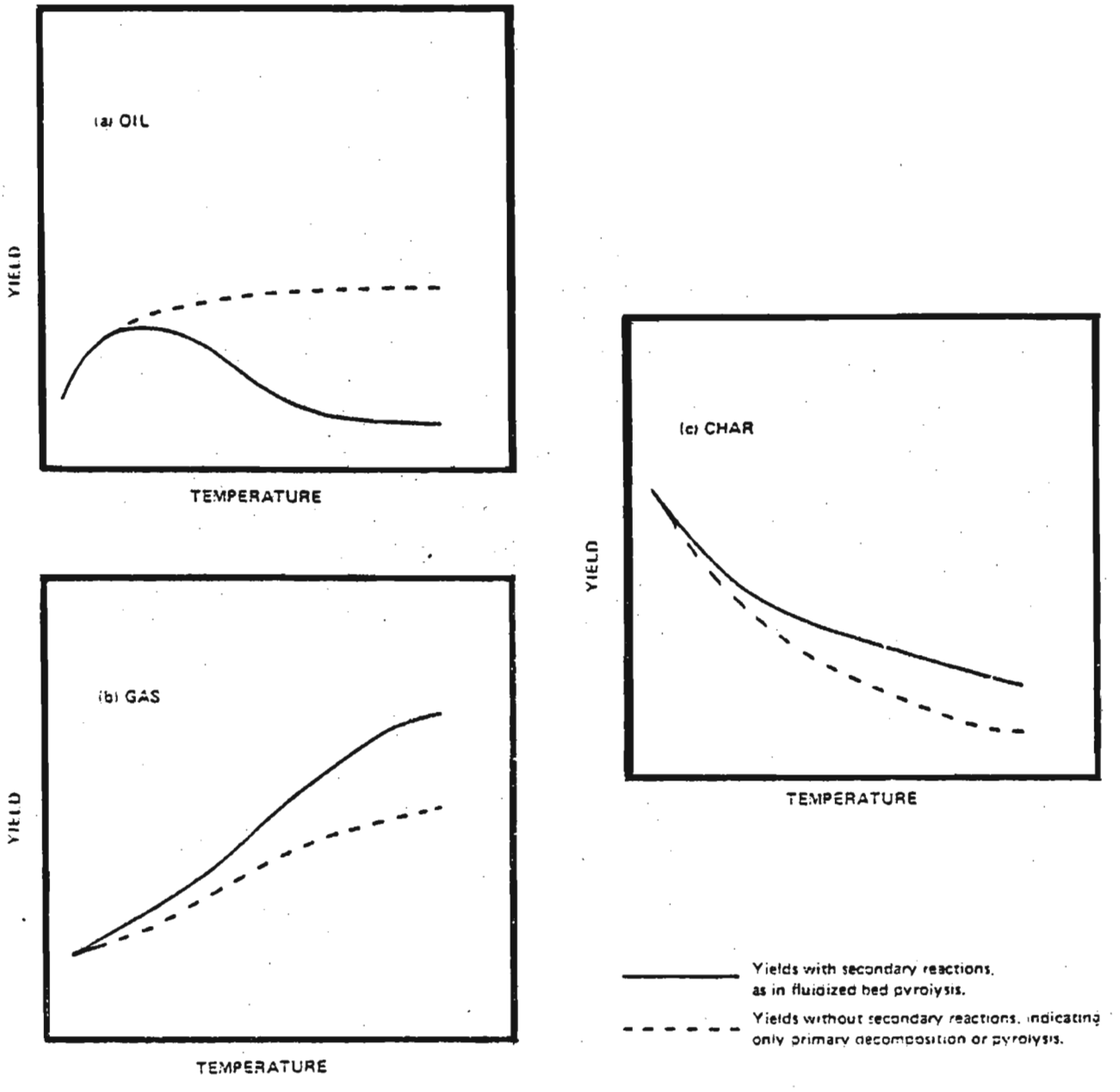

Figure 2 Schematic representation of effect of secondary reactions on pyrolysis yields at different temperatures.

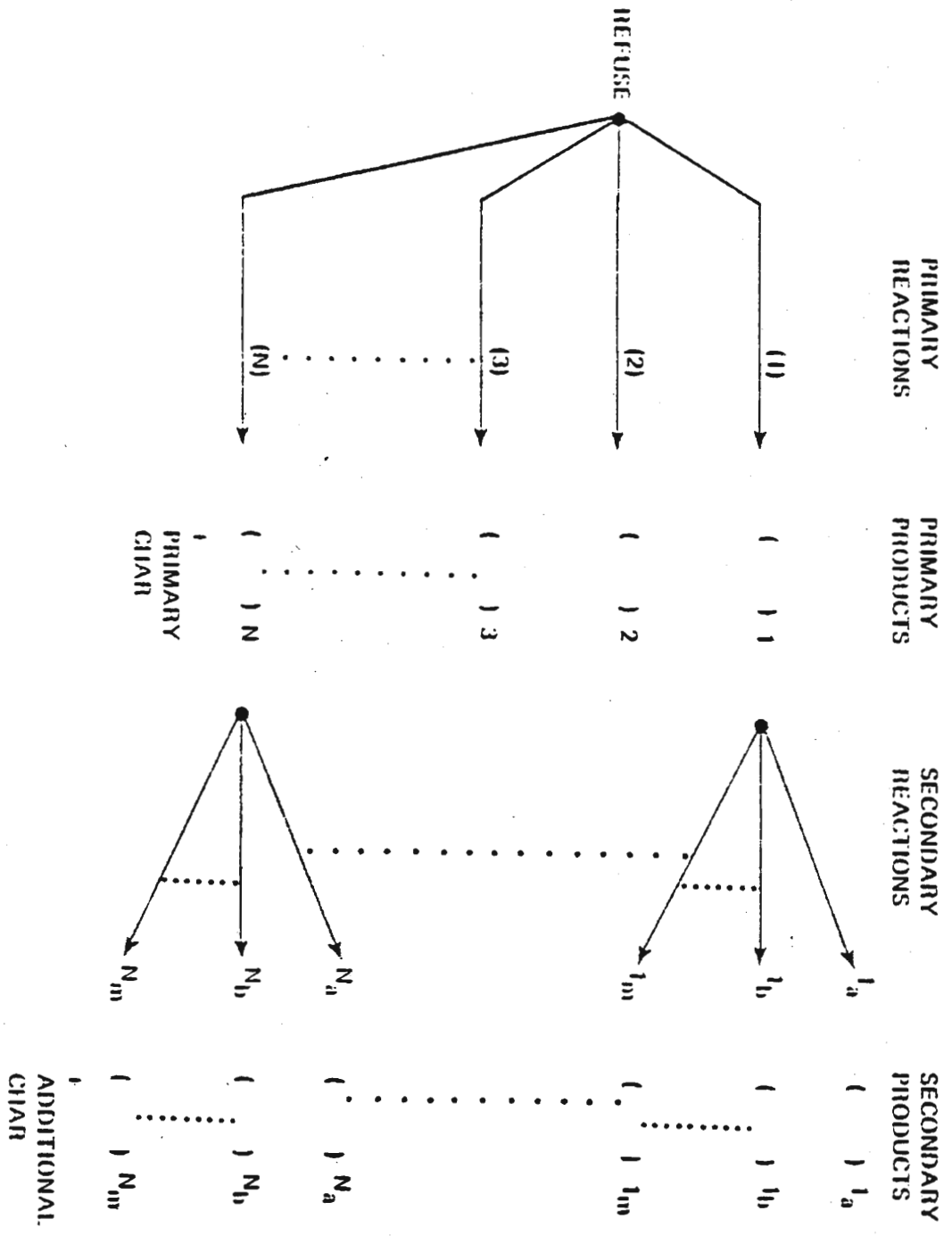

Figure 3 Overall Reaction Mechanism

Although the figure shows one volatile product for each primary or secondary reaction, the concept is sufficiently general to account for the possibilities that a given reaction may form multiple products or that a given product may be formed from more than one reaction.

This general reaction mechanism is needlessly complicated for a first approximation of what occurs in a waste pyrolysis system. To enable a reasonably simple determination of meaningful results we can condense the above model as follows:

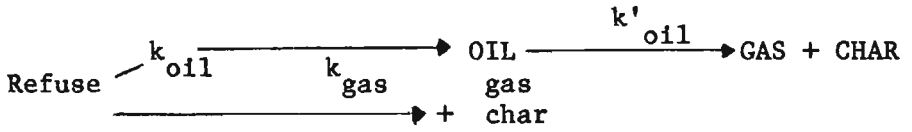

The primary volatile products are assumed to be only gas and oil, the formation of each of which is described by a global rate constant. Some of the oil is assumed to be converted to gas and char by a global secondary reaction having a rate constant k'. The terms oil and gas obviously include numerous compounds.

Given the foregoing picture, a model is developed below which describes oil yield from the fluidized bed pyrolyzer by considering both the primary pyrolysis and secondary reactions.

PRIMARY PYROLYSIS

As a first approximation, the particles are assumed to heat up instantaneously and to remain isothermal during the run. This assumption has been used in the analyses given here, but for cases where it is inadequate it can be replaced by calculation of the temperature distribution within the refuse elements as a function of time. Based on recent data on cellulose pyrolysis, pyrolysis of the various materials being studied in the ERCO program is assumed to be adequately represented as a single reaction first order in the mass of pyrolyzable material remaining, and having an Arrhenius type of temperature dependence. Thus:

$$dv_{oil}/dt = k_{oil} \left(V^{*}_{oil} - V_{oil}\right) \qquad (1)$$

and

$$k_{oil} = (k_o)_{oil} \exp\left(-E_{oil}/RT\right) \qquad (2)$$

where t is time, V_{oil} is the oil yield expressed as weight fraction of refuse fed, V^*_{oil} is the ultimate or asymptotic value approached by V_{oil} as time approaches a large value the exact size of which depends on temperature (i.e., $V_{oil} \rightarrow V^*_{oil}$ as kt becomes much larger than 1), k_{oil} is the first order rate constant for primary oil production, in the units of s^{-1}; (k_o) oil and E_{oil} are kinetic parameters commonly referred to as the pre-exponential factor (s^{-1}) and activation energy (kcal/mole), respectively, R is the gas constant (kcal/°K-mole) and T is absolute temperature (°K).

Solution of Equation (1) for a refuse element fed (and hence heated) at time t and then held at the experimental temperature until t = τ gives the following

$$V_{oil} = V^*_{oil} \left[1 - \exp\{-k_{oil} (\tau - t)\}\right] \qquad (3)$$

In the case of a pyrolyzer into which refuse is fed at a constant rate $\dot{m}$ (kg/hr) during the interval t=0 to t = τ, the value of τ - t for the different refuse elements range from τ for those fed at t=0 to 0 for those fed at t=τ. If the pyrolyzer is an isothermal and constant temperature fluidized bed, the cumulative oil yield at the end of the run of duration τ is

$$\text{Cumulative Oil Yield} = \int_0^T \dot{m} V^*_{oil} \left[1-\exp\{-k_{oil}(\tau-t)\}\right]dt \qquad (4)$$

Recognizing that the ultimate oil yield for the run would have been $mV^*_{oil}\tau$ and defining ϕ as the fractional completion of the oil formation process, i.e.,

$$\phi = \text{Cumulative Oil Yield}/m\dot{V}^*_{oil}\tau \ ,$$

solution of Equation 4 gives

$$\phi = 1 - \left[1 - \exp(-k_{oil}\tau)\right] /k_{oil}\tau \qquad (5)$$

Asymptotic forms of this equation are useful in the analysis of data.
When $k_{oil}\tau \ll 1$, $\phi \simeq k_{oil}\tau/2$. When $k_{oil}\tau \gg 1$, $\phi \simeq 1 - 1/k_{oil}\tau_t$.

SECONDARY REACTIONS

In accordance with the above discussion, some of the oil is assumed to be converted to char and gas according to the reaction

$$\text{Oil} \rightarrow \text{Char} + \text{Gas}$$

The rate of this reaction is assumed to be proportional to the concentration of oil vapor, and the fluidized bed is assumed to be well mixed with respect to solids and plug flow with respect to gas. The bed is isothermal and of constant temperature, and all entrained and carried-over char particles have properties characteristic of the bed temperature and residence time that would have been experienced if the particles had not been entrained. The average gas velocity prevails everywhere throughout the bed. Accordingly, the rate of oil evolution by pyrolysis is constant throughout the bed while the concentration of oil vapor increases from zero at the bottom of the bed to its largest value at the top. Figure 4 illustrates this approximate picture.

If a material (oil) balance is made around the fluidized-bed section, then the concentration of oil at any point x above the bed bottom (x = o) is given by: (In the remainder of the derivation of the model, the subscript oil is omitted for convenience.)

$$c = \frac{V^{*}_{oil} \cdot \dot{m} \ (1 - e^{-kt})}{m \cdot k' \cdot a} \left[1 - \exp\left\{-\frac{k' \cdot a}{v \cdot vol}\right\} \cdot x\right] \qquad (6)$$

when

V^{*}_{oil} = ultimate value of oil yield expressed as weight fraction of refuse fed (k_g oil/k_g refuse)

$\dot{m}$ = refuse feed rate (kg/hr)

k = first order rate constant for primary decomposition of refuse (s^{-1})

M = molecular weight of oils (kg/kg mole)

k' = rate constant for oil consuming secondary reaction (m/s)

v = gas velocity through bed (m/s)

x = distance from bottom of bed (m)

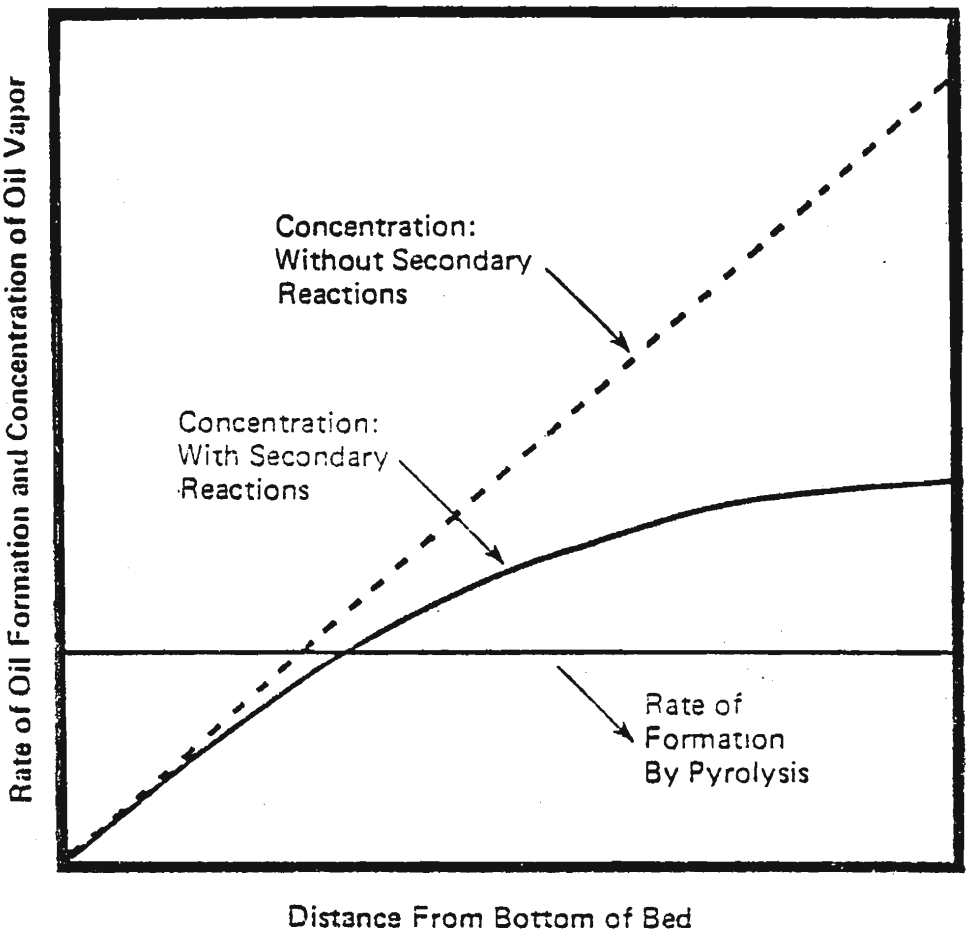

Figure 4 Assumed distribution of oil vapor in fluidized bed.

vol = volume of bed (m^3)

a = surface area of solids in bed (m^2)

Further, if we let θ be the cumulative oil yield up to time t (i.e., total oil yield carried from the bed during an experiment of duration t) expressed as a fraction of ultimate oil yield, then

$$\theta = \frac{\int_0^{\tau} C_{x=h} \cdot M \cdot v \cdot A \cdot dt}{\dot{m} \cdot V_{oil} \cdot t}$$

where A = cross-sectional area of bed, i.e., vol/h (m^2)
and h = bed height (m) during run.

Substituting for $c_{x=h}$ from Equation 6, integrating, and rearranging terms, we have

$$\theta = \frac{vA}{k' \cdot a}\left[1 - e^{\frac{-k'a}{aV}}\right]\left(1 - \frac{1}{kt}(1 - e^{-kt})\right)$$

or $\theta = \phi' \times \phi$ where

$\phi = 1 - \frac{1}{kt}(1 - e^{-kt})$ is the same as ϕ (Equation 5),

representing the oil yield in the absence of secondary reactions.

$\phi' = \frac{1 - e^{\frac{-k'a}{vA}}}{\frac{k'a}{vA}}$ is the fraction of oils consumed by secondary reactions.

When $\frac{k'a}{vA}$ and kt are both $<< 1$, as at low temperatures, $\phi \sim 1/2kt$ and $\theta \sim 1/2kt$. Therefore, parameters for k (k_o, E), the primary oil production rate constant, can be derived from the lower temperature data. At highter temperatures kt becomes large enough so that $\phi \simeq 1$ and $\theta \simeq \frac{1}{k'a/vA}$ and thus parameters for k', the secondary oil-consuming reaction rate constant, can be estimated from the higher temperature data.

For convenience of computations, the above equation may be rewritten as:

$$V_{oil} = V^*_{oil}(1 - \phi')(\phi) \qquad (7)$$

where

$$\phi = 1 - \frac{\left(1 - e^{-kt}\right)}{kt}$$

$$\phi' = 1 - \frac{\left(1 - e^{-k't'}\right)}{k't'}$$

$$k = k_o e^{-E/RT}$$

$$k' = k_o' e^{-E'/RT}$$

$$t' = a/vA$$

The time t in the correcation is a general parameter which indicates the duration of the experiment. In short experiments, the time of feeding and the time of sampling, in general, will not be the same. A complete derivation of the changes in Equation 7 may be found in Reference 4. With the inclusions of these minor changes, Equation 7 becomes

$$V_{oil} = V^*_{oil}\left[\frac{1-e^{-k'\ a/va}}{k'a/va}\right]\left[1-\left\{\frac{1-e^{-k\tau_s}}{k\tau_s}\right\}e^{-k(t_s - t_f)}\right] \qquad (8)$$

where the new parameters are

τ_s = sampling time

$(t_s - t_f)$ = time between the beginning of feeding and the beginning of sampling.

$(t_s - t_s)$ represents the contribution during sampling of all material fed prior to the begining of sampling.

EVALUATION OF PARAMETERS

The above model was used to analyze the pyrolysis data. Let us look at the parameters that must be determined. Restating Equation 8

$$V_{oil} = V^*_{oil}\left[\frac{1-e^{-k'a/va}}{k'a/va}\right]\left[1-\left\{\frac{1-e^{-k\tau_s}}{k\tau_s}\right\}e^{-k(t_s-t_f)}\right] \qquad (8)$$

where

V_{oil} ≡ Mass of oil leaving the bed during the sampling period, per unit mass of the refuse fed (lb/lb).

V^*_{oil} ≡ Value of V_{oil} for an infinitely long residence time of the solids in the bed with no secondary reactions.

t' ≡ a/vA, sec

$$\Phi' \equiv 1 - \frac{(1 - e^{-k't'})}{k't'}$$

$$\phi \equiv 1 - \frac{(1 - e^{-k\tau_s})}{k\tau_s} e^{-k(t_s - t_f)}$$

$$k \equiv k_o e^{-E/RT}$$

$$k' \equiv k_o' e^{-E'/RT}$$

The data from the individual pyrolysis experiments give us the parameters V_{oil}, τ_s, t', $t_s - t_f$, and T. R is the universal gas constant defined as R = 1.987 cal/°k-mole, with the temperature (T) in degrees Kelvin. V^*_{oil} must be between 0 and 1.

The remaining parameters must be fitted to the data. These are k_0', k_0, E', E V^*_{oil}. A complete computer fit of these five parameters was accomplished.

Figure 5 shows the "Computer Curve" that was generated by fitting the model of Equation 8 with the data that are available from our Sawdust experimental results. The values for the five fitted parameters for all materials are given in Table 1. For materials which did not have sufficient low temperature data, a point was added of zero production of pyrolytic oil at 100°C. This assumption of no pyrolytic oil production at 100°C is perfectly valid for the time period that we are considering.

A composite plot of curves for all Phase I materials that were curve fitted is shown in Figure 6. The curves for the different materials all have the same common shape, a steep increase in the pyrolytic oil production followed by a more gentle decrease in the yield of pyrolytic oil. The temperature at which the curves change slope varies between 200°C and 400°C. The shape of the curves confirms the approach that was taken in describing the reactions. There is a series of rapid primary reactions that form the pyrolytic oil from the feed. Then, after a certain temperature is attained, the secondary reactions become dominant and decompose the pyrolytic oil to a gas and a char product.

TABLE 1

PARAMETERS OF FITTED VARIABLES

	E KCAL/MOLE-°K	E' KCAL/MOLE-°K	k_o SEC-1	k_o' M/SEC	V^*_{OIL}
Sawdust (SAW)	43.8	17.4	10^{13}	3.8	.30
Paper (PAP)	43.8	15.7	8.9×10^{12}	5.0	.604
Paper + Sawdust (PAS)	43.3	17.1	9.9×10^{12}	4.8	.413
Corncobs (COB)	26.0	13.8	4.92×10^{10}	1.25	.256
Municipal Solid Waste (MWI)	29.7	14.5	3.4×10^{10}	2.88	.377
Waste Oil (WOL)	27.2	17.5	1.01×10^{9}	4.93	.692
Rice Straw	38.5	17.1	3.67×10^{11}	2.75	.336
Cotton Gin Waste	38.4	22.7	1.76×10^{12}	3.11	.299
Wheat Straw	43.0	16.1	4.58×10^{12}	3.64	.316
Industrial Sewage Sludge	43.5	20.0	1.98×10^{12}	3.46	.274
Pine Bark	39.8	16.6	4.98×10^{12}	3.42	.333

CONCLUSIONS

The model agrees very well with our data. This not only confirms the presence of secondary reactions, but also describes the rates at which these reactions take place.

The primary reactions at the lower temperatures dominate the overall reaction to such an extent that the peak in the curve occurs at almost the ultimate oil yield for that temperature. This again points to rapid primary reactions. After this rapid build-up in pyrolytic oil product, the primary oil yield would slowly increase with temperature asymptotically to a final value as predicted by a single reaction step. Near this maximum of the oil yield curve, the secondary reactions start to play an important role and dominate the overall reaction. This is evident in the decrease of the pyrolytic oil yield curve.

The differences in the peak pyrolytic oil production among the various materials is a result of the different ultimate oil yields that would be expected from the structure of the molecules at the temperature that the reaction occurs.

The pyrolytic oil curve, if plotted against a normalized V_{oil}/V^*_{oil}, would all peak at approximately the same value because of the rapid primary reactions. The shape of the curves is in very good agreement with the model and the work on primary cellulose pyrolysis conducted with the MIT strip heater.[5] The data from MIT shows an activation energy of 33.4 Kcal/mole^{-0}K with a pre-exponential factor of 6.79×10^9 sec^{-1} for cellulose.

The data from a wide variety of cellulosic-based materials gives activation energies of between 27.2 and 43.8 Kcal/mole^{-0}K with pre-exponential factors in the order of 10^9 to $\tau\, 10^{13}$ sec^{-1}. Considering that our materials are not the pure α-cellulose that MIT used, the agreement is excellent.

The curve labeled PAS is a mixture of paper and sawdust. The pyrolytic oil yield falls between the two curves for individual paper and sawdust. This is as should be expected since it is a combination of the two materials. But more important, this indicates that the exact shape of the curves and the ultimate oil yield will be closely related to the amount of α-cellulose that occurs in the mixture for all of the cellulosic-based materials.

The parameters for pre-exponential factor (k'_o) and activation energy (E') for the secondary reactions are very similar among the various materials indicating that the secondary reaction mechanism can, indeed, be approximated by the single reaction step. The model shows agreement with the data.

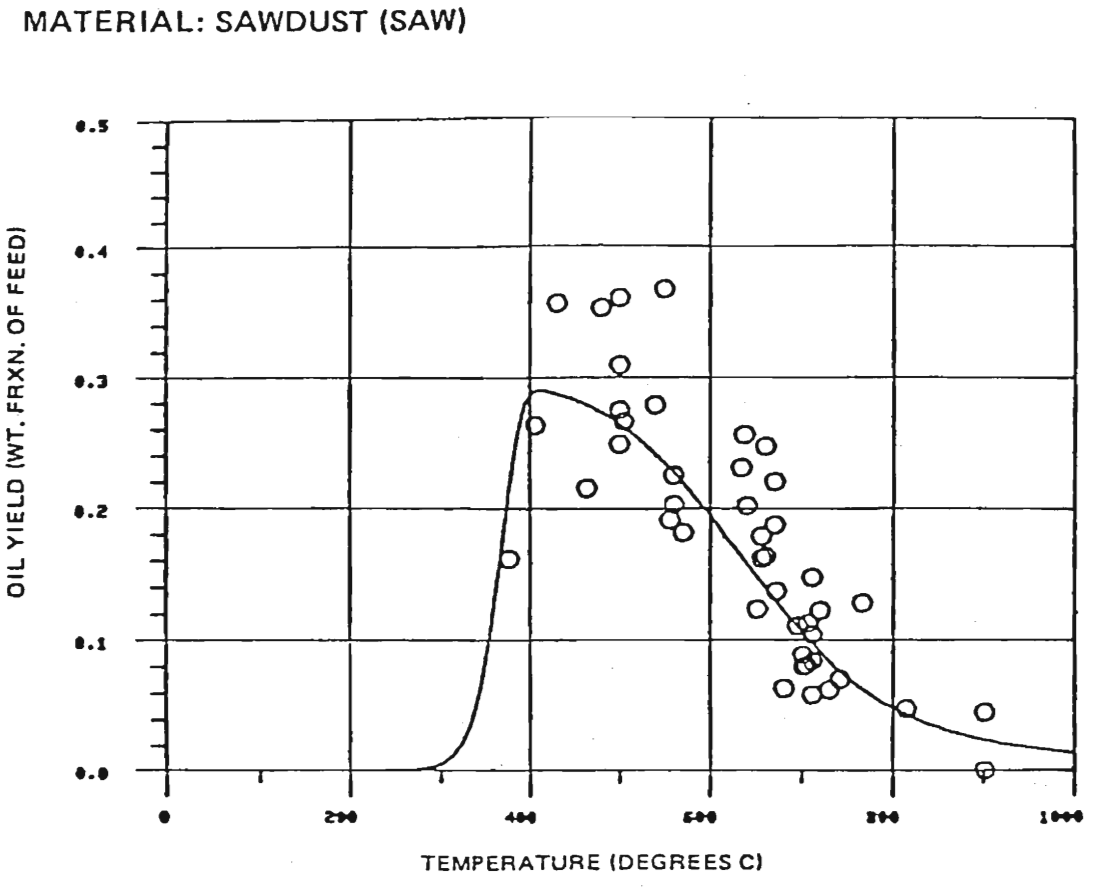

Figure 5 Model curve for pyrolysis oil yield data of sawdust.

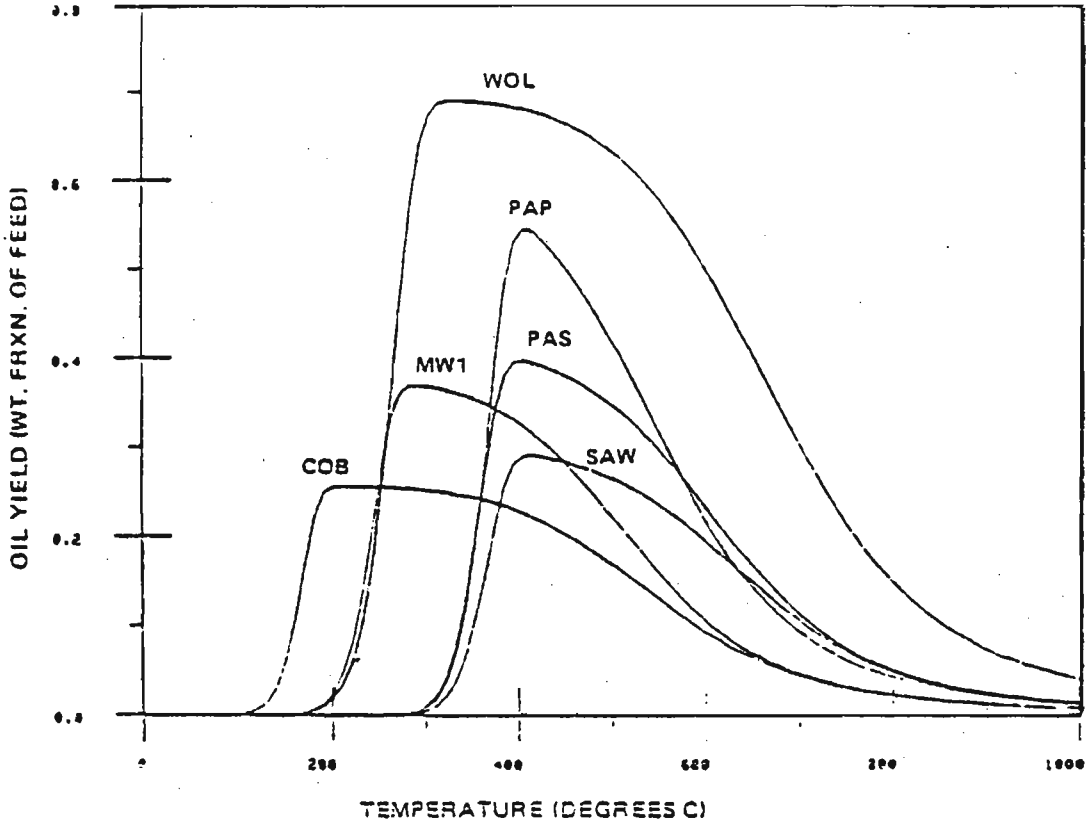

Figure 6 Model curve for pyrolysis oil yield data for various feed materials.

REFERENCES

1. Cheremisinoff & Morregi (Ed.), Energy From Solid Wastes, Ch. 9, Clean Liquid & Gaseous Fuels From Organic Wastes, Marcel Deicker, 1976.

2. Tatom et al - "Utilization of Agricultural, Forestry, and Animal Wastes for the Production of Clean Fuels," EPA Draft Final Report contract 68-02-1485, April 1975.

3. Ergun & Figueroa, "Direct Liquefaction of Biomass, Correlative Assessment of Process Development," presented at the 3rd Annual Biomass Energy Systems Conference, June 5-7, 1979.

4. Kosstrin et al - "Pilot Scale Pyrolytic Conversion of Mixed Wastes to Fuel," EPA Draft Final Report, March 1980. Contract 68-03-2340.

5. Lewellen, Peters & Howard - "Cellulose Pyrolysis Kinetics and Char Formation Mechanism," Sixteenth Symposium (Int.) on Combustion, Pittsburgh Pennsylvania, 1976.

THE CONVERSION OF BIOMASS DERIVED PYROLYTIC VAPORS TO HYDROCARBONS

Theodore C. Frankiewicz
Occidental Research Corporation
2100 S.E. Main
Irvine, CA 92714

ABSTRACT

A new process concept, termed pyrolysis/catalysis is introduced for the conversion of biomass to organic liquids of commercial value. The effective catalyst is a high SiO_2/Al_2O_3 ratio zeolite in its acid form which is supported on a low surface area, non-acidic solid. Using tetrahydrofurfural alcohol (Thfa) as a compound modeling biomass pyrolysis vapors, oxygen free - organic liquid yields of up to 70% were demonstrated for this catalytic conversion. An integrated pyrolysis/ catalysis process using α- methylglucoside in water as a feed resulted in 30% of the feed carbon being converted to organic liquids of interest.

INTRODUCTION

The research reported in this paper originated in Occidental Research Corporation's Resource Recovery program whose objective was the extraction of energy and materials from municipal solid waste (MSW). MSW organics are more representative of biomass in general than one might initially expect. Various studies on the composition of trash indicate that 90-95% of the organics are derived from paper, biomass waste, and processed cellulosics.[1],[2] Rubber plus plastics comprise less than 10% of the organics by weight and are frequently present at a less than 5% level. Because the carbohydrate content is so high, MSW organics can be assumed chemically to be cellulose in the presence of known levels of impurities. Work conducted with pure cellulose and with MSW in ORC laboratory and bench-scale pyrolysis reactors suggests this assumption is viable at least for the study of thermal reactions.

The chemical structure of cellulose, shown in Figure 1, is one of repeating glucose monomeric units joined by a relatively rigid β - glucoside linkage. Upon heating, the glucoside linkages may sever and the fragments formed would be capable of rearranging into organic

acids (R-C(=O)-OH), acetals (R-O-C(H)(R)-O-R), keto-alcohols (R-C(OH)-C(=O)-R), and polyhydric alcohols (R-[C(OH)]N-R) of varying molecular weights. Faster heating rates and higher temperatures tend to increase the yield of gaseous products and decrease tar and char formation.[3] It is interesting to note that relatively few oxygen-free products have been detected in cellulose pyrolysis experiments. Thermochemical calculations using the techniques of Benson [4] indicate why this is case. The results, see Figure 1(b), show that the carbon-carbon bonds in cellulose are weak compared to -C-OH and -O-H bonds. Thus, a set of strictly thermal reactions are not likely to lead to the formation of oxygen free hydrocarbons in high yields. Furthermore, the oxygenated fragment molecules formed upon pyrolysis also contain -C-O- bonds of equal or greater stability than -C-C-. This suggests that thermal conversion of these fragments to oxygen free hydrocarbons is similarly unlikely.

A major objective of the pyrolysis/catalysis process concept is to convert the highly oxygenated molecular fragments from the initial pyrolysis into oxygen-free hydrocarbons by catalytically rather than thermally breaking and rearranging -C-C- and -C-O- bonds. This is shown schematically in Figure 2.

Table 1 lists by functional characteristics, the kind of molecules that have been identified as cellulose pyrolysis products under a variety of conditions.[5] Generally any given species is produced in low yields which vary with the pyrolysis conditions used.

A characteristic common to most, if not all, organic oxygen functionalities of the molecular classes listed in Table I is their susceptibility to nucleophilic attack. As such, some form of acid catalyzed decomposition or transformation is possible for this broad spectrum of functional groups. Crystalline aluminosilicate minerals, i.e., zeolites, are well-known for their surface acidity and their ability to induce chemistry characteristic of acid catalysis. As will be shown, zeolites are good candidates for a catalyst which is capable of inducing a series of inter/intramolecular rearrangements, additions, scissions, etc. These can ultimately result in the desired deoxygenation of the oxygenated molecular fragments present in pyrovapor originating from MSW or biomass.

The feed material contemplated for use in this process was MSW organics which had been cleaned of most metals and glass through conventional shredding and air classification technology. Typically this material contains 20-30% moisture and possesses an MAF

TABLE 1. Cellulose Pyrolysis products which have been identified by various investigators are listed by functional characteristics [5].

Types of Molecule	Number Identified
Poly-functional oxygenates	15
Furan & Furan derivatives	12
Simple acids & esters	10
Simple carbonyls - Ketones	6
Aldehydes	7
Olefinic Carbonyls	4
Hydrocarbons	3
Carbohydrate Polymers	?

FIGURE 1

CELLULOSE STRUCTURE AND BOND STRENGTHS

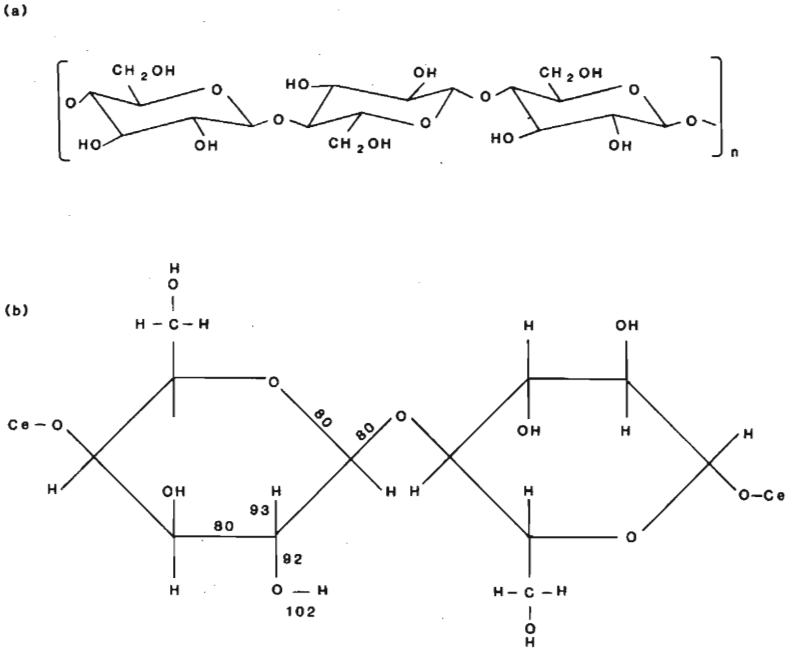

stoichiometry of $C_6H_{10}O_4$.[6] After drying and comminution to millimeter sized particles, the MSW organics are fed to a pyrolysis reactor at 500-550°C for periods of 0.5 to 5 seconds. At these temperatures, the products obtained are water (15%), char (30%), noncondensible gases (10%), and oxygenated hydrocarbons (45%). The latter were found to have the stoichiometry $C_5H_8O_2$[6]. Char yields are high due to the use of a solid heat carrier which provides considerable surface for char forming reactions. In an absolute sense, these yields may not be comparable to those where indirect heating is used.

As shown in Figure 2, the non-condensible gas and vaporous hydrocarbons are then to be passed over the appropriate zeolite catalyst for the production of substantial yields of high grade fuels and chemicals.

The purpose of this research was to identify the characteristics required for the catalyst to be used in pyrovapor conversion and to demonstrate the process concept.

A priori, the search for an appropriate catalyst was limited to high SiO_2/Al_2O_3 ratio zeolites for several reasons. First, the surfaces are strongly acidic and capable of inducing the kind of chemistry required for pyrovapor conversion.[7] Second, these highly acidic surfaces are not very susceptible to poisoning by organic bases since the latter tend to decompose on strong acid surfaces above 350°C.[8] Third, this class of zeolites is stable to steam and inorganic acids at temperatures up to 900°C. Finally, at SiO_2/Al_2O_3 ratios of 15 or above, zeolite surfaces change from hydrophilic to hydrophobic.[9] That is the ΔH of adsorption becomes higher for hydrocarbons than for water. Such a change is significant for the conversion of oxygenated molecules to hydrocarbons since at this point:

- water adsorption will not be limiting hydrocarbon reactions
- surface mobility of unreacted heteromolecules will be enhanced, and
- hydrocarbon intermediates will be retained on the catalyst surface where desired hydrocarbon formation reactions may occur.

The activity of de-aluminized mordenite, for example, has been studied by several laboratories and rather striking changes in reaction character are observed as the SiO_2/Al_2O_3 ratio increased.[9,10] Of particular interest is that mordenite with $R = SiO_2/Al_2O_3 < 15$ is capable of dehydrating alcohols but not effective at aggregatively condensing them to higher carbon number products. If $R > 15$, hydrocarbon formation reactions are observed and the overall reaction becomes decidedly exothermic.

FIGURE 2
PYROLYSIS - CATALYSIS IS AN APPROACH FOR GENERATING HYDROCARBONS

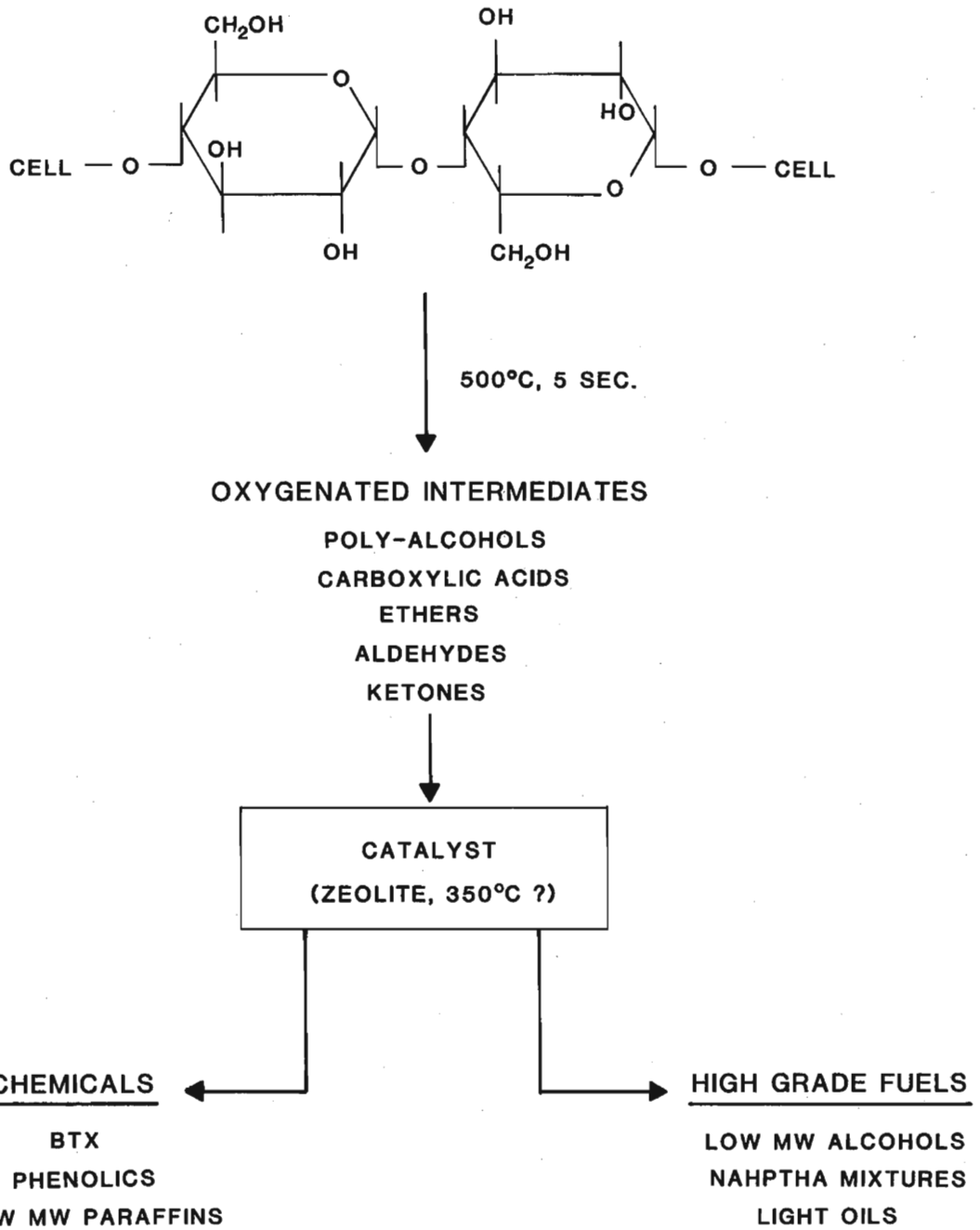

EXPERIMENTAL

Two sets of apparatus were used in this work. The first, shown in Figure 3 is a pulsed micro reactor connected through a heated transfer line to a microprocessor controlled gas chromatograph. Carrier gas for the g.c. was routed through the micro reactor. The latter was a 0.25" O.D. stainless tube which contained 0.1 to 1.0 cc of catalyst. Just upstream of the reactor was a heated chamber where either liquids or solids could be injected and vaporized or pyrolyzed at the desired temperature. Products flowed directly to the g.c. where they were analyzed with a two column program summarized in Table 2. The second apparatus consisted of a larger tubular reactor containing up to 10g. of catalyst which did not require a carrier gas and could be fed continuously. Products from the continuous reactor were then collected (gaseous) or trapped (liquid) and analyzed off-line according to the program of Table 2.

Although the purpose of the work under discussion is to develop pyrovapor conversion chemistry, the actual use of pyrovapor in this early work was neither practical nor desirable. Not practical because in-situ pyrovapor generation on this small scale complicates the experimental procedure and requires careful between run apparatus cleaning to prevent plugged lines and skewed analyses. The complicated nature of pyrovapor would make the extraction of chemical reaction information from the experiments considerably more difficult than it is already. Therefore, several compounds were examined for their suitability as model pyrovapor components. These included glycerol, aldol, 3-hydroxy-2-butanone, acetol, furfural, and tetrahydrofurfuryl alcohol. The last molecule, thfa, was ultimately chosen for study because it is similar in structure to about one fourth of those molecules which have been identified as cellulose pyrolysis products. It also has a stoichiometric composition of $C_5H_{10}O_2$, similar to the $C_5H_8O_2$ reported for pyrolytic oil, and the reaction of this molecule on the catalyst surface involves intermediates resembling those expected from most of the C4 and C5 polyfunctional oxygenates known to to be cellulose pyrolysis products.

The structure of the molecule is

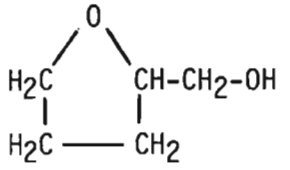

As will be seen in results to be discussed, the behavior of this molecule over a zeolite catalyst closely resembles the behavior of pyrovapor genarated from the considerably more complicated molecule α-methylglucoside.

TABLE 2. Time program functions for analyzing pulsed micro-reactor products with the in-line g.c.

TIME IN MINUTES	PROGRAM EVENT STATUS	COLUMN I FUNCTION	COLUMN II FUNCTION
0	System set for start of experiment	In Line.	Isolated.
.1	Column II brought in line to provide audible inject command	In Line. H_2 Separated	In Line.
2.2	Column II isolated to trap gases	In Line. $CO_2, C_2H_4, C_2H_6, C_2H_2$ Separated.	Isolated. O_2, N_2, CH_4, &CO Trapped.
11.7	Column II brought in line to elute trapped gases	In Line.	In Line. O_2, N_2, CH_4, &CO Separated.
18.0	Column II isolated for remainder of program	In Line. H_2O, C_3's Separated	Isolated.
37.0	Oven temperature is increased to 180°C at a rate of 10°C/minute	In Line. C_4's, C_5's, C_6's Separated	
60.0	Oven temperature is increased to 230°C at a rate of 10°C/minute	In Line. C_7's, C_8's, C_9's Separated	
92.0	Oven temperature is increased to 270°C at a rate of 10°C/minute	In Line. C_{10}'s, etc. Separated	

Col. I: 1/8" x 72" Poropar Q, 60-80 Mesh
Col. II: 1/8" x 84" 13X Molec. Seive, 80-100 Mesh

Figure 3

Flow Diagram Of Pulsed Micro-Reactor Apparatus For Use In The Catalytic Conversions Of Oxygenated Hydrocarbons To Fuels And Chemicals

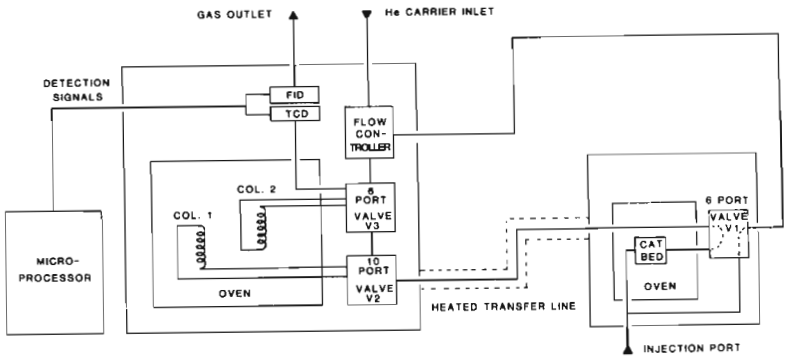

FIGURE 4

HYDROCARBON YIELDS VS. AMOUNT OF FEED FOR Thfa OVER A SERIES OF ZEOLITES AT 375°C

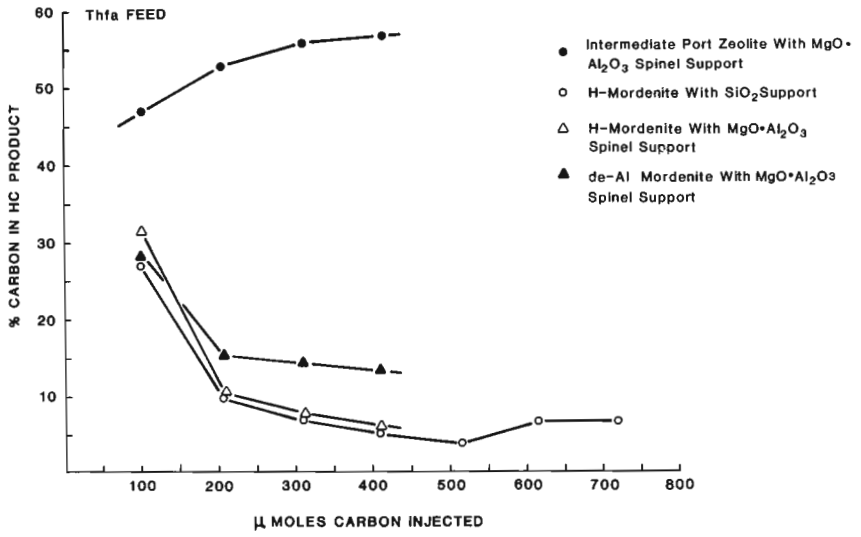

RESULTS & DISCUSSION

As a result of several screening experiments, two zeolites were chosen for further study. The first, mordenite, is a large port zeolite whose 6.4Å pore dimensions result from crystal channels bounded by 12 membered rings of oxygen atoms covalently bonded to the tetrahedral silica-alumina framework. Mordenite was used in its hydrogen form both as received from Norton Co., SiO_2/Al_2O_3=10, and in a de-aluminized form, SiO_2/Al_2O_3=62. The second zeolite was an intermediate port zeolite with SiO_2/Al_2O_3=38 and 5.7Å pore openings defined by 10-membered rings of oxygen atoms in the crystal framework. Examples of intermediate port zeolites are clinoptilolite, TMA offretite, silicalite, and ZSM-5.

Figure 4 shows the relative ability of the two zeolites to convert the pyrovapor model compound, Thfa, to oxygen free hydrocarbons. These experiments, performed in the pulsed micro-reactor clearly show the benefit of using the smaller, more shape selective zeolite pores to effect the desired chemistry. The pore dimensions of the intermediate port zeolite are too small to permit the formation of condensed ring hydrocarbons (coke) within the pores and this appears to be critical to maintaining catalytic activity. Not surprisingly, rates of coke formation are a major problem for this technology since hetero-atom containing hydrocarbons are known coke precursers.

The amount of catalyst coking observed was found to be a strong function of both the acid strength and surface area of the support solid used in conjuction with the active zeolite. Table 3 summarizes data in support of this conclusion. All runs listed in this table were conducted at 375°C with a weight hourly space velocity (WHSV) of 1 hr^{-1}. Vapor/catalyst contact time was ~1 sec. Surface acidities were bracketed through the use of a series of Hammett indicators whose colors are affected by the acid strength of surface adsorption sites.[11]

Experiments 38 and 42 from the table were identical and show the lowest catalyst coke loadings at the conclusion of the experiment. In each case, a neutral, low surface area solid support was used with the zeolite. Run 39 used a high surface area silica only slightly more acidic than the beads of Run 38, yet coke formation almost tripled. The use of neutral alumina with surface acidity very similar to that of fumed silica but with very low surface area again reduced coke formation. The worst result is Run 6 with 45% coke yield at a very early point in the experiment. In this case, the Al_2O_3 support used was both acidic and of high surface area.

Material balances for three similar experiments conducted at temperatures from 325° to 425°C are given in Table 4. In each case the experiment was continued until catalyst activity was negligible as evidenced by the cessation of gas production. In general catalyst activity was very high during the first 10% of the run, fairly uniform for the middle 80% and then dropped dramatically during the last 10%.

TABLE 3. Hammett acidity functions (H_o), surface areas, and level of coking observed in Thfa conversion for support solids used with an intermediate port synthetic zeolite. All catalyst formulations contained 10% active zeolite, 90% support solid

Expt	Support Solid	H_o	Surface Area (BET)	Feed to Catalyst Ratio	Reacted Carbon on Catalyst
38	Amorphous silica beads	>6.8	$<10 m^2/g$	1.0	2.2%
42	Amorphous silica beads	>6.8	$<10 m^2/g$	1.0	1.6%
39	Fumed silica	3.3-4.0	$150 m^2/g$	1.0	4.7%
B	Al_2O_3	3.3-4.0	$<10 m^2/g$	1.0	3.1%
35	Kaolin	1.5-3.3	$150 m^2/g$	0.1	16%
6	Al_2O_3	<1.5	$150 m^2/g$	0.1	45%
51	Silicalite	>3.3	$200 m^2/g$	1.5	14%

Experiment 38 at 375°C was the most successful run with the longest catalyst life, lowest coke yield, and highest oxygen free hydrocarbon yield. At lower temperatures, Thfa decomposed first to a tar-like substance which subsequently charred and deactivated the catalyst. At 425°C, zeolite surface cracking activity was too high and the resulting carbon formation quickly blocked the catalyst pores.

Catalyst coke levels were determined by an oxidation procedure where both steam and oxygen were used to oxidize carbon residues at temperatures of 550-600°C. After oxidation, the catalysts were found to be indistinguishable in activity from the fresh preparations.

Since the vapors produced in pyrolysis of biomass organics will be quite damp, several runs were made using 50% Thfa/50% H_2O as a feed. Experiment 41, also listed in Table 4 shows that neither catalyst performance nor catalyst life are affected by the high relative steam pressures.

TABLE 4. Material balances for the conversion of Thfa over 10% intermediate port Zeolite/90% low surface SiO_2 at a WHSV = 1 hr^{-1}

Expt	Temp.	Feed to Catalyst Ratio	% Oxygen Removal	Distribution of Carbon in Products			
				Gaseous	Catalyst Coke	Oxygenated Hydrocarbons	Hydrocarbons
48	325°C	.67	46%	1%	7%	53%	39%
42	375°C	1.0	78%	1%	2%	27%	70%
38	375°C	1.3	68%	3%	2%	32%	63%
49	425°C	.67	52%	5%	3%	48%	44%
The following expt. used 50% Thfa/50% H_2O as a feed							
41	375°C	1.0	75%	2%	2%	26%	70%

In order to demonstrate the conversion of a more complicated biomass related molecule, an aqueous solution of 33% by weight of α- methylglucoside ($C_7H_{12}O_5$) was prepared. This was fed into the dual chamber reactor shown in Figure 5. The first chamber was maintained at 550°C and vapor residence time, based on the volume of steam generated at 1 atmosphere pressure, was $\sim$5 seconds. The steam and organic vapor generated were then fed into the second chamber maintained at 375°C and contacted with the 10% intermediate port zeolite, 90% amorphous silica catalyst. Residence times in the catalyst reactor were 1 sec. The overall product distribution obtained after 1 hr. of running was

Pyrolysis char	15%	of carbon in feed stream
Catalyst coke	11%	
Gaseous product	20%	
Aqueous soluble organics	24%	
Organic liquid	30%	

These results indicate that a good yield of oxygen free organic liquids can be produced via the coupling of pyrolytic and catalytic conversion steps for the treatment of biomass related molecules.

Figure 5
Schematic Diagram Of 2-Stage Pyrolysis/Catalysis Reactor For Continuous Conversion Of Pyrolysis Vapors To Hydrocarbon Products

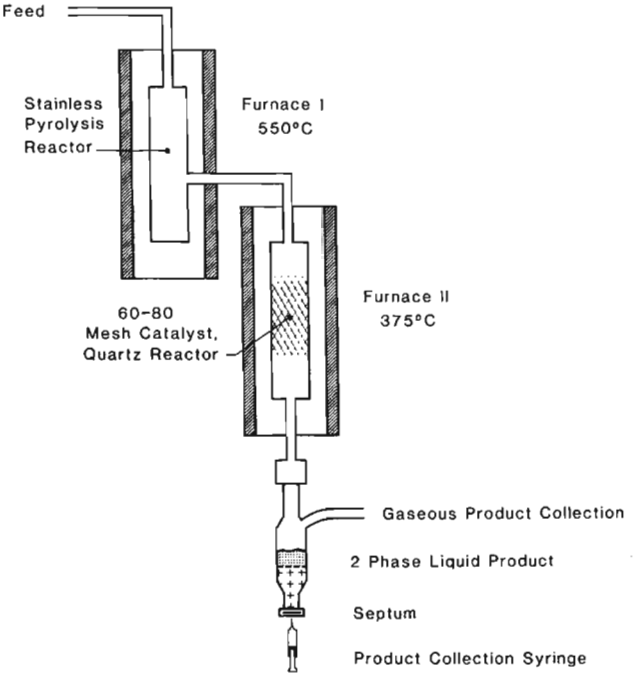

CONCLUSION

The use of high silica/alumina ratio zeolites for converting complex, highly oxygenated hydrocarbons to oxygen free hydrocarbons was shown to be technically feasible. Highly oxygenated organic vapors are generated in the pyrolysis of biomass at 500-550°C and these vapors may be catalytically converted over acidic zeolites to useful hydrocarbon liquids. Intermediate port zeolites with pore openings around 5.7Å appear to be most useful for effecting the conversion of interest since they are relatively resistant to coking. A low surface area, low acid strength support for the active zeolite is crucial to maintaining a reasonable catalyst lifetime by further reducing coke formation on the catalyst.

References

1. Kaiser, E.R., Combustion, Feb. 1977, p.26.

2. Jackson, F.R., Recycling and Reclaiming of MSW, Noyes Data Corp., N.J., 1975.

3. Lewellen, P.C., Peters, W.A., and Howard, J.B., 16th Symposium on Combustion, The Combustion Institute, Pittsburgh, PA., 1977.

4. Benson, S. W., Thermochemical Kinetics, J. Wiley & Sons, N.Y., 1968.

5. Molton, P.M., and Demmitt, T.F., Reaction Mechanisms in Cellulose Pyrolysis, a Literature Review, Battelle Pacific Northwest Laboratories (BNWL-2297), Richland, Washington, 8/77.

6. Pober, K. and Bauer, F.H., Chemtech, March 1977, p. 164.

7. Chang, C.D., and Silvestic, A.J., Journal of Catalysis 47, 249-259 (1977).

8. Butter, S.A., Jurewicz, A.T., and Kaeding, W.W., U.S. Patent 3,894,107, 7/8/75.

9. Kiovski, J.R. et.al., 5th North American Catalysis Society Meeting, Pittsburg, PA, 1977.

10. Givens, E.N., Plank, C.J., and Rosinski, E.J., U.S. Patent 4,052,472, 10/4/77.

11. Athinson, D., and Curthoys, G., Chem. Soc. Re. 8(4), 475-497(1979).

Acknowledgement: The contributions of Ryan Nelson to this experimental program are gratefully acknowledged.

HIGH TEMPERATURE ELECTRIC ARC, RF ENERGY AND COMBUSTION GAS HEATED PYROLYSIS OF POWDERED BIOMASS

David W. Goheen
Central Research Division
Pioneering Research Group
Crown Zellerbach Corp.
Camas, Washington 98607

ABSTRACT

Lignocellulosic materials are found almost everywhere on the earth's surface and, being part of the biological system, have the capacity to regenerate on a cyclic basis. Many proposals aimed at production of energy and chemicals from these renewable biomass materials are being presently studied. Nearly 20 years ago, high temperature pyrolysis of finely divided lignocellulose under controlled conditions was examined as a possible source of hydrocarbon chemicals and promising results were obtained. The basic products were acetylene and ethylene along with methane. Calculations showed theoretical yields of more than 40% for acetylene and yields up to 15% were obtained experimentally.

BACKGROUND

At the present time, most chemicals of commerce are prepared from petroleum, but it is now clear that alternative sources of chemical feedstocks will need to be developed if our modern industrialized societies are to be maintained. This report is a summary of work, described in more detail elsewhere(1) and undertaken some twenty years ago, aimed at production of hydrocarbon chemicals from renewable lignocellulosic materials. While the work at the time did not result in a competitive commercial process, it should be emphasized that, even during the period of major petrochemical expansion and incredibly low crude petroleum prices, it was found that acetylene could be produced from renewable lignocellulose at almost competitive costs to processes based on natural gas and petroleum.

In analyzing the potential of the world's biomass as a source of energy and chemicals, the tendency until very recently has been to dismiss the biomass as being incapable of any sizeable contribution to future needs. This erroneous assumption needs to be corrected at every opportunity. On a global basis, carbon is fixed by photosynthetic processes annually on a tremendous scale. By assuming that the carbon dioxide in the atmosphere is roughly in an equilibrium state, it can be calculated that carbon is fixed at a rate of between 10^{11} and 10^{12} metric tons per year and is converted back to carbon dioxide at approximately the same rate. This continuous removal and buildup is often referred to as the natural carbon cycle.

Thus, by tapping only a small portion of the carbon in the cycle mankind could theoretically solve all energy and material demands that can be foreseen both now and in the future. The problem is, of course, of a practical nature. A major portion of the biomass consists of materials that are widely scattered or are obtained as dilute aqueous solutions so that it is costly to collect them in one place suitable for conversion.

Lignocellulose from woody plants to a large extent overcomes the collection problem and, in fact, wood represents just about the only practical way that incident solar energy can be collected and stored for long periods at the present time. Thus, it represents a very usable and valuable raw material for potential conversion to energy and chemical products. One important consideration is the amount of wood available for conversion. Presently, the cut of wood in the world is about 8×10^8 metric tons and this figure is expected to increase to about 2×10^9 metric tons by the year 2000(2). That this cut can be reached and probably exceeded on a sustained basis was pointed out as long as thirty years ago by E. Glesinger in a book, "The Coming Age of Wood"(3). Glesinger believed that, world-wide, up to 14×10^9 metric tons of wood could be produced annually if sound timber management practices were adopted. It is reasonable to expect that the 2×10^9 metric ton figure will be reached by the year 2000.

It is difficult to estimate the fraction of the total cut that does not end up as a finished product. But taking into account the amount

of bark that is known to be discarded, the amount of lignin separated during chemical pulping, saw kerfs and tops and limbs that are not even brought in from the forest, a figure of about 33% is probably conservative. Thus, there are now available at least 2.6×10^8 metric tons of unused woody material and by the year 2000 there should be 6.7×10^8 metric tons of unused wood available for conversion. This theoretically could be obtained without increasing the annual cut that already occurs for all purposes for which wood is used. These figures are of roughly similar magnitude to crude petroleum production and greatly exceed the tonnage of all chemical products now obtained from petrochemical processing. In this connection, it is instructive to point out that in the United States more than four times as much cellulose is produced from chemical pulping of wood than all the synthetic plastics and polymers produced by the petrochemical industries.

The very large amount of unused organic material from trees has attracted the attention of many investigators and numerous schemes to convert it to more useful, lower molecular weight materials have been made. Procedures are known for conversion of cellulose and lignin into many chemicals of commercial value, but very few processes have been able to compete with petrochemical procedures for making the same chemicals. This was especially true in the two decades following World War II when petroleum was incredibly plentiful and inexpensive. Almost all of these conversion procedures have attempted the stepwise breakdown of the large naturally occurring polymers. Economic exploitation of these procedures has been hampered, not only by very low crude petroleum costs (prior to 1973) but also by the fact that the conversion schemes resulted in a multiplicity of products with low yields for each product.

There is, however, a completely different approach to the production of chemicals from lignocellulosic materials. By using inexpensive residues already collected such as sawdust, and subjecting them to very severe conditions so that the materials are degraded to a single product or, at most, a very few products that are easy to collect and purify, one can eliminate some of the economic problems.

Such a study on the rapid, high temperature pyrolysis of lignocellulosic materials was undertaken by the Crown Zellerbach Corporation nearly 20 years ago. Since World War II, a number of plants have been built that produce acetylene and ethylene by the rapid, high temperature pyrolysis of saturated hydrocarbons, particularly methane that occur in natural gas. A description of one of the procedures can be found in U.S. Patent No. 2,792,437(4). When natural gas is heated in a regenerative type furnace at temperatures of 1,204-1,482°C with retention times of .0001-0.2 second, the main product is acetylene. When the temperature is reduced to 927-1,204°C and the retention time is 0.01-0.2 second, a mixture of acetylene and ethylene is obtained; and when the temperature is lowered still further to 677-925°C and the retention time is 0.01-2.0 seconds, the main product is ethylene.

It has been known for many years that formation of acetylene is endothermic. It has also been known that, under equilibrium conditions,

it is the only thermodynamically stable hydrocarbon at high temperatures (in excess of 1000-1200°C); however, the thermal decomposition of hydrocarbons into acetylene is not a reaction that goes to complete equilibrium(5). Acetylene, although formed at high temperatures, decomposes rapidly into carbon and hydrogen. This explains the need for high temperatures with very fast quenching when hydrocarbons are pyrolyzed to produce acetylene.

Many processes for accomplishing the pyrolysis of diverse hydrocarbons and even mixtures of carbon and hydrogen have been developed. Heating can be by resistance furnaces, regenerative furnaces, induction furnaces(6,7), electric arcs(8,9), plasmas(10), and partial combustion(11,12). In all these reports, hydrocarbons (or carbon in a hydrogen atmosphere) were the feedstock for acetylene production. Only one pertinent reference was found to the high temperature pyrolysis of wood(13). In this case, wood was subjected to conventional charring at relatively low temperatures to give gaseous products, including methane. The gaseous mixture was then cracked yielding unsaturated hydrocarbons. No references, other than our work, to the rapid, high temperature pyrolysis of wood were uncovered.

As mentioned above, the possibility of producing acetylene led us to try rapid, high temperature pyrolysis of lignocellulosic materials since it was felt that only one or two products would be produced. Consequently, a laboratory research program, followed by a pilot plant evaluation of the economics of acetylene production was undertaken.

EXPERIMENTAL WORK AND DISCUSSION

Various ways of subjecting small samples of powdered lignocellulosic materials to very high temperatures were first investigated. The first experiments were conducted by blowing powdered kraft lignin through an arc in a "four-way" glass tube with dry nitrogen. A "four-way" glass tube of 20mm inside diameter was fitted with two copper wires about 1 cm apart in the middle of the tube. The wires were connected to a transformer capable of producing a potential of 15,000 V. The system was purged with nitrogen and an arc was struck between the wires. A sample of kraft lignin was introduced into one of the arms of the glass apparatus and this was carried through the arc by means of the nitrogen stream. The gases from the cell were passed through an infra-red cell and analyzed by IR spectroscopy. Carbon monoxide, carbon dioxide, hydrogen cyanide, and acetylene were found to be present in the gases. Quantitative data were not obtained in the first experiment, but acetylene was shown to be formed and was about 2.5% of the total gas stream. The same experiment was used in subsequent quantitative experiments. In these, weighed amounts of lignin were blown through the arc and helium was used as the sweep gas to prevent formation of hydrogen cyanide found when nitrogen was used as the carrier. The gases were collected in a calibrated volumetric cylinder by displacement of a saturated brine solution. Various types of lignin and also wood and cellulose were tried. The results are shown in Table 1.

TABLE 1

Material Pyrolyzed	Amount of Material	Volume Collected	% Acetylene in the Gases	Yield of Acetylene in %
Precipitated Kraft Lignin	0.4g	1,900ml	2.5	14
Desugared Calcium Base Spent Liquor Solids	0.6g	1,600ml	0.3	0.9*
Desulfonated Calcium Base Spent Liquor Solids	0.4g	1.750ml	2.5	13
Lignocarbon from Heating Calcium Base Spent Liquor with Acid	0.4g	1,600ml	0.8	4*
Powdered Douglas-Fir Wood	0.4g	1,700ml	2.5	13
Powdered Cellulose	0.5g	1,800ml	3.5	15

* Gases contained a considerable amount of H_2S.

These experiments showed that several lignocellulose materials gave unexpectedly large yields of acetylene when pyrolyzed in short times at high temperatures. Contrary to expectations, the presence of oxygen in the lignocellulose did not prevent formation of substantial amounts of hydrocarbons.

With this apparatus, there was no way of estimating the temperature of the arc, so a different heating method was devised. The arc in the "four-way T-tube" was replaced with a coil wound from No. 28 tungsten wire. The coil of about 1/8" diameter and one inch long was connected to copper wires and sealed into the system with rubber stoppers. After purging with helium, a current from a variable transformer was applied and the coil was heated to incandescence drawing 500 watts at 20 volts. The temperature was estimated by an optical pyrometer to be between 2000 and 2500°C. As before, kraft lignin was blown through the coil and a yield of 23% acetylene based on the lignin was obtained. The tungsten coil became brittle and broke after one run, probably owing to formation of tungsten carbide. A tantalum coil was also tried but this also broke after one run.

In the experiments using the arc and heated filaments, acetylene was the main organic product, and only small amounts of carbon monoxide, carbon dioxide, and free carbon were found. The yields were promising but the exact values were uncertain owing to the difficulty in determining the exact amount of material actually heated to the high temperatures. Thus, it was decided to investigate other furnace designs that could pyrolyze larger samples at known temperatures.

Induction furnaces, heated by means of high frequency currents in water-cooled copper coils, appeared to offer an attractive means of generating high temperatures in small, easily controlled regions. Consequently, an R_f generator was secured and experiments to design a small suitable laboratory furnace were carried out.

A 4-inch quartz tube was first tried. This was wrapped with a coil of 1/4-inch copper tubing with eleven turns. Water was passed through the tubing to keep it from melting. The ends of the coil were attached to the output terminals of the R_f generator. Taps were first used to drive the grids off the oscillator tubes of the generator, but it was soon found that a coil of about two turns of the copper tubing about 1/2-inch away from the main coil and connected to the grid-driving input terminals of the oscillating circuit worked better and gave balanced loads.

A carbon crucible 3" x 3" was used as the conductor to be heated and it was placed in the quartz tube near the middle of the copper coil. This design was found to be too large for production of high temperatures, so a smaller tube and crucible were used. With a 2 1/2-inch quartz tube and a carbon crucible of 1-inch diameter and 3-inches long, a temperature of 1650°C could be reached using the full output of the R_f generator. However, this type of furnace was not suitable for pyrolyzing lignin in a helium atmosphere. The high temperature and voltage caused ionization of the helium and the arc so formed actually

perforated the quartz tube. Argon was even worse as a carrier. Carbon dioxide did not ionize but reacted rapidly with the carbon crucible to form carbon monoxide. Thus, the latter gas was used as a carrier as it neither ionized nor reacted with the crucible.

A few experiments on lignin pyrolysis at temperatures of about 1500°C gave much carbon black but very little acetylene. It became obvious that this design resulted in far too long a residence time for the gases, so this approach was abandoned.

It was found that flake graphite had just the right properties to be intensely heated. In one test, a porcelain crucible containing flake graphite placed in a matrix of alumina was melted into the alumina (m.p., about 2093°C). Thus, a new furnace designed to utilize graphite as the heating element was designed in the following way: Two alumina blocks of about 2 1/2-inches in outside diameter were prepared. The bottom block had a hole which just fitted the combustion tube. Above this block was placed the other alumina block which had inside hole about 1/2 larger than the combustion tube. The space between the tube and block was filled with graphite. When the system was placed inside the copper coil and the R_f generator turned on, it was found that rapid and easy production of any temperature up to the melting point of the combustion tube could be obtained (above 1760°C). The hot graphite attacked the combustion tubes but they were found to hold up for two or three runs. Painting them with magnesium zirconate helped and allowed the tubes to be used for six or seven runs. A tube of silicon carbide was found to be very resistant to the graphite and initial pyrolyses were used with this tube in the newly designed furnaces.

The pyrolysis was very simple. The tube was loosely packed with broken pieces of combustion, the R_f generator turned on and the graphite was heated to the desired temperature. Then lignin was slowly dropped into the heated zone by means of a water-cooled copper tube extending to about 2-inches above the heated zone. Several experiments gave only about 4% acetylene yields. The reason for low yields was finally found to be porosity of the silicon carbide tubes, and use of these was discontinued as more than half the gases produced were being lost. Thus, porcelain combustion tubes painted with magnesium zirconate were used for subsequent runs. A series of runs was made using measured helium flow rates (ionization and arcing were not a problem in this design) and variable temperatures from 1760°C down to 1040°C. Results are shown in Table 2.

An inspection of the table shows that yields of acetylene and ethylene almost reverse themselves from the highest to the lowest temperatures and that a large fraction of methane formed in the pyrolytic reaction was not cracked even though the temperatures were high enough to do so. In an attempt to determine why the methane was not sufficiently cracked, a series of runs on natural gas (>90% methane) in the same furnace was made using about 10-15% methane in helium. Gases were collected in a 30-inch weather balloon and the extent of pyrolysis determined by IR analysis. Results were shown as partial pressures in

TABLE 2

Run	Amount of Lignin, g	Time of Addn., sec.	Temp. °C	Vol. of Gas, ml.	Helium Flow Rate ml/min.	Yld. of C_2H_2, %	Yld. of C_2H_4, %	Yld. of CH_4, %
1	2.9	30 sec.	1760	5,800	2,700	7.9	2.1	13.4
2	3.0	30 sec.	1704	6,900	2,700	8.0	2.8	16.1
3	3.0	30 sec.	1538	7,000	2,700	8.6	2.5	16.5
4	3.0	30 sec.	1482	6,100	2,700	5.8	2.2	15.0
5	3.0	30 sec.	1371	6,000	2,700	6.2	2.5	14.9
6	3.0	30 sec.	1260	7,300	2,700	5.2	4.7	22.7
7	3.0	30 sec.	1149	7,200	2,700	3.5	7.2	23.1
8	3.0	30 sec.	1040	7,900	2,700	3.2	6.5	22.1

the gases collected in the balloon. The pyrolyses were run until back pressure of the balloon equalled the pressure in the natural gas line. Data are shown in Table 3.

These data show that pyrolysis of methane is appreciable at about 1200-1260°C for this furnace design and proceeds very well at 1316°C. It is of interest to note that the partial pressure of acetylene reached a maximum and then held steady with increasing temperature, while the methane partial pressure steadily decreased with temperature. This was taken to mean that for any particular furnace design, there is a maximum allowable acetylene concentration. As the methane decomposes, it goes through an acetylene intermediate and finally is converted to carbon and hydrogen. It follows that a shorter hold time and higher temperature could allow greater concentrations of acetylene to be developed. This was shown to be the case in earlier experiments where partial pressures of acetylene in excess of 30mm were obtained by both the arc and heated coil pyrolyses.

From the data on methane (Table 3) it can be seen that at 1038°C, only a small amount of acetylene is produced, whereas the data on lignin pyrolysis (Table 2) shows that more acetylene is produced than from the methane at the same temperature. From this, the conclusion was drawn that acetylene from lignin and wood is formed by two different paths, the first by direct pyrolysis of the large molecules into smaller fragments and the second by pyrolysis of methane formed by more extensive degradation of the large molecules. This conclusion is supported by work on hydrocarbons. It is easier to make ethylene and acetylene from large hydrocarbon molecules than it is from methane(5). In addition to kraft lignin, other raw material feeds were studied. Cellulose worked well, but wood served even better. Results on wood are shown in Table 4.

Based on these laboratory results, a decision to build a bigger furnace and determine the commercial feasibility of preparation of acetylene from wood was made. It was realized that the yields obtained in the small furnace were probably not high enough to be commercially interesting, but it was felt that in a larger unit, better heat control and transfer would result in increased yields by converting more of the methane which was always formed in the laboratory sized unit. Theoretical consideration also led to the assumption that larger yields were possible. These were:

1. Wood has an elemental composition of close to 50% C, 6.0% H_2, and 44% O_2.

2. This gives an empirical formula of $C_{4.17}H_{5.9}O_{2.7}$.

3. Assuming that oxygen of the wood ends up equally or CO and H_2O and that carbon formation is not a major side reaction, the decomposition can be expressed as $C_{4.17}H_{5.9}O_{2.7} \rightarrow 1.41\,C_2H_2 + 1.35\,CO + 1.35\,H_2O + 0.19\,H_2$ and for 100 lb. of wood, 37 lb. C_2H_2 + 38 lb. CO + 24.5 lb. H_2O + 0.5 lb. H_2.

TABLE 3

Run	Nat. Gas Setting*	Helium Setting*	Temp., °C	Pressure of Methane, mm	Pressure of Ethylene, mm	Pressure of Acetylene, mm
1	4.3	12.0	R.T.	142	0	0
2	4.3	12.0	1,037	134	7.0	1.5
3	4.3	12.0	1,204	131	6.0	13.0
4	4.3	12.0	1,316	90	2.5	24.0
5	4.3	12.0	1,427	39	3.0	24.0
6	4.3	12.0	1,538	14	2.0	24.0

TABLE 4

Feed Material	Amt.	Temp., °C	Yield of Methane, %	Yield of Ethylene, %	Yield of Acetylene, %
Powdered Douglas-Fir Wood	2g	1427	18.5	4.6	13.0
Powdered Douglas-Fir Wood	2g	1482	15.8	5.7	11.4

4. The yield of acetylene could be as much as 37-40% of the wood. A yield of 25-26% was assumed to be reasonable. This was based on two points.

    a. Our laboratory apparatus gave about 1/2 the yield of acetylene from methane that is expected from a commercially perfected acetylene reactor using methane. Assuming a proportionate improvement for a commercially perfected reactor using wood, the laboratory yields of 10-15% could be doubled.

    b. The calculated theoretical yield from wood was about 40%. Commercial acetylene yields from methane is about 65% of theoretical. A similar yield from wood, thus would be about 26%.

A furnace was designed with a tangential reaction burner. Heat was supplied by burning natural gas and sawdust (30 mesh and less) was transported to the hot zone by a carrier gas (steam, CO_2, etc.). Product gases were removed through a 3/4-inch diameter graphite reaction tube fitted with a moveable quench probe. Acetylene was determined by gas chromatography. A schematic diagram is shown in Figure 1.

This reactor proved to have several undesirable features and was modified several times and finally a straight jet-type, burner-reaction design was adopted as the best. This is shown in Figure 2.

Numerous runs showed to optimum O_2 to methane (for heating) ratio to be 1:1.4. Highest acetylene yields were found to be at low sawdust rates but acetylene concentrations in the product gas were found to increase as the sawdust feed rate increased. Thus, optimum sawdust feed rate became a compromise between obtaining high yields and high acetylene concentrations in the product gas stream. A series of runs was made to determine the decomposition rates of acetylene under the optimum conditions of temperature, flow rate, and firing gas mixture ratios. These were plotted as a curve of acetylene concentration versus time. From this, the amount of wood converted to acetylene but not necessarily appearing as product acetylene was calculated. This was found to be 46%, which is in good agreement with the assumed theoretical yield of about 40%. Owing to excessive acetylene decompositions in all of the furnaces, we were not able to approach this yield. The best yields actually obtained in the jet-type reactor were 12% by weight of acetylene accompanied by 4% ethylene.

An experiment substituting hydrogen and carbon monoxide for natural gas for firing still produced acetylene showing that the hydrocarbon was not being produced by incomplete conbustion of methane used for firing. Some calculations were made concerning the energy absorbed in converting sawdust to acetylene. In our jet furnace, this was found to be 3,180 BTU/lb. of acetylene obtained. This figure was obtained from temperature, flow rates, and chromatographic analyses. This figure is considerably lower than the 5,150 BTU/lb. of acetylene necessary in the partial methane combustion processes. The figures refer only to energy required to convert the feedstock and do not take into account furnace losses and energy required to reach reaction

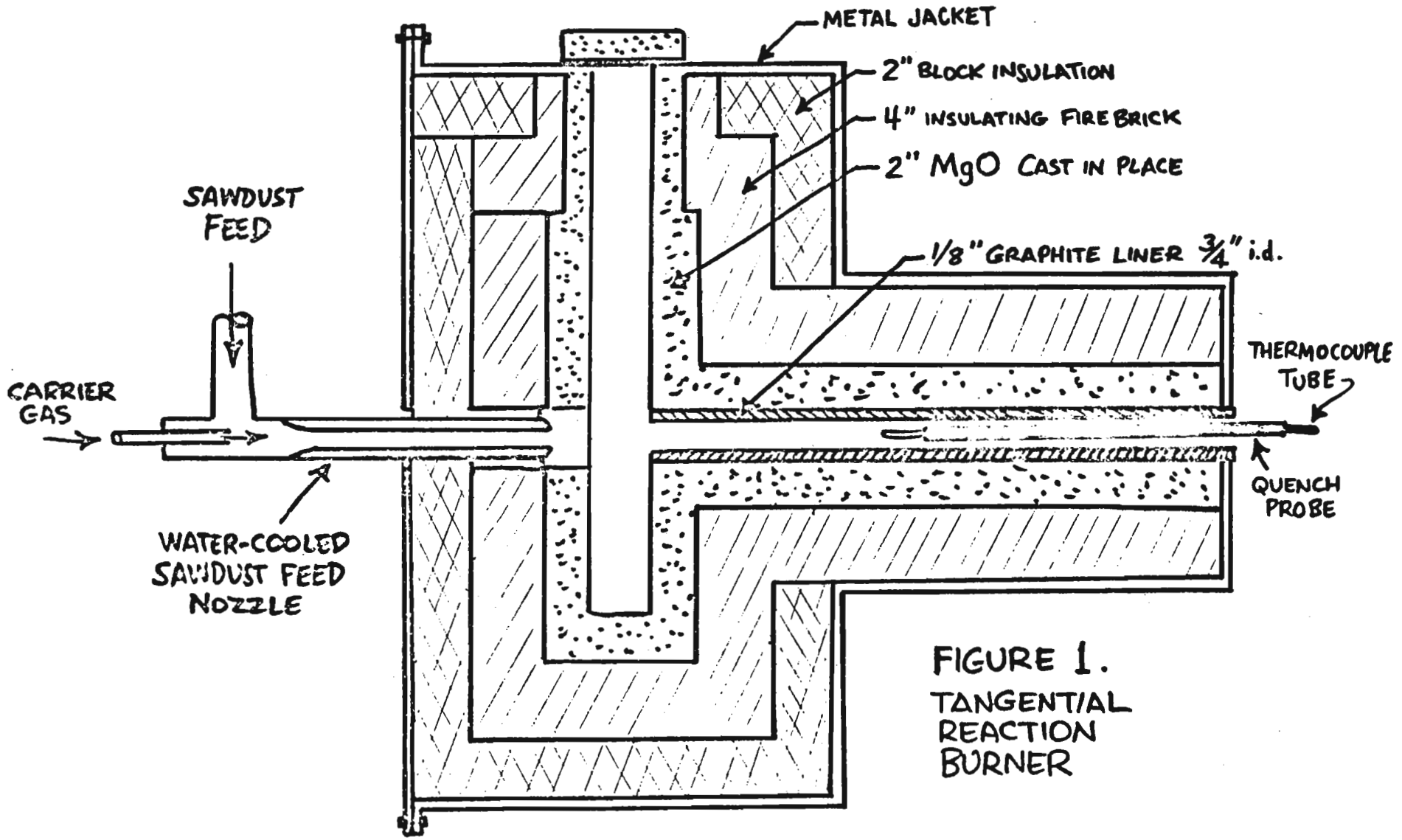

FIGURE 1.
TANGENTIAL REACTION BURNER

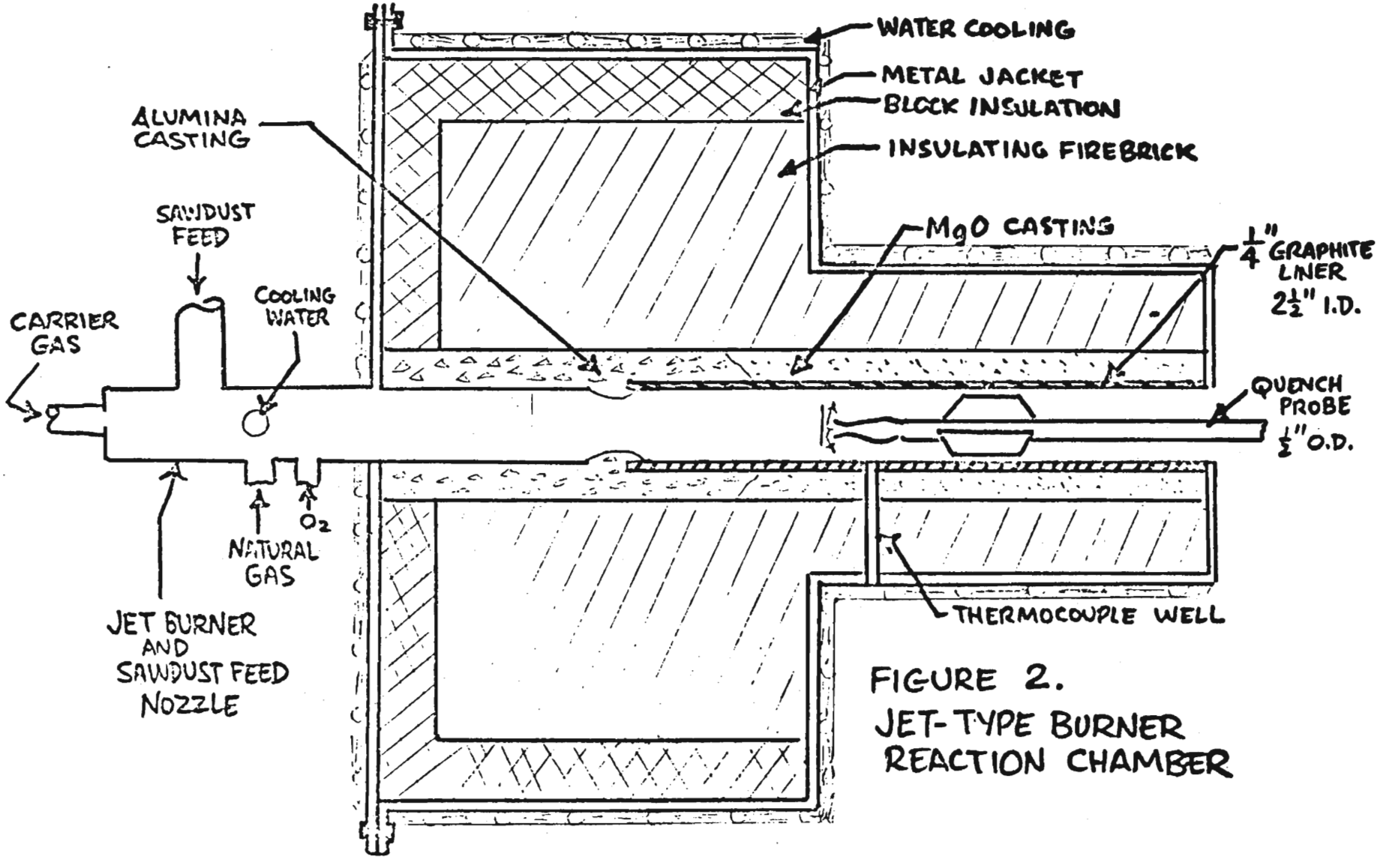

FIGURE 2.
JET-TYPE BURNER
REACTION CHAMBER

temperature.

In our furnace, it was found necessary to use relatively low temperatures (1204-1260°C) and relatively long reaction times. These combined to give low acetylene yields. The low temperatures meant that heat transfer was relatively slow to the wood particles so that initially formed acetylene decomposed before all the wood reached pyrolysis temperature. Thus, the presence of oxygen in the wood was shown to be a disadvantage. The ratio of added oxygen to methane had to be lower than the stoichiometric value since much oxygen was available from the wood and the temperatures attainable by chemical energy were lower than would be optimum for rapid heat transfer and conversion of the wood particles to gaseous products.

The possibility of using electric arc or corona discharge in combination with the combustion process was considered. After a complete economic feasibility showed that yields in excess of 30% acetylene would be necessary to compete on an equal basis with acetylene from natural gas, it was decided to terminate our study without building a large plant.

SUMMARY

Although we did not produce a commercially competitive process, we came close. The economic evaluation showed that production costs of acetylene from wood were about 25% higher than for acetylene from methane. Taking into consideration present day natural gas and wood waste costs, the acetylene from wood looks more attractive. Future plants to make hydrocarbons from renewable lignocellulose plants appear to be a certainty. These may be based on conventional hydrolysis or gasification routes, but may very well be based on rapid, high temperature pyrolyses similar to that described in this report.

REFERENCES

1. Goheen, D. W. and Henderson, J. T., The Preparation of Unsaturated Hydrocarbons from Lignocellulose Materials, Cellulose Chem. Technol. 12, 363-372 (1978).

2. Karlivan, V. P., New Aspects on Production of Chemicals from Biomass, Paper presented at World Conference on Future Sources of Organic Raw Materials, Toronto, Canada (July 10-13, 1978).

3. Glesinger, E., The Coming Age of Wood, Simon and Shuster, NY (1979).

4. Goins, R. R. and Begley, J. W., U.S. Pat. No. 2,793,437, May 14, 1957.

5. Lockwood, D. C., Pet. Ref. 39, No. 11, 223-226, 1960.

6. Weaver, T., Chem. Eng. Prog. 49, No. 1, 35-39 (1953).

7. Baddour, R. F. and Iwasyk, J. M., Ind. and Eng. Chem. Pro. Design and Dev. 1, No. 3, 169-176 (1962).

8. Pettyjohn, E. S., Nat. Pet. News, 38, No. 32, 597-604 (1946).

9. Schoch, E. P., Univ. of Texas, Pub. No. 5011 (1950).

10. Leutner, H. W. and Stokes, C. S., Ind. and Eng. Chem. 53, No. 5, 341-342 (1961).

11. Hale, A. B. and Parrish, S. E., U.S. Pat. No. 2,868,856, Jan. 13, 1959.

12. Elliot, J. and McClure, H. H., U.S. Pat. No. 2,945,074, July 12, 1960.

13. Cedarquist, K. N., Swedish Pat. No. 115,120, Oct. 9, 1945.

HIGH RADIATIVE HEAT FLUX PYROLYSIS OF THIN BIOMASS

K. A. Lincoln
Ames Research Center, NASA
Moffett Field, California

ABSTRACT

Some recent experimentation on the pyrolysis of cellulose resulting from intense thermal radiation is compared with similar work conducted 15-20 years earlier by the author and colleagues. Various aspects of flash-heating by high radiative flux are discussed, and several thermal radiative sources are compared. A refocused carbon arc, a xenon flash lamp, and lasers were used to pyrolyze cellulose over a wide range of radiant heat fluxes. Results show that the heating rate significantly influences the composition of the pyrolysis products. Critical attention is given to the methods of analyzing the vapors produced from flash-heating and to the interpretation of the resulting data.

INTRODUCTION

Historically the work reported on here received its impetus soon after World War II when the various effects of nuclear weapons were being vigorously investigated. One of those effects is fire damage; it is of greater importance at high weapon yield because the fire-ignition range exceeds the blast-damage range. With solid fuels, pyrolysis is usually the first step in the sequence of pyrolysis, ignition, combustion, and fire spread. In most burning of solid fuels it is the pyrolysis step that actually provides the reactants for the subsequent combustion reactions. Thus, it was concluded that if the composition of the pyrolysis products could be determined and if the factors that influence thermal decomposition ascertained, we would be in a better position to postulate combustion-reaction mechanisms and establish a more scientific basis for fire retardants and flame inhibitors.

Because typical fire kindling fuels — such as wood, paper, and cotton cloth — are of biomass origin, cellulose is their chief component. It has been found that small amounts of inorganic impurities have a large effect on the thermal decomposition reactions of cellulosic materials, and so care must be exercised in choosing only the same sample material when comparing results. Thus, for the purpose of providing a standard

supply of samples having uniform physical and chemical properties, specially prepared α-cellulose was formed into sheets of several discrete thicknesses with known amounts of carbon black included. For the work reported here, the samples contained 2% carbon black by weight, which provided an absorbance greater than 90% for the various radiant heat sources. This paper reports on work performed 15-20 years ago by the author [1] and colleagues [2], and compares it with recent results employing newer instrumentation but using the same supply of α-cellulose.

EXPERIMENTAL

Radiant Heating

Inasmuch as the emphasis in this paper is on the response of materials to thermal radiation, it would be well to briefly review some of the salient features of high-intensity radiant heating. When the irradiance level is extreme on an opaque body of high surface absorptance, energy deposition is limited to material very near the exposed surface, and ablation effects predominate over the relatively inconsequential diffusion of heat into the solid. Thus, to make flash-heating feasible, a sample must possess certain physical characteristics. For maximum temperature rise, a material must have a high optical absorptance in the spectral range of the radiant source and, if the entire sample is to be vaporized, it must have a high surface-to-volume ratio.

Among the advantages of radiant heating for flash-pyrolysis is that it is "clean," that is, only the light-absorbing material is heated; the container and other surrounding objects remain cool and do not contribute to the vapor products. The radiant pulses are very reproducible and can be very short and very intense, thereby enhancing the detection of certain thermally produced, reactive intermediates. The disadvantage of this type of heating is that it is difficult to measure the temperature of the heated material. We have met with some success using fast, electronic optical pyrometers, but care must be exercised to exclude light from the incident radiation and from induced light-emitting processes.

Radiant Thermal Sources

Among the earlier achievements of the weapon-effects work was the simulation of the thermal irradiance exposures from nuclear weapons, using a refraction-optics carbon-arc thermal source [3]; this source produced irradiance levels up to about 92 W/cm^2 on a 2.3-cm diameter uniform spot. The outstanding feature of this refocused arc was that the pulse shape and intensity could be controlled with shutters. The spectral distribution of the radiation approximated that of a 5500 K blackbody. Martin [2] has done an enormous amount of work using this thermal source to (1) measure the temperature profiles and to determine the ignition parameters of cellulose in air and (2) determine the pyrolysis products resulting from exposures of cellulose in inert atmospheres.

At a somewhat later time the quartz xenon flashlamp (flashtube) was introduced as a source of thermal radiation for the pyrolysis work [4].

Although this lamp has a spectral distribution similar to that of the carbon arc, the distribution varies with the applied voltage and approximates a 5000-7000 K blackbody; thus, the energy maximum is in the visible. The pulse shape and intensity can be varied to some extent by the electrical parameters in the power supply [5], but, most important, the output is very reproducible. To receive maximum heat flux the sample material was placed in a glass (or quartz) tube and positioned at the center of the helical flashlamp. The maximum peak irradiance employed was about 25 kW/cm^2 per surface. This had the advantage that a thin sheet of cellulose (up to about 3 cm^2) could be irradiated on both sides simultaneously.

The advent of the laser ushered in a new chapter in radiant pyrolysis. Although elegant optics can be incorporated into experiments, only very simple optics are required to direct the energy exactly where it is needed on a sample material. In this case the thermal source can be located remote from the target, and a sample can be heated conveniently inside a vacuum chamber or inert gas atmosphere. The greatest advantage is that the laser beam can be focused to heat a small part of a bulk material or to increase the flux density, and attenuators can be inserted easily into the beam to reduce the flux. With pulsed lasers it is very easy to monitor the energy of each pulse as well as the shape of the pulse. The latter can be varied somewhat by the electrical parameters in a manner similar to that of the flashlamp.

In the cellulose work reported here we have used neodymium-glass lasers (1.06 μm) only in the normal (or burst) mode to achieve longer heating pulses and to avoid, for example, plasma effects, inverse bremsstrahlung, and multiphoton absorbtion, all of which tend to prevail with the Q-switched mode. The beam cross-section, which is nongaussian and fairly uniform, was focused to 1-6-mm-diameter spots. Flux densities in the 2500-kW/cm^2 range on a 1-mm-diameter spot are easily reached, but in this work much lower values were used to simulate the phenomena of interest.

The disadvantage of normal-mode lasers is the very irregular intensity variations with time in their output, which is composed of a train of approximately 1-μsec spikes of random intensities. Despite this, the overall pulse shape and energy are very reproducible from pulse to pulse. Depending on the application, the monochromaticity may or may not be a disadvantage.

Instrumentation for Vapor Analysis

As might be expected, early on in this work the vapor pyrolysis products of cellulose were analyzed entirely by gas chromatography [6]. Figure 1 is a schematic of the exposure cell employed by Martin in his experiments in which he used the carbon-arc thermal source to pyrolyze cellulose directly in the stream of the helium carrier gas prior to its entry into the column of the gas chromatograph. The chamber was kept small to prevent the accumulation of volatiles in front of the sample; the helium flowed through the chamber continuously before, during, and after the exposure, thus serving as a nonoxidizing atmosphere to sweep away the products as they were formed. The stripping column was in the

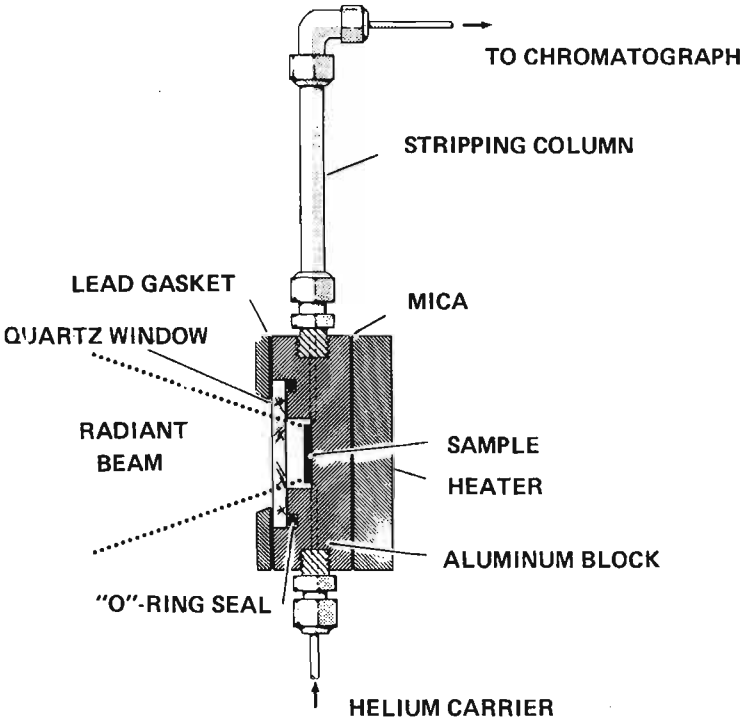

FIGURE 1. GAS CHROMATOGRAPHY EXPOSURE CELL FOR RADIANTLY HEATED SAMPLES.

stream to preclude the introduction of tarry substances and heavy viscous liquids from entry into the chromatographic column. In a smaller number of experiments the xenon flashlamp was employed as the thermal source. We found that small pieces of 2-mil cellulose sheets could be completely vaporized in a single flash that had a total energy as low as 8 J/cm^2 incident on both surfaces [4]. This provided a very convenient means of injecting the vapor products directly into the gas chromatograph, for the sample could be held in a segment of quartz tubing in the carrier-gas stream and positioned at the center of the helical flashlamp. This is clearly very similar to the procedure with the carbon-arc source, but it permitted extension to much higher flux densities.

Although gas chromatography is extremely effective in separating the various components in a gaseous mixture, it cannot detect short-lived species or transient intermediates or condensable components that fail to pass through the chromatography column. For this reason we turned to direct-inlet mass spectrometry and combined a flashlamp with a time-of-flight mass spectrometer [4], as shown in Figure 2. Here the samples are located within the ion-source housing and are vaporized by the brief thermal pulse directly into the ionizing electron beam with no slits or baffles between the point of vaporization and the ion gun. This instrumentation provided us not only with in situ analysis of the vapors, but also with time-resolved mass spectra, because the spectrometer generated up to 40 mass spectra per millisecond. Although this arrangement permits line-of-sight travel of molecules from the sample to the ionizing region, there are, nonetheless, ample opportunities for wall collisions and condensations on the walls of the test tube.

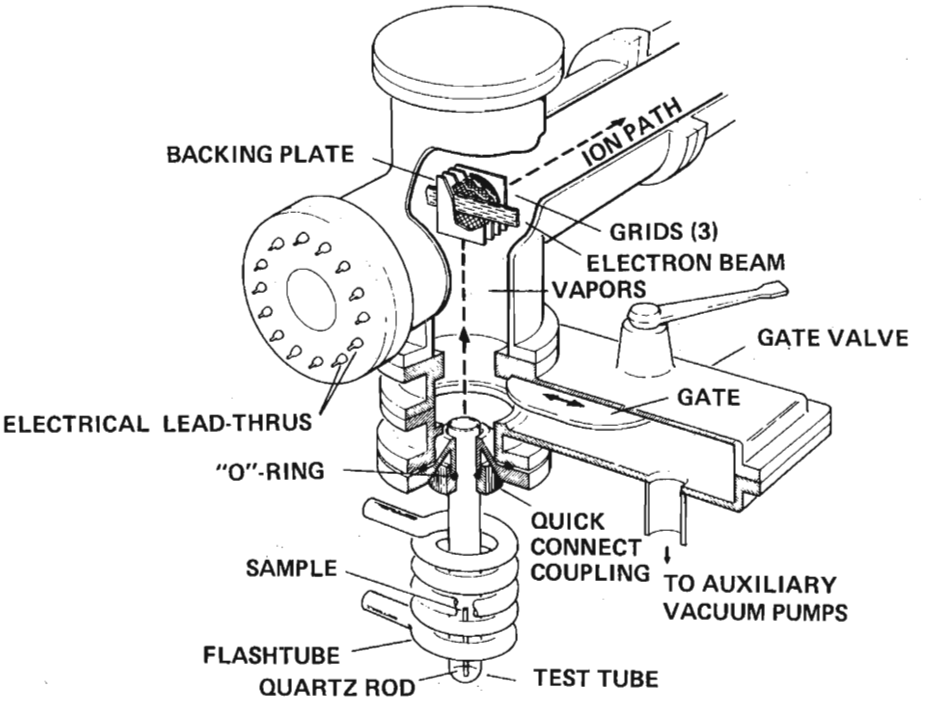

FIGURE 2. ION SOURCE OF TIME-OF-FLIGHT MASS SPECTROMETER WITH FLASHTUBE-HEATED, SOLID-SAMPLE INLET.

Consequently, when the pulsed laser was developed, we coupled one to the mass spectrometer [7] as shown in Figure 3. Now with the vaporizing material much closer to the ion gun, we could get a much better analysis of the condensables and short-lived species.

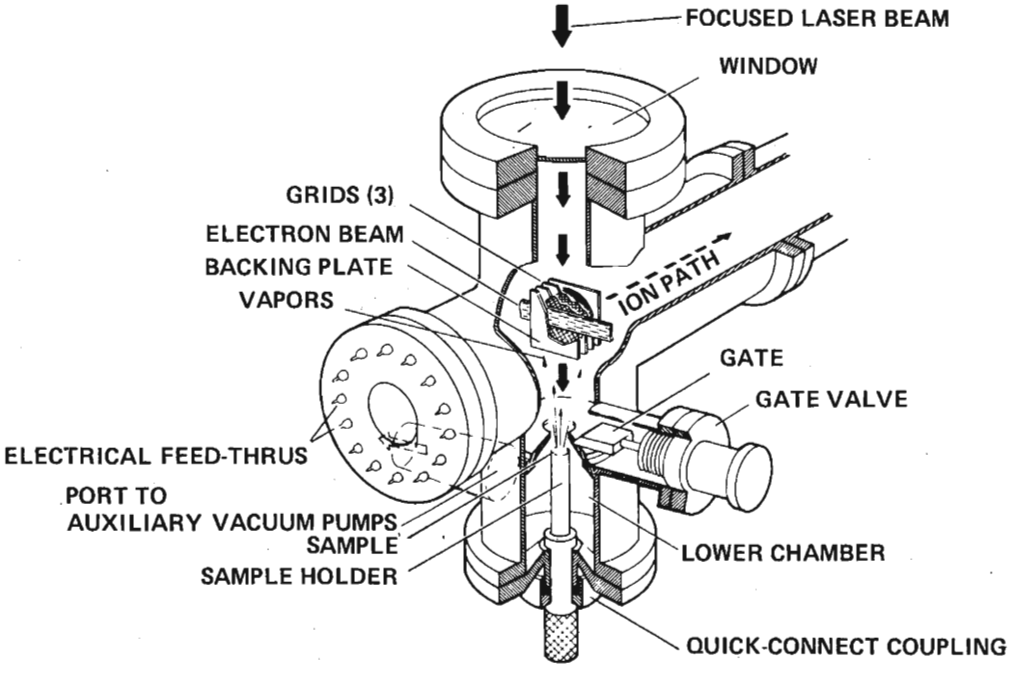

FIGURE 3. ION SOURCE OF TIME-OF-FLIGHT MASS SPECTROMETER MODIFIED FOR LASER VAPORIZATION OF SOLID SAMPLES.

At a later time the instrument shown in Figure 4 was developed at Ames Research Center; it is described in [8]. As before, this instrument was built around a time-of-flight mass spectrometer with provision for both pulsed- and CW-laser heating; it also has provision for varying the distance between the sample and the ion gun. This latter feature enabled us to measure the velocities of the vapor species. We found that the laser-produced vapors emerge from a planar surface (no crater formed) in an adiabatic free-jet expansion, just as though they had originated in a reservoir and exited via an orifice the size of the spot on the material from which they were vaporized by the laser. This is the subject of another paper [9], and is mentioned here only to give a more complete picture of the vaporization phenomenon.

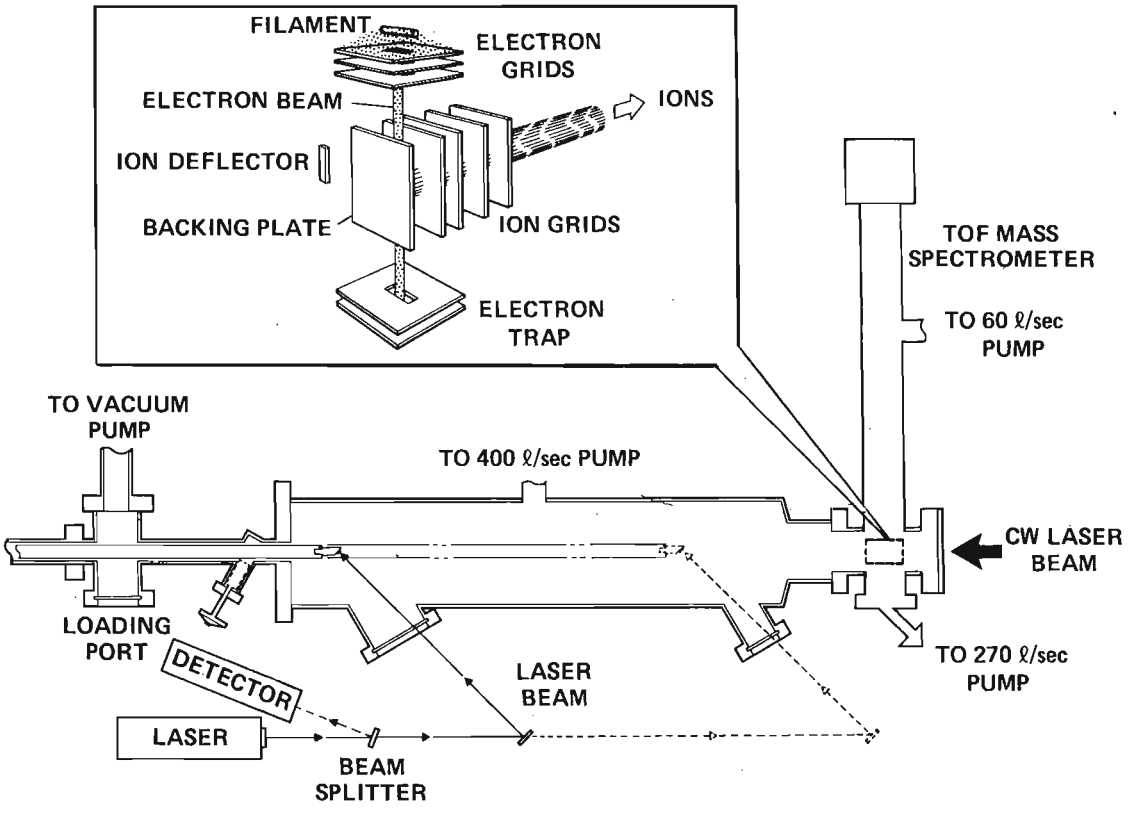

FIGURE 4. MASS SPECTROMETER AND VAPORIZATION CHAMBER FOR LASER-HEATED SAMPLES.

RESULTS AND DISCUSSION

Table 1 compares the pyrolysis products of cellulose that resulted from very different rates of heating. The first three columns summarize some of the work performed by Martin [2] in the early 1960's, using gas chromatography to analyze the volatiles and wet chemistry techniques for the tar fractions. Martin found the latter to be mostly levoglucosan (1,6-anhydro-β-D-glucopyranose), which is the monomer of α-cellulose. Complete listings of the approximately one dozen compounds that constitute the bulk of the volatile organics, along with their concentrations and the pyrolysis details, are included in his paper. It was concluded

that the rate of heating makes a profound difference in the products. This is also borne out by the data in column 4 of Table 1 by the results of flash-heating with the xenon flashtube, with its much higher irradiance, although the difference is more in relative concentrations rather than in kinds of compounds. Evidently the reactions leading to char formation are repressed, and the tars are vaporized at the higher flux. This observation is substantiated by some very recent work utilizing the Ames equipment on the same cellulose material. Figure 5 shows that the kinds of species are the same, but that their relative concentration is changed by the incident power level. This is the typical response of polymeric materials — higher flux breaks the polymer into smaller fragments (i.e., a larger proportion of low-molecular-weight compounds).

TABLE 1. PYROLYSIS PRODUCTS OF CELLULOSE
(Analyzed by Gas Chromatography)

	Thermal sources			
	Resistance furnace	Carbon arc	Carbon arc	Xenon flashtube
Irradiance, W/cm^2		6.3	46	12,000 (peak)
Temperature, °C	25 incr. to 350	~300	>600	>600
Exposure time	2.7 hr	10 sec	4 sec	1/2 msec
Atmosphere	In vacuo	He	He	He
Products based on weight percent of decomposed sample:				
H_2O	19	32	16	28
CO	3	3	13	37
CO_2	?	9	11	4
Volatile organics	~51	3	6	30
Tar	2	19	51	None
Char	25	~33	~3	~1
CO/CO_2 (molar ratio)	--	0.52	1.9	14.4

Table II summarizes the recent laser-mass spectrometric experimentation on α-cellulose performed at Ames Research Center. These data should correspond closely with those of column 4 of Table 1 except for the small difference introduced by expressing the products in weight percent in one table (Table 1) and in mole fractions in the other. However, there is a significant difference in the amount of volatile organics detected by the gas chromatograph and the mass spectrometer. Since the latter instrument makes an in situ measurement and detects nearly all of the vapors, we can infer that something was lost on the way to the column in the earlier work. Figure 5 also shows that high-molecular-weight compounds are present even at the high irradiance exposure. Parenthetically, it should be pointed out that most of the

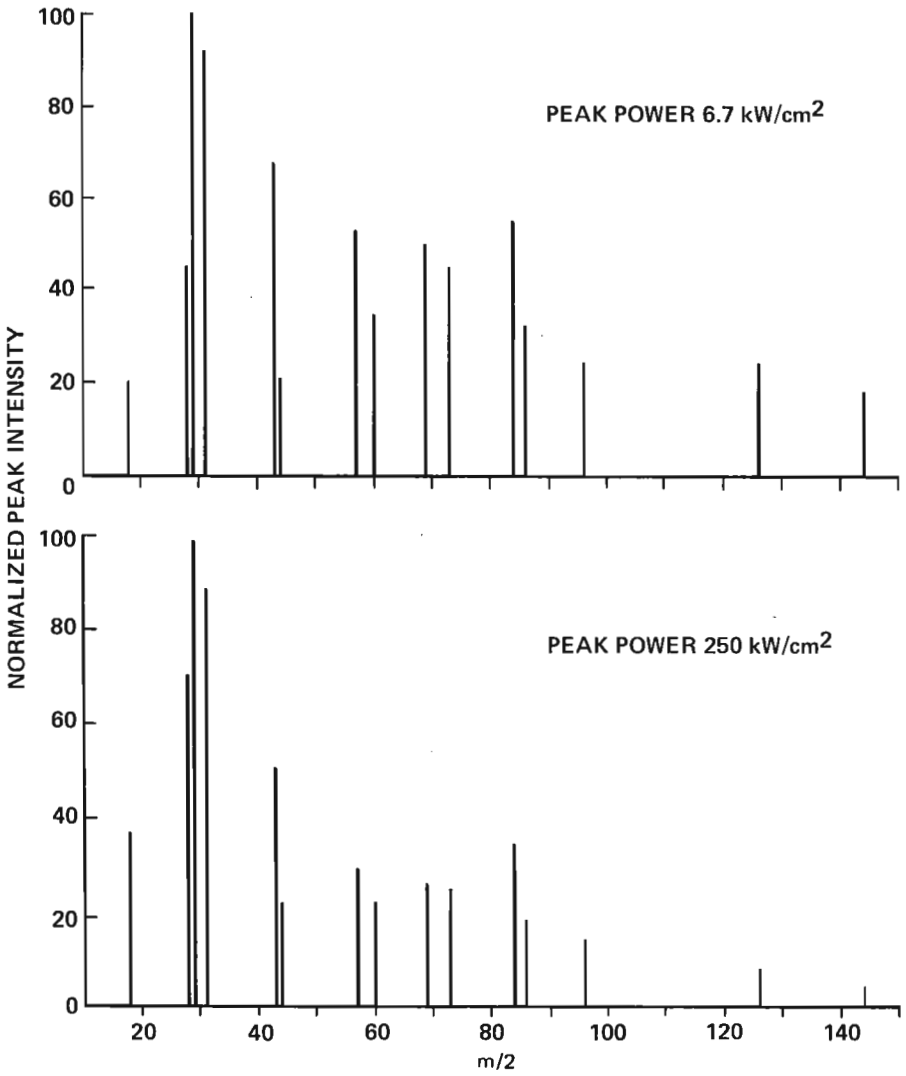

FIGURE 5. ABRIDGED MASS SPECTRA OF LASER-VAPORIZED α-CELLULOSE.

TABLE 2. PYROLYSIS PRODUCTS OF LASER-VAPORIZED CELLULOSE (Analyzed by in situ Mass Spectrometry)

Peak irradiance, kW/cm^2	6.7	250
Energy/pulse, J	1.1	1.1
Exposure time	0.4 msec	0.4 msec
Atmosphere	In vacuo	In vacuo
Mol fraction of products:		
H_2O	0.07	0.15
CO	0.03	0.07
CO_2	0.02	0.02
Volatile organics	0.88	0.76
Tar	None	None
Char	None	None
CO/CO_2	1.5	3.2

low m/z values in the mass spectra are fragments of higher-molecular-weight compounds, but the high m/z values verify that molecular weights of at least that value are present. The mass peaks at m/z 126 and 144 are believed to be from levoglucosan (MW = 162), an example of a volatile compound that would not be detected by the GC system.

To avoid certain errors in acquiring and intrepreting data from the in situ mass spectrometry, some subtle but important instrumental factors must not be overlooked, otherwise the relative concentrations of the condensable vapors with respect to the noncondensables can be severely distorted. This can be best explained by referring to Figure 6, which shows the envelope of one of the laser pulses from which the above data were derived plus the resulting total vapor pulse

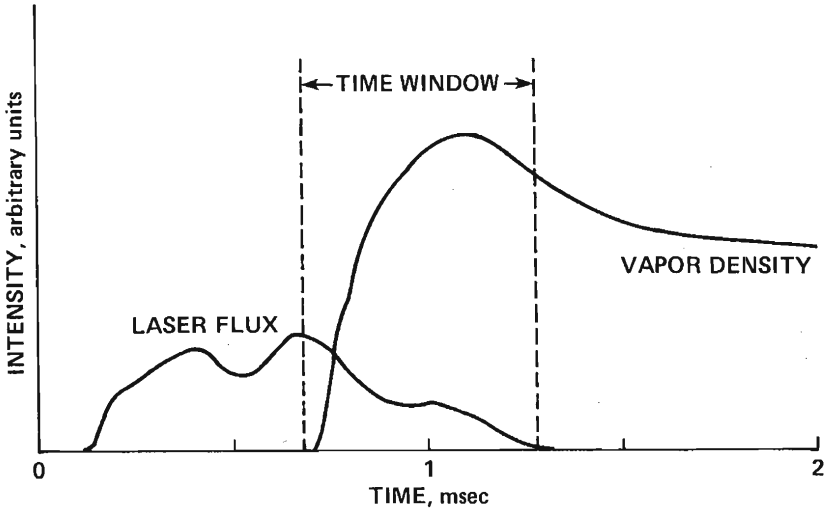

FIGURE 6. LASER PULSE AND RESULTING VAPOR PULSE FROM α-CELLULOSE.

as it emanated from the cellulose target and was detected by the mass spectrometer shown in Figure 4. Despite the irregular shape of the laser pulse in this case, the vapor cloud comes out in a smooth pulse which tails out for 100 msec or more. The condensable vapors are quickly lost to the container walls, but the noncondensable gases persist within the vacuum chamber and cause the long tail whose decay rate is dependent on the speed of the pumping units and the geometry of the system. When spectra are accumulated continuously (as was the case in all of the earlier work), the results tend to exaggerate the amount of noncondensables present. Recently this problem was avoided by gating the mass spectrometer "on" only during a time window of less than 1 msec when the vapor cloud emanating directly from the sample passed through the ion source; as a result, the spectrometer is "off" by the time most reflected vapors can reach the ion source, thus obviating the above discrimination against the condensables.

A large number of mass spectra were obtained from the flash-pyrolysis of α-cellulose, but they have not as yet been translated into their complete chemical components; however, some comparisons of spectra obtained in the earlier work with those obtained recently with the equipment depicted in Figure 4 (where the distance from the sample to the ion gun was about 50 cm) are very revealing. The recent continuous

spectra are quite similar to those obtained from the flashtube-heated samples via the arrangement shown in Figure 2. On the other hand the recent "window" spectra are nearly identical with those from the earlier laser-heated samples via the equipment depicted in Figure 3. In the latter case there is a much greater abundance of high-molecular-weight materials (i.e., more readily condensable organic compounds) evident in the spectra. This difference in spectra is not due to the difference in heating, but to the proximity of sample to ion gun — a factor that tends to give the condensables equal detectability. Hence, it is now evident that the condensable vapors and transient species were adequately included in the analyses only when the sample was close to the ion source or only when the vapor cloud was analyzed during the appropriate time window in cases where the sample was remote from the ion source.

This brief discussion of instrument parameters is included to point out the importance of the sampling techniques in any analysis designed to measure reliably all the products produced by the flash-pyrolysis of biomass. The above provides strong evidence that a large percentage of the condensable materials were lost to detection in the earlier work in which the cellulose was heated inside a quartz tube by a coaxial flashtube. This was the case in which the tubulation was an appendage to the mass spectrometer or in the carrier stream of the gas chromatograph; hence, we are drawn to the conclusion that many of the high-molecular-weight compounds (volatile organics) are missing or surpressed in the gas chromatography results of Table 1; this is particularly true of the data in column 4.

CONCLUDING REMARKS

This work has substantiated the premise that the rate of heating of cellulose makes a profound difference in the composition of the pyrolysis products. It can be inferred from this that pyrolysis proceeds along different reaction paths as the heating rate changes, but caution must be exercised in attributing all the results to this explanation. For example, the amount of char decreases with increasing irradiance to the point where none is produced by laser flash-heating. The surface temperature is believed to exceed 600 °C but not by very much. This is because the preponderance of unpyrolyzed organic molecules present in the vapor indicates that the temperature is significantly below that required to vaporize carbon; hence, it is unlikely that the char is vaporized. Moreover, as the char decreases the tar fraction tends to increase, and so these factors suggest that a change in reaction path occurs as the irradiance (and consequent heating rate) is increased.

Martin [2] has suggested that the char layer becomes hot enough to react endothermically with the mixture of pyrolysis products passing through it. This explanation is plausible at the heating rates produced by the carbon arc, but would appear less likely with the very high irradiances at short times produced by the laser. Under these conditions the tar also disappears, but this does not necessarily reflect a further change in the pyrolysis reaction path. In the first place, thermal cracking appears to occur because there is a shift toward more

smaller molecules with an increase in irradiance. Second, much of the tar really does not disappear, because the in situ spectra clearly show the presence of large molecules, even at the highest irradiance; this indicates that many of those components that make up the tar at lower temperatures are vaporized and escape the heated zone fast enough to avoid cracking. Note that under these conditions the high-temperature zone is extremely thin. The above observations and the data indicating that above some irradiance level a large increase produces only a small change in vapor composition support the conclusion that a maximum ablation temperature is reached and that no further change in reaction mechanism occurs.

It is important to emphasize that in the flash pyrolysis of materials by pulsed, high-flux thermal sources, only a thin layer of the surface of the exposed material is vaporized; thus, it is necessary to clean off the surface or remove it before a meaningful relationship between the vapor products and the bulk material can be established. We have found it most convenient to hit the surface of the sample with several "shots" from the laser prior to analyzing the vapor products produced by a subsequent laser "shot" on the same exposed surface. When samples are so thin that they are vaporized by a single flash, this is not possible; consequently, the vapors may contain a high percentage of surface contaminates.

Another caveat pertains to unsuspected errors that can be introduced by the sampling and analytical techniques employed to measure the relative concentrations of the vapor products from flash-pyrolysis. Where possible, it is best to make in situ measurements close to the vapor source under conditions that do not cause discrimination against high or low molecular weights or against condensable components. In this work we found that although the mass spectrometer itself caused little discrimination, the manner of injecting the vapors into the ion source was extremely critical.

REFERENCES

1. Lincoln, K. A., "Flash-Pyrolysis of Solid Fuel Materials by Thermal Radiation," Pyrodynamics 2 (1965), pp. 133-143.

2. Martin, S. B., "Diffusion-Controlled Ignition of Cellulosic Materials by Intense Radiant Energy," Tenth International Symposium on Combustion, The Combustion Institute, 1965, pp. 877-896.

3. Broida, T. R., "The Production of Intense Beams of Thermal Radiation by Means of a High-Current Carbon Arc and Relay-Condenser Optical System," USNRDL-417, Nov. 1953.

4. Lincoln, K. A., "Flash-Vaporization of Solid Materials for Mass Spectrometry by Intense Thermal Radiation," Anal. Chem. 37 (1965), p. 541.

5. Lincoln, K. A., "Thermal Radiation Characteristics of Xenon Flash-tubes," Appl. Opt. 3 (1964), pp. 405-412.

6. Martin, S. and Ramstad, R. W., "Compact Two-Stage Gas Chromatograph for Flash Pyrolysis Studies," Anal. Chem. 33 (1961), p. 982.

7. Lincoln, K. A., "Mass Spectrometric Studies Applied to Laser-Induced Vaporization of Polymeric Materials," High Temperature Technology. Proceedings of the Third International Symposium, 1967, Butterworths, London, pp. 323-332.

8. Lincoln, K. A., "A New Mass Spectrometer System for Investigating Laser-Induced Vaporization Phenomena," Int. J. Mass Spectrom. Ion Phys. 13 (1974), p. 45.

9. Covington, M. A., Liu, G. N., and Lincoln, K. A., "Free-Jet Expansions from Laser-Vaporized Planar Surfaces," AIAA J. 15 (1977), pp. 1174-1179.

Experimental Procedure

The system was adjusted for maximum light intensity before any experiments were conducted. At the focus of the shallow ellipse, light profiles were scanned with a calorimeter when possible. A thermocouple set inside the reactor was used to do the final adjustment and to give a crude evaluation of the flux level after the addition of the spherical mirror. With the spherical mirror in place, physical space limitations prevented the use of the calorimeter.

One and a half to two grams of white "Avicel" PH102 cellulose were weighed out and loaded in the feeder. The heater tapes and light were turned on and the system allowed to warm up. The downward gas flow through the feeder was set to between 50 and 70 cc/min. Following this, the carrier gas was fed downward through the top of the reactor at about 500 cc/min, purging the system of air for several minutes. All of the gas flows were monitored with rotometers.

The feeder was then started and run until all the 100-200 μm diameter cellulose particles had passed through the reactors. A typical run lasted about five minutes, depending on the amount of material in the feeder and the rate of feed.

After a run, the material collected in the bucket and the condensors was weighed. Material deposited on the reactor walls and tubing was collected by washing these surfaces with methanol followed by acetone. The volume of gas collected in the sample bag was also measured. The collected gases were then analyzed with a chromatograph.

Results

Several runs were performed and the amount of pyrolysis was minimal. To increase the residence time of the particles in the "hot spot" the light source was changed to a 2000W bulb, and a front surface spherical mirror was placed behind the reactor to increase the integrated flux incident on the surface of the particles. With careful adjustment of this spherical mirror the peak flux was increased to 150 W/cm^2. The light profile remained almost unchanged. These conclusions were reached by running the light bulb at a low voltage and using a thermocouple probe which had been "calibrated" against the calorimeter.

Under these circumstances there was an increase in the amount of cellulose which underwent pyrolysis. Nevertheless, more than 50% of the material was collected in its original form.

To improve the light absorptivity, black carbon was added to the white cellulose in a 1 to 9 blend by weight. At least 40% of the material was still not pyrolyzed.

Another configuration of the reactor was attempted. The steam was fed into the reactor from the bottom and now traveled counter-current to the direction of flow of the cellulose particles. This was intended to slow down the particles; thereby increasing their residence time in the light flux. Very high steam flows (up to 3 g/min) were used and no significant improvement in the pyrolysis was observed. One problem was the difficulty in handling particulates with different diameters. The terminal velocity of the particles is a function of the square of the diameter [19], thus their deceleration is a strong function of their size.

The experimental system described in the preceding sections was capable of marginal performance at best. The temperature of the quartz wall around the focus was not homogeneous due to the asymmetry of the configuration. This caused many particulates to miss the most intense radiation zone due to convection currents which developed in the gas flow.

To overcome the problems associated with this configuration an improved pyrolysis system was assembled, as described in the following section.

THE VERTICAL AXIS SYSTEM

Experimental Set Up

The vertical axis system employed two ellipses with major and minor semi-axes of 49.8 and 33.4 cm respectively to focus the light from a 5 kW tungsten-halogen bulb. A flat, front-surface mirror was used to redirect the light beam to a vertical orientation. This was to permit the use of an optical bench to support one ellipse and the bulb. Figure 4 illustrates the configuration.

The main advantages of this new configuration were the symmetry of the ellipses with respect to the reactor's axis, and its ability to position a cylindrical mirror concentric to the reactor. This mirror increased the length of the intense light zone by trapping some of the radiation inside the upper part of the reactor.

A minor complication with the system was the necessity of cooling the flat mirror to enable it to withstand large light intensities without shattering. The mirror lay against a water-cooled copper plate which functioned as a heat exchanger. Thermocouple readings showed that without cooling, the center of the mirror was heated to above 200°C by the focused light.

The cylindrical mirror was prepared by platinum ion sputtering both sides of a quartz tube. Radiant energy entered the reactor and was trapped within this cylinder. The mirror trapped a significant amount of radiation, since a temperature high enough to initiate wood pyrolysis [20] existed even at four inches above the focus. Unfortunately, the half-life of the platinum coating was not very long due to the degradation which occurred at these high temperatures. To extend the cylindrical mirror life, the feasibility of increasing the coating's

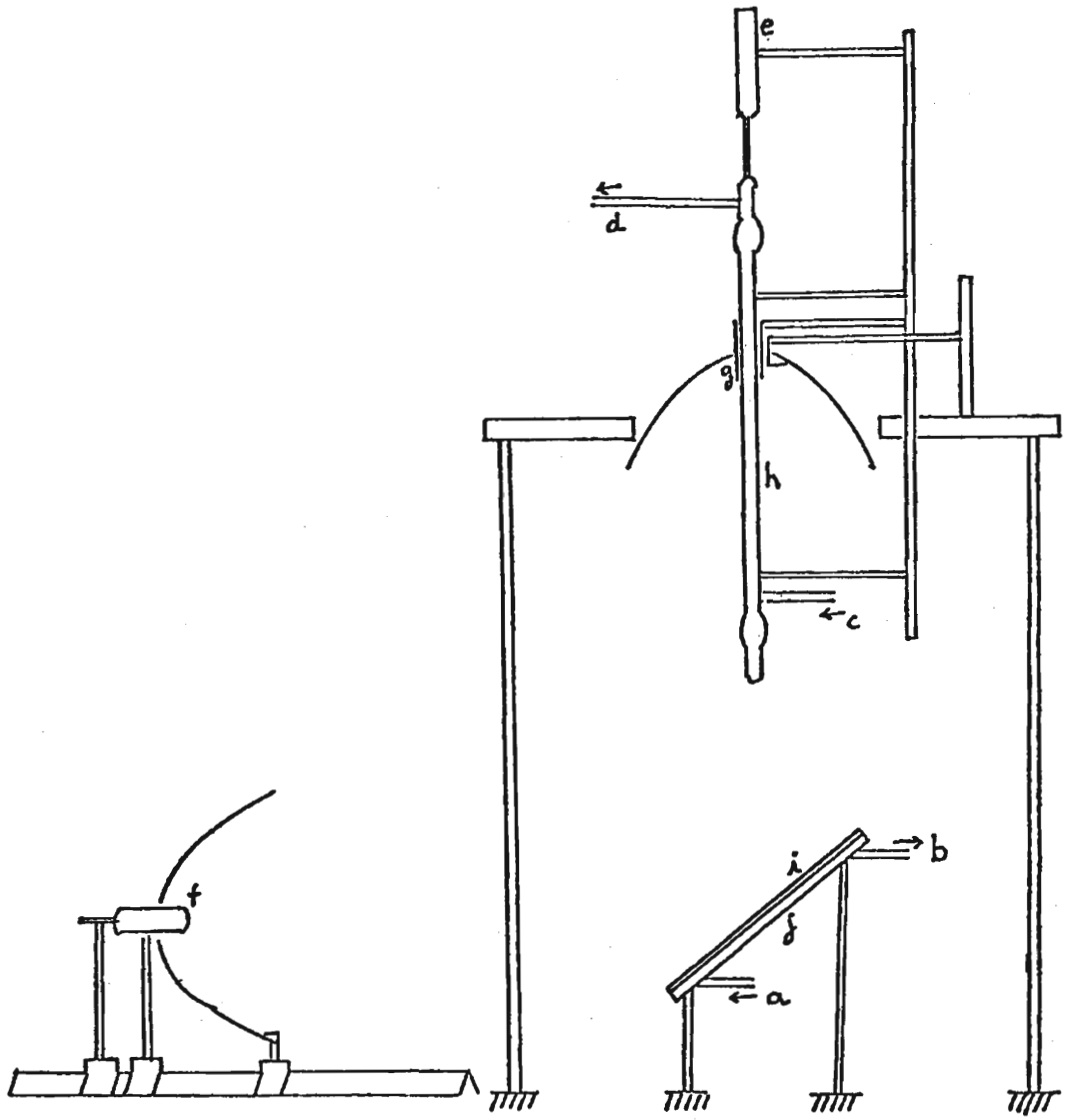

a- water inlet
b- water outlet
c- gas inlet
d- gas outlet
e- vibrating feeder
f- light source
g- cylindrical mirror
h- quartz reactor
i- plane mirror
j- cooling mirror jacket

FIGURE 4. EXPERIMENTAL LAYOUT FOR THE VERTICAL AXIS SYSTEM

thickness, or of using a different material for a preliminary coating, is being investigated. The cylindrical mirror was not used with the first experiments which employed a two inch diameter reactor.

The ellipsordal mirrors used in the horizontal system had to be replaced by larger units because of the additional heat generated by the 5 kW light bulb. Even these bigger ellipses required air cooling to prevent the temperature of their surface (aluminum coated with rodium) from rising above 250°C. This is the upper operating temperature recommended by the manufacturer. As noted earlier, symmetrical ellipses are not the most efficient system for collecting light radiated by extended sources, but the availability of relatively inexpensive large units outweighed the loss in efficiency. The decrease in efficiency is calculated to be on the order of 10% of what could be achieved with the best system investigated.

The first reactor used in this system was fabricated from two inch diameter quartz tubing. It consisted of a main body with spherical ball joints at the top and the bottom, as shown in Figure 4. This reactor was designed to accommodate an increased throughput of biomass. It was also hoped that the larger diameter would prevent the particulates from hitting the wall during their downward journey.

The particulate biomass material was introduced into the top of the reactor either by the vibrating feeder described earlier or by an Acrison model 150Z-A screw feeder.

The experimental procedure was the same as before; however the superheated steam, CO_2, or N_2 was introduced into the bottom of the reactor flowing upward countercurrent to the direction of the falling particulate matter. The teflon bags used previously for gas collection were replaced by a liquid displacement system to allow for greater accuracy in gas volume measurement.

Results

It soon became clear that very few of the falling particles were passing through the "hot zone" along the central axis of the reactor. Most fell along the wall. Temperature profiles obtained with the thermocouple showed that the center of the reactor was hotter than the wall area. This caused convection currents, moving outward from the central axis, to carry particulates out of the intense light zone. Even using a 5 kW bulb, the spot diameter was small compared with the two inch reactor diameter.

In view of the difficulty, a one inch diameter reactor was built, and the five inch long cylindrical mirror added. All of the other parts of the system remained the same.

With this arrangement, higher temperatures at the wall than at the center of the reactor were recorded. If pronounced convection currents formed, they would push particles to the center, thus improving pyrolysis. It is also evident that the particulates will travel at least

three inches in a zone where the temperature is high enough to induce pyrolysis.

Several runs, using Avical PH102 cellulose, Kraft lignin and ground corn cob material were conducted, but the amount of pyrolysis was never complete. Mass balances and gas analyses were performed and data from the best runs are presented in Table II.

Discussion of Results

From these results it is obvious that a good mass balance was achieved, but the amount of pyrolysis was never better than 50% by weight of the feed material. Complete pyrolysis is not an imperative result, since biomass can be submitted to more than one pass through the reactor in commercial applications.

The fact that the concentrated radiant energy available at the inner focus of the downward facing ellipse has the characteristics of both an upward and a downward facing beam has been a source of some difficulties. The effectiveness of a cavity as a radiant energy trap is reduced because the focused radiant energy has no dominant orientation. Also, a cavity designed to trap upward directed radiation tends to obscure the downward radiation. Although deep ellipsoids are much less expensive than large paraboloids, the complexity and operating characteristics of ellipsoidal systems make them less desirable than systems based on paraboloids.

The solids collected after an experiment consisted of unpyrolyzed feed material and char. A method of separating these two components has not yet been devised, but from visual inspection it appears that the mixture is mainly unpyrolyzed biomass. If the assumption is made that all of this mixture is unconverted feed material, then subtracting the total solids collected from the original sample weight gives the amount of solid material that was actually pyrolyzed. Using this method, it can be shown that the percentage yields of liquids from the feed material is 54%, 30%, 69%, and 24% for runs 1, 2 3 and 4 respectively.

The high percentage yield of liquids from Run 1 is probably due to the fact that the lignin, which was the feed material, is soluble in the cleaning solvents. This solubility caused some material which should have been accounted for as unpyrolyzed solids to be added into the liquids, thus distorting the results for this run.

A possible explanation for the difference in liquid production between the vacuum run and the remaining two runs is based on the heat transfer phenomena occurring in the reactor. It is well known [21] that solid biomass undergoes pyrolysis at temperatures below 500°C and that gas phase reactions should occur at temperatures of about 700°C. According to the currently accepted mechanism for cellulose pyrolysis [22,23], most of the pyrolysis products should be complex organic molecules (sugars). The high liquid yield obtained from the vacuum experiment seems to indicate that in this run the reactor was performing as expected, so that no gas phase reactions were occurring.

TABLE II

EXPERIMENTAL RESULTS FROM VERTICAL AXIS SYSTEM

		Run 1	Run 2	Run 3	Run 4
Day		4/29/80	5/9/80	5/13/80	5/29/80
Sample material		Lignin	PH-102 Cellulose	PH-102 Cellulose	Wood
Sample weight (gm)		1.01555	2.2303	2.4518	2.0504
Total solids collected (gm)		0.6454	1.0409	2.0951	0.7630
Total liquids collected (gm)		0.2008	0.3552	0.2456	0.3058
Carrier gas (at 50 cc/min)		N_2	N_2	N_2	N_2
Steam flow (gm/min)		0.898	1.25	vacuum	2.09
Total gas collected (cc)		500	1500.1	n.a.	969
Total gas produced (cc)		--	709.5	n.a.	--
Gas elementary composition		--	35.5% C (volume base)	n.a.	--
		--	28.5% H (volume base)	n.a.	--
		--	31.7% O (volume base)	n.a.	--
Gas detailed analysis (% by weight)	CO_2	--	10.6%	--	8.04
	H_2	--	1.99	--	17.10
	N_2	--	0	--	27.29
	CO	--	69.1	--	35.14
	CH_4	--	6.21	--	7.20
	C_2H_4	--	7.18	--	3.95
	C_2H_6	--	0.85	--	0.38
	C_3H_6	--	3.01	--	0.41
	C_3H_8	--	0.26	--	0.13
	C_4	--	0.78	--	0.36
	Total:		100.00		100.00
Gas calorific value (Btu/Scf)			491.5		

The inert gas which flowed upwards through the reactor in the other two runs may have had an adverse effect on the reactor's temperature profile. Ideally, the inert should help to decouple the solid and gas phase reactions by diluting and cooling the evolved volatile matter so that no gas phase reactions will occur. However, the inert will absorb heat from the falling particles and the wall by convection and conduction. If enough heat is transferred to the inert, it could in turn act to heat the pyrolysis products instead of cooling them, and thus cause gas phase reactions to occur. The occurrence of gas phase reactions would explain the lower liquid production from these two inert runs.

CONCLUSIONS

There are no inexpensive optical sources which adequately simulate the intense radiant energy flux available at the focus of a good solar furnace. Research efforts which require high flux levels on the bench should plan on constructing or accessing an arc image furnace with a xenon lamp. Many of the problems discussed in this paper could have been avoided through the use of an arc image furnace.

The products of radiant flash pyrolysis may be either liquid syrups or permanent gases, depending upon reactor conditions. Syrups are favored by low gas phase temperatures and short residence times, whereas permanent gases are favored by high gas phase temperatures. Thus the ability of the radiant flash pyrolysis reactor to decouple the gas from the solid phase temperature makes it unusually flexible, providing for the selective production of either liquids or gases. Clearly much more research is required to better define the limits of selectivity, and to identify markets for the syrups.

REFERENCES

1. Antal, M. J., Feber, R. C. and Tinkle, M. C., "Synthetic Fuels from Solid Wastes and Solar Energy," Proceedings of the World Hydrogen Energy Conference, Miami (1976).

2. Antal, M. J., "High Temperature Pyrolysis Using Solar Process Heat," Report on the Symposium and Workshop on the $5Mw_{th}$ Solar Thermal Test Facility, Houston (1976), ALO/3701-76/1.

3. Antal, M. J., "Tower Power: Producing Fuels from Solar Energy," in Towards a Solar Civilization, R. Williams ed., MIT Press, Cambridge (1978), pp. 80-84.

4. Antal, M. J., "Tower Power: Producing Fuels from Solar Energy," Bull. Atom. Sci., Vol. 32, (1976) pp. 58-62.

5. Antal, M. J., "The Conversion of Urban Wastes," International Symposium on Alternative Energy Sources, Barcelona, Spain (1977).

6. Antal, M. J., "Results of Recent Research on the Use of Pyrolysis/Gasification Reactions of Biomass to Consume Solar Heat and Produce a Useable Gaseious Fuel," Proceedings of the STTF Users Association 1978 Annual Meeting, Denver (1978).

7. Antal, M. J., "Solar Flash Pyrolysis: Syngas from Biomass," Proceedings of the Solar High Temperature Industrial Processes Workshop, (1978) Atlanta.

8. Antal, M. J., "The Effects of Residence Time, Temperature and Pressure on the Steam Gasification of Biomass," American Chemical Society Division of Fuel Chemistry (1979), Honolulu.

9. Antal, M. J., "Synthesis Gas Production from Organic Wastes by Pyrolysis/Steam Reforming," IGT's Conference on Energy from Biomass and Wastes (1978), Washington.

10. Antal, M. J., "Biomass Energy Enhancement. A Report to the President's Council on Envoronmental Quality" (1978).

11. Antal, M. J., Rodot, M., Royere, C., and Vialaron, A. "Solar Flash Pyrolysis of Biomass," ISED Silver Jubilee 1979 International Congress, (1979) Atlanta.

12. Moreira, J. R., and Antal, M. J., "Gasification of Biomass as a Source of Synfuels for Developing Countries," 2nd Miami International Conference on Alternative Energy Sources, (1979) Miami.

13. Antal, M. J., Rodot, M., Royere, C. and Vialaron, A., "Biomass Gasification at the Focus of the Odeillo (France) 1 Mw_{th} Solar Furnace," American Chemical Society Symposium on Thermal Conversion of Solid Wastes and Biomass (1979), Washington, D.C.

14. McDanal, A. J., "Optical Analysis of Paraboloidal Concentrator with Secondary Reflectors," 1979 International Congress - Joint Meeting with the American Section of the International Solar Energy Society, May 28 - June 1 (1979).

15. Handbook of Chemistry and Physics, 52nd Edition, The Chemical Rubber Co., Cleveland, Ohio, 1971/72.

16. General Electric, Commercial and industrial Lamp Catalog.

17. Rabl, A., Solar Energy 18 (1976), pp. 93-111.

18. Sherber, M. S., "High Irradiance Pyrolysis of Cellulose with Applications to Biomass Gasification with Solar Process Heat," BSE Thesis, Princeton University, Princeton, N.J., unpublished.

19. Bird, R. B., Steward, W. E., Lightfoot, E. N. "Transport Phenomena," John Wiley and Sons, Inc. (1960), p. 60.

20. Antal, M. J., "Biomass Energy Enhancement - A Report to the President's Council on Environmental Quality," (1978) Princeton University, Princeton, N.J.

21. Antal, M. J., "Thermochemical Conversion of Wood (Biomass) to Liquid and Gaseous Fuels," Internal Report, Department of Mechanical and Aerospace Engineering, Princeton University, Princeton, N.J., 1979.

22. Shafizadeh, F., "Industrial Pyrolysis of Cellulosic Materials," Proceedings of the 8th Cellulose Conference, T. E. Timell (editor), Interscience, (1975), N.Y.

23. Broido, A., "Kinetics of Solid Phase Cellulose Pyrolysis," in "Thermal Uses and Properties of Carbohydrates and Lignins," Shafizadeh, F. et al. (ed.), Academic Press, New York, 1976.

BENCH SCALE RADIANT FLASH PYROLYSIS OF BIOMASS

M. J. Antal
L. Hofmann
J. R. Moriera

Princeton University
Department of Mechanical and Aerospace Engineering
Princeton, NJ 08544

ABSTRACT

The results of continuing research at Princeton University on the radiant flash pyrolysis of biomass as a source of fluid fuels, industrial feedstocks and chemicals is described in this paper. Bench scale sources of intense, visible radiant energy have been used to simulate the concentrated solar flux available at the focus of solar towers. Windowed transport reactors have been developed, which act as cavity receivers for the focused radiant energy and provide a means for direct use of the radiation to rapidly pyrolyze the entering biomass. Detailed results of bench scale experiments are presented, which suggest the use of concentrated radiant energy as a selective means for the production of sugar related syrups from biomass by flash pyrolysis.

INTRODUCTION

The flash pyrolysis of biomass requires a source of high quality heat. Early work at Princeton [1-7] identified concentrated solar radiation as an attractive means for rapidly heating the biomass and thereby achieving flash pyrolysis. When used in this fashion the solar heat input is effectively stored in the form of a fluid fuel. This storage aspect overcomes some of the problems associated with the intermittent nature of solar heat. The energy of the biomass feedstock is preserved by the use of an external heat source for pyrolysis, so that the product energy leaving the reactor is equal to or greater than the feedstock energy entering the reactor. Because the solar heat input is only about 10% of the biomass energy throughput, the cost of the solar concentrator plays only a small role in the overall economics of the system. Thus the useful energy output of a solar concentrator system is magnified by about a factor of ten when the solar heat is used to pyrolyze biomass; in contrast with electric power production which reduces the useful energy output of the concentrator by a factor of three. Experimental work at Princeton suggests that the yields of valuable chemicals such as ethylene may be enhanced through the use of

radiant energy for flash pyrolysis [8,9]. Economic projections [10, 11] indicate that the enhanced production of chemicals from biomass using conversion methods based on radiant flash pyrolysis should be very attractive to the hydrocarbon processing industry. The use of concentrated solar radiation for biomass pyrolysis also holds promise for developing countries [12].

This paper describes bench scale experimental work using artificial sources of intense radiant energy which is being performed to support the development of radiant flash pyrolysis reactors. Because of our experience using the Odeillo $1Mw_{th}$ horizontal beam solar furnace [13], we initially chose to build an artificial source of intense radiant energy with a horizontal beam. One of the reactors taken to Odeillo was used with this horizontal beam furnace to recreate the Odeillo experiments under more controlled conditions. This reactor operated vertically, with the flux of radiation directed normal to the flow of the biomass particles. As discussed in the following sections, this experimental configuration was only marginally successful. More recent work has emphasized the development of vertical beam furnaces operating with axially concentric, vertical windowed transport reactors. This work has enjoyed better success, and has revealed the possibility of achieving very high yields of liquid products due to the unique ability of concentrated radiant energy to sustain two characteristic temperatures (gas and solid) within the reactor.

SOURCES OF INTENSE RADIANT ENERGY

Since solar radiation as intense as 1000 W/m^2 is sometimes available, and concentration ratios of 10,000 have been achieved [14], some experimental solar furnaces are able to supply radiation in excess of 1000 W/cm^2. To simulate these intense energy fluxes in the laboratory it was necessary to develop an optical system which could focus light from an artificial source. Currently available high intensity light sources are tungsten-halogen lamps, xenon lights, and carbon arcs. These lights produce radiation with a spectrum similar to that of a black body radiating at a temperature of about 3000°C, 6500°C or 5500° C, respectively. According to the Stefan Boltzman Law for a black body radiator, these temperatures produce theoretical maximum radiation intensities of 450, 10,000 and 5000 W/cm^2.

Xenon lights are the most intense of the three, but they have several disadvantages: a small arc size which leads to a small, intense spot of radiation when the light is properly focused, very expensive, complex RF equipment for lamp ignition, and a high level of ultra-violet radiation requiring various protective measures. Carbon arcs have light intensity instabilities associated with fluctuations in the distance between the carbon rods; they also produce undesirable gases when burned in air. Halogen-tungsten bulbs are the least intense of these lights, but can easily be ordered in a variety of physical sizes, configurations, and power levels. They are also the least expensive option, and present the advantage of simple control of the light intensity through a conventional variac.

Previous experiments had shown that biomass particles several hundred microns in diameter could be pyrolyzed by solar radiation of about 100-200 W/cm^2, if the residence time of the particles in the flux was on the order of 1/10 th of a second [13]. This light intensity should be attainable from tungsten-halogen bulbs, since their brightness temperature, T, is approximately 3200°K, and the emissivity of tungsten is .45 [15]. The heat radiated by a grey body is given by $q = \varepsilon\sigma T^4$ where $\sigma = 5.7 \times 10^{-8}$ $W/m^2°K^4$. It is easily shown that q = 270 W/cm^2 for a tungsten halogen bulb. For our application, tungsten halogen bulbs ranging in power from 750 to 5000 W were chosen.

THE OPTICAL SYSTEM

Since large plastic Fresnel lenses are very inexpensive, and narrow beam flood lights up to 1000 W are commercially available, an optical system which could utilize these two components was considered. Several of the flood lights could be distributed in a circle around the reactor. A separate Fresnel lens would focus each light onto the reactor's wall. This design was abandoned due to the necessity of keeping each Fresnel lens, which absorbs as much as 10% of the incident light, in a cooling bath, as well as the separate positional adjustments needed for each of the several sources.

Another configuration was analyzed in which several flood lights would illuminate a large parabolic mirror. This mirror would then concentrate all of the light into its focus. Since the typical divergence of the narrow beam flood light is at best 5° [16], the theoretical concentration ratio would be 400 times less than what could be achieved with solar radiation [17]. Some radiation intensity measurements were performed with the flood light and a 36 inch parabolic mirror. Light intensities no higher than 15 W/cm^2 were obtained.

Previous work with elliptical mirrors having an acceptance angle as large as 70% of the total solid angle had provided peak light intensities of 40 W/cm^2 [18], with the light distributed over several square centimeters. This system, together with a second ellipse, was the one finally chosen for use as a solar simulator. The second ellipse used the image produced at the secondary focus of the first ellipse as a light source, and re-imaged it to the primary focus of the second ellipse. This system was able to provide flux intensities up to 150 W/cm^2, distributed over an area very similar to that of the tungsten filament. For a point source, this arrangement should provide its maximum intensity when two symmetrical ellipses are used and set at a distance such that their secondary focii overlap.

Symmetrical ellipses can be very difficult to use in practical applications, because the large solid angle required for efficient light collection in one of the ellipses will interfere with the reactor mounted at the main focus of the other. Also, although there are a variety of relatively inexpensive tungsten filament light bulbs available up to 5000 W, they all present an almost constant irradiance per square centimeter. This means the higher the power of a bulb, the larger its filament area. Since large filaments depart appreciably

from point sources, it is difficult to anticipate their magnification in an optical system. For these reasons a computer simulation algorithm was developed to investigate the best optical configuration.

The algorithm was based upon ray tracing techniques, selecting a few thousand random rays through a Monte-Carlo calculation. Due to the bi-dimensional geometry used by the code, only an approximate simulation was performed for those configurations which have a lack of symmetry. A three dimensional code could easily be constructed to overcome this approximation, but the time required for computation would increase significantly. Several important points were learned from the code, some of which can be extracted from the data shown in Table I.

1. The largest dimension of the filament must always be parallel to the y-axis, instead of the x-axis (see Figure 2). Orienting the filament in this manner gives a better image (small magnification) and a higher light collection efficiency.

2. A configuration of two symmetrical ellipses does not necessarily give the maximum light collection efficiency for an extended light source. This is because some of the light emitted from the filament extremes will not be collected by the second mirror, even if their angle of departure, measured with respect to the line that contains both focii, is small.

3. The overall efficiency of the system increases when the ellipses are closer than the ideal position for a point source, since less light is missed by the second mirror.

4. The best distance of separation for the ellipses is not well defined since the size of the spot (magnification) is not strongly affected by the first 10% variation from the "ideal" position for a point source.

5. The addition of a spherical mirror to re-image light to the focus of the first ellipse, F1, theoretically can increase the system efficiency. From a practical point of view its inclusion is almost useless when deep ellipses are used, since the ellipses usually have a hole to allow for bulb positioning and the light re-imaged to F1 will either escape through this hole or will intercept the bulb base before reaching the primary reflector surface. A significant increase in light collection is observed only when a shallow ellipse is being used. A shallow ellipse plus a spherical mirror can be as efficient as a deep ellipse.

6. A two paraboloid system can also be used and the light collection efficiency as well as the magnification compete with the two ellipse system, provided a spherical mirror is added to re-image the forward light back to the focus. In particular, a commercial very narrow beam flood light with a divergence of 5°, plus a large paraboloid provided light intensities of the order of 50% of what was achieved with a two ellipse system.

TABLE I

COMPUTER CODE RESULTS

	Solid angle efficiency of 1st ellipse[5] (%)	Total efficiency of the system (%)	Image size along y direction (cm)
Large ellipse + shallow ellipse filament along y[1]; D[2]= 173.6 cm	75.5	34.8	.90
Large ellipse + shallow ellipse filament along y; D = 163.6 cm	78.2	37.5	1.12
Large ellipse + shallow ellipse filament along y; D = 153.6 cm	76.9	41.4	1.35
Large ellipse + shallow ellipse filament along x; D = 153.6 cm	77.6	30.0	1.58
Symmetrical shallow ellipses filament along y; D = 149.1 cm	46.5	21.5	1.08
Symmetrical shallow ellipses filament along y; D = 149.2 cm plus spherical mirror[3]	47.5	31.6	.90
Symmetrical shallow ellipses filament along y; D = 149.2 cm plus spherical mirror[4]	53.8	31.5	.90

1) Filament length, 3 cm.
2) D, distance between primary focal points of the two ellipses.
3) Spherical mirror, radius = 5 cm, thickness = 4 cm.
4) Spherical mirror, radius = 6 cm, thickness = 4 cm.
5) Provides useful test of the code. Geometrical efficiency for point source is 75%.

In summary, it is apparent that for filament sizes up to 5 cm the double ellipse system is relatively insensitive to slight variations in mirror displacement from the "best" configuration. (Figure 1)

Several measurements of light intensity distribution were made using a water cooled calorimeter or a thermocouple, and compared against the results from the computer code calculations. Figure 3 displays a comparison between typical experimental and calculated light intensity profiles.

THE HORIZONTAL BEAM SYSTEM

Experimental Set-Up

The main components of the optical system used for the horizontal beam experiment are a deep and shallow ellipse pair. The arrangement of the system is presented in Figure 2. The deep ellipse with semi-axes of 46.7 and 22.1 cm was used to collect light from the tungsten bulb. The shallow ellipse with semi-axes of 49.8 and 33.4 cm produced a focused bulb image inside the reactor. An optical bench was used to support the deep ellipse and the light bulb. The shallow ellipse was attached to a table. All three components could be displaced in the x, y and z directions. In the later experiments a 90 mm diameter spherical mirror was added to the system. This mirror reconcentrated the light after it crossed through the reactor in an attempt to use the light flux twice.

The light source for the first system was a 650 W quartz halogen bulb. In all the pyrolysis systems the light bulb received electrical power from a 120 V/60A variac to permit control of the light intensity.

The reactor used in the first pyrolysis experiment was fabricated from a one inch diameter quartz tube, 15 inches long, as depicted in Figure 1. Quartz was used as the material for all the reactors due to its ability to transmit and withstand intense radiant energy fluxes. A quartz bucket was placed in the bottom of the reactor to catch char and any unpyrolyzed material. The inlet and outlet lines of the reactor were wrapped with electrical heater tape and asbestos. Thermocouples and variacs allowed the temperature to be kept between 160 and 180°C. This prevented steam condensation but did not initiate pyrolysis of the biomass feed.

After leaving the reactor, the evolved volatile matter passed through a series of two condensers located in ice-water baths. The gases that left the second condenser were collected in teflon gas tight sample bags for later analysis.

Biomass, along with a continuous flow of inert gas, was introduced into the top of the reactor via a vibrating feeder. The gas flow was needed to aid in the solids feeding process, and also to prevent a flow of pyrolysis products or steam back into the feeder.

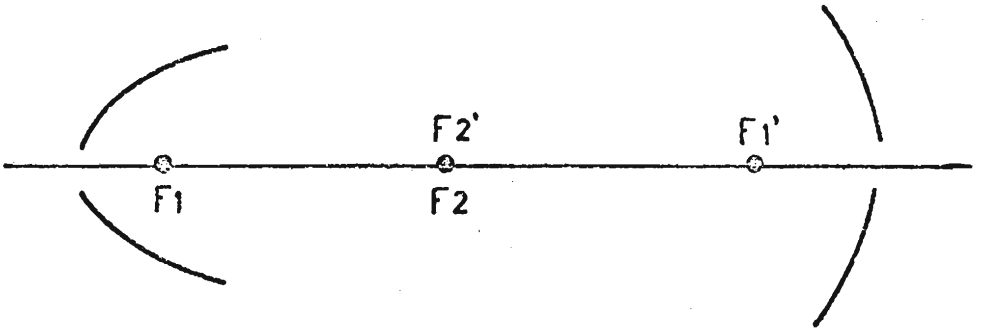

FIGURE 1. BEST CONFIGURATION FOR A TWO ELLIPSE SYSTEM

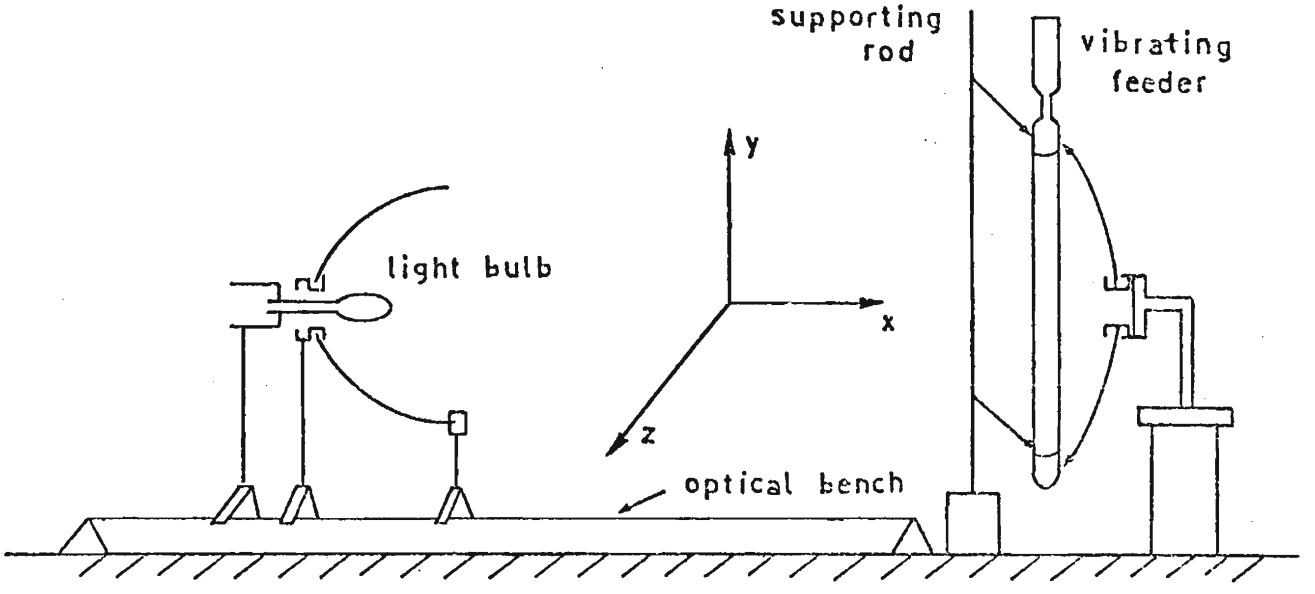

FIGURE 2. SKETCH OF THE HORIZONTAL AXIS SYSTEM.

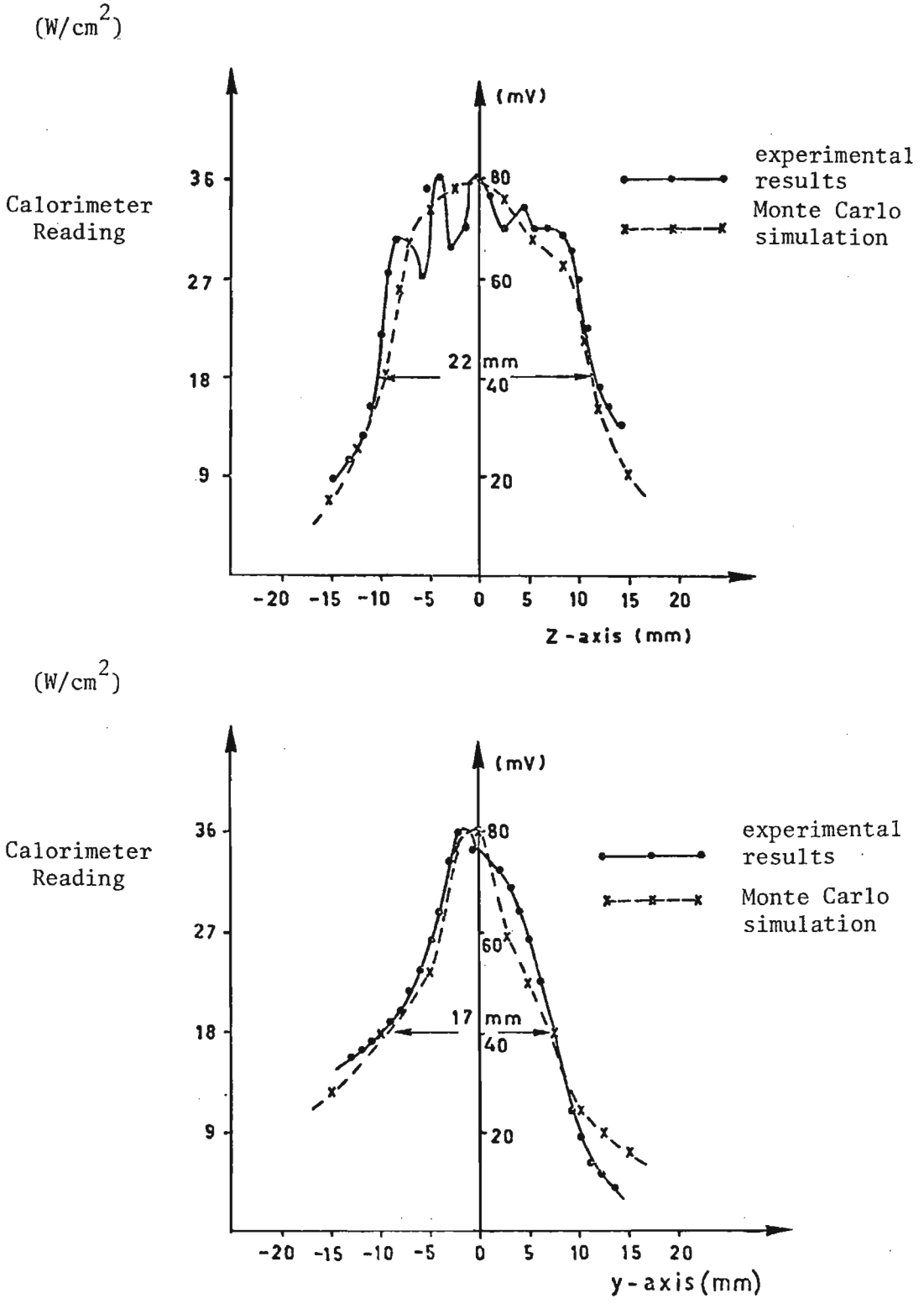

FIGURE 3. MEASURED LIGHT INTENSITY PROFILES (2000 W BULB AT 50 VAC).

A Comparison of Heating Techniques on the Pyrolysis of Douglas Fir

Kent J. Voorhees and Lloyd J. Hendricks
Department of Chemistry and Geochemistry
Colorado School of Mines
Golden, Colorado 80401

ABSTRACT

The effect of heating rate and heating times on the product distribution of the light hydrocarbons (methane, ethene, ethane, ethyne, propene, propyne-allene and butene) for the pyrolysis of Douglas Fir has been investigated. The methane/ethene ratio was affected to the greatest extent by varying the heating rate. A large methane/ethene ratio was observed for the slowest heating ratio (0.25°C/msec). The concentration of ethane-ethyne was observed to increase dramatically as longer constant temperature heating times were employed. It was speculated that char degradation produced the larger quantities of ethane-ethyne.

A review of the literature indicates there are many different techniques available for conducting pyrolysis experiments. It appears that many of these approaches were designed simply to provide heat without serious consideration of the resulting pyrolysis parameters (heating rate, heating time, etc.). Because the product distribution in the pyrolysate is dependent on these parameters, it is almost impossible to make any direct comparison between the various pyrolysis processes. In general, there has been no serious attempt to define the overall effect of the pyrolysis parameters on the product distribution. This paper presents an initial study on the determination of the effect of heating rate and heating times on the product distribution for the light hydrocarbons (methane, ethene, ethyne-ethane, propene, propyne-allene and 1-butene) resulting from pyrolysis of Douglas Fir.

EXPERIMENTAL

The product analyses were conducted using a Hewlett Packard 5710 gas chromatograph with a 1/8" x 8' stainless steel Chromosorb 101 column. The column was routinely temperature programmed from 30°C to 220°C at 12°C/min. Helium was used as the carrier gas. The signal from a flame ionization detector was electronically integrated using a Columbia Scientific integrator. Response factors as defined by Dietz [1] were used in all calculations.

The pyrolysis experiments for the heating rate studies were done on a Chemical Data System Pyroprobe unit using the filament probe. Heating profiles for the pryoprobe have been reported [2] to be non-linear during the last 20 percent of the heating process. Therefore, 1000°C was chosen for the final temperature with expectation that µg quantity samples would be completely pyrolyzed before reaching the non-linear portion of the temperature profile.

The preparation of the pyrolysis samples was accomplished by first grinding the wood to pass a 120 mesh sieve followed by suspending 5 mg of the particles in 1 ml ethyl alcohol. The suspended mixture (2 µl) was carefully applied across the center portion of the ribbon. Removal of the alcohol was accomplished by preheating the sample for 20 sec at 125°C. The interface for the pyroprobe was maintained at 200°C and final pyrolysis interval was 5 sec.

The heating time parameter was evaluated using a 10.6 micron continuous-wave carbon dioxide laser, with a maximum power output of about 20 watts. Fifteen watts were used for this study and was attained with a pressure of 20 torr in the 6-foot tube at a discharge current of 37.5 ma at 19.5 kV. The beam from the laser was focused down to about 1 mm diameter using a short focus germanium lens. Heat dissipation in the irradiated substrate prevents the size of the heated spot being made smaller than this size. At this power level and spot size, the power density was calculated as 7.4kW/cm^2. This spot size is much larger than theory would predict. Estimating the actual power density for the focused spot in air using the 1-inch focus lens suggests that the power level was about 0.80 MW/cm^2.

The sampling chamber for the laser pyrolysis products consists of an outer chamber, containing a nitrogen atmoshere at slightly more than atmospheric pressure, and an inner microchamber of about 0.6 cm^3 volume. The chamber is illustrated in Figure 1. The inner chamber is sealed to the sample material with a Teflon gasket. The focused laser beam was admitted at the front of this chamber through a sodium chloride window. At the bottom of the inner chamber is a jet for introduction of the sweep gas and at the top is the gas-sample exit. Because of the design of the microchamber, any leakage is always in such direction that the inert atmosphere of the outer chamber is

forced to pick up sample from the laser plume and carry it to the collection point.

The outer chamber, besides surrounding the sample in an inert atmosphere, also contained a drive screw attached to the sample-holder. This mechanism positioned the sample precisely for organic microstructure mapping, as well as rapidly moving the sample such that a fresh surface was supplied for pyrolysis. The equipment has been described in more detail [3].

The temperature measurement of the focused laser beam was made using an optical pyrometer [4]. The sensitive spot of the pyrometer has a size comparable to the laser spot size. Therefore, two readings of the weight-average temperature obtained at two different sample-to-pyrometer distances yields sufficient data, when combined with the projected spot size data, for the temperature distribution parameters to be calculated. A piece of fired Colorado clay crucible wall was used for the temperature measurement sample since it has a much slower ablation rate than most materials. This method gave a maximum temperature of 2255°C on that material, with a standard deviation of 1.55 mm in the spacial distribution of the temperature. With Douglas Fir, the temperatures were about 245°C higher than for the clay, but the rapid ablation rate prevented a complete temperature distribution measurement. The higher indicated temperatures in the wood were probably due to the very deep crater produced in the wood, which served as a more efficient black-body cavity than the shallower cavity in the clay crucible.

RESULTS AND DISCUSSIONS

The data illustrating the effect of heating rate on product distribution is shown in Table 1. The values represented in this Table are weight percentages for these compounds only. A sum of these weights when compared to all compounds, C_9 and smaller, comprised about 40 percent of the total weight. The numbers in Table 1 are averages of at least three pyrolysis runs.

The methane/ethene ratio appeared to be most severely affected by heating rate. At the fastest rate ($\sim$ 40°C/min) the methane value was lower than the ethene value. As the heating rate was decreased, a reversal was observed with the methane/ethene ratio reaching a final value of approximately 4:1 ratio at a heating rate of 0.25°C/msec. The other products monitored remain fairly constant.

An important experimental observation was recorded during these experiments. It is completely possible to shift the product ratios report in Table 1 at a given heating rate by simply doubling sample size. It cannot be overemphasized that near monolayers of finely divided

Table I

Summary of Heating Rate Studies with Pyroprobe

Time (msec) (heating time to 1000°)	25	100	500	2000	5000
Compound					
methane	23.8	39.4	40.8	44.4	41.7
ethene	38.5	36.8	28.1	23.9	10.5
ethane/ acetylene	8.4	8.6	8.8	6.1	6.6
propene	9.0	8.5	8.7	9.1	7.6
propyne/ allene	3.0	3.6	4.2	4.8	10.2
butene	14.3	11.6	14.1	11.3	17.8
Log Time (msec)	1.40	2.00	2.70	3.30	3.70

material must be applied to the ribbon in order to minimize the heat transfer problem.

The effect of heating time was measured using the CO_2 laser as the pyrolysis source. Table II summarizes the measured temperature for various heating times. The temperatures of greater than 2000°C for the 10 sec exposure probably did not represent the pyrolysis temperature of the sample. A more realistic assessment would be for the pyrolysis to occur at temperatures less than 1000°C. This is the approximate magnitude of temperature observed for the short pyrolysis times. The temperature increase observed for longer pyrolysis times probably result as a direct consequence of char buildup. The char can act as an insulation barrier and therefore reduce the amount of energy deposited to the sample.

Table II

Maximum Crater Temp in Wood as Function of Laser Pulse Duration

Time in Sec	Observed Temp °C
1	1100
2	1500
5	1920
10	2000

Table III summarizes the product distribution as a function of laser exposure time. Again, the numbers represented in Table III are averages of at least 3 separate measurements. Heating time seems to affect the ethane-ethyne concentration to the greatest extent. The increase in these products has been speculated as arising from char degradation to produce ethyne. This seems quite logical based solely on observed temperatures as a function of heating time. An experiment where primarily char was degraded at various heating times showed fairly uniform concentration of products with ethane-ethyne concentration higher than those from the short time experiments recorded in Table III. Table IV summarizes these data. We believe the comparison between Table III and IV clearly indicate the importance of the char layer in producing high quantities of ethane-ethyne.

Table III

Summary of Laser Exposure-Time Studies

Time (sec)	1	2	5	10
Compound				
methane	26.1	31.3	31.8	34.7
ethene	28.8	40.	28.9	23.4
ethane/ acetylene	8.2	8.6	23.7	30.6
propene	9.3	7.8	5.5	3.4
propyne/ allene	3.4	4.1	3.8	3.4
butene	24.2	8.4	8.0	4.8

Table IV

Laser Char Pyrolysis

	5 sec	10 sec
methane	32.5	37.1
ethene	14.4	15.0
ethane/acetylene	45.9	39.1
propene	2.5	3.1
propyne/allene	2.3	2.3
butene	2.3	3.3

The craters produced from a prolonged laser burn seemed to have the highest concentration of char around the edges of the hole. Therefore, if a wood sample could be prepared in a cylinder such that the maximum diameter of the wood sample was slightly less than the focused laser spot, much of the char formation and subsequent char degradation could be minimized. Laser pyrolysis (2 sec exposure) of a rod shaped portion of Douglas Fir 1 mm in diameter was conducted followed by product analysis. The products observed for this experiment are summarized in Table V. The product ratios for this analysis resembled the shorter exposure times rather than the two second run on the slab of Douglas Fir. Visually, the char layer formed was much thinner than those observed in the craters.

Table V

Summary of Various Laser Exposures

	Rod- 2 sec	Fresh Surface	2 sec*	1 sec*
methane	35.1	32.8	31.3	34.8
ethene	28.3	26.7	40.	23.2
ethane/acetylene	6.1	24.8	8.6	12.1
propene	10.2	5.3	7.8	11.1
propyne/allene	2.5	3.4	4.1	2.7
butene	17.7	6.9	8.4	15.9

*slab

The actual quantitative char formation was determined by physically removing the char followed by weighing. Likewise the aerosols were determined by trapping in a glass wool-Tenex trap. Table VI lists these two quantities plus the volatiles as determined by difference.

The data reported in this study represents a preliminary investigation; however, they demonstrate the important fact that significant product ratios can result from changing the pyrolysis parameters. A continuing study is presently underway to investigate other species as a function of the same pyrolysis parameters.

Table VI

Percentages of Laser Pyrolysis Products

gas 80.0% tar 4.1% Char 15.8%

Total 99.9%

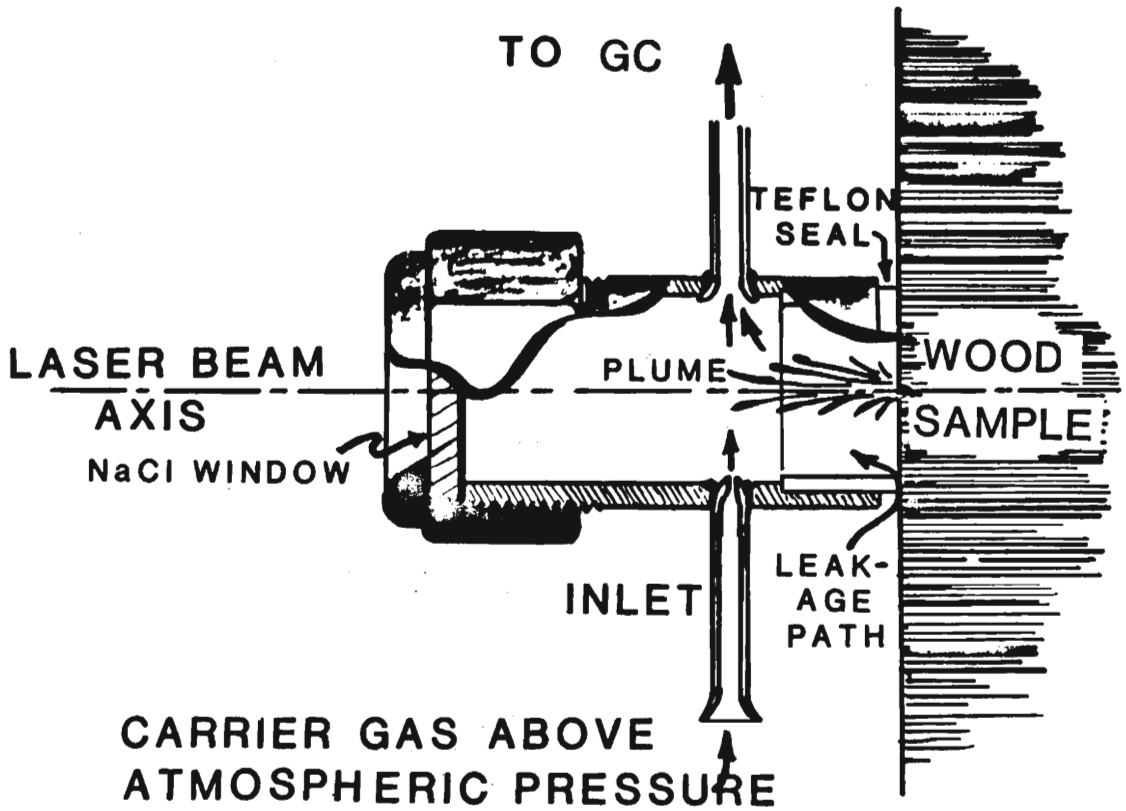

Figure 1. Laser Collection Apparatus

REFERENCES

1. W.A. Dietz, J. Gas Chromatogr., 5, 68 (1967).
2. G. Wells, K.J. Voorhees and J.H. Futrell, Anal. Chem., 52, 1782 (1980).
3. L.J. Hendricks, submitted to Rev. Sci. Inst.
4. L.J. Hendricks and S.P. Zobrist, submitted to Appl. Optics.

ABSTRACT

MICROWAVE PYROLYSIS OF BIOMASS

BY

Barbara Krieger
University of Washington

Microwave pyrolysis of biomass can occur by two mechanisms. The electromagnetic radiation can be absorbed by the biomass itself in proportion to the dielectric-loss factor. Or, in the presence of a low pressure gas, the radiation can cause arcing (ionization) in the gas surrounding the solid and a plasma can be formed.

The principal findings for dielectric-loss pyrolysis are as follows: The applicator geometry and design cause high temperatures to occur in dielectric-loss pyrolysis. Principally gases are formed in the perpendicular reactor geometry. For a recent design, using an angled reactor, mild pyrolysis to high molecular weight tars occurs.

The gases typically contain ~40% of the original biomass weight as carbon oxides and 5-10% of the original weight as H_2 and hydrocarbons such as methane and ethylene. As carbon content increases from cellulose < biomass < lignin, the residue (char) increases from 10 to 33%. Tar yields are quite variable, with 15-31% being typical. Less than half the tar reflects the chemical structure of the biomass (levoglucosan for cellulose; phenols, guaiacols for lignin). The remainder is condensed products such as naphthalene and anthracene. Using an angled reactor in the applicator shows increased phenolic compounds in the tar.

The principal findings for microwave plasma pyrolysis are as follows: The process is primarily one of gasification. The gases contain up to 14% (volume) of acetylene, in contrast to those described above. The size of the pellet affects all product yields, with smaller particles unexpectedly showing increased char and decreased gas and tar yields (for an equivalent batch reaction time to that of a large particle).

MICROWAVE DIELECTRIC-LOSS AND PLASMA PYROLYSIS BIOMASS

by Barbara Brockett Krieger
Univ. of Washington BF-10
Dept. of Chem. Engrg. Seattle, Washington 98195

INTRODUCTION - MICROWAVE DIELECTRIC-LOSS PYROLYSIS

Microwave pyrolysis of biomass can occur by two mechanisms. In the appropriate microwave reactor, the electromagnetic radiation can be absorbed by the biomass itself in proportion to the dielectric-loss factor which quantifies the ability of the material to dissipate electrical energy as heat. Or in the presence of a low pressure gas above a certain power level, the radiation can cause arcing (ionization) in the gas surrounding the solid and a plasma can be formed (1-6). Dielectric-loss heating occurs in the domestic microwave oven and in many drying applications including bonding and drying of wood(7). Details of the physical principles causing microwave heating and pyrolysis are described in Refs. (8-18).

The amount of microwave power absorbed depends on the local electric field strength and the temperature- and moisture-dependent dielectric constant of the material placed in the field (8-12). When the material does not absorb the radiation strongly (biomass-like substances) and the penetration depth is large, the field is not attenuated and uniform volume heating occurs. This results in a temperature distribution quite different from that found in heating by conduction (19). The heating is especially rapid for materials with high dielectric loss factors such as water or other materials with large dipole moments. Owing to volumetric heating, a potential advantage of microwave heating would be to process the rather large particles in which biomass is generally found. Refuse treatment (15) and waste rubber reclamation (20,21) have been found to be economic using microwave heating.

Wen and Tone (22) suggest that high temperature and high heating rate favor the production of gases from coal over tar and char production. This concept may indeed apply to biomass, but the exact regimes have not been demonstrated. However, when large particles of biomass experience intense heating, the very low thermal conductivity causes only the external particle surface to be rapidly heated. The interior is heated slowly at a rate governed by the thermal diffusivity of wood(23). If the conclusions of Wen and Tone apply to wood, the slow heating rates and lower temperatures at the particle interior will favor tar and char production,

thus decreasing gas yield from large particles of biomass. The forest products industry and others (24,25) have found particle size reduction to be a costly process. Thus, a principal motivation for this work has been to determine if microwave heating of biomass: gasifies large particles rapidly avoiding size reduction steps; gives unusual results; or offers an advantage over conventional pyrolysis using conduction heating.

EXPERIMENTAL APPARATUS

The details of the experimental apparatus, procedure, and reaction product analysis appear elsewhere(14,16). A waveguide applicator consists of a quartz tube through the broad face of an S-band waveguide . This configuration offers the possibility of a continuous process, easier scale-up, and easier product recovery than the resonant cavity exemplified by the home microwave oven. Although these applicators are quite efficient (26), the extremely low dielectric-loss factor of dry biomass (10-2 for wood versus 10+2 for water- Ref. 27) causes low absorption. For reasons described in detail elsewhere (7,14,16), a batch-type microwave reactor containing a single large cylindrical particle (1 cm diam, 1 cm high) is used. Helium sweeps the reaction products to a cold trap, and to continuous CO and total hydrocarbon analyzers. Tar fractions and grab samples of the gas are analyzed by gas chromatography or GC- mass spectrometry. Initial reactor pressures are 1-1.6 atm. Total batch reaction times are 1-5 minutes but most devolatilization is completed after one minute.

The characteristics of the reactants are given in Table 1 (increasing carbon content, left to right). These substrates are under-utilized wood or agricultural materials found in the Pacific Northwest. The anisotropy of biomass was removed by using small particles pelletized to the indicated densities. As discussed in Schwartz, et al (20), inorganic additives can increase microwave power absorption. Composition and amounts of these additives are also described in Table 1.

RESULTS

Photographs taken of split pellet cross-sections after very short reaction times show the black char coloration to be radially uniform (28). Identical pellets, heated rapidly by conduction from the surface (28) react in a shell- progressive manner with a sharp front between the black char and light- colored lignin. This demonstrates that the temperature distribution in dielectric-loss pyrolysis is the reverse of that found in heating by conduction, unless the re-

TABLE 1 - Reactant Characteristics

	Substrate[4]					
	Cellulose[1]	Red Alder[2]	Wheat Straw[2]	Cotton Wood[2]	Coal[3]	Lignin[1]
Elemental: (wt. %)						
Carbon	44.45	45.74	46.43	47.48	51.85	69.83
Hydrogen	6.17	6.65	6.70	6.22	4.66	5.67
Oxygen	49.38	37.46	33.71	35.86	17.45	24.50
Ash Content (wt. %)	0.01	0.29	5.52	0.48	8.23	1.00
Pellet Density (g/cm^3)	1.13	0.92	0.93	0.88	0.97	0.83
Pelletizing Pressure (psi.)	6,000	6,000	6,000	6,000	2,000	2,000

[1]Obtained from Rydholm (1965).

[2]Analyzed by Schwarzkopf Microanalytical Laboratory.

[3]Analyzed by Northwest Laboratories Inc.

[4]All substrates are pre-dried.

	Additive				
	NaOH	HCOONa	$NaHCO_3$	SiO_2	$Ca(OH)_2$
WT. % Substrate	0.6 2.8 6.6 Red Alder	8.3 Red Alder	6.7 Red Alder	1% Lignin	1% Kraft Lignin
WT. % Substrate	1.0 Lignin	1.0 Lignin	1.0 Lignin		1% Organosolv Lignin

TABLE 2 - Length of Induction Period As A Function of Composition

Substrate	Red Alder					Lignin	Cellulose	Wheat Straw	Cotton Wood	Coal
Type of Additive	NaOH			HCOONa	$NaHCO_3$					
Wt. % of additive	0.6	2.83	6.65	8.27	6.7	-	-	-	-	-
Induction time (min.)	2.4	1.85	1.40	1.30	1.9	0	∞	0	0	∞

action is highly exothermic.

Although microwave irradiation at any desired power level can be accomplished instantaneously, because the absorption is temperature- dependent (via the temperature-dependent dielectric-loss factor), the heating process exhibits an "induction period" of low absorption and slow temperature rise (14,20). During the period of maximum absorption (as indicated by power meters), the pyrolysis of cellulose, lignin, or biomass is rapid even for large pellets (28). An approximate, apparent first order rate coefficient for the lignin weight loss process is O(10) min-1 to be compared with approximately (50) min-1 from the weight loss data of Iatridis and Gavalas (29).* These are to be compared with a simple apparent rate for conduction heating, calculated as described in Russel, et al (30). For the thermal properties of lignin pellets used in this study, an approximate conduction constant is O(0.5) min-1. Bradbury, et al (31) report apparent rate coefficients for heating of 2.92 min-1 for finely powdered cellulose in an oven. These results are consistent with the conclusion that microwave heating of large particles is indeed rapid.

Table 2 summarizes the length of the induction period for microwave pyrolysis of several substances. Experiments were attempted to decrease the induction period (28). High density pellets were more quickly and successfully pyrolyzed (14,16). Additives to red alder (Table 1) shortened the induction period. Wheat straw with a higher inorganic (ash) content absorbed microwaves readily, however, coal (high ash) did not pyrolyze rapidly. This is attributed to the higher devolatilization temperatures of coal rather than poor absorption (28).

The presence of additives caused increased char production at the expense of the tar for sodium hydroxide additives to lignin. The results were similar for carbonates, silicates, and organic sodium salts. Since water is an effective absorber of microwave energy (responsible for the rapid cooking of foods in microwave ovens), water-retaining salts such as $Ca(OH)_2$ were used as additives. Wet substrates were also pyrolyzed. Since the loss factor of water was approximately 10+4 times that of wood, the water immediately evaporated (observed by a pressure rise) but reaction took place after the induction period observed for dry lignin. In some experiments, pellets fractured owing to extremely rapid water loss. As a result of poor absorption and unsuccessful attempts to improve it, high input power levels (1-2 kW) were necessary to accomplish biomass pyrolysis.

The applicator geometry influences the power absorbed by the

*The latter study used small lignin particles heated on a wire screen in two sec to a temperature of 750 C .

sample. Two different configurations have been tried, an applicator through which the reactor is "angled" (schematically shown in Ref. 14) and an applicator through which the reactor is perpendicular (shown in Ref.16). Although the former applicator absorbs less power itself, the power absorbed by the sample is small unless high input power levels are used. Mild pyrolysis of the biomass results, with high char yields and large quantities of tar being produced. The latter configuration causes more power to be absorbed by the sample and lower (0.8-1.5 kW) input power levels are required. Since the reactor walls (quartz) and gases surrounding the pellet are relatively transparent to microwave radiation,the walls and gases were cooler than the pellet in each case. Verification of this inverse temperature profile appears in Allan, et al (14).

Table 3 reports product yields exclusive of tar composition under identical conditions using the "perpendicular" reactor. Weight loss -time and temperature-time profiles appear elsewhere(14,16,28). Reported in Ref. 16 are comparisons between conventional and microwave pyrolysis products including tar composition.

DISCUSSION - DIELECTRIC-LOSS PYROLYSIS OF BIOMASS

The discussion will be limited to differences between biomass substrates under microwave pyrolysis since these conclusions are generalizable to other systems. Differences between microwave and conventional pyrolysis results are indicated as they apply to general pyrolysis mechanisms. It should be noted that results of any kind are related to the large particle size and density of the reactant.

The "induction period" or period before appreciable gas evolution was noted on the pressure transducers varies considerably and affects the overall pyrolysis (35). The length of the induction period is a function of the dielectric-loss factor and the heat of reaction since these affect the intrapellet temperature distribution. The dielectric-loss factor is itself temperature-dependent. The length of the apparent induction period is also determined by the temperature at which devolatilization occurs. TGA and DSC data in Ref. 33 and 34 for biomass and components show weight loss occurs at lower temperatures for wood and lignin (starting at 200-250 C) than for cellulose (starting at 350 C). This explains lignin's shorter induction period in Table 2. Density also affects microwave absorption (32) through its effect on intrapellet temperature distribution. The efficient pyrolysis of lignin may be due in part to the exothermic heat of reaction* which causes a more rapid internal

*Although disagreement exists (36-39), the heats of reaction generally accepted indicate that pyrolysis of cellulose is endothermic, lignin is exothermic, and wood is approximately thermoneutral.

temperature rise despite the reduced pellet density indicated in Table 1. This is offset by the swelling** behavior of lignin (or porosity increase) during devolatilization . The decrease in density causes slower overall pyrolysis for the lignin .

Lignin, wheat straw and black cottonwood absorb approximately 80% of the forward power and exhibit short induction periods. The data in Table 2, however, suggest ash (inorganic) content affects the induction period. Schwartz, et al (20) also report that certain additives caused a more rapid and controlled microwave curing process for rubber. Since lignin, wheat straw, and cotton wood have higher ash content, this could also explain their rapid microwave pyrolysis rate. Red alder does not react unless inorganic salts are present. The induction time is found to decrease with increasing additive and after this period (noted by a sharp pressure increase) reaction is vigorous. It is believed that the inorganic salts and ash can improve the absorption via: an increased dielectric-loss factor; acting as catalysts to lower devolatilization temperatures; or providing additional heat of reaction. They cannot be regarded as improving conduction heat transfer since volume heating occurs. The relative importance of these effects is discussed in Ref. (35). Little data exist regarding the dielectric-loss factor of mixtures or its temperature dependence.

The reactions products for each of the substrates in Table 3 are presented with (approximately) increasing C/H ratio left to right . The char yield follows the same trend. The high COx content of the gases from cellulose and biomass pyrolysis reflect their high oxygen content. Calculated as C/H, C/O, and H/O, the ratios increase from left to right in the table. The trend in H_2 and hydrocarbon content of the product gas follows all three ratios . The conclusion is that char and gas yield is determined in part by C/H/O content in high temperature microwave pyrolysis rather than by chemical structure. Yields are similar to thoe in conventional pyrolysis (using much smaller particles) at high temperatures and rapid heating rates.

The effect of additive concentration on the gas and char yield is shown in Fig. 1. It can be seen that the char yield is increased at the expense of the tar yield since gas yield is also increased. An elemental carbon and oxygen balance was performed on the substrates and is plotted in Fig. 2. The dotted line represents the calculated increase

**Lignin, like some coals, softens and swells whereas biomass and cellulose do not. The coal pyrolyzed in this study was a Washington sub-bituminous coal and did not soften.

TABLE 3 - Reaction Products - Dielectric-Loss Heating (wt %)

Fraction	Cellulose	6.7% NaOH+ Red Alder†	Wheat Straw	Black Cottonwood	Coal	Lignin
Residue	27.	25.8	17.8	10.6	DID NOT ABSORB	33.5
Volatiles & Polymeric film	43.	25.5* (14.2)**	27.9 (8.2)	31.4 (11.4)		19.6 (12.8)
Water	23.		8.2	10.1		8.6
Gases	4.	48.7	46.1	47.9		38.3
H_2		2.2	1.3	0.6		0.8
CO		26.	24.4	28.4		21.9
CO_2	4.	14.4	14.5	10.3		5.1
CH_4		1.6	2.6	4.6		4.4
C_2H_2		0.2	1.2	2.1		4.9
C_2H_4		4.1	1.5	1.3		1.8
C_2H_6		0.2	0.6	0.6		0.1

POOR ABSORPTION

†Red Alder couples only with additive present.
*By difference **( ) amount in cold trap.

TABLE 4 - Plasma Heating (wt %)

Fraction	Cellulose	Red Alder	Wheat Straw	Black Cottonwood	Coal	Lignin
Residue	2.9	9.2	23.1	9.7	49.8	39.8
Volatiles and Polymeric film	21.4	17.0	14.2	22.9	13.6	19.8
Water	9.1	6.2	13.0	8.3	5.6	8.6
Gases	66.6	67.6	49.8	59.1	30.9	31.9
H_2	1.8	2.4	1.1	1.2	1.4	0.5
CO	45.9	41.5	24.3	32.8	21.6	19.1
CO_2	5.9	11.1	16.1	13.0	3.6	4.0
CH_4	2.1	7.1	1.8	2.9	1.1	2.3
C_2H_2	7.7	4.4	4.4	5.9	1.9	4.6
C_2H_4	3.0	0.8	1.5	2.5	1.1	0.7
C_2H_6	0.3	0.2	0.7	0.8	1.2	0.7

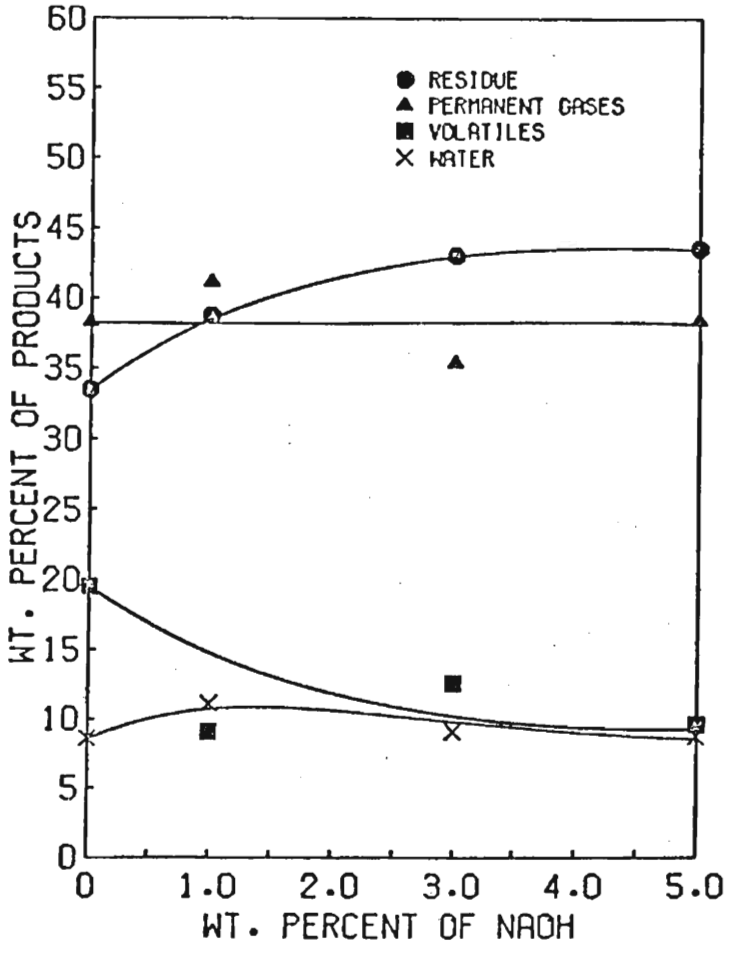

Fig. 1 The product distribution from the pyrolysis of lignin in dielectric loss mode as function of the weight percent of sodium hydroxide added. (The products are evaluated as weight percent of the original substrate including the additive.)

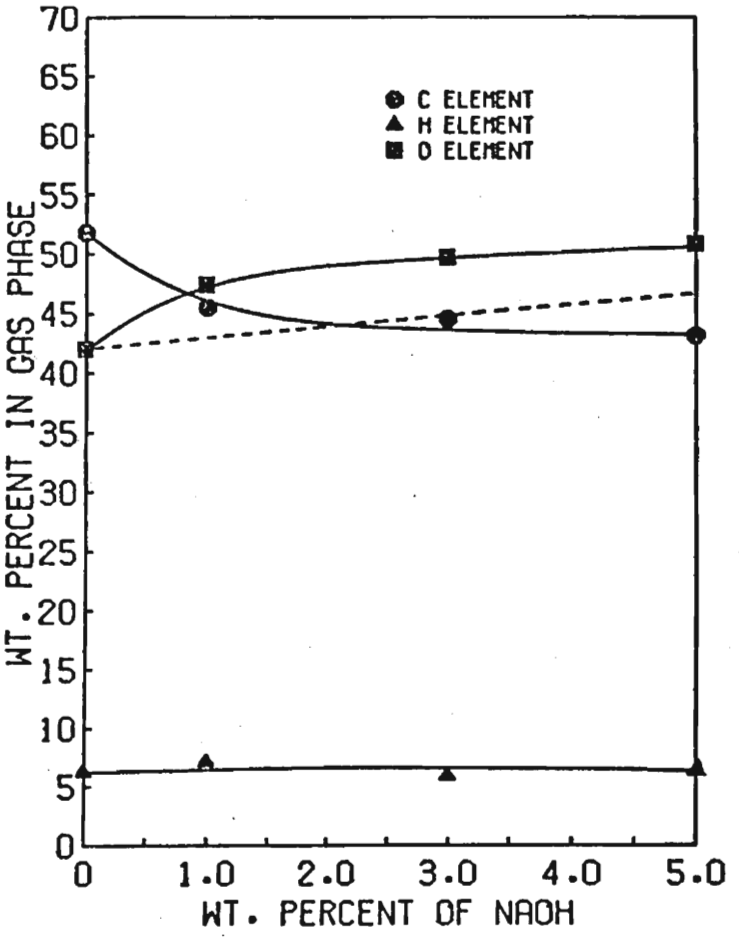

Fig. 2 The elements in gas product from the pyrolysis of lignin in dielectric loss mode as function of the weight percent of sodium hydroxide added. (The elements are evaluated as weight percent of the gas products.) The dotted line is the increased oxygen content attributable to the presence of NaOH.

in gas-oxygen content as a result of the presence of NaOH. The gas is seen to contain a larger amount of elemental oxygen than would be accounted for by the NaOH. This phenomena has been observed by Robertus et al in their large scale studies of biomass using mixed catalysts (40).

The tar components (16) indicate that one can expect fragments of the original chemical structure to appear in the tars. The tar from microwave pyrolysis of cellulose contains levoglucosan, the same compound found in conventional pyrolysis (14,31,41). The tar obtained from lignin and biomass contains phenols, guaiacols, and cresols - fragments of the lignin polymer. This also applies to lignins generated with different pulping processes. Organosolv lignin obtained from ethanol- water delignification is a lower molecular weight polymer than Kraft lignin (35). When the former is pyrolyzed, a low molecular weight tar that is completely soluble in tetrahydfuran is produced. Kraft lignin, a more condensed lignin, produces considerable (30-35%) char and a high molecular weight tar which is not soluble in THF.

Tars from both lignin and biomass contain condensed aromatics such as napthalene and anthracene which are not fragments of the original macromolecule. According to Sakai et al(42), these components are formed rapidly in secondary reactions during the high temperature (>850C) gas phase pyrolysis of simple hydrocarbons and olefins. However, it is worth noting that the initial internal surface area (about 5E+04 cm^2 , measured by BET) of the pellet is much greater (and at high temperature) than the relatively cool quartz reactor surface with a smaller (about 200 cm^2) surface area. It is reasonable to suggest that the increased temperature and greater area would enhance the rate of char-surface reactions over reactor surface reactions and be a factor in producing the condensed aromatics in the tar and the secondary reaction products in the gas.* Since the pellet is dense, the volatiles are at high pressure which would favor second-order reactions such as polymerization and condensation. However, the data are inconclusive as to the origin of these species.

If one broadly classifies acetylene and condensed aromatics as "high temperature products", Fig. 3 and Fig. 4 present results that indicate NaOH causes a gas and tar product distribution characteristic of a lower temperature as the amount of NaOH additive is increased. The limited data are inconclusive with respect to mechanism; however, Robertus, et al have investigated this aspect (40).

In Ref. 16, microwave pyrolysis of lignin is compared to results of Iatridis and Gavalas (29) who used an electrical-

*Berthelot long ago noted that acetylene forms benzene when passed over hot glass at high temperature.

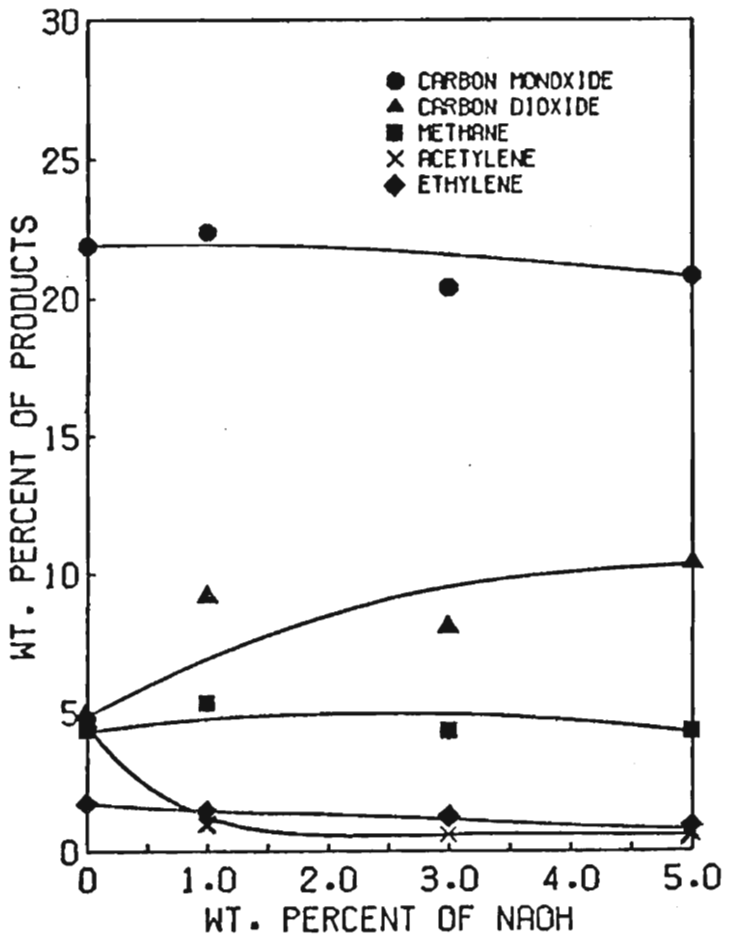

Fig. 3 The product distribution of gases from the pyrolysis of lignin in dielectric loss mode as function of the weight percent of sodium hydroxide added. (The products are evaluated as weight percent of the original substrate including the additive.)

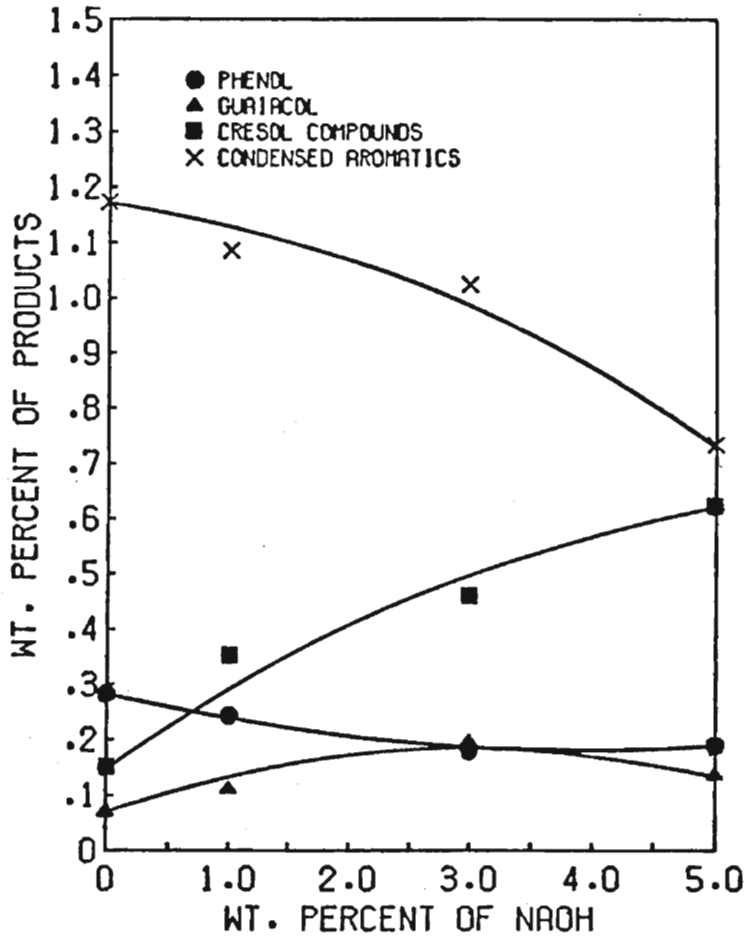

Fig. 4 The product distribution of tars from the pyrolysis of lignin in the dielectric loss mode as function of the weight percent of sodium hydroxide added. (The products are evaluated as weight percent of the original substrate including the additive.)

ly heated metal screen to rapidly pyrolyze small particles of lignin . The primary differences appear to be in the higher gas yield and the greater extent of secondary reactions to form condensed aromatics in microwave pyrolysis . This is attributed to a high intrapellet temperature.

INTRODUCTION--MICROWAVE-INDUCED PLASMA PYROLYSIS OF BIOMASS

Above certain power levels or at low pressure, arcing or ionization can occur in a microwave reactor. The resulting electrons are accelerated by the alternating field (2450 MHz) and their kinetic energy or "electron temperature" becomes very high (1). Although the electron concentration and its velocity determine the intensity of plasma heating, in a microwave reactor the heating may not be independent of the dielectric-loss factor of the substance, depending on how strongly the substance absorbs. At low pressure, only low power is needed to form a plasma, and primarily plasma heating occurs (owing to poor absorption by biomass). If solid biomass particles are present in a plasma, they experience rapid surface heating by electron bombardment. Volatiles are produced and the electrons quite effectively penetrate the "thick" boundary layer caused by volatiles outflow.* However, owing to surface cooling by the carrier gas, the rate of surface temperature rise is only 10-20 C/sec determined from optical pyrometer measurements (28,62,65).

When solids are heated by a plasma, it is generally true that the plasma does not penetrate the solid surface. Under certain conditions (62), plasma heating of a solid can be made to approximate a high heat flux which is spatially uniform and nearly constant with time. Since biomass is a rather poor heat conductor, the interior of a large particle is heated by conduction (as in combustion) and shell-progressive reaction occurs(62,63,65). If the gas-phase plasma reactions are known, the conclusions drawn from experiments designed to manipulate only intrapellet properties in a plasma reactor can be more widely applied to conventional, large pellet devolatilization In particular, since the high temperature, large pellet pyrolysis is limited by the rate of heat conduction in the pellet, the role of thermal diffusivity and particle size can be investigated. A review of attempts in the literature (49-61) to model the behavior of thermally- thick substances such as cellulose or biomass under rapid pyrolysis conditions appears in Ref. (48). From this review, it is concluded that particle size effects are extremely complex (57) and are generally imbedded in a dimensionless time. For this reason, our studies

*A rough comparison: net power to the biomass pellet in this study is about 5 watts/cm^2; combustion level heat flux is about 4-12 watts/cm^2 for cellulose according to Ref. (43).

have been carried out for the same dimensionless time when particle size is systematically varied.

Chemical reactions occuring in a plasma are severe fragmentation, rearrangement and free-radical reactions (6). These reactions have many applications today and general discussions appear in several books (1-6). Specific reactions of organic gases in plasma have been reviewed by Ref. (6) and organic solids such as coal (44) and refuse (45) have also been studied and reviewed in (46). The large particle of complex composition is generally not treated although plasma etching of semi-conductor surfaces has caused interest in this area (47). Principal motivations for this study are: to determine if plasma pyrolysis of large biomass particles offers advantages to conventional pyrolysis; and to understand the role of intrapellet properties especially for the high heat flux of plasmas.

EXPERIMENTAL DETAILS-MICROWAVE-INDUCED PLASMA PYROLYSIS OF BIOMASS

The apparatus details can be found elsewhere (46,62,65); the microwave applicator is the perpendicular configuration described above. Typical inert carrier gas pressures are less than 200 mm Hg and the batch reaction time is generally less than 45 sec to prevent study of the char gasification regime. Input power variation has been investigated (49) but it is generally set at the minimum which maintains a steady plasma . Gases such as CO_x and H_2 are added to determine those reactions occuring in the gas phase and to uncover the role of free-radical reactions. Pellet surface temperatures are measured by an infra-red optical pyrometer. Substrate composition and preparation is similar to that described earlier (28,46,62,64,65). Particle size varied from powdered lignin to lignin pellets of several configurations and characteristic dimension (65).

Experimental Procedure

The unraveling of product distribution variation in plasma pyrolysis is complex owing to the interdependence of temperature profile in the pellet and particle size, and to other effects such as residence time in the plasma or total pressure. Thus, a full factorial screening experimental design (65) was conducted. The four variables used in the 24 design (66) were: plasma reactor pressure; residence time in the plasma phase; particle size (characteristic dimension and aspect ratio); heat flux (particle surface area and aspect ratio). Large and small pellets were reacted for the same dimensionless time,

$$t_1/r_1^2 = t_2/r_2^2 \qquad (1)$$

(See Refs.48-61). In a separate study, density (thermal diffusivity) was also systematically varied (62,67).

Detailed product analysis was made as described in Ref. 16.

RESULTS - MICROWAVE-INDUCED PLASMA PYROLYSIS OF BIOMASS

Photographs of split pellet cross-sections after increasing batch reaction times indicate that the char and unreacted biomass are sharply separated by a black front that progresses inward*. Eq. 1 has been verified using the char thickness so measured. This data was also used to verify a simple conduction model to predict trends in intra-pellet temperature. The model used constant properties (different for char and lignin), and constant heat flux with the char-forming temperature and heat flux as parameters. It is described in Refs. 62 and 65. A typical product distribution in plasma pyrolysis is shown in Table 4. Table 5 briefly summarizes the effect of doubling particle size for constant pellet density and constant dimensionless reaction time using a factorial design. It was determined (62) that solely a change in particle density could produce the alterations in overall product yield such as those in Fig. 5. For species not strongly influenced by the plasma reactions, yields of specific compounds changed with a change in density as shown in Fig. 6. Effects of varying substrate and additive gases are reported in Ref. 28.

DISCUSSION- PLASMA PYROLYSIS OF BIOMASS

The results in Table 4 are consistent with the elemental composition of the biomass pyrolyzed. The high oxygen and hydrogen content of biomass and cellulose cause low char yields; the ash in wheat straw and the high carbon content as well as ash in lignin (and coal) are responsible for their higher char yields. The lower overall char yields in Table 4 (in contrast to those of dielectric-loss heating, Table 3) are attributed to the high effective temperature of plasma heating. The high gas yields are indeed remarkable in view of the 1 cm particle size.

Acetylene is found in high concentration when compared to thermal pyrolysis. A free radical mechanism of Mertz, et al (68) involving H atoms and CO is consistent with our findings since both added CO and H_2 cause an increase in acetylene yield (28).

The rate of weight loss in plasma pyrolysis is not as rapid as that occuring in dielectric-loss prolysis (28). However, by extending the heating period, the extent of gasification is quite high.

When pellet size is varied in a factorial design, the increase in fractional yield (independent of amount reacted) is

*This is consistent with very rapid reaction relative to heat conduction.

rather dramatic (see Table 5) and opposite from that predicted for large pellets (48-61). For equal actual reaction times of a small and large pellet, predictions are: more char, less gas and tar from the large particle. For equal dimensionless pyrolysis times , the gas yield is higher and char yield lower in the large pellet. Examination of simple heat conduction behavior reveals that the large particle is cooler at the interior and hotter at the exterior (where it has reacted). Consideration of the heating rate as a function of radius shows that it is lower for the large pellet. Thus the observed yields including the increased tar can be explained by the intrapellet temperature profile.

The gas and tar composition from the two different sized pellets reflects changes that show an increase in products characteristic of both lower and higher temperature pyrolysis. Methane yield is increased but so is the yield of condensed aromatics (65). Although the C_2H_2 yield increases with increas ing particle size, the factorial design results indicate the gas phase residence time (time in the plasma) also affects the acetylene yield, as expected from the mechanism of Mertz, et al.

Owing to the structure of a factorial design, Table 5 demonstrates the magnitude of gas composition change for solely a change in particle size. This concept is extremely important for the utilization of biomass which occurs naturally and as a by-product in an extremely wide variation of sizes. Table 5 and Figs. 5 and 6 demonstrate also that the dimensionless time is the important design variable for large particles.* It should be noted that for appropriately chosen heat flux and temperature conditions to give the desired products from a small particle, the use of large particles in the same reactor will increase the tar yield and cause a significant unreacted fraction. The role of thermal diffusivity in altering the intrapellet heating rate is clear from Fig. 5 where char, gas and tar production rates are altered by solely a change in density which has been shown (23) to determine the magnitude of the thermal diffusivity of wood. The limited data on gas composition changes (Fig. 6) when pellet density is changed show that products of interest (methane, ethylene) from large pellets can be influenced by the intrapellet heating rate.

OVERALL CONCLUSIONS

The study of plasma pyrolysis has provided insights that relate to the behavior of biomass under combustion conditions and has provided some data to illustrate the magnitude of the particle size and intrapellet conductivity effects (62,67) on product distribution. These conclusions have

---

Dimensionless time has been cast in many ways (48-61). The simplest often is (time)(thermal diffusivity)/(length*length).

TABLE 5

FACTORIAL DESIGN RESULTS:

EFFECT OF DOUBLING PARTICLE SIZE ON PRODUCT YIELD[1] FROM PLASMA PYROLYSIS

	Weight Percent Yield		% Change	
	Particle Size			
	6 mm	13 mm		Also Dependent On:[2]
Residue	68.4%	45.9%	- 33%	Particle external area (or heat flux)
Tar	17.7	27.5	+ 55	
Gases				
H_2O	0.5	3.3	+560	
H_2	0.6	1.1	+ 83	
CH_4	0.7	2.1	+200	
CO	8.5	14.5	+ 71	
CO_2	1.3	2.3	+ 77	
C_2H_2	2.1	2.5	+ 19	Residence time in plasma phase
C_2H_4	0.3	0.6	+100	
C_2H_6	0.2	0.3	+ 50	
Total	100.3	100.1		
% Unreacted	11.4	20.7	+ 82	Particle external area (or heat flux)

[1]Fractional Yield is based on initial particle weight less weight of unreacted lignin.

[2]Interactions determined from full factorial experimental design.

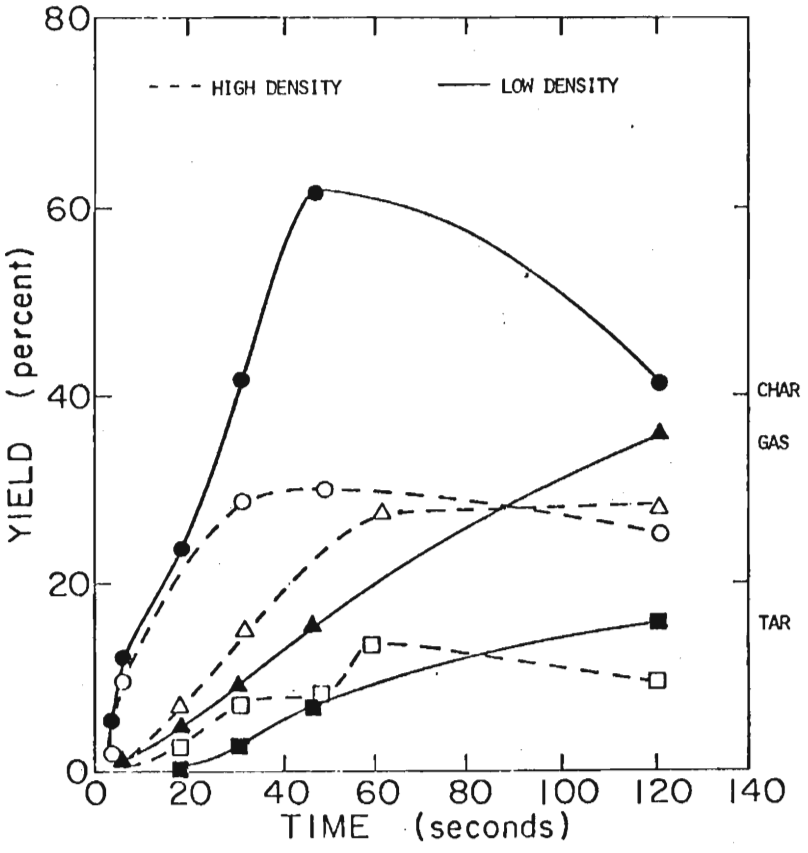

Fig. 5 Gross product distribution during reaction for low (solid line) and high (broken line) density pellet. O = char ± 6%. □ = condensible gases ± 7%. △ = permanent gases ± 0.1%.

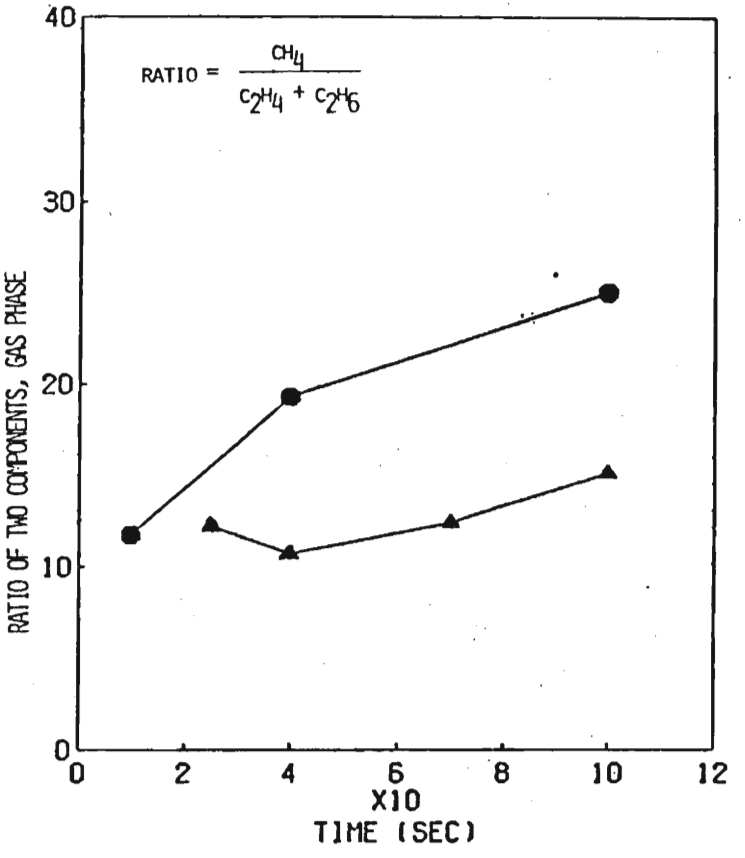

Fig. 6 Ratio of weight percent yield of methane to ethylene and ethane during reaction. ⬢ = high density pellet (1.2 g/cm^3). ▲ = low density pellet (0.9 g/cm^3).

wide application since an important usage of biomass is for fuel.

Plasma microwave pyrolysis is more easily executed than dielectric-loss microwave pyrolysis owing to the latter form of heating being very dependent on hardware design. Both microwave heating processes cause primarily gasification with low char yields especially in view of the large particles studied. The tar and gas composition reflects high temperature cracking and rearrangement reactions in the pellet, or in the case of plasma heating, in the gas phase. The plasma pyrolysis results presented here have implications for fast pyrolysis since even under the extremely severe heating conditions existing in the plasma, the physical properties of the large pellet affect the product distribution.

Both the dielectric-loss and plasma mechanisms for microwave heating accomplish rapid pyrolysis of large particles of biomass (wet or dry). The char and tar yield is low in both mechanisms, owing to rather rapid heating despite the large pellet size and high temperatures. This is consistent with similar results in the literature for coal.

Size reduction of biomass is costly. This study indicates that microwave pyrolysis can somewhat overcome heat transfer rate limitations and indeed speed the pyrolysis of large fragments of materials. Therefore it offers certain processings advantages. However, for materials with low dielectric-loss factors, the requisite power to initiate pyrolysis reactions is so high that currently, unless specific product distributions can be selected by the use of microwave heating, the scheme is not economically attractive. Little flexibility is available in choosing the frequency (which would improve coupling) since only certain bands are available for high-power commercial units. However, additives of appropriate composition and dielectric properties can alter the economics. The commercial feasibililty of microwave-induced reactions remains to be demonstrated. The use of dielectric-loss heating in the laboratory, however, to explore the role of heat transfer in biomass pyrolysis is valid.

ACKNOWLEDGEMENTS

The author is indebted to Ricky Chan, Martha Graef, Steve Slottee, Debbie Wiggins, and Donald Work for competent and enthusiastic performance of the experiments and analytical work during their studies. Others who have provided assistance and insight are K.V. Sarkanen and G.G. Allan, Dave Hanson, and Jim Callis. The National Science Foundation, Division of Problem Focused Research has supported this project.

LITERATURE CITED

1. McDonald, A.D., "Microwave Breakdown in Gases," John Wiley & Sons, 1966.

2. Hollahan, J.R. and A.T. Bell, "Techniques and Applications of Plasma Chemistry," Wiley-Interscience Publications (1974).

3. Bonet, C., "Thermal Plasma Processing," Chem. Eng. Prog., 72(12), 63 (1976).

4. Baddour, R. and R. Timmons, "The Application of Plasmas to Chemical Processing", edited by MIT Press, Boston, Mass., 1967.

5. Busch, K.W. and T.J. Vickers, "Fundamental Properties Characterizing Low-Pressure Microwave-Induced Plasmas as Excitation Sources for Spectroanalytical Chemistry," Spectrochimica Acta, 28B, 85-104 (1973).

6. Blaustein, B.D. and C. Fu, "Hydrocarbons from H_2 + CO and H_2 + CO_2 in Microwave Discharges: Le Chatelier's Principle in Discharge Reactions," Chemical Reactions in Electrical Discharges, Advances in Chemistry Series, American Chemical Society, Washington, D.C., 80, 250 (1969).

7. Work, D.W., "Microwave Pyrolysis of Organic Material," M.S. Thesis, Chemical Engineering, University of Washington (1977).

8. Copson, D.A., "Microwave Heating," 2nd Ed., AVI, New York (1975)

9. Püschner, H.,"Heating with Microwaves," Springer-Verlag, New York (1966).

10. Jolly, J.A., "Industrial Engineering Awareness of Industrial Microwave Power," J. Microw. Power, 14(1), 15 (1979).

11. Stucky, S.S. and M.A.K. Hamid, "Physical Parameters in Microwave Heating Processes," J. Mic. Power 7(2), p. 117 (1972)

12. Bhattacharyya, D. and D.C.T. Pei, "Application of Microwave Power in Heat Transfer Studies," J. Microwave Power, 8(3/4), 287 (1973).

13. Kase, Y. and K. Ogura, "Microwave Power Applications in Japan," J. Microwave Power, 13(2), 115 (1978).

14. Allan, G.G., B.B. Krieger and D.W. Work, "Dielectric-loss Degradation of Polymers. Cellulose." J. Poly. Sci., in press, 1980.

15. Tsutsumi, S., "Recycling of Waste Plastics," Chemical Economy and Engineering Review, 6(1):7-20 (Jan. 1974).

16. Chan, R.W.C. and B.B. Krieger, "Kinetics of Dielectric-Loss Microwave Degradation of Polymers, Lignin," Journal of Applied Polymer Science, accepted August 1980.

17. Ang, T.K., D.C.T. Pei and J.D. Ford, "Microwave Freeze Drying: An Experimental Investigation," Chem. Eng. Sci., 32, 1477 (1977).

18. Ang, T.K., J.D. Ford and D.C.T. Pei, "Microwave Freeze Drying of Food: A Theoretical Investigation," Int. J. Heat and Mass Trans., 20, 517-526 (1977).

19. Ohlsson, T. and P.O. Risman, "Distribution of Microwave Heating, Spheres and Cylinders," J. Microwave Pow., 13(4), 303 (1978).

20. Schwartz, H.F., R.G. Bossisio, M.R. Werthheimer and D. Couderc, "Microwave Curing of Synthetic Rubbers," J. Mic. Power, 8(3/4), 303 (1973).

21. Goodyear Corp., Technical communication with William Robinson (1979). U.S. Patent 4,002,587

22. Wen, C.Y. and S. Tone, "Coal Conversion Reaction Engineering," in Chemical Reaction Engineering Reviews, ACS Symp. Ser. 72, 1978.

23. McClean, M.C., "Wood Handbook," U.S. Forest Service and Forest Product Laboratories (1943).

24. Reed, T.B., "Energy Requirements in Biomass Densification," ACS, Div. Environ. Chem. Abstracts, Sept. 11, 1979, p. 199.

25. Solar Energy Research Institute, A Survey of Biomass Gasification, Vol. II, SERI/TR-33-239, July, 1979.

26. Gerling-Moore; manufacturer of microwave units, Palo Alto, California

27. Tinga, W.R. and S.O. Nelson, "Dielectric Properties of Materials for Microwave Processing," J. of Microwave Power, 8(1):23 (1973).

28. Chan, W.C.R., "Kinetics and Product Distribution in the Microwave Pyrolysis of Biomass," M.S. Thesis, University of Washington (1979).

29. Iatridis, B. and G.R. Gavalas, "Pyrolysis of a Precipitated Kraft Lignin," Ind. Eng. Chem. Prod. Res. Devl., 18, 127 (1979).

30. Russel, W., D. Saville and M.I. Greene, "A Model for Short Residence Time Hydropyrolysis of Single Coal Particles," A.I.Ch.E. J., 25, 65 (1979).

31. Bradbury, A.G., Y. Sakai and F. Shafizadeh, "A Kinetic Model for Cellulose," J. Appl. Poly. Sci. 23, 3271 (1979).

32. Kraszewski, A., "Model of Dielectric Properties of Wheat at 9.4 GHz," J. Microwave Power, 13(4), 293 (1978).

33. Milne, T. and D. Jantzen, "A Survey of Biomass Gasification," Vol. 2, Principles of Gasification, SERI/TR-33-239, July, 1979.

34. Shafizadeh, F. and G.D. McGinnis, "Chemical Composition and Thermal Analysis of Cottonwood," Carbohydrate Research, Vol. 16, p. 273, 1971.

35. Krieger, B.B., "Chemicals from Agricultural and Western Hardwood Residues," FINAL Reports, NSF Grant, 77-08979, 1980.

36. Roberts, A.F., "A Review of Kinetics Data for the Pyrolysis of Wood and Related Substances," Comb. and Flame, 14, 261 (1970).

37. Roberts, A.F., "Problems Associated with the Theoretical Analysis of the Burning of Wood," 13th Symp. (Intl.) on Combustion, Comb. Inst., 893 (1971)

38. Roberts, A.F., "The Heat of Reaction During the Pyrolysis of Wood," Comb. and Flame, 17, 79 (1971)

39a. Tang, W.K. and H.W. Eickner, "Effect of Inorganic Salts on Pyrolysis of Wood, Cellulose, and Lignin Determined by Differential Thermal Analysis," U.S. Forest Service Research Paper FPL82, January (1968).

39b. Tang, W.K., "Effect of inorganic Sals on Pyrolysis of Wood, Alpha-Cellulose, and Lignin Determined by Dynamic Thermogravimetry," U.S. Forest Service Research Paper FPL71, January (1967).

40. Robertus, R.J., L.K. Mudge, D.H. Mitchell, R.L. Cox, L.J. Sealock, Jr. and S.L. Weber, "Investigation of Gasification of Wood in the Presence of Mixed Catalysts," Paper 78d, AIChE 72nd National Meeting, San Francisco, California, November 1979.

41. Shafizadeh, F., R.H. Furneaux, T.G. Cochran, J.P. Scholl and Y. Sakai, "Production of Levoglucosan and Glucose from Cellulosic Materials," J. Appl. Poly. Sci., 23, 3525 (1979).

42. Sakai, T., K. Soma, Y. Sasaki, H. Tomingo and T. Kunugi, "Secondary Reactions of Olefins in Pyrolysis of Petroleum Hydrocarbons," Laboratory and Industrial Pyrolyses, ACS Symp. Ser. 32, 68 (1976).

43. Shivadev, U.K. and H.W. Emmons, "Thermal Degradation and Spontaneous Ignition of Paper Sheets in Air by Irradiation," Comb. and Flame, 22, 223 (1974).

44. Che, S.C.L., "Microwave Pyrolysis of Coals and Polynuclear Hydrocarbons," University of Utah, Ph.D. in Chemical Engineering, 1974.

45. Appell, H.R., Y.C. Fu, S. Friedman, P.M. Yavorsky and I. Wender, "Converting Organic Wastes to Oil," Report of Investigation, p. 7560, Bureau of Mines, 1971.

46. Graef, K.M., G.G. Allan and B.B. Krieger, "Rapid Pyrolysis of Lignin for Production of Acetylene, Biomass a Non-Fossil Fuel Source," ACS Symp. Ser. (1980).

47. Burggraaf, P.S., "Plasma Etching Technology," Semi-Conductor Intl., Dec., 1979; p. 49.

48. Slottee, J.S. and B.B. Krieger, "Effect of Particle Size on Volatiles Produced From Plasma Pyrolysis of Lignin," 89th National AIChE Meeting; Portland, Oregon, Paper (30d), August 17-20, 1980.

49. Kansa, J.E., et al., "Mathematical Model of Wood Pyrolysis Including Internal Forced Convection," Comb. and Flame 29, p. 311 (1977).

50. Panton, R.L. and J.G. Rittman, "Pyrolysis of a Slab of Porous Material," 13th Symp. (Intl.) on Combustion, Comb. Inst., 881 (1970).

51. Lee, C.K., R.F. Chaiken and J.M. Singer, "Charring Pyrolysis of Wood in Fires by Laser Simulation," 16th Symp. (Intl.) on Combustion, Comb. Inst., 1459 (1976).

52. Fan, L., et al., "Volume Reaction Model for Pyrolysis of a Single Solid Particle Accompanied by a Complex Reaction," The Canadian J. Eng. 56, p. 603 (1978).

53. Kung, H.C., "A Mathematical Model of Wood Pyrolysis," Comb. and Flame 18, 185-195 (1972).

54. Murty, K.A. and P.L. Blackshear, "Pyrolysis Effects in the Transfer of Heat and Mass in Thermally Decomposing Organic Solids," Eleventh Symp. (Intl.) on Combustion, 517-523 (1967).

55. Murty, K.A., "Thermal Decomposition Kinetics of Wood Pyrolysis," Comb. and Flame, 18 75 (1972).

56. Murty, K.A. and Blackshear, P.L., "An X-Ray Photographic Study of the Reaction Kinetics of α-Cellulose Decomposition," Pyrodynamics, 4 285 (1966).

57. Gavalus, G.R. and K.A. Willcs, "Intraparticle Mass Transfer in Coal Pyrolysis," A.I.Ch.E. J. 26(2) 201 (1980).

58. Crowl, D.A. and R.A. Riccirealli, "Transport Processes in Pyrolysis of Antrim Oil Shale," Energy Comm. 5(6) 425-470 (1979).

59. Martin, S., "Diffusion-Controlled Ignition of Cellulosic Materials by Intense Radiant Energy," Tenth Symp. (Intl.) on Combustion 877-896 (1965).

60. Tinney, E.R., "The Combustion of Wood Dowels in Heated Air," Tenth Symp. (Intl.) on Combustion, 925-930 (1965).

61. Freihaut, J.D., A.A. Leff and F.J. Vastola, "The Combined Influence of Chemical and Physical Factors Upon Coal Particle Temperature Profiles During Rapid Heating Pyrolysis," 173rd ACS Meeting, Division of Fuel Chemistry, New Orleans, 22 (1), (1977).

62. Wiggins, D., "Heat Transfer in The Degradation of Lignin in a Microwave Induced Plasma," Master Thesis, University of Washington, 1979.

63. Carberry, T.J., "Chemical and Catalytic Reaction Engineering," McGraw-Hill, N.Y. (1976).

64. Graef, K.M., "Reactions of Lignin in a Microwave Induced Plasma," M.S. Thesis, Chemical Engineering, University of Washington, 1978.

65. Slottee, J.S., "Effect of Particle Size and Other Variables on Volatiles from Plasma Pyrolysis of Lignin-A Statistical Experimental Design," M.S. Thesis, University of Washington (1980).

66. Box, G.E.P., J.S. Hunter and W.G. Hunter, Statistics For Experimenters, Wiley (1978).

67. Wiggins, D. and B.B. Krieger, "Effect of Heating and Quenching Rates on Volatiles Produced from Combustion-Level-Heat-Flux Pyrolysis of Biomass," 89th National AIChE Meeting; Portland, Oregon, Paper (36b), August 17-20, 1980.

68. Mertz, S.R., J. Asmussem and M.C. Hawley, "An Experimental Study of Reactions of Co and H_2 in a Continuous Flow Microwave Discharge Reactor," IEEE Trans. Plasma Sci., PS-2 (4), p. 297, 1974.

PRODUCT COMPOSITIONS AND KINETICS FOR RAPID PYROLYSIS OF CELLULOSE

M. R. Hajaligol, W. A. Peters,* J. B. Howard
and J. P. Longwell
Energy Laboratory and Department of Chemical Engineering
Massachusetts Institute of Technology
Cambridge, Massachusetts 02139

ABSTRACT

Systematic studies of the independent effects of temperature (300-1100°C), solids residence time (0-30s), and heating rate (<100-15,000°C/s) on the yields, compositions, and rates of formation of products from the rapid pyrolysis of 0.0101 cm thick sheets of cellulose under 5 psig pressure of helium have been performed. Temperature and sample residence time are the most important reaction conditions in determining the pyrolysis behavior, while heating rate effects are explicable in terms of their influence on these two parameters. A heavy liquid product of complex molecular composition accounted for 40 to 83 wt% of the volatiles above 400°C. Secondary cracking of this material increased with increasing residence time or temperature and was a significant pathway for production of several light gases. For short solids residence time the more volatile products included modest quantities of H_2 (∿1 wt.%), CH_4, C_2H_4, C_2H_6, C_3H_6 (∿0.2-2.5 wt.% each), and light oxygenated liquids such as acetone/furan mixtures, methanol, and acetaldehyde (∿0.8-1.5 wt.% each), most of which were formed primarily over the temperature range 500-800°C. At temperatures above 750°C for all holding times CO dominated the product gases, and attained a yield above 23 wt.% at 1000°C. Char yields decreased monotonically with increasing temperature to a minimum of ∿3 wt.% at temperatures of 700 and 800°C at solids residence times of 2 and 0s respectively.

INTRODUCTION

Previous research at M.I.T. and elsewhere [1,2] indicates that biomass pyrolysis offers promise for producing commercially interesting quantities of high heating value gases, and liquids suitable for replacing petroleum-based products such as distillate fuels, high octane motor fuel additives, and olefinic feedstocks. Realization of this potential, however, is critically dependent on identification of reaction conditions achievable in practical scale equipment. There have been many previous investigations of the pyrolysis of wood, cellulose and other forms of renewable materials. However, there still remains a great need for reliable systematic studies of the independent effects of commercially interesting reaction conditions such as temperature, heating rate, solids residence time, vapor phase residence time, pressure, presence of reactive gas, and sample dimension, and of the type of material, on the yields, compositions, and rates of pro-

* To whom correspondance may be addressed.

duction of pyrolysis gases, liquids and chars. This level of detail is needed to gain better fundamental understanding of, and to provide predictive modeling capability for, the thermal degradation of lignocellulosic and other biomass materials. It would also be useful in the selection, design, and optimization of thermal processes for converting renewable resources to clean fuels and chemical feedstocks. Further, since pyrolytic decomposition supplies the volatiles that allow ignition and support flaming combustion of most materials these data would also be of interest in studies on materials flammability, flame spread and stability, and related issues in fire research.

This paper presents recent results from an ongoing M.I.T. research program aimed at providing data and interpretive models responsive to the above needs. Effects of temperature, solids residence time and heating rate on the yields, compositions and rates of formation of products from the rapid pyrolysis of cellulose under a pressure of 5 psig of helium are the main focus. Subsequent communcations will furnish similar information on wood, lignin, and hemicellulose, and on cellulose at other pressures.

OBJECTIVES

The overall objective of this work was to determine quantitatively, by experimental measurements and associated modelling efforts, how reaction conditions affect the rapid thermal decomposition behavior of cellulose. Specific objectives were to measure product yields, compositions and rates of formation for ranges of reaction conditions of commercial and scientific interest including: temperature (300-1100°C), heating rate ($\leq$ 100-15,000°C/s), total pressure (0.0001-69 atm), sample size ($\sim$100-400 μm), and sample residence time (0-30 s).

APPARATUS AND PROCEDURE

Reactor Description

Laboratory scale batch reactors were employed in this work. These devices were designed to allow: a) total product collection for direct measurement of material and elemental balances; b) inversion of product yields from rapid thermal processes to kinetic parameters via non-isothermal models; and c) separation of collaborative effects of heating rate, residence time, sample size, extent of sample dispersion and temperature.

A schematic of one such reactor and the product collection equipment is shown in Fig. 1. This reactor vessel is designed for atmospheric pressure and vacuum pyrolysis work. It is a Corning Pyrex, cylindrical pipe, nine inches in diameter and nine inches long, closed at each end with stainless steel flanges, with electrical feedthroughs and gas inlet and outlet ports. Another version of this reactor capable of operation

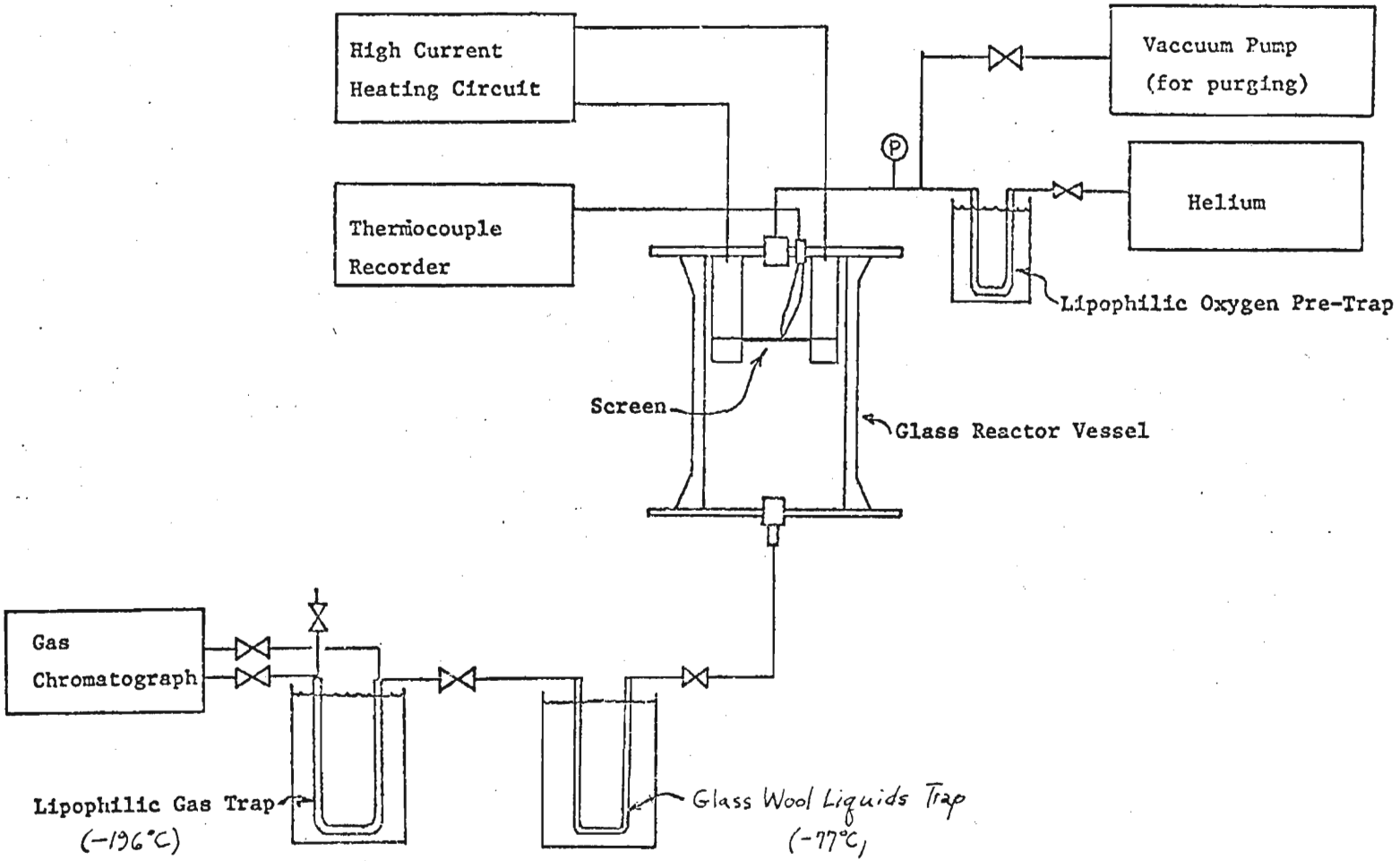

Figure 1. Captive Sample Apparatus

of up to 1500 psig is also available for studies of elevated pressures. The sample is heated inside a folded strip of 325 mesh stainless steel screen held between two massive brass electrodes mounted within the above vessel. The heating circuit consists of 100 and 50 amp variable transformers connected to two 100 amp relays which are in turn respectively activated by 0-1s and 0-60s timer switches. This system allows independent variation of the following reaction conditions over the indicated ranges; heating rates (100-100,000°C/s), final temperatures (200-1100°C), sample residence time at final temperature (0 - ∞ s). During operation most of the gas within the reactor remains close to room temperature so that upon exiting the immediate neighborhood of the hot stage, volatiles are rapidly diluted and quenched.

The time-temperature history of the sample over the entire run is measured in each experiment using a rapid response (time constant = 0.003 s) type K (chromel/alumel) thermocouple fabricated by joining 25.4 μm diameter bare wires to give an approximately 76 μm diameter bead. The thermocouple is placed within the folded screen and its output (millivolt range) is monitored by a fast response strip chart recorder.

Experimental Procedure

The cellulose samples used in this work were approximately 100 mg, thin strips of predried,[1] low ash (<0.007 wt.%) S & S No. 507 filter paper of dimensions 2 cm x 6 cm x 0.0101 cm thick and elemental composition C: 43.96 wt.%, H: 6.23 wt.%, and O: 49.82 wt.%. To begin a run a sample is placed between two folds of a preweighed screen which is then reweighed and inserted between the brass electrodes of the reactor. The thermocouple bead is inserted within the folds of the screen. The reactor is evacuated to a pressure of 0.1 mm Hg and flushed 3 to 5 times with helium, and then set at the desired pressure. The sample temperature is raised at a desired rate to a desired holding value which is maintained until the circuit is broken. The screen and remaining solid material then cool primarily by radiation and natural convection at an initial rate of around 200°C/s.

All products are collected in each run enabling total material balances and elemental balances to be directly determined (see below). The yield of char, which remains on the screen, is determined gravimetrically.

Those products which remain in the vapor phase within the reactor include gases, light liquids, and a small amount of material retained on glass wool at temperatures up to 100°C. The last is included in the product fraction operationally defined as tar. These three materials are collected by purging the reactor vessel with 3 to 5 volumes of helium and transporting them to two downstream traps. The first trap consists of a 36 cm long x 0.95 cm O.D., U-Shaped tube packed with

[1]The samples were dried in a dessicator over silica gel for at least 1 week prior to use.

glass-wool and is immersed in a bath of dry ice/alcohol (-77°C). The second (downstream) trap of the same geometry and dimensions, is packed with 50/80 mesh Porapak QS and is immersed in a bath of liquid nitrogen (-196°C). Those products which can be recovered from the traps by warming them to 100°C are analyzed gas chromatographically using a 3.66 m x 0.64 cm O.D. 50/80 mesh Porapak QS column, temperature programmed from -70°C to 240°C at a rate of 16°C/min with helium carrier gas at a 60 ml/min flow rate.

Hydrogen, which is recovered by direct sampling of the reactor atmosphere with a precision gas syringe, is analyzed on a 3.05 m x 0.32 cm O.D. 80/100 mesh, spherocarb column, operated isothermally at 0°C using nitrogen carrier gas at a flow rate of 30 ml/min. A thermal conductivity detector is used in both analyses.

Tar is operationally defined as material condensed: (a) within the reactor vessel at room temperature on the walls and flanges, and (b) in the glass wool trap described above and not evolved by heating to 100°C. It is recovered by washing the above locations with a 2:1 (v/v) mixture of methanol and acetone. Its yield is determined gravimetrically after evaporating the solvent.

Selected samples of char and tar are sent to a commercial laboratory for elemental analyses for carbon, hydrogen, and oxygen.

RESULTS OF APPARATUS VALIDATION EXPERIMENTS

All the data reported in this paper are for the thin strip cellulose samples described above. All yields are presented as a percent by weight of initial cellulose, unless otherwise specified. Selected experiments were performed to assess the validity of the experimental data and to determine the ranges of operating conditions where the above apparatus exhibits minimal contributions from secondary reactions. The results now follow.

Material and Elemental Balances

The apparatus described above gave very good total mass balances and reproducibility in the product yield and composition data. In most experiments the total material balance closure was 100±5% although in some runs only 90 to 95% of the original mass of the cellulose was accounted for. Elemental balances for carbon, hydrogen and oxygen were calculated for selected experiments from the data on volatiles yields and compositions, and elemental analyses of the product tar and char. Typical results for four runs are presented in Table 1 along with the total mass balances. The four balances are seen to be excellent for each of the cases. In this calculation the total amount of nitrogen, sulfur, and ash were assumed to be virtually zero.

Table 1. Carbon, Hydrogen, Oxygen, and Total Mass Balances for Cellulose Pyrolysis

Products	Peak Temperature 500°C				Holding Temperature[1] 400°C				Peak Temperature 750°C				Peak Temperature 1000°C			
	Total	C	H	O	Total	C	H	O	Total	C	H	O	Total	C	H	O
CO	.99	.42	-	.57	.25	.11	-	.14	15.82	6.78	-	9.04	22.57	9.67	-	12.9
CO_2	.3	.08	-	.22	1.45	.40	-	1.05	2.38	.65	-	1.73	3.36	.92	-	2.44
H_2O	3.55	-	.39	3.16	6.49	0.	.72	5.77	8.72	-	.97	7.75	9.22	-	1.03	8.19
CH_4	0.	0.	0.	-	0.	0.	0.	-	1.11	.83	.28	-	2.62	1.96	.66	-
C_2H_4	0.	0.	0.	-	0.	0.	0.	-	1.05	0.9	.15	-	2.18	1.87	.31	-
C_2H_6	0.0	0.	0.	-	0.	0.	0.	-	.17	.14	.03	-	.28	.22	.06	-
C_3H_6	0.	0.	0.	-	0.	-	0.	-	.70	.6	.1	-	.80	.69	.11	-
H_2	0.	-	0.	-	0.	0.	0.	-	.36	-	.86	-	1.18	-	1.18	-
CH_3OH	.25	.09	.02	.14	.21	.08	.03	.1	1.03	.39	.13	.51	.98	.37	.12	.49
CH_3CHO	.01	.01	.0	0.	.05	.03	0.	.02	1.58	.86	.14	.58	1.7	.93	.15	.62
C_4+ Ethanol	.00	0.	0.0	0.	0.	0.	0.	0.	.29	.15	.04	.10	.38	.2	.05	.13
AC + FU	0.07	.04	.01	.02	.16	.1	.02	.04	1.00	.62	.10	.28	.82	.51	.08	.23
$CHO(CH_3COOH)$	.12	.05	.01	.06	.0	0.	0.	0.	.85	.34	.06	.45	.58	.23	.04	.31
Tar	16.37	7.5	.97	7.9	83.35	38.28	4.95	40.32	59.92	27.77	3.63	28.63	49.12	22.89	2.98	23.25
Char	83.63	38.13	5.34	40.16	6.17	4.94	.24	.99	3.32	2.65	.1	.57	3.91	3.46	.13	.32
Total	105.25	46.32	6.74	52.23	98.36	43.96	5.96	48.43	98.8	42.68	6.59	49.53	99.86	43.92	6.9	48.88
Closure	105%	105%	108%	105%	98%	100%	96%	97%	99%	97%	106%	99%	100%	100%	111%	98%

[1] Holding Time = 30s

Extent of Secondary Reactions on the Screen Heater

The wire mesh screen used to support and heat the cellulose sample could cause catalytic or other secondary reactions during the cellulose decomposition. As part of the routine run procedure the screens are prefired in helium which contains a small amount of oxygen impurity. During this operation the latter is believed to react with chromium in the stainless steel to produce a layer of chromia which probably reduces the catalytic activity of the screen [3]. Nevertheless, to more quantitatively assess the role of surface effects experiments were performed to either passivate the screen to cracking or to augment its opportunity to cause cracking. To the former end a pyrolysis run was performed with a screen on which a layer of gold had been vacuum deposited while to the latter, runs were carried out using up to five layers of hot screen above the cellulose sample. Operating conditions in all cases were 5 psig of helium pressure, 1000°C/s heating rate, about 1000°C final temperature, and zero sample holding time. The results in all cases showed almost no difference in the product yields and compositions, except that in the multiscreen experiments there were changes in the small amount of the tar collected downstream of the reactor. While the total tar make was essentially unchanged, the yield of the latter constituent increased, from 2.8 wt.% with 2 layers of screen (normal operation) to 3 and ∿5.5 wt.% respectively with 3 and 5 layers. It was thus concluded that, except possibly for a very minor amount of cracking of heavier tar components to lighter ones, the surface of the screen heater exerted little influence on the data obtained in the above reactor.

Extent of Secondary Reactions Within the Sample

It is obvious that in any pyrolysis apparatus there is a maximum sample dimension above which heat and mass transfer limitations will exert a significant influence on the observed thermal decomposition behavior. Experiments were performed with the present equipment to determine if the conveniently available 0.0101 cm thick samples were small enough so that these effects would be unimportant. Runs were carried out under the conditions specified for the multiscreen tests, using samples of up to four times the above thickness. The results showed that doubling the thickness of the sample has no significant effect on the total cellulose decomposition or total yields of tar and volatiles. However, a four fold increase in sample thickness gave decreased tar production and a corresponding increase in total gas yield. The latter results may arise from enhanced secondary cracking due to increased tar and volatiles residence time within the thicker sample and from temperature variations due to thermal lags between the centerline and the surface of the sample. Heat transfer calculations showed that during heating at rates of up to 1000°C/s the temperature of the centerline of the 0.0101 cm thick sample should in the worse case lag its surface temperature by no more than 11-30°C.

Based on the above measurements and calculations it was thus concluded that the 0.0101 cm thick cellulose sheets are sufficiently small that contributions to their pyrolysis behavior from intra-sample heat and mass transfer effects can be neglected.

RESULTS AND DISCUSSION

Effects of Reaction Conditions on Product Yields and Compositions

Temperature

Data on the effects of temperature on the yields and compositions of char, tar and lighter volatiles from the pyrolysis of thin sheets of cellulose of the size and composition specified above are shown in Figures 2-6. These results were obtained in so-called peak temperature runs in which the sample was heated under 5 psig of helium, to the temperature indicated on the abscissa at a nominal rate of 1000°C/s, and then immediately allowed to begin cooling at an initial rate of 200°C/s. Figure 2 presents the results for char, tar and gas (including water) yields, which show that for these heating rates measurable decomposition of cellulose begins between 300 and 400°C. The extent of decomposition increases with temperature until almost 95 wt.% of the sample is converted to volatiles at 750°C. Most of the weight loss takes place between 500 and 700°C. Above 750°C the yield of char decreases from 6% to about 3% between 800 and 900°C. Because of cracking of volatiles which occurs at very high temperatures, it then increases very slowly with further temperature increases, reaching about 4% at 1000°C.

Tar yield increases with temperature to a maximum at around 700°C and then decreases with further temperature increases undoubtedly because cracking reactions become more favored at higher temperatures.

For significant yields of volatiles by cellulose pyrolysis under these conditions, the sample must remain above its decomposition temperature for a time which depends on the heating and cooling rate, final temperature, and operating pressure. For zero holding time conditions, complete reaction can be achieved at or above 750°C for a 1000°C/s heating rate. Most of the decomposition occurs during the heatup period. When peak temperature is reached, tar which could not escape the hot reaction zone during the heat up period could participate in secondary cracking to yield lighter volatiles. Tar yield in fact reaches a maximum at lower temperatures as holding time increases.

The total gas yield, which includes water, also increases as peak temperature increases, but at the temperature where tar yield goes through a maximum the slope of the gas yield vs. temperature curve increases. This is probably because the tar is cracked primarily to gases with little if any coke being formed.

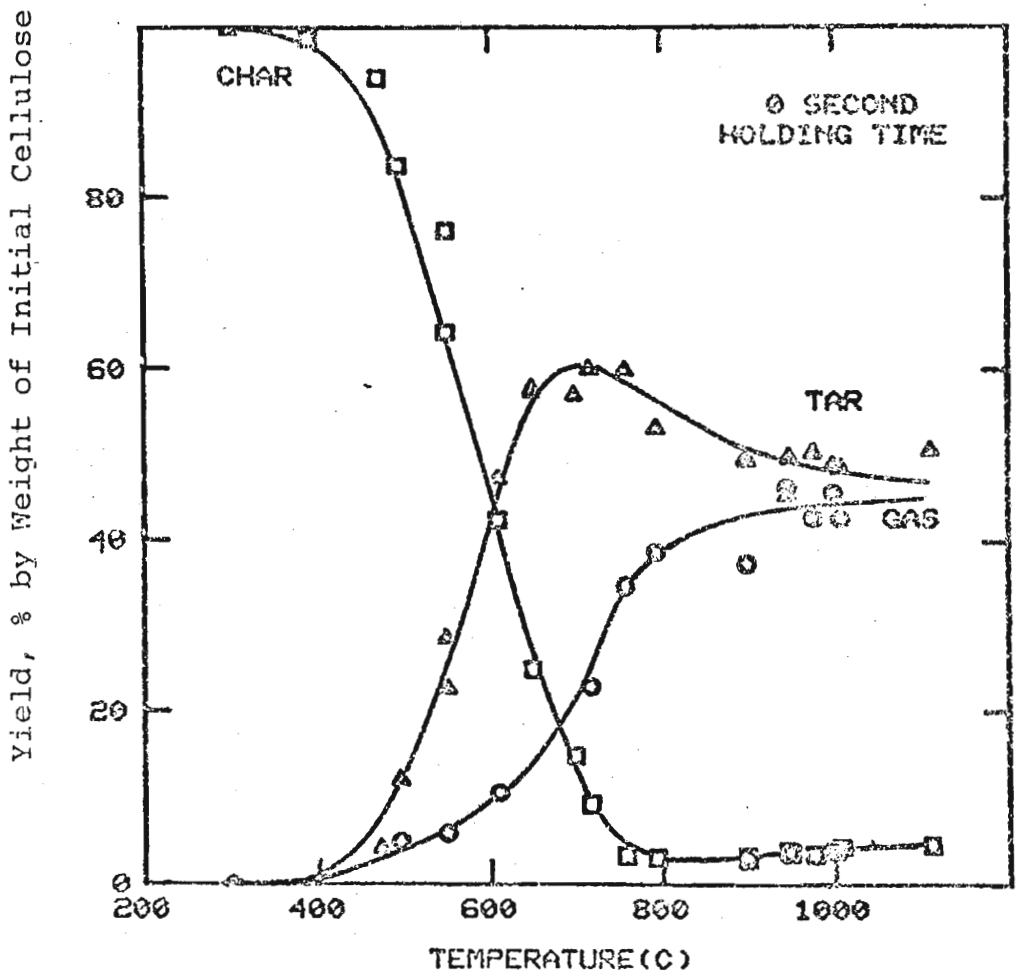

Figure 2. Effect of Peak Temperature on Yields of Char, Tar, and Gas

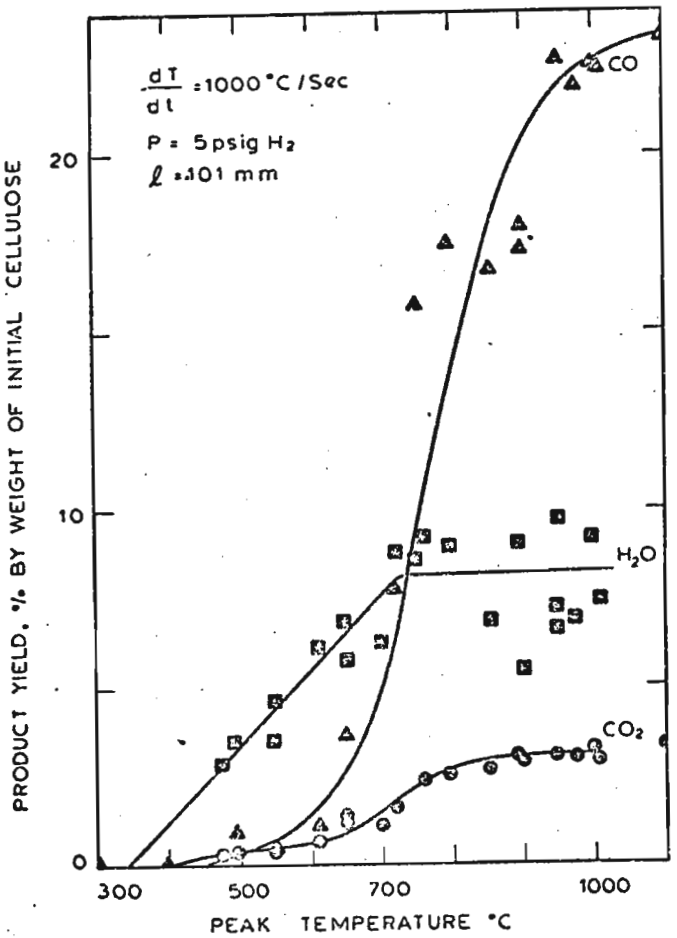

Figure 3. Effect of Peak Temperature on Yields of CO, CO_2, and H_2O

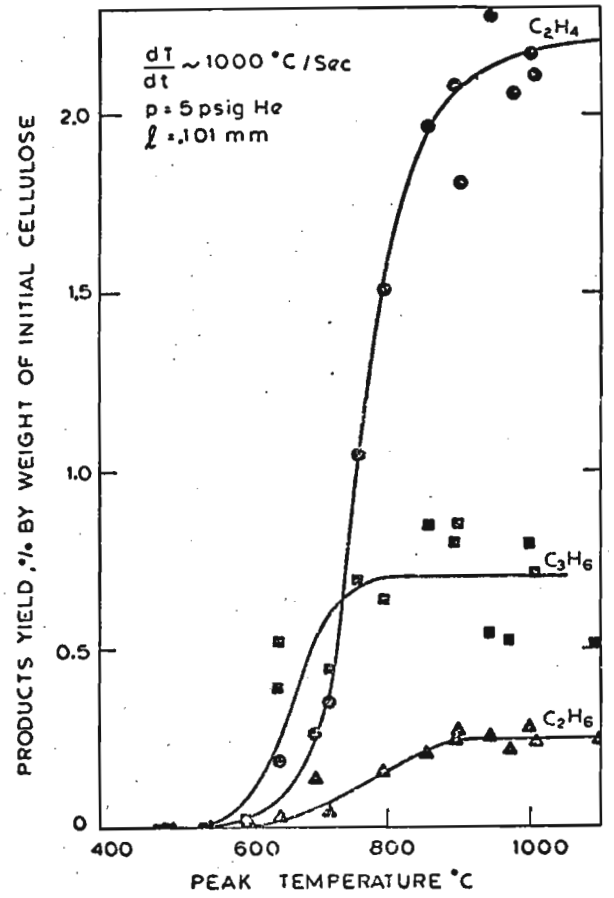

Figure 4. Effect of Peak Temperature on Yields of C_2H_4, C_2H_6, and C_3H_6

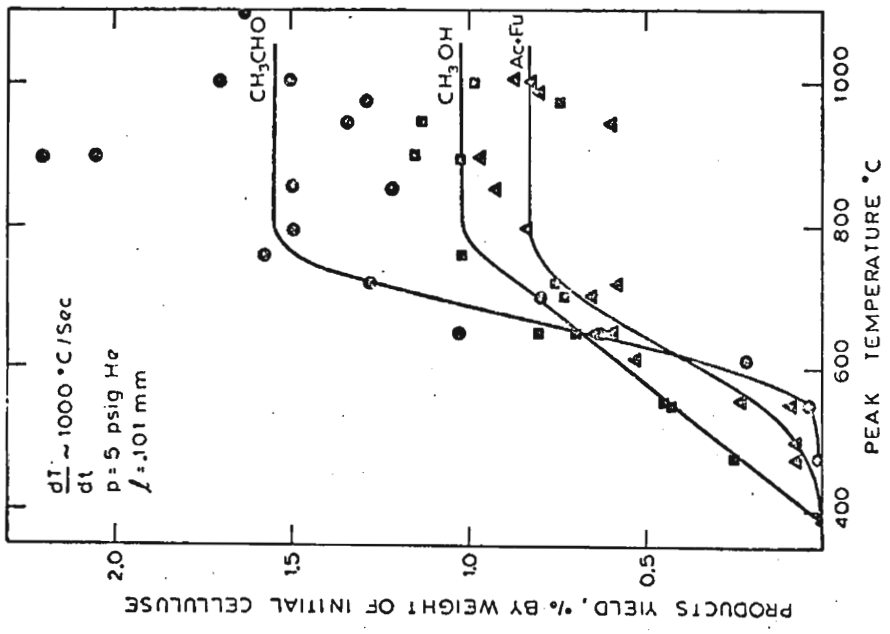

Figure 6. Effect of Peak Temperature on Yields of Acetaldehyde, Acetone + Furan, and Methanol

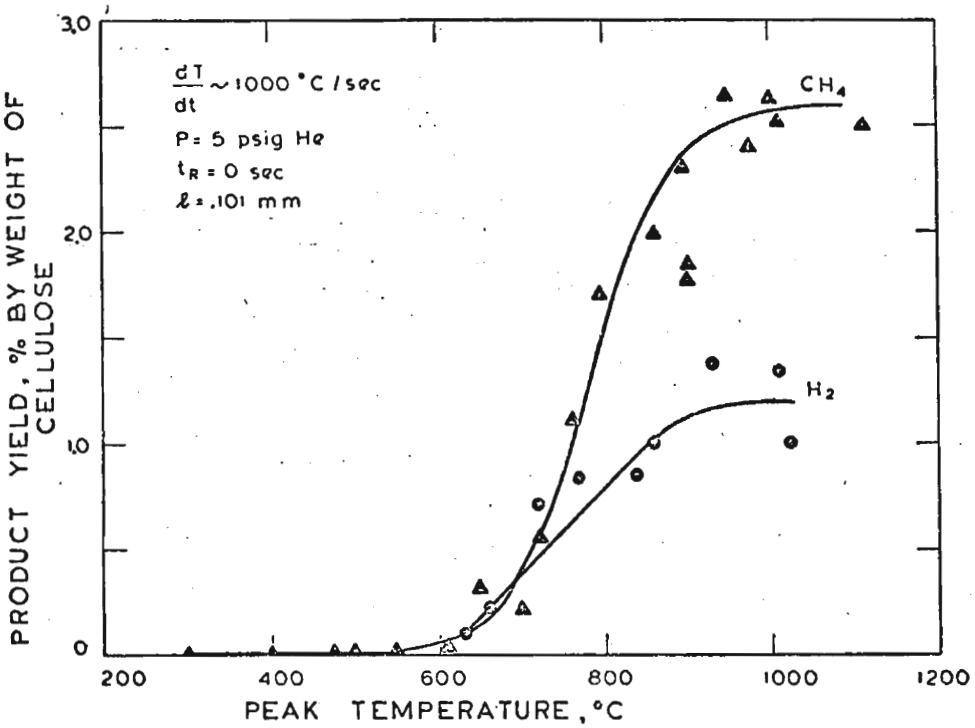

Figure 5. Effect of Peak Temperature on Yields of CH_4 and H_2

The influence of peak temperature on the yields of the indicated volatile products is shown as follows: Fig. 3: CO (23.3), CO_2 (3.2), H_2O (8.2); Fig. 4: C_2H_4 (2.2), C_2H_6 (0.25), C_3H_6 (0.70); Fig. 5: H_2 (1.2), CH_4 (2.6); and Fig. 6: acetone + furan (0.83), methanol (1.02), acetaldehyde (1.55). The yields of these products increase monotonically with temperature until the asympototes indicated here in brackets are reached at peak temperatures ranging from ∿700°C for H_2O, to ∿800°C for CO_2, C_3H_6, acetaldehyde, methanol, and acetone + furan, to 900-950°C for H_2, CH_4 and C_2H_4. The data on CO yields (Fig. 3) exhibit some scatter that arises from interferences from air impurity during the gas chromatographic analysis. It is nevertheless believed that a true asymptote for these conditions is attained at around 1000-1100°C. The yields of the light oxygenated liquids methanol, acetaldehyde, and acetone + furan may go through a maximum as temperature increases beyond ∿800-900°C but the scatter in the data preclude establishing this unequivocally. The existence of such maxima would not be unreasonable since these products can decompose at temperatures as low as 500°C.

During the early stages of the cellulose decomposition (i.e. over the peak temperature range 300-600°C at the 1000°C/s heating rate employed), the light volatiles are dominated by H_2O and some CO, CO_2, and light oxygenated liquids, but above 750°C CO is by far the most abundant gaseous product. From 300 to 600°C none of the above hydrocarbons, H_2 or the oxygenated light liquids from Fig. 6 attain yields of more than a few tenths of a percent, although the latter four compounds especially acetaldehyde are found in much larger amounts than the hydrocarbons. However above the 650-750°C temperature range where tar yield has peaked the yields of H_2, CO, CH_4, C_2H_4, and C_2H_6 increase markedly suggesting that a significant, and perhaps the dominant contribution to these products comes from secondary decomposition of the tar rather than from primary degradation of the parent cellulose.

Solids Residence Time

With the present apparatus, solids residence time or holding time is the period the sample and wire screen heater are maintained at some desired maximum temperature before initiating cooling. Volatiles generally have a very short residence time at final temperature because of the design of the reactor vessel and hot stage (Fig. 1). Figures 7 to 9 show the effects of variations in holding time over the range 0 to 30s on the yields of char, tar and gases respectively. Sample dimensions and all other operating conditions were as specified in the first part of this section. Below 800°C, increasing holding time at a constant temperature, augments both tar production (Fig. 8) and total weight loss (i.e. 100-char yield, Fig. 7). A similar effect is exerted on gas yields below about 750°C (Fig. 9). In each case the magnitude of the effect increases as the maximum temperature decreases. This behavior is believed to reflect the fact that at zero holding times and lower temperatures, decomposition of the cellulose is incomplete at the time final temperature has been reached. Providing

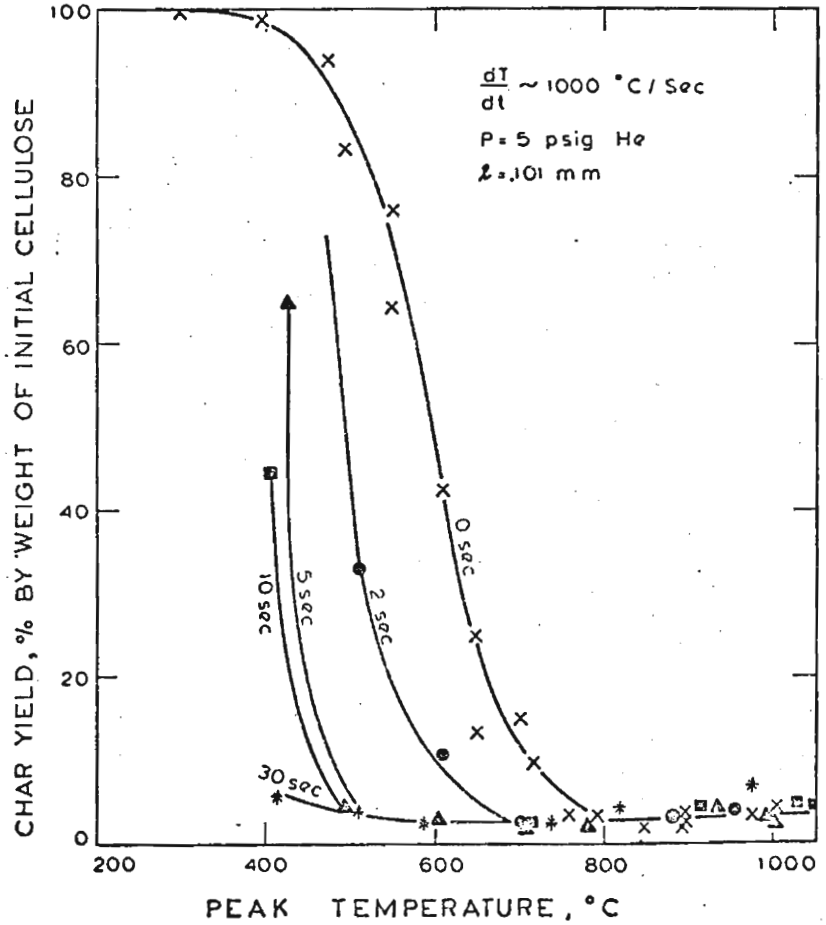

Figure 7. Effect of Solids Residence Time on Yields of Char

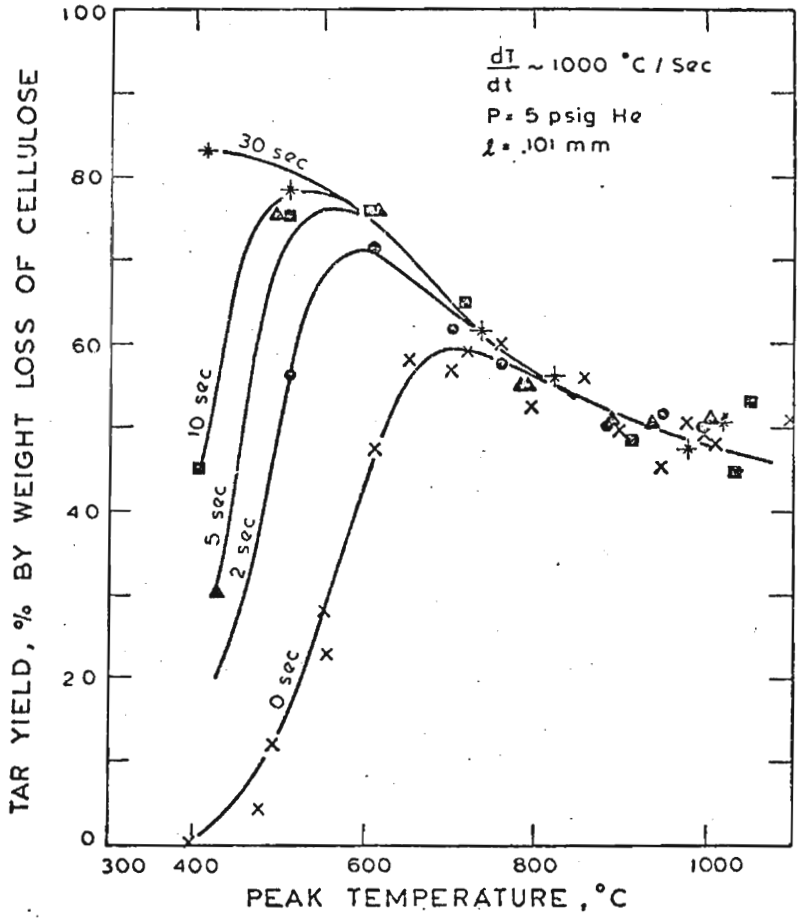

Figure 8. Effect of Solids Residence Time on Yields of Tar

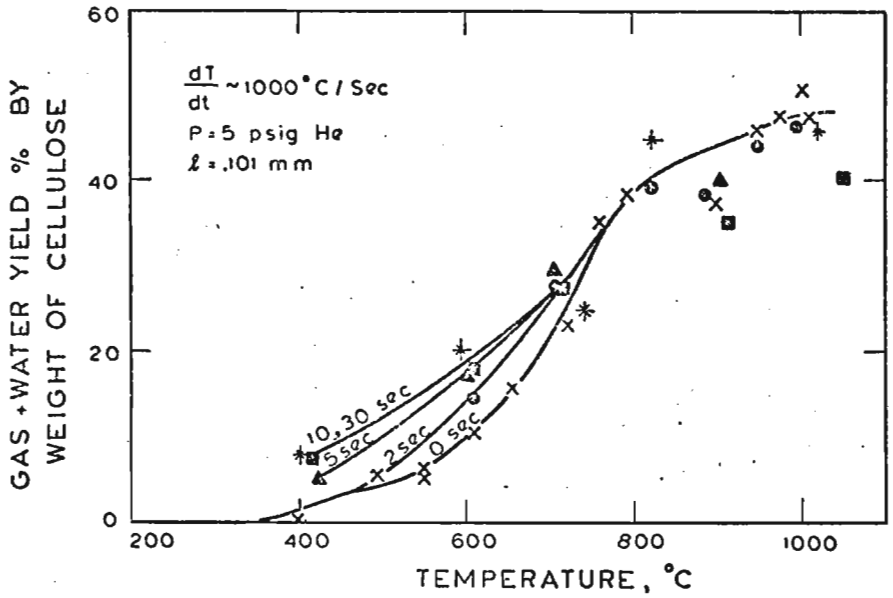

Figure 9. Effect of Solids Residence Time on Yields of Gas

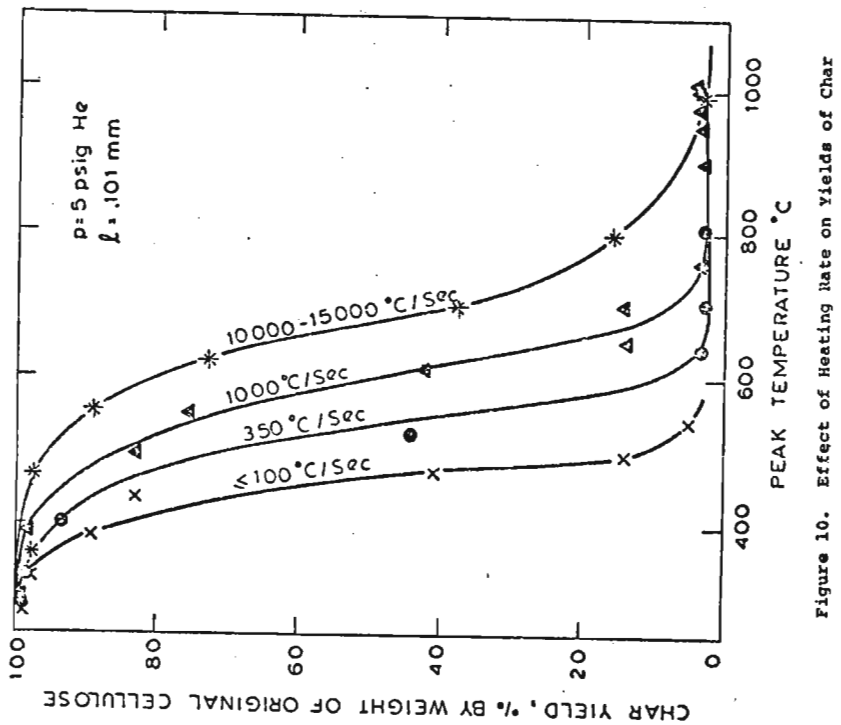

Figure 10. Effect of Heating Rate on Yields of Char

some holding time at these temperatures therefore allows further decomposition and hence the augmented yields of tar, and gas and the decline in char production. At temperatures greater than the thresholds indicated above there is essentially no effect of holding time since the reactions have become sufficiently rapid to give the maximum conversion realizable at that temperature even in zero holding times.

Figures 8 and 9 show that at a given holding time the temperature at which secondary cracking begins to dominate the global tar yield (i.e. the temperature of maximum tar production) corresponds quite well to that at which gas yields begin to increase substantially with temperature. These findings further support the picture that secondary reactions of tar play an important role in gas production under these pyrolysis conditions.

The effects of holding time on the low temperature yields of all the individual volatile products described above except water, are generally similar to those for the gas as a whole, i.e., increased yield with increased holding time. Water yield reaches an asymptote of 5.1 wt.% at a temperature of 600°C for holding times of 2 to 3 s and remains independent of temperature above 600°C. The asymptotic yields of CO_2 (3.0), C_2H_4 (1.9), C_2H_6 (0.22), C_3H_6 (0.68), and CH_4 (2.53) at 1000°C and 2-30 s shown here in brackets as wt.% are virtually the same as those for zero holding times as might be expected from Fig. 9, which shows no effect of holding time on the total gas make above 800°C. As temperature increased for these holding times the yields of acetaldehyde and of total light oxygenated liquids increased to maximum values of 1.8 and 4.7 wt.% respectively at around 800°C and then decreased with further temperature increases, undoubtedly due to increased time for secondary cracking of the oxygenates at higher temperatures.

Further details on the effects of holding time on the yields of individual volatile products determined in this work are presented elsewhere [4].

Heating Rate

Data on the effects of variations in heating rate over the range $\leq$ 100°C/s to 10,000-15,000°C/s, on yields of char, tar and gas for the other reaction conditions specified in the first part of this section are plotted in Figures 10-12 respectively. At a given peak temperature total conversion of the sample to volatiles (100 - char yield) increases as heating rate decreases. Similar behavior is exhibited by the yields of gas and, below about 750°C, of tar. These effects undoubtedly arise because at the lower heating rates more time is available for conversion reactions during the heatup period. Tar yields approach 85 wt.% of the cellulose at heating rates of $\leq$ 100°C/s and the maximum in the tar yield vs. temperature curve disappears at heating rates of 350°C/s and lower. These maxima have been interpreted as reflecting competition between: (a) escape of freshly formed tar from the elevated

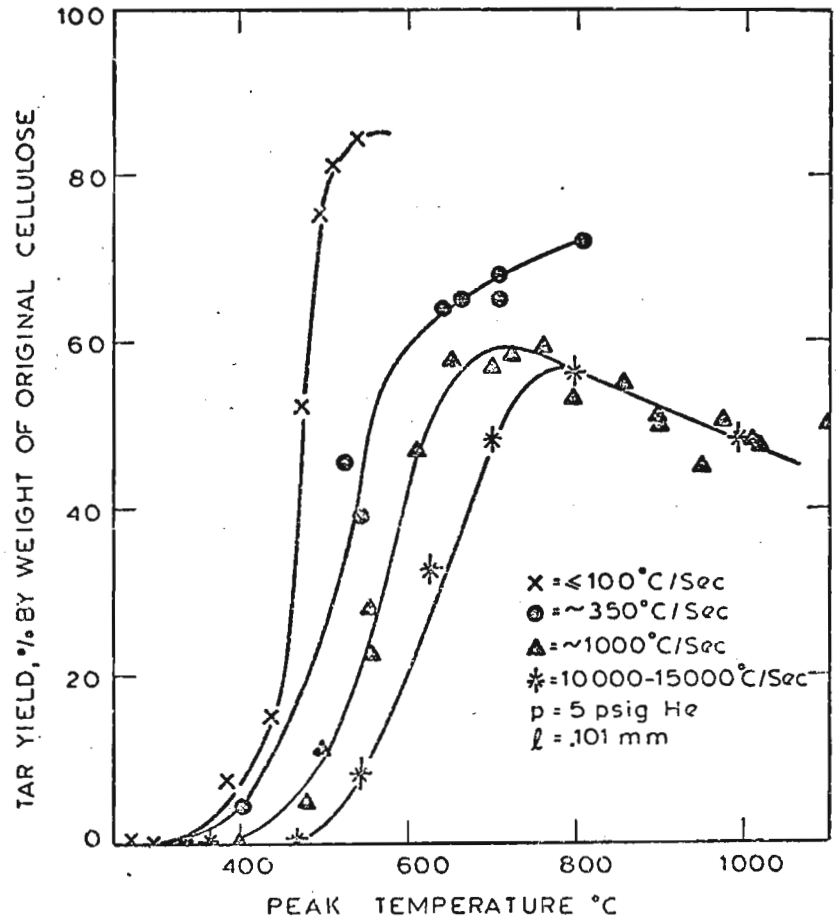

Figure 11. Effect of Heating Rate on Yields of Tar

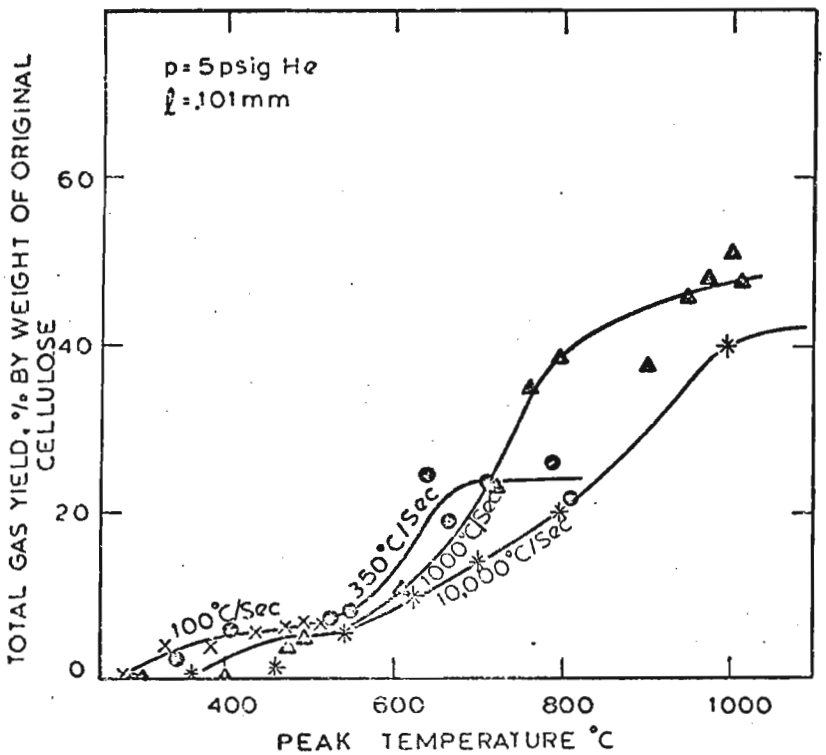

Figure 12. Effect of Heating Rate on Yields of Gas

temperature environment of the hot stage and decomposing sample, and (b) cracking of the tar in that environment. The maxima are believed to disappear because at the lower heating rates there is adequate time during the heatup period for most of the tar to be formed and then escape the immediate neighborhood of the screen before temperatures sufficiently high for extensive cracking to occur are attained.

Data have also been obtained on the effects of heating rate on the yields of most of the specific volatile products listed earlier and are presented elsewhere [4]. In general at lower temperatures their yields increase with decreasing heating rate.

Other Reaction Conditions

The effects of total reactor pressure and of sample thickness on product yields and compositions have also been studied and are presented elsewhere [4]. In brief, it was found that at a given temperature, as pressure is increased above 5 psig yields of char and most gases increase, tar yields decrease, while acetaldehyde, methanol, and acetone + furan behave as the gases at lower temperatures and as the tar at higher temperatures. This behavior undoubtedly reflects secondary cracking of tar and, at elevated temperatures, of these oxygenated light volatiles, and also implies that at higher temperatures, the latter compounds can contribute to the net make of hydrogen, CO, CO_2, and hydrocarbon gases. Increasing sample thickness from 100 μm to 193 μm had relatively little effect on the product spectrum, but a further increase to 400 μm resulted in decreased tar production and a corresponding increase in total gas yield.

Preliminary Kinetic Modeling

The data presented above, and other results on pressure effects reported in detail elsewhere [4], indicate that at higher temperatures and residence times secondary reactions of tar and of light oxygenated liquids such as acetaldehyde contribute extensively to the rates and extents of formation of light volatiles during the rapid pyrolysis of thin strips of cellulose. A rigorous kinetic model for the production of individual volatile products should therefore reflect multi-step chemical processes as well as any coupled effects of physical transport of tar or other volatiles in the neighborhood of, or possibly within, the decomposing sample. Results of modeling efforts to this end are presented elsewhere [4].

A more simplified modeling approach that has proved useful in the past for correlating similar data on the rapid pyrolysis of coal [5,6,7] was also investigated. In the simplest version of this analysis it is assumed that the cellulose decomposition directly yields a given reaction product i by a single independent reaction pathway also designated i:

$$\text{Cellulose} \xrightarrow{k_i} \text{Product i} \qquad (1)$$

and that the kinetics of this process can be modeled by a unimolecular first order reaction having a rate constant that may be written in the Arrhenius formalism:

$$\frac{dV_i}{dt} = k_{oi} e^{-E_i/RT} \quad (V_i^* - V_i) \qquad (2)$$

The experimental data for yields of specific products were fitted to this model, with a non-linear least squares regression code by integrating the non-isothermal form of Eq. (2) numerically using the experimentally measured time-temperature histories. Best fit values were obtained for the global kinetic parameters k_{oi}, E_i, and V_i^*. Table 2 presents the results for total weight loss and for several volatile products obtained under the experimental conditions given at the bottom of the Table. Theoretical yield curves calculated from these parameters generally gave good fits to the experimental yield data [4]. For many of the products the values derived for the activation energy and pre-exponential factor are reasonable for typical organic decomposition reactions [5,8]. However it is emphasized that these parameters should be considered only as useful tools for correlating the experimental data for the ranges of operating conditions under which they were measured. They should not be viewed as reflecting the detailed chemistry of cellulose decomposition to specific volatile products [1].

CONCLUSIONS

The captive sample reactor described above is a useful tool for studying the separate effects of temperature, heating rate, pressure, and solids residence time on the rapid thermal decomposition behavior of thin samples of cellulose, wood and other forms of biomass for pressures of 1 atm and above. Excellent material balances and data reproducibility are obtained. With the aid of suitable models kinetic parameters for the primary decomposition of the sample and secondary reactions of its volatiles may be derived from the integral product yields measured with this system.

Temperature and sample residence time are the two most important parameters in determining the rapid thermal decomposition behavior of cellulose. Heating rate effects can be interpreted in terms of their influence on these two reaction conditions. Thus for a fixed solids residence time and heating rate, gas yield always increases with increasing temperature, until some asymptote is attained, tar yield increases to some maximum and then declines with further temperature increases, and char yield decreases to around 3 wt.% but at high temperatures rises slightly probably due to carbon deposition from secondary reactions. At lower temperatures char yields decrease and gas and tar yields increase when either solids residence time is increased or heating rate is decreased. At higher temperatures

Table 2. Summary of Best-Fit Kinetic Parameters for Single Reaction Model of Cellulose Rapid Pyrolysis[1]

Product	E,kcal/g-mole	$Log_{10}k_o,s^{-1}$	V*,wt.%
Total Weight Loss	31.79	8.30	94.08
CH_4	60.04	13.00	2.41
C_2H_4	49.82	10.82	2.07
C_2H_6	41.55	9.06	0.26
C_3H_6	60.67	14.93	0.67
H_2	27.29	6.17	1.16
CH_3OH	49.35	13.42	0.92
CH_3CHO	55.1	13.56	1.54
Butene & Ethanol	42.54	9.9	0.32
Acetone & Furan	43.04	11.07	0.81
CHO (Mainly Acetic Acid)	58.18	12.8	1.19
H_2O	24.62	6.71	8.04
CO	52.74	11.75	21.64
CO_2	23.42	5.39	3.08

[1]Data are for the temperature range 300-1000°C, a nominal heating rate of 1000°C/s, solids residence times of 0 s and a total pressure of 5 psig. Sample size was 6 cm x 2 cm x 0.0101 cm thick.

however these two parameters have no significant influence on these yields because of the dominant influence of temperature alone.

The product spectrum from the thermal degradation of cellulose at a 1000°C/s heating rate, with zero holding time at final temperature, is characterized by evolution of chemical water from an initial decomposition at around 330°C, followed by small amounts of CO_2 and CO beginning at around 400 and 440°C respectively. Yields of most volatile products except tar increase monotonically as temperature increases and generally attain asymptotic values at temperatures between 700 and 900°C.

Modest quantities of H_2 (∿1 wt.%), CH_4, C_2H_4, C_2H_6, C_3H_6, (∿0.2 - 2.5 wt.% each) and light oxygenated liquids such as acetone/furan mixtures, methanol, and acetaldehyde (∿0.8 - 1.5 wt.% each) are formed primarily over the temperature range 500-800°C. Under zero residence time conditions carbon monoxide dominates the gaseous products above 750°C and attains a yield of above 23 wt.% at 1000°C.

Most of the tar product is material condensed in the reactor at room temperature. Based on preliminary characterization by elution chromatography and gas chromatography [9] it is believed to contain at least several hundred compounds. Its yield can be from 60 to 83 wt.% of the cellulose depending on temperature and solids residence time. At higher temperatures (400 to 700°C depending on solids residence time) the yield of this product decreases with further temperature increases undoubtedly due to secondary cracking.

This secondary cracking of tar is believed to be a significant pathway for production of H_2, CO, and several light hydrocarbon gases such as CH_4, C_2H_4, and C_2H_6.

Char yield decreases monotonically with increasing temperature under these conditions to a minimum of ∿3 wt.% at temperatures of 700 and 800°C at solids residence times of 2 and 0 s respectively. At solids residence times from 0 to 30s further temperature increases above 800°C result in modest increases in char yield, probably as a result of carbon deposition arising from secondary cracking of tar and light oxygenated volatiles.

ACKNOWLEDGEMENTS

Financial support for this work is provided by the United States Department of Energy under Grant No. DE-FG02-79ET00084 administered by the Solar Energy Research Institute and is gratefully acknowledged. Dr. Alex Kotch is the Technical Monitor for this project. Financial support for the construction of the reactor facility used in these studies, and for complementary research on biomass pyrolysis liquids was provided by the Edith C. Blum Foundation of New York and is also

greatly appreciated. Important contributions to the experimental and modeling work have been made by Dr. H. D. Franklin and Messers. R. Caron, J. Curme, and P. Houghton. Mr. P. Bhadha provided valuable data on the global chemical composition of the pyrolysis tars.

NOMENCLATURE

E_i	the activation energy for reaction i, kcal/g-mole
k_{oi}	the pre-exponential factor for reaction i, s^{-1}
ℓ	sample thickness, mm
p	total reactor pressure, psig
R	the gas constant, kcal/g-mole-°K
T	the absolute temperature, °K
V_i	the yield of product i at time t, wt.% of the cellulose
V_i^*	the ultimate yield of product i, (i.e. at $t = \infty$), wt.% of the cellulose

REFERENCES

1. Lewellen, P.C., W.A. Peters, and J.B. Howard, "Cellulose Pyrolysis Kinetics and Char Formation Mechanism", Sixteenth Symposium (International) on Combustion, The Combustion Institute Pittsburgh, (1977), 471.

2. Peters, W.A., "Literature Incentives for the Production of Clean Fuels and Chemicals from Biomass by Thermal Processing", In-house Literature Review, M.I.T. Energy Laboratory, June (1978).

3. Yurek, G.J., Personal Communication (1978).

4. Hajaligol, M.R., "Rapid Pyrolysis of Cellulose", Sc.D. Thesis, Department of Chemical Engineering, Massachusetts Institute of Technology, Cambridge, Massachusetts, in preparation (1980).

5. Suuberg, E.M., W.A. Peters, and J.B. Howard, "Product Composition and Kinetics of Lignite Pyrolysis", Ind. Eng. Chem. Process Design Develop., 17, 37 (1978).

6. Suuberg, E.M., W.A. Peters, and J.B. Howard, "A Comparison of the Rapid Pyrolysis of a Lignite and a Bituminous Coal", in Thermal Hydrocarbon Chemistry, p. 239, Advances in Chemistry Series, No. 183, A.G. Oblad, H.G. Davis, and R.T. Eddinger, Ed., Am. Chem.

Soc., Washington, D.C. (1979).

7. Suuberg, E.M., W.A. Peters, and J.B. Howard, "Product Compositions and Formation Kinetics in Rapid Pyrolysis of Pulverized Coal - Implications for Combustion", Seventeenth Symposium (International), on Combustion, 117, The Combustion Institute, Pittsburgh (1979).

8. Benson, S.W., The Foundations of Chemical Kinetics, McGraw-Hill, New York (1960).

9. Bhadha, P.M., "Fractionation of High Molecular Weight Biomass Pyrolysis Tars", Unpublished 10.90 Report, Department of Chemical Engineering, Massachusetts Institute of Technology, Cambridge, Massachusetts (1980).

ABLATIVE PYROLYSIS OF MACROPARTICLES OF BIOMASS

J.P. Diebold
Solar Energy Research Institute
1617 Cole Boulevard, Golden, CO 80401

ABSTRACT

Recent research has revealed that macroparticles of biomass can be pyrolyzed with a "solid convection" heat transfer technique to result in surface regression rates of over 3 cm/sec, which is 3 ½ orders of magnitude faster than that attained with conventional gaseous and radiative heat transfer techniques. The extremely high heat fluxes attained by this technique pyrolyze the macroparticles of biomass without forming the usual layer of char (char usually insulates the substrate to force a slow pyrolysis reaction to occur with macroparticles). This observed laboratory phenomena is being used in the design of a unique 100 lb/hr research reactor to fast pyrolyze 1 cm wood chips in which the chips will be entrained into a reactor which utilizes centrifugally-enhanced, solid-convection heat transfer.

INTRODUCTION

In considering a chemical process, selecting a process which makes a high valued product rather than a mediocre valued product has an obvious economic advantage, if all other things are equal. That is why the conversion of biomass wastes to high octane gasoline rather than a boiler fuel was selected for further study at the Naval Weapons Center in the early 1970's. Conceptually, the process involved the very selective fast pyrolysis of the biomass to gases containing significant amounts of reactive hydrocarbons such as ethylene and propylene. These gases were compressed, purified, and then under heat and pressure the reactive hydrocarbons were reacted with themselves without catalysts to form low molecular weight polymers. The polymerization reaction is self-limiting such that about 90% of the polymers boil in the gasoline range. With polymer gasoline made in this manner, but from pure ethylene, the unleaded octane number was found to be in the low 90's. Polymer gasoline made from pyrolysis gases had the same distillation curve as that made from pure ethylene, indicating that the initial presence of acetylene, propylene, and butenes in the pyrolysis gases has little effect on the product. This allows the use of a very simplified gas purification system since the various C_2^+ hydrocarbons (larger than methane) do not need to be separated from each other. Gasoline yields of about 75 gallons per dry, ash-free ton of biomass were projected based on values obtained from the pyrolysis of municipal solid waste derived feedstock (ECO II by Combustion Equipment Associates) (1).

The process is relatively energy intensive such that the byproduct

fuel gases, tars, and char (if any) would all be burned for process energy. The yields of the intermediate olefins were shown to increase with the amount of steam usage. This means that any improvement in the energy efficiency of the process, which can be converted to steam production, can be related to a small incremental increase in the potential yield of olefins. For example, a study of the energy required to recirculate carrier gases revealed that carbon dioxide required significantly more energy than the use of steam or the byproduct fuel gases. Furthermore, unless the capital expense of a larger hydrocarbon absorption tower, compressor, and a gas turbine (for energy recovery) were less than for a steam boiler, steam appeared to be a more energy efficient carrier than diluent gas. This conclusion is reinforced by the petrochemical industry's use of steam as the diluent gas when cracking naphtha to ethylene. Other means of increasing the system's efficiency would, of course, include the extensive use of heat exchangers to recover heat for steam generation. The low temperature waste heat, such as that formed by steam condensation at atmospheric pressure, would be used to heat air for feedstock drying (2).

In addition to these more obvious methods of increasing the energy efficiency of the process, the possible elimination of unnecessary, superfluous process steps was examined and found to have real potential. Figure 1 shows that the energy required for the conversion of 1 cm chips to 100 μm powder is a small portion of the energy contained in the feedstock. However, in a typical industrial situation the energy put into the biomass for grinding is in the form of mechanical energy so that the true energy penalty for grinding is 3 to 4 times as high depending on thermal to mechanical conversion efficiencies. For 100 μm particles, this amounts to $7\frac{1}{2}$ % of the energy contained in the feedstock or 10 to 15% of the energy available for process energy, which is quite significant. In addition, the hot ground feedstock would most likely be put into temporary storage where it would be allowed to cool and thereby lose all the energy put into it by the grinding step. Consequently, one of the valid criticisms of state-of-the-art fast pyrolysis is that a finely powdered feedstock is necessary to obtain the high heating rates for the particles to avoid the undesirable side reactions of pyrolysis such as char and water formation. A significant decrease in the process energy required could be attained if one could use 1 cm chips rather than 100 μm powders for fast pyrolysis feedstocks.

The last effort with the China Lake entrained-bed pyrolysis reactor before the program was phased out at the Naval Weapons Center was the pyrolysis of pure cellulose, lignin, and birch flour. Due to mechanical difficulties with the system, only a preliminary screening of these feedstocks was obtained. The cellulose and the birch flour both produced about 12 to 14% by weight of the desired hydrocarbon product (C_2^+). This was considerably lower than had been attained with the ECO II material and is thought to represent suboptimal reaction conditions. The very significant results of this work concern the very small amount of char formed and its physical shape. From the cellulose pyrolysis, only 0.1% of the feedstock was converted

FIG. 1 **Biomass Grinding Power Requirements**

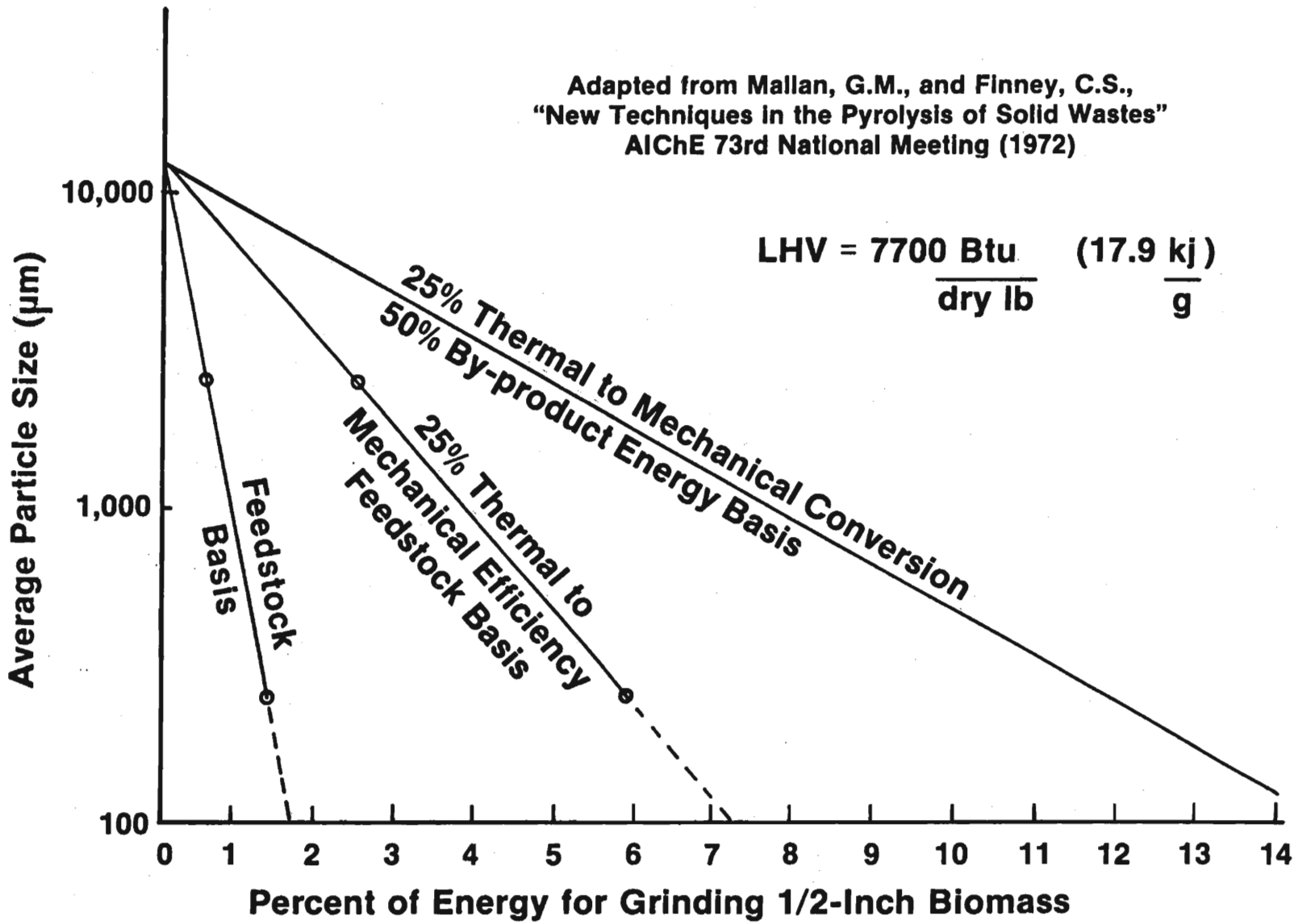

to char and part of that is thought to have been reactor scale. This result was predicted by the work done at MIT (3) in which a few milligrams of cellulose were sandwiched between electrically heated screens. However, the China Lake work demonstrated the phenomena in a continuous flow reactor with over 5 kilograms of cellulose involved in the reaction. This represents a scale-up of the phenomena by 4 or 5 orders of magnitude. The birch flour pyrolysis resulted in a 1 $^1/_2$ % conversion to char which reflects the higher ash content of the wood flour. The calculated ash content for both the cellulose and the birch char is very similar at about 30%. This similarity in ash content may indicate that the very fine ash had a catalytic effect to cause condensation reactions to occur on its surface until the resultant tars decomposed to char to block the movement of reactants to the catalytically active sites. Examination of the birch-flour char confirmed that it was not typical of slow char forming reactions. Most of this char had no structure resembling the fibrous feedstock. Instead, the char had the appearance of being an agglomeration of 1 μm spheroidal particles as shown in Figures 2 through 4 (4,5). This type of char formation is contrary to the classical concept of pyrolysis and char formation, in which the virgin feedstock has a char layer through which heat must be conducted in counter flow to the off-gassing pyrolysis products. This concept of pyrolysis, although valid for slow pyrolysis, does not appear to be applicable to fast pyrolysis. One of the apparent anomolies noted in the ECO II pyrolysis work at China Lake was that the char had about the same bulk density as the ECO II feedstock (6). This was disturbing at the time because the slow pyrolysis concepts require that the feedstock particle be hollowed out by the process. This removal of 85% of the mass should have greatly reduced the bulk density even after allowing for some physical shrinkage of the outside dimensions. The char anomaly was not resolved until the birch flour char was examined microscopically and found not to be composed of skeletal remnants. The lack of char formation on the pyrolyzing surface of the biomass has a major impact on the ability to transfer heat into the particle.

The formation of char on the surface of slowly pyrolyzing biomass serves to act as a thermally insulating layer. Through this layer, the pyrolysis gases pass in counter-current flow relative to the heat needed for pyrolysis. This transpirational cooling of the char by the gaseous pyrolysis products (mostly steam formed by the slow dehydration reaction) greatly reduces the heat flux and consequently the pyrolysis rates. The rate of pyrolysis as measured by the equilibrium rate of advance of the char-wood interface is very slow and is about 3 $^1/_2$ cm per hour with radiative and free convective exposure to temperatures of 500 to 1000°C (ASTM-E119) (7). In contrast to this slow rate, the pyrolysis of 250 μm particles in an estimated 50 ms residence time in the China Lake entrained flow reactor suggests a fast pyrolysis rate in excess of 900 cm per hour or 0.25 cm per second. Although this estimated rate is very high, the maximum rate of pyrolysis probably was not attained due to the intermittant contact of the turbulently entrained particle with the hot tube wall.

Fig. 2 SEM Photograph of Birch Char (147X)

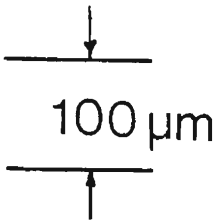

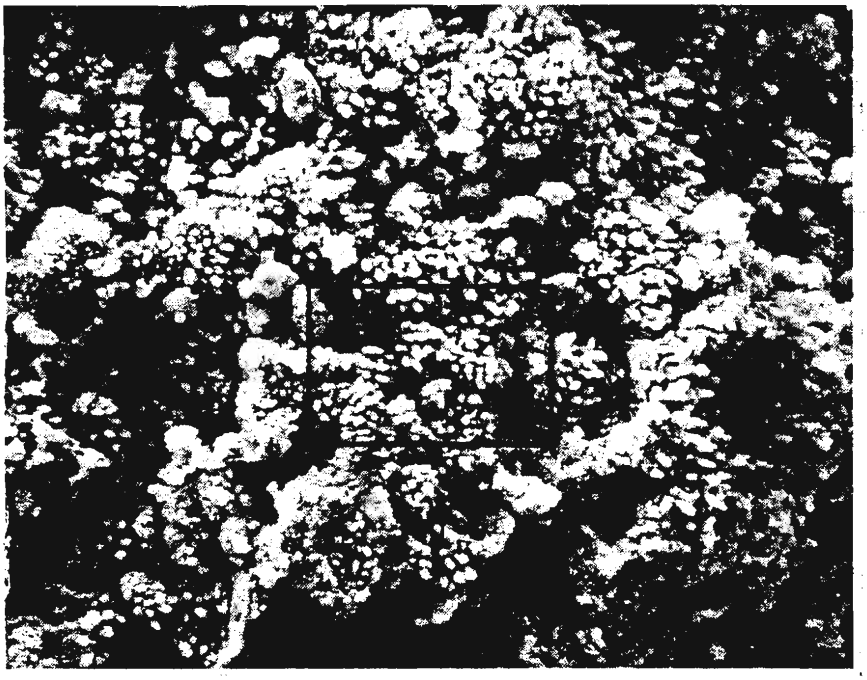

Fig. 3 SEM Photograph of Birch Char (853X)

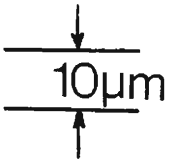

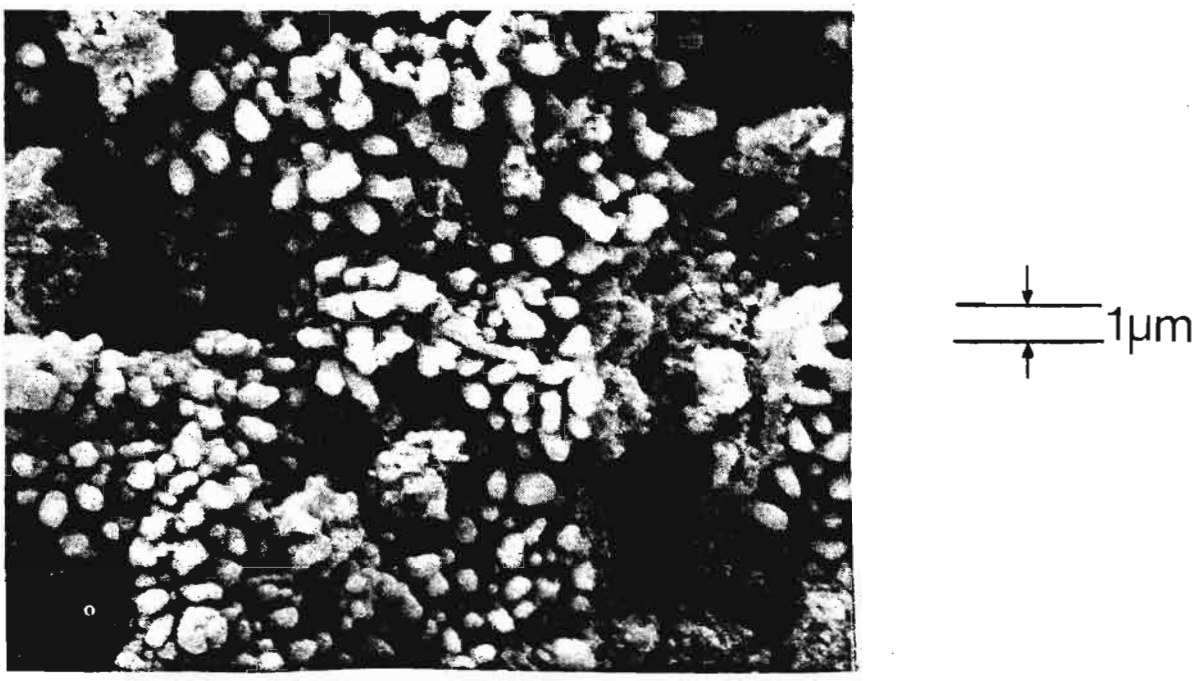

Fig. 4 SEM Photograph of Birch Char (2500X)

The importance of physical contact of the pyrolyzing biomass particle with the hot wall is readily apparent with the proper assumptions. If it is assumed that the wall temperature is 1800°F (∿1000°C), that the surface of the pyrolyzing biomass is at 600°F (315°C), and the absorptivity is a generous 0.85, then the radiative heat flux to the particle is about 35,000 BTU/hrft^2 (∿12 w/cm^2). One concept of pyrolysis is that the biomass decomposes first to pyrolytic oils. With the same relative temperatures, conducting heat through a thin 10 μm layer of this pyrolytic oil having an assumed conductivity of 0.08 BTU ft/ft^{2}hr°F results in a phenomenal heat flux of nearly 3 •10^6 BTU/hrft^2 (1000 w/cm^2). Whether or not this high heat flux to the virgin substrate could be attained in reality depends upon how well the assumed conditions can be met. The reactor wall temperature would be very difficult to maintain in a steady state since petrochemical cracking furnaces typically have heat fluxes of only 10,000 to 50,000 BTU/hrft^2 (3 to 15 w/cm^2) even in the radiative sections. Without resorting to focused light energy sources (e.g., laser or solar power tower), high heat fluxes to the wall could be supplied by condensing sodium vapors as in a heat pipe. At these fluxes the temperature drop through a 0.1 inch (0.25 cm) stainless steel wall is on the order of several hundred degrees. However, if the pyrolyzing particle were to be in a dilute entrained flow and in relative motion to the hot reactor wall, the heat flux to the particle could be much higher than the average heat flux through the wall. This "forced solid convective" heat transfer would allow the wall to recover its initial temperature between the passage of each particle. The particle must be kept in firm contact with the wall to maintain the high conductive heat flux. Maintaining the liquid pyrolytic oil film at a minimum thickness requires that the particle be forced to the wall to extrude the oil out. Relative motion between the wall and the particle will also aid in wiping off the oil (and any char) as it is formed. The required conditions for fast pyrolysis of macroparticles appeared to fit an externally heated cyclone reactor as will be discussed, but the demonstration of the concept was needed before committing the necessary resources to build a unique reactor design.

ABLATIVE HOT-WIRE PYROLYSIS

The demonstration of the physical rate at which pyrolysis proceeds is very difficult in an entrained flow reactor. However, a few conceptual changes to the discussion above allows for a very easily constructed qualitative experimental apparatus. If the biomass macroparticle is held stationary while the hot stainless steel surface slides past, the physical rate of pyrolysis could be measured. Since the biomass is rapidly offgassing, air will have a very difficult time to diffuse into the pyrolysis site. If the quantity of pyrolysis products formed is kept small, they will cool before they have mixed with sufficient air to ignite.

To demonstrate the fast pyrolysis of macroparticles (e.g., tongue depressors) a hacksaw frame was fitted with a 0.010 inch (254 μm) diameter nichrome wire. The wire was electrically insulated from the frame and attached to a transformer to provide about 20 volts. With

this simple arrangement, one can "saw" through biomass as though it were a thermoplastic like polyethylene or polystryene. The sawing action produces smoke which normally does not ignite. The width of the cut is slightly less than the width of the cutting wire. If the "sawing" action is started without the wire being hot, only a negligible cut can be made. Turning on the electricity to the wire results in the saw suddenly having a lubricated feeling as the biomass pyrolyzes to form the oils and vapors. It is not definitely known at this time if the biomass forms only liquids which then vaporize or if some gases are formed concurrently with the liquid. However, the formation of gases between the biomass and the hot steel surface would drastically reduce the heat transfer rates. Microscopic examination of the best "cut" (pyrolyzed) surfaces reveal no char present and that the cell structure can be clearly seen through a light-colored tar layer which appears as a coat of varnish. The hypothesis that wood pyrolyzes first to tar with very little concurrent gas formation is supported by the lack of a foamed appearance on the "cut" surface. Thin pieces of biomass cut fastest with the least evidence of char formation due to the wire cooling too much with the thicker sections. The red hot wire is visibly cooled and darkened as it passes through even thin biomass such as paper or wood veneers.

A more sophisticated experimental apparatus was constructed to obtain quantitative data for the hot-wire-fast-pyrolysis phenomena. A small DC motor was obtained and fitted with a double spool so that while the nichrome wire was winding off one side of the spool, the other side could be winding it back up. The wire passes over an electrically conductive graphite pulley to the pyrolysis zone and then to another graphite pulley. A microswitch was placed so that the deflection of the hot wire could signal the start and end of the cut. This elapsed time divided by the width of the biomass gives the physical rate of pyrolysis. The wire also passes around an odometer wheel which trips a microswitch for every revolution. By counting the blips on a recorder, wire speed is ascertained. The pressure at the wire-biomass interface is calculated from the biomass weight, the thickness of the biomass and the wire. Measurement of the temperature of the wire as it enters and exits the biomass would provide indications of heat of reaction, heat transfer rates, and pyrolysis temperatures. It appears that optical pyrometry is the most promising approach to the wire temperature measurements. Automatic commercial optical pyrometers unfortunately are made to look at larger "targets" than the thin wire. Manually operated "disappearing filament" optical pyrometers are impossible to operate accurately in the second or so available to take the measurement. The little known technique of using infrared sensitive film to record temperatures appears to be very promising for the hot wire system, but technical difficulties and priorities have thus far precluded obtaining quantitative wire temperature data. However, with wire temperatures estimated to be at 1500 to 1800°F (800 to 1000°C), hand-held hardwood tongue depressors have been cut at rates of 1 cm/sec and 3 cm/sec at wire speeds of 10 and 20 cm/sec respectively. With thin birch veneer, cutting rates of 3 $1/2$ cm/sec were attained with wire speeds of about 10 cm/sec. Preliminary transient heat transfer calculations suggest the biomass is heated

only to a depth of about 20 μm, which implies a heating rate of about $5 \cdot 10^5$ °C/sec.

Other means of attaining ablative pyrolysis which were demonstrated included a "friction saw" made of a smooth disk of stainless steel fitted to a hand-held rotary saw. A relief was machined into the disk to minimize the rubbing contact of the sides of the disk on the walls of the cut. The friction of the circumference of the disk against the wood caused it to locally heat enough to cause pyrolysis. The charless cutting front passed through the wood fast enough to avoid charring the wall of the cut. The resulting cut surface was very smooth and had a polished appearance. The use of a friction saw to cut aluminum and stainless steel has been known for quite some time, but its usefulness to cutting wood is a newly recognized phenomena.

A hand-held tesla coil used for checking out electronics was also used to demonstrate fast pyrolysis. With very short duration discharges through a wooden tongue depressor, very small, crooked, charless holes were formed initially. Longer duration discharges resulted in larger diameter holes which had charred walls and through which light could pass.

Although much more data need to be generated with the hot wire apparatus, the tentative conclusions are that: biomass can indeed be pyrolyzed without the formation of an insulative char layer and that pyrolysis rates, which are 3 $1/2$ orders of magnitude greater than slow pyrolysis rates, can be achieved with the proper combination of steel surface temperatures, relative motion, and pressure. Due to all of the implications that fast pyrolysis of macroparticles was indeed demonstrated in the laboratory, an engineering demonstration of the concept was given top priority.

ENGINEERING DEMONSTRATION OF ABLATIVE FAST PYROLYSIS OF MACROPARTICLES

Initial concepts for the engineering demonstration of the macroparticle pyrolysis involved the use of 1 cm wood chips entrained by a supersonic steam flow into a toroidally shaped reactor. The chips would be centrifuged to the outside wall of the toroid where they would be pyrolyzed. However, it was soon realized that this design would use only a small portion of the toroidal surface for heat transfer, i.e., the major diameter of the toroid. Subsequently, the tangential entry for the feedstock was changed from a simple angle to a compound angle which would cause the particles to travel a helical path as they traveled around the inside of the toroid. The particles would then extract heat from the entire inside surface of the toroid. The relative diameters of the toroid under consideration were such that the particle was being subjected to extremely high "g" forces due to the helical motion in the toroidal tube and relatively low "g" forces due to the toroid itself. After comparing ease of construction, it was decided to straighten out the toroid to form a simple cyclone reactor.

The cyclone reactor design is conceptually very simple, as shown in

Figure 5. The biomass, as large as 1 cm particles, are accurately metered to the steam ejector with a gravimetric weigh feeder. This screw feeder is on an electronic scale which constantly adjusts a volumetric feeder to deliver a desired mass rate of a nominal 100 lbs/hr (45 kg/hr). A twin screw in the feeder will be used with finely powdered feedstock, whereas a 45 mm single screw will be used with wood chips. The steam ejector uses 100 lbs/hr of superheated steam at 200 psig (1450 kPa) and 1400°F (760°C). The steam serves to entrain the particles into the 6 inch (15 cm) diameter by 28 inch (71 cm) cyclone reactor at speeds up to 375 ft/sec (114 m/s), as well as to dilute the gases and thereby reduce the partial pressure of the pyrolysis products. If 1 cm cubes of biomass were to be fed at 100 lbs/hr (45.4 kg/hr) there would be 30 particles per second spaced an average of 10 ft (3 m) apart in the steam ejector stream. In the cyclone reactor, the biomass particles initially experience 19,000 "g's" to force them to the red hot wall, as shown in Figure 6. This produces a force of about 30 lbs (140 N) under a 1 cm cube of biomass or about 140 psia (1000 kPa) between the wall and the cube. If the tar is wiped off the biomass as fast as it is formed, the tar will be under the fast moving 1 cm chip for only 0.1 ms. Three electric heater systems are to provide the energy needed for pyrolysis. These heater systems will be independently controlled and the energy consumption independently monitored. Although the solid biomass particles are trapped in the cyclone reactor for an estimated 300 ms until the 1 cm particle is vaporized, the gases and vapors are free to leave through the exit located on the center line of the cyclone. The average gaseous residence time in the cyclone is estimated to be between 75 and 175 ms. A purged three inch (7 $\frac{1}{2}$ cm) diameter quartz sight glass will be located near the tangential entry so that the pyrolyzing particles may be photographed with SERI's 10,000 frame per second movie camera.

Downstream of the cyclone reactor is a 2 inch (5 cm) diameter vapor cracker reactor which is 17 feet (5 m) long. The gases and vapors will have an additional 70 to 150 ms residence time in the vapor cracker. The vapor cracker will be electrically heated by six independently controlled and monitored heaters. Due to the inability of large solids to escape the cyclone reactor, all tar vapors will have a chance to be cracked, whereas in a purely entrained-flow situation the larger particles are still producing tar vapors at or near the exit of the system.

Gas samples may be withdrawn from three locations in the cyclone pyrolysis reactor and six locations in the vapor cracker. This reactor system will be able to generate data related to the energy requirements at the various stages of pyrolysis as well as determining the intermediate product distribution of the gases at various residence times and temperature histories (cracking severities). The independently controlled heater sections will allow a variety of temperature profiles to be forced onto the cyclone reactor and the vapor cracker. The capabilities of this reactor system are very similar to that used by the Europeans to study hydrocarbon cracking to produce olefins (9). The use of Incoloy 800H for the cyclone reactor

FIG. 5

Ablative Macroparticle Pyrolysis Flow Schematic

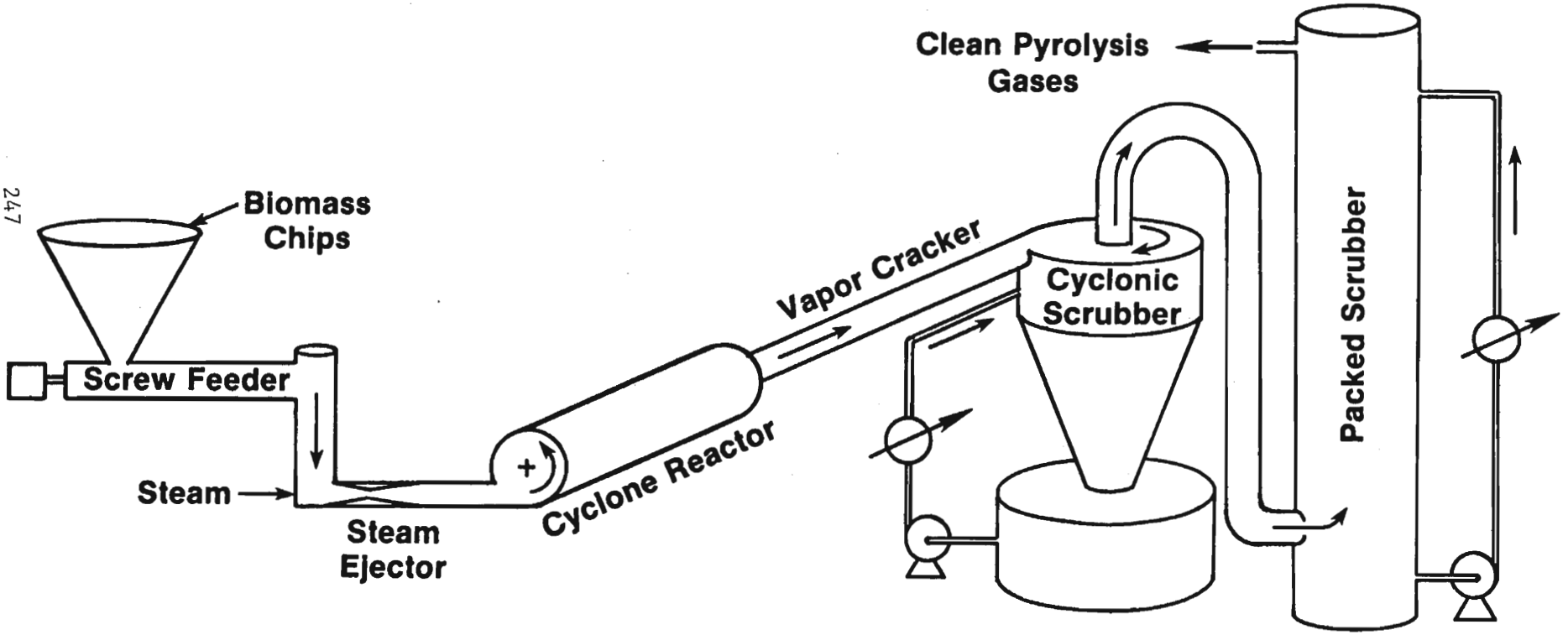

FIG. 6 **Macroparticle Pyrolysis Concept**

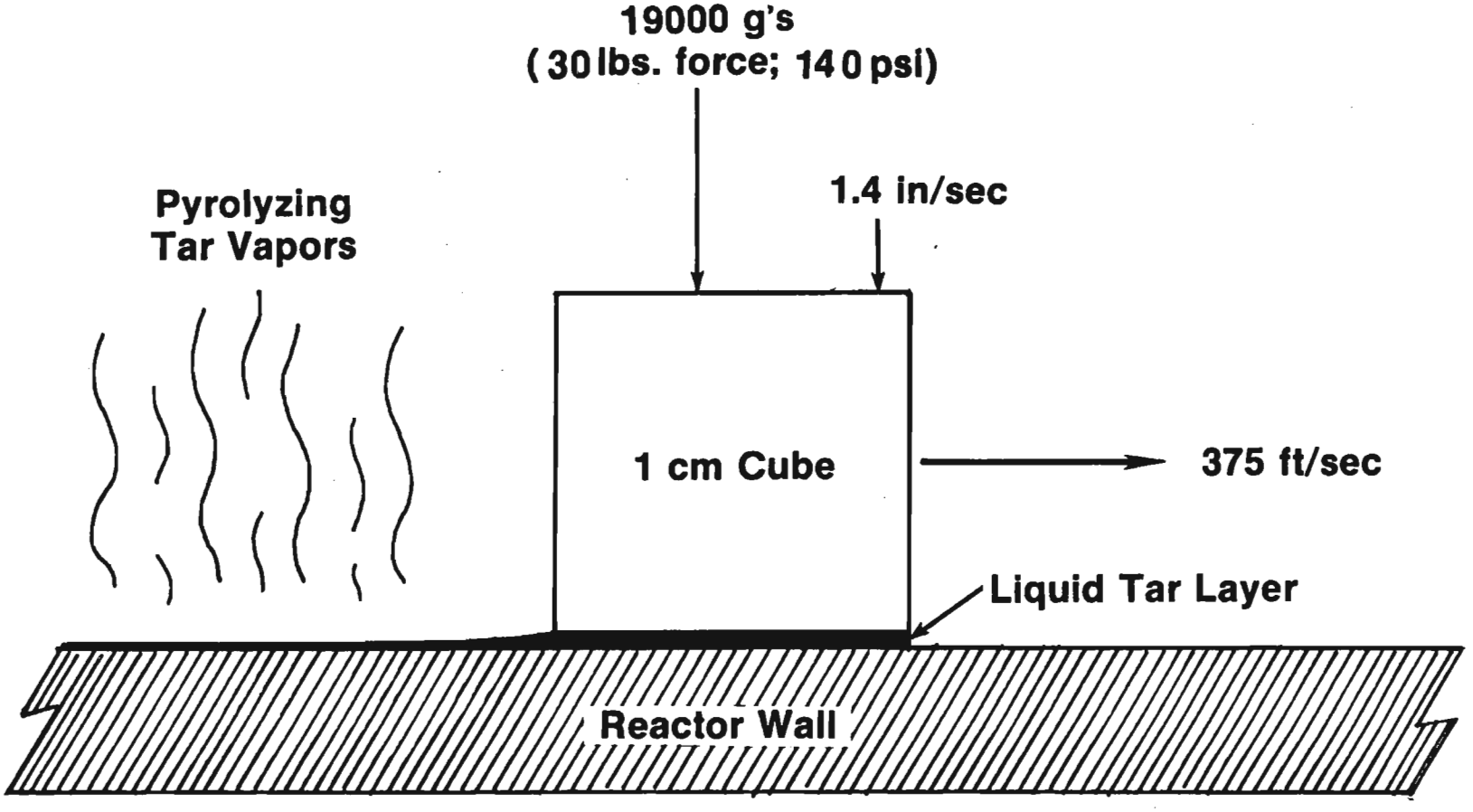

and the vapor cracker reflects naphtha cracking state-of-the-art (10). The use of the gravimetric weight feeder system will allow the instantaneous comparison of biomass flow into the reactor to gas flow out of the system and provide several data points per experimental run. The capabilities of this new reactor system are relatively sophisticated compared to previous reactors.

Downstream of the vapor cracker, the pyrolysis stream will be quenched and cooled to slightly below the steam dew point in a cyclonic scrubber using high pressure water sprays. The small amount of anticipated char, tar, and ash will accumulate primarily in this cyclonic spray system. A small amount of char-tar-ash slurry will be constantly slipstreamed to the flare for incineration. The cooled gaseous stream will then go to an irrigated packed scrubber where steam will condense and help to coalesce the anticipated entrained tar mists. The cooled, clean gases will then pass to an orifice meter before being flared off. The entire pyrolysis reactor system will be operated at only slightly above atmospheric pressure to maximize the olefin formation in the gases. Conversion of these gases into gasoline, alcohols, or petrochemical feedstocks will be addressed in future programs.

The major components for this 100 lb/hr macroparticle engineering demonstration have been ordered with deliveries to begin in mid-October 1980. The equipment will be assembled next to SERI's oxygen gasifier unit with a probable completion date of late December 1980. Shakedown and experimentation will commence in January 1981.

CONCLUSIONS

New insights into biomass fast pyrolysis have revealed that char formation can be a secondary rather than a primary reaction, so that virtually no char is formed with the proper heat flux and primary tar removal. This hypothesis was shown to be valid when using a red-hot wire drawn across macroparticles of biomass such as wood veneer and tongue depressors. Pyrolysis rates 3 $\frac{1}{2}$ orders of magnitude greater than slow pyrolysis were demonstrated. Because the heating is localized, only the pyrolyzing surface is heated so that the size of the particles is of very little importance. Additional data will be generated with the hot wire apparatus to look at wire temperature, speed, and pressure relationships.

A practical 100 lb/hr (45 kg/hr) reactor to utilize these insights into fast pyrolysis has been designed and is being procured. This engineering demonstration reactor will be able to pyrolyze particles up to 1 cm in diameter and is the smallest size reactor practical for these large particles. The system will be operating during FY81 to demonstrate the ablative fast pyrolysis of biomass macroparticles to produce gases rich in olefins for gasoline, alcohol, or petrochemical production.

ACKNOWLEDGEMENTS

The close interaction with Dr. T.B. Reed in the development of the hot wire pyrolysis concepts is acknowledged and was much appreciated. The use of the friction saw for wood cutting was conceived and demonstrated by Dr. Reed. Mr. Michael Soltys suggested the use of the tesla coil for fast pyrolysis. The SEM photos were taken by Mr. Rowland McNeil of the Naval Weapons Center, China Lake.

REFERENCES

1. Diebold, J.P. and G.D. Smith "Noncatalytic Conversion of Biomass to Gasoline", ASME sponsored Solar Energy Conference, San Diego, CA, March 12-15, 1979., 79-Sol-29.

2. Diebold, J. and G. Smith "Commercialization Potential of the China Lake Trash-to-Gasoline Process", Chapter 11 in Design and Management for Resource Recovery, Volume 1, Energy from Waste, edited by T.C. Frankiewicz. Ann Arbor Science Publishers. (1980).

3. Llewellen, P.C., W.A. Peters, and J.B. Howard "Cellulose Pyrolysis Kinetics and Char Formation Mechanisms", Fire and Explosion Research: Sixteenth Symposium on Combustion. The Combustion Institute, pp. 1471-80, 1976.

4. Diebold, J.P. "Preliminary Results in the Fast Pyrolysis of Biomass to Lower Olefins", ACS Division of Petroleum Chemistry Sponsored Symposium on Alternate Feedstocks for Petrochemicals, Las Vegas, NV, August 24-29, 1980.

5. Diebold, J.P. "Research into the Pyrolysis of Pure Cellulose, Lignin and Birch Wood Flour in the China Lake Entrained-Flow Reactor", SERI/TR-332-586., June 1980.

6. Diebold, J.P., G.D. Smith, and C.B. Benham "Conversion of Organic Wastes to Unleaded, High Octane Gasoline", Final Report to the Environmental Protection Agency, contract EPA-IAG-D6-0781, September 1979.

7. Schaffer, E.L. "An Approach to the Mathematical Prediction of Temperature Rise Within a Semi-Infinite Wood Slab Subjected to High-Temperature Conditions", Pyrodynamics, Vol. 2, pp. 117-132, (1965).

8. Diebold, J.P., C.B. Benham, and G.D. Smith "R&D in the Conversion of Solid Organic Wastes to High Octane Gasoline" presented to the American Institue of Aeronautics and Astronautics sponsored Symposium on Alternate Fuels Resources, Santa Maria, CA. March 25-27, 1976. AIAA Monograph Volume 20.

9. Van Damme, P., S. Narayanan, and G.F. Froment, "Thermal Cracking of Propane and Propane-Propylene Mixtures: Pilot Plant Versus Industrial Data", AIChe J., 21, 1065 (1975).

10. Chambers, L.E. and W.S. Potter "Design Ethylene Furnaces: Part 2: Maximum Olefins", Hydrocarbon Processing, March 1974, 95-100.

FLUIDIZED BED PYROLYSIS TO GASES CONTAINING OLEFINS

J. L. Kuester
College of Engineering and Applied Sciences
Arizona State University
Tempe, Arizona 85281

ABSTRACT

Recent gasification data is presented for a system designed to produce liquid hydrocarbon fuel from various biomass feedstocks. The factors under investigation were feedstock type, fluidizing gas type, residence time, temperature and catalyst usage. The response was gas phase composition. A fluidized bed system was utilized with a separate regenerator-combustor. An olefin content as high as 39 mole % was achieved. Hydrogen/carbon monoxide ratios were easily manipulated via steam addition over a broad range with an autocatalytic effect apparent for most feedstocks.

INTRODUCTION

A process to convert biomass materials to quality liquid hydrocarbon fuels has been under development at Arizona State University since 1975. An indirect liquefaction approach is utilized, i.e., gasification followed by catalytic liquid fuels synthesis. The advantage of indirect liquefaction (vs. direct) is minimization of oxygenated compounds in the liquid hydrocarbon fuel product. The use of catalysts in the liquid fuels synthesis results in very mild processing conditions, i.e., low pressures, temperatures and residence times.

The potential products from the system are indicated on Figure 1. The medium Btu pyrolysis gas (500 + Btu/SCF) conceivably could be used as a fuel gas. The project objective however has always been to tailor the gas composition with respect to carbon monoxide, hydrogen and olefins for use as a synthesis gas for the liquid fuels system. The first reactor in the liquid fuels system contains a Fischer-Tropsch type catalyst. The condensible hydrocarbon phase is a narrow range light paraffinic fuel (C_5 - C_{17}) which can be readily tailored to match diesel, kerosene or jet fuels. If a high octane gasoline is desired, a conventional catalytic reforming step is used to achieve the desired effect.

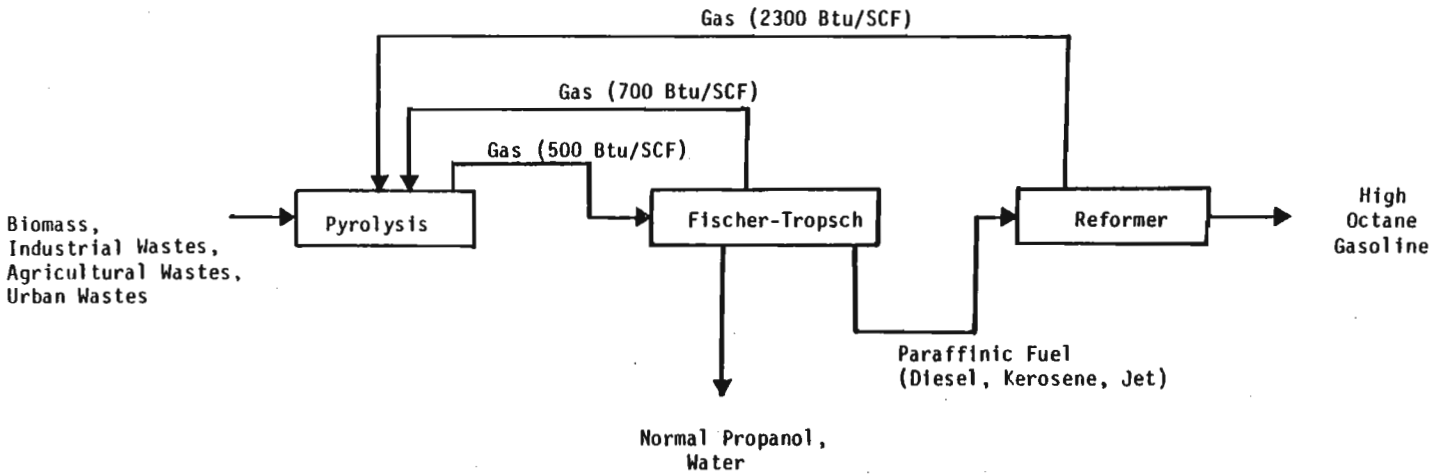

Figure 1.

Basic Chemical Conversion Scheme

A secondary condensible phase from the Fischer-Tropsch step is essentially a binary of normal-propanol and water. The off gases from the liquid fuels reactors are heavy in the low molecular weight paraffins (C_1 - C_5) and thus are of high heating value. It is anticipated that these would be recycled back to the gasification system.

The research scale process has a capacity of about 25 lbs/hr of feedstock. A flow diagram is shown in Figure 2. A fluidized bed with separate regenerator is employed for the pyrolysis step. The heat transfer medium can either be catalytic or inert. The system (both functionally and operationally) is a direct analogy to a catalytic cracker in a petroleum refinery which has been successfully employed since the 1940's. A fluidized bed is also used for the Fischer-Tropsch step (to control the temperature). The reformer is a fixed catalytic bed. Equipment and procedure development have accompanied factor studies for the chemical reactor systems. Previous experimental results for the process have been reported in several publications [1-5]. These include a 2^2 factorial design (temperature, feed rate) for pyrolysis, a 2^3 central composite design (CO, H_2, C_2H_4 feed composition) and temperature, pressure, catalyst loading studies for the Fischer-Tropsch system and a 2^3 central composite design (temperature, pressure, feedrate) for the catalytic reformer. In each case, the responses were the product yields and composition. Additional physical properties were reported (octane number, cetane number, heating values, specific gravity, etc.). In this paper the following additional studies will be presented:

1) gasification data for alternative feedstocks,
2) temperature effects on gasification performance,
3) steam and residence time effects on gasification performance, and
4) water gas shift catalyst effects.

FEEDSTOCK STUDY

A large number of feedstocks were investigated through the gasification step. (Table 1). The industrial wastes refer to by-products of industrial processes. The forest residues tested are all cut by the U. S. Forest Service in the southwest United States for water conservation purposes and burned in the field. Environmental pressures will preclude burning in the future. Eco-Fuel II is a preprocessed municipal refuse. Almond prunings are cut and burned in the almond orchards and thus represent an environmental problem. Russian thistle (tumbleweeds), raw guayule, water hyacinth and peat represent materials that might be harvested deliberately for energy production purposes. Some of the feedstocks were tested at the initiative of the Principal Investigator while others were at the request of the industrial concerns, government agencies and other University laboratories. Elemental and ash analysis for some of the feedstocks are listed in Tables 2 and 3. As indicated, the carbon, hydrogen, oxygen and nitrogen compositions are similar for the biomass materials. The sulfur content is very low except for preprocessed municipal refuse (Eco-Fuel II). The ash content does vary significantly for the materials, ranging from negligable for the synthetic polymers to over 15% for a few materials (e.g., Eco-Fuel II, Russian thistle, water hyacinth).

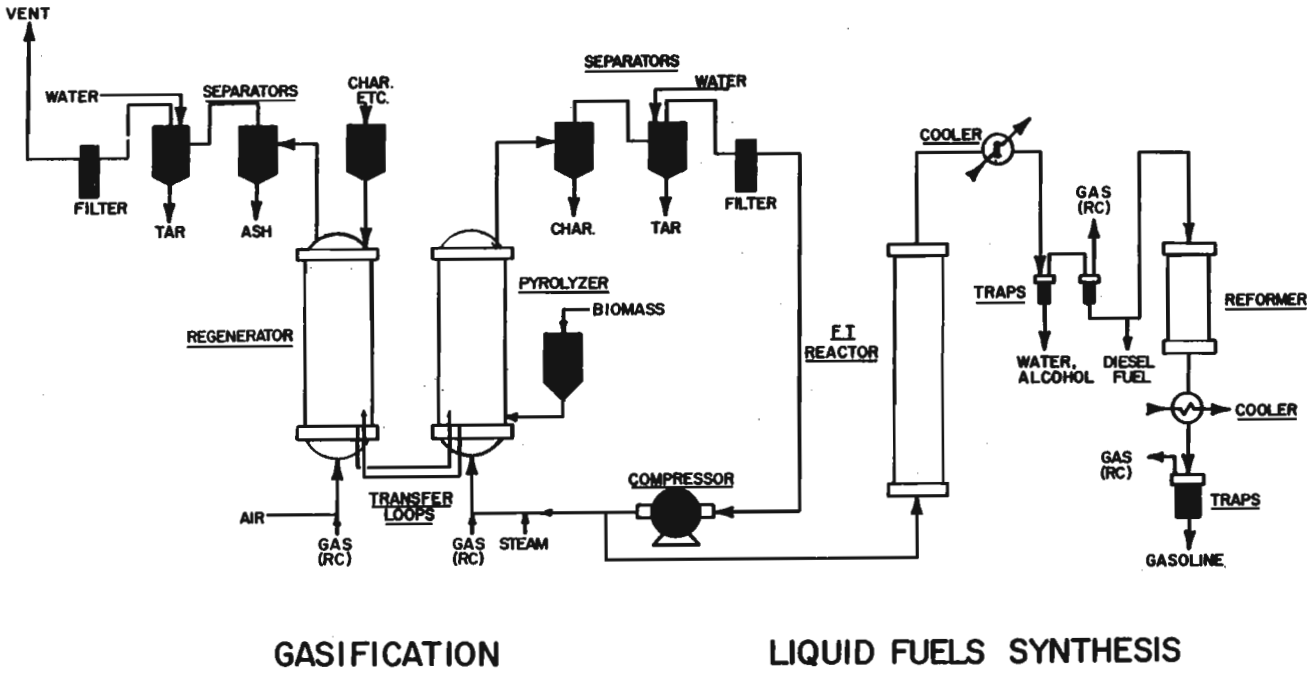

Figure 2.

CONVERSION SYSTEM SCHEMATIC

Table 1

FEEDSTOCKS

Industrial Wastes

- Sawdust
- firbark
- guayule bagasse
- guayule cork
- jojoba meal
- almond hulls
- almond shells
- paper chips
- polyethylene
- polypropylene

Forest Residues

- creosote bush
- sugar sumac
- Arizona cypress
- pringle manzanita
- Wright silktassel
- pointleaf manzanita
- shrub live oak
- hairy mountain mahogany
- Utah juniper
- pinion pine
- mesquite

Urban Wastes

- Eco-Fuel II

Agricultural Wastes

- almond prunings

Energy Crops

- Russian thistle
- raw guayule
- water hyacinth
- peat

Table 2

FEEDSTOCK ANALYSIS
(WT %)

Sample Marking	% Nitrogen	% Sulfur	% Ash	% Loss On Ignition
Guayule - Cork	0.91	0.34	3.53	96.47
Guayule - Bagasse	0.66	0.11	3.27	96.73
Guayule - Raw	0.81	0.18	5.14	94.86
Jojoba Meal	3.94	0.36	3.04	96.96
Water Hyacinth	1.87	0.53	18.97	81.03
Almond - Hulls	0.88	0.08	5.91	94.09
Almond - Shells	0.68	0.03	8.75	91.25
Almond - Cured Prunings	1.01	0.21	25.44	75.46
Eco II - Brockton	0.50	1.44	24.41	75.59
Sawdust	0.28	0.12	7.03	92.97
Paper Chips	0.13	0.08	0.58	99.42
Russian Thistle	1.33	0.19	15.45	84.55
Peat	0.97	0.15	7.63	92.37
Polyethylene	0.09	0.17	0.04	99.96
Polypropylene	0.13	0.03	0.03	99.97

Table 3

FEEDSTOCK ANALYSIS
(WT%)

	Eco Fuel II (Brockton)	Paper Chips	Guayule Bagasse
C	38.0	41.7	40.2
H	4.9	5.7	4.7
O	31.4	52.1	48.4

Table 4

PYROLYSIS OPERATING CONDITIONS

Temperature, °F	1200-1700
Pressure, psig	0-1
Residence Time, Sec	3-6
Feed Rate, lbs/hr	2-15
Heat Transfer Media	sand

Gasification operating conditions for the feedstock survey runs are listed in Table 4. The runs were performed over a period of several months and some equipment modifications were implemented (e.g., feeder modification). Pyrolysis gas composition data is shown in Tables 5-7. Gas phase yield measurements varied from 50-97% but were subject to some experimental error due to lack of a continuous feedback measurement from the solids feeder and occasional coating of the venturi gas flow meter.

The operating conditions for the gasification data should not be considered optimal but are representative of the state-of-the-art of the system at the time the runs were performed. Thus for a given feedstock, improvements in performance are anticipated,

All the cellulosic feedstocks yield a gas with a heating value of about 500 Btu/SCF. The gas from the synthetic polymers has a much higher heating value due to the absence of oxygenated compounds. The gas composition results are masked somewhat by the variation in operating conditions for the different runs. However, several conclusions can be drawn:

1) The more cellulosic type feedstocks yield the lowest total olefin content (generally in the 5-15 mole % range).
2) Materials containing hydrocarbon materials (e.g., oils, latex, synthetic polymers) result in total olefin yields in the 10-25 mole % range.
3) Pure synthetic carbon chain polymers result in total olefin yields of over 30 mole %.
4) Hydrogen/carbon monoxide mole ratios of 0.25 to 0.95 are encountered for dry feedstocks without steam addition (excluding the synthetic polymers).
5) H_2S was not detected for any feedstock. This includes high sulfur materials such as Eco-Fuel II. This is of significance with regard to potential effects on catalyst activity downstream.

Previous studies [1-5] on the system have indicated that an optimal pyrolysis gas composition for maximizing liquid hydrocarbon fuel yields is 20 mole % + olefins and a H_2/CO ratio of 1-1.5. Selected feedstocks are capable of producing the desired amounts of olefins (e.g., guayule cork). Without steam addition, all the materials (except the synthetic polymers) result in a suboptimal H_2/CO mole ratio.

TEMPERATURE STUDY

Gas phase composition results for paper chip feedstock are shown in Figure 3. Only the major components are included in the analysis (H_2, CO, C_2H_4, C_2H_6, CH_4, CO_2). Recycle pyrolysis gas was used for fluidization. The feedstock was dry and steam was not fed to the system. However, the recycle gas is saturated with water after passing through the wet scrubbing system. The results shown in Figure 3 indicate an apparent water gas shift effect with increasing temperature with a corresponding decline in paraffin and olefin production. When considering that gas phase yields increase with increasing

Table 5.

PYROLYSIS GAS COMPOSITION (mole %)[1]

Feedstock:	Almond Hulls	Almond Shells	Almond Prunings	Poly-ethylene	Polypro-pylene	Paper Chips	Peat[2]
H_2	28.08	26.03	25.70	14.19	13.57	14.77	45.05
O_2	0.00	0.00	0.16	0.00	0.00	0.23	0.00
CO	35.44	38.06	42.68	0.96	0.69	58.86	18.48
CO_2	13.92	12.15	5.97	0.23	0.00	3.27	16.29
H_2S	0.00	0.00	0.00	0.00	0.00	0.00	0.00
CH_4	14.96	17.21	14.88	43.56	42.43	14.76	10.69
C_2H_2	0.05	0.06	0.17	0.61	1.18	0.10	0.12
C_2H_4	4.01	3.09	5.68	19.29	13.34	3.70	4.15
C_2H_6	1.29	1.72	1.05	6.78	6.13	2.26	1.88
C_3 olefins	1.23	0.54	0.21	5.30	9.77	1.21	1.21
C_3H_8	0.03	0.06	0.00	0.00	0.00	0.08	0.09
C_4 olefins	0.12	0.10	0.08	0.59	3.64	0.18	0.19
C_4H_{10}	0.00	0.00	0.01	0.02	0.06	0.00	0.01
C_5H_{12}	0.01	0.01	0.00	0.00	0.00	0.00	0.02
C_5 + olefins	0.86	0.97	3.41	7.49	9.20	0.57	1.83
total unsaturated	6.27	4.76	9.55	33.28	37.13	5.76	7.38
H_2/CO ratio	0.79	0.68	0.60	14.78	19.67	0.25	2.44

1 - water, nitrogen free basis
2 - Steam fluidization with recycle pyrolysis gas to sparges (other runs with total recycle gas)

Table 6.

PYROLYSIS GAS COMPOSITION (mole %)[1]

Feedstock:	Fir Bark	Sugar Sumac	Raw Guayule	Guayule Bagasse	Guayule Cork	Russian Thistle	Water Hyacinth	Sawdust	Jojoba Meal	Eco-Fuel II
H_2	16.58	28.89	17.28	25.02	20.57	26.37	23.00	15.13	11.96	15.74
O_2	0.10	0.00	0.00	0.07	0.17	0.00	0.00	0.42	0.41	0.05
CO	53.42	31.88	34.98	39.61	22.14	36.08	42.43	55.57	37.56	50.40
CO_2	2.99	10.57	8.51	6.11	3.77	14.62	13.94	5.31	10.32	3.20
H_2S	0.00	0.00	0.00	0.00	0.00	0.00	0.00	0.00	0.00	0.00
CH_4	18.07	15.16	26.17	15.36	26.03	16.23	14.34	16.37	23.21	15.03
C_2H_2	0.05	0.01	0.04	0.21	0.05	---	0.00	0.10	0.00	0.00
C_2H_4	5.71	5.75	5.57	7.14	14.80	3.21	3.52	2.63	9.15	6.04
C_2H_6	1.60	2.85	2.31	0.63	4.79	1.69	1.62	2.36	3.44	3.60
C_3 olefins	0.37	1.81	1.50	0.00	3.04	0.61	0.57	1.13	2.01	2.03
C_3H_8	0.01	0.41	0.05	0.13	0.16	0.02	0.02	0.09	0.03	0.10
C_4 olefins	0.18	0.65	0.56	0.06	0.83	0.14	0.13	0.20	0.45	0.51
C_4H_{10}	0.02	0.08	0.01	0.00	0.08	0.01	0.00	0.01	0.01	0.11
C_5H_{12}	0.00	0.00	0.04	0.00	0.00	0.01	0.08	0.00	0.80	0.00
C_5 + olefins	0.91	2.20	2.97	5.64	3.58	1.02	0.35	0.67	1.78	3.13
total unsaturated	7.22	10.42	10.64	13.05	22.30	4.98	4.57	4.73	13.39	11.71
H_2/CO ratio	0.31	0.91	0.49	0.63	0.93	0.73	0.54	0.27	0.32	0.31

1 - water, nitrogen free basis

Table 7.

PYROLYSIS GAS COMPOSITION (mole %)[1]

Feedstock:	Arizona Cypress	Pringle Manzanita	Creosote Bush	Pinion Pine	Wright Silktassel	Utah Juniper	Pointleaf Manzanita	Shrub Live Oak	Hairy Mountain Mahogany	Mesquite
H_2	26.64	24.99	25.99	25.82	25.64	28.83	24.46	27.99	27.61	33.01
O_2	0.07	0.04	0.03	0.44	0.04	0.05	0.34	0.07	0.04	0.06
CO	38.40	40.68	39.43	41.78	38.69	39.54	35.50	41.28	37.84	44.35
CO_2	7.04	6.76	7.70	4.39	5.43	6.41	10.58	4.53	4.76	5.10
H_2S	0.00	0.00	0.00	0.00	0.00	0.00	0.00	0.00	0.00	0.00
CH_4	15.82	15.10	15.61	15.68	16.56	16.20	14.08	16.86	15.32	12.11
C_2H_2	0.01	0.11	0.02	0.14	0.17	0.11	0.15	0.11	0.30	0.03
C_2H_4	6.40	6.29	6.48	6.33	7.30	6.56	5.64	5.56	10.26	2.61
C_2H_6	1.65	1.29	0.93	1.87	1.68	1.60	2.00	1.12	1.53	0.18
C_3 olefins	0.65	0.44	0.45	0.28	0.53	0.43	1.21	0.15	0.67	0.00
C_3H_8	0.02	0.01	0.05	0.01	0.05	0.02	0.08	0.01	0.04	0.17
C_4 olefins	0.21	0.10	0.18	0.08	0.15	0.12	0.29	0.09	0.16	0.01
C_4H_{10}	0.03	0.02	0.02	0.01	0.03	0.04	0.12	0.01	0.02	0.00
C_5H_{12}	0.00	0.00	0.00	0.00	0.00	0.00	0.00	0.00	0.00	0.00
C_5 + olefins	3.07	4.17	3.11	3.17	3.74	0.11	5.56	2.22	1.44	2.36
total unsaturated	10.34	11.11	10.24	10.00	11.89	7.33	12.85	8.13	12.83	5.01
H_2/CO ratio	0.69	0.61	0.66	0.62	0.66	0.73	0.69	0.68	0.73	0.74

1 - water, nitrogen free basis

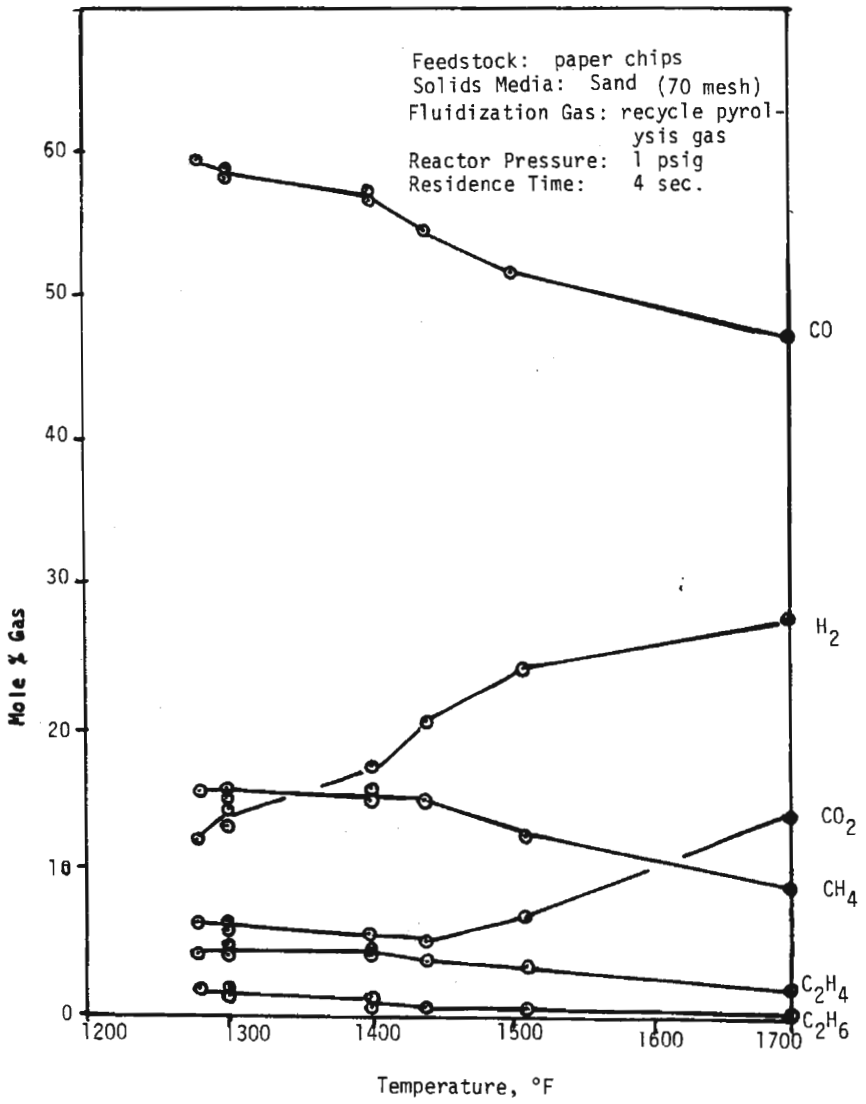

Figure 3.

PYROLYSIS GAS COMPOSITION vs. TEMPERATURE

temperature and that an optimal balance of carbon monoxide, hydrogen and olefin production is desired, it is apparent that temperature alone is insufficient as a control variable in the gasification system.

FLUIDIZING GAS, RESIDENCE TIME, CATALYST STUDY

It is difficult to isolate the effects of fluidizing gas type and composition and residence time in a fluidized bed system. Thus for a given reactor size, lower residence times are achieved by increasing the gas throughput. This is constrained by proper particle size to prevent excessive solids carryover. Experimentation in this area consisted of steam addition to the system with fixed reactor dimensions and particle size. Results for various feedstocks are shown in Tables 8-10. The steam was superheated to approximately 600°F via a coil in the gasification system combustor. With this system, the reactor temperature was lowered with a significant amount of steam addition to the pyrolyzer. For fir bark and guayule cork feedstock (Tables 8, 9), an increase in unsaturated compounds and H_2/CO ratio were observed with steam addition. An autocatalytic water gas shift reaction effect is apparent in each case. This could be due to the presence of mixed metal oxides in the ash content of the biomass (similar to commercial water gas shift catalyst composition). Eco-Fuel II feedstock did not exhibit as significant a water gas shift effect (Table 10). However, the H_2/CO ratio was increased by a factor of 7 when a section of the reactor overhead line was packed with a commercial water gas shift catalyst. In general, it appears that the H_2/CO ratio can be manipulated with steam addition for virtually any feedstock candidate. If an autocatalytic effect is not present, a simple fixed bed shift catalyst section will achieve the desired result. Olefin production appears more complicated. The most dramatic effect occurred with guayule cork feedstock with an increase from 22 to 39% with steam addition. This however corresponded to a substantial reduction in residence time (8 to 1 seconds) and may also be feedstock dependent. Current research is aimed at lowering the residence time to less than one second via a combination of steam addition and recycle off gas from the liquefaction system. The liquefaction off gas normally would be depleted of hydrogen and olefins and thus use of this gas would avoid an effective increase in residence time with respect to these components as is the case when recycling pyrolysis gas.

SUMMARY, CONCLUSIONS, CONTINUING RESEARCH

The particular experiments emphasized in this paper lead to the following conclusions:

1) A wide variety of feedstocks can be processed through the gasification system to a gas with a heating value of 500 + Btu/SCF.
2) Some feedstocks are more attractive than others with regard to producing a high olefin content. This appears to be related to hydrocarbon content of the material.
3) The H_2/CO ratio can be manipulated over a wide range in the gasification system with steam addition. Some feedstocks require the aid of a water gas shift catalyst while others appear to exhibit

Table 8.

STEAM EFFECT - FIR BARK FEEDSTOCK

	No Steam	Partial Steam
Operating Conditions:		
temperature, °F	1400	1250
pressure, psig	0.9	0.9
residence time, sec.	4	3.2
feed rate, lbs/hr	5	5
heat transfer media	sand	sand
fluidizing gas	pyrolysis gas	pyrolysis gas + steam
Pyrolysis Gas Composition (mole %)[1]:		
H_2	16.58	29.24
O_2	0.10	0.14
CO	53.42	44.41
CO_2	2.99	3.33
H_2S	0.00	0.00
CH_4	18.07	10.60
C_2H_2	0.05	0.03
C_2H_4	5.71	7.30
C_2H_6	1.60	0.54
C_3 olefins	0.37	1.93
C_3H_8	0.01	0.06
C_4 olefins	0.18	0.46
C_4H_{10}	0.00	0.00
C_5H_{12}	0.00	0.00
C_5 + olefins	0.91	1.89
total unsaturated	7.13	11.58
H_2/CO ratio	0.31	0.66

1 - water, nitrogen free basis

Table 9.

STEAM-RESIDENCE TIME-RECYCLE EFFECTS
(Guayule Cork Feedstock)

	No Steam	Steam
Operating Conditions:		
temperature, °F	1300	1200
pressure, psig	0.9	0.9
residence time, sec	8	1
feed rate, lbs/hr.	5	5
heat transfer media	70 mesh sand	70 mesh sand
fluidizing gas	recycle pyrolysis gas	recycle pyrolysis gas + steam
Pyrolysis Gas Composition (mole %)[1]:		
H_2	20.57	24.51
O_2	0.17	0.47
CO	22.14	10.87
CO_2	3.77	10.76
H_2S	0.00	0.00
CH_4	26.03	10.95
C_2H_2	0.05	0.04
C_2H_4	14.80	16.67
C_2H_6	4.79	3.24
C_3 olefins	3.04	6.49
C_3H_8	0.16	0.25
C_4 olefins	0.83	2.65
C_4H_{10}	0.08	0.21
C_5H_{12}	0.00	0.00
C_5 + olefins	3.58	12.88
total unsaturated	22.30	38.73
H_2/CO ratio	0.93	2.25

1 - water, nitrogen free basis

Table 10.

STEAM EFFECT - ECO-FUEL II FEEDSTOCK

	No Steam	Steam	Steam + Water-Gas Shift Catalyst
Operating Conditions:			
temperature, °F	1250	1180	1260
pressure, psig	0.9	0.9	1.5
residence time, sec.	4	5	5
feed rate, lbs/hr	4	4	8
heat transfer media	sand	sand	sand
fluidizing gas	pyrolysis	pyrolysis gas + steam	pyrolysis gas + steam
Pyrolysis Gas Composition (mole %)[1]:			
H_2	16.81	23.62	42.59
O_2	0.09	0.08	0.00
CO	50.62	45.24	17.18
CO_2	2.30	3.74	12.52
H_2S	0.00	0.00	0.00
CH_4	15.92	11.34	16.45
C_2H_2	0.02	0.05	0.11
C_2H_4	7.14	7.90	5.03
C_2H_6	3.43	2.26	3.67
C_3 olefins	1.72	2.51	1.03
C_3H_8	0.11	0.17	0.03
C_4 olefins	0.25	0.78	0.30
C_4H_{10}	0.04	0.06	0.02
C_5H_{12}	0.00	0.00	0.02
C_5 + olefins	1.56	2.23	1.05
total unsaturated	10.67	13.42	7.52
H_2/CO ratio	0.33	0.52	2.48

1 - water, nitrogen free basis

an auto-catalytic effect to achieve the conversion.

4) H_2S content (beyond the gasification system wet scrubber) is negligible for the feedstocks surveyed.
5) The water gas shift reaction appears to be enhanced with an increase in pyrolysis reactor temperature over the range of 1300 - 1700°F.

Continuing research includes integrated system performance assessment, alternative feedstock characterization and factor studies for gasification (e.g., catalyst usage, alternate heat transfer media, steam usage, recycle effects, residence time study) and liquefaction (e.g., improved catalysts, catalyst activity characterization). An additional task in progress includes the characterization of various feedstocks by compound types and corresponding correlation with reactor system performance.

ACKNOWLEDGEMENTS

The work described in this paper is supported by the U. S. Department of Energy (Contract No. DE-AC02-76CS40202, Alternate Materials Utilization Branch), The U. S. Department of Agriculture (Grant No. 59-2043-0-2-094-0, Science and Education Administration) and The Arizona Solar Energy Commission (Contract No. 205-80). Feedstocks were supplied by Golden Byproducts, Inc., Phillips Petroleum, Colony Farms, U. S. Forest Service, Centro de Investigacion en Quimica Aplicada, Office of Arid Land Studies (University of Arizona), Environmental Research Laboratory (University of Arizona), Combustion Equipment Associates, San Carlos Apache Indian Reservation and Weyerhaeuser Corporation.

REFERENCES

1. Kuester, J. L., "Conversion of Cellulosic and Waste Polymer Material to Gasoline," presented at the American Chemical Society Symposium on Thermal Conversion of Solid Wastes, Residues and Energy Crops, Washington, D.C., September, 1979.

2. Kuester, J. L., "Conversion of Cellulosic Wastes to Liquid Fuels" presented at Engineering Foundation Conference on Municipal Solid Waste as a Resource: The Problems and the Promise, Henniker, New Hampshire, July, 1979 (published by Ann Arbor Press).

3. Kuester, J. L., "Liquid Hydrocarbon Fuels from Biomass," presented at The Biomass as a Non-Fossil Fuel Source Symposium, American Chemical Society, Honolulu, April, 1979 (published in Preprints and Symposium Series).

4. Kuester, J. L., "Liquid Fuels from Biomass," presented at the AIAA/ASERC Conference on Solar Energy, Phoenix, November, 1978 (published in Proceedings).

5. Kuester, J. L., "Conversion of Waste Organic Materials to Gasoline," Proceedings of the Fourth National Conference on Energy and the Environment, Cincinnati, October, 1976.

PYROLYSIS EXPERIMENTS AT CHINA LAKE USING A TUBULAR ENTRAINED FLOW REACTOR

J. P. Diebold* and C. B. Benham**

*Biomass Thermal Conversion and Exploratory Research Branch, SERI.

**Solar Thermal Research Branch, SERI.

ABSTRACT

Data were obtained from 38 pyrolysis tests conducted on a municipal solid waste feedstock using an entrained flow pyrolysis apparatus. Additional data were obtained from 5 tests made using birch flour and cellulose as feedstocks. Conditions were sought which maximized quantities of olefins produced per unit mass of feedstock. Exploratory tests were made varying reactor temperature, residence time, carrier gas composition, and dilution (ratio of carrier gas to feedstock flow rates). No effects of carrier gas composition upon pyrolysis gas composition were found with respect to olefin yields. In general, olefin production was greater for shorter residence times and greater dilution of the feed by steam and carbon dioxide carrier flow. The effects of temperature upon total olefin yield were not clear due to the narrow range of reactor temperatures explored. However, in general total olefin yields were relatively constant over the temperature range of 700-850°C for short residence times of less than 0.2 sec. In addition to saturated and aromatic hydrocarbons, nearly 20 g of olefins per 100 g of feed were obtained using the municipal solid waste feedstock, although a 14 1/2% yield of olefins was the average attained in the short residence time reactors. For the birch flour and cellulose feedstocks the olefin yields were about 10 g per 100 g of feed. The greater olefin yields obtained with municipal solid waste were attributed to the possible presence of plastics in the feed and/or to the proprietary processing used to produce ECO II.

INTRODUCTION

The pyrolysis data on municipal solid waste (MSW) presented in this paper was obtained as part of a project sponsored by the Environmental Protection Agency and carried out at the Naval Weapons Center at China Lake, California. The goal of the project was to develop a process for producing gasoline from MSW. The process flowsheet, described in detail in Ref. 1, required fast pyrolysis of the organic portion of MSW to produce significant quantities of unsaturated hydrocarbons (primarily olefins). These hydrocarbons would be compressed, separated from the other gases, and polymerized to produce polymer gasoline. The potential for fast pyrolysis of MSW to produce large yields of olefins had been reported by Finney and Garrett in Ref. 2, and this work along with data from Refs. 3-6 formed the basis for the gasoline flowsheet.

The goals of the pyrolysis effort were to build a continuous-flow pyrolysis reactor which would supply pyrolysis gases to the gas separation and gasoline synthesis subsystems and to verify the large olefin yields reported in Ref. 2.

Subsequent to the EPA sponsored project, Diebold conducted further tests with the pyrolysis apparatus using pure cellulose and birchwood flour as feedstocks. This work was sponsored by the Solar Energy Research Institute at Golden, Colorado. The goal of this effort was to determine the amounts of olefins obtainable from lignocellulosic feedstocks using the China Lake entrained flow reactor.

Table 1. FEEDSTOCK PROPERTIES

Material	Average Particle Size μm	Feedstock Composition (wt% Dry Basis)							Dry Major Empirical Formula	HHV (kJ/dry gram)[a]
		Ash	C	H	O	S	N	CI		
ECO II (drum T47)	188	12.46	45.50	6.20	34.22	0.98	0.27	0.37	$C_6H_{9.74}O_{3.39}$	19.77
ECO II (drum T51)	270	9.73	49.64	6.40	32.38	1.04	0.22	0.59	$C_6H_{9.28}O_{2.93}$	22.19
Dry Cellulose + 12% Ash	---	12.0	39.11	5.47	43.42	0	0	0	$C_6H_{10}O_5$	15.38
Cellulose Avicel PH-102	100	0.03	43.44	6.39	50.11	0.001	0.02	0	$C_6H_{10.6}O_{5.20}$	17.23
Birch Flour	< 180	0.40	48.75	6.36	44.40	0.02	0.08	0	$C_6H_{9.40}O_{4.11}$	19.38

[a] 1 kJ/g = 430 Btu/lb.

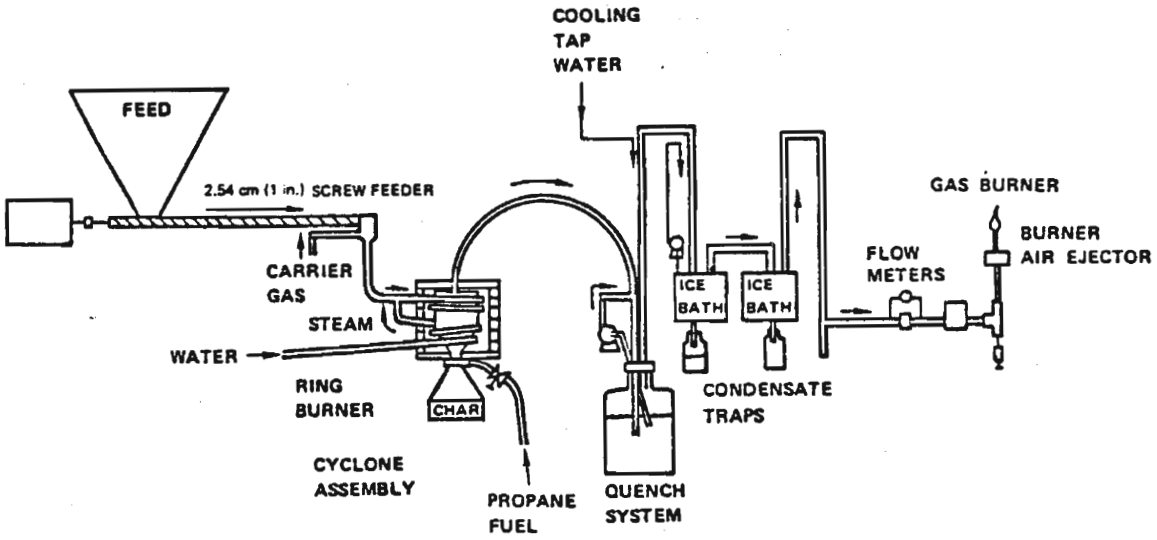

Figure 1. Long-Residence-Time Pyrolysis Reactor.

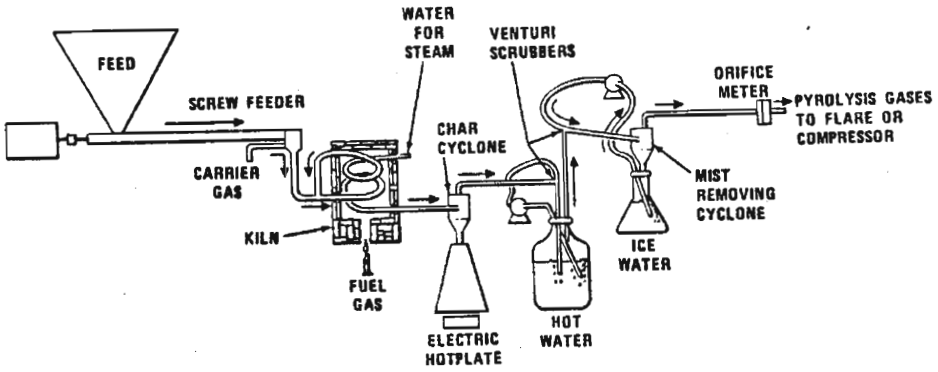

Figure 2. Entrained Tubular Pyrolysis Reactor.

FEEDSTOCKS

The solid waste feed chosen for the pyrolysis evaluation was "ECO-II™ fuel" produced by Combustion Equipment Associates, New York. During the manufacture of ECO II (Ref. 7), the inorganic fraction of the trash is removed first. Then, the organic fraction is treated with mineral acids in a proprietary process to embrittle the cellulosic materials. The embrittled material is then ball-milled at elevated temperatures (93 to 204°C). ECO II is a non-fibrous, free-flowing material having an average particle size of about 250 μm. An analysis was performed on two of the drums to determine variability, since the material shipped was the product of a process variable study. The results of those analyses are shown in Table 1 along with data on a hypothetical feedstock comprised of cellulose and 12% ash. The most noticeable difference between the ECO II fuel and cellulose containing 12% ash is that the ECO II has 5 to 10% more carbon and 5 to 10% less oxygen. This difference may be due to a combination of plastics content and pretreatment of the ECO II fuel.

Cellulose was purchased from the FMC Corporation, Philadelphia, Pa. under the trade name Avicel PH-102. It is a white, crystalline, free-flowing powder having a nominal particle size of 100 μm. Birch wood flour was purchased having a particle size of < 180 μm (minus 80 mesh). Properties of Avicel PH-102 and birch flour are also listed in Table 1.

APPARATUS

The pyrolysis apparatus consisted of a solids feeding system, pyrolysis reactor, and quench system. The feed system consisted of a Vibra Screw™ feeder having a screw auger 2.54 cm in diameter. This unit had a variable speed transmission to vary the feed flowrate. The feed was entrained from the screw by a carrier gas and pumped toward the pyrolysis reactor by an ejector also driven by carrier gas. Immediately upstream of the pyrolysis reactor, the mixed flow was entrained by a second ejector driven by superheated steam. This design allowed the use of different gases to be used as carrier and allowed the ratio of carrier gas to solid flow rate to be varied. Since the screw feeder hopper was not sealed, there was a concern about entrainment of air with the feed which would preferentially oxidize the unsaturated hydrocarbons in the pyrolysis reactor. Therefore, a slight positive pressure (< 5 cm of H_2O) was maintained on the screw by adjusting the flowrate of carrier gas used to entrain the solids from the end of the screw. While this slight positive pressure ensured that no air was entrained with the feed, it also made impossible attempts to achieve a complete mass balance for the system since some of the carrier gases escaped through the hopper.

Two differently configured entrained-flow pyrolysis reactors were used. The first design, depicted in Fig. 1, consisted of a 2.8 m long coil of type 304 stainless steel tubing having an inside diameter of

1.6 cm on the inlet of a cyclone separator. Both the coil and cyclone were contained within a propane-fired kiln. Most of the char was removed by the cyclone separator. This design provided about 0.3 to 0.4 seconds residence time in the coil and 5 to 10 seconds within the cyclone.

A second pyrolysis reactor design (Fig. 2) was used to achieve shorter residence times. The cyclone separator was removed from the kiln leaving only the coil within the kiln. Two different lengths of coil, 2.1 m and 6.1 m, were used to provide even greater control over residence time. Quenching of the pyrolysis gas was accomplished in a water bath, and two cold traps were used to remove tars. An air-driven ejector provided air for the premixed-flame flare and simultaneously provided suction on the system to assist in pumping the gases through the system.

INSTRUMENTATION AND DATA ACQUISITION

Data recorded for each run included run time, weight of solids fed, carrier gas flow rate, steam flow rate, weight of char produced, pyrolysis kiln temperature, pyrolysis exit gas temperature, pyrolysis gas flow rate and pyrolysis gas composition. The weight of solids fed was determined by weighing the feed in the hopper before and after each run. The collected char which included ash, was dried and weighed. Carrier gas and steam flowrates were calculated from the measured pressures upstream of sonic orifices. Temperatures were measured using type K thermocouples--attached to the outside wall of the pyrolysis coil until run 14 and thereafter immersed in the pyrolysis gas flow at the coil outlet. Pyrolysis gas flowrate was measured using a 1.23 cm diameter orifice with corner pressure taps. The pressure drop across the orifice and the average molecular weight of the gases (as determined by the gas chromatograph) were used to calculate the product gas mass flowrate. Gas composition was determined using a Model AGC-111H Carle gas chromatograph.

LONG RESIDENCE TIME REACTOR RESULTS

Data was obtained from 13 tests using the reactor configured as shown in Fig. 1 and using ECO-II as the feedstock. A data summary for these tests is presented in Table 2. As can be seen from the table, the tests were conducted at several different operating conditions. Carrier gases employed in the first 6 runs were methane, carbon monoxide, and mixtures of hydrogen, methane and carbon monoxide. The next 6 tests used both carbon dioxide and steam, and test 13 used a mixture of hydrogen, methane and carbon monoxide as well as steam. Pyrolysis temperatures varied from 716 to 860°C. Carrier gas flowrates varied from 0.23 to 0.73 kg per kg of dry feed, and moisture content of the feed varied from 1 to 15%. Due to a loss of carrier gas back through the screw feeder the values for the yields of the gases used as carrier are of poor accuracy and are not presented. Trends of composition as a function of temperature for tests 7 through 12 are shown in Fig. 3. The production of ethylene generally increased with temperature, whereas that of propylene

Table 2. PYROLYSIS DATA SUMMARY

Run	Pyrolysis Reactor Type	Feed Type	Wt% H_2O In Feed	Pyrolysis Temp. °C	Wet Feed Kg/h	Carrier Gas Type	kg/kg Dry Feed: Carrier Gas	kg/kg Dry Feed: Steam[a]	Dry Feed g/m³ Gases	Residence Time Sec	Grams Product/100 Grams Dry Feed: CH_4	C_2H_2	C_2H_4	C_2H_6	C_3H_6	C_3H_8	C_4H_8	C_5^+ C_6^+	H_2	CO	CO_2	Char	C_2-C_4 Unsat.
1	Cyclone	ECO II	1	760	3.83	CH_4	0.37	0.01	302	>5	?	0.1	8.2	1.0	1.8	?	0.5	?	0.3	24.1	6.7	24.0	10.6
2	↓	DRUM	15	790	2.39	Mix	0.67	0.18	175	↓	?	0.1	11.6	1.0	1.4	↓	0.4	↓	?	?	10.8	23.7	13.5
3	↓	T51	10	815	3.43	CO	0.45	0.11	297	↓	6.6	0.2	7.4	0.6	0.7	↓	0.3	↓	0.6	↓	8.6	15.7	8.6
4	↓	↓	10	850	3.98	CO	0.29	0.11	461	↓	4.1	0.2	4.3	0.2	0.2	↓	0.1	↓	0.4	↓	4.1	15.0	4.8
5	↓	↓	10	815	3.05	Mix	0.23	0.11	330	↓	?	0.2	7.8	0.6	0.5	↓	0.1	↓	?	↓	8.8	18.6	8.6
6	↓	↓	10	732	3.60	CH_4	0.52	0.11	300	↓	?	0.1	5.7	1.1	2.3	↓	1.3	3.6	0.5	19.4	5.4	20.5	9.4
7	↓	↓	1	732	4.22	CO_2	0.24	0.67	175	4.3	3.6	0.1	5.7	0.8	1.7	↓	0.7	2.1	0.4	18.2	?	12.2	8.2
8	↓	↓	1	732	3.86	↓	0.24	0.74	148	3.9	7.0	0.3	5.9	0.8	1.4	↓	0.7	1.8	0.6	20.6	↓	12.3	8.3
9	↓	↓	1	788	4.08	↓	0.29	0.70	147	3.7	5.2	0.3	7.3	0.6	1.0	↓	0.4	3.2	0.8	23.0	↓	12.2	9.0
10	↓	↓	1	682	3.91	↓	0.33	0.65	176	4.6	3.4	0.2	5.2	0.9	2.2	↓	1.3	3.4	0.4	18.8	↓	18.9	8.9
11	↓	↓	1	552	3.85	↓	0.31	0.74	237	6.3	0.8	0	1.5	0.3	0.7	↓	0.3	1.6	0.1	7.0	↓	27.7	2.5
12	↓	↓	1	860	1.71	↓	0.73	1.13	96	5.8	5.2	0.6	6.9	0.3	0.3	↓	0.1	4.0	1.3	21.8	↓	4.6	7.9
13	↓	↓	1	716	3.12	Mix	0.28	0.91	138	4.6	?	0.2	5.0	0.9	1.5	↓	0.7	1.7	?	?	7.4	7.0	7.4
14	Coil	ECO II	1	700	2.84	CO_2	0.73	1.0	126	0.195	5.6	0.5	7.6	0.7	2.8	0.6	2.2	3.5	0.7	19.6	?	11.7	13.1
15	6.1 m	DRUM	↓	740	4.22	↓	0.46	0.7	172	0.178	3.2	0.5	6.1	0.5	2.1	0.1	1.7	3.2	0.5	22.0	↓	?	10.4
16	↓	T51	↓	810	3.09	↓	0.57	0.9	120	0.171	4.2	0.6	8.1	0.8	3.3	0.2	2.5	1.8	0.7	30.1	↓	?	14.5
17	↓	↓	↓	750	3.13	↓	0.99	1.2	95	0.133	5.1	0.8	9.4	1.0	3.3	0.2	2.2	3.2	0.8	36.8	↓	23.0	15.7
18	↓	↓	↓	730	1.77	↓	1.74	2.4	56	0.139	4.5	1.0	11.4	0.9	3.9	0.2	2.5	3.4	0.9	35.9	↓	?	18.8
19	Coil	↓	↓	730	3.43	↓	0.90	1.1	111	0.050	2.5	0.5	6.7	0.6	2.0	0.1	1.8	3.7	0.6	22.2	↓	16.1	11.0
20	2.1 m	↓	↓	780	1.86	↓	1.65	1.9	62	0.052	3.5	1.3	9.4	0.6	2.3	0.1	1.5	3.0	0.9	27.4	↓	12.5	14.5
21	↓	↓	↓	770	2.31	N_2	1.03	1.6	68	0.045	5.2	1.6	9.5	0.9	2.5	0.1	2.5	1.9	1.2	42.5	9.6	22.7	16.1
22	↓	↓	10	760	1.91	CO_2	1.79	2.3	56	0.049	4.1	1.2	11.3	0.7	2.3	0.2	2.1	5.0	0.9	34.8	?	17.9	16.9
23	↓	↓	1	720	2.16	↓	1.59	1.9	67	0.053	3.1	0.9	9.1	0.8	2.0	0.1	2.0	5.8	0.7	27.1	↓	12.7	14.0
24	↓	↓	↓	700	2.14	↓	1.61	1.9	68	0.054	3.0	1.0	9.1	0.7	2.4	0.1	2.4	3.9	0.7	27.0	↓	14.3	14.9
25	↓	↓	↓	760	2.34	↓	1.46	1.8	68	0.049	3.8	1.2	10.5	0.8	2.5	0.1	2.3	2.3	0.8	32.3	↓	20.4	16.5
26	↓	↓	↓	830	2.72	↓	1.26	1.6	70	0.044	4.3	1.4	10.7	0.7	2.0	0.1	1.8	2.9	0.9	34.7	↓	10.3	15.9
27	↓	↓	↓	810	2.12	↓	1.63	2.3	55	0.043	3.9	1.4	10.7	0.8	1.7	0.1	1.5	5.2	1.0	32.3	↓	17.2	15.3
28	↓	↓	↓	820	2.57	↓	1.30	1.7	66	0.044	4.6	1.3	10.3	0.8	2.4	0.1	2.0	2.9	1.0	38.3	↓	?	16.0
29	↓	↓	↓	820	3.47	↓	0.99	1.2	86	0.042	3.9	1.3	9.1	0.7	1.6	0.1	1.6	3.4	0.9	30.2	↓	25.0	13.6
30	↓	↓	↓	770	3.79	↓	0.90	1.1	102	0.046	3.3	0.5	8.1	0.4	2.8	0.2	2.4	4.4	0.7	29.6	↓	17.2	13.8
31	↓	↓	↓	840	2.20	↓	1.54	1.9	60	0.046	4.5	1.4	10.0	0.6	2.1	0.1	1.4	2.8	1.1	34.3	↓	18.2	14.9
32	↓	↓	↓	750	2.29	↓	1.50	1.8	69	0.051	3.3	1.1	9.2	0.8	2.8	0.1	2.4	3.9	0.8	29.6	↓	15.8	15.5
33	↓	ECO II	↓	743	2.36	CO_2	1.15	1.7	78	0.056	1.6	0.7	6.0	0.5	1.0	0.1	1.0	2.1	0.3	13.2	↓	?	8.7
34	↓	DRUM	↓	732	2.75	↓	1.13	1.5	96	0.059	2.7	0.9	7.5	0.7	2.0	0.1	2.0	3.4	0.5	22.8	↓	?	12.4
35	↓	T47	↓	760	1.25	↓	1.23	3.1	48	0.064	3.1	1.2	8.7	0.5	1.6	0.1	1.9	2.8	0.6	22.9	↓	20.2	13.4
36	↓	↓	↓	738	3.42	↓	0.77	1.2	112	0.055	3.5	1.1	8.8	0.6	2.2	0.1	2.2	4.4	0.6	26.4	↓	?	14.3
37	Coil	↓	↓	761	0.84	↓	1.83	4.7	33	0.198	6.2	2.1	13.5	0.6	1.7	0.1	1.8	3.1	1.0	36.4	↓	?	19.1
38	6.1 m	↓	↓	759	3.81	↓	0.71	1.0	121	0.161	4.1	0.9	8.8	0.7	2.3	0.1	2.1	3.4	0.6	26.0	↓	18.5	14.1
39	Coil	Cell.	0	744	5.63	CO_2	0.16	0.7	142	0.114	4.3	0.8	5.9	0.6	1.4	?	0.6	4.6	1.3	58.2	?	0.001	8.7
40	6.1 m	Cell	↓	754	2.26	↓	0.40	1.2	84	0.167	6.7	0.8	9.3	0.8	0.6	↓	0.2	1.2	2.5	79.2	↓	?	10.9
41	↓	Birch	↓	765	1.68	↓	0.53	1.9	65	0.169	9.8	0.7	8.6	0.5	0.9	↓	0.6	0.8	3.0	63.4	↓	0.028	10.8
42	↓	↓	↓	732	2.11	↓	0.44	2.5	58	0.121	8.1	0.9	7.1	1.1	1.8	↓	1.5	1.7	1.9	59.0	↓	0.016	11.3
43	↓	↓	↓	704	1.52	↓	0.52	4.1	37	0.108	6.2	0.7	6.2	1.0	1.7	↓	1.1	2.6	1.8	53.1	↓	0.015	9.7

[a]Includes H_2O in feed.

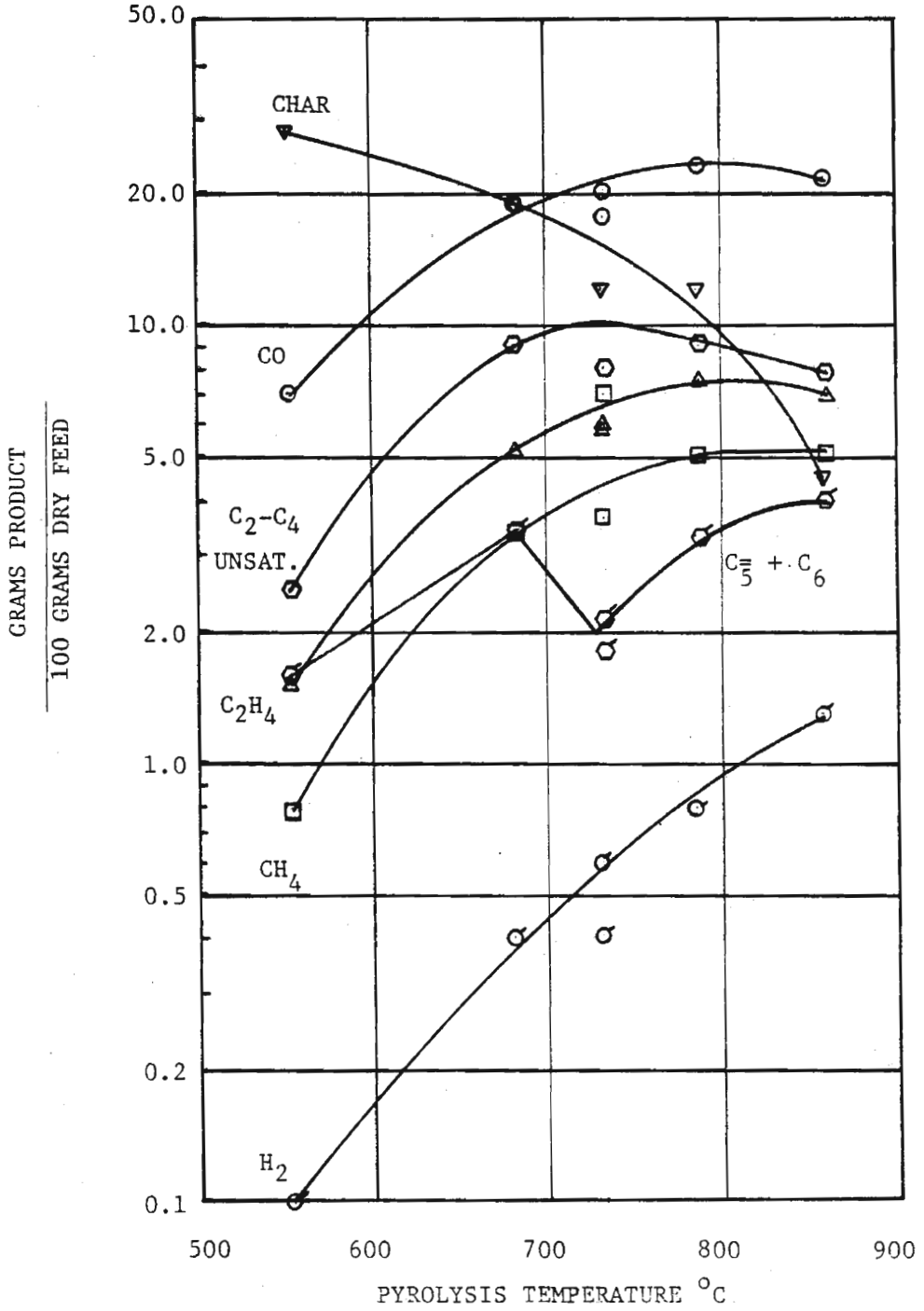

FIG. 3. PYROLYSIS PRODUCTS VS. PYROLYSIS TEMPERATURE WITH THE LONG RESIDENCE TIME REACTOR

and butylenes decreased. Although it is possible that some of the propylene and butylenes were themselves pyrolyzed at the higher temperatures to account for the increase in ethylene production, data in Ref. 8 suggest that these olefins as well as ethylene were more likely polymerizing at these conditions to form a mixture containing about half benzene and half "coal" tars. The increase with temperature of the unknown material, backflushed by the gas chromatograph and labeled "$C_5 + C_6 +$", suggests that this polymerization may indeed have taken place. The location of the cyclone separator in the pyrolysis furnace gave the gases a calculated residence time of 4 to 5 seconds, which appears to have been long enough for polymerization of the heavier olefins to take place at the higher temperatures.

Samples of char from run 10 (682°C) and run 12 (860°C) were tested for heat of combustion in a Parr bomb. A value of 17.9 kJ/g (7710 Btu/lb) was reported for the char from the lower temperature pyrolysis, and a value of 15.1 kJ/g (6504 Btu/lb) was reported for the char formed at the higher temperature. This trend is consistent with the greater gasification occuring at the higher temperature. Based on the weight of the ash recovered from these tests, the char from run 10 contained 58.7% ash and that from run 12 contained 50.1%. Based on the ash content of the feed, run 10 should have produced 16.6% char compared to the measured 18.9%.

As indicated previously, the use of steam and carbon dioxide as carrier gases, rather than hydrogen, methane, and/or carbon monoxide, did not appear to result in major shifts of the weights of desired pyrolysis products. To verify this observation, run 13 was made using a carrier gas consisting of steam and a mixture of 19% by volume hydrogen, 39% carbon monoxide, and 42% methane. The pyrolysis products from this run were not greatly different from those made using steam and carbon dioxide except that the C_2+ hydrocarbons were all slightly lower than usual. It appeared that if there is a small effect of carrier gas on the desired products, carbon dioxide is a preferred carrier gas. This implied that an important function of the carrier gas is one of diluting the products to decrease bimolecular reactions (polymerization) and subsequent tar formation during pyrolysis.

The use of steam as part of the carrier gas allowed the system to operate with a decreased noncondensable carrier flowrate and decreased the eventual dilution of the C_2+ hydrocarbons with carrier gas.

SHORT RESIDENCE TIME REACTOR RESULTS

It was realized that the product gases were being held at the pyrolysis temperature for such a long time (~ 5 seconds) that a portion of the olefins was polymerizing to tars and char. A 1.9-centimeter diameter stainless steel tube, 6.1 meters long was formed into a 41-centimeter diameter coil for the new pyrolysis reactor as shown in Fig. 2. This resulted in a calculated residence time in the pyrolysis coil of about 150 milliseconds with the flowrates then in use. A thermocouple probe was placed at the exit of the pyrolysis coil so that the pyrolysis products impinged upon it. The product gases then passed through a

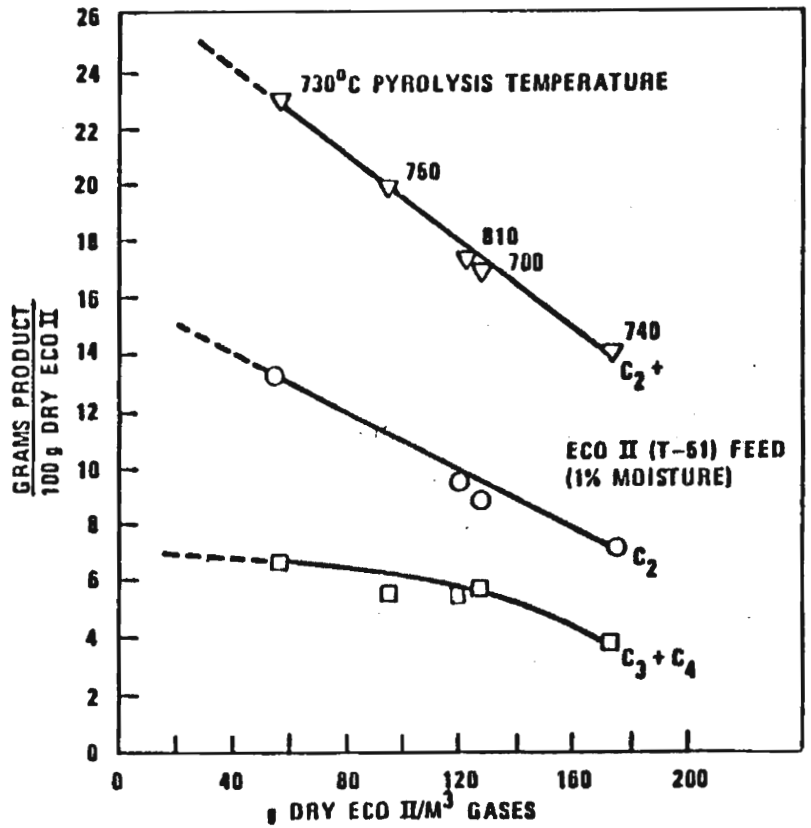

Figure 4. Products vs. Concentration in 6.1-meter Reactor.

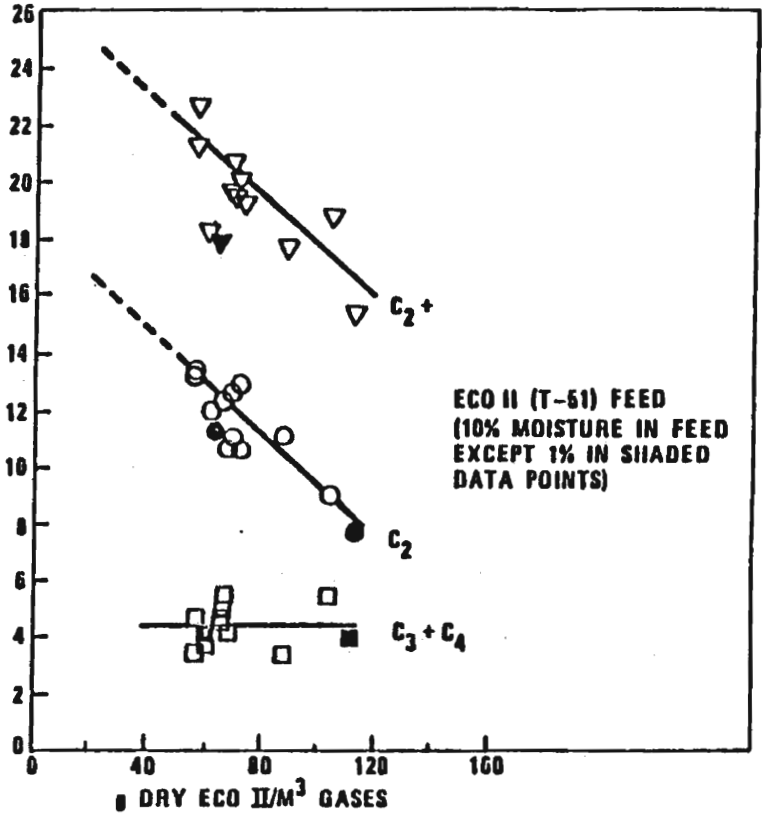

Figure 5. Products vs. Concentration in 2.1-meter Reactor.

1.2-meter length of noninsulated 1.9-centimeter tubing which cooled the gases below about 550°C before they entered the 38-centimeter diameter cyclone separator. The cyclone separator was moved out of the kiln. The steam accumulator was moved to inside the pyrolysis kiln and the steam lines were shortened and better insulated; these changes produced much higher steam temperatures (approaching the pyrolysis temperature). The cyclone and the length of tubing connected to the quench jug were insulated with fiberglass. Runs 14 through 18 were made with this arrangement. The pyrolysis results for the entrained tubular reactor are shown in Table 2.

As will be discussed in detail, the data suggested that the residence time in the pyrolysis coil was still too long, so a 2.1-meter length of tubing was shaped into a shorter reactor. This length of coil resulted in a calculated residence time of about 50 milliseconds. The kiln was rebuilt at that time to provide higher pyrolysis temperatures. Runs 19 through 36 were conducted with this shorter reactor tube. The large cyclone was removed after run 25 so that, through run 38, the char and tars were both collected in the quench jug, as shown in Fig. 2.

Nineteen pyrolysis runs were made using drum T-51 ECO II (a product of Combustion Equipment Associates) for the feedstock with the long tubular pyrolysis reactor, as shown in Table 2. These experiments resulted in the realization that between 700 and 840°C pyrolysis temperature has a relatively minor role in affecting the pyrolysis products with residence times less than 150 milliseconds. The controlling variable appears to be definitely related to the relative concentration of the feed or more specifically the partial pressure of the pyrolysis gases in the reactor. Figure 4 shows that with the 6.1-meter pyrolysis coil there is a pronounced relationship of yield of product as a function of the weight of feed per cubic meter of pyrolysis gases (at the pyrolysis temperature). Figure 5 is similar but shows data generated with the 2.1-meter pyrolysis coil. In both cases, the more dilute pyrolysis conditions gave rise to a greater production of desirable hydrocarbons as well as to carbon monoxide and hydrogen by-product gases. Initially it was assumed that the increased hydrocarbon yields were due to a decreased residence time in the reactor. However, when the 2.1-meter coil replaced the 6.1-meter coil and reduced the residence time by two-thirds with no further increase in hydrocarbon production, it was realized that dilution was the key variable. In fact, the longer coil produced slightly greater amounts of products at the same dilution values, indicating more complete pyrolysis of the larger feed particles. The residence times indicated were calculated using a very simplistic approach; the volumetric flow rate of the gross pyrolysis gases and the steam (at the pyrolysis temperature) were divided into the volume of the pyrolysis reactor. The pyrolysis temperature was simplistically chosen to be that of the gas stream exiting the reactor.

The minor role played by temperature in this "high temperature" pyrolysis regime is seen in Fig. 6. With a variation in pyrolysis temperature of nearly 150°C, there appears to be an increase in the ethylene production of perhaps 10%, but no significant increase in overall ($C_2 + C_3 + C_4$) nor C_2+ fractions was observed. It should be noted that the C_2+

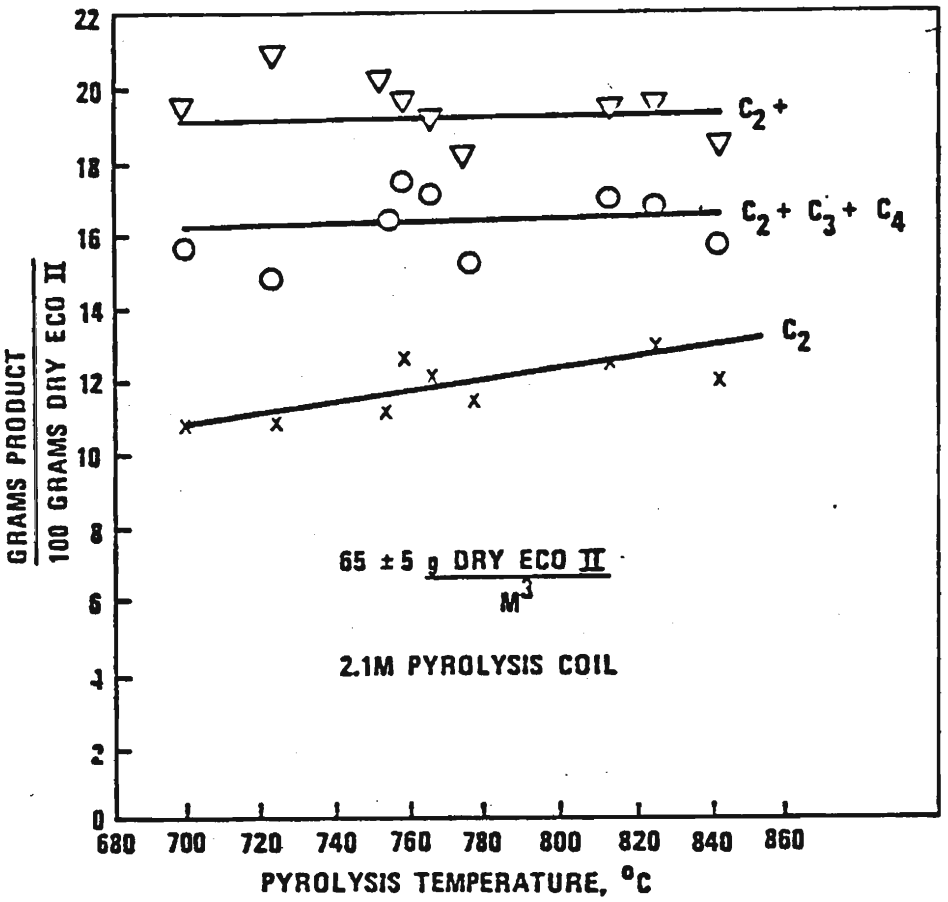

Figure 6. Products vs. Temperature

fraction includes significant amounts of ethane which can be recovered and recycled to the pyrolysis reactor to be cracked to ethylene with expected yields of over 90% as well as the $C_5^{=} + C_6$ (aromatic liquids) which could be used as a high octane gasoline blending stock.

The use of nitrogen as the carrier gas in run 21 was made primarily to determine if the increase in the amount of carbon dioxide carrier gas was responsible for the apparently large increase in ethylene formation. The gas chromatograph, used for the analysis, elutes ethylene immediately after carbon dioxide, and there is some overlapping of the two peaks. There was concern that part of what was thought to be the ethylene peak was actually only carbon dioxide. The use of nitrogen as the carrier gas resulted in a relatively small amount of carbon dioxide in the gross gases (3% by volume) and good peak separation, but did not adversely affect the apparent production of ethylene. It was concluded that the ethylene data were valid. This same run did alter the interpretation of the propane and propylene data and resulted in their values being reduced slightly. These results are reflected in the data presented after run 13. No major shifts in the C_2+ hydrocarbon fraction

were observed in changing the carrier gas from carbon dioxide to nitrogen in the run. There did appear to be significant increases in the carbon monoxide and hydrogen production with this run and a reduction in the amount of C_5+ material.

The variable partial loss of the carbon dioxide carrier gas backing up through the feed hopper makes the carbon and oxygen balances relatively unreliable. The use of steam in the pyrolysis process and water in the quench system makes the hydrogen balance difficult also. An examination of run 21, which used nitrogen as the carrier gas, shows good closure on the overall mass balance (1.006 kilograms out per kilogram in) and the carbon balance (1.018 kilograms out per kilogram in). The amount of water formed by pyrolysis needed to close the hydrogen balance is 0.108 kilogram of water per kilogram of dry feed. The oxygen balance very nearly closes without the hypothesis of water formation; i.e., 0.975 kilogram oxygen out per kilogram oxygen in or 0.009 kilogram water per kilogram of dry feed. Small differences in feed composition and/or a small error in the relatively difficult hydrogen analysis of the feed probably account for these discrepancies. It is concluded that little water is formed during fast pyrolysis of biomass and that the amount will be greatly affected by the extent of the water gas shift reaction taking place.

Experimental pyrolysis runs were conducted to evaluate the use of a different lot of ECO II feed (lot T-47), the reduction of the amount of carbon dioxide carrier gas used, and the use of the longer 6.1-meter pyrolysis coil. Lot T-47 of ECO II appeared to be similar to the T-51 lot, but with some differences: 188 μm (T-47) vs. 270 μm (T-51) average particle size; 12.5% ash vs. 9.7% ash; and a heat of combustion (higher heating value) of 19.8 kJ/g (8507 Btu/lb) vs. 22.2 kJ/g (9550 Btu/lb). There has been some concern that the lower heating value for lot T-47 was indicative of a lower plastics content and that this would result in a significantly lower yield in desirable hydrocarbons, since plastics like polyethylene are pyrolyzed at these conditions to form very high yields of desirable olefins such as ethylene and propylene. Taking the pyrolysis runs as a whole, it appears that the hydrocarbon production from lot T-47 is about equivalent to that from lot T-51, with the result that slightly better energy conversions to hydrocarbons were observed with lot T-47 due to the lower energy content of the feed.

The use of the longer pyrolysis coil for runs 37 and 38 confirmed previous runs (14 through 18) with respect to relatively good hydrocarbon production with a lower kiln temperature (ΔT) due to the larger heat transfer surface and residence time. In fact, it was observed that the temperature of the exiting pyrolysis gases (measured with a sheathed thermocouple probe) was 25 to 50°C hotter than the pyrolysis kiln (also measured with a sheathed thermocouple). This probably reflects a slightly exothermic pyrolysis reaction occurring at the elevated temperatures and/or large temperature variations within the kiln itself. Using lot T-47 feed with 10% moisture gave similar results on a dry feed basis as were obtained with lot T-51 having only 1% moisture, as shown in Fig. 4.

In runs 35 through 37 the steam flow was irregular. The problem with the steam flow was in part due to the "weeping" of the steam pressure relief valve and in part due to a cracked fitting. This leakage and pressure fluctuation resulted in uncertainties in the actual dilution present in the pyrolysis reactor for these four runs. Run 28 has no known boiler water leakage, although the steam pressure still had considerable fluctuation (125 ± 25 psi). The steam fluctuation was apparently due to a small change in the boiler waterline which allowed the water to accumulate in a horizontal section until the surface tension was overcome and the water was dumped into the hot section of the boiler. These factors resulted in variable steam flows, which were averaged for the purpose of comparing the runs.

PYROLYSIS TESTS USING CELLULOSE AND BIRCHWOOD FLOUR

A few tests were conducted with the short-residence-time pyrolysis reactor using pure cellulose and birchwood flour to determine if the high olefin yields obtained from ECO II could be obtained from lignocellulosic biomass materials (Ref. 9). The preliminary data from these tests are shown in Table 2. A comparison of the C_2 - C_4 unsaturated hydrocarbons (last column) listed in Table 2 with the average values for ECO II reveals that the cellulose and birch flour produced only about 70% of the amount of these hydrocarbons as the ECO II feedstock, but at the same time produced much more methane. The greater amount of hydrocarbons obtained from the MSW feedstock may be due to plastics in the ECO II feed or may be caused by the chemical pretreatment used in preparing the ECO II material. Due to feeding problems, both the cellulose and the birch flour tended to pass through the reactor unevenly which probably resulted in a low effective dilution and consequently lower olefin yields. Additional experimentation needs to be conducted with both natural biomass feedstocks as well as biomass material which has undergone the proprietary processing used to prepare ECO II. SERI now has such a material in hand made from sugar cane biogasses (AGRIFUEL™ by Combustion Engineering Associates) and will test it in the near future. The amount of char produced by cellulose was 0.1% and by birch flour 1.5%-which is one to two orders of magnitude less than that contained in ECO II.

CONCLUSIONS

Significant yields of unsaturated hydrocarbon (approximately 15 weight percent) as well as saturated and aromatic hydrocarbons were obtained from a commercially available pretreated municipal solid waste feedstock (ECO-II). Results of tests conducted with an apparatus providing residence times greater than 5 seconds indicated that ethylene yields increased with temperature to the highest pyrolysis temperature of 860°C. However the quantity of higher molecular weight olefins showed a decrease after about 650°C. Using a pyrolysis reactor providing residence times less than 0.2 seconds, no clear temperature for maximum olefin production was found. However, larger amounts of carrier gas relative to the quantity of solids fed apparently produced more olefins. One plausible explanation for this result is that higher partial pressures of reactive intermediates produced in the pyrolysis reaction form tars and char rather than low molecular weight olefins. Variation of carrier gas composition had no significant effect upon pyrolysis gas composition indicating that shifting of products based upon equilibrium chemistry does not occur at a rapid rate at the conditions employed.

Olefin yields obtained from pure cellulose and birch wood flour using the short-residence-time pyrolysis reactor were about 70% those obtained from ECO-II. The greater yields of olefins from the MSW feedstock is believed to be due to the presence of plastics, although the chemical pretreatment of this material may contribute to olefin production. The char yields from the cellulose and birch flour were only 0.1% and 1.5% respectively, compared to 10 to 25% for the municipal solid waste feedstock.

REFERENCES

1. Diebold, J. P., C. B. Benham, and G. D. Smith. "Conversion of Organic Wastes to Unleaded, High-Octane Gasoline." Final Report. EPA IAG-D6-0781. Cincinnati, OH: Industrial Environmental Research Laboratory; 1980.

2. Finney, C. S., and D. E. Garrett. "The Flash Pyrolysis of Solid Waste." Presented to 66th Annual Meeting of AIChE, paper 13-E. November 1973.

3. Lincoln, K. A. "Flash-Pyrolysis of Solid-Fuel Materials by Thermal Radiation." Pyrodynamics, 2, pp. 133-143; 1965.

4. Brink, D. L., M. S. Masoudi, and R. F. Sawyer. A Flow Reactor Technique for the Study of Wood Pyrolysis. Presented at: Fall meeting, Western States Section, The Combusion Institute, El Segundo, CA. October 1973.

5. McFarland, J. M., et al. "Comprehensive Studies of Solid Waste Management." NERC Report No. 72-3, National Environmental Research Corp. Contract 2 ROI-EC-00250-01, Environmental Protection Agency. May 1972.

6. Mallon, G. M. and L. E. Compton. "Gasification of Carbonaceous Solid," U.S. Patent 3,846,096. 1974.

7. Beningson, R. M., et al. Production of ECO-FUEL®II frokm Municipal Solid Waste. CEA/ADL Process. Proceedings of 80th AIChE National Meeting, Boston, MA. Paper 30e. September 1975.

8. Dunstan, A. E., E. N. Hague, and R. V. Wheeler. "Thermal Treatment of Gaseous Hydrocarbons; I. Laboratory Scale Operation." Ind. Eng. Chem., 26(3):307-314.

9. Diebold, J. P. "Research into the Pyrolysis of Pure Cellulose, Lignin, and Birchwood Flour in the China Lake Entrained-Flow Reactor", SERI Report No. TR-332-586, Solar Energy Research Institute, Golden, CO., June, 1980.

AN EXPERIMENTAL INVESTIGATION INTO FAST PYROLYSIS OF BIOMASS USING AN ENTRAINED FLOW REACTOR

M. BOHN AND C. BENHAM*

Abstract

Pyrolysis experiments were performed using an entrained flow pyrolysis reactor and two different feedstocks-a powdered material derived from municipal solid waste (ECO-II)^{TM} and wheat straw. All entrained-flow tests were conducted with reactors having a length of either 30 cm. or 90 cm. Steam was used as the carrier gas for all tests. Reactor wall temperature was varied from 700°C to 1400°C. Gas composition data from the ECO-II tests were comparable to data reported previously by Diebold using an ECO-II feedstock. Trends were found in ethylene yield as a function of reactor wall temperature and residence time. The trends suggest that it may be possible to correlate gas yield with a single parameter which includes temperature, reactor length, and steam-to-biomass flow rate ratio. The important conclusion from the wheat straw tests is that olefin yields are about one half that obtained from ECO-II. Evidence was found supporting the idea that high olefin yields from ECO-II are due to the presence of plastics in the feedstock.

Batch experiments were run on wheat straw using a Pyroprobe^{TM} . The samples were heated at a high rate (~20,000°C/sec.) to 1000°C and held at 1000°C for a variable period of time from 0.05 seconds to 4.95 seconds. These results revealed that two different mechanisms occur. For times up to 0.15 seconds, volume fractions of ethylene, propylene, and methane increase while that of carbon dioxide decreases. After that period, those species are no longer generated and only carbon monoxide and hydrogen are produced. The change in mechanism may be related to poor thermal contact of portions of the sample with the probe. Data at 0.15 seconds compare quite well with data from the 30 cm. reactor at 1000°C except for the lack of acetylene in the Pyroprobe data. This suggests that the sample was not heated as rapidly by the Pyroprobe as in the entrained flow reactor which provides heating rates of approximately 5000°C/sec.

*Solar Thermal Research Branch
Solar Energy Research Institute
Golden, Colorado

Introduction

Destructive distillation (pyrolysis) of biomass materials is an ancient art which has become the object of renewed interest during the past few years. This renewed interest stems from the continuing energy dilemma and the realization by many scientists and engineers that biomass is a viable feedstock for producing fuels and chemicals which are now derived from petroleum feedstocks.

The thrust of the effort within the Solar Thermal Research Branch at SERI is toward producing diesel fuel from gases obtained from an entrained flow pyrolysis reactor. The feedstocks of primary interest are agricultural non-food materials such as wheat straw and corn stalks. A catalytic process for converting olefins, carbon monoxide and hydrogen to liquid hydrocarbons was described by Kuester.

Since the hydrocarbon yield from a catalytic process is influenced by the relative amounts of hydrogen, carbon monoxide and unsaturated hydrocarbons, it is important for us to understand the interrelationship of the large number of pyrolysis variables which influence gas composition.

Much of the effort in pyrolysis during the past few years has been directed towards detailed studies of the pyrolysis mechanism (see reference 2-9). Welker presents a review of the literature on pyrolysis and ignition of cellulosic materials. Typically, these studies involved small samples of a given material heated at a few hundred degrees centigrade per minute and resulted in gas composition, char yield, and kinetics data. An entrained flow reactor on the other hand is one practical implementation of continuous pyrolysis which can provide heating rates on the order of $1000^{o}C$/sec.

Several researchers have reported data from entrained flow pyrolysis reactors. Finney and Garrett reported high yields (>20 wt %) of ethylene using a finely divided municipal solid waste feedstock in a steam carrier flow, a reactor temperature of about $800^{o}C$, and a short residence time (<1 second). Brink studied pyrolysis of wood, kraft black liquor, and municipal solid waste in a reactor having a heating rate of about $1000^{o}C$/second, a maximum temperature of $840^{o}C$ and a residence time of about 3 seconds. The carrier gas used was nitrogen. Rensfelt studied pyrolysis of a variety of feedstocks including wood, straw, municipal solid waste, peat, coal and graphite. The reactor was capable of heating rates to $1000^{o}C$/second and temperatures were varied from $500^{o}C$ to $1000^{o}C$. Carrier gases used included steam, hydrogen, and nitrogen. Ethylene yields obtained using municipal solid waste were comparable to those obtained by Diebold with pyrolysis tests on municipal solid waste feedstock (ECO-II) which is a commercially available material from Combustion Equipment Associates, New York. In the Diebold experiments pyrolysis temperatures ranged from 700 to $800^{o}C$, residence times from 50 to 200 ms, and ratios of steam to biomass

flow rates from 1:1 to 5:1. A combination of steam and carbon dioxide was generally used as the carrier gas. Three runs were made using nitrogen in place of carbon dioxide. The two primary results obtained from this study were that large amounts of olefins (>20 wt %) were obtained in the pyrolysis gases and that the greater the dilution of the biomass with carrier gas, the greater the yield of olefins. Diebold, in a separate study used the same apparatus to obtain data using pure cellulose and birch flour as feedstocks. These materials produced less than one-half the amount of olefins produced using the ECO-II feedstock. McFarland obtained about 4 wt% ethylene using large particles (1.25 cm.) of municipal solid waste in an entrained flow reactor operated at about 800°C.

In spite of the considerable amount of data obtained from the previously mentioned studies, a clear picture of which variables are important and what influence these variables have upon gas composition has not been determined.

The SERI Entrained Flow Pyrolysis Reactor

As mentioned in the previous section, one of the goals of the SERI program is to allow more extensive entrained flow reactor measurements than reported in previous works. Measurements of interest include the effect of reactor length, reactor temperature, and carrier flow to biomass flow ratio on pyrolysis gas composition. In this section we describe the SERI entrained flow reactor, instrumentation and experimental procedures.

As shown in figure 1, biomass is metered into a mixing chamber by a screw feeder where it is entrained by a flow of superheated steam. Water flow rate delivered to the boiler/superheater is measured by a rotameter and the temperature of the steam entering the mixer is also monitored. For smooth delivery, the water is supplied to the boiler/superheater by a piston tank pressurized to about 14 atmospheres by nitrogen.

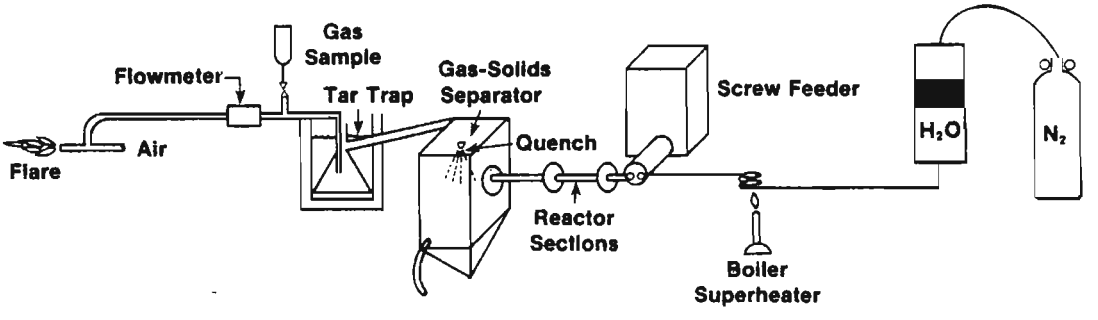

Figure 1. SERI Entrained Flow Pyrolysis Reactor.

The entrained biomass/steam flow enters the reactor which is electrically heated vycor or stainless steel tubes with 13 mm. inside diameter. Electrical heating has been provided either with a tube furnace for the vycor tube or by nichrome coils placed near the steel reactor tube. For the vycor tube, reactor temperature was determined by the temperature setting chosen on the furnace. For the steel tube, power input to the nichrome coils was provided by variacs and the temperature was monitored by chromel/alumel thermocouples. The thermocouples are supported by small steel tubes welded perpendicular to the reactor and held in close contact to the reactor tube by high temperature ceramic cement. Reactor length is adjusted from 15 to 150 cm. by adding or removing reactor sections. Power supplied by the variacs was measured.

Downstream of the last reactor section, a cold water spray quenches the reaction and condenses the steam carrier. At this point, pyrolysis gases and solid particles are separated. The gases then pass through two tar traps consisting of dry ice/water baths and small gas samples are drawn into 150 cc evacuated stainless steel sample bottles downstream of the tar traps. A flow meter section then measures pyrolysis gas molecular weight and mass flow before the gases are flared with a bunsen burner. The entire system is operated slightly below atmospheric pressure due to suction provided by the air ejector. Gas analysis including hydrocarbons through C_5 is provided by a Hewlett-Packard model 5840 gas chromatograph.

Flow rate of the biomass particles is measured by a mass balance upon which the screw feeder rests. In addition to the reactor wall temperature probes, gas temperature is measured at several stations along the reactor by chromel/alumel thermocouples immersed in the flow through the reactor wall. The probes are made from 0.005" wire and are gold plated to minimize emissivity and thereby reduce sensitivity to radiation from the reactor wall. All data are recorded by a microcomputer based data acquisition system. This system also controls the steel reactor temperature by closing a feedback loop between the wall temperature probes and stepper motors which turn the variacs. Gas sampling ports are also provided at several stations along the reactor length to allow one to measure gas composition as a function of extent of reaction.

Typically, the reactor and the steam are brought up to temperature together. When steady conditions are reached, the screw feeder is turned on and the reactor temperature is allowed to re-equilibrate to the original temperature. At this time gas samples are taken. A run of about five minutes is required to allow solids feed rate to be accurately determined, but for purposes of debugging feed or entrainment problems, runs of thirty minutes have been used.

Results

For purposes of comparing results from the SERI reactor with previous experiments, references 13 and 14, we ran experiments with ECO II fuel as the biomass feedstock. Temperatures from 700°C to 1200°C were used with a 90 cm. reactor and temperatures from 1000°C to 1400°C with a 30 cm. reactor. Steam to biomass ratio was approximately 1:1. The ECO II particles have an average size of 240 micron.

Diebold, reference 14, has shown that steam/biomass ratio can strongly influence ethylene yield. We have taken data for 1:1 ratio from the SERI reactor and from reference 14. Reference 13 does not report the steam/biomass ratio used in those experiments. The feedstock used in reference 13 was not ECO II but a municipal waste with a composition of $C_6H_{9.3}O_{4.2}$ while ECO II is reported, reference 14, to have a composition of $C_6H_{9.8}O_{3.3}$. In addition, particle sizes may have been somewhat larger as the size reported in reference 13 was "<0.5mm". Residence times were calculated for the SERI reactor according to the method used in reference 14 (volumetric flow rate of gases in the reactor at gas exit temperature divided by reactor volume) while residence times used in reference 13 were reported to be generally >0.4s.

Volume fraction of ethylene is shown in figure 2. The continuous curves are the data for the SERI 90 cm. and 30 cm. reactors and from reference 13 while the individual points are from reference 14. Absolute scaling of data from reference 14 is difficult because carbon dioxide was used as a carrier for those experiments and gas composition was reported on a carbon dioxide-free basis.

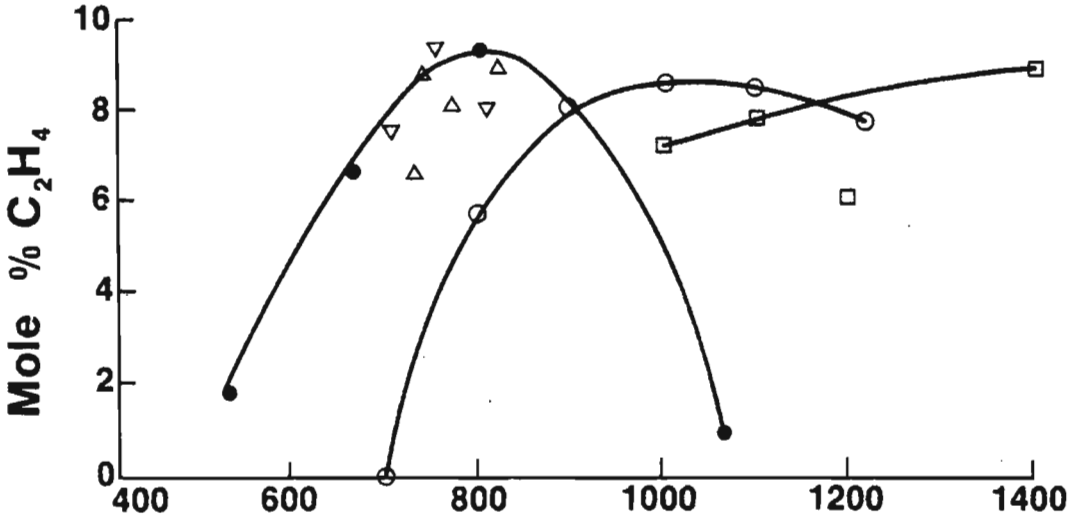

Reference	Steam Bio	Residence Time
□ Present	1 : 1	0.012 s
○ Study	1 : 1	0.037 s
△ 14	1 : 1	0.05 s
▽ 14	1 : 1	0.15 s
● 13	?	0.4 s

Figure 2. Ethylene Yield vs. Reactor Temperature and Residence Time.

Figure 2 shows a well defined trend (except for the reference 14 data) of ethylene peaks occurring, at low temperatures for longer residence times. A decrease in ethylene yield at high temperatures is generally regarded a result of secondary gas phase reactions which convert the unsaturated hydrocarbons to higher molecular weight hydrocarbons. The dependence on residence time in an entrained flow reactor has not been shown before, but can be explained in terms of heat transfer limitations.

Species evolution from the particles depends on the rate of increase of particle temperature and the heating period (residence time). A short reactor operating at a given temperature could produce a gas composition similar to that produced by a longer reactor operating at a lower temperature. The exception would be the olefins which may be produced in greater volume fraction in the short reactor due to the higher heating rate. This appears to be the case in figure 2. The ethylene peak for the 30 cm. reactor is higher than that for the 90 cm. reactor. Note that the longest residence time peak (from reference 13) is even higher but a direct comparison of yields from reference 13 should not be made because steam/biomass ratio is unknown for those data. More data for other residence times and steam/biomass ratio should confirm this dependence of gas composition on residence time and temperature and could lead to a correlation between these three parameters.

This same trend is exhibited in figures 3, 4, and 5 in which gas composition is plotted as a function of reactor temperature for the 90 cm. reactor, for the 30 cm. reactor, and for the data from reference 13, respectively. The trends, especially for carbon monoxide, hydrogen, methane, and carbon dioxide are shifted towards higher temperatures in the short reactor. A noticeable difference between reference 13 data and the 90 cm. data, figure 4 and 5, is the decrease in carbon monoxide and the increase in hydrogen and carbon dioxide for the entire temperature range. This suggests the water-gas shift reaction which could be related to catalytic materials in the solid waste or the long residence times used in reference 13.

Experiments were also run with wheat straw as the biomass feedstock. As discussed in an earlier section, wheat straw is a potential feedstock for a process upon which our research is focused. That process is the pyrolysis of agricultural non-food products and the catalytic conversion of the resulting pyrolysis gases (primarily hydrogen, carbon monoxide, and olefins) to diesel fuel.

Results for a 30 cm. reactor with particle size $\sim$150 micron, and steam to biomass ratio of approximately 1:1 are shown in figure 6. The most important result is that the wheat straw produces approximately half the ethylene as does the ECO II feedstock. Possible reasons include the presence of plastics in the ECO II as well as the fact that the ECO II is chemically pre-treated by acid hydrolysis to assist in grinding. The latter explanation seems less plausible because tests with an electrically heated platinum wire on small batches of acid treated

newsprint gave an increase in olefin yield from 10.1 to 11.2 wt % compared to non-treated newsprint. In addition, Finney has reported entrained flow reactor results on untreated municipal waste in which half the paper fibers were removed, presumably increasing the fraction of plastics in the feedstock. Those results indicated ethylene yields of 21% by volume which is considerably higher than that reported for ECO II yields. We therefore conclude that the presence of plastics is responsible for the high olefin yields reported for fast pyrolysis of municipal wastes.

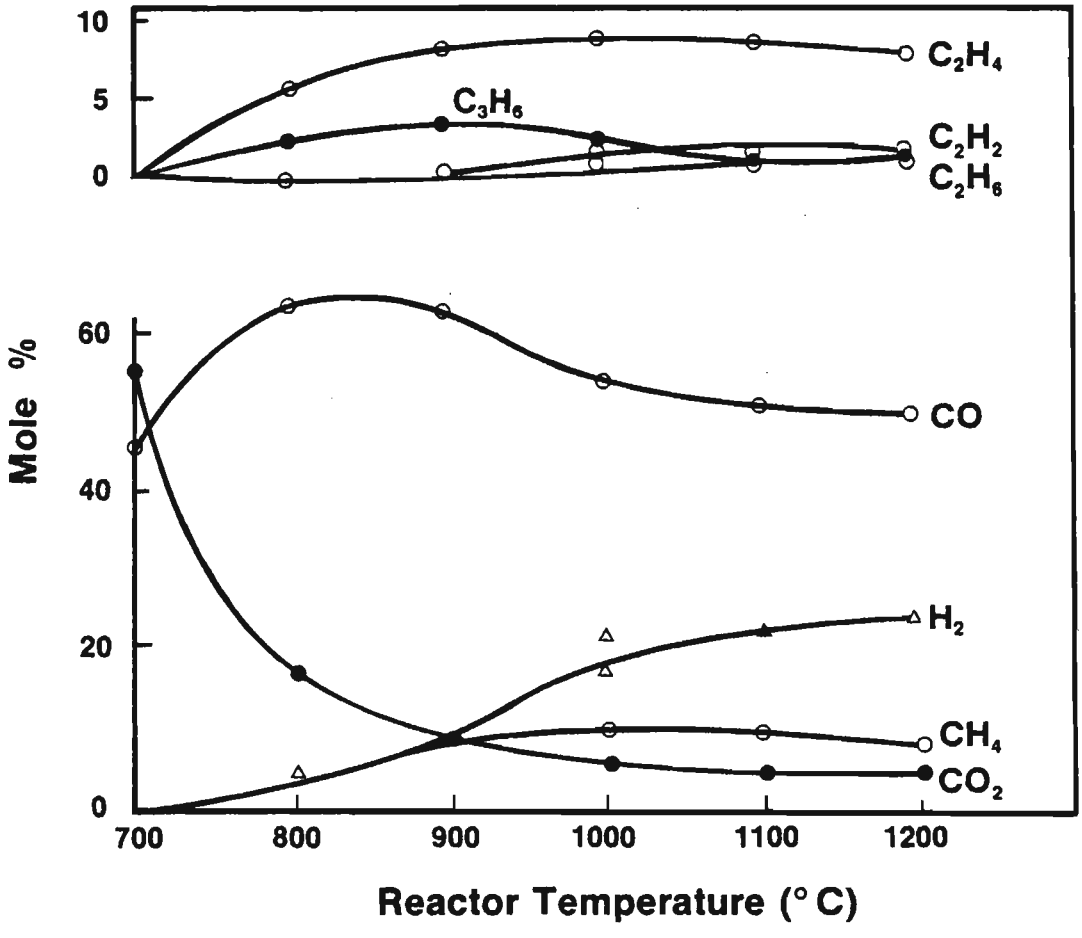

Figure 3. Gas Composition vs. Reactor Temperature, 90 cm. Reactor, ECO II.

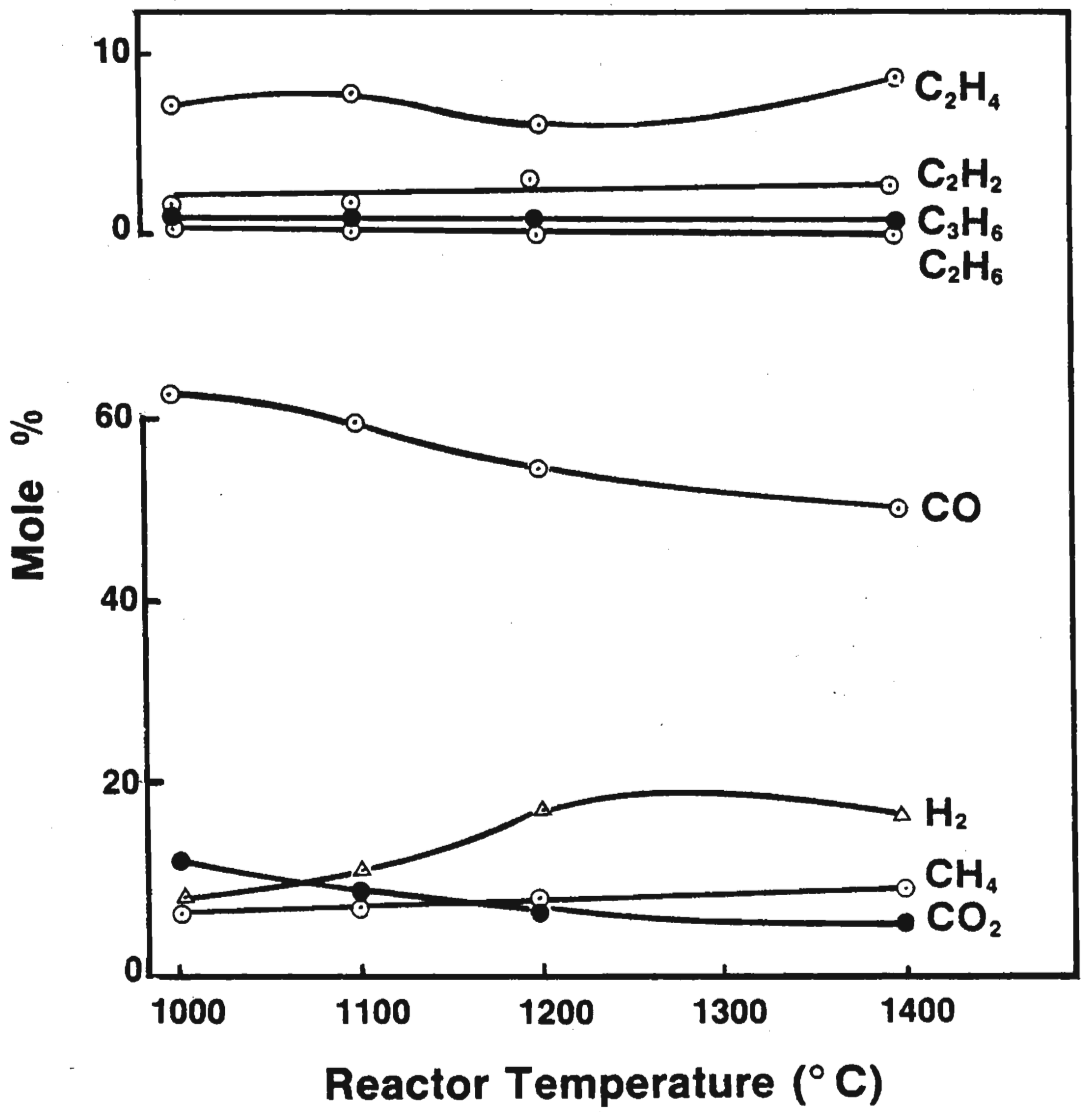

Figure 4. Gas Composition vs. Reactor Temperature, 30 cm. Reactor, ECO II.

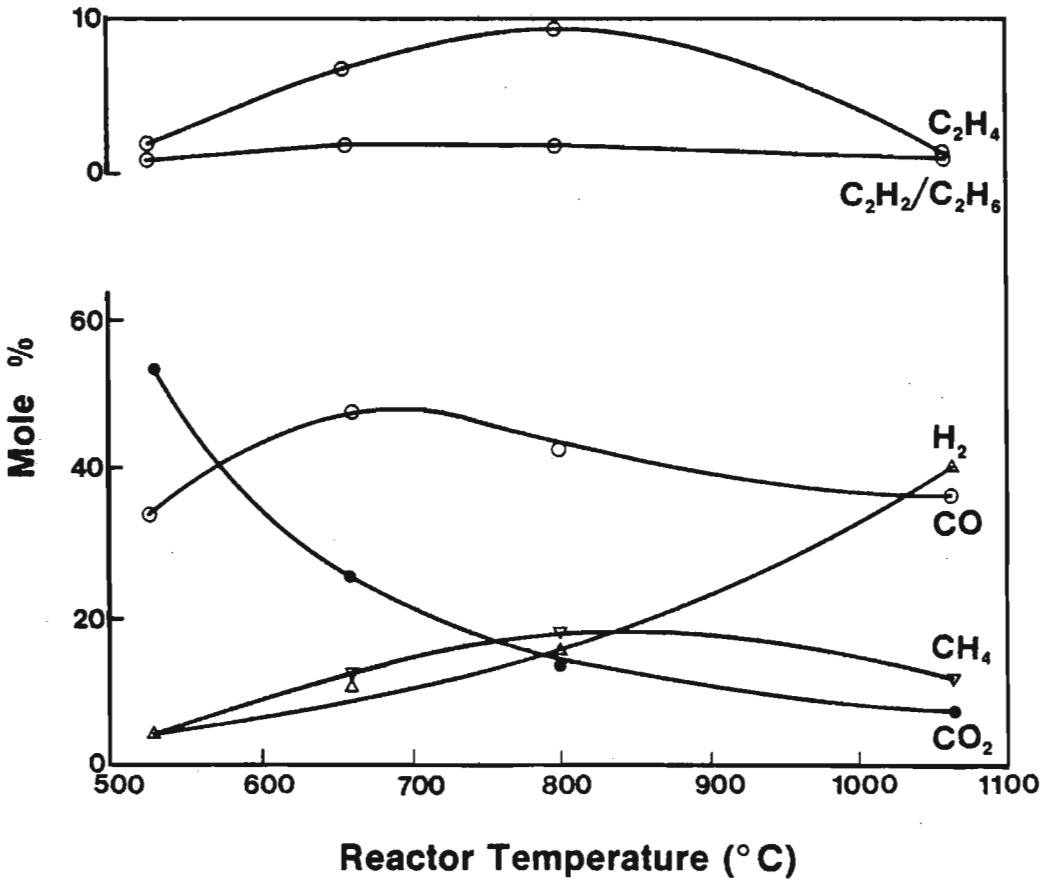

Figure 5. Gas Composition vs. Reactor Temperature, Reference 13, Solid Waste.

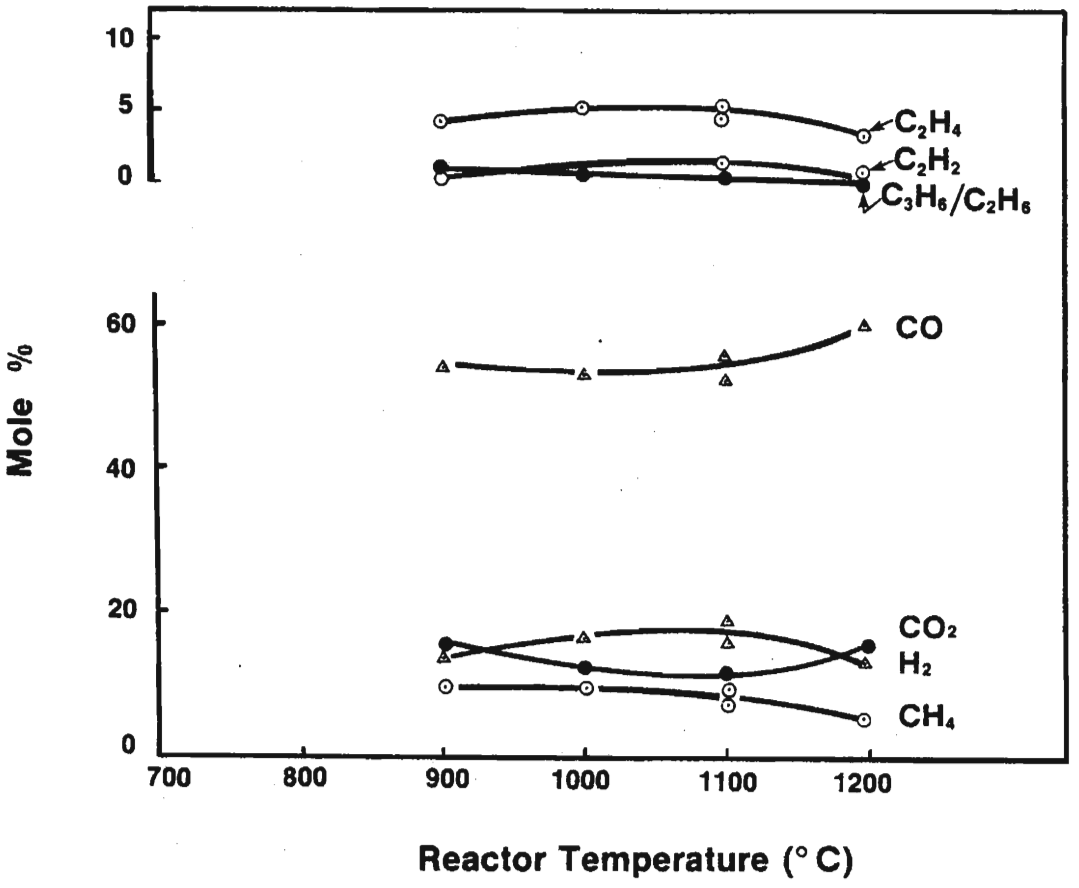

Figure 6. Gas Composition vs. Reactor Temperature, 30 cm. Reactor, Wheat Straw.

To complement our reactor experiments we have been using an electrically heated platinum wire to study fast pyrolysis of small batches of prospective feedstocks. This method is useful for screening feedstocks as well as for quickly determining operating regimes in which the reactor experiments may be interesting. The registered tradename of the device is Pyroprobe (Chemical Data Systems, Inc.) and has been used by many researchers for similar purposes. Our work, however indicates that some caution in interpreting results from the Pyroprobe is in order.

The Pyroprobe allows one to heat the platinum wire along a prescribed temperature-time curve. Specifically, the temperature can be programmed to increase linearly to a given temperature, and then hold that temperature for a given period of time. We used the device to heat small (200µg) samples of fine wheat straw on a temperature ramp of 20,000°C/sec up to 1000°C and then hold the sample at that temperature for times ranging from 0.05 seconds to 4.95 seconds.

In figure 7, we plot the gas composition versus the time which the probe was held at 1000°C. There are clearly two regimes for holding times less than or greater than 0.15 seconds. This suggests two different mechanisms. At 0.15 seconds the maximum ethylene, propylene, and methane mole fractions occur. For holding times longer than this, the fraction of those components and also of carbon dioxide decreases at the same rate on the log-log scale while the hydrogen increases and carbon monoxide fraction is essentially constant. The linear decrease in the four species after 0.15 seconds holding time can be shown to imply that either those four species cease to be generated or are generated at rates which are related in an unusual way. The most likely explanation is that the four species are produced up until 0.15 seconds and after that are diluted by the increasing amounts of hydrogen and carbon monoxide.

The change in mechanism may be related to poor contact of the particles with the probe. Microscopic examination of a probe after applying the particles by what seems to be the most effective method (applying a distilled water/wheat straw slurry to the element and then evaporating the water) revealed that the particles contacted the probe in only a very few isolated points. For holding times up to 0.15 seconds these contact points are very rapidly heated and produce increasing quantities of olefins (and decreasing quantities of carbon dioxide which is consistent with our low temperature reactor experiments). During this time, it is possible that the portions of the sample not in direct contact with the probe are heated much more slowly producing char. After 0.15 seconds, portions of the sample in direct contact with the probe have completely pyrolyzed leaving the char to continue heating slowly and producing hydrogen and carbon monoxide. In addition, gases evolved from the particles in direct contact with the probe, could force the particles from the probe thereby greatly reducing the heating rate of the sample. A close examination of the residue left on the probe after short holding times could help verify these explanations.

Comparing the gas composition after 0.15 seconds at 1000°C (which seems to be the gas composition most representative of the 20,000°C/sec. heating rate) with that for the 30 cm. reactor at 1000°C, figure 6, we find they are quite similar with one exception. Pyroprobe data at these conditions is consistently lacking any meaningful quantities of acetylene, while the reactor consistently yields acetylene. A lack of acetylene implies a lower temperature reaction in the probe experiments than in the reactor experiments. Although the probe was heated at 20,000°C/sec to 1000°C it appears that the particles lagged the probe temperature due to poor thermal contact with the probe. It is difficult to determine the particle temperature except indirectly by comparison with probe runs for higher final temperatures. However, an analysis of particle heating rates for the entrained reactor suggests that heating rates of 5000°C/sec may be reasonable and therefore we expect that the particles heated with the probe were heated at less than 5000°C/sec, and achieved temperatures less than that achieved by the particles in the 30 cm. reactor.

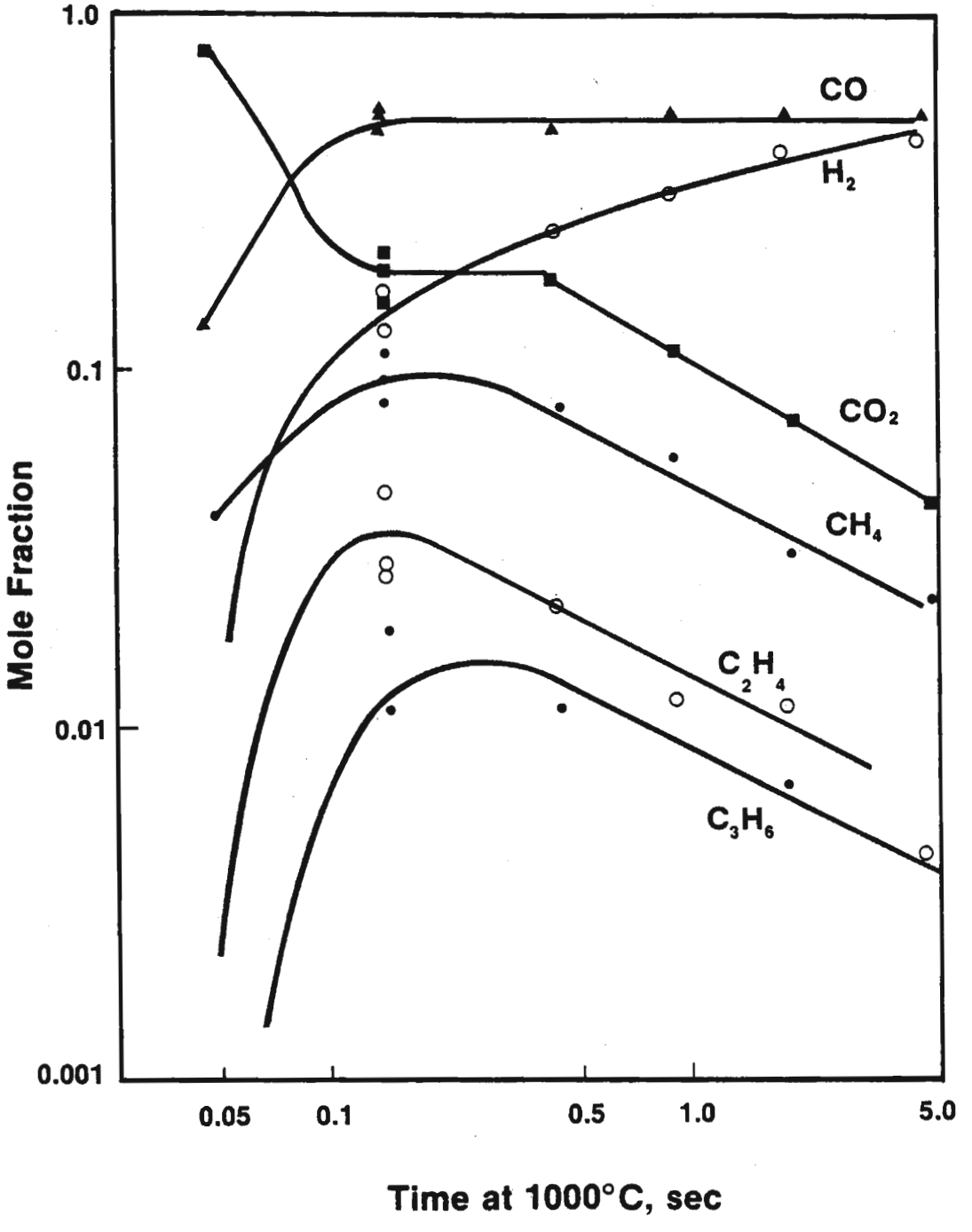

Figure 7. Gas Composition vs. Holding Time (1000°C), Wheat Straw, 20,000°C/sec.

Conclusions

Entrained flow reactor pyrolysis experiments on a municipal solid waste feedstock (ECO II) resulted in olefin yields comparable to that reported previously. However, trends in the data, namely ethylene yield as a function of reactor temperature and residence time which had not been seen before, were found. The trends suggest that it may be possible to correlate gas yield with a parameter which includes temperature, reactor length and steam/biomass ratio.

Experiments were also performed with an agricultural non-food product, wheat straw. The most important result of those experiments was that olefin yields were about half that of the ECO II feedstock. The most likely explanation is the presence of plastics in the ECO II feedstock.

Pyroprobe experiments with wheat straw reveal that two mechanisms affect the gas composition resulting from heating at 20,000°C/sec to 1000°C and then holding at 1000°C for a variable period. For periods up to 0.15 seconds, volume fractions of ethylene, propylene, and methane increase while that of carbon dioxide decreases. After that period the species are no longer generated and only hydrogen and carbon monoxide are generated. The change in mechanism may be related to poor thermal contact of portions of the sample with the probe. Data at 0.15 seconds compare quite well with the 30 cm. reactor results at 1000°C except for the lack of acetylene in the pyroprobe data. This suggests that the sample was not heated as rapidly by the pyroprobe as in the entrained flow reactor.

Future Work

We plan to run more experiments on wheat straw and other agricultural non-food products in the entrained flow pyrolysis reactor. Data from these experiments will include gas yield as a function of reactor length, reactor temperature, and steam/biomass ratio. Trends from these data will be used to develop correlations which will be useful for engineering scale-up of the reactor and to help explain pyrolysis mechanisms.

Acknowledgement

The assistance of Mr. G. Bessler in design and construction of the apparatus, the assistance of Mr. R. Kemna in construction and operation of the apparatus, and the assistance of Mr. P. Bergeron in gas chromatographic analysis are appreciated.

REFERENCES

1. Kuester, J.L., "Conversion of Cellulosic Wastes to Liquid Fuels," presented at the Engineering Foundation Conference on Municipal Solid Waste as a Resource, Henniker, New Hampshire, July 1979.

2. Antal, M.J., "The Effects of Residence Time, Temperature and Pressure on the Steam Gasification of Biomass," presented at the American Chemical Society Symposium, Honolulu, Hawaii, April 1979.

3. Baker, R.R., "Thermal Decomposition of Cellulose," Journal of Thermal Analysis, Vol. 8, pp. 163-173, 1975.

4. Broido, A., and Nelson, M.A., "Char Yield on Pyrolysis of Cellulose," Combustion and Flame, Vol. 24, pp. 263-268, 1975.

5. Stamm, A.J., "Thermal Degradation of Wood and Cellulose," Ind. Eng. Chem., Vol. 48, pp. 413-417, 1956.

6. Lipska, A.E., and Parker, W.J., "Kinetics of the Pyrolysis of Cellulose in the Temperature Range 250-300 ^{o}C," Journal of Applied Polymer Science, Vol. 10, pp. 1439-1453, 1966.

7. Antal, M.J., Friedman, H.L., and Rogers, F. E., "Kinetic Rates of Cellulose Pyrolysis in Nitrogen and Steam," presented at the Fall Meeting, Eastern Section, The Combustion Institute, Hartford, Connecticut, November 1977.

8. Antal, M.J., Friedman, H.L., and Rogers, F.E., "Kinetics of Cellulose Pyrolysis in Nitrogen and Steam," Combustion Science and Technology, Vol. 11, 1979.

9. Lewellen, P.C., Peters, W.A., and Howard, J. B., "Cellulose Pyrolysis Kinetics and Char Formation Mechanism," Sixteenth International Symposium on Combustion, August 1976.

10. Welker, J.R., "The Pyrolysis and Ignition of Cellulosic Materials: A Literature Review," J. Fire and Flammability, Vol. 1, p. 12, 1970.

11. Finney, C.S., and Garrett, D.E., "The Flash Pyrolysis of Solid Waste," presented at the 66th Annual Meeting of the AICHE, paper 13-E, November 1973.

12. Brink, D.L., Masoudi, M.S., and Sawyer, R.F., "A Flow Reaction Technique for the Study of Wood Pyrolysis," presented at the Fall Meeting, Western States Section, The Combustion Institute, El Segundo, California, October 1973.

13. Rensfelt, E., et al., "Basic Gasification Studies for Development of Biomass Medium-Btu Gasification Processes," presented at the Energy from Biomass and Wastes Symposium, Washington, D.C., August 1978.

14. Diebold, J.P., Benham, C.B., and Smith, G.D., "Conversion of Organic Wastes to Unleaded High Octane Gasoline," Final Report EPA IAG-D6-0781, Cincinnati, Ohio, Industrial Environmental Research Laboratory, 1980.

15. Diebold, J.P., "Research into the Pyrolysis of Pure Cellulose, Lignin, and Birch Flour in the China Lake Entrained Flow Reactor," SERI/TR-332-586, Golden, Colorado, 1980.

16. McFarland, J.M., et al., "Comprehensive Studies of Solid Waste Management," SERL Report No. 72-3, National Environmental Research Corp., Contract 2 RO1-EC-00250-01, EPA, May 1972.

FLASH PYROLYSIS OF BIOMASS IN SWEDEN

C. Ekström, E. Rensfelt[+]
The Royal Institute of Technology
Dept. of Chemical Technology
S-100 44 Stockholm, Sweden

ABSTRACT

Biomass has been shown to be a very special raw material for gasification giving a high yield of volatiles and a low yield of char which is highly reactive. These properties are accentuated by flash pyrolysis, a high heating rate process. Char yield is still lower (10 % of m.a.f) and even more reactive. The char fraction after long residence time (final carbonization of flash char) is almost independent of the temperature between 650 and 1000°C. Depending on temperature, residence time and presence of a catalytic surface, the secondary gas reactions can yield anything between a syngas and a methane-rich and/or ethylene-rich medium-BTU-gas. Ethylene and methane are shown to be at least partly secondary products from thermal cracking of the tar fraction. The main part of the hydrocarbon liquids initially produced are rather easily converted even thermally to e.g. hydrocarbon gases and carbon black. A residual fraction of the tar (5 % on m.a.f. basis) needs some kind of a catalyst to be converted.

The paper describes the experimental apparatus and procedure used to investigate flash pyrolysis. Experimental results are presented together with a short commentry. Finally, the importance of these results for the process development of fuel gas, syngas and chemical feedstock are mentioned.

1. INTRODUCTION

Experimental studies on pyrolysis and gasification of peat, solid waste and biomass were initiated in late 1974 in Sweden at the Royal Institute of Technology. Experiments were conducted in small batch reactors with heating rates from 10 to 100°C/min. The pyrolysis reactions were found to be much faster than could be resolved by these heating rates (1). Information regarding the Garret (Occidental) Flash Pyrolysis Process (solid waste) and a Russian milled peat flash pyrolysis process lead to a dicision to investigate further the rapid-rate heating pyrolysis (1976) (2), (3). In (1977) studies on secondary tar conversion were initiated, to investigate both the production of ethylene thermally and syngas and fuel gas catalytically (4), (5), (6).

This paper presents the basic experimental methods and apparatus used

[+]Present address: Studsvik Energiteknik AB,
Dept. for Chemistry and Environment
Environmental Chemistry
S-611 82 Nyköping, Sweden

together with the results mainly pertaining wood. Results for peat and solid waste have to some extent been published wlsewhere (1), (6), (7).

2. EXPERIMENTAL APPARATUS

The flash pyrolysis apparatus is shown in Figure 1. The powdered fuel (particle size normally less than 0.6 mm) is fed continuously by the screw feeder and falls through the electrically heated reactor tube (500-1000°C). The char particles then fall into the char hopper under the reactor, while the finer char particles are separated by the cyclone and the dust filter. The liquid products condense in the tar condenser and the tar water condenser after which the tarry aerosol is retained in the cotton filter. The amounts of outlet gas is measured by the gas meter. Gas samples, which are taken after the cotton filter, are first completely dried using a drying agent before being analyzed using a gas chromatograph.

The fuel throughput range is approximately 0.1 to 0.5 kg dry fuel/hour. Experiments have shown the limit where increased throughput results in a decrease in the thermal decomposition of the fuel (4-7 g/m^2,s related to the heated reactor surface). Results from Russian experiments with flash pyrolysis of peat also indicate a limit in the same order of magnitude (3).

Normally nitrogen is used as carrier gas but other gases and/or steam can also be used. Although not normally done, the carrier gas stream not passing the screw feeder can be preheated. The total carrier gas flow varies between approximately 5 and 65 ml/s at STP (5 ml/s through the feeder).

In order to achieve a flow without too much pulsation, a vibrating screw feeder is used. A tube parallel to the screw, ensures equalization of pressure in the fule hopper and the rest of the system in case of pressure fluctuation.

The vibrations from the screw feeder are damped by a bellow immediately after the screw. The tube section before the reactor is cooled by air in order to keep a reasonably low temperature above the reactor entrance.

The reactor consists of a replaceable inconel 600 tube (in some experiments a quartz tube) with an inner diameter of 2 cm and a heated length of 1 m. It is heated electrically by eleven individually controlled kanthal spirals wound round a quartz tube surrounding the reactor tube. The temperature profile inside the reactor is measured by a chromel-alumel thermocouple, adjustable to any height.

The residence time for a given particle size (the maximum speed relative the gas stream is very much dependent upon particle size) can be varied over a wide range by combining two methods:

1. Using different carrier gas flows.
2. Varying the heated length of the reactor.

Experimental Apparatus

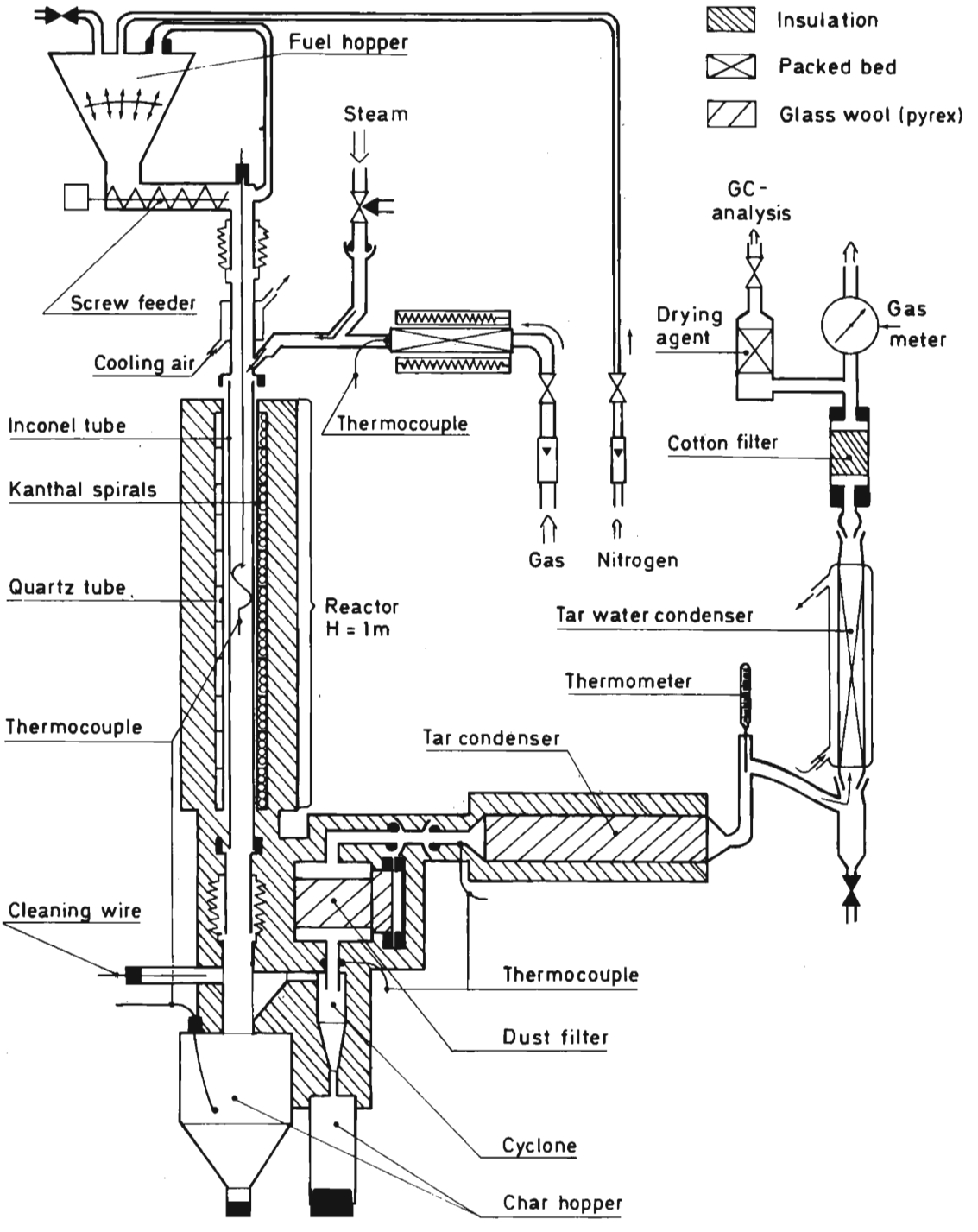

Figure 1

The thermal expansion of the reactor tube is taken up by a bellow before the char separating system. The above described reactor oven has been used since summer 1977. Previous to this, the oven consisted of six vertical kanthal spirals which only were controlled as a whole unit, i.e. the shape of the temperature profile and the heated length were unvariable.

The whole char separating system, except the char hoppers, is kept at 300-500°C by heating tapes in order to prevent condensation of the liquid products, and at the same time keeping the temperature well below the reactor temperature.

If blockage occures in the cyclone inlet, it can easily be removed during an experiment by using the moveable cleaning wire.

The above described char separating system has been used since 1978. In earlier experiments, e.g. those discussed below in paragraph 6, all products passed the cyclone, the unseparated dust being caught at the beginning of the tar condenser. This dust was removed and weighed separately after the experiments. With this system, however, bigger particles often gathered in the horizontal cyclone inlet if the carrier gas flow was too low to blow them into the cyclone.

All liquids are condensed in two steps, the tar condenser and the tar water condenser, after which tarry aerosol, that is always formed, is caught in the cotton filter. The first step, the tar condenser, is heated by heating tapes. The temperature at the inlet is kept between 300 and 500°C, and is then lowered along the condenser to 50-150°C at the outlet in order to achieve better separation between tar, carbon black and tar water. Also, experiments have shown that, if the tar condenser is heated as mentioned above, the amounts of aerosol is markedly reduced compared to if the tar condenser is not heated. A probable explanation is, that if the gas stream is cooled too rapidly the water starts to condense at the same time as the tar. This yields a very stable aerosol.

The tar condenser and the tar water condenser are filled with glass wool and ceramic fillers respectively.

In the experiments presented in paragraph 5.1.2 the condensing system was moved and a second vertical reactor for further conversion of the gas phase (i.e. both gases and liquids at room temperature) was connected between the dust filter and the tar condenser. This reactor had a quartz tube with a heated length of 1.1 m and an inner diameter of 3 cm. It was heated by an oven similar to the pyrolysis oven but with 12 individually controlled kanthal spirals.

Gas samples could in this case also be taken between the dust filter and this second reactor.

3. EXPERIMENTAL PROCEDURE AND CALCULATION OF RESULTS

Before an experiment, the fuel hopper is loaded with dried fuel (moisture content about 1.6 % for biomass, 1.4 % for peat and 0.5 % for

solid waste) and after that air in the fuel hopper is removed by nitrogen. The screw feeder is then calibrated. All ovens and heating tapes are heated to desired temperatures and the temperature profile in the reactor (and in the cracking reactor when that is being used) is measured. The carrier gas flow is measured by the gas meter.

An experiment is started by turning on the screw feeder. During experiment, the outlet gas amounts are continuously measured by the gas meter. Normally three gas samples are taken during one run (0.5-1 h) and analyzed for N_2, O_2, H_2, CO, CO_2, CH_4, C_2H_2, C_2H_4 and C_2H_6 contents. Also, the temperature profiles in the reactors are measured. The temperatures from all thermocouples are continuously recorded. During the experiments presented in paragraph 5.1.2 the temperature in the cracking reactor was adjusted to three levels while the pyrolysis reactor temperature was held constant. Then, one gas sample was taken after the cotton filter for each temperature level, and two gas samples were taken before the cracking reactor.

After the experiments, all separated char is taken and weighed; all tubes in the char separation system, the cyclone, the char hoppers and the reactor tube are brushed. The glass wool in the dust filter is weighed before and after a run. The total amount of liquid products is calculated from the weight differences between, before and after a run of all parts in the condensing system, including the cotton filter. It is not possible to achieve complete separation of the different components carbon black, tar and tar water. Therefore, the percentage contents of these components in the liquid phase are estimated visually for each condenser and the yields of each component is calculated from these estimates. They are therefore marked with dotted lines in Figure 4 and 5. The errors in these estimations are probably systematic, so it should be possible to compare the results from different runs.

The yields of gaseous products and the dry product gas composition are calculated from:

- Measured carrier gas flow before experiment
- Measured total gas flow during experiment
  It is assumed that this gas flow is saturated with water vapour, about 2 vol-% at room temperature
- The analyzed gas samples

The average nitrogen content in the dry gas samples is compared to the nitrogen content in the total dry gas flow during experiment calculated by comparing this with the measured carrier gas flow. The average between those two contents, or the one with the believed lowest experimental error, is then used for further calculations.

The total yield of all products, i.e. char, liquids and gases, is compared to the total fuel feed calculated from the calibration of the screw feeder. The total product yield is normally 90-100 % of the total fuel feed.

The temperature referred to as the reactor temperature is the estimated average temperature 80 cm from the reactor inlet (with maximum heated

reactor length) during a run. Depending on the shape of the temperature profile, it is sometimes adjusted up to 10°C. Examples of temperature profiles, see Figure 2. (In the experiments discussed in paragraph 6 with the old reactor oven, see paragraph 1, the shape of the temperature profile was somewhat different and therefore the average temperature 70 cm from the reactor inlet was used).

The solids residence time is calculated from the gas velocity in the reactor and the maximum speed of the particles relative the gas, which in turn is calculated from particle and gas data. For these calculations, the reactor is roughly divided into three zones based on the temperature profile:

Zone 1: The temperature increases from 100°C to the reactor temperature. The residence time in this zone was 0.1-0.3 seconds for biomass particles between 0.4 and 0.6 mm.

Zone 2: Constant reactor temperature. The length of this zone was varied between different runs, which resulted in residence times from 0.04 to 1.4 seconds.

Zone 3: Temperature decreases from reactor temperature to 400-500°C at reactor exit. Residence time was 0.1 to 0.3 seconds.

The used residence time is defined as the total residence time in these three zones. In Figure 2 the temperature profiles for five of the experiments presented in Figure 4 are shown, together with number of heated kanthal spirals, carrier gas flows and the resulting residence times of the solids. The residence time decreases rapidly with increased solid particle size, and this limits the maximum particle size that can be used.

4. REACTIONS INSIDE THE CHAR PARTICLES

4.1 Results

Results from pyrolysis of wood at different heating rates are shown in Figure 3. It can be seen that flash pyrolysis (heating rate in the order of 1000°C/s) at temperatures above 600°C results in less char than pyrolysis with low heating rates (20°C/min). It can also be seen that the amount of char after final carbonization is almost temperature independent above approximately 650°C.

The weight loss by flash pyrolysis of wood at different solids residence times are shown in Figure 4. At a final temperature of 760-775°C the necessary residence time for complete devolatilization is little more than 1 s.

Char from flash pyrolysis has been heated slowly (20-50°C/min) to the same final temperature as with flash pyrolysis and held there for 15 min (Figure 4) and 20-60 min (Figure 3) respectively. Other experiments

Examples of temperature profiles

Number of heated elements	Carrier gas flow ml N_2/s STP	Solids residense time, s
▽ 11	4.7	1.17
○ 11	17,7	1.04
□ 11 *	41.4	0.82
● 5	16.9	0.71
■ 2	17.2	0.41

*One oven element broken

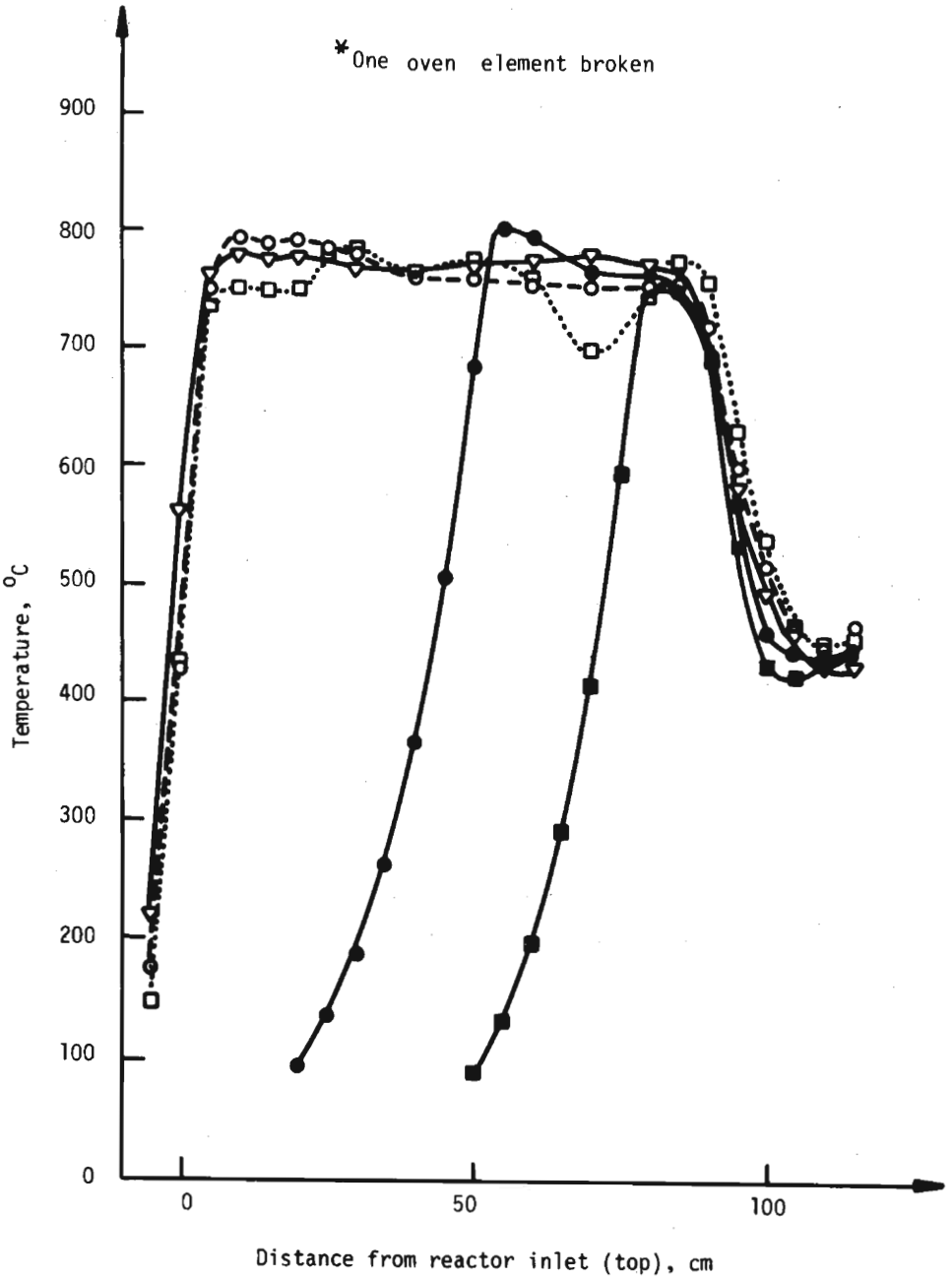

Figure 2

Pyrolysis of poplar wood at different heating rates and temperatures

Particle size: 0.4 - 0.5 mm

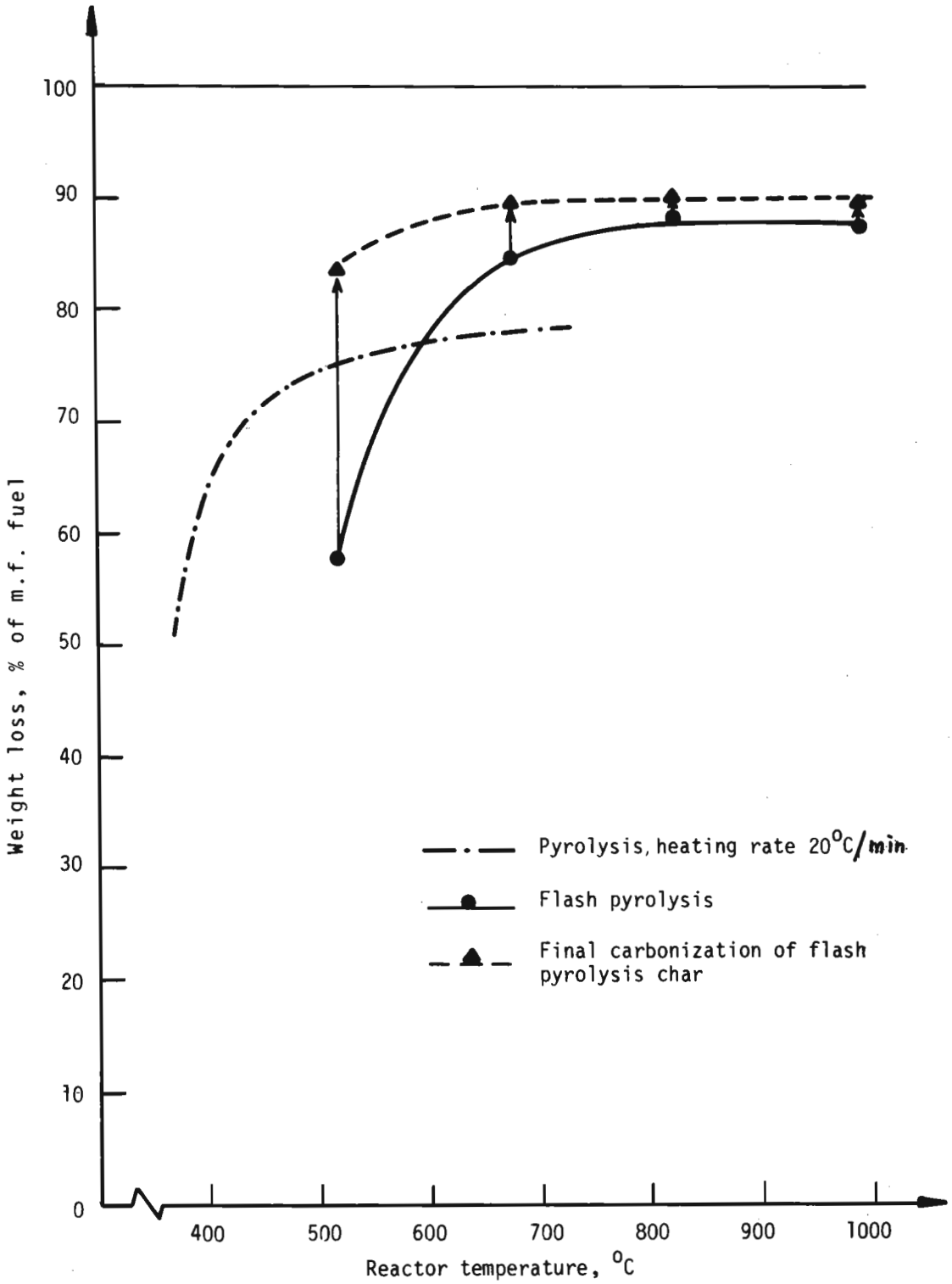

Figure 3

Flash pyrolysis of Salix Q 701-2
at different residence times

Particle size: 0.5 - 0.6 mm
Pyrolysis temperature: 760 - 775 °C

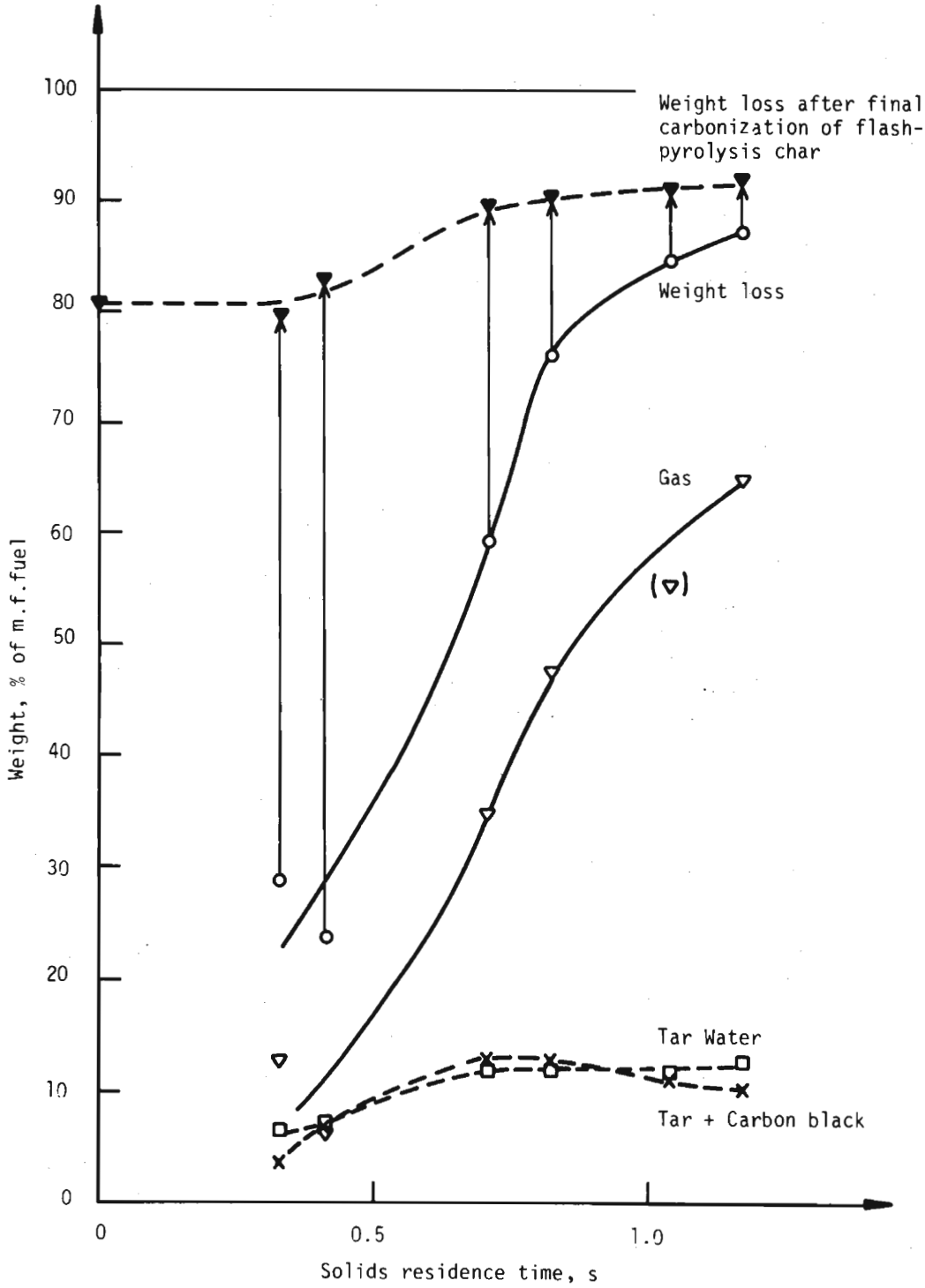

Figure 4

have shown that this final devolatilization is completed in less than 10 min.

The results in Figure 3 and 4 show that high heating rate, i.e. flash-pyrolysis, gives less char than low heating rate, over the whole investigated temperature range providing that the residence time at the final temperature is long enough for complete devolatilization. From Figure 4 it can be seen that, for flash pyrolysis, the char yield after complete devolatilization is nearly constant for residence times longer than 0.7 s in the flash pyrolysis reactor. This may be the time necessary for the particles to reach the final temperature and for the primary reactions to be completed.

Experiments with steam-gasification of char, has shown that char from flash pyrolysis is much more reactive than char from pyrolysis with low heating rate (2-3 times higher reaction rate at a given temperature). This char property is related to the chemical char structure and not to physical properties like surface area (9).

4.2 Discussion

The markedly reduced char yields from flash pyrolysis with final devolatilization of the char compared to the char yields from pyrolysis with low heating rate can be explained by the theory presented by Shafizadeh and Brunner (10), (11). At low temperature (< 300°C) slow dehydration of cellulose takes place producing a product, which is more stable than cellulose against the fast depolymerization to primary volatiles, occuring at higher temperatures. High heating rates provide shorter time for the dehydration to take place than low heating rates, which results in a more unstable material left for depolymerization to primary volatiles and therefore lower final char yields.

The char yield is also dependent on the mass transfer of primary volatiles out of the char (12). Very slow escape of volatiles (for example big particles) especially at low temperatures results in secondary charring reactions.

The primary pyrolysis reaction leads in all cases to char as one product in the range of experimental parameters that we have studied. Particle size distribution and macro structure of the wood feed is reflected in the properties of the produced char.

The very strong temperature dependence of the char yield from flash-pyrolysis (Figure 3) at temperatures below 750°C is probably a kinetic effect. Above 750°C, the solids residence time in the flash pyrolysis reactor is enough for almost complete devolatilization, i.e. the temperature dependence on the reaction rate at higher temperatures could not be seen in these experiments.

Such a strong dependence on temperature for the necessary time for complete pyrolysis has also been shown by Shafizadeh at temperatures between 300 and 425°C (10).

Flash pyrolysis of poplar wood
Composition of product gas at different reactor temperatures

Particle size: 0.4 - 0.5 mm

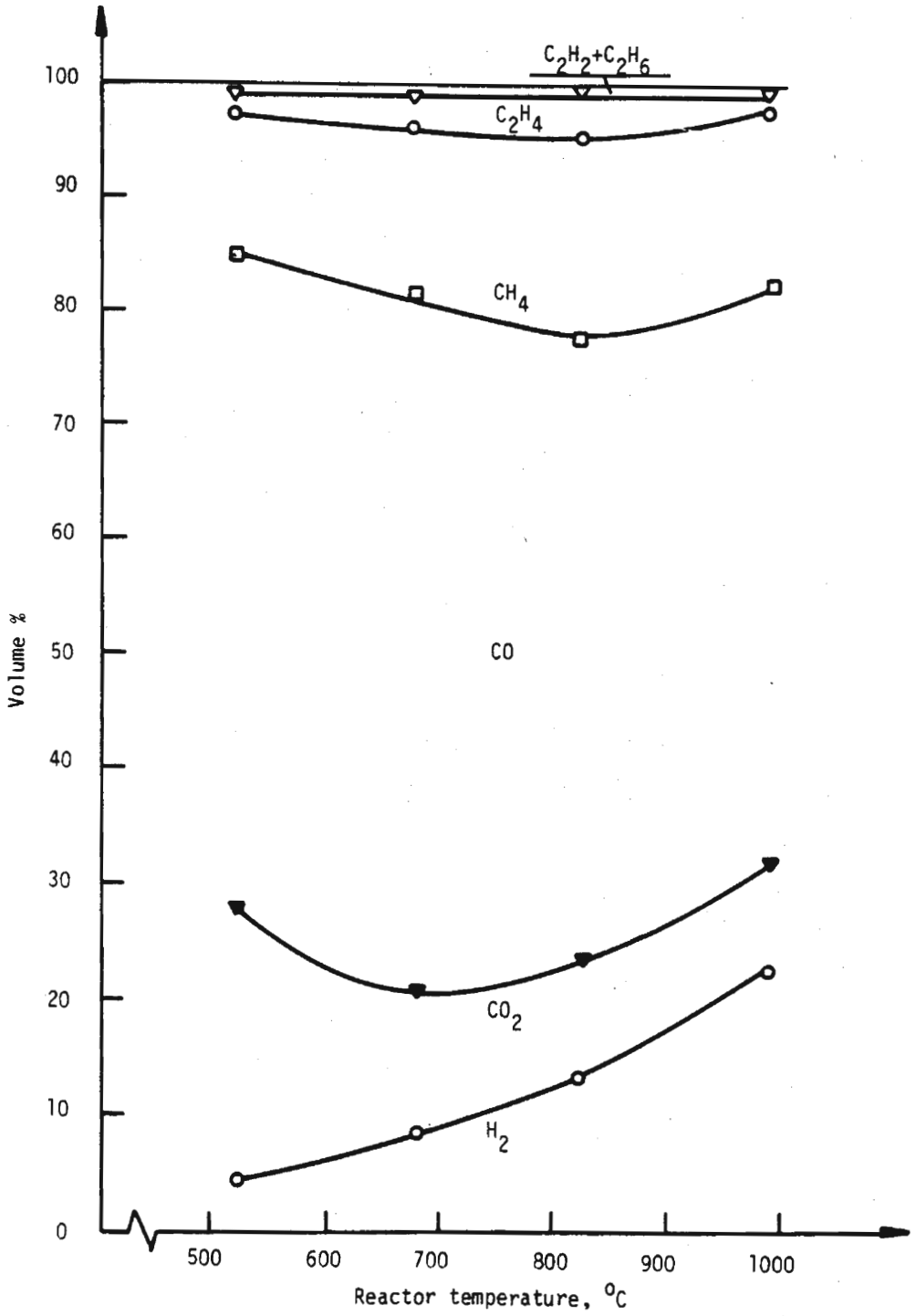

Figure 7

Flash pyrolysis of poplar wood
Gas production at different reactor temperatures

Particle size: 0.4 - 0.5 mm

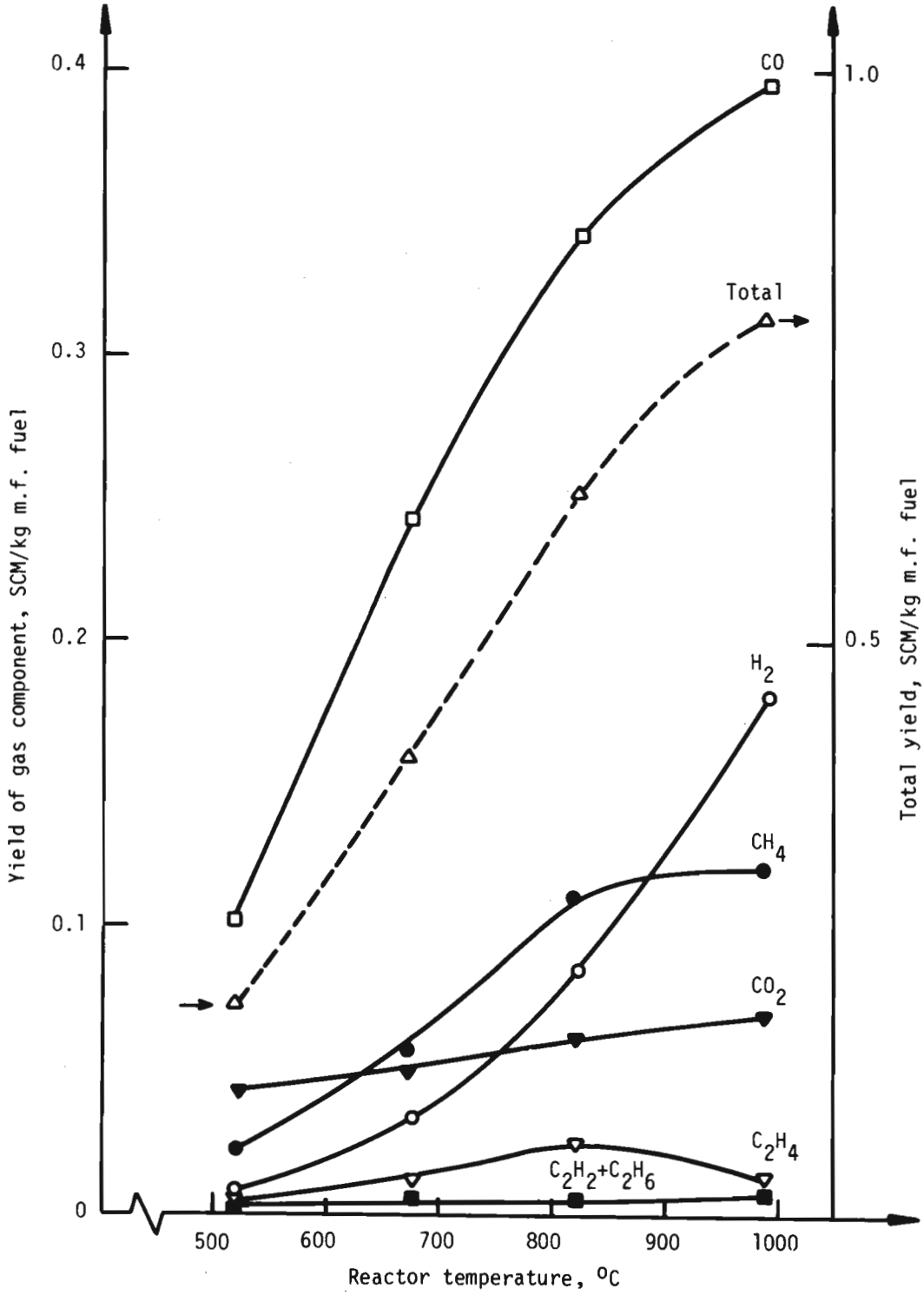

Figure 6

It should be observed that our results do not show whether the chemical reaction or the heat and mass transfer inside the particles is the rate-determining step.

5. SECONDARY GAS PHASE REACTIONS

5.1 Results

5.1.1 Flash Pyrolysis Experiments

The yields of volatiles at different solids residence times when pyrolyzing wood at 760-775°C are shown in Figure 4. A slight maximum yield of tar + carbon black (carbon black is formed in the gas phase at higher temperatures, see part 5.2.3) is found after 0.7-0.8 s.

The product distributions at different reactor temperatures are shown in Figure 5. The total yield of the liquid fraction by flash pyrolysis is about half that of the "primarily" produced liquids (1). This corresponds to a much higher and with temperature rapidly increasing gas yield.

The production of different gases as a function of reactor temperature for biomass is shown in Figure 6. The CO_2-yield is nearly constant in the measured temperature range and the CH_4-yield does not increase markedly above a temperature of 850°C. The C_2H_4-yield is maximized between 800 and 850°C for all investigated fuels.

The product gas composition at different reactor temperatures is shown in Figure 7. The gas composition is far from that corresponding to thermodynamic equilibrium for the two reactions:

$$CO + H_2O \rightleftharpoons CO_2 + H_2$$
$$CH_4 + H_2O \rightleftharpoons CO + 3H_2$$

In order to reach thermodynamic equilibrium, both CO and CH_4 should react with some of the pyrogenetic water. The high content of hydrocarbons give the product gas a relatively high heating value (3300 to 4200 kcal/SCM).

5.1.2 Flash Pyrolysis followed by Further Conversion of the Gas Phase

In these experiments the gas phase from the flash pyrolysis reactor passed a second cracking reactor after the char had been separated (see end of paragraph 2).

The results for different conditions are shown in Figure 8, 9 and 10. The temperature in the pyrolysis reactor was held constant while the temperature in the cracking reactor was varied between 500°C and 950°C in each experiment. Results with pyrolysis temperatures between 521°C and 913°C are presented. As the conditions varied during one experiment, only products that could be measured continuously, i.e. the gas (gas at room temperature) could be used for calculating the results. Gas samples were taken before the cracking reactor and after the liquid condensing

Flash pyrolysis of poplar wood
Product distribution at different reactor temperature

Particle size: 0.4 - 0.5 mm

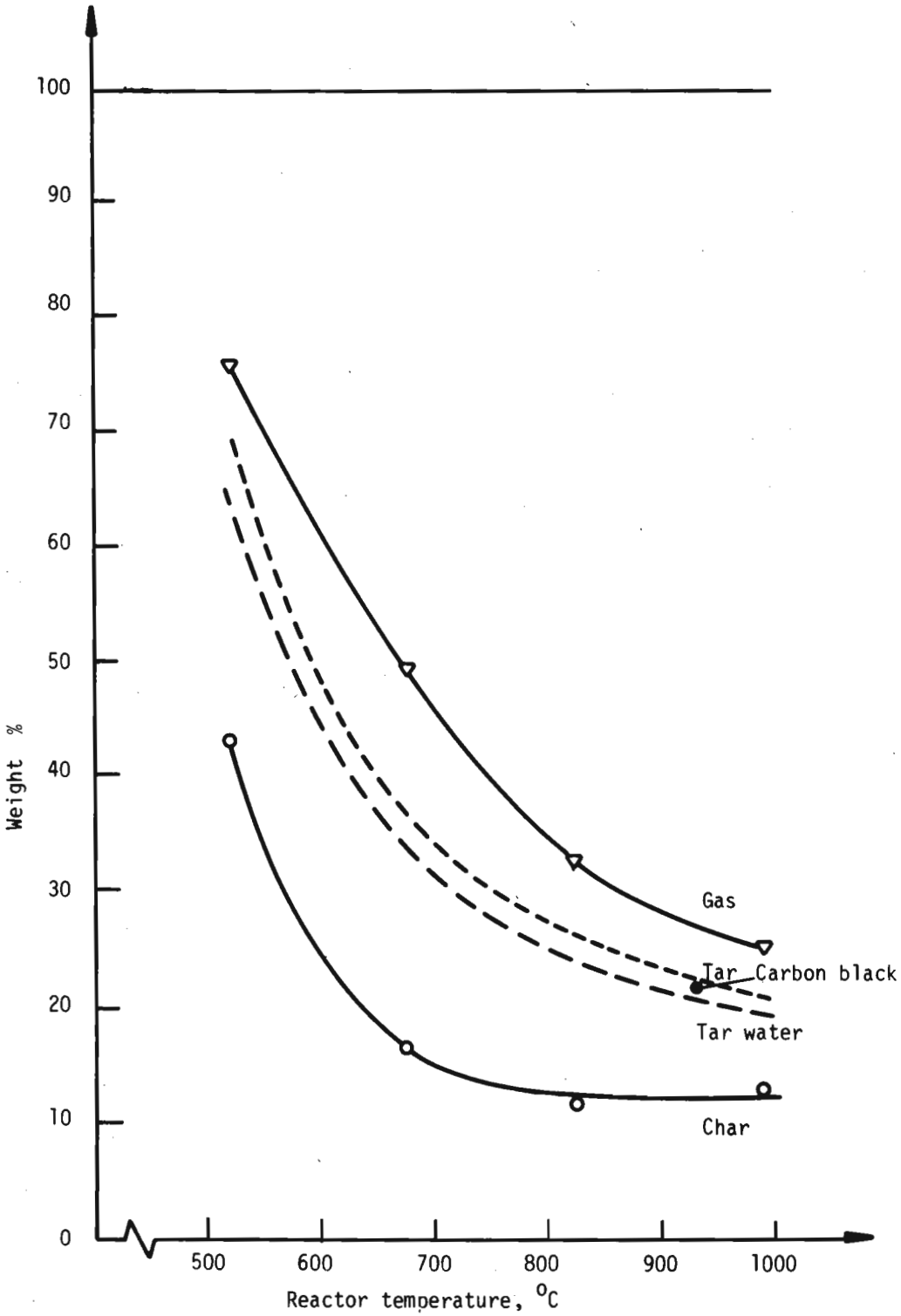

Figure 5

system. The only way to see if an increase in gas yield came from tar and carbon black, and not from reactions between gases and pyrogenetic water, was to calculate and compare the C-content in the product gas from different conditions.

As can be seen in Figure 8, a small part of the tar and/or carbon black from flash pyrolysis has been cracked, but that part increases, when the temperature in the cracking reactor increases. Cracking at lower or at the same temperature as in the flash pyrolysis reactor results only in small reduction of the tar and/or carbon black yield.

The production of methane and ethylene is shown in Figure 9 and 10 respectively. A higher gas phase temperature than in the flash pyrolysis reactor, after separation of the char, results in increased production of both methane and ethylene. For ethylene, there is a maximum yield at about 700°C, except for cracking after flash pyrolysis at low temperature (521-542°C).

The product gas composition at a given temperature in the cracking reactor was similar to the gas composition only after flash pyrolysis at the same temperature, i.e. the gas was still far from thermodynamic equilibrium.

5.2 Discussion

The volatiles that have escaped from the char can undergo further secondary reactions in the gas phase to form different hydrocarbons, hydrogen, carbonoxides and carbon black. The results presented above clearly show that the rate at which primary volatiles are converted increases markedly with increased temperature, especially above 500°C. This has also been shown by Antal (14), (16) and Shafizadeh (10) for cellulose. Antal has also shown that steam reforming reactions probably do not dominate the secondary reactions.

When discussing results from pyrolysis experiments, it is important to separate the influence of:

a) Heating rate
b) Solids residence time
c) Gas phase residence time

5.2.1 Thermal Cracking of Tar

As already mentioned the total yield of liquid products from flash-pyrolysis is about half as much as that from pyrolysis with low heating rate. In the latter case, volatiles formed at temperatures below 500°C have time to leave the reactor without being further heated, i.e. undergoing a minimum of secondary gas phase reactions, while in the co-current flash pyrolysis reactor, all the volatiles have to pass the hotest zone where they can undergo secondary reactions. An experiment with flash-pyrolysis of solid waste at about 500°C, i.e. too low temperature for rapid thermal cracking, also gave rather high yields of tar (about 30%). These results are similar to those from the Occidental Flash Pyrolysis Process (2), (17).

Flash pyrolysis followed by thermal cracking
Carbon content in product gas

Fuel: Poplar wood
Particle size: 0.13 - 0.40 mm
Filled dots: Flash pyrolysis 1 - 2 s

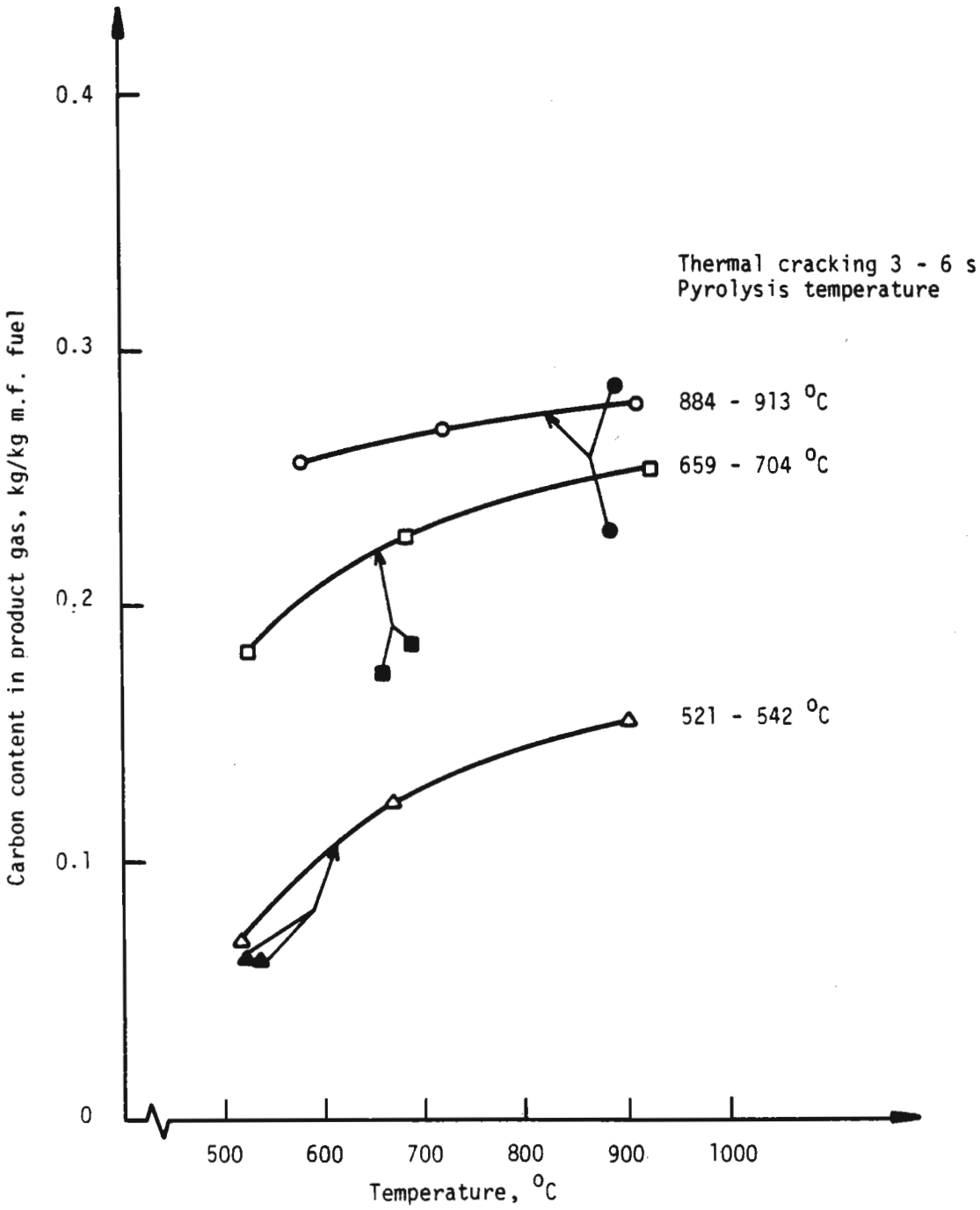

Figure 8

Flash pyrolysis followed by thermal cracking
Methane production

Fuel and legend same as in figure 8

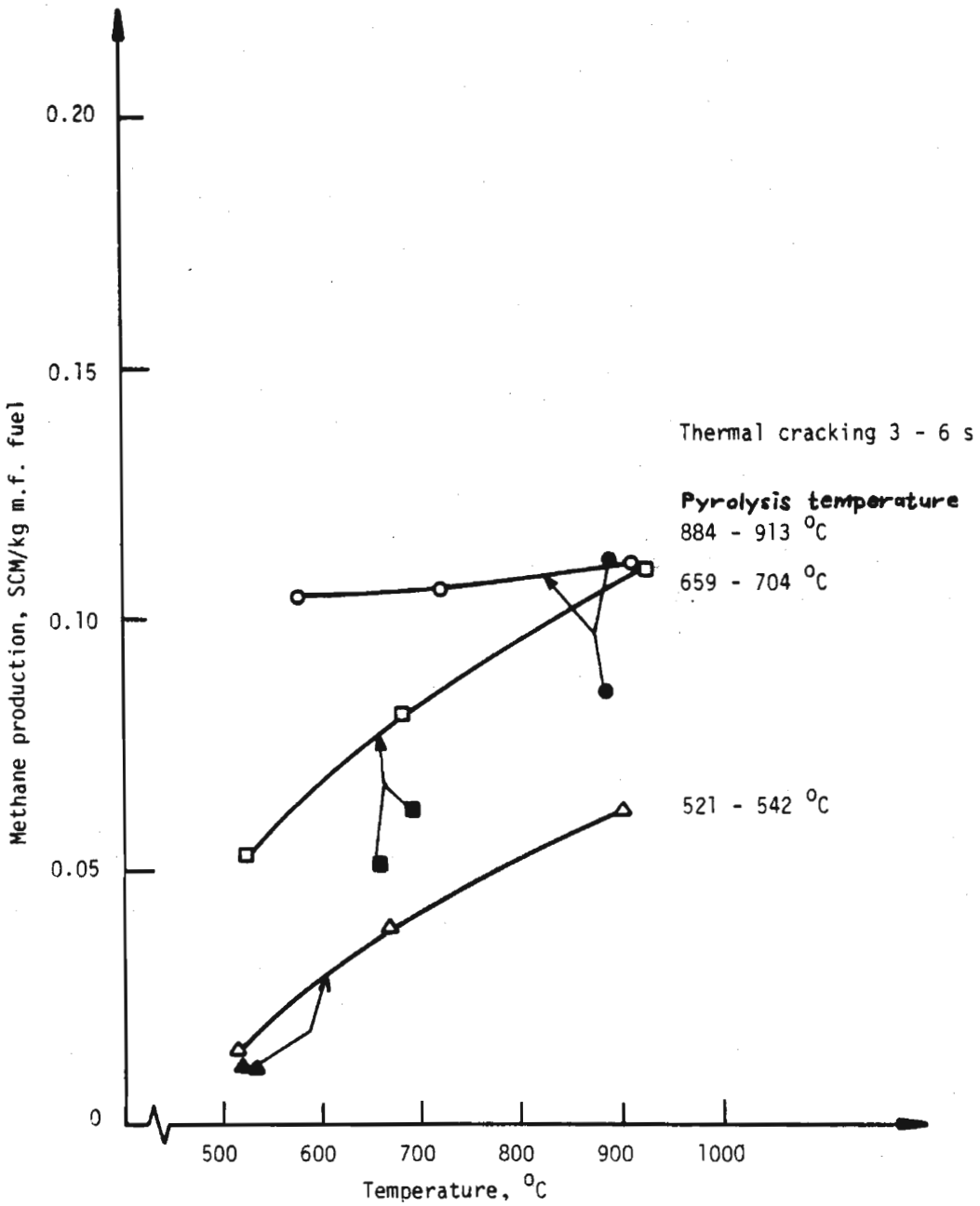

Figure 9

Flash pyrolysis followd by thermal cracking
Ethylene production
Fuel and legend same as in figure 8

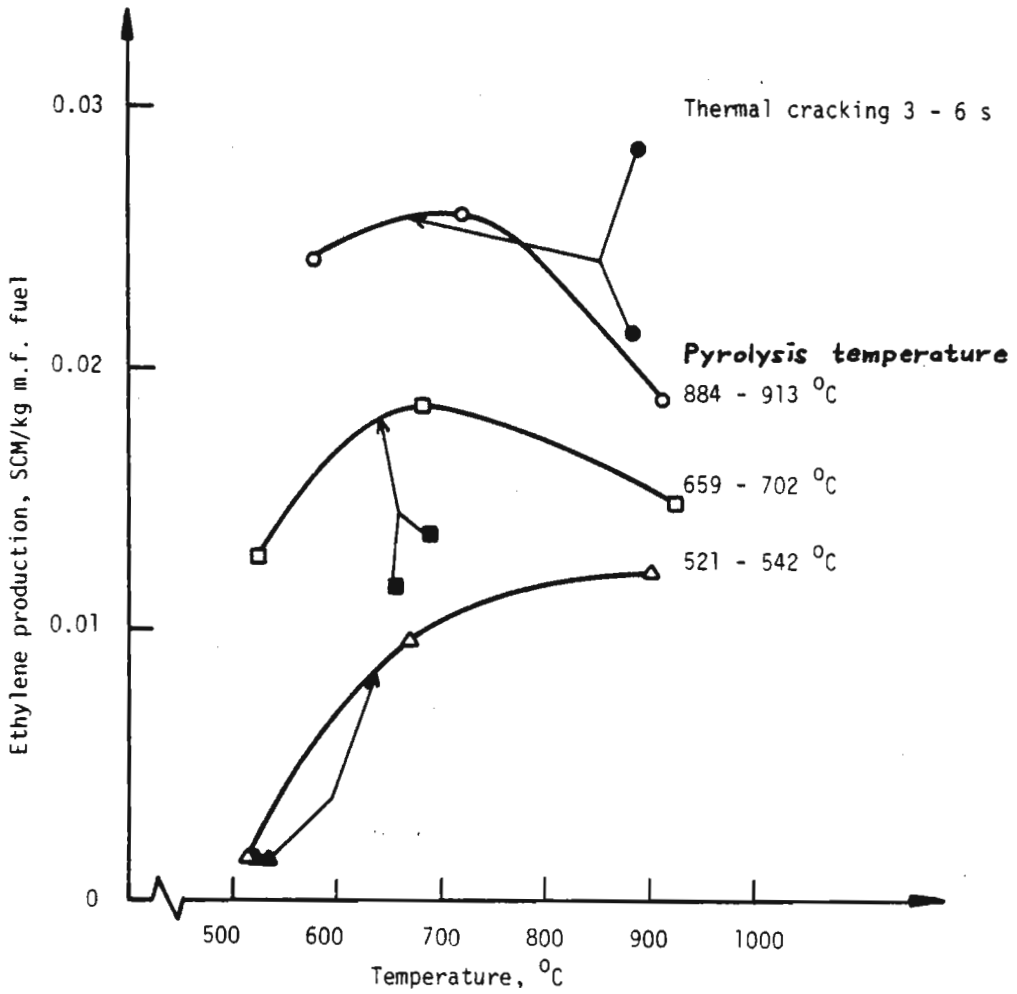

Figure 10

However, for wood, the tar yield is rather low after flash pyrolysis at 500°C (about 12 %). As can be seen in Figure 3 and 5, the total yield of volatiles after flash pyrolysis also is rather low at 500°C, and increases markedly with increased temperature up to 750°C. As mentioned before, the rate of thermal cracking of tar increases markedly with temperature, and these effects together makes the tar yield for biomass rather constant over a wide temperature range. At high temperatures (above 750°C) both the rate of primary pyrolysis and the rate of thermal cracking are rather high. As can be seen in Figure 4, almost complete devolatilization is achieved after 1 s, and the parallel rapid thermal cracking of the tar and devolatilization of the fuel results in only a slight maximum in total yield of tar and carbon black after 0.7-0.8 s.

The results presented in paragraph 5.1.2 show, that the remaining tar after flash pyrolysis does not undergo considerable thermal cracking if the gas phase pass a second oven at the some or somewhat lower temperature than in the flash pyrolysis reactor. Also, the amounts of tar left after Antal's pyrolysis experiments with low heating rate, followed by thermal cracking, were similar to those found after flash pyrolysis (14), (16).

The above mentioned indicates that only some of the hydrocarbons in the tar can undergo rapid thermal cracking (below 950°C), while the others decompose very slowly. Experiments has shown that these last mentioned hydrocarbons, and also carbon black, can be converted by catalytic steam reforming (4), (5), (6).

5.2.2 Formation and Breakdown of Lower Hydrocarbons

The results presented in paragraph 5.1.2 show that a great deal of the methane and ethylene from flash pyrolysis is formed in the gas phase by thermal cracking of tar. This has also been shown by Antal (14). The rate of breakdown of C_2H_4 and other unsaturated hydrocarbons increases markedly with temperature and partial pressure (13), (14), (15) which explains the maximum yields of ethylene at 700°C for flash pyrolysis followed by thermal cracking and 800-850°C for flash pyrolysis only. It also increases in presence of pyrolyzing biomass (15).

Diebold et.al have also shown, that the ethylene yield can be raised by increased dilution of the gas phase (resulting in lower partial pressure)(18).

The results in paragraph 5.1.2 also show, that increased temperature in the pyrolysis reactor results in increased yield of methane and ethylene after the thermal cracking step. This indicates, that the yield of primary tar, from which those hydrocarbons are formed, increases with increased pyrolysis temperature, or that high heating rates result in the formation of methane and ethylene directly from the solid phase.

5.2.3 Formation of Carbon Black

Experiments with flash pyrolysis of peat and solid waste show that carbon black is formed in the gas phase from hydrocarbons in the tar (1), (6). When pyrolyzing wood, it is formed at all temperatures above

500°C, but for peat and solid waste it is formed first above 750°C and 600°C respectively. According to Lavrov (19) and Berezina and Magaril (20) soot is formed from different hydrocarbons with benzpyrene as an important intermediate.

It should be observed that carbon black is formed in the gas phase at high temperatures and is condensated together with the tar. This is not the case for char produced by secondary charring reactions, which occure inside the char and at low temperatures. See paragraph 4.2.

6. COMPARISON OF WOOD, SOLID WASTE AND PEAT

Flash pyrolysis of all these fuels give principally the same products, and they also seem to undergo the same reactions, although the yields of the products differ.

The char yields after final carbonization of wood and the combustible part of solid waste are nearly the same, a little more than 10 % of m.f. and m.a.f. fuel respectively above 650°C. For low moor peat it is much higher, 30-35 % of m.f. peat (1), (6). It is very interesting to notice that the reduction in char yield due to high heating rate tends to be 8-10 % on a m.a.f. basis for all fuels investigated. That means a 50 % reduction in char yield for wood and solid waste but only 20 % for peat.

The total yield of liquid products do not differ much between wood and peat, about 35 % and 30 % respectively at 600°C and about 13 % for both fuels at 1000°C. Solid waste give higher yields, about 45 % at 600°C and about 30 % at 1000°C. A great deal of this difference is due to the much higher yield of pyrogenetic water for solid waste.

Consequently, the product gas yield is much higher for wood than for peat, and especially for biomass it increases markedly with increased temperature. For solid waste the gas yield is about the same as for peat, but it reaches its maximum at a lower temperature, about 800°C.

Although the gas yields differ for the investigated fuels the composition of the product gas are very similar. For wood the CO-content in the dry product gas is higher and the H_2-content is lower than for peat and solid waste. Also, the maximum content of C_2H_4 is about twice as much for solid waste and peat as for wood. The high hydrocarbon content for all fuels result in rather high heating values of the product gas.

7. POTENTIAL USES FOR FLASH PYROLYSIS

7.1 Chemical Feedstock - Ethylene

In a special study attempts were made to optimize the ethylene yield from flash pyrolysis. A maximum of 4 weight % ethylene on a m.a.f. basis was achieved (15). As mentioned in paragraph 5.2.2 the reaction rate for the breakdown of ethylene increases with temperature and is also higher in presence of pyrolyzing biomass. As has been seen above, the

yield of volatiles is independent of temperature above 650°C (with long particle residence time, Figure 3) and the ethylene is to a large extent a secondary product from volatiles. This means that further studies should be directed towards processes with a primary step with high heating rate and long residence time for particles but short residence time for gases and a moderate temperature (600°C). A fast fluidized bed is one example of this reactor type. The secondary step after high temperature removal of fly ash can be fully optimized regarding temperature and residence time for maximum ethylene yield. The important questions regarding suitable methods for introducing heat to both these steps have not yet been closely investigated. Some factors indicate that indirect heating is most interesting:

a) Steam crackers for ethylene production operates at atmospheric pressure, and the secondary step in a plant for making ethylene from solid fuels would be rather similar to a conventional unit.

b) The extremely low temperature (600°C) at which heat has to be supplied to the primary gasifier.

7.2 Medium-BTU Gas

Production of syngas and fuel gas can also utilize flash pyrolysis as an important step. Low exit temperature and a very rich medium-BTU gas is possible by combining concurrent fluid bed gasification, high temperature dust removal and suitable catalyst for product gas adjustment. Such processes have been presented lately and a PDU will be built in Sweden (6), (21). System studies on the wood to methanol process have indicated that oxygen blown processes are superior to airblown/indirect heat transfer processes (21). Fuel gas production with indirect heating might be interesting due to the smaller scale and the lower reactor temperature.

ACKNOWLEDGEMENT

The authors are indepted to Professor Olle Lindström, by whom this research work was initiated, for his many helpful suggestions and encourageing support. Grant support from Swedish National Board for Energy Source Development and Swedish Board for Technical Development are gratefully acknowledged.

REFERENCES

1. Rensfelt, E. et al., "Basic Gasification Studies for Development of Biomass Medium-Btu Gasification Processes", IGT-Conference on Energy from Biomass and Wastes, Washington, D.C. (1978).

2. Levy, S.J., "San Diego County Demonstrates Pyrolysis of Solid Waste", Environmental Protection Publication SW-80d.2, US Government Printing Office, Washington, D.C. (1975).

3. Reprintseva, S.M., "An Experimental Investigation of the Thermal Dissociation of Milled Peat Using Radiant Heating", The Thermal Dissociation of Dispersed Solid Fuels, Nauka Technika, Minsk (1965).

4. Marklund, A., Olsson, S., "Katalytisk Krackning av Pyrolystjära", KT-77-02-01, The Royal Institute of Technology, Dept. of Chemical Technology, Stockholm (1977).

5. Ekström, C., Espenäs, B-G., "Termisk krackning och katalytisk ångreformering av pyrolystjära från biomassa", KTU 80-23, The Royal Institute of Technology, Dept. of Chemical Technology, Stockholm (1980).

6. Rensfelt, E., et.al., "New Possibilities for Gasification of Peat at Low Temperature", 6th International Peat Congress, IPS, Duluth, Minnesota (1980).

7. Lindman, N., "Gasification Research at the Royal Institute of Technology, Stockholm, Sweden", 11th Biomass Thermochemical Conversion Contractors Meeting, U.S. DOE, Richland, Washington (1980).

8. Gavriltshik, Je.I., et.al., "Pyrolysis of Peat Bertinate during Shorttime Thermolysis", Torf.Prom. No 9 (1972), p.p.19-23 (In Finish).

9. Blomkvist, G., et.al., "Investigation into Factors Affecting the Reactivity of Peat Char", 6th International Peat Congress, IPS, Duluth, Minnesota (1980).

10. Shafizadeh, F., "Utilization of Biomass by Pyrolytic Methods", TAPPI Forest Biol./Wood Chem. Conf., Madison (1977), p.p. 191-199.

11. Brunner, P., "Examination of the Pyrolysis of Cellulose for the Production of Activated Carbon from Wastes", ISWA Information Bulletine No 23 (1977), p.p. 2-11.

12. Lewellen, P.C., Peters, W.A., Howard, J.B., "Cellulose Pyrolysis Kinetics and Char Formation Mechanism", Fire and Explosion Research: 16th Symp. on Combustion, The Combustion Institute (1976), p.p. 1471-80.

13. Huffman, W.J., et al., "Ammonia Synthesis Gas and Petrochemicals from Cattle Feedlot Manure", Clean Fuels From Biomass and Wastes Symp. Papers, Orlando, Florida (1977), p.p. 249-278.

14. Antal, M.J., "The Effects of Residence Time, Temperature and Pressure on the Steam Gasification of Biomass", Symp. on Biomass as a Non-Fossil Fuel Source, American Chemical Society, Honolulu (1979).

15. Lindström, L., et al., "Eten via flash-pyrolys av trä - en experimentall studie", KTU 78-40, The Royal Institute of Technology, Dept. of Chemical Technology, Stockholm (1978).

16. Antal, M.J., "Synthesis Gas Production from Organic Wastes by Pyrolysis/Steam Reforming", IGT-Conference on Energy from Biomass and Wastes, Washington, D.C. (1978).

17. Preston, G.T., "Resource Recovery and Flash Pyrolysis of Municipal Refuse", Waste Age, May (1976), p.p. 83-98.

18. Diebold, J., Smith, G., "Conversion of Trash to Gasoline", NWC Technical Publication 6022, Naval Weapons Center, China Lake, California (1978).

19. Lavrov, I.V., "Some Questions of the Theory of the Pyrolysis of Methane and Possible Mechanisms of the Formation of Soot", Khimiya Tverdogo Topliva, Vol. 10, No. 2 (1976), p.p. 100-107.

20. Berezina, Z.N., Magaril, R.Z., "The Formation of Pyrocarbon in the Pyrolysis of Individual Hydrocarbons", Khimiya Tverdogo Topliva, Vol. 11, No. 5 (1977), p.p. 156-159.

21. Waldheim, L., Rensfelt, E., "Development of a Swedish Biomass Gasifier for Synthesis Gas Production", 11th Biomass Thermochemical Conversion Contractors Meeting, U.S. DOE, Richland, Washington (1980).

CYCLONE REACTOR FOR FLASH PYROLYSIS OF SOLID PARTICLES
Application to the fast pyrolysis of wood by use of solar energy.

J. LEDE, F. VERZARO, B. ANTOINE and J. VILLERMAUX
Laboratoire des Sciences du Génie Chimique
(Chemical Engineering Science Laboratory)
CNRS-ENSIC, 1, rue Grandville 54042 NANCY FRANCE

ABSTRACT

The purpose of the present paper is to present the results obtained on the study of a continuous reactor suitable for fast pyrolysis of biomass (wood particles). The cyclone, the advantages of which are underlined, seems to be one the most adapted device for reactions occuring in less than 1 second. The results presented are relative to theoretical and experimental investigations concerning chemical reaction, residence time distribution of carrier gas and solid particles, heat transfer processes and study of the competition between chemical process and conduction of heat within the reacting solid. The correlations deduced from these studies are used for the calculation of the characteristics of a fast pyrolysis cyclone reactor capable to operate in a solar concentrator of a given power.

INTRODUCTION

A possible solution to the present problems of energy is to produce synthetic fuels from biomass and particularly from wood. Different routes can be followed for energetic valorization of wood : combustion, gasification (with air or O_2), pyrolysis (slow and fast), hydrolysis, fermentation and liquefaction. Among the thermal processes, fast pyrolysis is deserving attention because of the large yield of gases evolved, tar and char production being minimized by fast heating. The evolved gas has a higher heating value than in the case of usual gasification. It contains large percentages of CO and H_2 and appreciable amounts of hydrocarbons such as C_2H_4 and C_2H_2.

Gasification and fast pyrolysis reactions are endothermic and a source of heat is required. Heat can be produced by the combustion of a part of the wood feedstock (usual gasifiers), of an external fuel or of a part of the reaction products. Use of concentrated solar energy would bring the following advantages :

. Saving of biomass (up to 30 %), the entire feedstock being used for the reaction itself

. Saving the cost of an oxygen unit

. Gas evolved not diluted in N_2 and CO_2

. Very clean source of energy

. The focal volume is a region of high concentration of energy : these are ideal conditions to ensure high heat flux at the wood surface (fast pyrolysis conditions). Moreover, each gaseous molecule evolved, immediately penetrates into a cold non absorbing gaseous medium : these are favorable conditions for quenching of products.

. The energy evolved by combustion of the products represents the sum of the solar energy stored during photosynthesis (formation of biomass) and during the endothermic reaction (in the solar concentrator).

Our purpose is to study a new type of reactor for solar fast pyrolysis of wood.

PROGRAMM OF THE STUDY

The problem will be examined with a chemical engineering approach as follows :

. Research of the principal characteristics of the chemical reaction itself

. Selection of the type of reactor suitable for the reaction

. Hydrodynamic studies (residence time measurements for carrier gas and solid)

. Studies of heat transfer processes in the reactor

. Theoretical and experimental investigation of competition between heat transfer and chemical processes at the particle level.

. Prediction of the possible performances of a cyclone reactor operating in a given solar furnace.

PRINCIPAL DATA CONCERNING THE CHEMICAL REACTION

1. Analysis of gaseous products

The results of preliminary experiments have been published elsewhere [1,2]. These experiments have been carried out with Douglas fir and beech sawdust samples in discontinuous operation (free falling in an electric furnace of known temperature or across the focal zone of an image furnace) and in continuous operations (constant flowrate of sawdust in the image furnace device or in a small vortex reactor with walls heated at 1323 K [3].

A fairly good agreement has been observed in the results in account of the different experimental conditions.

The gas contains a large proportion of CO and H_2 (more than 70 % of the total volume) and appreciable amounts of C_2H_4 (around 7 % of total volume). H_2 and C_2H_2 concentrations increase with temperature while CO, CO_2 and C_2H_4 concentrations decrease [2,4].

The mass yield of gas increases with temperature. Volume of gas evolved above 1273 K corresponds to about 1 m^3 NTP per kg of wood pyrolysed.

2. Water effects

Experiments made with wet samples show that water plays a significant role above 973 K : mass yield of gas, H_2 and CO proportions increase [2,4].

Water has also a significant importance when brought as steam, as proved by other types of experiments.

The end cross section of a beech wood rod (5, 8, 10 and 16 x 10^{-3} m diameter) is set up at the focus of an image furnace (made with 2 parabolic mirrors 1.5 m in diameter associated with a carbon arc discharge providing a heat flux of the order of 3.5 x 10^6 w m^{-2} at the focus). The reactive part of the wood rod is placed inside a pyrex reactor fed by a constant steam flowrate. The rod is automatically moved forwards as the volatilization reaction proceeds, with a linear velocity of the order of 3 x 10^{-4} m s^{-1}. Gasification yields are close to 100 % with H_2/CO ratio greater than 1 [5].

Experiments with wet wood and under steam atmosphere show that continuous operation would profit by using steam as a carrier gas.

3. Heat of reaction

Reaction is endothermic above 973 K and the heat of reaction reaches about 10 % of the heat of combustion of wood at 1273 K [4]. This value increases in the presence of water and reaches 30 % for a theoretical complete reaction giving only CO and H_2 (5600 KJ x Kg^{-1}) [2].

SELECTION OF A REACTOR ADAPTED TO FAST PYROLYSIS

The problem is to choose a continuous reactor suitable for a reaction occuring between solid particles (wood) and a gaseous phase (H_2O) for reaction times smaller than one second. Figure 1 shows that among the different gas solid reactors available, free falling reactors, transported beds and vortex devices (cyclone) are recommended for reactions occuring between 10^{-3} and 10 s, with small particles sizes (between 10^{-6} and 10^{-3} m). One can expect they are the most adapted to fast pyrolysis of biomass.

The best known vortex device is the cyclone which is generally used to separate fine particles from a gas. Its advantages for past pyrolysis are the following :

. Low residence time for solid (fast pyrolysis condition) and for carrier gas (quenching condition)

. The shape of the cyclone is such that it can be easily set up inside a solar cavity

. Chemical Engineering studies of the cyclone operating as a chemical reactor have not been extensively published, offering a large and interesting field of research

. One can expect that ashes and unreacted particles will be automatically separated from gaseous products (separator aspect of the cyclone).

In the conventional configuration (Figure 2) the gas solid mixture tangentially enters the cyclone and is forced into a constrained vortex. Under the influence of centrifugal force, solid particles are forced towards the walls. The gaseous vortex flow is reversed in the lower portion of the cyclone leaving most of the entrained particles which are collected at the bottom while clean gas escape at the top.

RESIDENCE TIME STUDIES

Studies of the hydrodynamics of carrier gas and wood particles have been made at room temperature.

1. Residence Time Distribution (RTD) of the gas

These experiments have been previously described [1,6]. Air flows in a conventional cyclone (1.25 x 10^{-1} m diameter) under steady state conditions. A pulse of H_2 is injected at the inlet. A catharometer detector records the outlet concentrations signal, the shape of which is analysed on a computer as a function of the gas flow rate.

Reactors	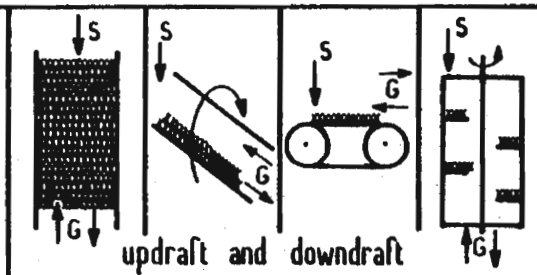				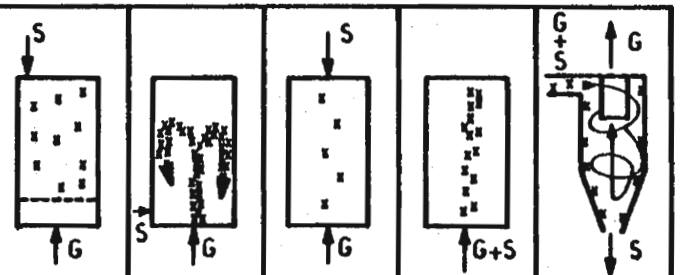				
	updraft and downdraft								
	fixed bed	rotary kiln	moving grate	multiple hearth	fluidised bed	spouted bed	free falling	pneumatic transport	cyclone
particles d_p (m)	10^{-3} _ 3×10^{-1}				10^{-5} _ 10^{-2}			10^{-5} _ 10^{-3}	10^{-6} _ 10^{-3}
particles t_s (s)	10^{3} _ 10^{5}				10^{2} _ 10^{4}			1 _ 10^{2}	5×10^{-3} _ 10

S : solid G : gas

FIGURE I : Different types of gas solid reactors.

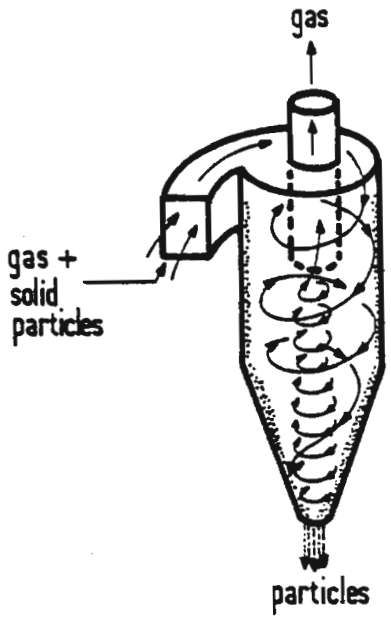

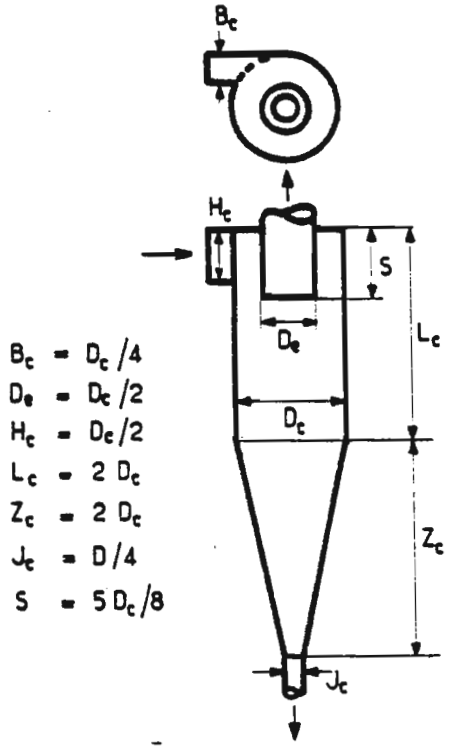

FIGURE II : Conventional cyclone reactor.

The flow pattern in the cyclone can be represented by a plug flow zone (fraction β of the total volume) followed by a well stirred zone (fraction α of the total flow rate) more or less by passed by the gas (figure 3). The relative importance of these two zones have been correlated as a function of the entrance Reynolds number Re_o :

$$\beta = 10^{-7} \, Re_o^{\,2} \qquad (1)$$

$$1 - \alpha = 3.72 \times 10^{-11} \, Re_o^{\,3} \qquad (2)$$

(Re_o is calculated with inlet duct hydraulic diameter).

Figure 3 shows that for $Re_o < 500$ the cyclone can be assimilated to a stirred reactor while for $Re_o > 3000$ it works like a plug flow reactor. Intermediate conditions must be avoided because of by pass.

2. Residence Times of particles

Two optical cells are set up at the inlet and at the bottom of the cyclone. Each cell is made with a phototransistor facing an infrared light emitting diode. A pulse of a small quantity of wood sawdust is introduced at the inlet of the cyclone (1.25×10^{-1} m diameter) and passes across the first cell. A pulse is delivered and starts a timer which is stopped when the particles leave the cyclone through the second cell. A microprocessor board computes the elapsed time and gives the residence time of the particles on a display unit. Figure 4 gives the results obtained with different particle sizes as a function of Re_o. The solid residence time t_S is surprisingly higher than t_G for high values of Re_o. For low values of Re_o, t_S tends to the free falling time while $t_G \to \infty$.

It seems advisable to work with $\frac{t_S}{t_G}$ ratios close to 1, in conditions where results obtained on gas RTD could apply to solid particles. These conditions correspond to Re_o around 6000 where the cyclone is working like a plug flow reactor (as shown by gas RTD measurements).

HEAT TRANSFER STUDIES

1. Heat transfer between the heated walls and the carrier gas

These experiments have also been previously described [1,6]. A small stainless steel conventional cyclone (1.68×10^{-2} m diameter ; 9.64×10^{-6} m^3 volume and $3,2 \times 10^{-3}$ m^2 surface) fed by a known flowrate of argon is placed at the focus of an image furnace operating with a 4000 W xenon lamp. Gas temperatures at the inlet (T_o) and at the outlet (T_S) are measured by thermocouples while wall temperature (T_W) is estimated with an optical pyrometer. The measurements are made as a function of Re_o.

A theoretical analysis taking into account the results obtained on gas RTD leads to the following relationship [6] :

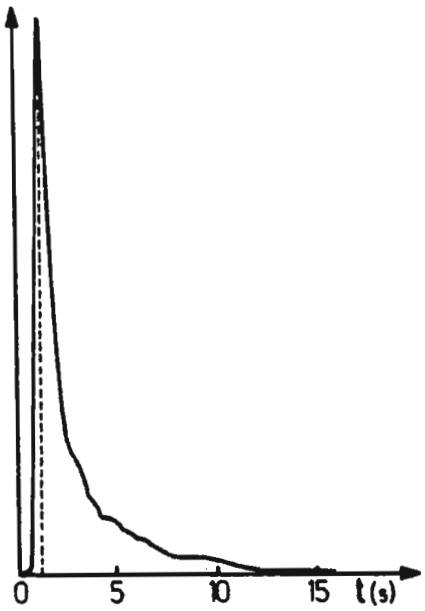

(a) Outlet concentration signal

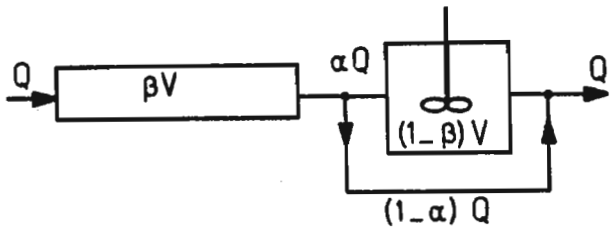

(b) Model for residence time distribution

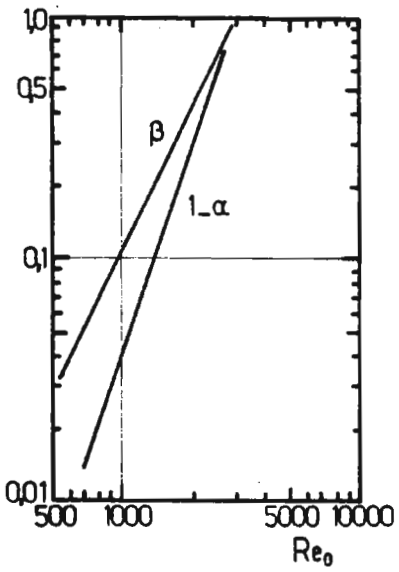

(c) variations of parameters α and β vs Reynolds number Re_o

FIGURE III : Flow pattern of the gas in a cyclone.

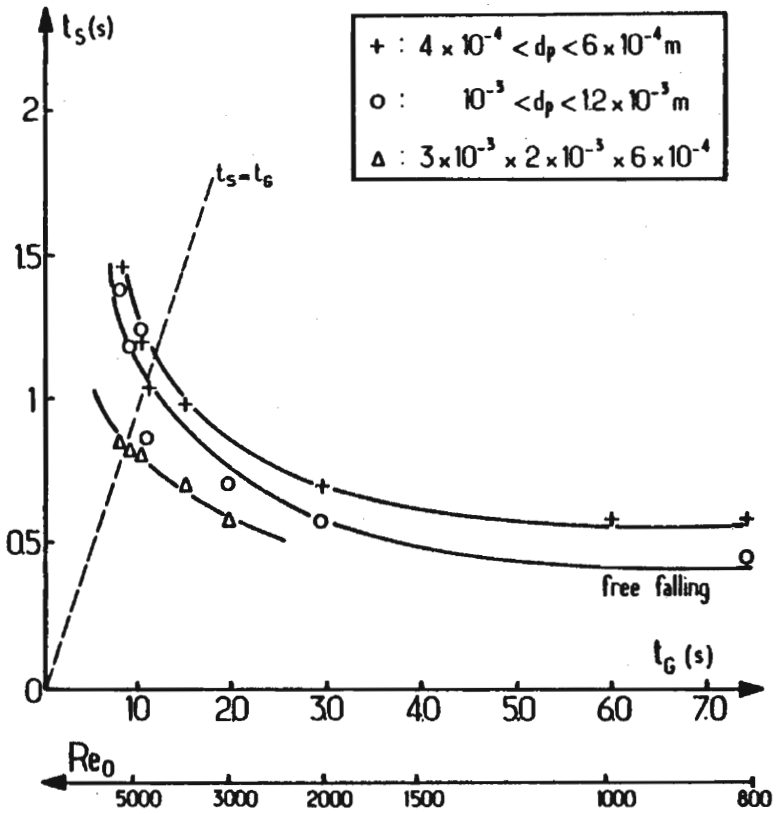

.a. Variations of t_s vs t_G and Reynolds number Re_o for different particle sizes.

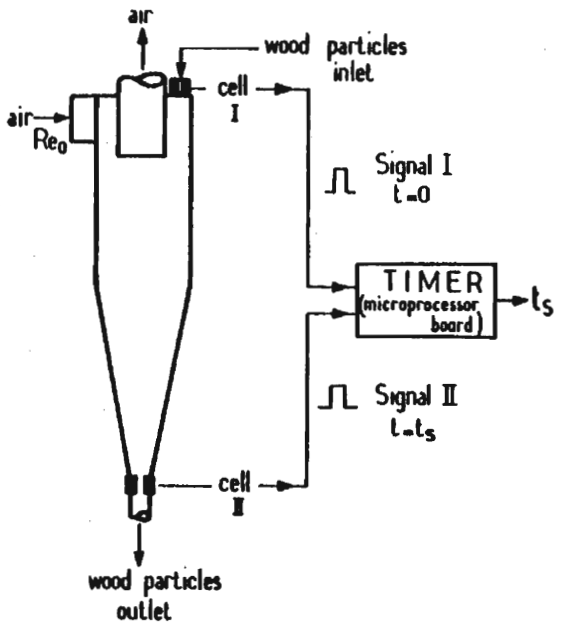

.b. Schematic diagram of apparatus

FIGURE IV : Residence time measurements of wood particles in a cyclone.

$$\frac{T_W - T_S}{T_W - T_o} = \exp(-N)\left(1 - \alpha + \frac{\alpha}{1 + \frac{1-\beta}{\alpha} N}\right) \qquad (3)$$

where $N = \frac{h\ S}{Q_m\ Cp_G}$ is a number of transfer units.

α and β are given by (1) and (2) when Re_o is known. h is the overall heat transfer coefficient

$$h = \frac{\lambda_o\ Nu_o}{d_H}$$

Nu_o beeing the Nusselt number calculated with d_H (hydraulic diameter of the cyclone = $4\ \frac{V}{S}$).

For $Re_o > 3000$ one can verify that $\frac{T_W - T_S}{T_W - T_o} = \exp(-N)$.

Experimental measurements of T_o, T_S and T_W have been made for $600 < Re_o < 1600$ and the following relationship has been proposed(fig.5)

$$Nu_o = 1.35\ Re_o^{0.38} \qquad (4)$$

Values of Nu_o are greater than those corresponding to a turbulent flow in a cylindrical duct. For $Re_o = 1500$ the mean residence time (calculated at 988 K) is 6.2×10^{-2} s. This corresponds to a heating rate greater than 10^4 K S^{-1}.

For $Re_o > 3000$ h is of the order of 50 watts m^{-2} K^{-1}.

2. Heat transfer between the gas and the particles

Wood particles can be heated by forced convection (heat transfer coefficient h_c) and by free convection (heat transfer coefficient h_L).

For spheres, h_c and h_L can be estimated thanks to the correlations [7] :

$$\frac{h_c\ d_p}{\lambda_G} = 2 + 0.6\left[\frac{\eta_G\ Cp_G}{\lambda_G}\right]^{1/3}\left[\frac{\rho_G\ u_r\ d_p}{\lambda_G}\right]^{1/2} \qquad (5)$$

$$\frac{h_L\ d_p}{\lambda_G} = 2 + 0.6\left[\frac{g\ d_p^3\ \rho_G^2\ \Delta T}{\eta_G^2\ T}\right]^{1/4}\left[\frac{\eta_G\ C_{p_G}}{\lambda_G}\right]^{1/3} \qquad (6)$$

For wood sawdust ($d_p = 2 \times 10^{-4}$ m, $T_s = 1200$ K, $T_o = 300$ K) one calcu-

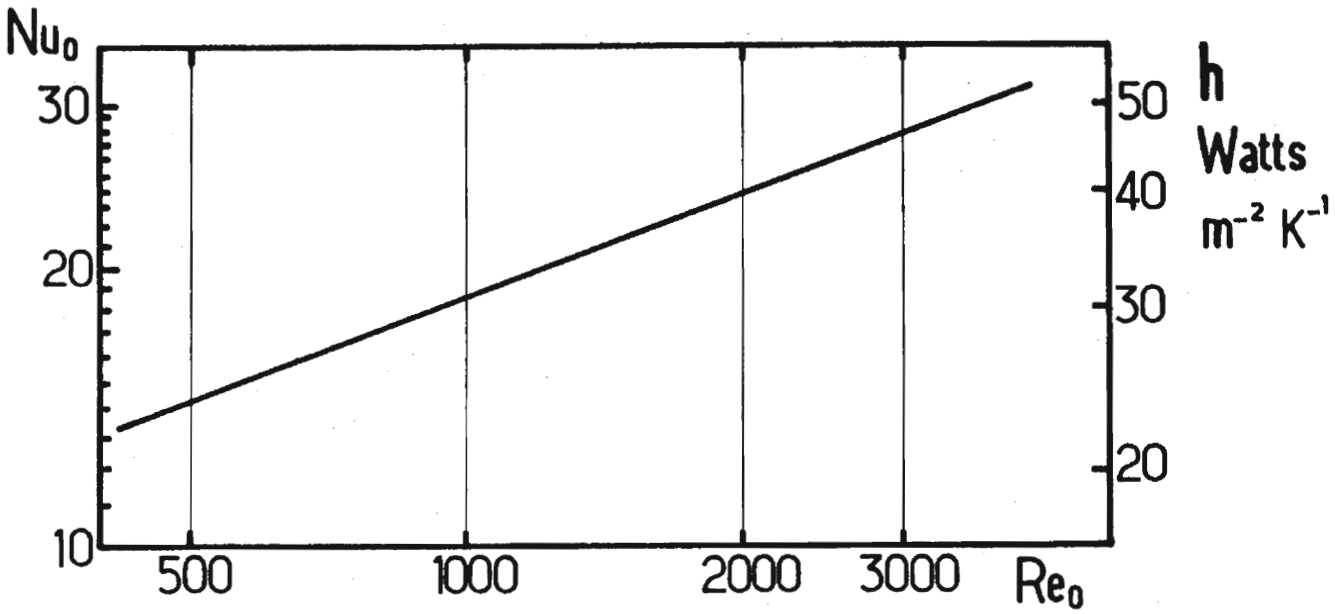

FIGURE V : Heat transfer between the gas and the walls of the cyclone. Variations of Nusselt number Nu_o and overall heat transfer coefficient h vs Reynolds number Re_o

lates the following orders of magnitude :

h_c = 700 watts m^{-2} h^{-1} and h_L = 800 watts m^{-2} K^{-1}

3. Heat transfer between the particles and the heated walls

. Radiative heat transfer

The heat transfer coefficient h_R can be estimated as [7] :

$$h_R = \varepsilon\sigma(T_W^2 + T_s^2)(T_W + T_s) \qquad (7)$$

with ε = 0.5, T_W = 1200 K and T_S = 300 K

one finds h_R = 65 watts m^{-2} K^{-1}

This transfer process is probably of minor importance.

. Direct transfer between the particles and the wall

This transfer process is probably the most efficient one because of the strong frictions occuring when the grains forced to the walls undergo intensive whirling motions on the heated surface. Experimental measurements of these effects would be of major importance but have not been performed yet.

As a conclusion, many heat transfer processes contribute to a fast heating of the particles and we can assume that surface temperature of particles is rapidly equal to the temperature of the carrier gas. The validity of such an assumption can be checked by the results of chemical experiments : fast pyrolysis of sawdust has been carried out in a small cyclone (1.68×10^{-2} m diameter). The gas temperature was measured to be 1143 K. The chemical analysis of gases gave results close to those observed in an electric furnace at 1173 K, a value close to 1143 K [2].

ANALYSIS AT THE PARTICLE LEVEL (Study of the competition between chemical process and conduction of heat within the solid)

1. Theoretical point of view [8]

Consider a particle undergoing a high intensive heating at its external surface and suppose that the solid decomposes to gaseous products. A model has been proposed [8] to represent the thermal volatilization of particles in conditions of heat transfer limitations between the external surface and the internal parts of the particles.

The problem has been treated with four different boundary conditions : constant surface temperature ; constant heat flux at the surface ; convective heat exchange with the gas at constant temperature ; radiative exchange with the hot wall.

Two extreme situations can be imagined :

. The chemical processes are much slower than heat conduction in the solid. The volatilization is then controlled by chemical reaction. The temperature of the whole solid is nearly uniform and the reaction occurs in the whole volume : the particle is said to valatilize in "chemical regime".

. The chemical processes are much faster than heat conduction. A steep temperature gradient appears close to the surface, in the first internal layers, where the reaction occurs, while the deeper parts of the particle remain cold. In such a case, volatilization is controlled by the competititon between chemical reaction and diffusion of heat. Even in this extreme condition, diffusion of heat must be taken into account and the concept of a surface reaction is irrelevant : the particle is said to volatilize in "ablation regime".

The processes involved in these two extreme situations can be respectively represented by two characteristic times :

the reaction time :

$t_R = \frac{\rho_s}{r}$ where $r = k \exp - \frac{E}{\mathcal{R}T}$ is the chemical reaction rate (Kg $m^{-3} s^{-1}$)

the thermal conduction time :

$t_T = \frac{L_o}{\alpha_T}$ where L_o is the radius of the particle and α_T its thermal diffusivity

Let $M = \frac{t_T}{t_R} = \frac{L_o^2 r}{\rho_S \alpha_T}$ (8) be a thermal "Thiele modulus" :

In chemical regime : $M << 1$

In ablation regime : $M >> 1$

In the case where the surface is maintained at constant temperature (equal to the temperature of the gas) one can show that the time t_F required for a particle to disappear in ablation regime is given by :

$$t_F = b \sqrt{t_T \, t_R} \qquad (9)$$

where b is a constant factor depending on the heat of reaction.

The experimental measurement of t_F allows the calculation of M thanks to the relation :

$$M = b^2 \frac{L_o^4}{\alpha_T^2 \, t_F^2} \qquad (10)$$

According to the value of M, the volatilization regime (chemical or ablation) can be determined.

t_T can be estimated $\left(\frac{L_o^2}{\alpha_T}\right)$ and with help of relations (8) and (10) it is possible to calculate t_R and to deduce the value of r, the chemical rate that would be observed if no diffusional limitation occured.

Notice that it is also possible to determine the linear ablation velocity u_L thanks to the relation :

$$u_L = \frac{L_o}{t_F} = \frac{1}{b\rho_s}\left(\frac{\lambda_s r}{C_{p_s}}\right)^{1/2} \qquad (11)$$

2. Experimental determination of the volatilization regime in a cyclone fed with calibrated sawdust

A stainless steel cyclone (1.68×10^{-2} m diameter) is heated at the focus of an image furnace. The cyclone is fed in continuous operation by a constant flowrate of beech wood particles ($1.5 - 2 \times 10^{-4}$ m diameter) fluidized in argon (known entrance Reynolds number Re_o). The outlet temperature of the gas T_s and the unreacted fraction f_s of wood are measured as a function of Re_o.

Taking into account the results previously obtained on RTD of gas and assuming the same behaviour for solid particles one can write [6] :

$$Re_o < 500 \qquad f_s = \int_o^{t_F/\bar{t}} \left(1 - \frac{t}{t_F}\right)^3 \exp\left(-\frac{t}{\bar{t}}\right) d\left(\frac{t}{\bar{t}}\right) \qquad (12)$$

$$Re_o > 3000 \qquad f_s = \left(1 - \frac{\bar{t}}{t_F}\right)^3 \qquad (13)$$

$\bar{t}$ is the mean residence time.

Experimental results are shown on table 1.

TABLE 1

Gas flowrate $m^3 s^{-1}$ (NTP)	Solid flowrate $Kg\ s^{-1}$	Re_o	T_s(K)	$\bar{t}$ (s) (750 K)	f_s	t_F(s)
1.33×10^{-4}	2.37×10^{-4}	3200	1141	27.5×10^{-3}	0.113	53×10^{-3}
1.38×10^{-4}	2.46×10^{-4}	3320	1126	26.5×10^{-3}	0.111	51×10^{-3}
2.37×10^{-4}	5.62×10^{-4}	7600	1088	15×10^{-3}	0.423	60×10^{-3}

The values of complete volatilization times t_F are calculated according to (13). The fact that t_F is relatively independent of $\bar{t}$ is a proof of the validity of the model.

From relation (10) it is possible to calculate M = 15 (with $t_F = 5 \times 10^{-2}$ s and b = 2.79 [6]) : this shows that fast pyrolysis of 2×10^{-4} m particles of wood in a cyclone occurs in ablation regime (M > 1).

The velocity of the ablation front u_L is calculated to be of the order of 2×10^{-3} m s^{-1}.

The above estimations are only orders of magnitude that it would be inresting to confirm in further experiments with different particles sizes.

PRESENT INVESTIGATIONS

This research is now being pursued along the following lines :

1. Residence time of particles are studied in other cyclones of different sizes

2. The nature of products obtained by flash pyrolysis in electrically heated cyclone fed by argon or by steam is compared

3. The behaviour of the cyclone is observed when the loading ratio

$$R = \frac{\text{solid flow rate (Kg } s^{-1})}{\text{gas flow rate (Kg } s^{-1})}$$

is increased. Ratios up to R = 10 can be achieved without appreciable alteration in the cyclone working conditions.

4. Different ways of heating the cyclone by solar radiation are studied. Two possibilities can be considered :

. The cyclone, quite opaque, is set up in an absorbing cavity.

. The upper part of the cyclone is transparent (window) and concentrated solar radiation penetrates into the reactor which plays the role of a cavity. The wood particles are heated up by the processes previously described and also by direct absorption of light.

Only the first arrangement will be considered in a first step.

A theoretical study has been made to calculate the distribution of radiative flux in a cavity inside which a reactor is set up [9]. Different cavities have been considered : cold cavities with specular or diffusive reflecting walls and hot cavities with diffusing walls. Calculations have been conducted in order to enhance absorption by lateral cylindrical walls with respect to the upper flat surface of the cyclone. The hot cavity is found to give the best theoretical performance.

NUMERICAL APPLICATION

In so far as the correlations proposed in the present study are supposed to hold, one can predict the performances of a cyclone in which fast pyrolysis of wood is carried out in a solar concentrator with a given power P.

The calculations are made under the pessimistic assumption that heat required to heat up water and wood at high temperature is not recovered.

The initial temperature of wood and steam is chosen equal to 433 K.

The reactor is supposed to operate in conditions of plug flow assumption ($Re_o > 3000$).

For a conventional cyclone with a D diameter :

$$V = 2.135\ D^3$$

$$S = 11.66\ D^2$$

$$d_H = \frac{4V}{S} = 0.733\ D$$

$$d_o = \frac{D}{3}$$

Relations (3) allows calculation of T_W required to ensure a given value of T_S (for example 1073 K)

For $Re_o > 3000$: $\frac{T_w - T_s}{T_w - T_o} = \exp(-N)$

$$N = \frac{h\ S}{Q_m\ C_{p_{Go}}} \qquad \text{with} \qquad h = \frac{\lambda_o\ Nu_o}{d_H}$$

No heat transfer measurement has been made with steam, but we can anticipate that the 1.35 factor in (4) depends on the nature of the gas. Suppose as a first approximation that $Nu_o = 2\ Pr\ Re^{0.38}$ (for argon Pr = 0.67).

Thanks to the general expression of Re_o

$$Re_o = \frac{4\ Q_m}{\pi\ \eta_{G_o}\ d_o} \qquad (14)$$

we can write

$$\text{Log}\ \frac{T_w - T_o}{T_w - T_s} = 121.5\ \frac{\lambda_o\ Pr}{C_{p_{Go}}\ \eta_{Go}}\ \frac{1}{Re_o^{0.62}} \qquad (15)$$

with the following values for steam :

$C_{p_{Go}} = 1977 \text{ J Kg}^{-1} \text{ K}^{-1}$

$Pr = 1.09$

$\lambda_o = 29.5 \times 10^{-3} \text{ W m}^{-1} \text{ K}^{-1}$

$\eta_{G_o} = 146 \times 10^{-7} \text{ N s}^{-1} \text{ m}^{-2}$

$$\text{Log}_n \frac{T_w - T_o}{T_w - T_s} = \frac{135.4}{Re_o^{0.62}} \qquad (16)$$

For example if $Re_o = 3000$; $T_o = 433$ K ; $T_s = 1073$ K, it is possible to calculate :

$T_p = 1473$ K

Suppose, now, the cyclone is set up in a cavity placed at the focus of a solar concentrator with a given power P and that it is desired to pyrolyse a massic flow rate $R \times Q_m$ of wood. It is possible to calculate Q_m and D (cyclone characteristic).

$$P = R\, Q_m\, C_{p_S} (T_s - T_o) + Q_m\, C_{p_G} (T_s - T_o) + R\, Q_m\, \Delta H$$

with P = 6000 W

R = 10

$C_{p_S} = 2800 \text{ J Kg}^{-1} \text{ K}^{-1}$

$C_{p_G} = 2117 \text{ J Kg}^{-1} \text{ K}^{-1}$

$\Delta H = 14 \times 10^3 \text{ J mole}^{-1} = 583 \times 10^3 \text{ J Kg}^{-1}$

we calculate :

flow rate of steam $Q_m = 2.5 \times 10^{-4} \text{ Kg s}^{-1}$

flow rate of wood $Q_{m_S} = 2.5 \times 10^{-3} \text{ Kg s}^{-1}$ ($\simeq$ 9 Kg/hour)

The corresponding cyclone can be calculated to have a diameter $D = 2.2 \times 10^{-2}$ m.

For P = 6000 W and R = 1, the calculations give :

$Q_m = Q_{ms} = 1.6 \times 10^{-3} \text{ Kg s}^{-1}$ ($\simeq$ 6 Kg/hour)

and $D = 1.43 \times 10^{-1}$ m

For R = 10 the mean residence time is $\bar{t} = 28 \times 10^{-3}$ s.

The size of particles entirely volatilized after a time $t_F = \bar{t} = 28 \times 10^{-3}$ s can be calculated thanks to relation (10). Let us choose M = 20 in order to be in ablation regime, with $\alpha_T = 1.4 \times 10^{-7}$ m^2 s^{-1} and b = 2.8 [6] we calculate :

$$d_p \simeq 1.6 \times 10^{-4} \text{ m}$$

For R = 1, $\bar{t}$ = 1.1 s and d_p value increases to 10^{-3} m.

All these calculations are, of course, orders of magnitude.

NOTATIONS

b	constant factor
C_{pG}	heat capacity of gas $\left(\text{at } \frac{T_s + T_o}{2}\right)$
C_{pG_o}	heat capacity of gas (at T_o)
C_{p_s}	heat capacity of wood
d_H	hydraulic diameter of the cyclone
d_p	particle diameter
d_o	inlet duct of the cyclone : hydraulic diameter
D	cyclone diameter
E	activation energy
f_s	unreacted fraction
h	overall heat transfer coefficient
h_c	forced convection heat transfer coefficient
h_L	free convection heat transfer coefficient
h_R	radiative heat transfer coefficient
k	preexponential factor
L_o	half initial thickness of a particle
M	thermal Thiele modulus
N	number of transfer units
Nu_o	Nusselt number (at T_o)
Pr	Prandtl number
Q_m	massic flow rate of gas
Q_{ms}	massic flow rate of solid
R	loading ratio
Re_o	entrance Reynolds number
r	chemical reaction rate
S	internal surface of the cyclone
$\bar{t}$	gas mean residence time $\left(\text{at } \frac{T_o + T_s}{2}\right)$
t_F	time required for a particle to disappear
t_G	gas mean residence time (at T_o)
t_s	solid mean residence time
t_R	chemical reaction time
t_T	thermal conduction time

T_o inlet temperature
T_o outlet temperature
T_s wall temperature
T_w wall temperature
u_r relative rate of gas and particle
u_L linear ablation velocity
V volume of the cyclone
α stirred zone fraction (flow rate)
α_T thermal diffusivity of wood
β plug flow zone fraction (volume)
ΔH enthalpy of reaction
ε emissivity of the solid
η_G viscosity of the gas $\left(\text{at } \frac{T_s + T_o}{2}\right)$
η_{Go} viscosity of the gas (at T_o)
λ_G thermal conductivity $\left(\text{at } \frac{T_s + T_o}{2}\right)$ of gas
λ_s thermal conductivity of solid
ρ_G density of the gas $\left(\text{at } \frac{T_s + T_o}{2}\right)$
ρ_s density of solid
σ Stephan constant

REFERENCES

[1] J. LEDE, Proceedings of Solar Fuels Workshop, STTFUA Albuquerque (USA) (1979)

[2] J. LEDE, P. BERTHELOT, J. VILLERMAUX, A. ROLIN, H. FRANCOIS, X. DEGLISE, Revue Phys. Appl., 15, 545 (1980)

[3] J. LEDE, F. VERZARO, J. VILLERMAUX, Revue Phys. Appl., 15, 535 (1980)

[4] X. DEGLISE, C. RICHARD, A. ROLIN, H. FRANCOIS, Rev. Gén. Therm., 227 (1980)

[5] J. LEDE, B. ANTOINE, J. VILLERMAUX, C. RICHARD, H. FRANCOIS, X. DEGLISE, to be published

[6] J. VILLERMAUX, F. VERZARO, J. LEDE, Part II, Rev. Gén. Therm., 227 (1980)

[7] J. SZEKELLY, J.W. EVANS, H.Y. JOHN, Gas Solid Reactions, Academic Press (1976)

[8] J. VILLERMAUX, B. ANTOINE, Part I, Rev. Gén. Therm., 227 (1980)

[9] C. ROYERE, to be published

[10] N.B. VARGAFTIK, Tables on the thermophysical properties of liquids and gases, John Wiley (1975)

FAST PYROLYSIS ON A MOLTEN LEAD BATH

J. M. Skaates
Department of Chemistry and Chemical Engineering
Michigan Technological University
Houghton, Michigan

HISTORY OF LEAD BATH PYROLYSIS

Molten lead as a heat source for biomass or fossil fuel pyrolysis has a long history. Here we note only that in 1923 Henry Ford contracted with Piron Coal Distillation Systems to build a plant in Detroit to carbonize 4000 tons per day of coal by means of a steel conveyor belt floating on a pool of molten lead [1].

The inventor of the lead bath pyrolysis process described in this paper is Dr. Martin Fassell, a metallurgical engineer and former director of research of Howmet. Dr. Fassell conceived the process primarily as a means of disposing of mixed municipal solid waste and generating a medium Btu gas.

In 1974 the Resource Recovery Systems Division of the Barber-Colman Company, with Dr. Fassell as Division Manager, initiated a pilot plant study of the process with the goal of maximizing the production of fuel gas and a high value aromatic fraction. Test runs on wood chips, agricultural wastes, and other types of biomass were carried in a 908 kg/day (1 ton/day) pilot plant unit. Development work on the process continued until 1978, when Barber-Colman closed out the Resource Recovery Systems Division and donated the lead bath pyrolysis process, including all technical files, experimental units, and patent rights, to Michigan Technological University. The Center for Waste Management Programs (CWMP), a research division of Michigan Technological University, has continued development of the process on a limited scale. Small-scale studies of lead bath pyrolysis have been carried out to explore some of the major parameters affecting product distribution.

DESCRIPTION OF THE PROCESS

Pyrolysis of biomass for the production of liquid and gaseous fuels involves thermal degradation of the cellulose and lignin according to a particular temperature-time path. Pyrolysis schemes that have been proposed differ according to the following points:

1. method of heating the biomass
2. temperature-time-history of the biomass
3. temperature and environment encountered by the primary gases liberated in biomass pyrolysis

Various methods of heating biomass are:

1. heating by contact with a heated solid surface (rotating drum)
2. heating by contact with hot gases (fluidized bed)
3. heating by contact with a liquid metal surface (molten lead bath)
4. heating in a molten salt bath

In the continuous lead bath pyrolysis process solid organic wastes are subjected to a high-temperature, low-contact-time pyrolysis followed by a rapid quench of the off-gas to preserve valuable chemical species. The solid feed to the pyrolysis system is comminuted until the particles are 0.6 cm (1/4 inch) or less in the longest dimension. The feed is then placed in an airlocked hopper and metered into the pyrolysis furnace by a screw conveyor. The 980 kg/day pilot plant unit designed by Dr. Fassell is a brick-lined refractory furnace 6.1 m (20 ft) long (Figure 1). The feed from the screw conveyor drops onto the molten lead hearth and is pyrolyzed at 760°C in the absence (or near absence) of oxygen. The lead is kept in circulation by a turbine pump. A rake mechanism sweeps the char to the end of the hearth where it is conveyed out of the furnace to cool (in the absence of oxygen). The residence time of the solid biomass on the hearth is 45 to 90 seconds, depending on the speed of the raking mechanism.

The gas processing system used in the 908 kg/day Barber-Colman pilot plant unit consisted of a water quench, followed by an oil scrubbing system to recover benzene, toluene, and other high molecular weight organics. The remaining gas was a medium Btu fuel gas, part of which was used to fire the radiant heaters above the hearth. The technical development files contain results of a number of runs of biomass feed to the 908 kg/day pilot plant unit:

Table 1

PRODUCTS FROM BIOMASS PYROLYSIS

Product	Percent of dry biomass for feed of Rice hulls	Sugar Maple Sawdust
Water	21.0	27.7
Char	14.4	18.3
Ash	17.1	0.9
Gases (excluding aromatic and olefins)	30.7	38.1
BTX	0.5	0.7
Olefins	1.2	1.5
Tars and pitch	9.6	0.6
Water-soluble organics	-	2.3
Unaccounted for	5.5	9.9
	100.0	100.0

In all cases the gas recovered from the scrubbers was a medium Btu fuel gas having a heating value of about 18.6 MJ/m^3 (500 Btu/scf). The composition of the fuel gas is given in Table 2:

LIQUID METAL PYROLYSIS FURNACE

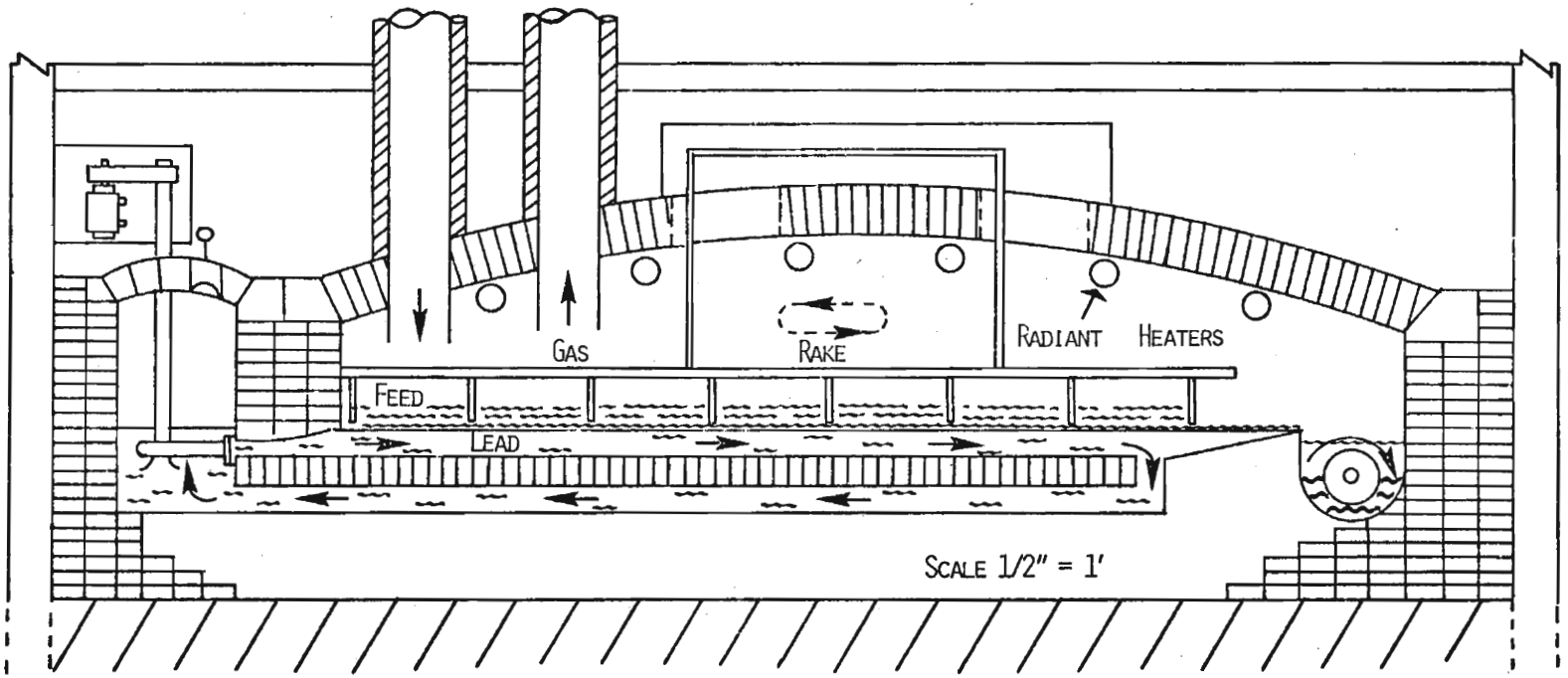

FIGURE 1 FURNACE CROSS-SECTION

Table 2

COMPOSITION OF MEDIUM BTU FUEL GAS (DRY BASIS)

Component	Mole Percent
Hydrogen	36.8
Carbon Monoxide	35.2
Carbon Dioxide	25.6
Nitrogen	1.3
Ethane	1.1
	100.0

The Barber-Colman reports refer to energy balance calculations indicating that the medium Btu fuel gas plus aromatics contain about 80% of the heating value of the biomass feed. Twenty percent of the feed heating value would be required to fuel the pyrolysis furnace, leaving sixty percent for other purposes.

STATUS OF THE PROCESS

The continuous lead bath pyrolysis process achieves in an economically feasible way the objectives of rapid heating of biomass, a high pyrolysis temperature and quick removal and quenching of primary pyrolysis products. These are basic requirements if the yields of valuable products are to be increased, and tar and char minimized. The design of the furnace, the solid feed system, and the raking mechanism are based on Dr. Fassell's life-long experience with high-temperature metallurgical operations.

Development of the continuous lead bath pyrolysis process was incomplete when Barber-Colman abandoned the project. The gas scrubbing system on the pilot plant unit was primitive. As expected, considerable trouble was encountered with phenolic tar deposits on the gas take-off line and in the scrubbers. The further use or disposal of the char raked off the hearth was a question mark, as this char contained from 1 to 2% lead by weight. Crucial variables, such as lead temperature, water content of the biomass feed, and furnace atmosphere had not been explored to determine their effect on product yield. Finally, an economic evaluation of the process, including biomass collection and transportation costs, capital cost of the pyrolysis system, and cost of cleanup of waste streams, had not been made.

DEVELOPMENT WORK AT MICHIGAN TECH

Background

The Center for Waste Management Programs (CWMP), a mission-oriented research unit of Michigan Technological University, was assigned the task of evaluating and further developing the continuous lead bath pyrolysis process. Due to the cost of operating the 908 kg/day pilot

unit, CWMP chose to conduct experiments on a smaller scale to explore the chemistry of the process. The questions addressed were:

1. Would gas production and benzene-toluene-xylene (BTX) yield be significantly improved by operating the process at a higher temperature?

2. What is the mechanism of contamination of the char by lead? What methods would be effective in separating the lead from the char?

Although the scrubbing system on the pilot plant unit was crude and had severe tar fouling problems, it was felt that these problems could be solved by applying technology developed for coal gasification and for the partial oxidation of heavy residua.

Effect of Operating Temperature

The 760°C operating temperature was chosen by Dr. Fassell to avoid two problems. According to Dr. Fassell, furnaces with reducing atmospheres operating below 720°C pose the risk of explosion in the event of furnace failure and air in-rush. On the other hand, operating above 800°C on solid municipal waste would result in the softening and melting of glass waste on the lead hearth. Since the latter is not a factor with biomass feed, it was decided to explore biomass pyrolysis at a series of temperatures up to 1000°C. A computer-aided search of the literature on cellulose and lignin pyrolysis indicated that, to a rough approximation, these components pyrolyze independently when biomass is heated. Accordingly, samples of cellulose (Whatman 50 filter paper) and lignin (Westvaco Indulin AT kraft pine lignin) were studied. To trace the effect of high temperature pyrolysis on hydroxy and methoxy groups attached to the aromatic ring in lignin, a model compound (guaiacol, or 2-methoxy-phenol) was chosen for study [2].

The apparatus used in these studies consisted of a one-liter round bottom quartz flask inserted in a 200-1200°C vertical Lindberg furnace (Figure 2). The flask cover had ports for sample introduction, argon purge, gas withdrawal, and a thermowell. The lead was contained in a crucible machined from spectroscopic grade graphite. The purity of the lead was 99.92%. Pyrolysis gases were removed through a quartz take-off tube directly above the lead surface, and were analyzed by gas chromatography. A typical chromatogram contained 20 to 24 peaks, of which 14 were known. The unknown peaks were eluted after CO_2 and before benzene. Total pyrolysis gas evolved could be determined by a gas buret. Tars were collected on quartz wool inserted into the electrically-heated quartz take-off line.

Total gas production from the pyrolysis of cellulose, lignin, and guaiacol is reported in Figure 3. Gas production increases more steeply with temperature for guaiacol than for lignin or cellulose.

Pyrolysis gas composition as a function of pyrolysis temperature is reported in Figures 4 to 11. Replicates of runs indicated that the

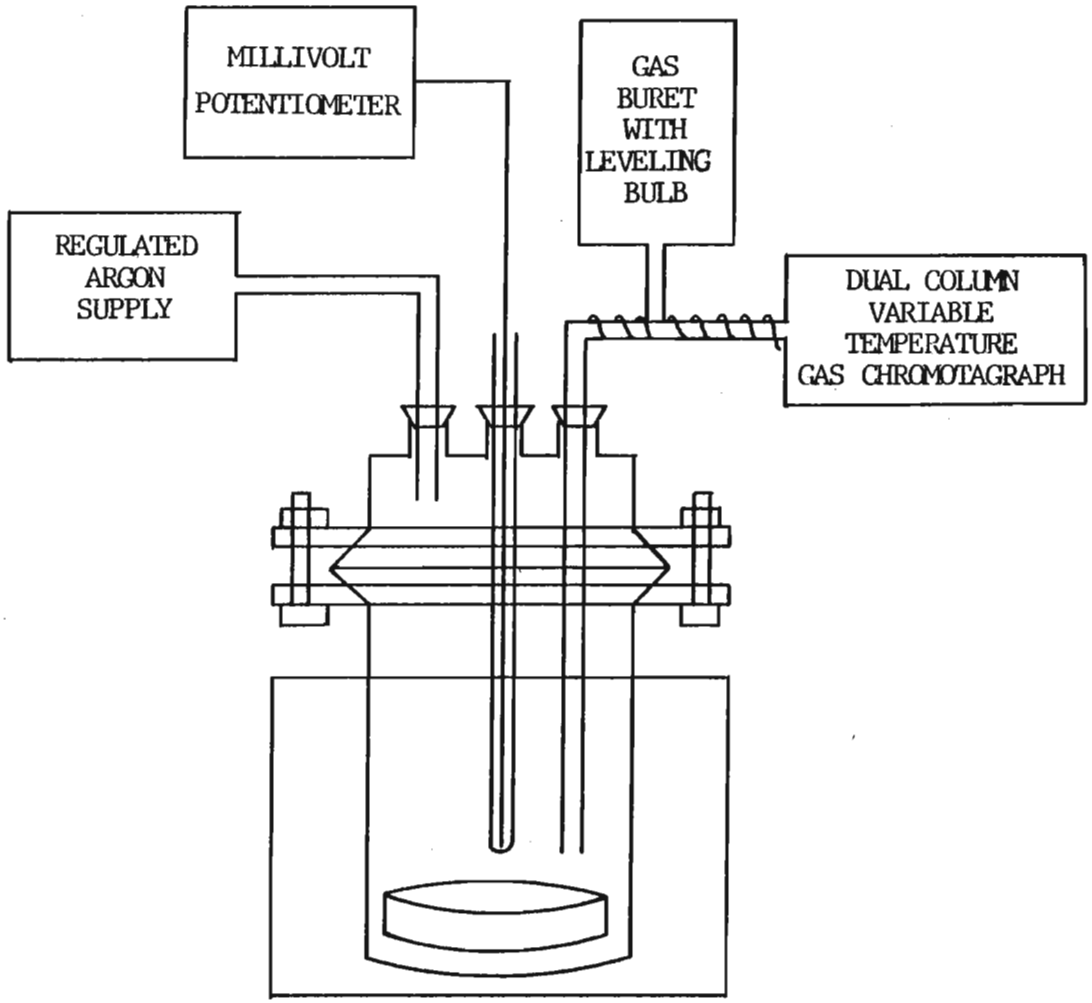

FIGURE 2 SMALL-SCALE PYROLYSIS UNIT

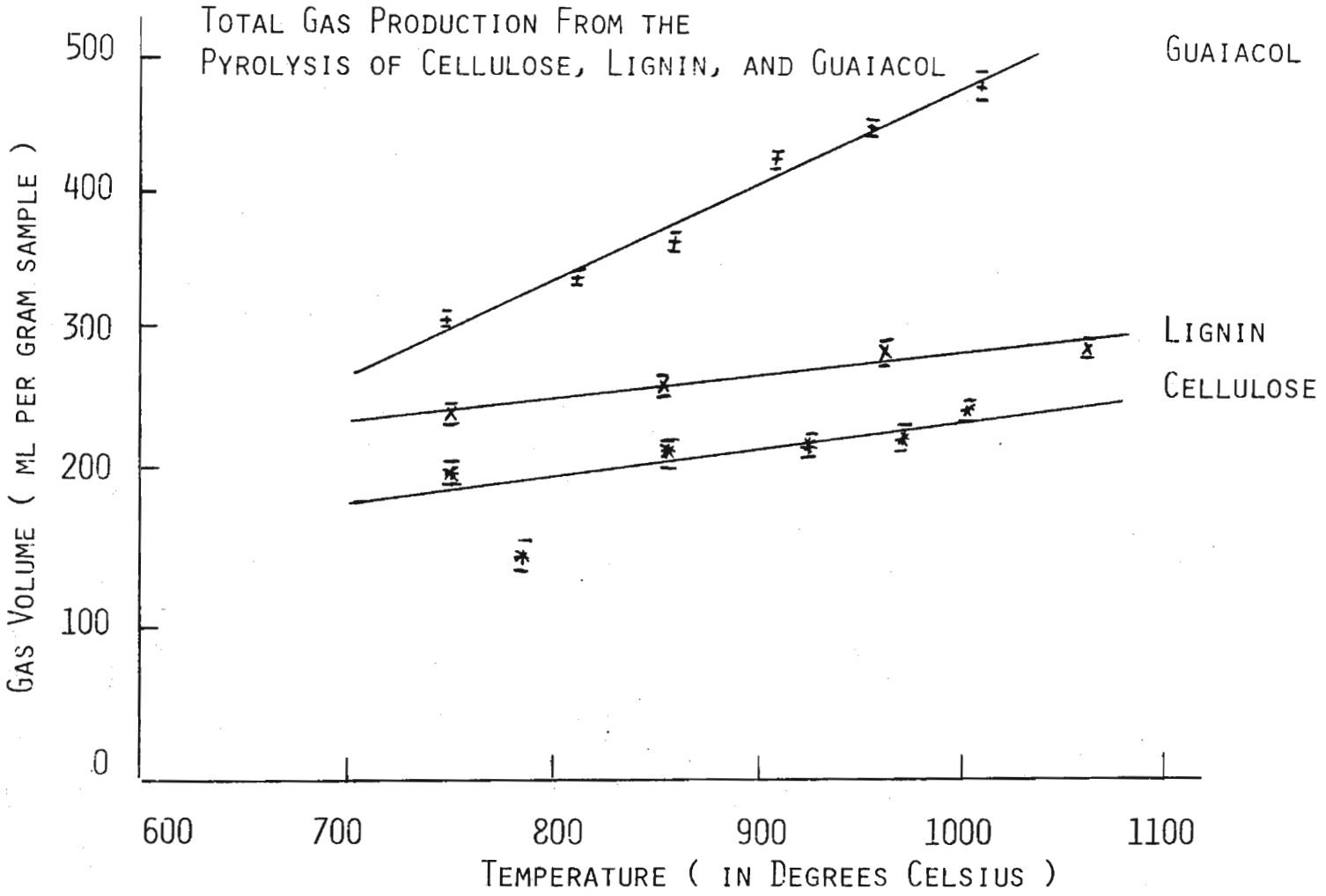

FIGURE 3 TOTAL DRY GAS PRODUCTION AT STANDARD TEMPERATURE AND PRESSURE

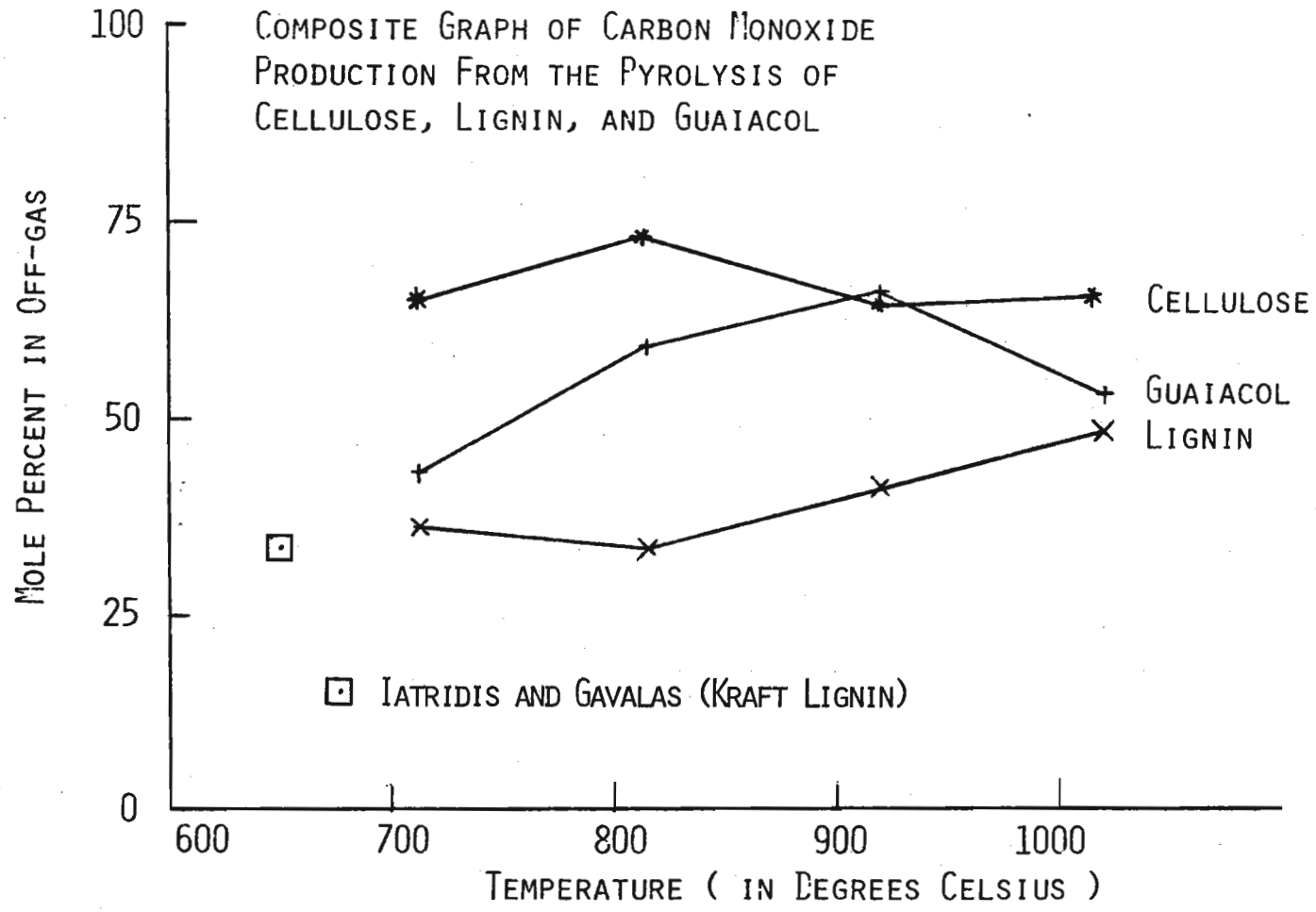
COMPOSITE GRAPH OF CARBON MONOXIDE PRODUCTION FROM THE PYROLYSIS OF CELLULOSE, LIGNIN, AND GUAIACOL
MOLE PERCENT IN OFF-GAS
100
75
50
25
0
600
700
800
900
1000
TEMPERATURE (IN DEGREES CELSIUS)
CELLULOSE
GUAIACOL
LIGNIN
IATRIDIS AND GAVALAS (KRAFT LIGNIN)

FIGURE 4

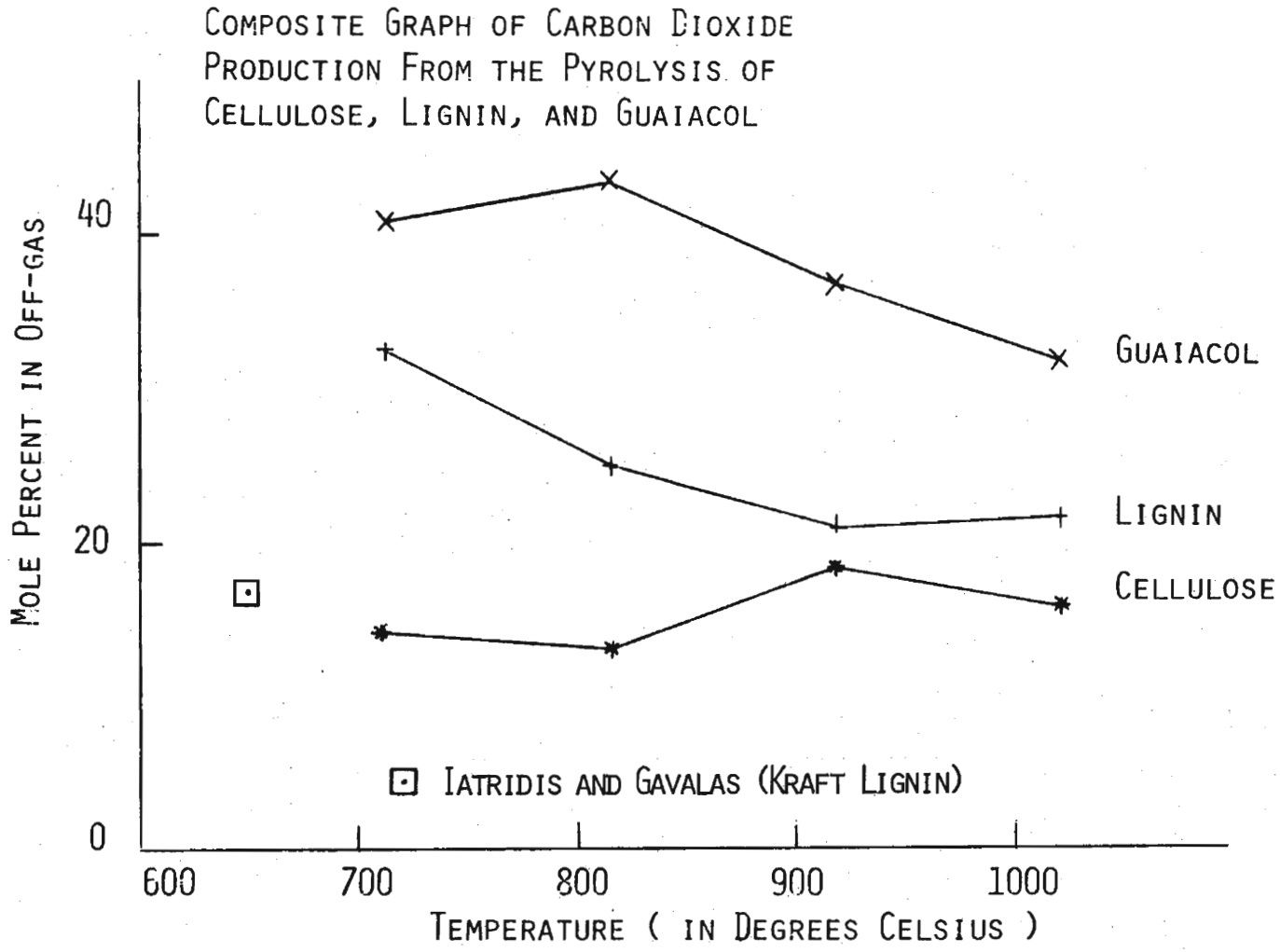
COMPOSITE GRAPH OF CARBON DIOXIDE
PRODUCTION FROM THE PYROLYSIS OF
CELLULOSE, LIGNIN, AND GUAIACOL
MOLE PERCENT IN OFF-GAS
40
20
0
GUAIACOL
LIGNIN
CELLULOSE
IATRIDIS AND GAVALAS (KRAFT LIGNIN)
600
700
800
900
1000
TEMPERATURE (IN DEGREES CELSIUS)

FIGURE 5

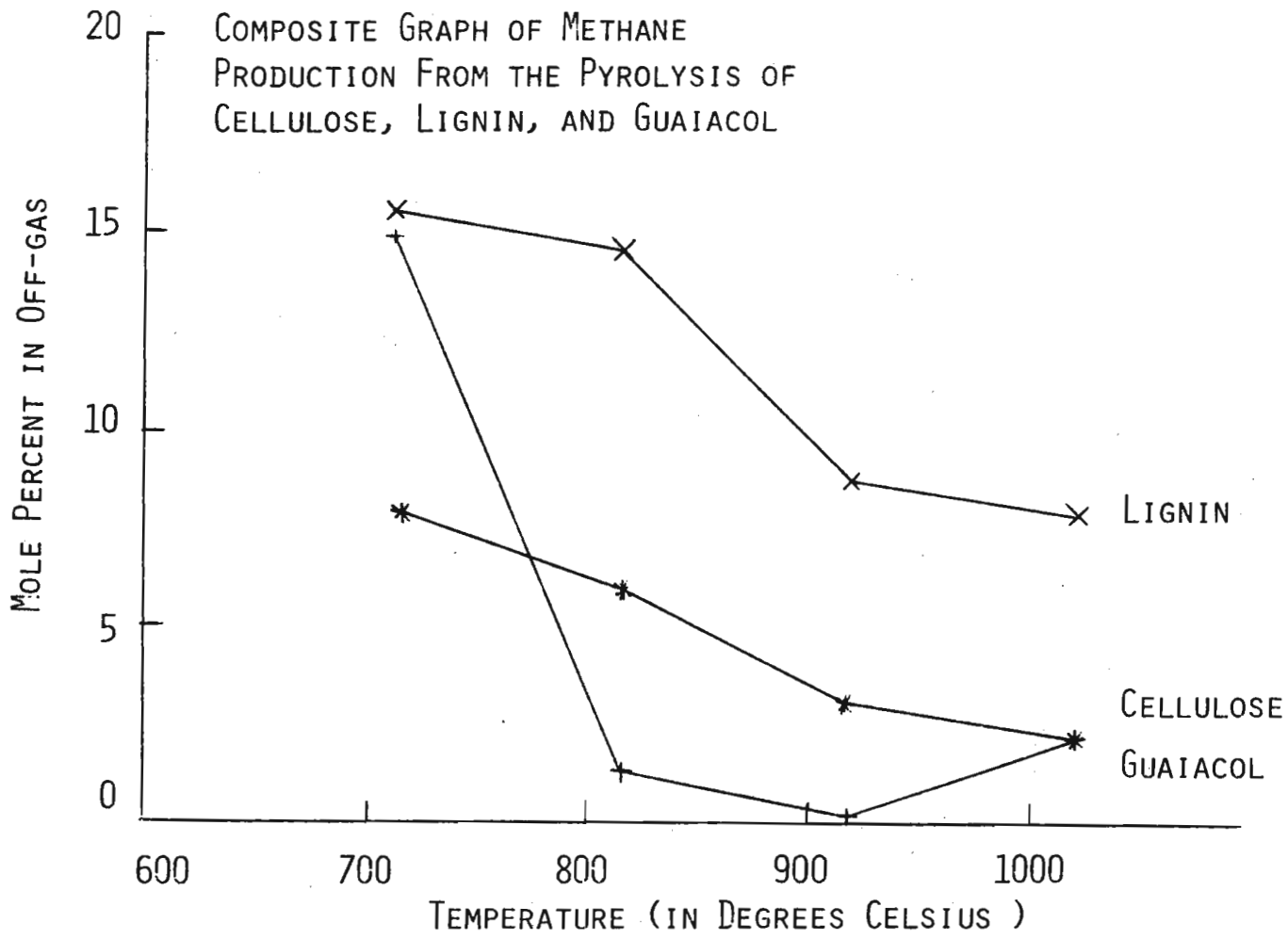
Composite Graph of Methane Production From the Pyrolysis of Cellulose, Lignin, and Guaiacol
Mole Percent in Off-gas
20
15
10
5
0
600
700
800
900
1000
Temperature (in Degrees Celsius)
Lignin
Cellulose
Guaiacol

Figure 6

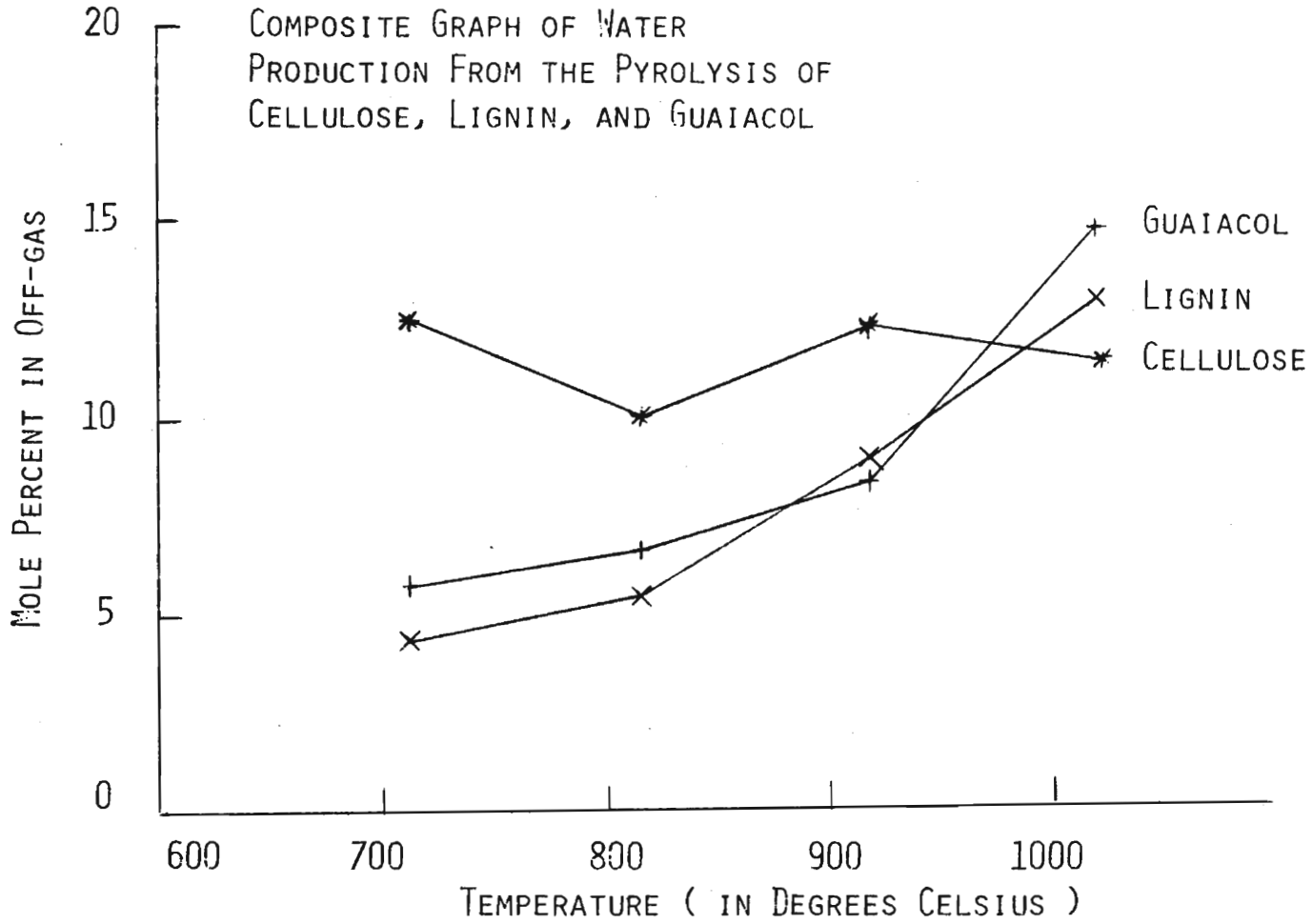
Composite Graph of Water
Production From the Pyrolysis of
Cellulose, Lignin, and Guaiacol
Mole Percent in Off-gas
20
15
10
5
0
600
700
800
900
1000
Temperature (in Degrees Celsius)
Guaiacol
Lignin
Cellulose

Figure 7

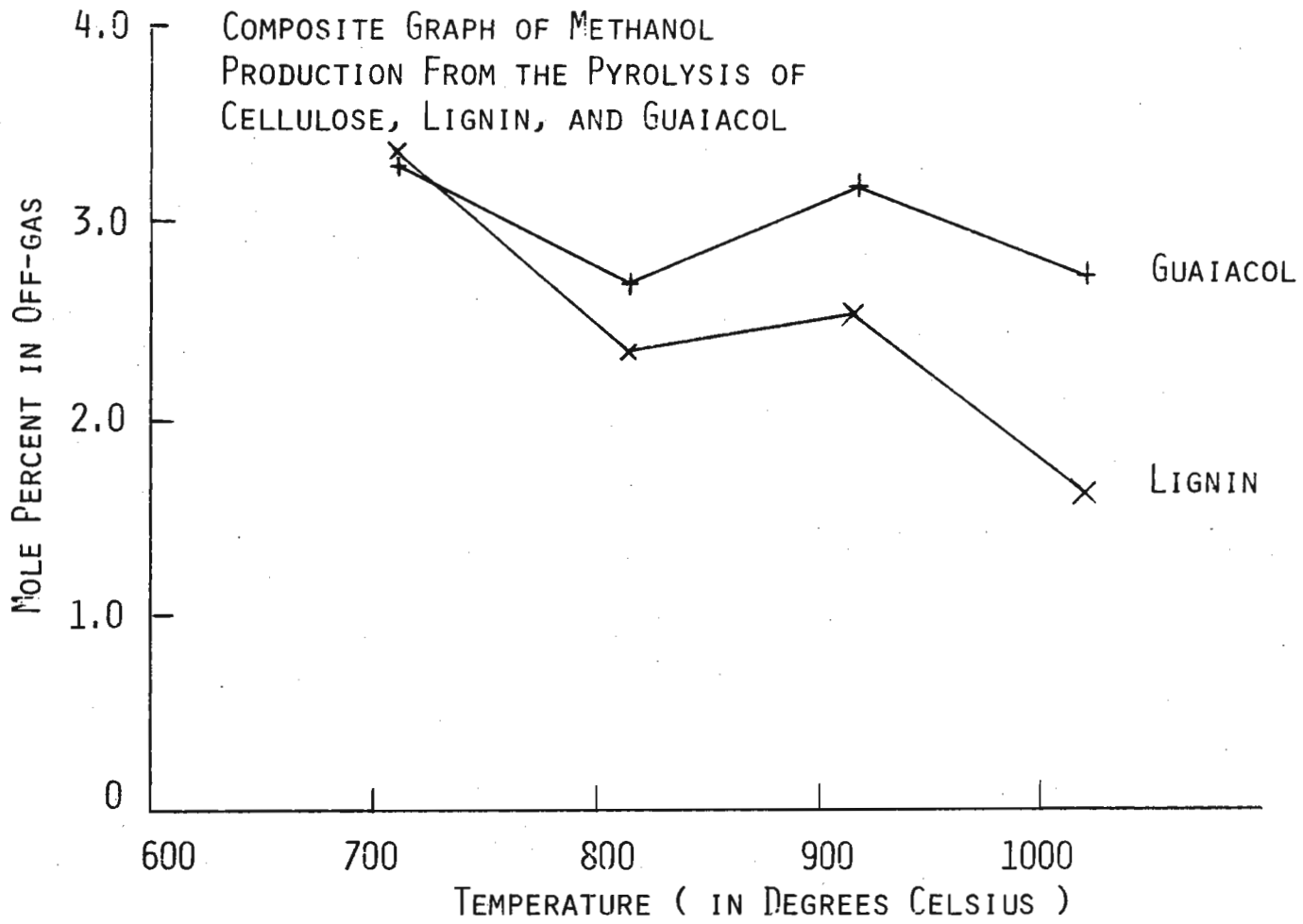
Composite Graph of Methanol Production From the Pyrolysis of Cellulose, Lignin, and Guaiacol
Mole Percent in Off-gas
4.0
3.0
2.0
1.0
0
600
700
800
900
1000
Temperature (in Degrees Celsius)
Guaiacol
Lignin

Figure 8

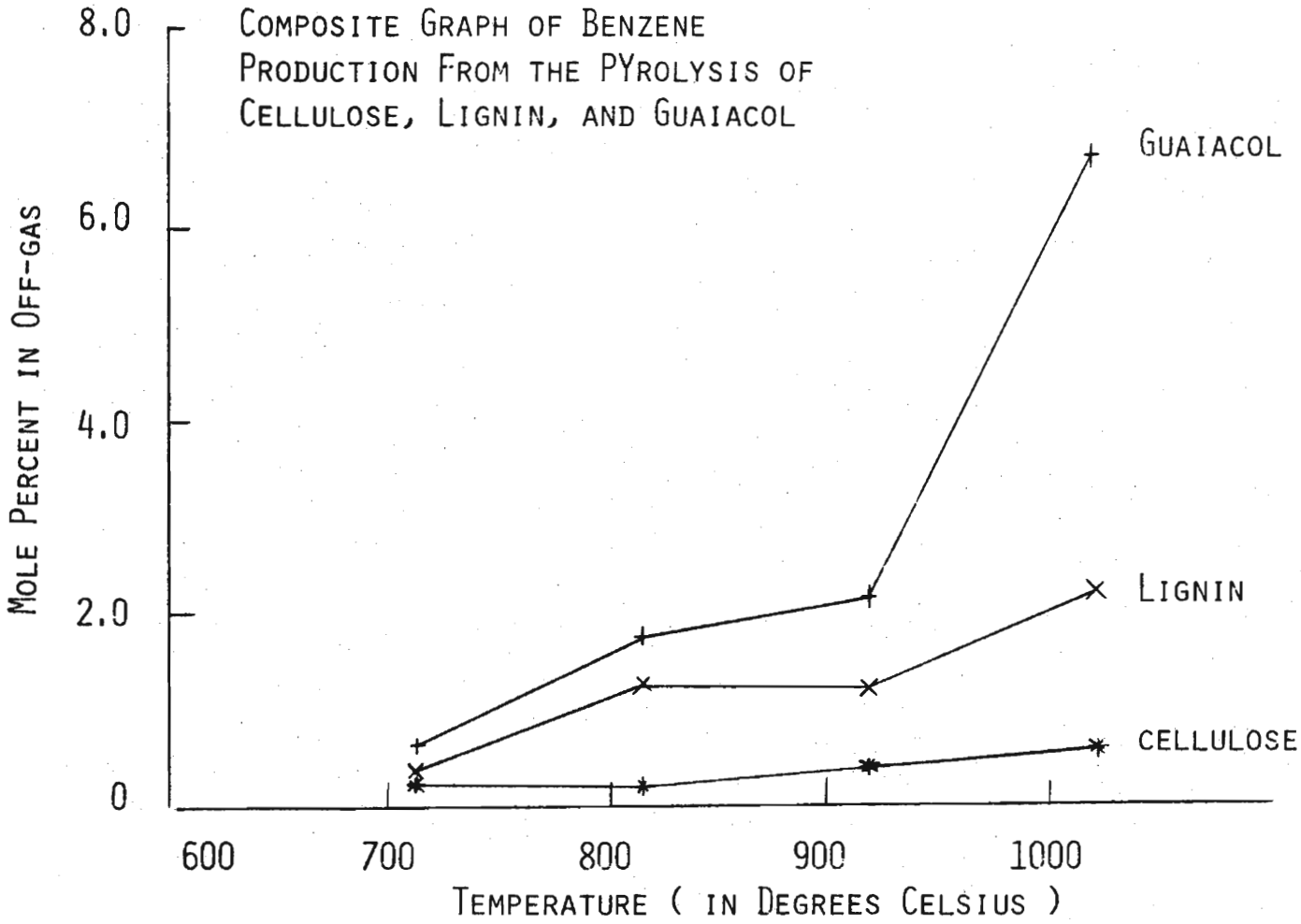
Composite Graph of Benzene Production From the PYrolysis of Cellulose, Lignin, and Guaiacol
Mole Percent in Off-gas
8.0
6.0
4.0
2.0
0
600
700
800
900
1000
Temperature (in Degrees Celsius)
Guaiacol
Lignin
cellulose

Figure 9

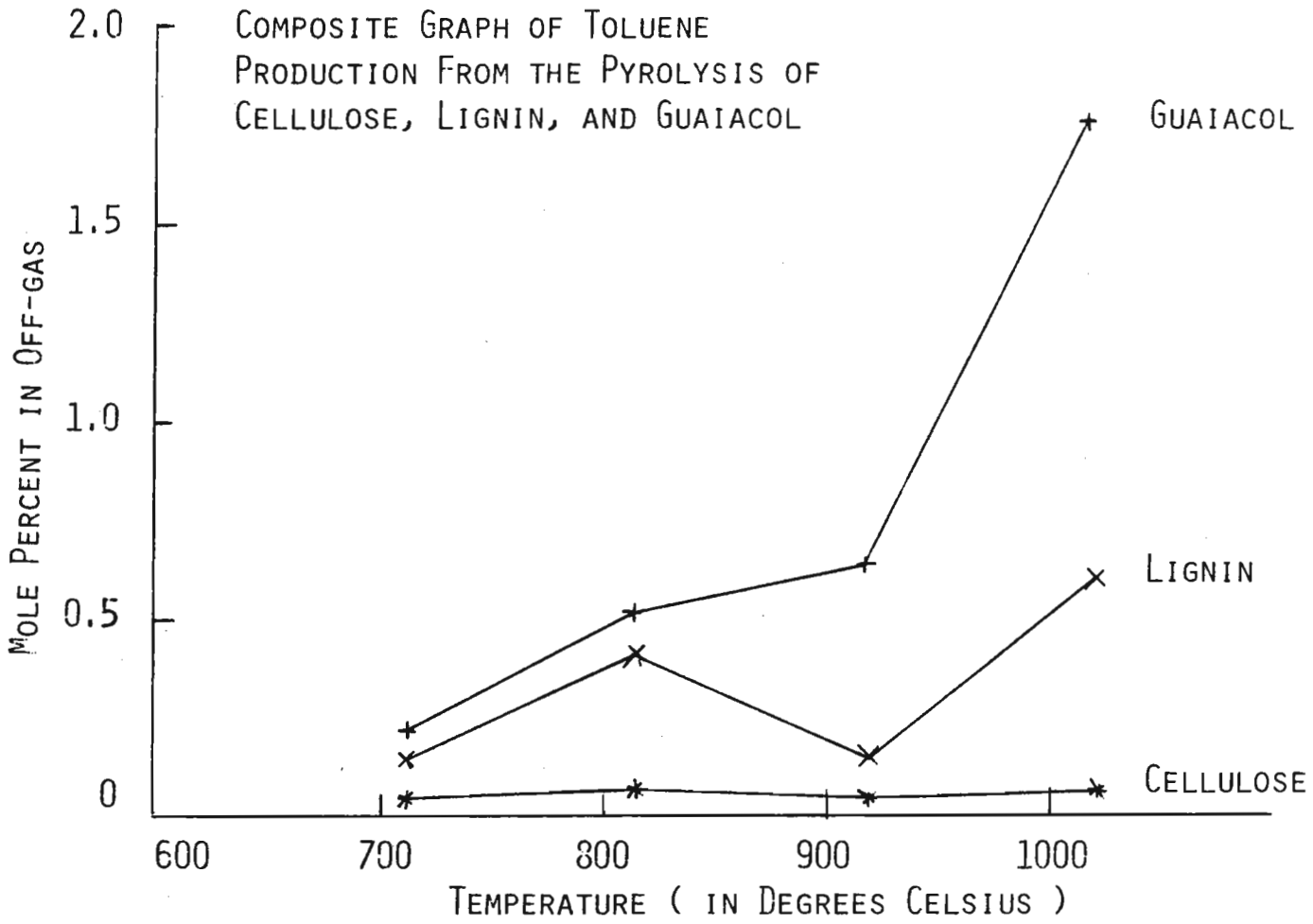
COMPOSITE GRAPH OF TOLUENE
PRODUCTION FROM THE PYROLYSIS OF
CELLULOSE, LIGNIN, AND GUAIACOL
GUAIACOL
LIGNIN
CELLULOSE
MOLE PERCENT IN OFF-GAS
2.0
1.5
1.0
0.5
0
600
700
800
900
1000
TEMPERATURE (IN DEGREES CELSIUS)

FIGURE 10

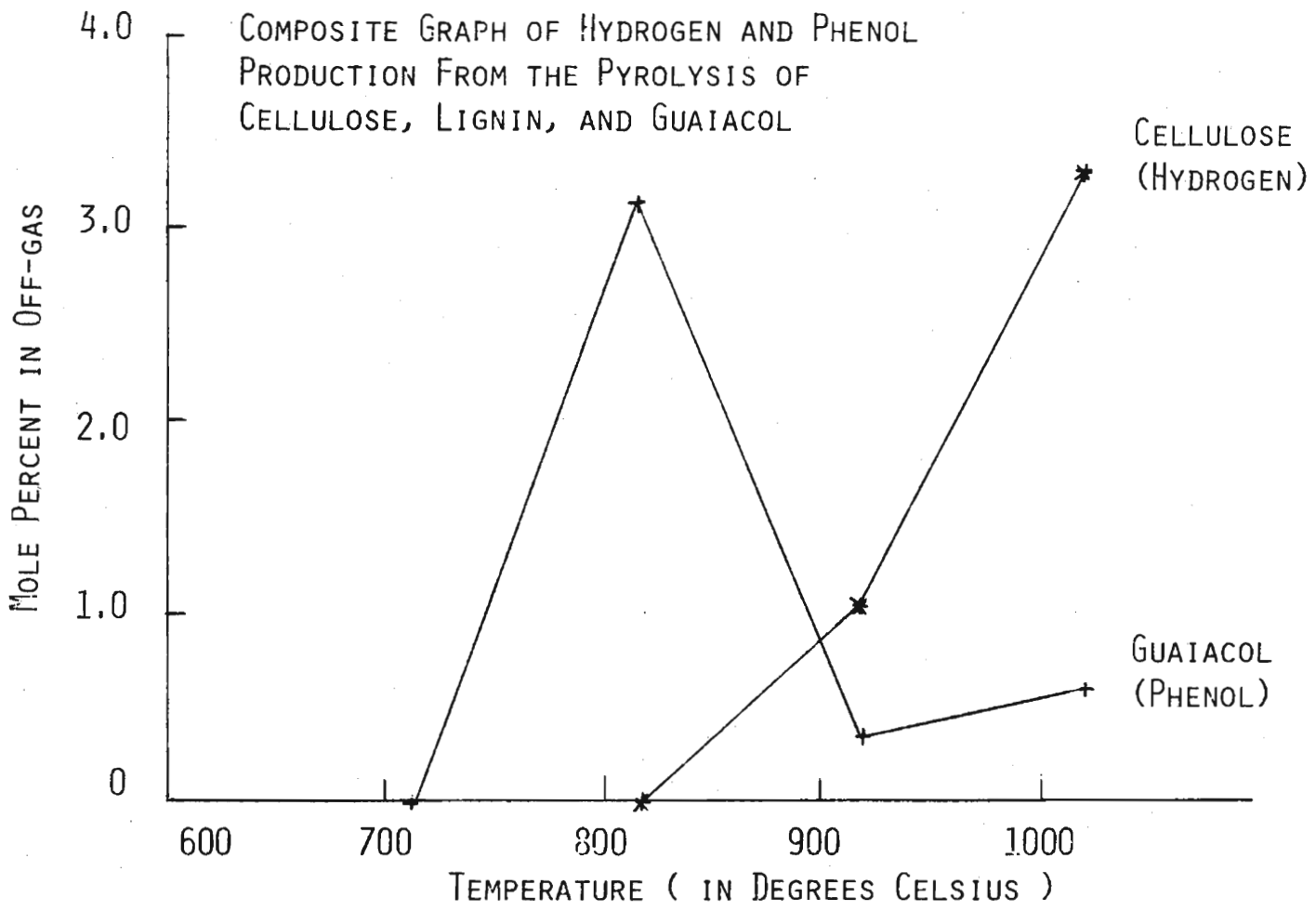
Composite Graph of Hydrogen and Phenol
Production From the Pyrolysis of
Cellulose, Lignin, and Guaiacol
Cellulose
(Hydrogen)
Guaiacol
(Phenol)
Mole Percent in Off-gas
4.0
3.0
2.0
1.0
0
600
700
800
900
1000
Temperature (in Degrees Celsius)

Figure 11

reproductibility of the reported percentages is about ± 3%. The gas compositions determined are different in several aspects from those reported for the pilot plant unit operating on sawdust and other biomass (Table 1). The lower CO_2 content from the pilot plant unit reflects removal of CO_2 in the water scrubber. The low hydrogen content of the gas from the small experimental unit probably reflects conversion to water by reaction with oxygen entrained with the entering cellulose or lignin. Due to a more elaborate method of solid feed introduction, the atmosphere in the pilot plant unit was probably more reducing than that in the small experimental unit.

Of greatest interest is the increase in the yield of benzene and toluene with increasing temperature. The yields from guaiacol were significantly higher than from lignin or cellulose. The Barber-Colman files contain a report of an anomalous run on wood chips where a high yield (12%) of BTX was found. We have been unable to attain this yield for cellulose or lignin in the temperature range 700 to 1000°C.

Few literature data are available which can be directly compared with our results. Iatridis and Gavalas [3] pyrolyzed a precipitated kraft lignin in helium at 1 atmosphere over the temperature range 400 to 650°C. Their samples were held between two folds of a stainless steel wire cloth functioning as a resistance heater. They found methane, CO, CO_2, and methanol as major products, with single ring phenols reaching a maximum yield of about 3% at 650°C. Their yields of CO and CO_2 at 650°C are plotted in Figures 4 and 5.

Lead Contamination of Char

A study was made of factors affecting the contamination of char by lead in the lead bath pyrolysis of wood waste [4]. One-quarter inch lengths of 0.8 cm dowel stock were pyrolyzed at temperatures from 730°C to 1050°C. The effect of residence time on the lead hearth was also investigated, with times from 10 seconds to 120 seconds being studied. The char produced had a void fraction of 0.4, and a surface area of 360 m^2/g, as determined by BET adsorption of nitrogen. The char samples were extracted with 7 $\underline{M}$ HNO_3, and the lead content of the filtrate determined by atomic adsorption spectroscopy. It was found that the lead content of the char was affected much more by pyrolysis contact time than by pyrolysis temperature. After ten seconds of pyrolysis at 800°C the wood char contained 135 ppm lead. This increased to 240 ppm after 120 seconds of pyrolysis.

Scanning electron microscope photographs of the internal and external surfaces of the long time char revealed that bulk metallic lead did not enter the interior of the char even after 100 minutes on the lead bath. This conclusion was confirmed by an electron microprobe study of a cross-section of a short time char sample. Although macroscopic drops of lead near the external surface of the char were visible in the electron microscope photographs, calculations showed that these represented only a small fraction of the total lead content of the char. This would indicate that physical adsorption of lead vapor on the pore walls was the predominant mechanism of lead contamination.

Thus, a possible method of removing lead from the char would be to blow the hot char with steam after it is raked off the lead hearth.

References

1. Piron, E. H., and Crawford, R. M., "The Piron Coal Distillation Process" Proceedings of the International Conference on Bituminous Coal, Carnegie Institute of Technology, November 15-18, 1926, pp 729-746

2. Blankinship, Richard M., MSc Thesis, Michigan Technological University, 1979

3. Iatridis, B., and Gavalas, G. R., Ind. Eng. Chem. Prod. Res. Dev. 18, 127-130 (1979)

4. Alsgaard, David W., MSc Thesis, Michigan Technological University, 1979

Abstract

In the continuous lead bath pyrolysis process biomass is ground to less than 0.6 cm in the longest dimension and fed by a screw conveyor onto the surface of a molten lead bath maintained at 760°C. Gases liberated in this high temperature, short contact time pyrolysis are water quenched, and the aromatics removed in an oil scrubber. The gas leaving the scrubber is a medium Btu fuel gas. The char formed on the molten lead hearth is removed by a raking mechanism after a residence time of 45 to 90 seconds.

To explore the effect of temperature on product distribution, samples of cellulose, lignin, and a model compound (guaiacol) were pyrolyzed on a pool of lead in a small laboratory unit. Pyrolysis temperatures ranged from 750°C to 1000°C. Total gas production increased with increasing temperature. Benzene yield from lignin increased from 0.4% at 720°C to 2% at 1000°C.

Separate studies of contamination of the char by lead revealed that pyrolysis contact time was more important than pyrolysis temperature. The predominant mechanism of char contamination by lead was adsorption of lead vapor on the pore walls.

PREPARATION OF POWDERED FEEDSTOCK FROM BIOMASS WITH STEAM

Q. Nguyen and G. Noble
Iotech Corporation Ltd., Ottawa, Ontario Canada

ABSTRACT

Pretreatment is prerequisite for effective enzymatic saccharification of lignocelluloses. Steam explosion pretreatment fractionates lignocelluloses into three main components: highly accessible cellulose which retains the basic crystalline structure, hemicellulose rendered hot water soluble and thermoplastic lignin soluble in aqueous ethanol and dilute sodium hydroxide solution. The biomass is subjected to saturated steam at 3450-6900kP (500-1000psi) for 5 seconds to 5 minutes then explosively released to atmospheric pressure. The substrate is pulverized into a powder, 60% of which passes through 200 mesh screen. Glucose and xylose yields of 90% and 75% of theoretical respectively are obtained after 24 hour enzymatic hydrolysis of steam exploded aspen. Highly reactive lignin can be recovered with 80% yield. The estimated operating cost of the steam explosion is $7.50/OD ton of biomass. At this low cost, the Iotech process achieves many pretreatment requirements in one step. Total utilization of biomass is achieved since the high quality lignin can be used for chemical feestock.

INTRODUCTION

Effective pretreatment at a low cost is a key factor in the commercial utilization of lignocelluloses for chemicals by biological conversion processes. The most desirable pretreatment would give maximum yields of the three main components of biomass, namely cellulose, hemicellulose and lignin, in suitable forms for subsequent processing. One of the major deterrents in the enzymatic saccharification of biomass is the lignin-hemicellulose complex embeding in the cellulose structure. To make the cellulose accessible, this lignin-carbohydrate complex must be broken up. The pretreated biomass substrate should also be in a finely divided form to achieve high specific surface area.

Delignification by pulping processes does not achieve effective utilization of biomass since the use of high value lignin is often neglected. Other methods for enhancing cellulose accessibility such as: swelling with sodium hydroxide solution, comminution, irradiation are

either ineffective or very expensive. Iotech Corporation Ltd. has developed a patented pretreatment process which satisfies the requirements mentioned above.

THE STEAM EXPLOSION PROCESS

The explosion processes for pulverizing permeable material such as wood, coal, ore, minerals etc., have been known for quite some time [1]. The basic principle is to impregnate the material to be exploded with a suitable fluid (usually steam) at high pressure and temperature for a certain period of time in a pressure-tight cylindrical shape vessel, then suddenly release the pressure. The decompression causes an instantaneous expansion of the fluids occupying inside the pores or cells resulting in size reduction of the exploded materials. High temperature also weakens the structure of many materials, adding to the degree of pulverization.

Extensive optimization tests have been carried out with aspen wood (Populus Tremuloides) because it is the most abundant hard wood species in Canada which has not yet been fully utilized. Hybrid poplar clones have been developed to give very high biomass yields with short rotations.

In typical process conditions, green wood chips are steamed at 3450-6900kP (500-1000psi) for 5 seconds to 5 minutes in the gun as shown in Figure 1. At the end of the cook, the steam inlet is shut off and the discharge valve is opened. The chips extrude through an orifice at the gun nozzle and into a cyclone collector where excess steam is flashed off and recovered. Exploded wood has an average moisture content of 63% based on wet weight as compared to 50% of input chips. The cyclone we use is under-sized and unheated. There is a considerable amount of steam blowing downwards and condensing on exploded wood being collected in a bin placed beneath the cyclone. With a properly designed collector, we believe that the moisture content can be reduced to less than 60%.

The following variables were found to be significant to the extent of size reduction: temperature, steaming time and pressure drop when the explosion takes place. Sufficient time must be allowed for the center of the chips to reach the softening temperature, $> 220^{o}C$, at which the fiber structure fails [2]. The degree of pulverization was found to increase with larger pressure drop. However, the effect of pressure was less significant beyond 4800kP (700psi).

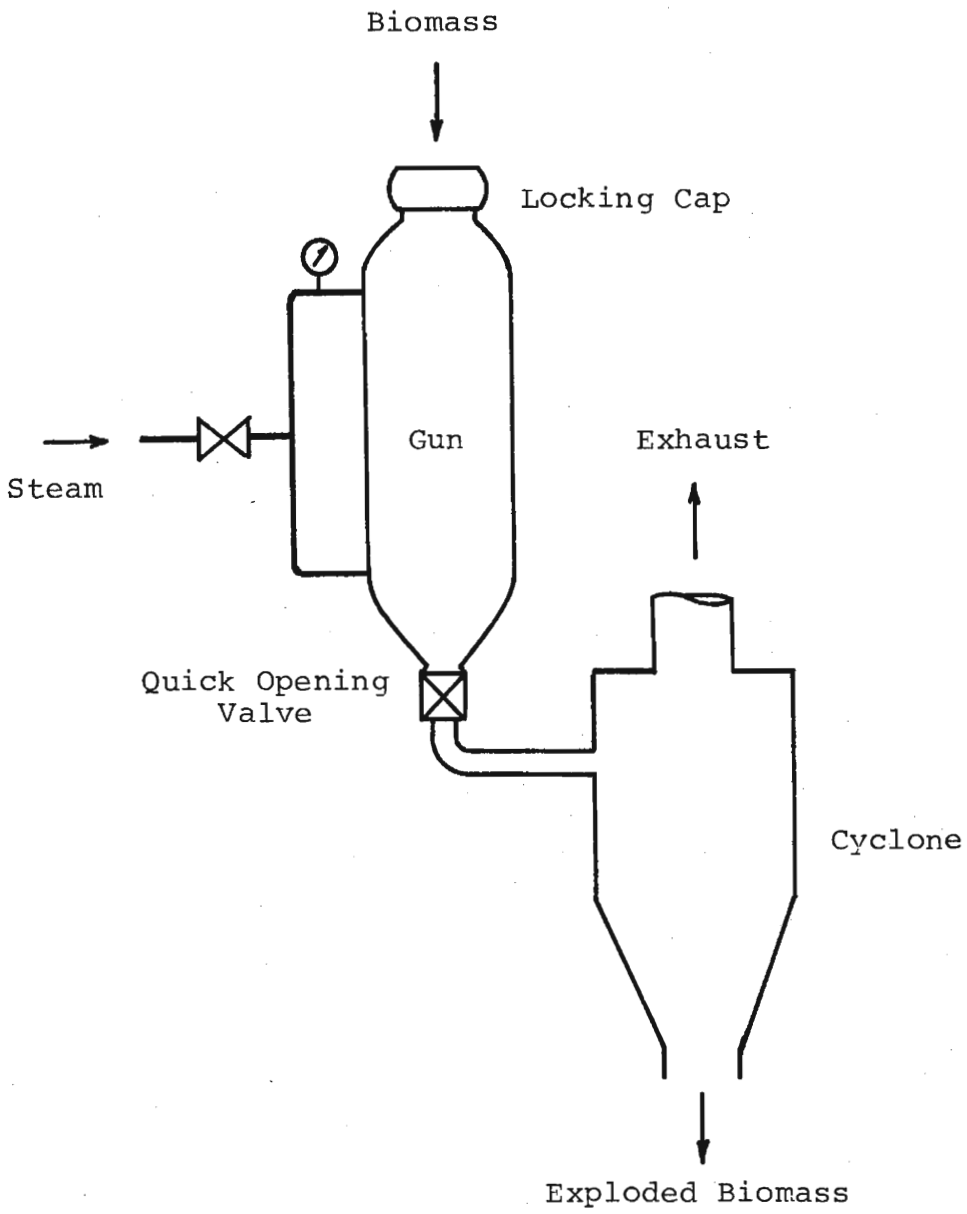

FIGURE 1
SCHEMATIC DIAGRAM OF THE GUN

Other less important variables were: chip size, moisture content of chips, gun nozzle configuration. Heat penetrates to the center of the small chips faster than to the center of large chips. With cooking time adjusted accordingly, similar results were obtained from hammer milled chips and commercial chips. Drier chips required slightly shorter cooking time. The use of constricting dies with similar cross-sectional area in the gun nozzle such as: circular, star shape, perforated plate, had little effect. Some of the dies created more shear to the extruded fibers but also slowed down the discharge rate resulting in smaller pressure drop. Straws with their delicate structure and low lignin content required less severe treatment as compared to wood.

STEAM HYDROLYSIS OF LIGNOCELLULOSE

High pressure steam rapidly hydrolyses the acid groups attached to the hemicellulose into acetic acid and uronic acid which then attack the lignin-hemicellulose complex and the amorphous cellulose regions. Hydrolysis occurs at the glycosidic bonds, the bonds of lignin-hemicellulose complex and the and ether linkages of lignin. Only the amorphous cellulose regions are subjected to attack by the available weak acids since the tight structure of highly crystalline cellulose is impermeable. Steam hydrolysis of lignocelluloses in the gun was found to be first order reaction and the rate approximately doubles at a temperature increase of 10^{o}C. Prolonged cooking also causes oxidation and degradation of hemicellulose and condensation of lignin. Dehydration of xylose yields furfural, some of which can condense with the lignin. At high temperature the hydrolysis rate of hemicellulose is much faster than the degradation rate of the product. Therefore, it is necessary to use high pressure steam and short cooking time to obtain high yields of xylose. Because of the short cooking times required it is advantageous to have the instant discharge feature of the gun which enables one to terminate the reactions and to cool down the product in a split second.

EXPLODED ASPEN WOOD AND ITS UTILIZATION

About 60% of exploded aspen wood passed through the 200 mesh screen (0.074 mm opening) of a Bauer-McNett fiber classifier. The degree of pulverization increases as steam pressure goes up. The fiber classification results of aspen wood processed at four different pressures are shown in Table 1. The size distribution of input chips is given in Table 2. Each sample was cooked to a similar degree of hydrolysis. Finer fiber size may be obtained

if cooking time is increased for higher operating pressure shots.

TABLE 1
FIBER CLASSIFICATION OF EXPLODED ASPEN WOOD

Screen mesh	2000 (290)	3033 (440)	3792 (550)	4481 (650) kP psi
	% exploded wood			
48 < 1 < 28	46.3	34.4	23.2	4.4
100 < 1 < 48	9.2	16.9	2.6	15.1
140 < 1 < 100	15.5	4.5	22.8	18.8
200 < 1 < 140	2.6	4.9	5.3	4.3
1 < 200	26.4	39.3	46.1	57.4

TABLE 2
SIZE DISTRIBUTION OF HAMMER MILLED ASPEN WOOD

Screen Opening, mm		Tyler Equiv. Mesh	Weight Percent
Retained by	9.51	0.371 in.	17.9
"	4.76	4	38.6
"	3.36	6	22.6
"	1.00	16	16.5
Pass	1.00	16	4.4

Exploded aspen has the appearance of peat moss. The brown colour is attributed to the hydrolysed lignin and the sugars. Because of its finely divided form the product can be dried quickly by blowing hot air over it. With the presence of water soluble hemicellulose, the fibers tend to stick together in small lumps upon drying.

Exploded aspen can be fractionated into three main components: cellulose, hemicellulose and lignin by solvent extraction. Most of the hemicellulose can be extracted with hot water, more than half of which is free pentose. Under optimum conditions less than 20% of the original hemicellulose is degraded. Over 90% of the lignin can be extracted with 0.1N NaOH solution at room temperature and 80% is recovered by precipitation with acid. About 20% of the original lignin is rendered water soluble. A lignin fraction respresenting 51% of the original amount in the wood was extracted with ethanol. The lignin was fractionated with methanol and benzene mixture and the number-average molecular weights of the fractions were obtained with a vapour pressure osmometer [3]. 19% of the above lignin had a molecular weight of 463 or lower. 39% had a molecular weight of 664 or lower, and the highest molecular weight observed was only 3340. The remaining lignin in the pulp had higher molecular weight. The isolated lignin softens at 120-130^{o}C, when moisture is present the softening temperature drops to 90-100^{o}C.

The caustic washed pulp is over 90% alpha cellulose. The cellulose retains the basic crystalline structure [4]. The degree of polymerization varies from about 800 to the limit 200 depending on the extent of the hydrolysis.

The effects of temperature and cooking time on sugars yields and on lignin extractable with caustic soda are shown in Figure 2. At low processing temperature and pressure long cooking time is required to achieve maximum cellulose accessibility, but considerable degradation of hemicellulose also occurs and the lignin is heavily condensed and less reactive. The maximum yields of the three components also do not arise at the same time. At high temperature and short time conditions, 90% glucose and 75% xylose yields and high quality lignin have been obtained. The prospect of ethanol fermentation of xylose is good, therefore, the potential ethanol yield from exploded aspen is substantially increased. A lignin formaldehyde resin has been successfully formulated and tested. Figure 3 summarizes one of many possible ways of utilization of exploded biomass.

COST ESTIMATE

A detailed engineering design of the steam explosion process gives an estimated operating cost of $7.50/OD ton of biomass. The operating cost includes costs of capital, maintenance, labour and steam. The cost of steam is a relatively small factor in the cost economics when the recovered steam can be utilized.

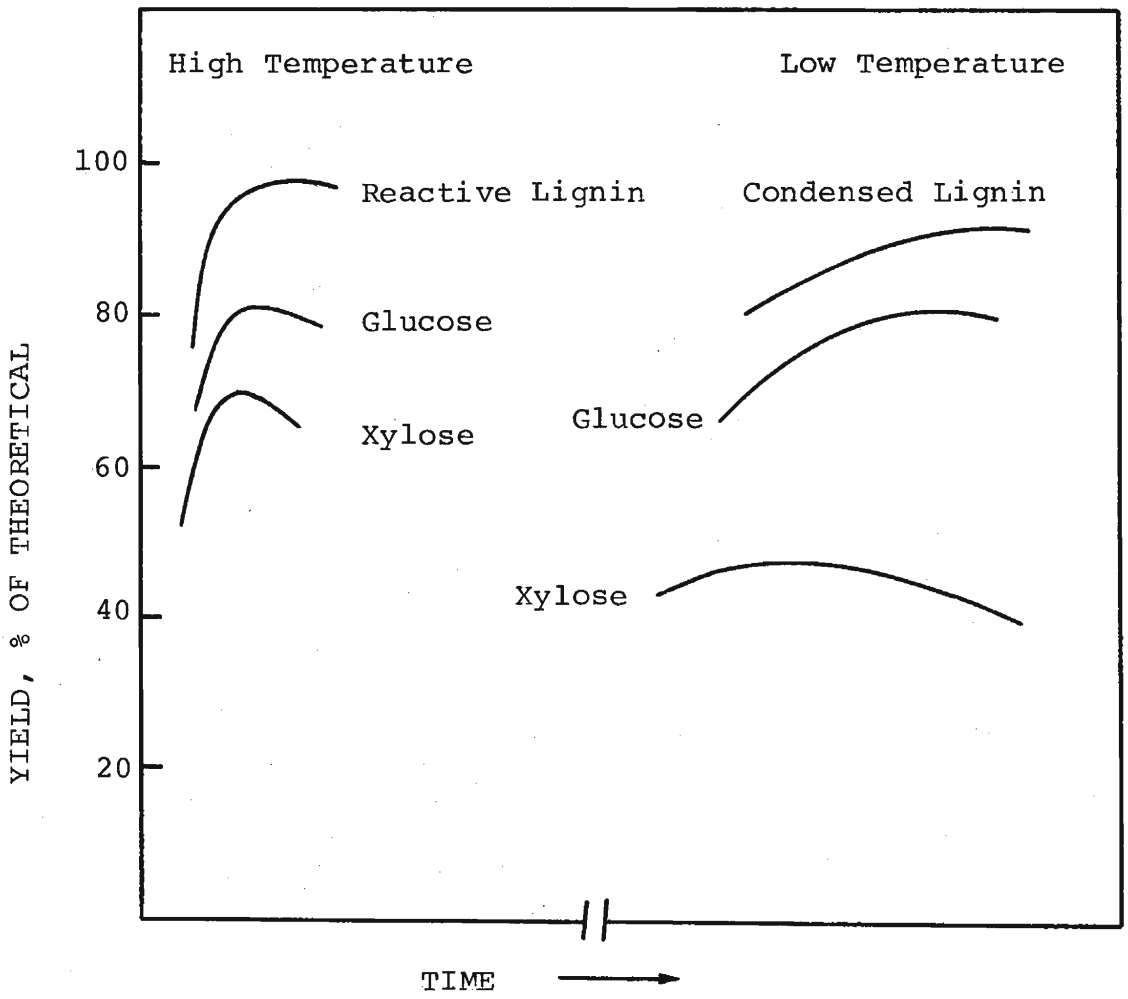

FIGURE 2
EFFECT OF TEMPERATURE AND COOKING TIME ON SUGAR YIELDS AFTER 24-HOUR ENZYMATIC HYDROLYSIS AND ON LIGNIN EXTRACTABLE WITH 0.1N NaOH SOLUTION

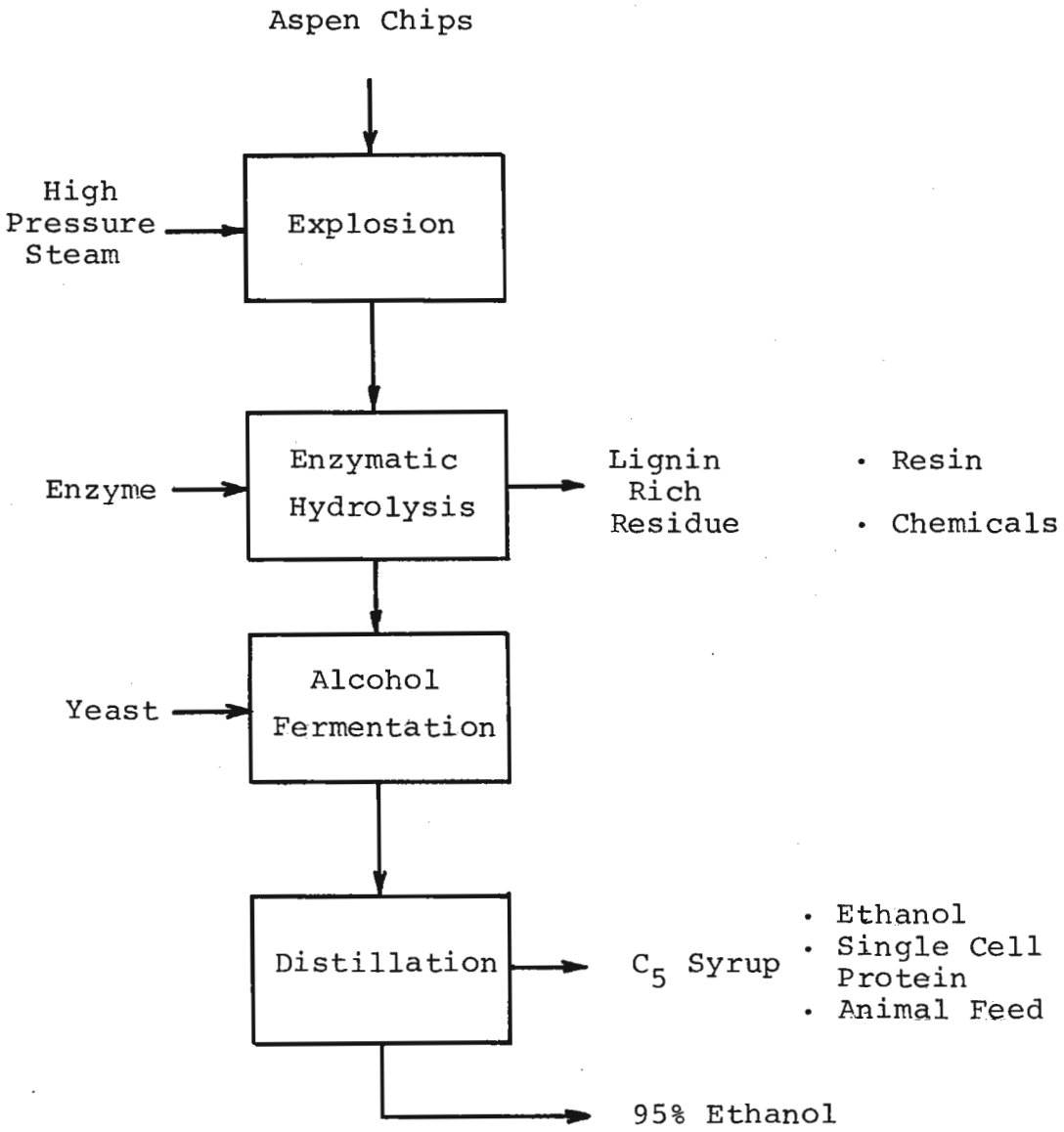

FIGURE 3
SCHEMATIC DIAGRAM FOR THE UTILIZATION OF EXPLODED ASPEN

Energy requirements for comminuting dry pine shavings to various screen sizes were reported by Millet et al [5]. At a size equivalent to Iotech exploded wood the energy cost alone was estimated at $30/ton. This figure does not include the cost of drying and capital related expenses which would push the cost of milling even higher.

CONCLUSION

Steam explosion is a low-cost pretreatment process which achieves several desirable effects in one step:

a) The carbohydrates are highly accessible to enzymes.

b) The lignin is recovered in a suitable form for conversion into useful chemicals.

c) The biomass is pulverized into a powder thus increasing the active surface area.

d) The product is sterilized by steam so that risk of contamination in the downstream biological processes is reduced.

REFERENCES

1. Meigs, D., "Explosion Unit Operation of the Process Industries", Chem. & Met. Eng., (Feb. 1941), pp. 122-125.

2. Baldwin, S.H. and Gorring, D.A.I., "The Thermoplastic and Adhesive Behaviour of Thermomechanical Pulps from Steamed Wood", Svenok Papperstidnig, II (1968):18, pp. 646-650.

3. Brownell, H.H., Contract Report No. 65-80-528, Forintek Canada Corp., Ottawa, Canada, 1980.

4. Marchessault, R.H. and St.-Pierre, J., "A new understanding of the carbohydrate system", CHEMRAWN I, Pergammon Press, Toronto, Canada, 1978, pp. 613-625.

5. Millet, M.A., Baker, A.J., and Satter, L.D., "Physical and Chemical Pretreatments for Enhancing Cellulose Saccharification", Biotechnol. & Bioeng. Symp. No. 6, John Wiley & Sons Inc., 1976, pp. 125-153.

THE EMBRITTLEMENT TREATMENT OF WHEAT STRAW FOR CONVERSION TO A POWDER+

A. A. Ghazee
University of Dayton Research Institute
Dayton, Ohio 45469

N. L. Hecht
University of Dayton Research Institute
Dayton, Ohio 45469

Introduction

In this project conducted at the University of Dayton (UDRI), fifteen pounds of wheat straw were treated with HCl and converted to a fine powder. The treatment used was based on the procedures established in a previous program to develop cellulose embrittlement processes to produce RDF-powder from MSW. Twelve pounds of powder were sent to SERI for evaluation in its pyrolysis facility. In addition powder samples were analyzed to determine the effectiveness of the embrittlement process and characterize the powder obtained from the wheat straw.

Background - Cellulose Embrittlement

In recent years, we have begun to look with renewed interest upon a variety of cellulose waste materials as a promising alternate source of energy. Cellulose wastes are categorized as biomass materials which in the 1800's served as a primary fuel source for the United States. Biomass materials can be converted to liquid, solid, or gaseous fuels by a number of chemical, biological, and thermal processes.

Most of the organic waste in municipal and industrial refuse as well as agricultural wastes are termed biomass since they are plant materials. Included in this category are waste paper and wood products (newsprint, cardboard, furniture, packaging materials, etc.), crop and food processing residues (straw, corn cobs, husks, etc.), logging and wood manufacturing residues (branches, stumps, bark, sawdust, etc.) as well as manure and sewage sludge.

The major constituents of most biomass materials are cellulose, hemicellulose and lignin. The quantities of each of these constituents vary depending on the type of plant material, the type of processing it received and whether it is a paper or wood product. A tabulation of the general composition for several important types of biomass materials is presented in Table I.

+This work was sponsored by SERI

TABLE I

BIOMASS MATERIAL COMPOSITIONS

Biomass Material	Composition (%)				
	Cellulose	Hemicellulose	Lignin	Mineral Matter	Waxes, Resins, etc.
Hardwoods	40-55	24-40	18-25	1	2-12
Softwood	45-50	25-35	25-35	1	2-12
Grasses, straw, etc.	25-40	25-50	10-30	2-9	?
Leaves	15-20	85	-	-	tr
Newsprint	40-50	20-40	18-30	1-4	tr
Waste Paper	60-80	20-30	2-10	2-6	tr

Most biomass materials are cellulosic compounds composed of 30-50 percent α-cellulose, 20-40 percent hemicellulose and 10-25 percent lignin. Cellulose is a linear glucose polymer of D-anhydroglucopyranose units linked by β-1-glucosidic bonds as shown in Figure 1. Hemicellulose is a polysaccharide intimately associated with cellulose but with a lower molecular weight. Lignin is a complex polyhydric polymer containing condensed phenolic, open phenolic, condensed ether, open ether and alcoholic groups. These three major constituents are combined into a fibrous structure which makes up the main body of most plant material.

Wood fiber serves as a good model to demonstrate the complex interrelationship of the cellulose, hemicellulose and lignin constituents. A cross section of a wood fiber ash shown in Figure 2 consists of a central cavity (lumen) surrounded by two concentric layers. The inner layer (middle layer) adjacent to the lumen consists of an inner and outer skin which is mostly cellulose and hemicellulose encasing a middle lamella which is mostly lignin. The outer layer (primary wall) serves as an elastic membrane around the outside of the fiber and consists mostly of cellulose, hemicellulosic materials, and some lignin. The zone between wood fiber cells is principally lignin. The cellulose fibers in the inner and outer skins are helical around the fiber axis.

The cellulose in the wood fiber has a fibrous morphology consisting of crystalline and amorphous areas. The molecular weight and chain length are variable and in most cases only average values can be determined.

Wood fibers, because of their pore structure and general cellular nature have a large internal surface area and are highly adsorbent. They have a particularly strong affinity for water. Dry cellulose fibrous materials under normal atmospheric conditions contain 15-30 percent moisture. Water can be in the fibrous structure as bound water, capillary water or imbibed water. Bound water is held by adsorption on the surface of the cellulose crystallites. This water is strongly bonded to the cellulose and no longer exhibits the properties of "free water". Capillary water is found in the fiber pores but is not intimately bound to the cellulose fibers. Imbibed water fills the lumen and coarse pores of the fiber and remains as free water.

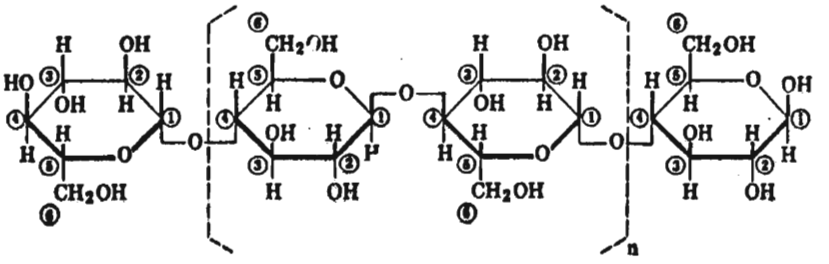

Figure 1. Chemical Structure of Cellulose

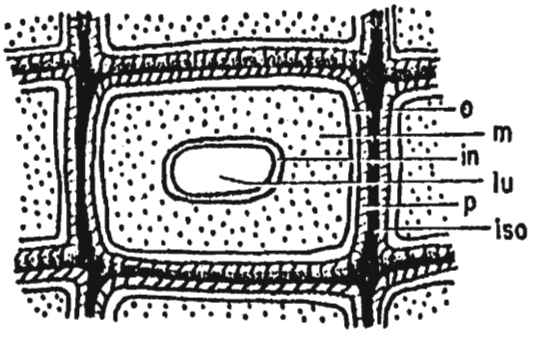

Figure 2. Cross Section of a Wood Fiber with Adjoining Areas: (o) outer layer, secondary wall; (m) middle layer, secondary wall; (in) inner layer, secondary wall; (lu) lumen; (p) primary wall; (iso) isotropic intercellular substance.

Thermal treatments alone can be used to degrade cellulosic materials. Heating above 200°C (392°F) for long periods will result in a loss of fiber structure as well as loss of hygroscopicity. Significant degradation can even be observed at temperatures of 150°C (302°F). Initial studies at the UDRI showed that thermal treatments resulted in moderate embrittlement of cellulosic materials. It is believed that this occurs by the formation of hydrogen or ether bonding between adjacent cellulose molecules.

Treatment of cellulosic materials with oxidizing agents will also cause a breakdown to products of lower molecular weight. These products can vary from practically unchanged fibers to a friable powder. In screening studies performed at the UDRI it was found that exposure of shredded newsprint to Cl_2 (an oxidizing agent), resulted in substantial embrittlement of paper. However, considerable Cl_2 was adsorbed by the paper when it was exposed to the embrittlement treatment. It would appear that ozone or H_2O_2 might be a more desireable oxidizing agent since it would not present potential corrosion or pollution problems if it were adsorbed by or reacted with the cellulosic material during treatment.

Mineral acid treatments have been found to be very effective for the embrittlement of cellulosic materials. Nitric, sulfuric, and hydrochloric acid treatments have proved to be the best reagents in the studies conducted at UDRI and in work reported by Combustion Equipment Associates (CEA). The work performed at CEA served as the basis for the development of a proprietary process for converting MSW to a powder fuel (Eco Fuel-II). The results of the studies at UDRI showed that HCl was the most effective embrittlement agent tried. In addition, it was found that longer treatment times and higher treatment temperatures increased the embrittlement of the cellulose samples.

An understanding of the chemical processes which result in the embrittlement of cellulosic material by HCl treatment is of fundamental importance. Such an understanding would provide a basis for modification and improvement of the present process, and could provide a rationale for subsequent development of alternative processes which avoid the use of expensive and highly corrosive agents such as HCl.

One of the anticipated results from the exposure of moist cellulosic materials to HCl is the hydrolysis of glycoside bonds in the polysaccharide backbone. Vicosity measurements on cupriethylendiamine solutions prepared from HCl-treated filter paper have in fact confirmed this expectation. Exposure to very low levels of HCl causes a dramatic decrease in the solution viscosity, indicating a decrease in the degree of polymerization (DP). In spite of this decrease in DP, however, these lightly treated cellulosic samples were not significantly embrittled. Based on these observations, it was concluded that embrittlement was not solely the result of a decrease in the DP of cellulose. Our conclusion was reinforced by common experience with over-pulping in the paper industry. Paper produced from pulp having a low DP have certain undesirable characteristics, but friability is not included as one of these. Clearly some other chemical changes must occur subsequent to the hydrolysis process.

A clue to the nature of the embrittlement process was provided by the properties of filter paper which had been heavily treated with HCl. Such samples failed to completely dissolve in the cupriethylenediamine reagent. Like the extent of embrittlement, the lack of solubility appeared to qualitatively correlate with the level of HCl treatment of the filter paper sample. However, meaningful viscosity measurements could not be conducted with these samples owing to their lack of complete solubility.

Unfortunately time and funds were not available to conduct definitive experiments which would indicate the cause for the reduced solubility of the highly embrittled samples in the reagent. Moreover, a causal relationship between reduced solubility and embrittlement has not been established for these extensively treated filter papers. Nonetheless, we suspect that the observations that were made are related, and we have developed a working hypothesis on the data available. Assuming that the cross-linking occurs via the formation of ether linkages as shown in Figure 3, the following reactions in the cellulose can be predicted:

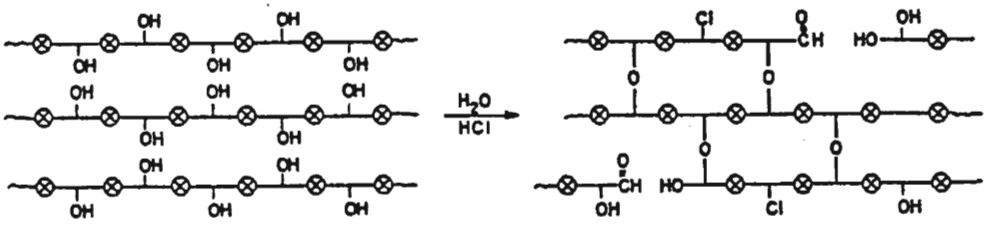

Figure 3. Possible Embrittlement Mechanism; Hydrolysis and Crosslinking of Adjacent Cellulose Chains by Oxygen Bridges.

1) Rigidization with attendant ease of fracture;
2) Decrease in solubility as the molecular shape changes from a long extended form with readily accessible OH groups to a more spherical form with reduced surface area and inaccessible OH groups;
3) A rapid decrease in molecular weight or DP as the reactive glycoside linkages are cleaved, followed by a slowing of the decrease in DP as cross-linking takes place; and,
4) A decrease in the quantity of retained HCl as the process temperature is increased. The ether cross-links are thought to be formed by the reaction of OH groups with chlorinated cellulose, and the subsequent loss of HCl. Higher process temperatures should lead to more complete cross-linking and loss of HCl.

Powder Preparation

The major emphasis of this project was the production of powder from wheat straw for analysis. About 15 pounds of wheat straw were obtained from SERI to be used as the feedstock for the embrittlement treatments. The wheat straw was processed in the UDRI Pilot Unit for the production of minus 45 mesh powder.

Five pound batches were embrittled in the reactor unit at a treatment temperature of 310° F using a 72 percent hydrogen chloride, 28 percent nitrogen reactant gas mixture for a treatment time of 5 minutes. The embrittled straw was ball milled for 30 minutes and then screened for 10 minutes. A tabulation of the powder preparation conditions is presented in Table II.

The reactor unit (shown in Figures 4 and 5), built by the UDRI, was designed to process 2.5 to 5 pounds of material with a continuous flow of reactant gases. The reactor was constructed from a 30 gallon carbon steel drum coated with a 20 mil thickness of Emralon* 314 (50% Teflon - 50% epoxy). The reactor is supported in a Unistrut frame such that it could be loaded and unloaded by tilting it about a horizontal axis

*trade name

TABLE II

POWDER PROCESSING CONDITIONS

Quantity material processed	5 lb
Processing temperature	310°F
Processing time	5 minutes
HCl flow rate	0.93 ft^3/min
N_2 flow rate	0.36 ft^3/min
HCl adsorbed	2.3% by wt
Ball mill time	30 minutes
Screening time	10 minutes

between two vertical Unistrut channels. The wheat straw was introduced at the top and the lid was sealed with a specially designed silicone rubber gasket and locking ring to prevent leakage. Three 1800-watt drum heaters were installed on the outside of the reactor for heating. A stainless steel screen with 0.33 inch diameter holes was installed at the bottom of the reactor to ensure an even distribution of the gas, and a Teflon relief valve was installed on the lid to provide safety from excessive pressures. All temperature measurements were made with a digital thermometer.

Hydrogen chloride was supplied from a 60 pound HCl cylinder, and N_2 was drawn from an existing N_2 cylinder bank. A 5 kW heater was used to heat the N_2. Two glass rotameters, 0-3.5 cubic feet/minute were used to measure the rate of the reactant gases flowing through the reactor.

The scrubber unit consisted of a polyvinyl chloride-lined 55 gallon drum containing 22.2 gallons of 0.15N sodium hydroxide solution. The unreacted gases were dispersed through a 6 inch diameter fritted glass funnel into the NaOH solution. Efficiency of the scrubber was tested by introducing a known quantity of HCl, and titrating a 0.34 ounce sample from a 16.9 ounce aliquot of the scrubber solution with 0.1N HCl. A series of tests showed that the titrimetric data could account for approximately 95% of the quantity of HCl calculated from flow measurements.

After the reactor was charged with wheat straw, it was sealed and heated to the desired temperature with the drum heaters. Upon reaching the specified temperature, a moderate flow of HCl and N_2 was begun. The HCl fow was maintained for a short time to provide the desired quantity of this reactant. The reactor was then purged with N_2 for an additional 0.5 hour. Gas flow rates and times were recorded from the control

PROCESS FLOW DIAGRAM

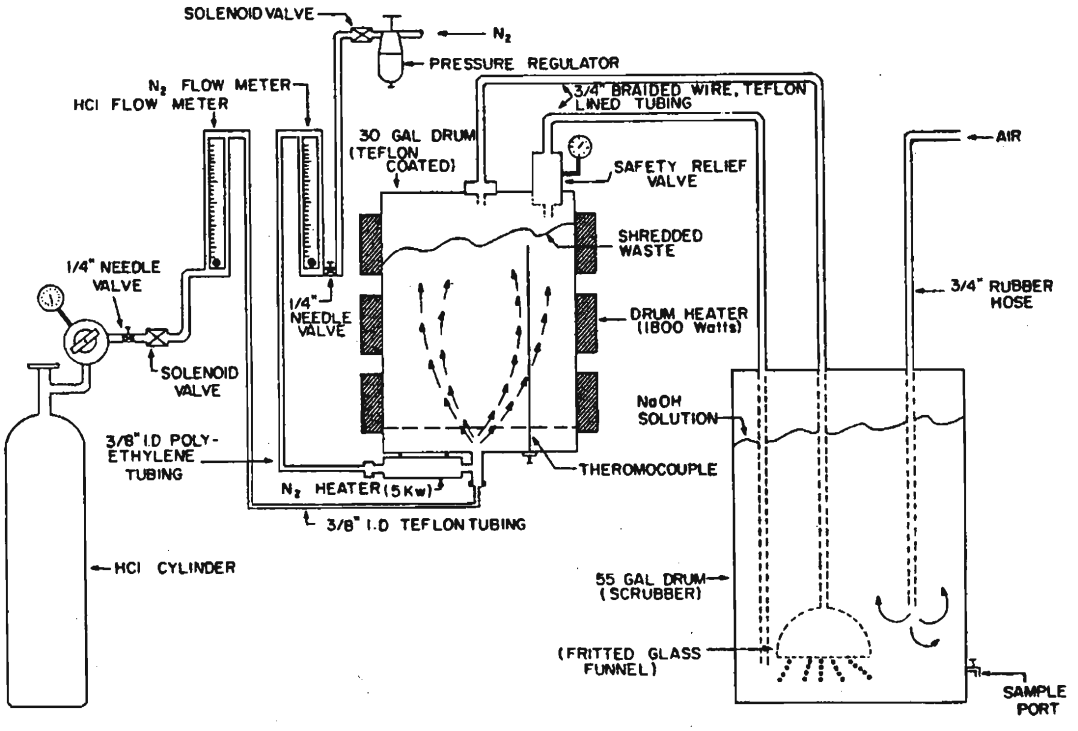

Figure 4. Process Flow Diagram for Pilot Reactor.

panel. Unreacted HCl and the N_2 passed out the top of the reactor through a 0.75 inch Teflon lined tube and into the scrubber unit described above. Two aliquots of the scrubber solution were titrated with 0.1N HCl to account for the amount of unreacted HCl. The input to the reactor was calculated from the flow rate of HCl at the measured pressure and temperature. Output of HCl from the reactor was calculated from the change in normality of the NaOH solution. The retention of HCl could be determined by the difference in these two values.

After chemical treatment, the wheat straw was ball milled for 30 minutes. The ball mill unit consisted of a 13 quart ceramic jar filled with 30 pounds of 0.5 x 0.5 inch ceramic cylindrical grinding pellets. The jar was rotated on a pair of 2 inch diameter hard rubber rollers, one of which was chain driven by a 186.4 watt electric motor. The ball milled powder was then screened through a Tyler RoTap sieve shaker for 10 minutes to obtain minus 45 mesh powder.

Powder Characterization

Samples of the powder produced were obtained for chemical, physical, and thermal analysis. In addition, samples were sent to the Galbraith Laboratories, Inc. for selected chemical analysis.

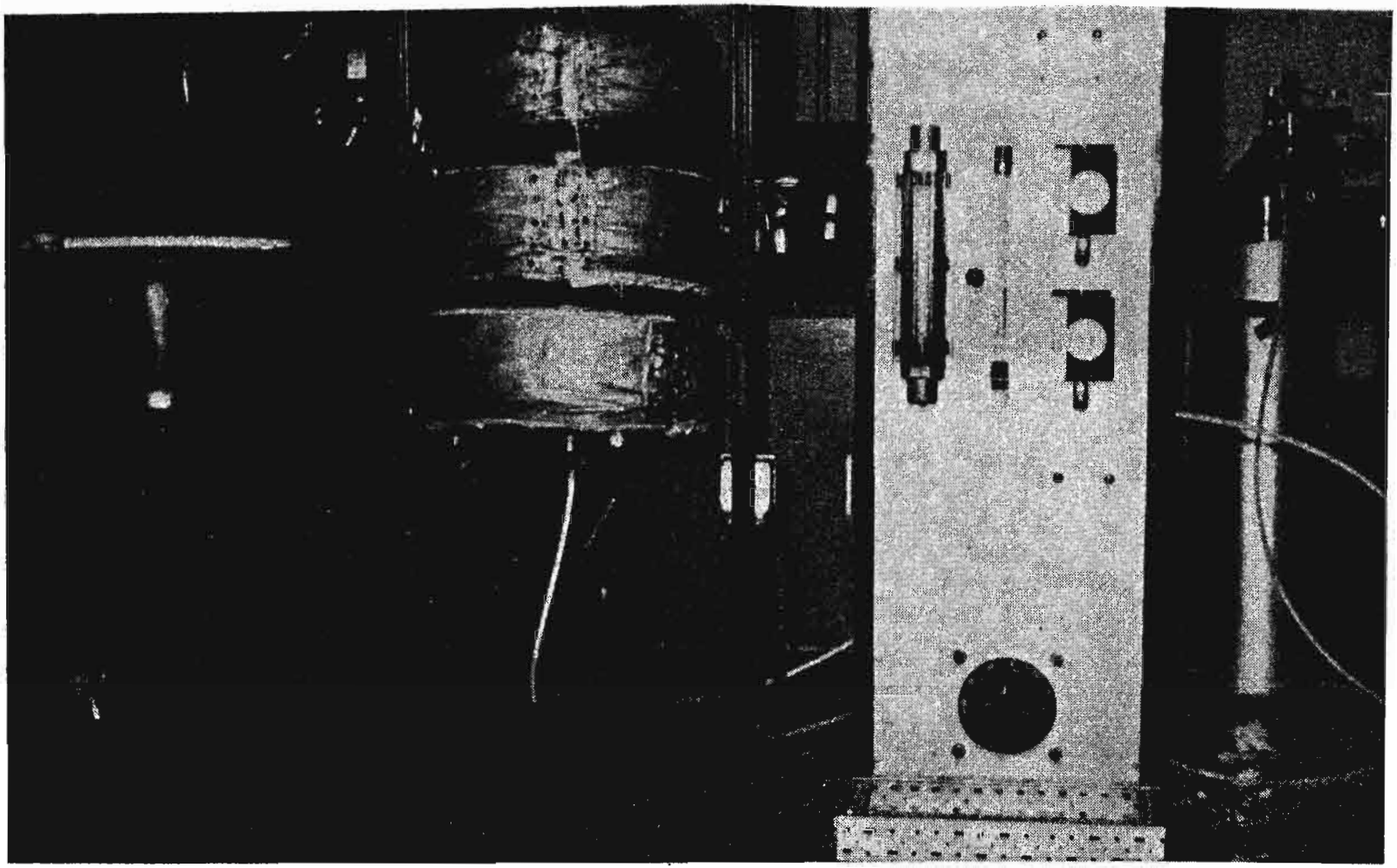

Figure 5. Pilot Reactor

Particle size distribution and morphology of the powder samples were measured to better characterize the physical nature of the powder. The particle size distribution was measured using a Tyler RoTap Sieve Shaker and the results are shown in Table III. All of the data reported represent the average values calculated from five or more measurements.

TABLE III

PARTICLE SIZE DISTRIBUTION OF POWDERED WHEAT STRAW

Particle Size mesh	Quantity %
+45	34.7
-45+100	26.5
-100+200	32.7
-200	6.1

Using a scanning electron microscope and EDXA (Energy Dispersive X-ray Analysis) the morphology and inorganic elements of the untreated straw, the straw converted to powder, and ash samples from both were studied. Representative electron micrographs are shown in Figures 6 through 13.

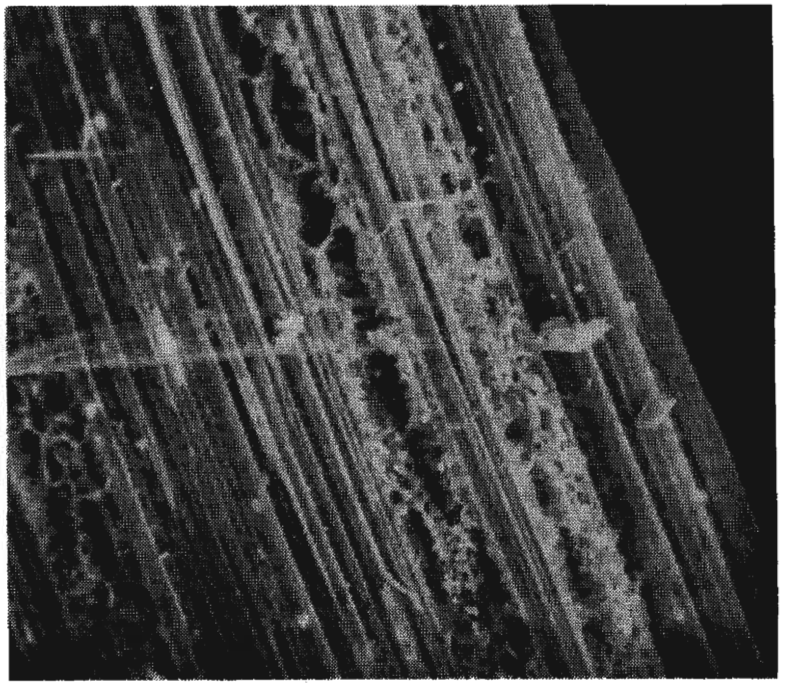

Figure 6. Wheat Straw at 100X

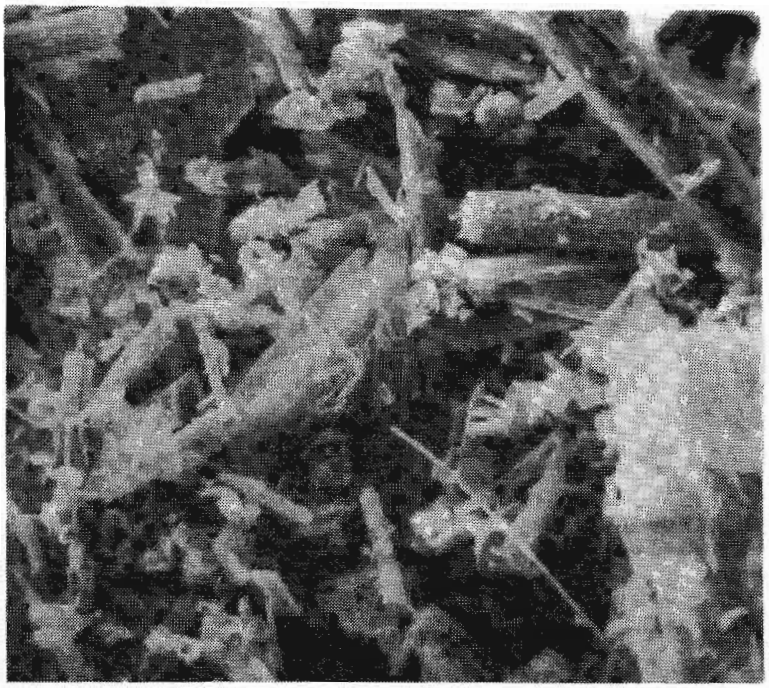

Figure 7. Powdered Straw at 100X.

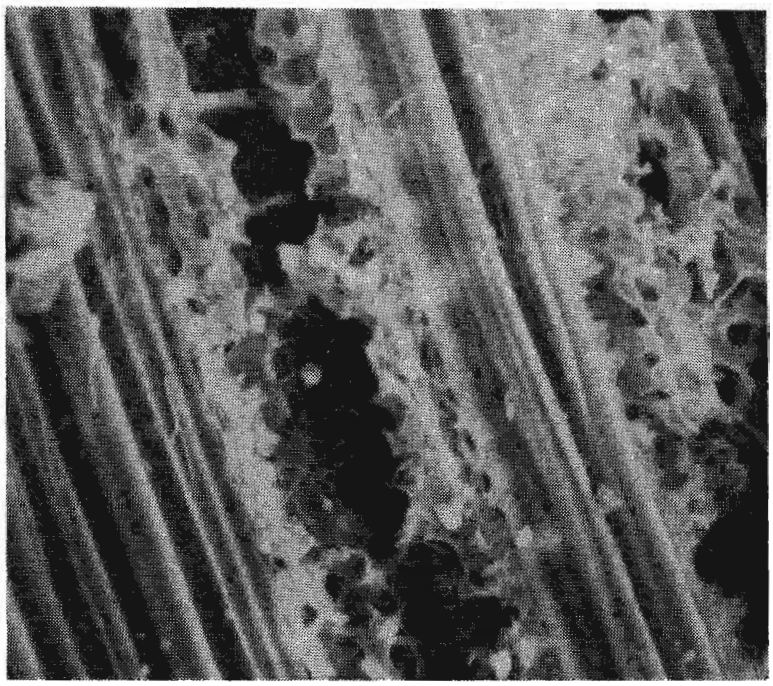

Figure 8. Wheat Straw at 300X.

Figure 9. Powdered Straw at 300X.

Figure 10. Ash from Wheat Straw at 100X.

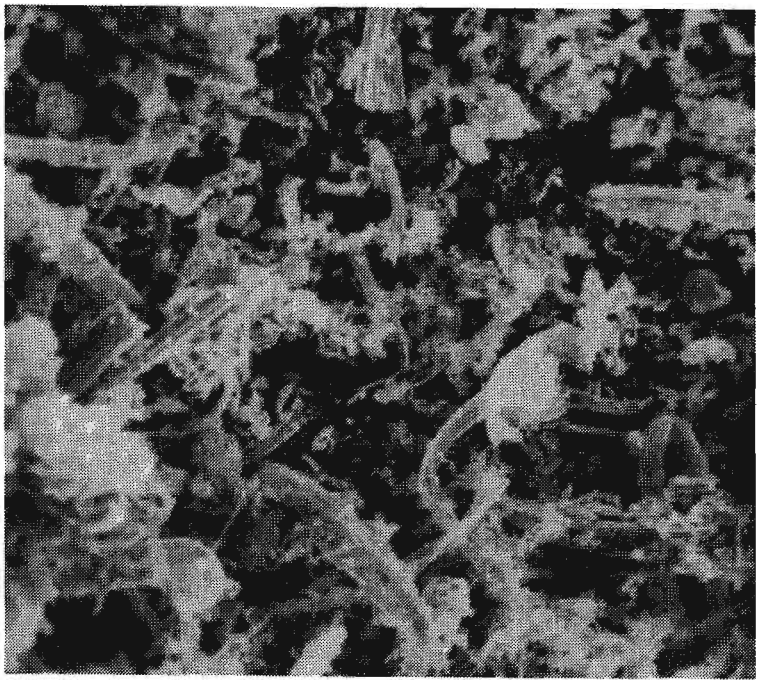

Figure 11. Ash from Powdered Straw at 100X.

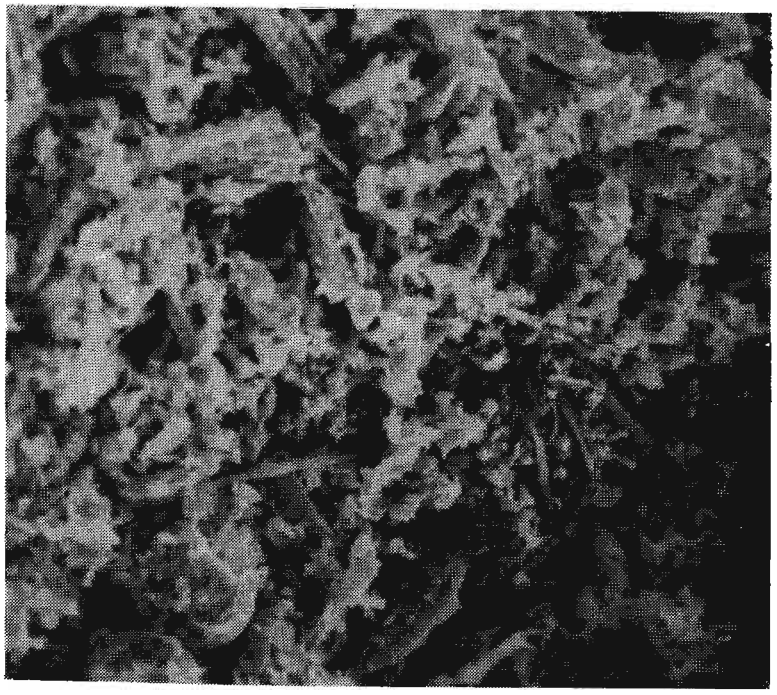

Figure 12. Ash from Wheat straw at 300X.

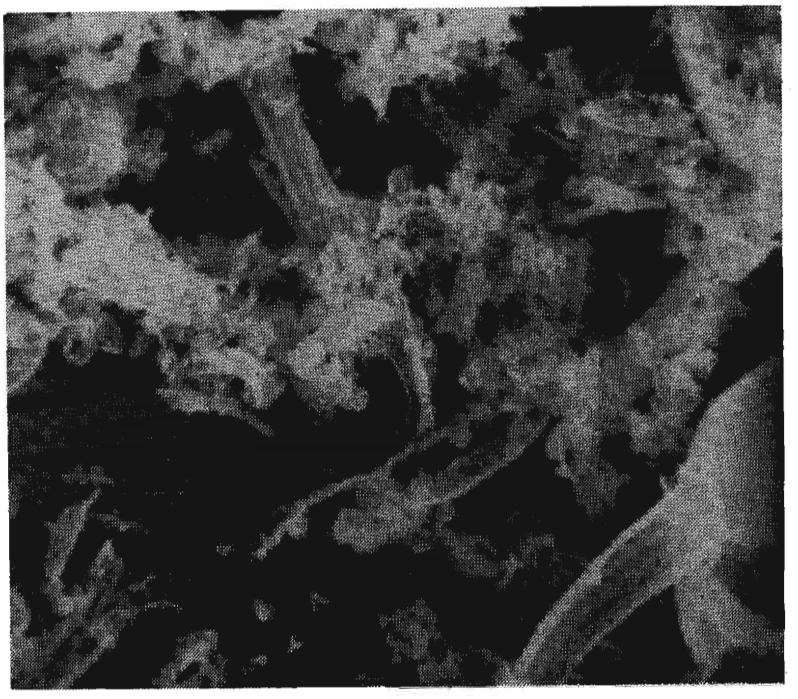

Figure 13. Ash from Powdered Straw at 300X.

The EDXA scans obtained for the untreated straw, powdered straw and the ash from both materials are shown in Figures 14 to 17. The elements identified for each sample are compiled in Table IV.

TABLE IV

ELEMENTAL ANALYSIS BY EDXA

Wheat Straw	Powdered Straw	Ash from Straw	Ash from Powder
Al	Al	Si	Si
Si	Si	Cl	Cl
Cl	Cl	K	K
K	K	Ca	Ca
			Fe*

*The Fe found in the ash from the powdered straw may be a contaminant picked up during grinding.

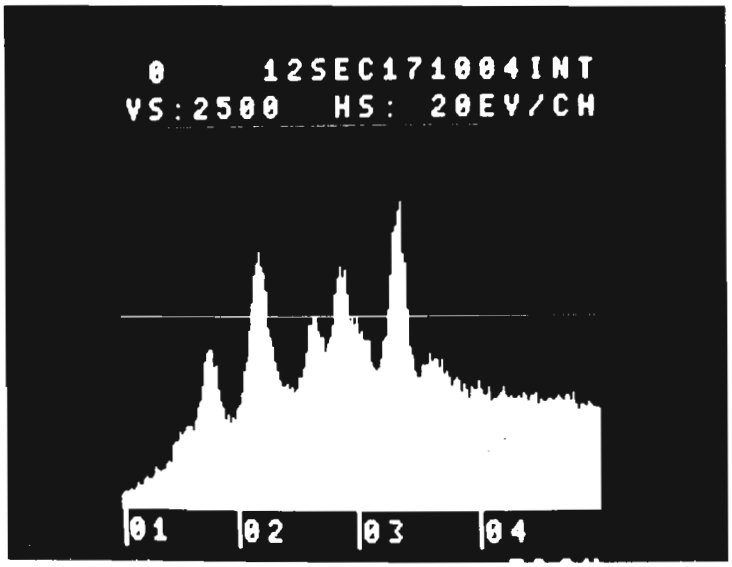

Figure 14. EDXA Scan for Wheat Straw.

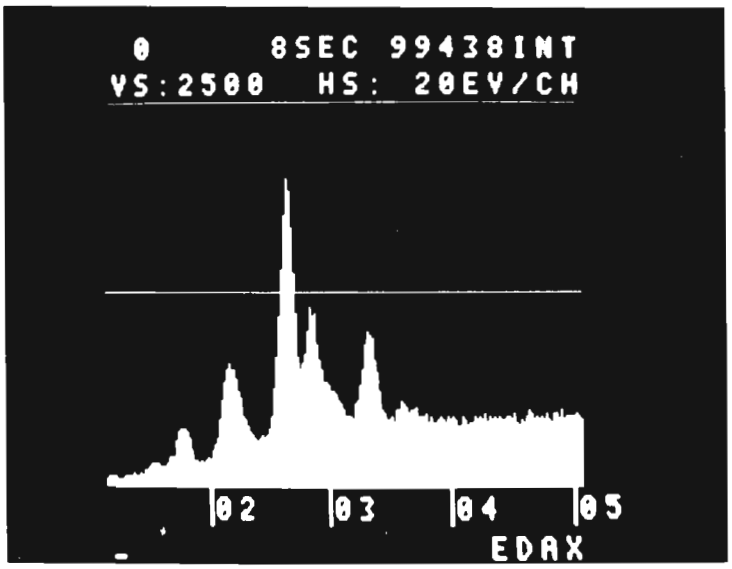

Figure 15. EDXA Scan for Powdered Straw.

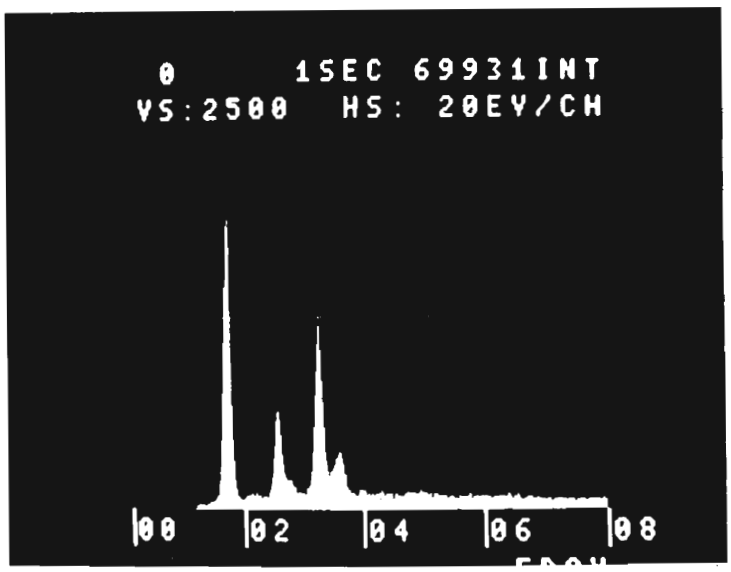

Figure 16. EDXA Scan for Ash from Wheat Straw.

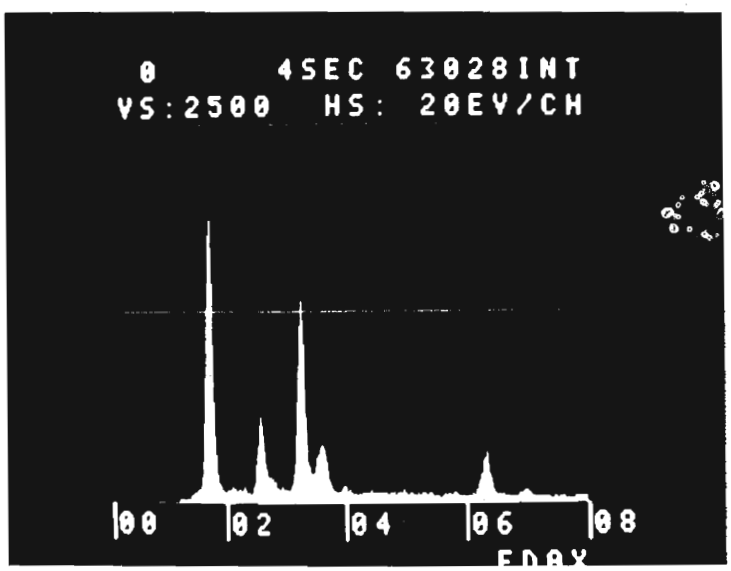

Figure 17. EDXA Scan for Ash from Powdered Straw.

Ash samples were prepared from the wheat straw and powder following ASTM standard D 271. The wheat straw had an average ash content of 6.8% and the powdered straw had an average ash content of 9.5%. The heat content of the wheat straw and the powdered straw was measured using 1 gram samples in a Parr Adiabatic Bomb Calorimeter following ASTM standard D 2015. The wheat straw had an average heat content of 7050 BTU per pound and the powdered straw had an average heat content of 6931 BTU per pound.

The chemical analysis of both the wheat straw and the powdered straw was conducted at the Galbraith Laboratories Inc. of Knoxville, Tennessee. The results of these analyses are presented in Table V.

TABLE V

CHEMICAL ANALYSIS

Element	Wheat Straw %	Powdered Straw %
C	43.27	41.51
O	43.83	40.90
H	6.10	5.69
N	0.12	0.15
Cl	0.38	2.70
SubTotal	93.70	90.95
Loss on Ignition	94.18	90.26

Discussion of Results and Conclusions

In this work, wheat straw was readily converted to a fine powder by the use of cellulose embrittlement techniques developed for powdering MSW. From the preliminary study conducted it appears that the wheat straw is more easily embrittled than was observed for MSW subjected to the same treatment conditions. The powder obtained consisted of short choppy fibers primarily minus 45 mesh (354μ) in size. The heat content of the powder was 6931 BTU/per pound and the ash content averaged about 9.5 percent. Compared to the untreated wheat straw the powder had a higher ash content and a slightly lower heat content. In addition, the powder has a lower carbon, oxygen and hydrogen content but a much higher chlorine content. It is believed that some hydrogen, carbon and oxygen are volatilized during the embrittlement process while some hydrochloric acid is adsorbed.

Procedures for converting wheat straw to a fine powder have been established. The powder obtained appears to be an effective feedstock for biomass conversion processes. However, the mechanisms of the process are not completely understood and need further elucidation. The identification of effective alternative embrittlements reagents, particularly reagents (HNO_3, H_3PO_4, etc.) that would not leave residues which

could be corrosive or detrimental to the environment are also needed.

It would appear that a variety of biomass materials, particularly cellulose wastes from industrial and agricultural sources (stalks, husks, bark, wood and crop residue, etc.), could also be converted to powdered feedstock for fuel production. However, more work is needed to develop effective processing procedures for powdering the variety of biomass materials which might be available for conversion.

Based on these observations the following recommendations for future work are proposed: (1) further elucidation of the embrittment mechanism; (2) identification of alternate embrittlement reagents; and (3) extension of the embrittlement process to other biomass materials.

PURIFICATION AND USES OF FAST PYROLYSIS GASES MADE FROM BIOMASS

Michael S. Graboski
Chemical and Petroleum-Refining Engineering Department
Colorado School of Mines
Golden, Colorado

ABSTRACT

The fast pyrolysis of biomass and MSW provides a product gas rich in olefins. The raw product gas is useful for the manufacture of pure ethylene and motor fuels. This paper explores gas cleanup and processing requirements for the production of ethylene and fuels and discusses the economics of synthesis. It is concluded that alcohol motor fuels represent an attractive conversion route for fast pyrolysis gas.

INTRODUCTION

Much has been written about the use of biomass as a supplement for petroleum and natural gas energy sources. Depending on the conversion route, that is, gasification, pyrolysis or liquefaction, a wide variety of products are possible. Direct liquefaction of biomass is technologically far behind gasification and pyrolysis. Gasification and pyrolysis represent distinctly different conversion paths. Figure 1 highlights these differences. In gasification the aim is to produce synthesis gas (a mixture of CO and H_2) for fuel or chemicals production by oxidizing the carbon matter using air or oxygen, steam and CO_2. Bulk chemicals including methanol, ammonia and methane are the obvious chemical products from synthesis gas although the manufacture of higher alcohols and hydrocarbons is certainly feasible. Pyrolysis on the other hand yields a mixture of gases, tars and char by supplying heat indirectly to the solid. The rate of heating dictates the product distribution. Slow heating rates (10-100 C/min) yield a mixture of gas, tar and char. The tar and char yields are large. Flash pyrolysis of biomass with a solid heating rate on the order of 1000 C/sec. provides a feedstock rich in olefins and only a small amount of char and tars.

Olefins may be readily converted to many different petrochemicals and fuels including alcohols, gasoline, plastics, glycols and ethers. An important question is "which route is most attractive?" This depends on a variety of factors including plant scale, location and technology.

PYROLYSIS TECHNOLOGY

A number of research and demonstration projects have had as their purpose, the production of olefinic and paraffinic hydrocarbons from the thermal decomposition of biomass. These include Mallan and Compton (1974), Diebold and Smith at China Lake (1979), Benham at SERI, (1980), Kuester at Arizona State (1978), and Antal at Princeton University (1979) to name a few. The project which is farthest along developmentally and for which a large body of data are available in the open literature for olefin production is that of Diebold.

In the China Lake process, shown in Figure 2, pulverized biomass is steam pyrolyzed in a short residence time, atmospheric pressure, high temperature reactor similar to that employed in petroleum cracking. Reaction temperatures of 1300-1500F and residence times of 10-1000 milliseconds have been employed in a reactor capable of processing several pounds of biomass per hour. The reactor used was 3/4-inch ID by 7 feet long. The principle biomass fuel employed is a preprocessed municipal solid waste trade named ECO-II. Some tests have also been conducted on cellulose and birch flour. Benham (1980) has recently investigated various wood flours and straws in a similar apparatus. The nature of the experimental apparatus employed is such that the reactor is non-isothermal and the residence time is ill-defined. Additionally, the heat is supplied indirectly through the vessel wall, confounding the temperature history of the solid. It is therefore difficult to interpret the results of the experiments in a quantitative fashion to determine the optimum operating conditions for ethylene yield.

Table 1 compares yields obtained from the China Lake Process with those obtained for other hydrocarbon feedstocks. While the hydrocarbon portions are similar in relative amounts, the biomass yields are lower because of the large quantity of CO and CO_2 produced. These are a result of the high oxygen content of the feedstock. Figure 3 gives a more detailed product analysis for ECO-II feedstock. Other feedstocks such as cellulose and birch flour yield somewhat less olefins and almost no char. More CO and CO_2 are produced because of the higher oxygen content.

While the composition of biomass and petroleum feedstocks greatly differ, it is apparent that the same types of free radical reactions take place since the product distributions are somewhat similar. Little is known about the thermal degradation of oxygenated species. Experiments on the cracking of acetaldehyde show that the principal products are light paraffins, olefins, carbon monoxide and hydrogen. Antal (1979) and others have shown that olefins are not the primary pyrolysis products issued from the solid but result from gas phase cracking. The effect of ash components and feedstock pretreatment and preparation might have an effect on the yield. The nature and amount of the heavy hydrocarbons and char produced must be better quantified. More experimentation is needed to model the chemistry.

GAS CLEANUP TECHNOLOGY

Figure 4 shows two possible schemes for pyrolysis gas cleanup. Gas exiting the reactor must be rapidly cooled so that the pyrolysis reactions are quenched. Experience shows that the rapidity of the quench and ultimate ethylene yield are related. To minimize secondary reactions, the product mixture must be cooled below 900-1000 F in tens of milliseconds. This can be directly accomplished using oil or water sprays at the expense of inefficient heat recovery in the production of pyrolysis steam. Modern plants employ transfer line exchangers (Mol (1973)), which are short-residence time, single pass heat transfer units.

Typically, the residence time is on the order of 10-20 milliseconds total in these units with temperature reduced below 1000 F in about 2 milliseconds. High pressure steam is readily recovered for use in the pyrolysis plant. Transfer line exchangers are used to reduce the temperature to between 600 F and 1100 F for gas and oil cracking respectively. In the later case, the temperature must be kept high enough to eliminate fouling in the exchanger due to condensation of heavy tars. In the case of biomass feedstocks, the potential for fouling exists due to a combination of tars, char, and ash. Care therefore must be taken in the exchanger design to eliminate condensation problems. Following the transfer line exchanger, the reaction mixture may have to be further quenched depending upon the temperature of the gas mixture. The quench may be accomplished using a light oil fraction or organic laden condensate derived from the plant.

In the case of MSW feedstock, considerable solid residue exits the pyrolyzer. Hot cycloning of the gas appears to be advantageous for recovering solids and permitting further heat recovery from the gas.

In the pyrolysis system cooling to 700 F to 900 F in the transfer-line exchanger should permit cycloning of residual char, ash and slag without tar condensation. The dew point of the product mixture is not well known and this temperature is therefore very tentative. The gas-steam-tar mixture must then be cooled and scrubbed to remove the condensables.

When dealing with biomass feedstocks such as wood flours, the quantity of ash and char produced is negligible. In this instance, cleanup can proceed as in the MSW case or can be simplified by direct quench to an oil or water scrubber. The later scheme is less expensive but is also less energy efficient. The feasibility of such a water quench/scrubber has been demonstrated in the Union Carbide Purox process. Table 2 compares features of oil and water scrubbing.

In either case, oil mist is carried through the separator in micron size droplets. These can be recovered by a variety of techniques. The two principle methods involve filter type devices termed mist eliminators and electrostatic precipitators (ESP). The latter are more costly but can give essentially complete recovery of oil from the gas stream. Mist eliminators are much lower in efficiency. Table 3 gives some data on oil recovery for scrubbers, mist eliminators and precipitators. A good review of oil mist elimination techniques is given by Bennett (1980).

Some tars produced are water soluble. Little information has been reported on the nature of the tars from biomass flash pyrolysis. Therefore, proper design of a recovery system cannot be carried out at this time. One alternative would be to recycle the tar-water mixture to the cracker to provide additional ethylene. At this point, the gas consists primarily of C_6 and lighter components.

CHEMICAL SYSTHESIS

The fast pyrolysis gas can be processed to yield a variety of products. Three simple alternatives are olefins recovery for subsequent chemical systhesis, gasoline manufacture and mixed alcohols manufacture.

Ethylene is an important intermediate in the petrochemical industry. The major uses of ethylene (Stinson (1979)) are low density polyethylene (27%), high density polyethylene (16%), ethylene glycol and oxide (19%), ethylene dichloride (15%), and ethylbenzene (8%). The bulk of the U.S. ethylene comes from cracking of hydrocarbons. In 1979, the U.S. capacity was 33 billion pounds per year with an 88 percent onstream factor. Ethylene demand is strongly dependent on the consumer economy. During recessions, demand falls; in the current recession period, the onstream factor for the ethylene industry is approximately 66 percent.

Ethylene demand is projected to grow to 41 billion pounds by 1985. Capacity is expected to keep pace with demand. The trend in ethylene production is toward heavier feedstocks which means more capital intensive facilities and high production costs. The price of ethylene has moved strongly from 14¢/lb. in mid-1979 to 24¢/lb. in mid 1980 due to increased feedstock prices. Large commercial plants typically are on the order of one billion pounds per year, while small regional facilities are on the scale of 100 million to 500 million pounds per year. The yield of ethylene from a 100 TPD biomass facility is estimated to be 7 MM lb/year and 60 MM for a 1000 TPD facility. Because of higher production costs, there must be a ready market within the region to offset transportation costs. Therefore, olefin production is very site specific.

Gasoline and alcohol production are suitable alternatives for fuel purposes. Each has a ready, dependable market. Additionally, the politics of energy makes this type of venture attractive. Alcohol production has three important advantages over gasoline production. First, the gallon output of an alcohol plant is greater than that for a gasoline plant. Second, the alcohol product may qualify for a 40¢/gallon tax credit under the windfall profits tax bill. Third, the octane rating of the alcohol product is much greater than the polygasoline produced from olefins.

Table 4 (Christiansen (1980)) presents a comparison of several projections on liquid hydrocarbon demand through the year 2000. These studies show that from the year 1985 to 2000, demand will continue to grow. These studies are probably not realistic as the U.S. is currently seeing a reduction in imports due to conservation resulting from pricing and federal legislation mandating the production of higher performance transportation vehicles. It is possible that there will be, more nearly, a zero growth in consumption through 1985. This still means that an import rate of 7 MM BB/D must be maintained.

Figure 5 (C&E NEWS, July 1980) shows the projected change in octane requirements for the motor gasoline pool over the next decade. This figure reflects a combination of the banning of lead and the higher octane requirements of the new Detroit products. Currently, the EPA requires a minimum octane (R+M)/2 of 87 for the unleaded gasoline. However, better fuel economies mean higher compression ratios, and it is expected that the future pool of unleaded gasolines will have a regular grade with an octane of 89 and a premium grade with an octane of 93.

At this moment, refiners are facing pressures from all directions: Detroit is pushing the compression ratios up because of tough EPA requirements on fuel economy, and at the same time, that government agency has limited the use of lead compounds to 0.8 gr/gal of gasoline until October 1, 1980, when it will be phased down to 0.5 gr/gal. In addition, the gasoline pool is competing for BTX (Benzene-Toluene-Xylene) that might otherwise go to chemical feedstocks; therefore, it is facing possible shortening supplies of aromatics. This gloomy overall picture has left refiners with only a few alternatives to boost octane ratings.

The possibilities appear to be:

Lead compounds like TEL and TML (tetraethyl lead and tetramethyl lead)

MMT (methyl-cyclopentadienyl manganese tricarbonyl)

MTBE (methyl tert butyl ether)

TBA (tert butyl alcohol)

Reformate (Aromatic fraction consisting of C_7-C_9 compounds).

Alcohols; methyl fuel, methanol, and ethanol, Sun Tech methanol-TBA blend

By definition, octane number is the percent of 2,2,4-trimethyl pentane (isooctane) that must be blended with n-heptane to give the same knock behavior in a laboratory engine as the fuel tested. RON (Research Octane Number) reflects performance at full open throttle at low speed (acceleration) and MON (Motor Octane Number) is a performance index of even driving with full open throttle and high speed or partly open throttle at high or low speed.

On October 27, 1978, EPA (Environmental Protection Agency) banned MMT. The agency said that MMT producer Ethyl Corp. (Richmond, Va.) failed to prove that the additive does not raise hydrocarbon levels in auto emissions. According to EPA estimates, without MMT, refiners will have to increase processing rates by 6% and deal with shortening supplies of aromatics. California was the first to react when the EPA imposed a ban on MMT, on the grounds that unleaded gasoline containing the additive did not meet the state's vehicle emissions standard for

hydrocarbons. Furthermore, the California Air Resources Board (CARB) said that MMT emissions are toxic and blamed the additive for plugging exhaust-gas recirculation valves and causing scale buildup.

With respect to TBA, the EPA approved its use in gasoline up to 7% by volume, effective January 1979 (News of the Week 1979). Oxirane has been using the alcohol at commercial scale for ten years and no consumer-related problems have been reported. But TBA is not widely available and the construction of a plant for the sole purpose of making TBA is apparently not economically feasible. At the present time, the alcohol is used mainly in Gulf Coast refineries and goes into gasoline distributed in the East via product pipelines, apparently because production is not enough to treat gasoline in other areas.

MTBE, another octane booster, appears as a very attractive alternative because of its higher octane number and negligible water miscibility. Furthermore, the EPA approved the use of the additive as an octane booster at concentrations of 7% or less by volume. But it is produced from isobutylene and methanol, and because of limitations on the amount of isobutylene produced in the U.S. by refineries and olefins plants, only enough MTBE is available to make up 3% of the gasoline pool. Other studies are more pesimistic.

For 1980, the unleaded gas demand will be 46% and will reach 64% of the total U.S. gasoline consumption by 1984. Treating the entire 3.2 million bbl of unleaded gasoline expected to be used per day in 1980 would require 21.4 billion pounds per year of the ether. If the estimated production for 1980 is 1.3 billion pounds per year, that means that only 6% of the unleaded gasoline would be treated at a 7% level of MTBE.

Ethanol from fermentation is another alternative receiving considerable attention, but according to a study of the U.S. Department of Energy (DOE), "if all practicably available farm land were used for farm crop plantings in excess of those required for food production, the ethanol produced from the crops and crop residues would satisfy no more than 8% of today's (March 1978) total liquid fuels energy demand." Economics of the process are improving since a 40¢/gal federal excise tax is being considered.

One of the main reasons for the sudden popularity of MTBE is that it will increase the refiners availability of aromatics. Reformate is the most immediate answer to octane improvement. Furthermore, improved technology and catalysts for catalytic reforming will allow better yields and products to be achieved. But alcohol fuels produced from coal or biomass have the potential to treat the U.S. gasoline production without additional crude oil imports. Reformate, one of the highest octane ingredients of gasoline, contains about 40% aromatics plus naphthenes, olefins, and straight-run paraffins. But higher severity operation, which reduces yield and boosts costs, is required to raise reformate's octane. In addition, refiners have to face competition from

the petrochemical industry. The chemical demand for BTX normally runs about 3 billion gallons per year, while the amount consumed in gasoline is roughly seven times that. There are other factors working against the use of BTX in the gasoline pool. Benzene has been listed as a hazardous pollutant under the Clean Air Act and nothing prevents the EPA from banning benzene outright at some future point. Refiners may choose not to use it at all instead of installing controls and monitoring equipment. Toluene and xylene have not been listed as hazardous and are not now subject to regulation.

All these restrictions and bureaucratic obstacles leave refiners with alcohols as the other alternative. Reformate, MTBE, and TBA will be only minor components of an overall strategy to increase octane ratings, whereas alcohols from coal and biomass will play a major role.

OELFIN RECOVERY

The most commonly used scheme for olefin recovery utilizes cryogenic gas processing. A typical flow scheme is shown in Figure 6. The raw gas off of the pyrolysis furnace must be compressed to 450 to 800 psia for processing. Because of the large quantity of CO_2 present in the gas, the CO_2 along with other acid gases including H_2S and HCl must be removed at this point. For such applications, a variety of scrubbing systems are available. A suitable choice is the Benfield hot carbonate process. It has the important advantage that hydrocarbons are not soluble in the potassium carbonate scrubbing agent. The CO_2 must be removed at this point because it will cause icing in the demethanizer. The gas mixture is dried and cooled to -250 F where hydrogen is recovered. The mixture is distilled in the demethanizer to recover CO, CH_4 and H_2 as a fuel gas. A C_2 splitter is then used to recover pure ethylene. An ethane stream and a C_2^+ stream can be recycled for further cracking.

GASOLINE MANUFACTURE

In order to polymerize ethylene to gasoline, the raw gas must first be compressed. After compression, the CO_2 must be scrubbed and the olefins concentrated. This can be accomplished by scrubbing with an aromatic absorption oil. Acetylene must also be hydrogenated to ethylene. This is a simple fixed bed step which can be accomplished with the available hydrogen in the steam. In the most complicated alcohol system, these steps must also be employed.

The polymerization of olefins to form gasoline may be carried out thermally or using a catalyst. The catalytic process involves a phosphoric acid catalyst. In the case of ethylene, depending on the temperature, naphthenes, aromatics and paraffins are formed along with olefins. The light cut (<110C) is generally paraffinic while the heavy ends are aromatic (>220C)(Ipatieff, and Pines (1935)). Catalytic polymerization takes place at 350 F to 750 F and 200 to 1500 psia.

Figure 7 shows a typical flow sheet for a cat-poly unit. Generally, 60-80 percent conversion per pass is attainable. Alkanes in the feed along with CO, and H_2 pass through the reactor intact along with unconverted olefins and therefore, a recycle stream is necessary. The liquid polymer consists of a gasoline fraction with a boiling range between 190 F and 360 F and a heavy gas/oil. By properly controlling the temperature the gasoline fraction can be maximized.

The motor octane number of the cat-poly gasoline produced from ethylene is typically about 82. The research octane number is reportedly higher. Compared with alkylates, the antiknock performance is inferior. Upgrading might be necessary to produce a higher quality motor blending fuel.

THERMAL POLYMERIZATION

Thermal polymerization requires temperatures on the order of 900-1300 F and pressures between 800 and 1200 psi (Keith and Ward (1935)). The thermal process produces a produce containing about 2/3 olefins with the remainder being naphthenes and paraffins. Additionally, a considerable amount of heavy oil is produced. Gasoline from the thermal process has a very low octane number, typically ranging from 68-72. Thus, thermal polymer product would have to be reformed to increase the octane level for blending. The flow sheet for the thermal process is similar to that for the catalytic process.

PRODUCTION OF MIXED ALCOHOLS

Reasons

There are a number of reasons to consider the synthesis of mixed alcohols from fast pyrolysis gas. These may be broadly divided into economic and utlization classifications. Like the production case of hydrocarbon fuels, the plant facility is not only eligible for a 10 percent investment tax credit but also for an additional 10 percent energy tax credit at least through 1985. In the case of the solid waste disposal facilities, the Windfall Profits Tax Bill allows the use of tax exempt Industrial Development Bonds to build facilities to produce alcohol or other fuels. During this period of unprecedented high interest rates, this is an important consideration. Finally, and most important, the alcohol fuels tax exemption has been extended through 1992. This tax credit amounts to 40¢/gallon of 95% alcohol and 30¢/gallon for 70% alcohol added to gasoline in a 10% amount if the alcohol is derived from sources other than coal, gas or petroleum. Alcohols produced chemically from fast pyrolysis gas appear to satisfy the law.

From a utilization point of view, the alcohols also look attractive. Based on the fast pyrolysis gas, a fuel blend containing the composition shown in Table 5 can be obtained.

Table 6 presents octane numbers for typical oxygenated fuels. From Table 6, it can be seen that these compounds are capable of

providing substantial octane improvement on blending. Ethers are particularly attractive in that they boost the MON as well as the RON.

Figures 8, 9, 10, 11 (Keller, 1979) suggest that the alcohol blend from fast pyrolysis will yield a motor fuel with suitable vapor pressure, volatility and phase separation resistance due to water.

Technology

Two principle synthesis routes for alcohol manufacture from olefins are direct hydration using an acid catalyst and indirect hydration using sulfuric acid. Additionally, higher alcohols, in this case principally propanols, can be manufactured using the oxo-process and its modifications. For preparation of fuel grade alcohol, the indirect hydration process appears to be the most useful.

Indirect Hydration

The indirect hydration process (Kirk-Othmer (1963)), as shown in Figure 12, employs sulfuric acid as a reactant. At temperatures of 70-80 C and acid strengths of 95-99%, ethylene is rapidly adsorbed to yield ethylhydrogen sulfates. Industrially, these ractions are carried out at 150-200 psi with feeds containing 35% or more ethylene.

$$C_2H_4 + H_2SO_4 \text{ ------} C_2H_5SO_3$$

$$2C_2H_4 + H_2SO_4 \text{ ------} (C_2H_5)_2(SO_4)$$

The quantity of the mono and di-sulfates present depend on the ethylene partial pressure and liquid residence time.

The crude pyrolysis gas contains ethylene, propylene and butylene as well as saturates, CO, CO_2 and H_2. To carry out the above reaction, propylene and butylene must be removed because these will tend to polymerize. The most convenient way to effect this removal is to wash the raw gas with cold, diluated H_2SO_4. Typically, 85% acid is satisfactory to effect $C_3^=$ removal and 70% for $C_4^=$ removal. Additionally, heavier tars should be removed prior to ethylene adsorption.

A number of process improvements would greatly enhance process economics. These are listed in Table 7.

Past studies have shown that even at atmospheric pressure with low olefin content gases, high ethylene recovery is possible. Bury and Ollander studied the adsorption of ethylene from coke oven gas containing 3% ethylene and effected 70% removal in 1 1/2 minutes gas contact time. This suggests that fast pyrolysis gas can be treated at or above atmospheric pressure with a minimal amount of preprocessing. Eliminating the CO_2 stripping step and olefin concentration step are important in process economics.

After adsorption, the mixed acid/ethylhydrogensulfate is diluted with about 1.5 volumes of water and held for 3/4-1 hour at about 90 C. The crude alcohol is stripped from the mixture and is sent to purification. The resulting acid stream, containing 60-70% aqueous acid is reconcentrated by vacuum evaporators to about 93%. The acid is brought to full strength by the addition of oleum. The acid reconcentration step is expensive and should be the target of research.

Distillation of the crude alcohol will yield the desired dry product. Little or no phase equilibria data are available for the design of such a separator. A significant process improvement would be to replace the distillation step by a more suitable technology.

Economics

The economics of these processes have been recently evaluated by SAI (1979). Table 8 gives efficiency data and Table 9 summarizes the capital costs and economics for each process adjusted to a zero dump fee for MSW. These economics may be unrealistic in terms of the fuel cost because of the cost for preprocessing the solid waste. However, they are satisfactory for comparison purposes.

For plant sizes of 100 ton/day and 1000 tons/day capacity, Table 9 shows the relative costs of the products in comparison to early 1980 prices. Considering the tax credit for alcohols, the 1000 ton/day capacity plant shows economic promise, particularly for alcohol manufacture.

Table 10 reflects a recent study by the Institute of Gas Technology (C&E News, August 11, 1980). The point of Table 10 is that the cost of imports and domestic fuels cannot be directly compared. There are a number of benefits from domestic production which can be quantified including reduced inflation, competition, employment and national security. The study suggests that a domestic synfuel barrel can be sold for twice the price of an imported barrel with the same effect on the economy. Implementation of an industry based on such reasoning can be accomplished only by government assistance.

CONCLUSIONS

The production of an olefin rich synthesis gas is technically feasible. Such a gas is suitable for the recovery of ethylene, manufacture of gasoline or mixed alcohols. The later route appears to be the most economically feasible. A number of R&D areas have been identified which must be investigated for process optimization.

REFERENCES

1. Antal, M.J., Edwards, W.E., Friedman, H.C., Rogers, F.E., "A Study of the Steam Gasification of Organic Wastes," Final Report, EPG University Grant No. R804836010 (1979).

2. Benham, C., Private Communication, Solar Energy Research Institute, Golden, CO (1980).

3. Bennett, R., A Survey of Biomass Gasification Volume III, Ch. 12, Solar Energy Research Institute (1980).

4. Christiansen, A.P., "Evaluation of MEBP as a Gasoline Extender," M.S. Thesis, Colorado School of Mines, T-2303 (1980).

5. Diebold, J., Smith, G., "Commercialization Potential of the China Lake Trash to Gasoline Process;" Municipal Solid Waste as a Resource: The Problems and Promise Conference, July 13-17, 1979.

6. Griswold, C.F., "Steam Pyrolysis of Tosco Shale Oil for Production of Chemical Intermediates," M.S. Thesis, CPR, Colorado School of Mines, Golden, CO (1976).

7. Ipatieff, U.N., Pines, Herman, "Polymerization of Ethylene under High Pressures in the Presence of Phosphoric Acid," I&EC 27, 1364 (1935).

8. Keith, P.C., Ward, J.T., "3.5 Cents Per Gallon is Manufacturing Cost of Polymerized Gasoline," National Petroleum News, 52-62 (Nov. 20, 1935).

9. Keller, J., "Alcohol Gas Motor Fuel?", Hydrocarbon Processing 58 (5), 127 (1979).

10. Keuster, J.L., "Urban Wastes as an Energy Source," Energy Systems: An Analysis for Engineers and Policy Makers, Marcel Dekker (Jan. 1978).

11. Kirk Othmer Encyclopedia of Chemical Technology V8, 431-436, V16, P568-571, John Wiley and Sons (1963).

12. Mallan, George, Compton, L.E., Occidental Petroleum, "Gaseous Hydrocarbons from Municipal Waste," U.S. 3,846,096 (Nov. 5, 1974).

13. Mol, A., "Which Heat Recovery System?" Hydrocarbon Processing 52 (7), P109-112 (July 1973).

14. Science Applications Incorporated, "Evaluation of the NWL-Diebold Pyrolysis Gas Process," SAI #79-019-GLN (1979).

16. Stinson, S.C., "Ethylene Technology Moves to Liquid Feeds," C&E News, p. 32 (May 1979).

TABLE 1

	COMPARISON OF YIELDS, WT %		
	SHALE OIL	NAPHTHA	BIOMASS
METHANE	19	19	6
C_2-UNSATURATES	30	26	16
C_3 + C_4-UNSATURATES	19	19	6
CARBON MONOXIDE	--	--	40
CARBON DIOXIDE	--	--	15
HYDROGEN	1	1	1

TABLE 2 FEATURES OF OIL AND WATER SCRUBBING

	Oil Scrubbing	Water Scrubbing
Disposal of purge liquid	Thermal oxidation with heat recovery or recycle after fractionation	Water treatment before discharge
Oil droplet removal considerations	Entrainment and saturation of gas stream with oil	Oil entrainment from H_2O
Makeup quality	Oil might require fractionation to achieve proper boiling range material	Condensate quality water
Metallurgy	Carbon steel equipment is probably adequate if no water condensation occurs	Water will be acidic due to contaminants in gas: stainless steel scrubber required
Source of scrubbing medium	Available if oil produced by process can be used; otherwise must be imported	Readily available

TABLE 3 SUMMARY OF MIST ELIMINATION SURVEY RESULTS

Device	Plate Scrubber	Packed Scrubber	Spray Scrubber	Venturi	Mist Eliminator	Wet ESP
Pressure drop (in. H_2O)	10	0.24-0.5[d]	1 - 3	10 - 30	1 - 3	1
Droplet size (microns) at percentage removal	5 at 80	1.5 at 50	2 at 50	5	5 - 10 at 50	1 at 100
Circulation (gpm/1000 acfm)	2-50	2-50	30-100	5-20	3-5[c]	Variable
Capital cost	(a)					(b)
Operating cost	Power	Power	Power	Power	Minimal	Minimal
Maintenance cost	Nominal	Nominal	Nominal	Nominal	Nominal	High

[a]Plate scrubber is the most expensive wet scrubber; venturi is the least expensive wet scrubber.

[b]Wet ESP is the most expensive of all devices considered.

[c]Three to five gpm/ft^2 of mist eliminator cross-sectional area.

[d]Pressure drop per foot of packed height.

TABLE 4

Expected Liquid Hydrocarbon Demand

(expressed as million barrels/day of crude oil equivalent)

	1973	1974	1985 (Pace)	2000 (Chem. Systems)	2000 (Low Imports) (Chem. Systems)
Gasoline	6.7	6.6	6.6	9.0	9.0
Naphtha/JP-4[a]	0.2	0.5	0.4	---	---
Kerosine/Jet A	1.4	1.3	1.4	2.6	2.6
Diesel No. 2	2.7	2.5	4.0	3.6	3.6
Residual	2.8	2.6	4.4	4.5	4.5
Asphalt, Lubes, etc.	0.7	0.6	1.6	1.5	1.5
Fuel Gas/Petrochemicals	1.8	1.8	2.3	4.5	4.5
TOTAL	16.3	15.7	20.7	25.7	25.7
OIL SOURCES					
Imports	6	5.6	8.6	10.0	6.0
Domestic Crude + NGL	10.3	9.8	12.1	12.5	12.5
Shale Oil	0	0	0	2.5	2.5
Coal Liquids	0	0	0	1.0	5.0
TOTAL	15.3	15.7	20.7	26.0	26.0

[a]Petrochemical use of naphtha or gas oil not included

TABLE 5

TYPICAL MIXED ALCOHOL FUEL FROM PYROLYSIS GAS

	Wt. %
Ethanol	73.0
Isopropanol	10.0
Sec-Butanol	8.0
Diethylether	7.0
Di-isopropylether	1.0
Dibutylether	1.0

TABLE 6

OCTANE NUMBER OF OXYGENATED HYDROCARBONS

COMPOUND	RON	MON
Methanol	106-115	86-92
Ethanol	110	92
n-Propanol	-	90
Isopropanol	106	99
n-butanol	100	-
Sec-butanol	110	92
Isobutanol	107	-
Tertbutanol(TBA)	113	110
MTBE	117	101
Di-isopropylether	103	99

TABLE 7

ALCOHOL SYNTHESIS RESEARCH

1. Eliminate or Minimize
   - A. Compression
   - B. CO_2 Stripping
   - C. Ethylene Concentration
2. Develop New Alcohol Recovery System
3. Improve Acid Reconcentration Technology

TABLE 8

EFFICIENCIES FOR BIOMASS PYROLYSIS(MSW)

Feedstock	Ethylene	Product Gasoline	Mixed Alcohols
Biomass Feed, TPD	100	100	100
Biomass Fuel, TPD	44	44	44
Biomass for Power, TPD	13.5	5.1	7.4
TOTAL Biomass Feed, TPD	157.5	149.1	151.4
Products			
Ethylene, TPD	10.0		
Gasoline, BBL/D		106	
Alcohol, GAL/D			7073
LPG,TPD	8.79		
Fuel Gas, MMSCFD(HV)	1.48(446)	1.50(434)	1.39(434)
C_5^+ Oil Fraction, TPD			3.30
Major Product Efficiency,%	16.4	24.3	25.4
Overall Efficiency,%	55.4	50.4	54.6

TABLE 9

SUMMARY OF ECONOMICS FOR

A MSW FAST PYROLYSIS FACILITY

Item	Ethylene	Gasoline	Alcohols** *
100 TPD capital cost, $mm *	8.2	11.0	9.1
yield	10 TPD	4,452 gal/D	7073 gal/D
selling price at * * 20% DCF ROI	$0.48/lb.	$3.30/gal.	$1.84/gal.
selling price at 20% ROI for 25% reduction in capital	$0.36/lb.	$2.60/gal.	$1.29/gal.
$10 increase in fuel fee	+7¢/lb.	+27¢/gal.	+21¢/gal.
25% increase in yield, ROI	26%	25%	27%
selling price for 20% DCF ROI, 1000 TPD plant	$0.22/lb.	$2.14	$1.05/gal.
current selling price	$0.24/lb.	$0.98/gal.	$>1.00/gal.

*Chemical Feedstock

* * Assumes a zero price for MSW feedstock

* ** Alcohols may net an additional 40¢/gallon credit

TABLE 10

Benefits accrue from oil import reduction of 500,000 bbl per day

$ per barrel[a]	Year 1	Year 3	Longer term
Direct benefit	$37.00	$38.49	$40.00
Indirect benefits			
Oil price effect	12.41	19.07	12.41
Inflation effect	9.92	23.04	11.90
Employment effect	7.32	22.92	8.78
Security effect	6.71	6.71	6.71
TOTAL	**$73.36**	**$110.23**	**$79.80**

[a] Based on 1980 dollars. Source: Gas Research Institute

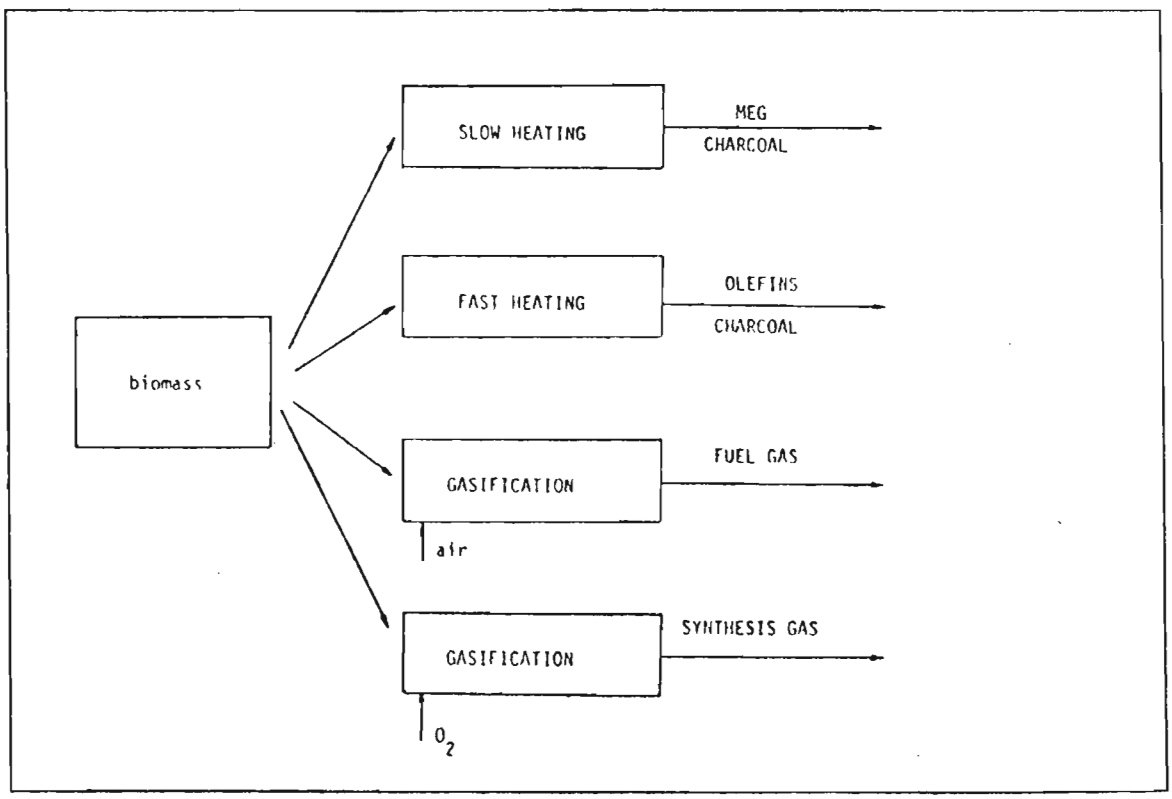

Figure 1. Biomass Processing Routes

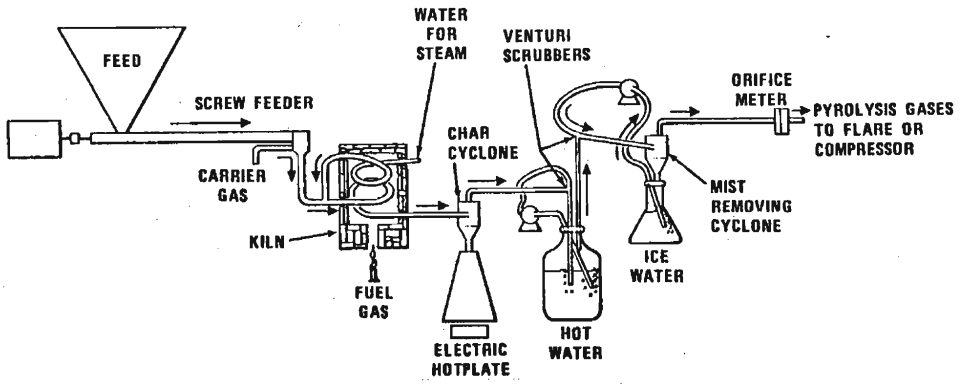

Figure 2. Pyrolysis Schematic (April 1977)

(Source: NAC TP 6022)

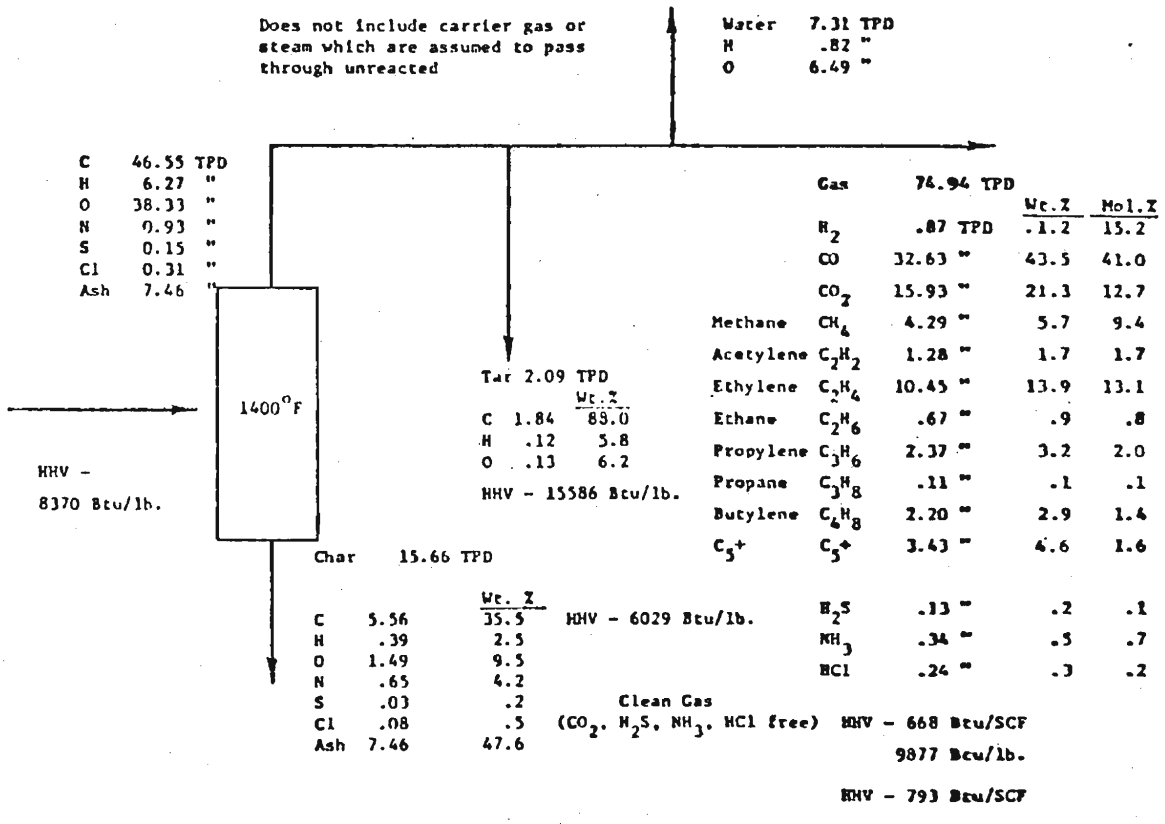

Figure 3. Material Balance Around Pyrolyzer.
(Source: Gladney,F., "Technical, Economic, and Environmental Feasibility Study of China Lake Pyrolysis System," Dow Chemical Inc., for EPA, March 1979.)

FIGURE 4

PRYOLYSIS CLEANUP UNIT OPERATIONS

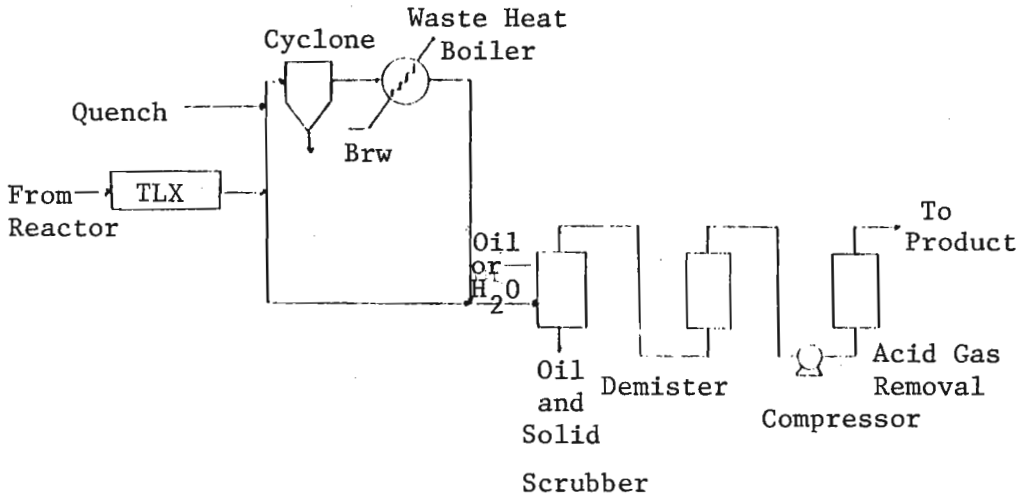

FIGURE 5

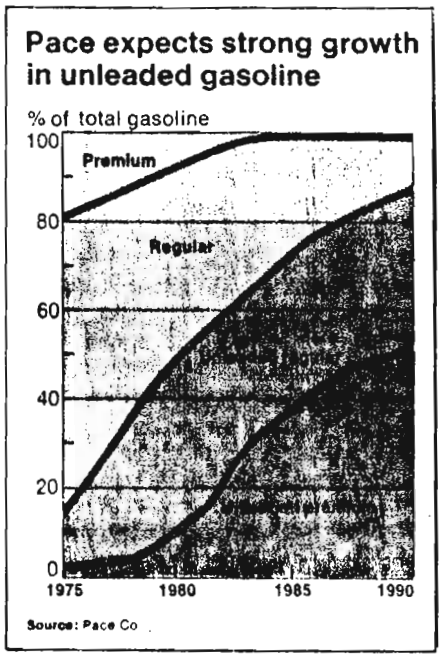

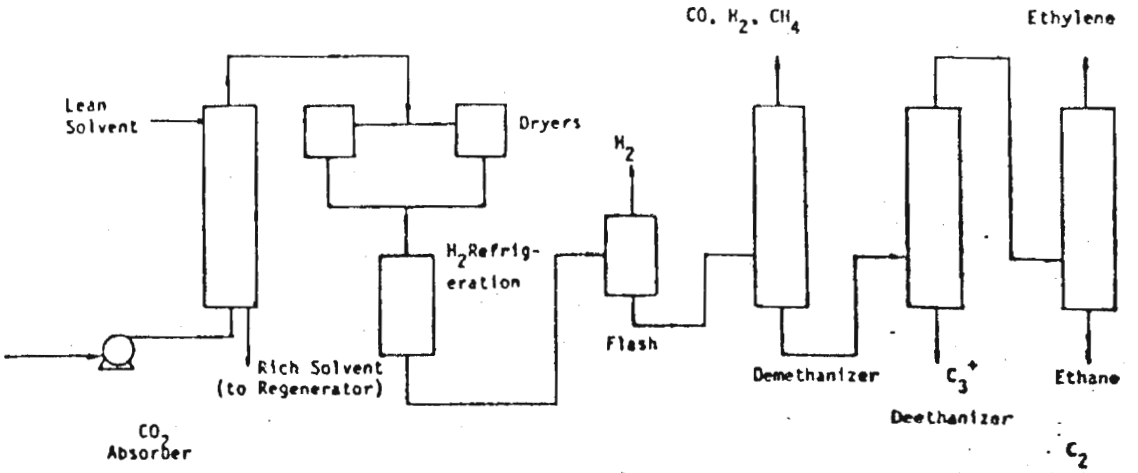

FIGURE 6. Ethylene Recovery System

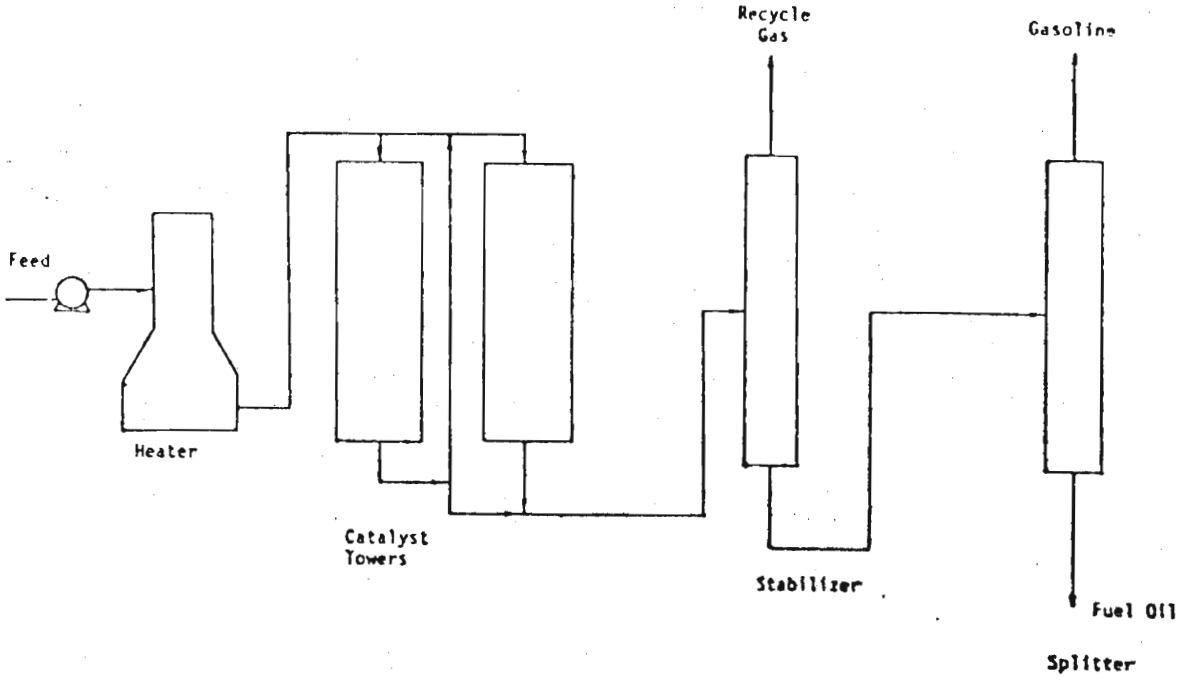

FIGURE 7. Flow Diagram for Catalytic Polymerization Process

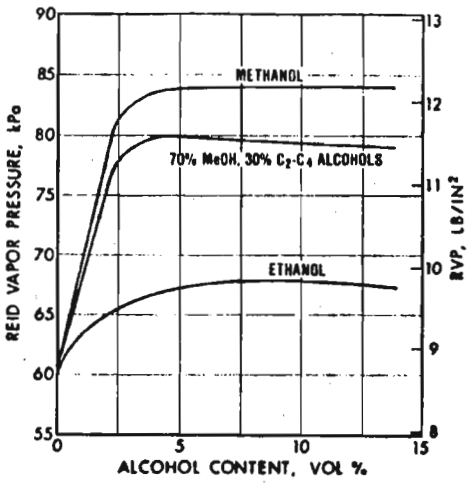

FIGURE 8 Reid Vapor Pressure Of Alcohol Blends

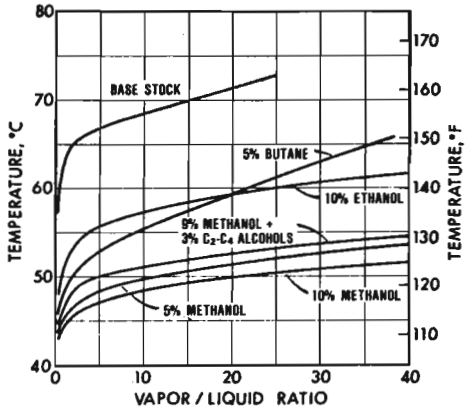

FIGURE 9 Vapor Liquid Ratios For Blends

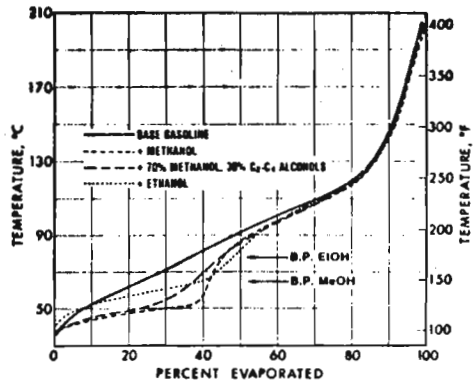

FIGURE 10 Distillation Curves For Alcohol Blends

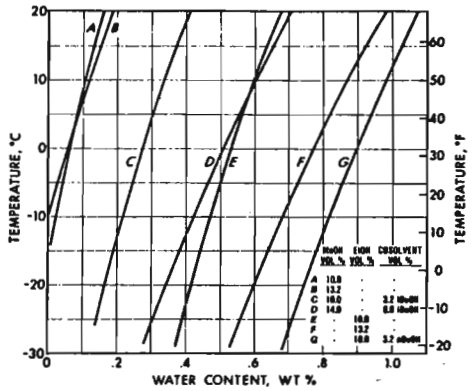

FIGURE 11 Cosolvents Can Improve Water Tolerance

(Source: Hydrocarbon Processing, 58, (5), 127 (1979))

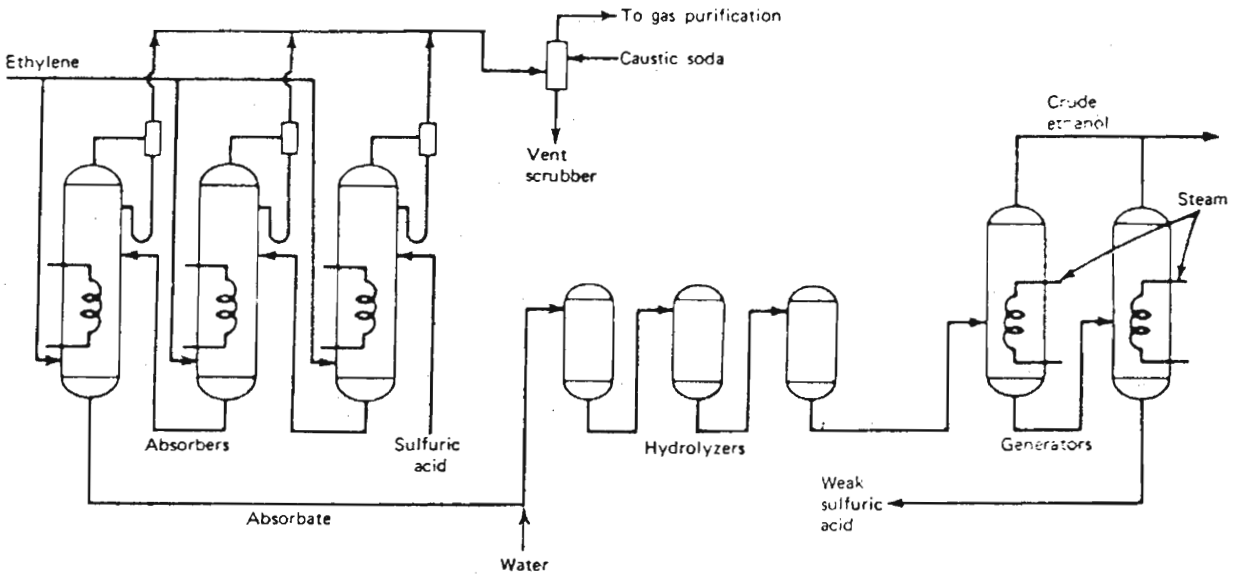

FIGURE 12 Manufacture of ethyl alcohol by esterification–hydrolysis (indirect hydration).

SPECIALISTS' WORKSHOP ON FAST PYROLYSIS OF BIOMASS

OCTOBER 19-22, 1980

COPPER MOUNTAIN, COLORADO

Michael Antal
Department of Mechanical &
Aerospace Engineering
Princeton University
Princeton, NJ 08544
609/452-5136

Charles Benham
SERI
1617 Cole Boulevard
Golden, CO 80401
303/231-1754

Paul W. Bergeron
SERI
1617 Cole Boulevard
Golden, CO 80401
303/231-1768

Mark Bohn
SERI
1617 Cole Boulevard
Golden, CO 80401
303/231-1755

Rashmikant M. Contractor
E. I. du Pont de Nemours & Co.
CR & D Dept., Experimental Sta.
Wilmington, DE 19898
302/772-3111

Ray Desrosier
SERI
1617 Cole Boulevard
Golden, CO 80401
303/231-1436

James Diebold
SERI
1617 Cole Boulevard
Golden, CO 80401
303/231-7250

Clas G. V. Ekstrom
Dept. of Chemical Technology
Royal Institute of Technology
S-100 44 Stockholm
Stockholm, Sweden S-10044
08/787-8994

Ted Frankiewicz
Occidental Research Corporation
P. O. Box 19601
Irvine, CA 92713
714/957-7257

A. Ghazee
University of Dayton
Dayton, OH 45469
513/229-3016

David W. Goheen
Pioneering Research Group
Central Research Division
Crown Zellerbach Corporation
Camas, WA 98607
206/834-4444

Michael S. Graboski
Colorado School of Mines
Chemical & Petroleum Refining
Engineering
Golden, CO 80401
303/279-0300 Ext. 2764

Herbert M. Kosstrin
P. O. Box 2325
245 Summer Street - 11th Floor
Boston, MA 02107
617/973-0309

Alex Kotch
SERI
1617 Cole Boulevard
Golden, CO 80401
303/231-1823

SPECIALISTS' WORKSHOP ON FAST PYROLYSIS OF BIOMASS

OCTOBER 19-22, 1980

COPPER MOUNTAIN, COLORADO

Barbara B. Krieger
University of Washington
Benson Hall BF-10
Seattle, WA 98195
206/543-2216 2250 (Message)

James Kuester
College of Engineering
Arizona State University
Tempe, AZ 85281
602/965-5071

J. Lede
Laboratorie des Sciences du
Genie Ghimique
1, Rue Grandville - 54042
Nancy Cedex, France
8-336-6623

Kenneth Lincoln
NASA-Ames Research Center
Mail Stop 234-1
Moffett Field, CA 94035
415/965-5373

Tom Milne
SERI
1617 Cole Boulevard
Golden, CO 80401
303/231-1440

S. Narayanan
Stone & Webster Engineering Corp.
One Penn Plaza
250 West 34th Street
New York, NY 10001
212/760-3619

Quang Nguyen
IOTECH Corporation
220 Lavrier Ave. - W
Ottawa, Ont. Canada KIP 529
613/238-4126

William A. Peters
M.I.T. Energy Laboratory
Room 66-460, M.I.T.
Cambridge, MA 02139
617/253-3433

Tom Reed
SERI
1617 Cole Boulevard
Golden, CO 80401
303/231-1437

John Scahill
SERI
1617 Cole Boulevard
Golden, CO 80401
303/231-7351

Fred Shafizadeh
School of Forestry & Department
of Chemistry
University of Montana
Missoula, MT 59801
406/243-6212

J. Michael Skaates
Department of Chemistry &
Chemical Engineering
Michigan Technological University
Houghton, MI 49931
906/487-2177

Mike Soltys
SERI
1617 Cole Boulevard
Golden, CO 80401
303/231-1449

Clayton Smith
SERI
1617 Cole Boulevard
Golden, CO 80401
303/231-1200

SPECIALISTS' WORKSHOP ON FAST PYROLYSIS OF BIOMASS

OCTOBER 19-22, 1980

COPPER MOUNTAIN, COLORADO

Meyer Steinberg
Brookhaven National Laboratory
Upton, Long Island, NY 11746
516/345-3036

Don Stevens
Battelle Northwest
P. O. Box 999
Richland, WA 99352
509/375-2260

Kent Vorhees
Department of Chemistry
Colorado School of Mines
Golden, CO 80401
303/231-0300

☆ U.S. GOVERNMENT PRINTING OFFICE: 1980—777-084/437